Vol. 172, June 1, 1985
Complete in one issue

ISSN 0003-2670

ANALYTICA CHIMICA ACTA

International journal devoted to all branches of analytical chemistry

ELSEVIER

ANALYTICA CHIMICA ACTA

International journal devoted to all branches of analytical chemistry
Revue internationale consacrée à tous les domaines de la chimie analytique
Internationale Zeitschrift für alle Gebiete der analytischen Chemie

PUBLICATION SCHEDULE FOR 1985

	J	F	M	A	M	J	J	A	S	O	N	D
Analytica Chimica Acta	167	168	169	170/1 170/2	171	172	173	174	175	176	177	178

Scope. *Analytica Chimica Acta* publishes original papers, short communications, and reviews dealing with every aspect of modern chemical analysis both fundamental and applied.

Submission of Papers. Manuscripts (three copies) should be submitted as designated below for rapid and efficient handling:

Papers from the Americas to: Professor Harry L. Pardue, Department of Chemistry, Purdue University, West Lafayette, IN 47907, U.S.A.

Papers from all other countries to: Dr. A. M. G. Macdonald, Department of Chemistry, The University, P.O. Box 363, Birmingham B15 2TT, England. Papers dealing particularly with computer techniques to: Professor J. T. Clerc, Universität Bern, Pharmazeutisches Institut, Baltzerstrasse 5, CH-3012 Bern, Switzerland.

Submission of an article is understood to imply that the article is original and unpublished and is not being considered for publication elsewhere. Upon acceptance of an article by the journal, authors will be asked to transfer the copyright of the article to the publisher. This transfer will ensure the widest possible dissemination of information.

Information for Authors. Papers in English, French and German are published. There are no page charges. Manuscripts should conform in layout and style to the papers published in this Volume. Authors should consult Vol. 170 for detailed information. Reprints of this information are available from the Editors or from: Elsevier Editorial Services Ltd., Mayfield House, 256 Banbury Road, Oxford OX2 7DH (Great Britain).

Reprints. Fifty reprints will be supplied free of charge. Additional reprints (minimum 100) can be ordered. An order form containing price quotations will be sent to the authors together with the proofs of their article.

Advertisements. Advertisement rates are available from the publisher.

Subscriptions. Subscriptions should be sent to: Elsevier Science Publishers B.V., Journals Department, P.O. Box 211, 1000 AE Amsterdam, The Netherlands. Tel: 5803 911, Telex: 18582.

Publication. *Analytica Chimica Acta* appears in 12 volumes in 1985. The subscription for 1985 (Vols. 167–178) is Dfl. 2400.00 plus Dfl. 264.00 (p.p.h.) (total approx. US $986.70). All earlier volumes (Vols. 1–166) except Vols. 23 and 28 are available at Dfl. 215.00 (US $79.60), plus Dfl. 15.00 (US $5.60) p.p.h., per volume.

Our p.p.h. (postage, packing and handling) charge includes surface delivery of all issues, except to subscribers in the U.S.A., Canada, Japan, Australia, New Zealand, P.R. China, India, Israel, South Africa, Malaysia, Singapore, South Korea, Taiwan, Pakistan, Hong Kong and Brazil who receive all issues by air delivery (S.A.L. — Surface Air Lifted) at no extra cost. For the rest of the world, airmail and S.A.L. charges are available upon request.

Claims for issues not received should be made within three months of publication of the issues. If not they cannot be honoured free of charge.

For further information, or a free sample copy of this or any other Elsevier Science Publishers journal, readers in the U.S.A. and Canada can contact the following address: Elsevier Science Publishing Co. Inc., Journal Information Center, 52 Vanderbilt Avenue, New York, NY 10017, U.S.A., Tel: (212) 916-1250.

ANALYTICA CHIMICA ACTA
VOL. 172 (1985)

ANALYTICA CHIMICA ACTA

International journal devoted to all branches of analytical chemistry

ELSEVIER Amsterdam–Oxford–New York–Tokyo

Anal. Chim. Acta, Vol. 172 (1985)

0003-2670/85/$03.30

Printed in The Netherlands

Analytica Chimica Acta, 172 (1985) 1—12
Elsevier Science Publishers B.V., Amsterdam — Printed in The Netherlands

FLOW INJECTION SYSTEM FOR STRIPPING VOLTAMMETRY

JOHN A. WISE[a] and WILLIAM R. HEINEMAN*
Department of Chemistry, University of Cincinnati, Cincinnati, OH 45221 (U.S.A.)
PETER T. KISSINGER
Department of Chemistry, Purdue University, West Lafayette, IN 47907 (U S.A.)
(Received 17th August 1984)

SUMMARY

A flow system for quantifying traces of heavy metals by anodic stripping voltammetry (a.s.v.) is described. This system is optimized for simplified, rapid sample processing using either linear-sweep or differential-pulse stripping waveforms. The linear-sweep excitation signal can be used effectively for concentrations in the ng ml^{-1} range at a rate of approximately 30 samples per hour. The differential-pulse waveform lowers the detection limits to concentrations as low as 20 pg ml^{-1}, in a sample volume of 1 ml at a rate of approximately 9 samples per hour. The advantages of the system include improved efficiency of sample preconcentration during the deposition step (especially for sub-milliliter samples), simplified operation, ready adaptability to automation and on-line monitoring, no sample deoxygenation, minimal sample pretreatment, and easy matrix exchange between the deposition and stripping steps. The utility of this system is demonstrated with indium and for the determination of lead in blood.

Anodic stripping voltammetry (a.s.v.) is the electroanalytical method of choice for quantifying very low concentrations of metal ions. Detection limits in the subnanomolar range are possible for many metals as a result of the preconcentration step. Previous work has demonstrated the good detection limits and multi-element capability of a.s.v. in thin-layer electrochemical cells [1—4]. An inherent advantage of this technique is the ability to handle small samples (50—200 μl) of low concentration efficiently by minimizing sample dilution. These systems, however, rely solely on diffusion for mass transfer of the analyte to the working electrode during deposition, thereby limiting their ability to preconcentrate the sample rapidly. The addition of convective mass transfer to the thin-layer cell configuration to increase the preconcentration efficiency while at the same time retaining small sample volumes would be highly advantageous.

This paper describes an a.s.v. system based on a thin-layer cell that is analogous to the commercially available type for liquid chromatography/electrochemistry. Sample flows through the thin-layer cell during which time metal ions are deposited in a mercury film electrode. The subsequent

[a]Present address: The Goodyear Tire and Rubber Company, 142 Goodyear Boulevard, Akron, OH 44316, U.S.A.

0003-2670/85/$03.30

stripping step is by either linear-scan voltammetry or differential-pulse voltammetry. Although it has been evaluated primarily with respect to the determination of indium ions for its ultimate use in an electrochemical immunoassay [6], the system exhibits general applicability to other problems such as the determination of lead in blood.

The adaptation of stripping voltammetry to flowing systems has also been explored in other laboratories, as reviewed by Wang [7]. This work demonstrates a flow system with a lower detection limit (50 pg ml^{-1} for indium) than any system reported thus far.

EXPERIMENTAL

Equipment

Flow system. A schematic drawing of the a.s.v. flow system is shown in Fig. 1. The oxygen removal system is described in the operations manual for the BAS amperometric controller (Bioanalytical Systems, West Lafayette, IN). A mercury pool electrode in the eluent flask was added for in situ pre-electrolysis of the supporting electrolyte. The h.p.l.c. pump (Eldex A-60-S) produced a flow rate that could be varied between 0.1 and 3.0 ml min^{-1}. A 3-cm guard column packed with 5-μm amino-bonded phase (Brownlee Labs) was used to provide sufficient back-pressure to ensure efficient pump operation. All tubing and connections were of 316 stainless

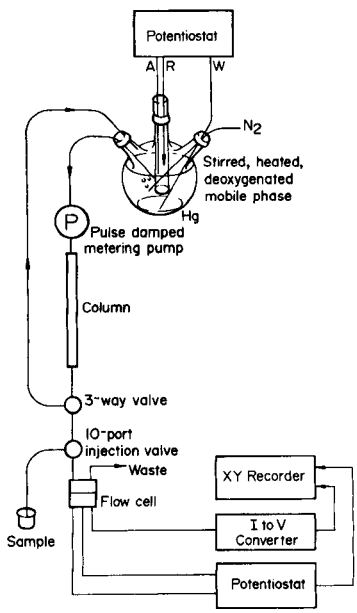

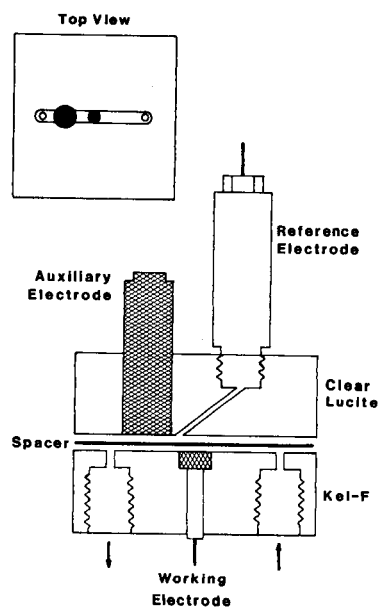

Fig. 1. Schematic drawing of the flow injection/a.s.v. system. See text for details.

Fig. 2. Thin-layer flow cell for flow injection/a.s.v. See text for details.

steel, Teflon, or Kel-F. The switching valve was a Model 70-30 (Rheodyne). The injection valve was a Valco 10-port valve arranged for use with two different sample loops. The five sample-loop volumes utilized were 20, 100, 200, 500 and 1000 μl.

The electrochemical transducer used for this system was an adaptation of a BAS thin-layer flow cell and is depicted in Fig. 2 [6]. The working electrode portion of the cell (MF 1019; BAS) was made of Kel-F and contained a glassy carbon electrode (3.2-mm diameter) along with the flow inlet and outlet ports. The gasket that defines the thin-layer volume was 0.127 mm thick, and had a channel width of 2 mm, yielding a total cell volume of approximately 4 μl. The auxiliary electrode portion of the cell was machined from clear Lucite and contained a wax-impregnated graphite auxiliary electrode (4.6 mm diameter) located downstream from the position of the working electrode. The Lucite half also contained an additional port for the Ag/AgCl reference electrode (MF 2075; BAS).

Electrochemical instrumentation. Potentiostatic control of the thin-layer cell was provided by either a PAR-174A Polarographic Analyzer (Princeton Applied Research Corp.), a CV-27 Voltammograph or a BAS-100 Electrochemical Analyzer (both from BAS). The potentiostat used for pre-electrolysis of the supporting electrolyte in the eluent flask was of conventional operational amplifier design, utilizing a high-current control amplifier [8]. A Houston Instruments Omnigraphic 2000 x-y recorder or a digital plotter was used to record stripping voltammograms.

Reagents

Standard solutions were prepared by diluting atomic absorption standards (Aldrich Chemical Co. for indium and Fisher Scientific Co. for others) with appropriate volumes of supporting electrolyte. The supporting electrolyte (0.1 M sodium acetate/0.05 M nitric acid, pH 4.75) was prepared from h.p.l.c.-grade sodium acetate (Fisher Scientific Co.) and Ultrex nitric acid (J. T. Baker Chemical Co.). Stock solutions of 1 M sodium acetate was pre-electrolyzed for 240 h at −1.5 V vs. SCE in a separate pre-electrolysis cell and then diluted with Type I water from a Nanopure Water System (Barnstead-Sybron) before transfer to the eluent flask for further pre-electrolysis and deoxygenation. Preformed mercury films were deposited from a 0.012 M mercury(II) nitrate/1.0 M potassium nitrate solution.

Procedures

Mercury film formation. The 1-ml sample loop was filled with the acidified 0.012 M mercury(II) nitrate solution. It was then injected at a flow rate of 0.10 ml min^{-1}. After 10 s, voltage was applied with the working electrode at −0.70 V vs. Ag/AgCl, and the mercury film was deposited for 10 min. The potential was then scanned linearly to 0.10 V where it was held for 1 min to strip oxidizable impurities from the film. The mercury film electrode (MFE) was then ready for use. Because a new film was generated

so easily, the cell typically was cleaned at the end of each day by wiping the MFE with a tissue and a new film was applied each morning; however, the same film can be used for a week.

Stripping coulometry was used to estimate the film thickness. After the deposition procedure, the potential of the MFE was stepped from −0.700 V to +0.700 V, and the current response resulting from the oxidation of the mercury on the electrode surface was integrated. Several such experiments indicated that film thickness was typically 300 μm, assuming a uniform distribution of mercury.

A.s.v. experiments. After the 1-min cleaning time for the MFE, the sample was injected into the flow stream. After allowing time for the sample to reach the cell, the potential of the MFE was stepped to −1.00 V. Twenty seconds after the sample had exited from the cell, the positive scan was initiated at a rate of either 20 mV s^{-1} for linear-sweep stripping or 5 mV s^{-1} for differential-pulse stripping. The parameters used for the differential pulse anodic scan were 5 mV s^{-1} scan rate, 25 or 50 mV modulation amplitude, depending on the required resolution, 0.5-s pulse interval, and variable current range depending on the concentration of the analyte. The potential scan was stopped at +0.10 V, and this potential was held for 10 s before proceeding to the next sample. Flow rates and sample volumes were optimized for different concentration ranges. The resulting deposition times were between 30 s and 5 min with total quantitation times per sample between 2 and 8 min.

Determination of lead in blood. A 100-μl aliquot of blood drawn from children or pregnant women was added to 2.9 ml of Metexchange reagent (Environmental Science Associates) by the Environmental Health Department at the University of Cincinnati College of Medicine. The samples were usually held for approximately three days before being sent to the laboratory, although they were ready for processing essentially immediately after preparation.

Upon arrival, the content of each cuvette was thoroughly mixed on a vortex mixer and then transferred to a 12 × 75-mm sterile polystyrene culture tube. Each tube was then centrifuged for 5 min to separate the cells. The supernatant solution was drawn into the 100-μl sample loop and injected (flow rate 0.10 ml min^{-1}). After 5 s, the potential of the MFE was stepped from +0.10 V to −1.00 V vs. SCE using a CV-27 Voltammograph. After another 90 s, a linear potential sweep with a positive scan was initiated at a rate of 50 mV s^{-1}. The scan was terminated at +0.10 V and the next sample was drawn into the loop and injected.

Calibration plots were obtained by making standard additions on the Lo Level Controls supplied with each Metexchange kit. This plot was used to correlate stripping peak current to sample concentration and then mathematically to the lead concentration in blood.

RESULTS AND DISCUSSION

Design criteria for flow system and flow cell

The flow system permits supporting electrolyte which has been pre-electrolyzed to remove reducible metal ion impurities and deoxygenated in the three-arm flask to be pumped through a 10-port sample injection valve and then through a thin-layer electrochemical cell. Other than clean-up of mobile phase, there are only three differences between this flow system and a conventional apparatus for liquid chromatography with electrochemical detection (l.c.e.c.). One difference is the addition of two nonmetallic inert fittings, one at each side of the pump head. These fittings are essential if the potentiostat utilizes hard ground for the working electrode. If the stainless steel tubing and fittings are not isolated from the grounded pump, sample deposition takes place in the sample loop and solvent breakdown occurs in the supply tubing for the mobile phase, producing bubbles that can be trapped in the check valves. To avoid these problems, special fittings were machined from Teflon or Kel-F for each check valve to isolate the remainder of the tubing. Kel-F was preferred because of its lower oxygen permeability.

The second consideration is to minimize the tubing length and volume between the injection valve and the flow cell. This reduces the time between sample injection and the beginning of the deposition step as well as allowing the system to be flushed clean more quickly. The third feature involves a switching valve located before the injection loop to permit mobile phase to be cycled through most of the system while the thin-layer cell is being assembled or disassembled. This procedure saves mobile phase while allowing for recirculation to keep the system clean.

Initial research was done with a commercially available cell (BAS). While these thin-layer flow cells work well, the cell design that evolved during the course of the research and which is pictured in Fig. 2 has three significant advantages. First, the top half of the cell is clear, allowing the user to observe the working electrode. This makes it possible to determine whether the mercury film formation is adequate and also to see if, or where, bubbles are trapped within the cell. Second, the auxiliary electrode is located within the thin-layer channel, but downstream from, instead of directly opposite, the working electrode. This prevents any possible electroactive components generated at (or cathodically stripped from) the auxiliary electrode from interacting at the working electrode. Third, the Teflon gasket which provides the thin-layer spacing has a narrower channel width (2 mm vs. 4.8 mm) than the original version. A channeling effect in these cells directs the flow straight from inlet to outlet through the cell [9]. It appears that the width of this flow path is inversely proportional to flow rate. This effect produces a variable dead volume along each edge of the cell. The narrower channel reduces this dead volume, reduces the working electrode surface area, and insures that the sample flow passes directly over the working electrode.

Because samples are not deoxygenated, oxygen from the sample can diffuse into the cell dead volume during the deposition step. The reduction in dead volume minimizes the time necessary for the medium exchange to deoxygenate the flow cell effectively between the deposition and stripping steps. The fact that the working electrode now reaches from edge to edge of the cell alleviates a memory effect caused by the stripping of metals into the dead volume area around the electrode and their subsequent redeposition with the next sample. It also serves to reduce the background noise observed during the stripping step. Because of the channeling effect, the edges of the electrode contribute little to the useful signal; however, the reduction of oxygen trapped in the edge volume does add to the background current level. The narrower channel alleviates this problem and improves the signal/noise ratio by reducing the unnecessary surface area.

Oxygen removal and pre-electrolysis

Removal of oxygen from the sample prior to injection into the flow system is not necessary because a medium exchange takes place before the stripping step. No difference in stripping voltammograms was observed between samples that had or had not been deoxygenated. It is important, however, to use a supporting electrolyte which is as free of oxygen and trace metal contaminants as possible for samples with trace or ultratrace concentrations. Oxygen was removed by elevating the temperature to 50°C and bubbling nitrogen into the eluent flask. The 6 ft. of 1/8-in. stainless steel tubing between the flask and the pump is sufficiently long to allow the carrier solution to cool to room temperature before being pumped through the system.

A mercury pool working electrode, a platinum wire auxiliary electrode, and a saturated calomel reference electrode were also added to the flask. The potential of the working electrode was held at −1.50 V to pre-electrolyze the buffered carrier solution. The entire unit was mounted above a magnetic stirring motor to increase mass transfer to the mercury pool. In this way, blank levels of constituent metals in the supporting electrolyte were held well below nanomolar levels as determined by checking standard additions to the supporting electrolyte.

Dependence of metal deposition efficiency on flow rate

The dependence of metal deposition efficiency on flow rate was evaluated by alternating 20-μl injections of a blank buffer solution and the same buffer solution with 1.0 μg ml^{-1} indium ion at several different flow rates. The resulting current during deposition was integrated, and the blank value was subtracted from the sample value at each flow rate. The measured charge was then divided by the calculated charge required for complete reduction of the sample to give the percentage deposited. Results are presented in Fig. 3. This curve is in good agreement with similar curves calculated for flow cells with similar channel thicknesses. For the system described, 0.20 ml min^{-1} was

found to be a good balance between limit of detection, time of quantitation, and pump capability (metering precision is poorer at low flow rates) when low concentrations were quantified. At this flow rate, approximately 60% of the metal ion in each sample was deposited in the MFE. For samples of higher concentration, faster flow rates or smaller sample volumes can be used to shorten the deposition time and increase the sampling rate.

Linear-sweep a.s.v.

For samples in the middle-to-high ng ml^{-1} range, the linear-sweep stripping waveform can be used effectively. Indium(III) was chosen as a test species because of its well documented and well defined electrochemistry as well as the relatively low levels at which it is found in the supporting electrolyte. This latter feature enabled detection levels to be evaluated without extensive pre-electrolysis of supporting electrolyte as would be the case with lead, cadmium, zinc and other ubiquitous metal ions.

Figure 4 shows a series of stripping voltammograms recorded on standard indium(III) solutions. Excellent correlation between peak current and

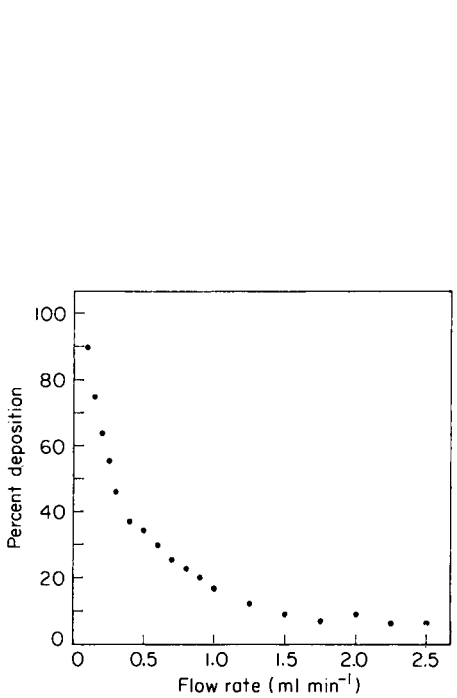

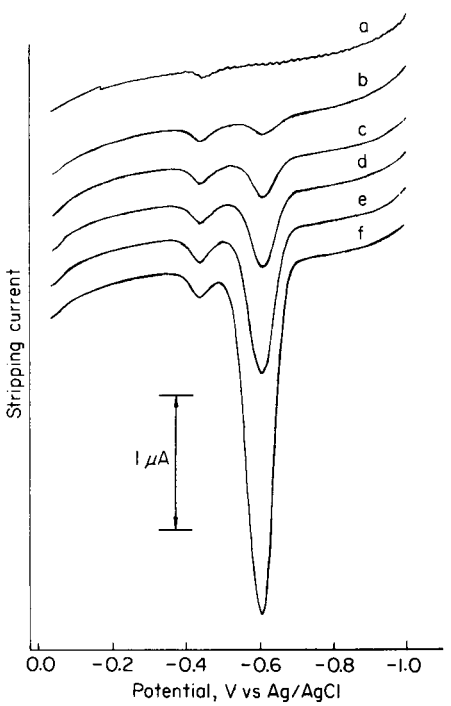

Fig. 3. Effect of flow rate on deposition efficiency for indium.

Fig. 4. Linear-sweep stripping voltammograms recorded after 200-μl injections of standard indium(III) solutions. Flow rate 0.25 ml min^{-1}; scan rate 20 mV s^{-1}. Indium concentration: (a—f) blank, 20, 50, 100, 200 and 500 ng ml^{-1}, respectively.

concentration was observed over a wide range of sample concentrations and flow rates, as is illustrated in Fig. 5. While the sensitivity is better at lower flow rates, quantitation time can be significantly reduced without a drastic loss of sensitivity at higher flow rates (up to 1 ml min^{-1}). For a 200-μl sample volume, a volumetric flow rate of 1 ml min^{-1}, a linear potential-scan rate of 20 mV s^{-1} and a 15-s equilibration period between the deposition and stripping steps, it is possible to process 30 samples per hour at these levels.

The flow need not be interrupted during the stripping step. In fact, continuous flow is advantageous with these thin-layer flow cells because it reduces the likelihood of bubble formation within the cell and allows the cell to be cleaned by mobile phase before the next sample. No difference in peak stripping current was observed between voltammograms recorded under stopped flow and continuous flow conditions.

The linear-sweep waveform can be used effectively at lower concentrations if a larger sample volume is pre-electrolyzed. However, this translates into longer quantitation time per sample.

Differential-pulse a.s.v.

As in stripping voltammetry in large volumes of solution, the detection limit can be improved compared to linear scan techniques by using the differential-pulse waveform for the stripping step. The stripping peak current for indium was optimized by systematic variation of the pulse height, the pulse interval, and the scan rate. The effect of pulse amplitude at different scan rates on the peak stripping current is shown in Fig. 6. At each scan rate, the sensitivity increased almost linearly with pulse height up to 50 mV and then increased less rapidly as predicted by theory [10]. Some of this

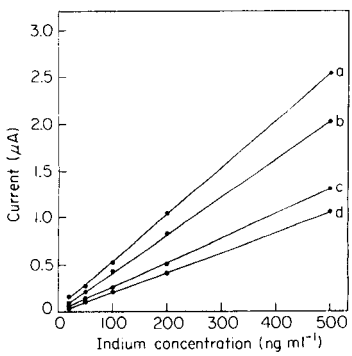

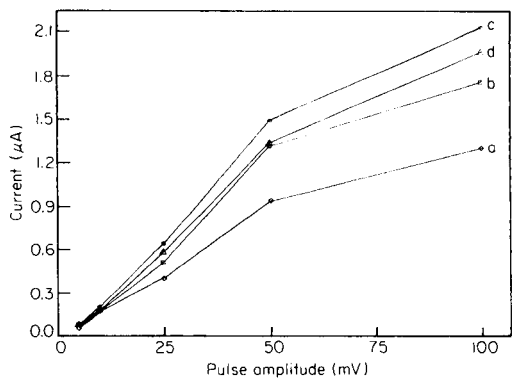

Fig. 5. Plot of peak stripping current vs. indium(III) concentration at different flow rates: (a—d) 0.25, 0.50, 0.75 and 1.0 ml min^{-1}, respectively. Scan rate 20 mV s^{-1}.

Fig. 6. Effect of pulse amplitude at different scan rates on the peak stripping current for indium (100 ng ml^{-1}, 200-μl injections, flow rate 0.5 ml min^{-1}) Scan rate: (a—d) 1, 2, 5, 10 mV s^{-1}, respectively.

deviation may result from *iR* drop caused by uncompensated resistance in the thin-layer cell during the rapid and large potential excursions. Although the peak stripping current is greatest at a 100-mV pulse amplitude, more reproducible results were obtained for a 25-mV or 50-mV pulse height. Figure 7 shows that greater sensitivity was observed at shorter pulse intervals when a scan rate of 5 mV s^{-1} with a 25-mV pulse amplitude was used.

The conditions for near maximum sensitivity are 5 mV s^{-1} scan rate, 50-mV pulse amplitude, and a 0.5-s pulse interval. Although the peak stripping currents are slightly lower at a differential-pulse scan rate of 10 mV s^{-1} than at 5 mV s^{-1}, the significant decrease in quantitation time more than compensates for the loss of sensitivity, unless the sample concentrations are near the limit of detection.

As noted above, the 10-port injection valve permits the use of different sample volumes for different concentrations. Increasing the sample size to 1 ml gives a deposition time of 300 s at a 0.20 ml min^{-1} flow rate and allows metal ions at the pg ml^{-1} range to be quantified at a rate of approximately 9 samples per hour. For indium concentrations over the range 50—1000 pg ml^{-1}, peak current varied linearly with concentration. A least-squares fit of peak stripping current (nA) vs. concentration (ng ml^{-1}) gave a slope of 46.7 ± 1.2, a *y*-intercept of —1.84 ± 0.65, a standard error of estimate of 1.89 and a correlation coefficient of 0.9994. Relative standard deviations for three runs at each concentration were in the range 6—12%. Similarly linear response was obtained for higher indium concentrations (1—8 ng ml^{-1}).

Typical differential-pulse stripping voltammograms for indium are shown in Fig. 8. For the eight standard solutions between 1 ng ml^{-1} and 8 ng ml^{-1}, the correlation coefficient was 0.999. The peaks at —0.47 and —1.05 V are lead and zinc impurities in the buffer solution used to dilute the indium standard.

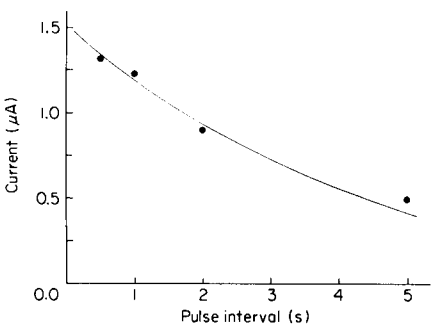

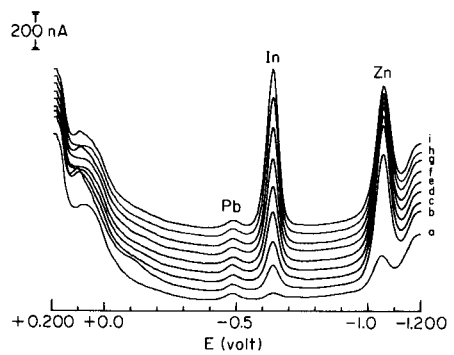

Fig. 7. Effect of pulse interval on peak stripping current (5 mV s^{-1} scan rate, 25-mV pulse amplitude, 0.5 ml min^{-1} flow rate).

Fig. 8. Differential-pulse stripping voltammograms recorded after 1.00-ml injections of standard indium solutions: (a—i) blank, 1.0, 2.0, 3.0, 4.0, 5.0, 6.0, 7.0 and 8.0 ng ml^{-1}, respectively. Flow rate 0.5 ml min^{-1}, scan rate 5 mV s^{-1}, pulse amplitude 25 mV.

Determination of lead in blood

The determination of lead in blood is one of the commonest determinations of a metal in a biological sample, and served as a representative system to evaluate the capabilities of flow injection/a.s.v. for real samples.

The Metexchange reagent is effective in releasing lead from red blood cells. Results with this reagent correlate well with results obtained by standard acid digestion procedures [11, 12]. The experimental section describes the modifications of the ESA procedure used here. Best results were obtained when samples were centrifuged to remove the blood cells which tended to drag across the electrode surface, causing sharp current spikes and building up on the upstream edge of the MFE, thus altering the flow path.

The results from this study were generally in good agreement with those obtained by using the ESA instrumentation (Fig. 9). At low lead concentrations, the flow injection/a.s.v. values were typically higher than those obtained with the ESA technique. Standard-addition studies for lead in the range 5—9 ng showed that the ESA procedures consistently underestimated the amount of lead by as much as 1—3 ng.

Figure 10 shows results from the flow injection/a.s.v. procedure along with those obtained by four other methods plotted against results obtained at the National Bureau of Standards by isotope dilution mass spectroscopy (i.d.m.s.). The samples in this comparison were bovine blood from the Center for Disease Control (CDC). The CDC values are a consensus of

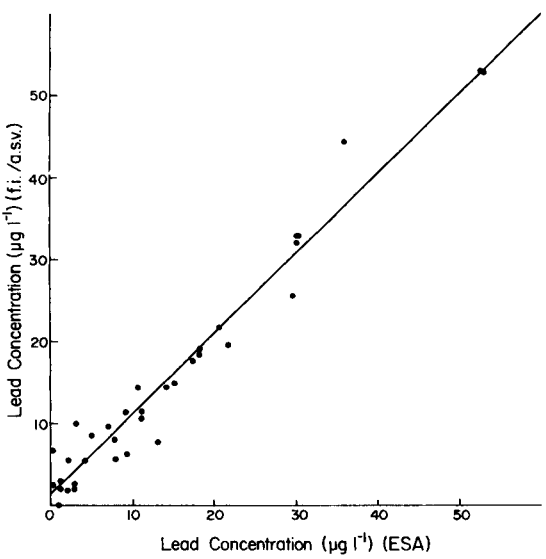

Fig. 9. Correlation plot of results obtained by the flow injection/a.s.v. procedure vs. the ESA procedure for lead in blood. Least-squares fit: $y = (0.947 \pm 0.036)x + (15.6 \pm 6.66)$ with $s_{yx} = 31.01$ and $r = 0.94$.

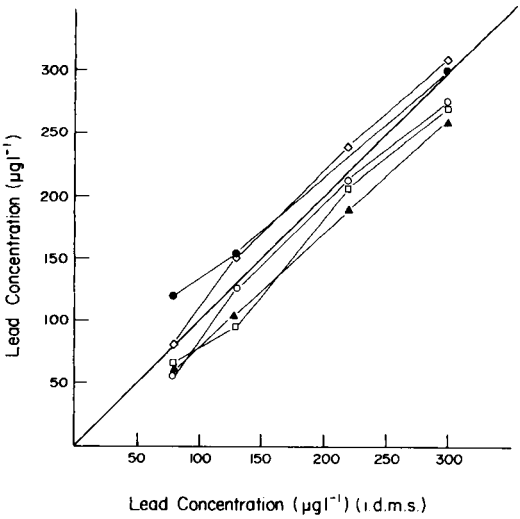

Fig. 10. Comparison of results for lead in bovine blood by five methods with results by i.d.m.s.: (○) a.s.v., University of Cincinnati Environmental Health; (●) a.a.s., University of Cincinnati Environmental Health; (◇) CDC Reference Labs; (□) ESA, a.s.v.; (▲) flow injection/a.s.v.

determinations made by six CDC reference laboratories which used acid digestion procedures with both a.s.v. and electrothermal atomic absorption spectrometric (a.a.s.) detection. The a.s.v. values from the University of Cincinnati Department of Environmental Health were obtained with the ESA Model 3010 Trace Metal Analyzer. The ESA/a.s.v. values are those reported by Environmental Science Associates after their own in-house determinations. Two trends are apparent from this correlation plot: the best correlation with i.d.m.s. values is achieved by the flow injection/a.s.v. technique, and flow injection/a.s.v. is the only technique which maintains linearity at the low end of the concentration range. The intercept of the flow injection/a.s.v. plot indicates some systematic error, probably because of incomplete release of lead from the red blood cells before they are separated from the reagent mix.

We acknowledge the Department of Environmental Health for their assistance. This work was supported in part by NSF Grant CHE8217045.

REFERENCES

1 W. R. Heineman, T. P. DeAngelis and J. F. Goelz, Anal. Chem., 47 (1975) 1364.
2 T. P. DeAngelis and W. R. Heineman, Anal. Chem., 48 (1976) 2262.
3 T. P. DeAngelis, R. E. Bond, E. E. Brooks and W. R. Heineman, Anal. Chem., 49 (1977) 1792.
4 D. A. Roston, E. E. Brooks and W. R. Heineman, Anal. Chem., 51 (1979) 1728.

5 D. W. Paul, T. H. Ridgway and W. R. Heineman, Anal. Chim. Acta, 146 (1983) 125.
6 M. J. Doyle, H. B. Halsall and W. R. Heineman, Anal. Chem., 54 (1982) 2318.
7 J. Wang, Am. Lab., 15(7) (1983) 14.
8 D. W. Paul, Ph.D. Dissertation, University of Cincinnati, 1980.
9 R. E. Shoup, G. S. Mayer and L. A. Allison, The 1983 LCEC Symposium, Indianapolis, IN, May, 1983.
10 J. Osteryoung and K. Hasebe, Rev. Polarography Jpn., 22 (1976) 1.
11 G. Morrell and G. Giridhar, Clin. Chem., 22 (1976) 221.
12 B. Searle, W. Chan and B. Davidow, Clin. Chem., 19 (1973) 76.

Analytica Chimica Acta, 172 (1985) 13—30
Elsevier Science Publishers B.V., Amsterdam — Printed in The Netherlands

THE IMPORTANCE OF CONCENTRATION EFFECTS AT THE ELECTRODE SURFACE IN ANODIC STRIPPING VOLTAMMETRIC MEASUREMENTS OF COMPLEXATION OF METAL IONS AT NATURAL WATER CONCENTRATIONS

A. M. ALMEIDA MOTA[a], J. BUFFLE*, S. P. KOUNAVES and M. L. SIMOES GONCALVES[a]

Department of Inorganic and Analytical Chemistry, University of Geneva, Sciences II, 30, quai E. Ansermet, 1211 Geneva 4 (Switzerland)

(Received 1st November 1984)

SUMMARY

The influence of the ligand/metal ion concentration ratio on the shape, peak current and peak potential of curves obtained by anodic stripping voltammetry (a.s.v.) at the hanging mercury drop electrode is described, particularly with respect to the use of a.s.v. for speciation of metal ions at very low concentrations as is often found in natural waters. The lead(II)/triethylenetetramine system is used as a model of a fully labile reversible system. It is shown that the total metal ion concentration at the electrode surface (C_M^0) during the stripping step may be much larger (30—300 times in typical conditions) than that in the bulk solution (C_M), the exact value depending on the deposition time t_d. Consequently, changes in the peak characteristics are observed when the ligand/metal concentration ratio in the bulk of the solution, C_L/C_M, is less than 1000. Semi-empirical equations, experimentally tested, are given, which enable C_M^0/C_M to be estimated for a specified solution and a.s.v. conditions, which correct for the "surface concentration effect" when a.s.v. is used to measure complexation, and which describe the influence of the parameters such as stirring efficiency, radius of the mercury drop and C_L/C_M. The implications of the results are discussed for determinations of total metal ion in complex media, of speciation based on peak-potential shifts or stripping voltammetric curves, and of complexation capacity.

Anodic stripping voltammetry (a.s.v.) is widely used for the determination and speciation of trace metals in natural waters because the techniques can be applied directly, even at the extremely low concentrations found in these samples [1—3]. The a.s.v. procedure includes the deposition step, where the metal ion M is reduced on the electrode surface during time t_d, at a constant deposition potential, E_d, and the stripping step, in which the metal is oxidized back into solution by scanning the potential towards more positive values. The deposition is, of course, a preconcentration step, thus the metal ion concentration at the electrode surface (C_M^0) during the stripping step, is much larger than that in the bulk solution (C_M).

[a]Present address: Centro de Quimica Estrutural, Instituto Superior Tecnico, 1096 Lisboa, Portugal.

0003-2670/85/$03.30

Although this surface concentration effect is of no particular importance in the case of an uncomplexing medium, in a complexing medium it may drastically influence the ligand-to-metal concentration ratio, and so the concentration gradient of M at the electrode surface will be modified, as well as the shape of the current/potential curve [4—6]. Obviously, this effect will be negligible when the bulk ligand concentration (C_L) is so large that it is in great excess even at the electrode surface during the stripping step. Unfortunately, this is not the case for many ligands found in natural water systems.

Figure 1 indicates typical ranges of concentrations of the commonest metal ions determined by a.s.v., and of the most important dissolved aquatic ligands (more details are available elsewhere [7]). Except for a few inorganic

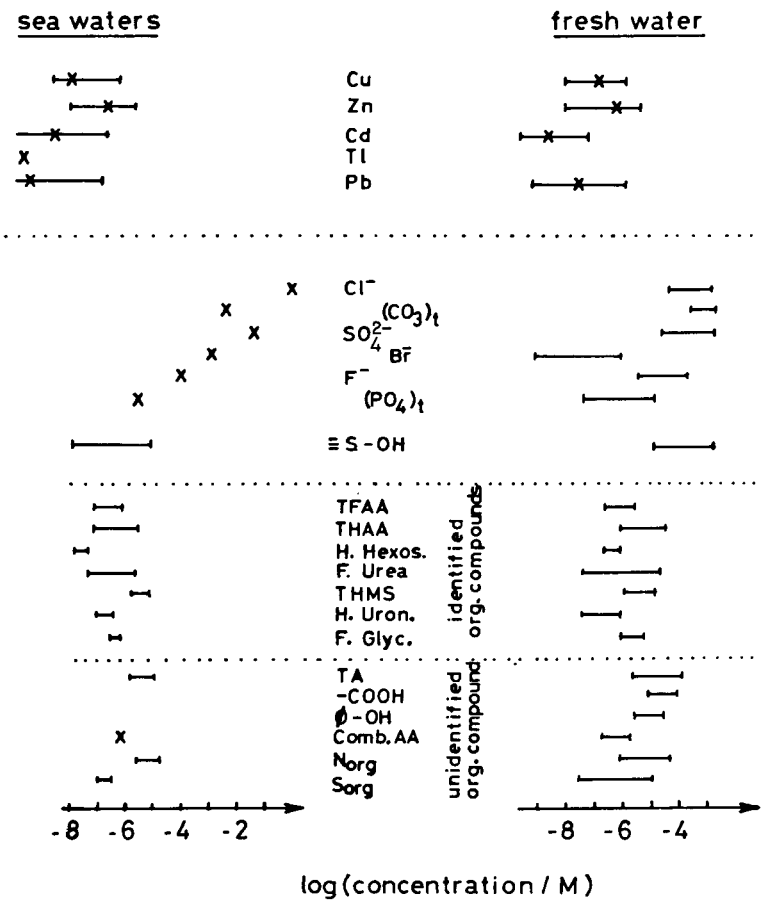

Fig. 1. Concentration ranges (——) and average values (x) of metals and ligands in water. Concentration units (molarity) relate to monomers (identified compounds and Comb-AA), functional groups (TA, —COOH, ∅—OH), or donor atoms (N_{org}, S_{org}). H. Hexos., hydrolysable hexosamines; H. Uron., hydrolysable uronic acids; F. glyc., free glycolic acid; N_{org}, S_{org}, organic N and S; TFAA (THAA), total free (hydrolysable) amino acids; THMS, total hydrolysable monosaccharides; F. Urea, free urea.

ligands such as Cl^-, HCO_3^- and SO_4^{2-}, $C_L/C_M \approx 100$ for most of the ligands and C_L/C_M may sometimes be as low as 10. It is then very important to establish whether a ratio between 10 and 100 in the bulk solution is large enough to ensure an excess of ligand at the electrode surface. The aims of this paper are first to evaluate quantitatively the influence of C_L/C_M on certain a.s.v. peak characteristics (current (i_p), potential (E_p), and shape), then to estimate the minimum ratio above which this effect is negligible, and finally to provide a procedure allowing one to correct for this effect when it is not negligible.

In studies of trace metal in natural waters, these aspects are particularly relevant in the following situations: (1) if the total concentration of M is calculated from i_p vs. C_M calibration data, without complete elimination of the ligand in the medium; (2) if the stability constants of labile ML complexes are measured from the shift in E_p with C_L [8]; (3) if complexation of M is evaluated by recording i_p vs. E_d curves (stripping polarography) [9—12]; and (4) if the complexation capacity and complexation constants are calculated from i_p vs. C_M standard addition curves [6, 13—15]. The last three cases will be discussed here.

The above effect was tested by using lead(II) and triethylenetetramine (TETA). In the conditions used, this ligand forms a well defined 1:1 complex [16]. In order to test specifically the surface effects, the bulk composition of the solution was held constant. Hence, in most cases, the increase in C_M^0 was obtained by increasing t_d at constant C_M, and the parameters i_p and E_p were used to follow the resulting effect of surface concentration. This effect was also investigated by using a medium-exchange system, in which the solution in the cell is changed between deposition and stripping.

EXPERIMENTAL

Reagents and apparatus

All reagents were of analytical grade (Merck) except for TETA which was of 99% purity (Fluka). Stock solutions were 0.1 M potassium nitrate acidified to pH 5.5, 1.00×10^{-2} M lead nitrate acidified to pH 3.0, 4.90×10^{-2} M TETA neutralized to pH 8.0 (concentration verified by an acid-base titration), and triethanolamine buffer solution at pH 7.5 with a concentration 10 times that of TETA.

The precision of the pH measurements was ±0.01 pH unit (Metrohm pH meter E-603). Buffer solutions of pH 4.00 and pH 7.00 (Merck) were used for calibration.

A Tacussel PRG5 polarograph was used for all experiments. The reference electrode, to which all potentials are referred, was Ag/AgCl/sat. KCl/0.10M KNO_3. The working electrode was a Metrohm (EA-290) hanging mercury drop electrode (HMDE), with a cone-shaped capillary end (the immersed length was 1.7 cm; the outside (o.d.) and inside diameters (i.d.) were 4.55 and 0.1 mm respectively). Because the geometry of the electrochemical cell strongly influences the reproducibility of the deposition step, a special plexi-

glas cell was built (Fig. 2, I) which would ensure reasonably reproducible stirring efficiency. Stirring was provided by a synchronous motor (Metrohm E-504), and a teflon-covered magnetic bar (4 mm diameter), the length of which (1.5 cm) was appropriate to the internal bottom diameter of the cell in order to prevent lateral movement. The bottom of the cell was conical, in order to prevent fallen mercury drops from impeding the rotation of the stirrer. The immersed parts of the platinum counter electrode (1 cm long, 1 mm diameter) and the reference electrode bridge (1 cm long, 3 mm diameter) were positioned about 0.7 cm above the endplane of the HMDE capillary. Purified nitrogen for degassing was introduced by means of a polyethylene capillary tube (1 mm o.d.).

The radius of the mercury drops (r_0), was determined by weighing a fixed number of drops, as a function of the divisions indicated on the HMDE (for 2, 5, 10 divisions, r_0 = 0.032, 0.044 and 0.055 ± 0.002 cm, respectively).

The average thickness of the diffusion layer ($\bar{\delta}$) in the solution during the deposition step was evaluated by recording the current, i_d, in an uncomplexing solution and at a sufficiently negative potential so that $C^0_{Pb} = 0$, and then by using the equation [17]: $\bar{i}_d = nFSD_{Pb}C_{Pb}/\bar{\delta}$, where $\bar{i}_d$ is the average value of i_d and is independent of time at sufficiently negative values of E_d (Fig. 3), n = 2, F = 96 494 C, S is the surface area of the Hg drop, D_{Pb} is the diffusion coefficient of Pb^{2+} in solution (8.3×10^{-6} cm^2 s^{-1}) [18], and C_{Pb} is the total concentration of Pb^{2+} in solution (10^{-4} M).

By using a variable-speed motor, it was found that $\bar{\delta}$ increases with $(1/\omega)^{1/2}$, where ω is the rotation speed of the stirrer. With the synchronous

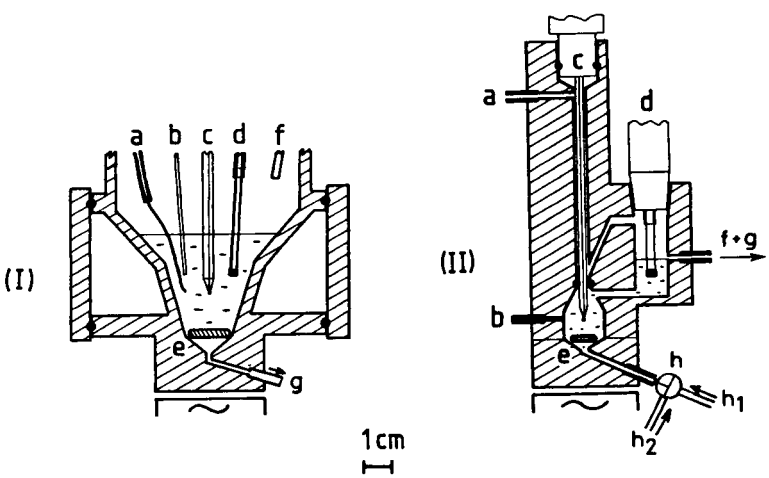

Fig. 2. Plexiglas cells for a.s.v.: (I) under classical conditions; (II) with medium exchange. Parts: (a) nitrogen entrance; (b) Pt electrode; (c) HMDE; (d) reference electrode; (e) stirrer; (f) exit for nitrogen (and solution for cell II); (g) exit of solution (and Hg drops for cell I); (h) three-way stopcock for entry of deposition solution (h_1) and stripping solution (h_2).

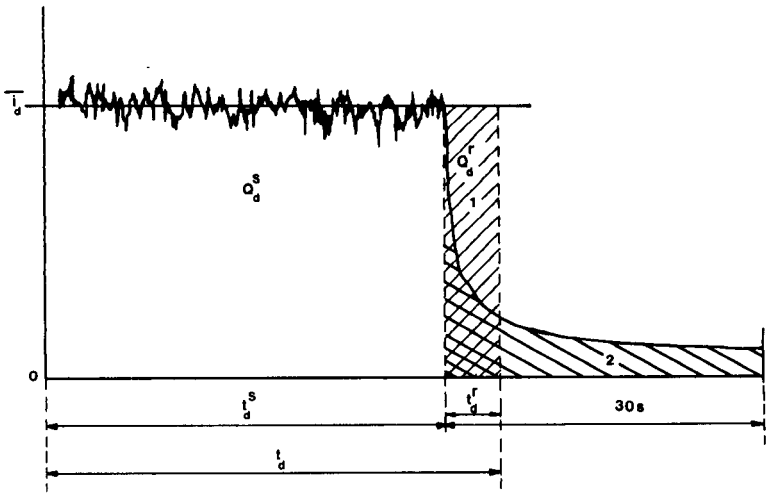

Fig. 3. The reduction current i_d as a function of deposition time t_d. t_d^r is a fictitious time, such that $t_d^r \bar{i}_d = Q_d^r$ = area 1 = area 2 = correction term to be applied to t_d^s for evaluating the true value of $Q_d = Q_d^s + Q_d^r$.

motor, $\bar{\delta}$ was found to be $(1.2 \pm 0.1) \times 10^{-3}$ cm. This value was measured before each experiment.

The polarographic cell used for medium exchange is shown in Fig. 2(II). Each solution was fully degassed before entering the polarographic cell (inlet h) and a flow of nitrogen was maintained in the cylindrical part around the capillary in order to prevent any penetration of air into the cell. Two reservoirs of degassed solution were connected to inlet h: a "deposition" solution of Pb(II)/TETA (h_1), and a "stripping" solution of 0.10 M potassium nitrate at pH 5.5 (h_2).

Procedure

All measurements were made at 25.0 ± 0.1°C, in 0.10 M potassium nitrate. Experiments in the absence of TETA were done at pH 5.5 in order to prevent the hydrolysis of lead(II). In the presence of TETA, the solutions were buffered with triethanolamine at pH 8.0. It was checked that under these conditions the hydroxide and triethanolamine complexes of lead(II) should be negligible compared to the Pb/TETA complex.

For all the deposition steps, a potential of −0.700 V was applied, while stirring, for a time t_d^s. Then the stirring was stopped, and the solution was allowed to rest for 30 s. The stripping step was then started by scanning the potential in the anodic direction at 20 mV s^{-1}.

As can be seen in Fig. 3, the deposition that continues during the rest period, t_d^r, may be significant, especially when t_d^s is short. The total quantity of electricity corresponding to the deposition is given by $Q_d = Q_d^s + Q_d^r$,

where Q_d^s and Q_d^r are the quantities of electricity corresponding to the stirring and rest periods, respectively. Dividing through by $\bar{i}_d$, the constant average deposition current, gives $Q_d/\bar{i}_d = Q_d^s/\bar{i}_d + Q_d^r/\bar{i}_d$ or $t_d = t_d^s + t_d^r$. Here t_d is the "corrected" deposition time proportional to the total amount of lead deposited in the drop, and t_d^r is the correction term. By recording curves similar to that in Fig. 3, for $C_L = 0$ and various concentrations of lead ions ($C_{Pb} = 10^{-4}$ M, 10^{-6} M, and $\approx 10^{-8}$ M, corresponding to the concentration of lead(II) contaminations), it was observed that t_d^r is independent of C_{Pb} and depends only on the mode of stirring. In the present conditions, it was found that $t_d^r = 5$ s. This correction was applied in all cases and only t_d values are reported below. The same type of correction was applied in the case of medium exchange, but t_d^r was found to be larger (25 s).

For the determination of the stability constants of the Pb/TETA complex, all E_p values (for cathodic sweep or a.s.v. techniques) in the presence of TETA, and the corresponding values in its absence, to which they are referred, were measured within the same set of experiments. All errors reported below are standard deviations, σ, defined as $\sigma = [\Sigma_i (x_1 - x)^2/(N-1)]^{1/2}$, where N is the number of determinations.

Electrochemical characteristics of the lead(II)/TETA system

The reported values of the acid-base constants of TETA and of its stability constant with lead(II), are given in Table 1. Cathodic sweep voltammetry was used to test the electrochemical behaviour of the Pb(II)/TETA system with $C_{Pb} = 10^{-5}$ M, $C_L = 9.1 \times 10^{-3}$ M and pH 8.02. According to the usual criteria [19], ($E_p - E_{p/2} = 28$ mV, and independence of E_p, $i_p/v^{1/2}$ and $E_p - E_{p/2}$ from the scan rate v, $E_{p/2}$ being the potential corresponding to $i_{p/2}$) it behaves as a labile reversible system, in the range $10 < v < 40$ mV s^{-1}.

For both a.s.v. and cathodic sweep voltammetry, the ratio of the peak currents, in the absence (pH 5.5) and presence (pH 8) of TETA, i_p^{nc}/i_p^c,

TABLE 1

Characteristics of the lead(II)/TETA system[a]

Reaction	T (°C)	Constant	Logarithm of stability constant	Ref.
L + H ⇌ LH	25	β_1^H	9.74	16
L + 2H ⇌ LH	25	β_2^H	18.82	16
L + Pb ⇌ PbL	20	β	10.4	16
L + Pb ⇌ PbL	25	β	10.18 ± 0.03[b]	This work

[a]TETA = L = NH_2—CH_2—CH_2—NH—CH_2—CH_2—NH—CH_2—CH_2—NH_2. All data are for an ionic strength of 0.1 M. [b]Average of four determinations by differential-pulse cathodic sweep voltammetry with $C_{Pb} = 2 \times 10^{-5}$ M and C_L varying between 0.98×10^{-3} and 1.95×10^{-2} M.

were found to be 1.00 ± 0.05, and were independent of the values of C_{Pb} and C_L, provided that TETA was in large excess (>30 for cathodic sweep voltammetry and >1000 for a.s.v.). This result implies that $D_{PbL} = D_{Pb}$. Consequently, the shifts in E_p in cathodic sweep voltammetry and in differential-pulse cathodic sweep voltammetry were used, as a further test of the electrochemical behaviour of the system, to compute the stability constant of the Pb(II)/TETA complex, according to Eqns. 2 and 3 (see below). The value shown in Table 1 is slightly smaller than the literature value, which may be due to the difference in temperature. In any case, considering the small amount of data available in the literature, the correspondence of the data in Table 1 was considered as satisfactory. In particular, the good agreement between the cathodic sweep voltammetry and the differential-pulse results, both for i_p^{nc}/i_p^c and $E_p^{nc} - E_p^c$, is a further confirmation of the lability of the complexation reaction. The suffixes nc and c stand for noncomplexing ($C_L = 0$) and complexing ($C_L \neq 0$) media respectively.

THEORY, DEFINITIONS AND QUALITATIVE DESCRIPTION

Discriminating between complexation at the electrode surface and in the bulk solution

For the lead(II)/TETA system described above, the degree of complexation of lead(II) in the bulk solution is given [20] by

$$\alpha = C_{Pb}/[Pb^{2+}] = 1 + \beta[L] = 1 + \beta(C_L - [PbL])/\alpha_H \quad (1)$$

where $\alpha_H = 1 + \beta_1^H[H] + \beta_2^H[H]^2$; C_{Pb} and C_L are the total concentrations of lead(II) and TETA, and $[Pb^{2+}]$, [L] and [H] are the free metal ion, ligand and proton concentrations. When a.s.v. is used to quantify lead(II) in this system, the resulting curve depends on the degree of complexation of lead(II) at the electrode surface, both during the deposition step (α_d^0), and the stripping step (α_s^0). Therefore, it is easy to compute the value of α from the characteristic parameters of the peak, E_p and i_p, only when $\alpha = \alpha_d^0 = \alpha_s^0$. As will be shown below, this is valid when $C_L \gg C_M$. Then Eqn. 1 reduces to

$$\alpha = 1 + \beta C_L/\alpha_H \quad (2)$$

In such a case, for a labile, reversibly reduced system like Pb(II)/TETA, the DeFord and Hume method [21, 22], initially developed for d.c. polarography, can be applied to the a.s.v. technique

$$\ln \alpha = (nF/RT)(E_p^{nc} - E_p^c) + \ln (i_p^{nc}/i_p^c) \quad (3)$$

In the particular case of the lead(II)/TETA system, it was observed that $i_p^{nc} = i_p^c$ so that the second term in Eqn. 3 vanishes. By combining Eqns. 2 and 3, β can easily be calculated, when α is a measured parameter.

Condition for $\alpha = \alpha_d^0$ during the deposition step

The reduction of complexes without an excess of ligand in d.c. polarography has been discussed in detail [22]. For the reduction of metal complexes

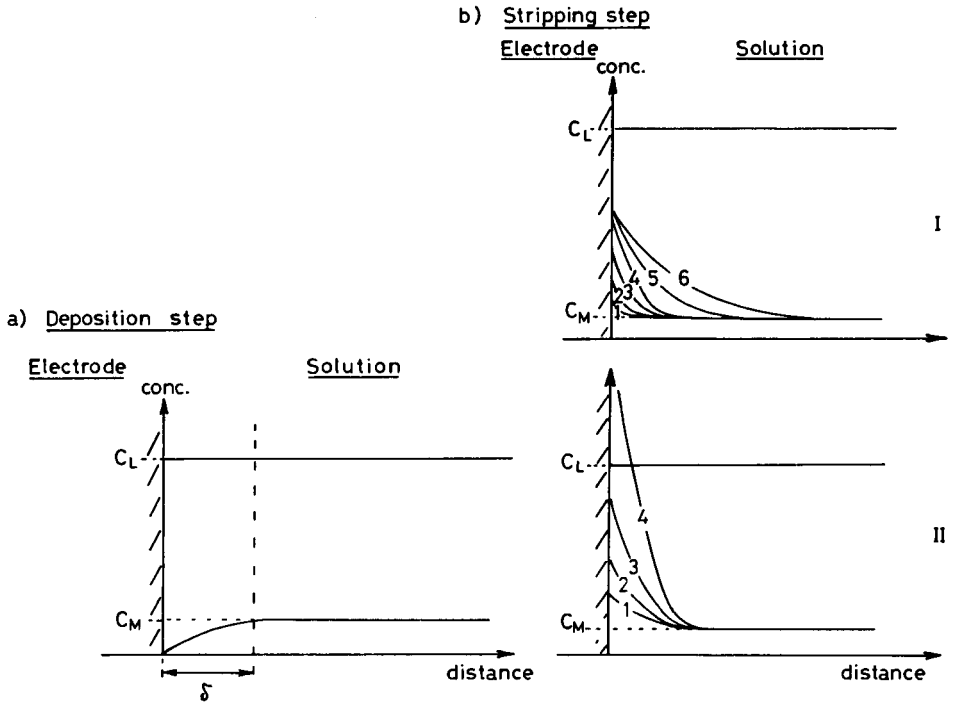

Fig. 4. Concentration gradients at the electrode surface during: (a) the reduction of M; (b) the stripping step for (I) various potentials, $E(1) < E(2) < E(3) < \ldots < E(6)$, at constant t_d, and (II) various t_d, $t_d(1) < t_d(2) < \ldots < t_d(4)$, at the peak potential. $C_L = [PbL] + [L] + \Sigma_i[LH_i]$.

to the metallic state, the consumption of M and the resulting liberation of L at the electrode surface (Fig. 4a), lead to the condition $\alpha_d^0 > \alpha$. Obviously, the difference between α_d^0 and α increases when going from the foot of the wave to the plateau. In d.c. polarography this results in a deformation of the reduction wave, and the same effect may be expected when constructing "pseudo polarograms" by stripping polarography.

However, if C_L is sufficiently large to fulfil the necessary condition for application of Eqn. 2 (e.g., $C_L/C_M > 20$), it will be even larger at the electrode surface; thus one can estimate that the difference between α_d^0 and α is $\leqslant 5\%$. It is maximal (5%) on the plateau of the wave.

Conditions for $\alpha = \alpha_s^0$ during the stripping step

In contrast to the deposition step, the metal ion concentration during the stripping step is larger at the electrode surface than in the bulk solution (Fig. 4b). Consequently, one can expect that $\alpha_s^0 < \alpha$. The size of the difference between these two parameters depends on the surface concentration of M liberated during the stripping step. This was computed theoretically [5]

for reversible systems in the absence of ligands for mercury film and hanging drop electrodes. For the HMDE, when E_d is chosen on the plateau of the reduction wave, and the scan rate of the stripping step is large enough (>5 mV s^{-1}) so that the bulk concentration of M^0 in the mercury drop is not changed during the stripping, it was shown that at the peak potential, E_p

$$C_M^0/C_M = (1/0.44)(D_{Ox}D_R)^{1/2}\, t_d/r_0\delta \qquad (4)$$

where D_{Ox} and D_R are the diffusion coefficients of the metal ion in solution and of the metal in mercury, respectively. It should be noted that C_M^0/C_M is independent of v, in contrast to i_p which increases with $v^{1/2}$ [18]. From Eqn. 4, using typical parameter values and with t_d = 3 min, it is possible to estimate that $C_M^0/C_M \approx 50$, i.e., surface concentrations much larger than bulk ones may be reached during the stripping step. Figure 4(b) shows the concentration gradients of M and L at E_p, when the stripping occurs in the presence of an "excess" of complexing agent: (e.g., C_L/C_M = 30): for a short t_d, $C_L^0 \approx C_L$ is still much larger than C_M^0 and $\alpha_s^0 = \alpha$. However, for large t_d, C_M^0 may become larger than C_L^0 so that $\alpha_s^0 \ll \alpha$. From the above estimate of C_M^0/C_M, it may be expected that $C_L/C_M > 1000$ is needed in the bulk solution, in order to ensure that $C_L^0/C_M^0 > 20$ at the electrode surface (for t_d = 3 min).

A qualitative description of the shape of the a.s.v. curves can be understood from Figs. 4(b, I) and 5. Figure 4 (b, I) shows the concentration gradients of M at different potentials during the stripping step for a given value of t_d. The surface concentration of M increases in the potential range corresponding to the rising portion of the a.s.v. curve, and remains constant from then on (cf. [5]). When t_d is small enough, $C_L^0/C_M^0 \approx C_L/C_M$ for all potentials, and a peak with a normal shape is obtained. For intermediate values of t_d, $C_L^0 > C_M^0$ for all potentials, but C_L^0/C_M^0 is much smaller at E_p than at the foot of the peak (see Fig. 4b, I). As a consequence, α_s^0 decreases all along the peak, and the resulting peak is broadened (Fig. 5, curve 1).

Finally, for still larger values of t_d, L becomes fully saturated at the electrode surface ($C_L^0 \approx C_M^0$) at a potential, $E_{sat} < E_p$. For $E > E_{sat}$, $\alpha_s^0 \approx 1$, thus the oxidation is greatly decreased, until the potential reaches a value corresponding to that for the oxidation in an uncomplexing medium. In such cases, a shoulder appears in the a.s.v. curves (Fig. 5, curves 2 and 3) for systems such that $E_p^{nc} - E_p^c(0)$ is large enough ($E_p^c(0)$ is the value of E_p^c at t_d = 0, see Fig. 6). The height of the shoulder, i_{sh}, depends mainly on C_L, and does not vary when t_d increases (Fig. 6). Hence, for extremely large values of t_d, the largest part of M^0 is reoxidized as free M^{2+}, giving rise to the corresponding a.s.v. peak, and the relative contribution of the shoulder to the total current becomes increasingly smaller, although its absolute value remains constant.

The influence of t_d on the a.s.v. peak parameters, E_p^c, i_p^c and i_{sh}, as described above, is shown in Fig. 6.

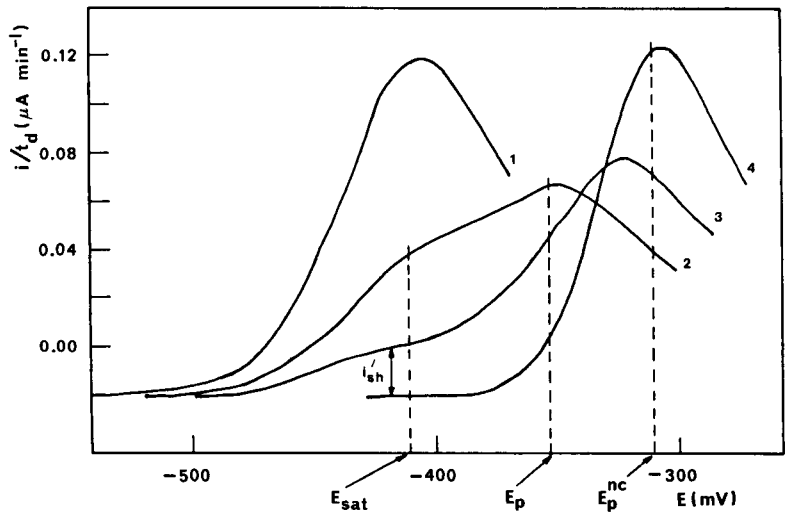

Fig. 5. "Normalized" anodic stripping voltammograms (i/t_d vs. potential) of lead ion (C_M = 1.00 × 10^{-6} M): (1—3) in presence of TETA (C_L = 0.98 × 10^{-4} M) for t_d = 1, 7 and 25 min, respectively; (4) in the absence of TETA. Other experimental conditions: 10^{-3} M triethanolamine, pH 8.02, μ = 0.10 M (KNO_3); T = 25.0° C; r_0 = 0.032 cm; v = 20 mV s^{-1}; $\bar{\delta}$ = 1.2 × 10^{-3} cm. E_{sat} and E_p are given for curve 2 (see text) $i'_{sh} = i_{sh}/t_d$.

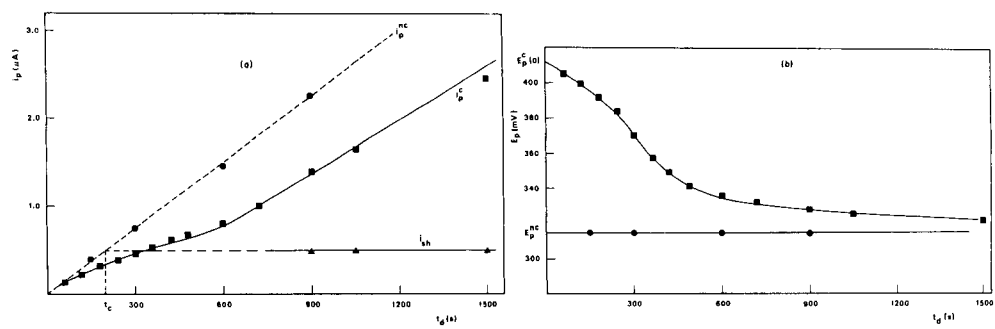

Fig. 6. Changes in the characteristic parameters of a.s.v. peaks (E_p, i_p) as a function of t_d: (●) points corresponding to the a.s.v. peak of the metal in the absence of the ligand; (■) points corresponding to the a.s.v. peak of the metal in the presence of the ligand; (▲) points corresponding to the a.s.v. peak shoulder height i_{sh}. Experimental conditions as in Fig. 5.

Definition of critical deposition time

From the above description, it is clear that the ratio C_M^0/C_M is a critical factor for correct interpretation of the a.s.v. parameters (E_p or i_p) obtained in any complexing medium. At present, there is no theoretical relationship which allows one to predict the values of i_p, E_p, or C_M^0/C_M, in conditions where there is no excess of ligand at the electrode surface during the stripping step.

The usefulness of Eqn. 4 for this purpose was therefore tested in the following part of this work. Although it is rigorously valid only in the absence of ligands, it may be expected that the influence of each of its parameters should be similar in complexing media and that it could be used as a semi-empirical equation for analytical prediction. In this respect, the lead(II)/TETA system is very suitable, because it was shown that the diffusion coefficients of the free and complexed forms of lead(II) are equal.

In order to test Eqn. 4 rigorously, it would be necessary to measure C_M^0 as a function of t_d. This is not possible, and so use was made of the fact that a shoulder appears in the a.s.v. curves when $C_M^0 \approx C_L$ and remains constant for $C_M^0 > C_L$, even for a very large t_d when $C_M^0 \gg C_L$ (Figs. 5 and 6). The height of this shoulder (i_{sh}) was then used to define a critical deposition time, t_c (as shown in Fig. 6), corresponding to the minimum value of t_d for which TETA is considered to be saturated at the electrode surface. Then one has $C_L^0 = C_L = C_M^0$, and

$$t_c = K(r_0\delta/D_{Ox}D_R)(C_L/C_M) \quad (5)$$

The experimental measurement of t_c was chosen so that the condition $C_L^0 = C_L = C_M^0$ was reasonably fulfilled. Even though this may not be rigorously true, t_c can be considered as a useful semiempirical parameter for testing the influence of the factors in Eqn. 5. Because Eqn. 4 was not deduced for the presence of ligands, the numerical constant K could be different from 0.44, but its order of magnitude should be similar. The influence of the selected parameter on the interpretation of the results was tested by defining another critical deposition time, $t_c(E)$, from the E_p^c vs. t_d curve (Fig. 6). This curve may be considered as a complexiметric titration curve of L by M inside the diffusion layer, the potential jump corresponding to the end-point of the titration. Because the break in this curve is always more clearly measurable than the inflection point, it was used to define $t_c(E)$ (Fig. 6). In all cases tested, the effects of the parameters of Eqn. 4 on t_c and $t_c(E)$ were similar. However, the measurement of $t_c(E)$ was less precise and only the results obtained with t_c are reported here.

RESULTS

Influence of r_0, $\bar{\delta}$, *and* C_L/C_{Pb}

The changes in t_c with r_0, $\bar{\delta}$, and C_L/C_M are given in Table 2 and Fig. 7. As predicted by Eqn. 5, a linear relationship is observed between t_c and $r_0\bar{\delta}(C_L/C_M)$. From the slope of the line $(6.0 \pm 0.4) \times 10^4$ s cm^{-2}, with the values $D_{Ox} = 8.3 \times 10^{-6}$ cm^2 s^{-1} and $D_R = 1.24 \times 10^{-5}$ cm^2 s^{-1} [23], it was calculated that $K = 0.61 \pm 0.04$. From the discussion of the critical deposition time this value of K is in reasonably good agreement with the theoretical value of 0.44 in Eqn. 4. This result confirms the quantitative influence of r_0, $\bar{\delta}$, *and* C_L/C_M on the a.s.v. peak parameters, and shows that Eqn. 4 provides an estimate of C_M^0, even in the presence of a ligand.

TABLE 2

Values of t_c found for different values of the experimental parameters r_0, $\bar{\delta}$ and C_L/C_M (errors were $r_0 = \pm 0.002$; $\bar{\delta} = \pm 10\%$; $t_c = \pm 12$ s)

r_0 (cm)	$\bar{\delta}$ (cm)	C_L/C_M	t_c (min)
0.055	1.2×10^{-3}	98	6.2
0.044	1.2×10^{-3}	136	7.1
0.044	1.2×10^{-3}	98	5.2
0.044	1.2×10^{-3}	65	3.4
0.044	1.7×10^{-3}	98	7.6
0.044	2.3×10^{-3}	98	11.0
0.032	1.2×10^{-3}	98	3.4

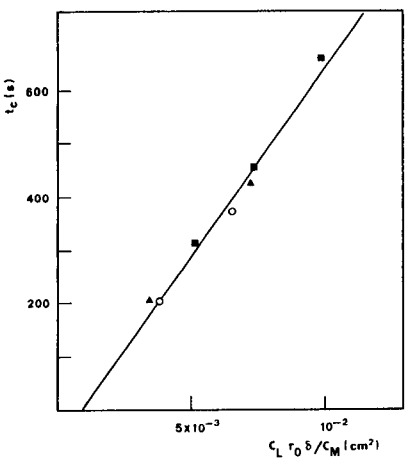

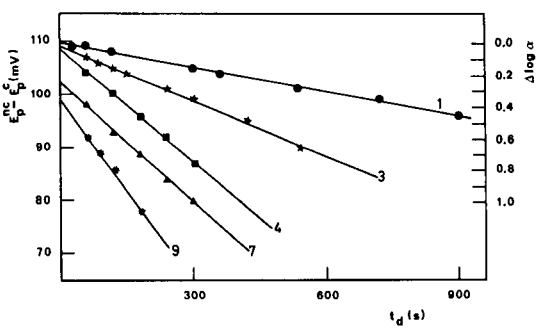

Fig. 7. Influence of the experimental parameters $\bar{\delta}$, r_0, C_L/C_M, given in Table 2, on the critical deposition time t_c. (The point at $t_c = 11$ min is less reliable, because a very long electrolysis time (45 min) was used for measurement of i_{sh}. (○, ■, ▲) Variations of r_0, $\bar{\delta}$, and C_L/C_M, respectively (see Table 2).

Fig. 8. Change of $E_p^{nc} - E_p^c$ and $\Delta\log(\alpha)$ with t_d, for $t_d < t_c$. Plots correspond to the experimental conditions presented in Table 3 with the same number: (●) 1; (★) 3; (■) 4; (▲) 7; (∗) 9. The axis $\Delta\log\alpha$ relates to line 3 only.

The E_p^c vs. t_d curves, and measurements of β

Figure 8 shows the change in E_p^c with t_d, expressed as $\Delta E_p = E_p^{nc} - E_p^c$, for $t_d < t_c$. Linear relationships were always obtained within experimental error. This property makes it possible to evaluate β by extrapolating ΔE_p to $t_d = 0$ [$\Delta E_p(t = 0)$], i.e., to conditions where $\alpha_s^0 = \alpha$. The $\Delta E_p(t = 0)$ values were then used with Eqns. 2 and 3 to compute β. The values obtained in this way for various values of r_0, $\bar{\delta}$, C_L/C_M and pH, are reported in Table 3. All these values are statistically identical, within experimental error, and the average

TABLE 3

Stability constant (log β) evaluated from the intercept of the linear relations (ΔE_p, t_d) with slopes a, for different values of the experimental parameters r_0, $\bar{\delta}$, C_L, C_L/C_M and pH[a]

No.	$\bar{\delta}$ (cm)	C_L (10^{-4} M)	C_L/C_M	pH	Slope (μV s^{-1})	log β
1	1.2×10^{-3}	4.90	1225	7.80	15.3 ± 0.3	10.28 ± 0.01
2	1.2×10^{-3}	4.90	612	7.81	23.2 ± 0.3	10.27 ± 0.01
3	1.2×10^{-3}	4.90	306	7.81	34.8 ± 0.7	10.25 ± 0.01
4	1.2×10^{-3}	4.90	136	7.81	72 ± 2	10.25 ± 0.01
5	1.2×10^{-3}	4.90	65	7.80	137 ± 8	10.21 ± 0.03
6	1.2×10^{-3}	0.98	98	8.05	77 ± 8	10.23 ± 0.06
7	1.7×10^{-3}	0.98	98	8.05	76 ± 2	10.25 ± 0.01
8	2.3×10^{-3}	0.98	98	8.08	43 ± 2	10.27 ± 0.02
9	1.2×10^{-3}	0.98	98	8.02	117 ± 7	10.20 ± 0.03
10	1.2×10^{-3}	0.98	98	8.06	88 ± 5	10.27 ± 0.03

[a]Scan rate 20 mV s^{-1}, r_0 = 0.044 cm for all except nos. 9 and 10, for which r_0 = 0.032 and 0.055 cm, respectively.

value, log β = 10.25 ± 0.03, is in agreement with that found by differential-pulse cathodic sweep voltammetry (Table 1).

It must be pointed out that in the present a.s.v. determination of log β, the chief sources of error are those incurred from the measurement of $\Delta E_p(t = 0)$ (±2 mV), and pH (±0.01). These errors produce errors of 0.07 and 0.02 log unit in β, respectively.

Figure 8 shows that not only does E_p^c increase linearly with t_d (for $t_d < t_c$), but that the slopes of the lines depend on the same parameters as t_c. In this time range, TETA never reaches saturation at the surface, but α_s^0 decreases gradually when t_d increases. On the basis of this property, it is possible to derive a semiempirical equation (see Appendix) for the change in ΔE_p with t_d

$$\Delta E_p = \Delta E_p(t = 0) - (1/K')(RT/nF)(D_{Ox}D_R)^{1/2}(C_M/C_L)t_d/r_0\bar{\delta} \quad (6)$$

with $\Delta E_p(t = 0) = (RT/nF)$ ln $(\beta C_L/\alpha_H)$; K' is an empirical constant, and should have a value close to 0.44 (Eqn. 4).

The slopes of the straight lines ΔE_p vs. t_d, are given in Table 3, and are plotted as a function of $C_M/(C_L r_0 \bar{\delta})$ in Fig. 9. A linear relationship is obtained with a slope of (5.7 ± 1.8) × 10^{-4} mV cm^2 s^{-1}. Then by using the above values of D_{Ox} and D_R, the value of K' obtained is 0.50 ± 0.16.

Effects of medium exchange on the a.s.v. curves

The medium-exchange system was used to verify that changes in the a.s.v. peak parameters with t_d, were due to phenomena occurring during the stripping step, and not during the deposition step.

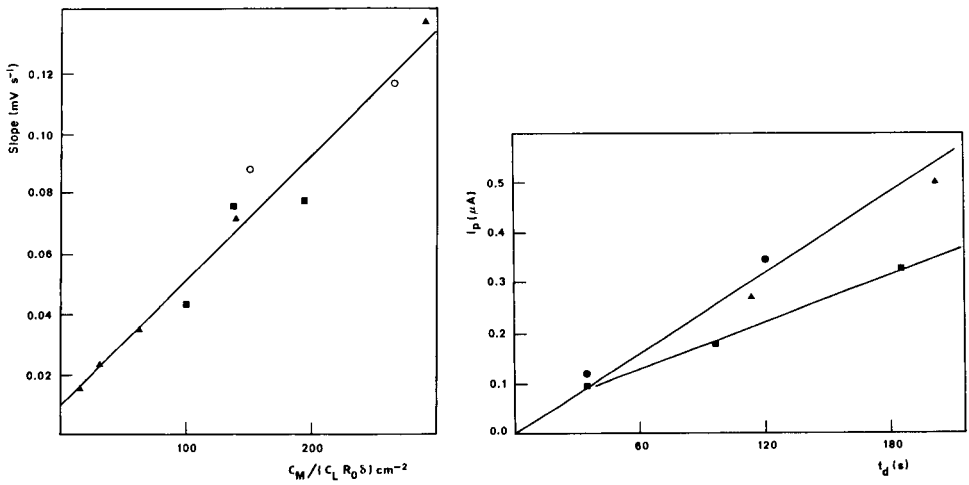

Fig. 9. Influence of the experimental conditions $\bar{\delta}$, r_0 and C_L/C_M on the slopes of the ΔE_p vs. t_d data. Experimental conditions are given in Table 3. The symbols (○, ■, ▲) are the same as in Fig. 7.

Fig. 10. Peak current i_p vs. t_d of the a.s.v. curves: (●) in the absence of TETA; (■) in the presence of TETA, without changing the solution; (▲) in the presence of TETA, by changing the solution. Each point is the average value of 3—7 determinations. In all cases, experimental errors on i_p varied between 1 and 5% and $C_{Pb} = 1.0 \times 10^{-6}$ M. For (■) and (▲), $C_L = 4.6 \times 10^{-5}$ M.

Figure 10 shows i_p vs. t_d relationships in the absence of TETA, and in the presence of TETA without and with medium exchange after the deposition step. It is clear that, without medium exchange, an i_p vs. t_d curve similar to that in Fig. 6 is obtained, whereas, with medium exchange, the points fall on the same straight line as that obtained in the absence of TETA. Not only does this result confirm that the observations described above are due to the stripping step, but also that the diffusion rate of Pb^{2+} and PbL during the deposition step are identical.

DISCUSSION

The results described above show the necessity of considering the concentrations of reagents at the electrode surface when a.s.v. techniques are applied in media containing complexes. The dependences of i_p and E_p on t_d show that the influences of the important factors on C_M^0 are adequately predicted by Eqn. 4 and that this equation can even give a reasonably good estimate of C_M^0. This is particularly useful, because it allows predictions about the best analytical conditions to be used in order to avoid surface concentration effects with the HMDE. A similar equation is available for mercury film electrodes [5]. Because in many cases r_0, $\bar{\delta}$, D_{Ox} and D_R do not vary over a

large range, average values of these parameters (r_0 = 0.04 cm, $\bar{\delta} = 2 \times 10^{-3}$ cm, $D_{Ox} = D_R = 10^{-5}$ cm, numerical constant = 0.5) give a useful and widely applicable relationship to calculate the order of magnitude of C_M^0/C_M: $C_M^0/C_M \approx 0.25\ t_d(s)$. As discussed above, this makes it possible to calculate that in most complexing media, the ligand/metal ratio in the bulk solution must be larger than 1000 in order to avoid a surface effect.

Figure 6 shows that when this condition is not met, the currents measured are at least 30% below those that should be obtained in the absence of a surface effect. An even larger discrepancy is obtained when the diffusion coefficient of the complex is lower than that of the free metal ion. This may be important for determinations of total metal concentration when the ligands of the test solution have not been eliminated previously. It may also be very important in attempts to measure the complexing properties of a metal ion in an unknown medium by stripping polarography. Because the importance of this effect will vary along the stripping polarographic wave, it may be expected that not only the limiting current, but also $E_{1/2}$ and the Tafel slope could be modified.

Influence on measurements of complex stability constants

From Fig. 8, it is possible to estimate the error incurred in log α, when the peak potential, E_p, is used to compute α from Eqn. 3 without extrapolating its value to $t_d = 0$. The value for $\Delta \log \alpha = (nF/RT)(\Delta E_p(t = 0) - \Delta E_p)$ is given in Fig. 8 for curve 3. For example, it can be seen that for t_d = 85 s, an error of 0.1 log unit is made for log α. From all the cases studied here, it can be generalized that C_L/C_M must exceed 1000 if an error smaller than 0.05 log unit is needed. This work suggests that two methods can be used to obtain correct α values, despite the surface effect. First, α can be measured from the shift in E_p extrapolated to $t_d = 0$. In cases when $D_{ML} \neq D_M$, the values of i_p^c and i_p^{nc} must also be used in Eqn. 3. Because i_p^c is also affected by surface effects, i_p^c/t_d must be extrapolated to $t_d = 0$, to give $(i_p^c/t_d)_{t=0}$. The ratio $(i_p^c/t_d)_{t=0}/(i_p^{nc}/t_d)$ must then be introduced into Eqn. 3. The second possibility is to use stripping polarography with medium exchange between deposition and stripping. This procedure has the advantage of being potentially applicable not only to labile complexes, as in the preceding case, but to any kind of complexation reaction, because the peak current is then directly proportional to the quantity of metal deposited during the reduction step. The method is, however, much more delicate to apply with the HMDE, especially in preventing penetration of oxygen, and accounting for any reduction during the medium exchange.

Application to measurements of complexation capacity

Complexation capacity is defined, for natural waters, as the overall concentration of all the complexing sites of the medium able to bind a given metal ion M. It is often obtained by making standard additions of the metal ion to the test medium and measuring the a.s.v. or d.p.a.s.v. peak currents as

a function of C_M. Ideally, before the saturation of the ligands, the increase of i_p is smaller than with standard solutions, whereas a linear increase, with the calibration slope, is observed for an excess of metal ion [24]. The value of C_M at the break corresponds to the complexation capacity. This assumes that the complexes formed are electrochemically inert. For labile complexes, the surface concentration effect can simulate, but must not be confused with, a complexation capacity curve [6]. Indeed, because C_M and t_d play an equivalent role in Eqn. 4, the curve $i_p = f(C_M)$ at constant t_d has a similar shape to the $i_p = f(t_d)$ curve at constant C_M (Fig. 6). Such i_p vs. C_M curves are shown for the Pb/TETA system in Fig. 11, as well as the corresponding i_p vs. t_d curves. The equivalence of t_d and C_M is clearly shown here: for a given value of C_L, the change in i_p depends on $t_d C_M$ only if the other experimental conditions remain constant, i.e., C_M^0 can be changed by variations in both the deposition time and in the value of C_M. A similar curve was reported by Bhat and Weber [13] for the addition of cadmium to fulvic acids, which could be due to the above surface effect. For conditions when $D_{ML} < D_M$, the "break" in the capacity curve (at t_d = 10 min in Fig. 6) is even better defined, as i_p decreases in the first part of the curve. This break is related to saturation of the ligand at the electrode surface, but not in the bulk solution. When such a break is interpreted as a bulk complexation capacity, the capacity can be underestimated by a factor of 50—100 [6].

Because it was demonstrated above that t_c is directly proportional to C_L (Eqn. 5), it would be attractive to measure the complexation capacity by titrating the ligand within the diffusion layer by varying t_d, instead of by adding metal ion to the bulk solution. This would have the advantage of keeping the value of C_L/C_M constant (and preferably low) in the bulk solu-

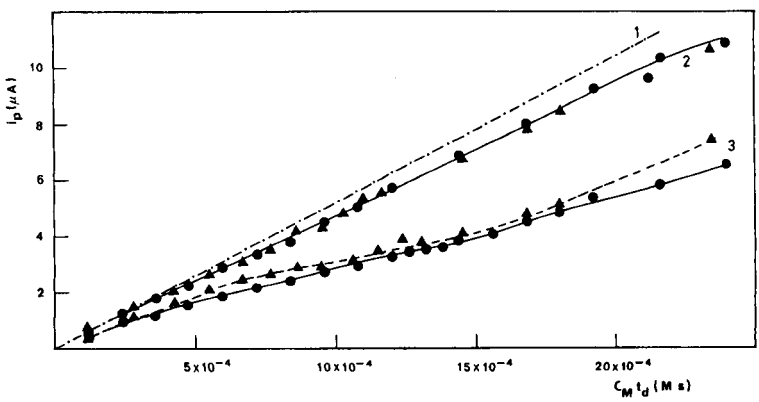

Fig. 11. Change in i_p with t_d and C_M. Curves: (1) C_L = 0, pH 5.5 (the same curve was obtained for $C_L \rightarrow \infty$ and pH 8.0); (2) $C_L = 2 \times 10^{-3}$ M and 3×10^{-2} M triethanolamine at pH 8.00; (3) $C_L = 4 \times 10^{-4}$ M and 4×10^{-3} M triethanolamine at pH 8.00. (●) t_d = 2 min with variable C_{Pb}; (▲) $C_{Pb} = 2 \times 10^{-6}$ M with variable t_d. In all cases E_d = —0.750 and v = 20 mV s^{-1}.

tion during the whole procedure, hence minimizing possible coagulation or aggregation effects. Despite its apparent elegance, it is doubtful that such a procedure would give accurate results under practical conditions. One reason is that the measurement of t_c requires the existence of a sufficiently well-defined shoulder on the a.s.v. peak. This occurs in the case of a very stable "simple" complex like Pb(II)/TETA, but not with the mixtures of comparatively weak complexes often found in natural waters. Another operational parameter could be used, such as the jump in the E_p vs. t_d curve, but these "characteristic" parameters would be difficult to find in practical media containing mixtures of ligands with different complexation and diffusing properties.

Surface concentration effect in d.p.a.s.v.

Differential-pulse a.s.v. is more generally used than a.s.v. for application to natural waters, because of its greater sensitivity and its relatively symmetrical peak shapes. Althouth the modulation in potential during the stripping step will produce a variation of the corresponding concentration of metal ion at the surface for the same t_d, the order of magnitude of the average value of C_M^0 in d.p.a.s.v. will be the same as for a.s.v. However, because of its much greater sensitivity, a smaller t_d can be used with d.p.a.s.v., thus minimizing the surface concentration effect. For practical reasons, it is difficult to use $t_d < 60$ s (i.e., $C_M^0/C_M < 20$) whatever the technique, at least with the HMDE. Thus the surface effect is not negligible, even with d.p.a.s.v., and it can be expected to play an important role in any system containing natural ligands.

The authors gratefully acknowledge the technical assistance of M. L. Tercier, F. Bujard and C. Bernard. This work was supported by the Swiss National Foundation (Project 2.413/0.82) and by the Junta Nacional de Investigacao Cientifica e Tecnologica (Contract 315.81.57).

APPENDIX

During the stripping step, the ligand at the electrode surface becomes more and more saturated as the applied potential, E, is scanned to more positive values. This influences the concentration gradients, and in turn, the current and the position of the peak potential. Nevertheless, for $t_d \ll t_c$ (small decrease in free ligand concentration at the surface compared to the bulk solution, Eqn. 3 can be used as a first approximation by replacing α, with its value at the electrode surface, α_S^0. $\alpha_S^0 = 1 + \beta[L]^0$, where $[L]^0$ is the concentration of free L at the surface. Further, neglecting the second term in Eqn. 3 and because $\beta[L]^0 \gg 1$, gives $\Delta E_p \approx (RT/nF) \ln (\beta[L]^0)$. $[L]^0$ must be estimated from the diffusion fluxes of L, its protonated forms and ML at the surface. However, if all these species have similar diffusion coefficients, the approximate mass balance equation at the surface will be $C_L^0 = C_L = [L]^0\alpha_H^0 + [ML]^0$, and $C_M^0 = [M]^0 + [ML]^0$. Because the system is well buffered, $\alpha_H^0 \approx \alpha_H$. Under the conditions used here, L is not saturated and the ML complexes are very stable, so that $C_M^0 \approx [ML]^0$. Finally, C_M^0 is evaluated from Eqn. 4, where the numerical constant is replaced by K'. Combining these conditions with the above equations for ΔE_p, C_L^0 and C_M^0 yields

$$\Delta E_p = (RT/nF)\{\ln(\beta C_L/\alpha_H) + \ln[1 - (1/K')(D_{Ox}/D_R)^{1/2}(C_M/C_L)t_d/r_0\bar{\delta}]\} \quad (A1)$$

For $t_d \ll [r_0\bar{\delta}/(D_{Ox}D_R)^{1/2}](C_L/C_M)$. Eqn. A1 reduces to a linear relationship

$$\Delta E_p = (RT/nF)\{\ln(\beta C_L/\alpha_H) - (1/K')(RT/nF)(D_{Ox}D_R)^{1/2}(C_M/C_L)t_d/r_0\bar{\delta}\} \quad (A2)$$

The ΔE_p values were computed from both Eqns. A1 and A2 with the values of K', r_0, $\bar{\delta}$, D_{Ox} and D_R found in this work, and using values of C_L/C_M = 50, 100 and 300. It was found that for the difference in the two ΔE_p values to be less than 2 mV (i.e., to achieve a linear dependence of E_p vs. t_d, the t_d values had to be less than 1, 2 and 6 min, respectively. In practically similar conditions, the E_p vs. t_d curves were found to be linear over a larger range of t_d, a result that may well be due to the approximate nature of the above mathematical treatment.

REFERENCES

1 A. Zirino, in M. Whitfield and D. Jagner (Eds.), Marine Electrochemistry, Wiley, Chichester, 1981, Ch. 10.
2 H. W. Nurnberg, in P. Ahlberg and L. O. Sundelof (Eds.), Structure and Dynamics in Chemistry, 1978, p. 270.
3 W. Davison and M. Whitfield, J. Electroanal. Chem., 75 (1977) 763.
4 J. E. Spell II and R. H. Philp Jr, J. Electroanal. Chem., 12 (1980) 281.
5 J. Buffle, J. Electroanal. Chem., 125 (1981) 273.
6 J. Buffle, A. Tessier and W. Haerdi, in C. J. Kramer and J. C. Duinker (Eds.), Complexation of Trace Metals in Natural Waters, Martinus Nijhoff, D. W. Junk Publishers, The Hague, 1984, p. 301.
7 J. Buffle, in H. Sigel (Ed.), Metal ions in Biological Systems, Vol. 18, M. Dekker, New York, 1984, Ch. 6.
8 H. Bilinski, R. Huston and W. Stumm, Anal. Chim. Acta, 84 (1976) 157.
9 H. W. Nurnberg, P. Valenta, L. Mart, B. Raspor and L. Sipos, Z. Anal. Chem., 282 (1976) 357.
10 M. Branica, D. M. Novak and S. Bubic, Croat. Chem. Acta, 49 (1977) 539.
11 A. Zirino and S. P. Kounaves, Anal. Chem., 49 (1976) 56.
12 M. S. Shuman and J. L. Cromer, Anal. Chem., 51 (1979) 1546.
13 G. A. Bhat and J. H. Weber, Anal. Chim. Acta, 41 (1982) 95.
14 I. Ružić, Anal. Chim. Acta, 140 (1982) 99.
15 M S. Shuman and G. P. Woodward, Environ. Sci. Technol., 11 (1977) 809.
16 R. M. Smith and A. E. Martell, Critical Stability Constants, Vol. 2, Plenum Press, New York, 1975.
17 W. Davison, J. Electroanal. Chem., 87 (1978) 395.
18 M. V. Stackelberg, M. Pilgram and V. Toome, Z. Electrochem., 57 (1953) 342.
19 E. R. Brown and R. F. Large, in A. Weissberger (Ed.), Techniques of Chemistry, Vol. I, Part 2a, Wiley-Interscience, New York, 1971, Ch. 6.
20 A. Ringbom, Complexation in Analytical Chemistry, Interscience, New York, 1963.
21 D. D. DeFord and D. N. Hume, J. Am. Chem. Soc., 73 (1951) 5321.
22 J. Heyrovsky and J. Kuta, Principles of Polarography, Academic Press, New York, 1966, Ch. 8 and 12.
23 Z. Galus, Diffusion Coefficients of Metals in Mercury, Pure Appl. Chem., 56 (1984) 635.
24 Y. K. Chau and K. Lum Shue Chan, Water Res., 8 (1974) 383.

Analytica Chimica Acta, 172 (1985) 31—37
Elsevier Science Publishers B.V., Amsterdam — Printed in The Netherlands

ANODIC STRIPPING VOLTAMMETRIC DETERMINATION OF ANTIMONY IN GUNSHOT RESIDUE

ROBERT C. BRINER*, SUPAPORN CHOUCHOIY[a] and RANDALL W. WEBSTER[b]

SEMO Regional Crime Laboratory, Southeast Missouri State University, Cape Girardeau, MO 63701 (U.S.A.)

RONALD E. POPHAM

Department of Chemistry, Southeast Missouri State University, Cape Girardeau, MO 63701 (U.S.A.)

(Received 4th September 1984)

SUMMARY

Anodic stripping voltammetry (a.s.v.) at a mercury film on a glassy carbon working electrode was utilized to determine the amount of antimony from hand swabs. The procedure described is useful for determining 10—120 ng of antimony found in the residue on the hands of an individual suspected of discharging or handling a firearm. The voltammogram provides an elemental pattern recognizable as gunshot residue containing small amounts of antimony and much larger amounts of copper and lead. The amount of antimony in a variety of gunshot-residue samples was determined by both anodic stripping voltammetry and graphite-furnace atomic absorption spectrometry for comparison purposes. Anodic stripping voltammetry is excellent for observation of the multielement pattern which proves to be very useful for gunshot-residue samples.

Law enforcement agencies are becoming increasingly dependent on the analysis of physical evidence provided by crime laboratory personnel to establish sufficient grounds for arrest and eventual prosecution. The ability to establish rapidly if an individual has recently fired or handled a hand gun can provide valuable information in investigations of suspected suicides, armed assaults and homicides involving the illegal use of fire-arms.

Harrison and Gilroy [1] observed in 1959 that metal components such as barium, lead, antimony and copper used in bullets and primer materials were deposited on the firing hand after discharge of a firearm. This deposit, referred to as gunshot residue (GSR), has been analyzed by a large variety of instrumental techniques capable of quantifying the picogram to microgram quantities of metals found in the residue. Bratin and Briner [2] provided an extensive review of the literature pertaining not only to the techniques used for trace metal analysis but also the detection of trace organics in GSR.

---

[a] Present address, 133 Friendship Village, Sukhumvit 77, Prakanong, Bangkok, Thailand.
[b] Permanent address: Hannibal Police Department, Hannibal, MO 63401, U.S.A.

0003-2670/85/$03.30

Presently, most crime laboratories depend on flame and flameless atomic spectrometry of the metals Sb, Pb, Ba and Cu [3, 4] and/or scanning electron microscopy with x-ray spectrometry to attempt to ascertain the presence or absence of GSR on the hands of a suspect or victim [5, 6]. The analyses are time-consuming, require considerable technical expertise and rather expensive instrumentation. Proper interpretation of the data is complicated by the fact that finding elevated levels of metals such as Sb, Ba, Cu, and Pb may not be due to GSR but rather environmental or occupational exposure of the suspect to one or more of these heavy metals [7]. The amounts found may vary considerably depending on sampling technique, inherent variation of residue deposition from shot to shot, even when the same gun is used, the type of gun and ammunition, as well as the technique chosen to analyze the samples [5].

Considering the problems associated with obtaining and interpreting the data, it is not surprising that some crime laboratories often do not attempt to work with GSR samples. At best, they may choose to send the samples to a larger analytical laboratory, which often results in serious delay before the information becomes available. The purpose of this work was to investigate the use of anodic stripping voltammetry (a.s.v.) to provide a rapid, inexpensive technique for the initial screening of suspected GSR samples. The results indicate that the determination of antimony with simultaneous qualitative indication of the presence of lead and copper in a suspected GSR sample provides an excellent screening device well within the capability of any forensic laboratory. The technique is nondestructive, which allows additional testing, if necessary. The procedure described is similar but far simpler than the application of a.s.v. to GSR previously described in the literature [8—10]. The results and detection limits obtained for antimony are comparable to those reported by Brihaye et al. [11] who used differential pulse anodic stripping voltammetry with a hanging mercury drop electrode. Results for antimony are reported for both a.s.v. and graphite-furnace atomic absorption spectrometry (a.a.s.) on both laboratory samples and field samples submitted to this regional laboratory by local law enforcement agencies as physical evidence in cases under investigation.

EXPERIMENTAL

Apparatus and reagents

Voltammetric measurements were made with a CV-1B Voltammetry Controller (Bioanalytical Systems) equipped with a Simpson d.c. millivoltmeter (Model 2830) and a Houston Omnigraphic Series 100 X-Y recorder. A 10-ml electrochemical cell was used with a platinum wire counter electrode, Ag/AgCl reference electrode, and a working electrode consisting of a thin film of mercury deposited on a glassy carbon electrode with a surface area of 7.07 mm^2. Atomic absorption measurements were made with a HGA-2200 graphite furnace (Perkin-Elmer) with ramp controller mounted on either a Perkin-Elmer 360 or Jarrell-Ash 82-500 atomic absorption spectrometer.

All reagents were standard ACS grade and were used as received. Antimony standards were prepared from a 1000 ppm Sb standard reference solution in 5% nitric acid (Fisher Scientific).

Procedures

Standard and GSR sample preparation. A GSR sample collection kit consists of five cotton-tipped, plastic-handled swabs in separate plastic vials, a 5% (v/v) nitric acid solution in a squeeze bottle and two pairs of plastic disposable gloves. Four discrete samples for suspected GSR were collected by wetting the cotton-tip swab with four drops of 5% nitric acid and swabbing the appropriate area of each hand: right back (RB), right palm (RP), left back (LB), and left palm (LP). Plastic gloves were worn at all times by the examiner and a new pair of gloves was used for each hand. The cotton swabs were then cut from the handle and placed in the appropriately labeled vial. The fifth swab was used as a reagent (5% nitric acid) blank. Then 1.00 ml of 4.0 M hydrochloric acid containing 0.02 M hydrazine sulfate was added to each vial and allowed to soak for at least 1 h. Comparison standards were prepared by adding from 10 to 100 ng of standard antimony solution directly to the cotton swab using a 0—20-μl Gilson variable microliter pipet and treating them exactly as described for GSR samples. Care must be taken not to touch the cotton tips.

Procedure for a.s.v. Standard or GSR sample (0.5 ml) prepared as described above was pipetted into the electrochemical cell containing 3.5 ml of the specified electrolyte to which 100 μl of 0.01 M mercury(II) chloride had been added. Nitrogen was bubbled through the solution with stirring for 180 s to remove dissolved oxygen. Simultaneous deposition of both the film of mercury and the analytes on the glassy carbon electrode was done for 540 s with stirring and 60 s without stirring at a potential of —1.00 V between the working and reference electrodes. Anodic stripping was then done by scanning the potential from —1.00 V to +0.10 V at a rate of 20 mV s^{-1}. A continuous blanket of nitrogen was supplied during both deposition and stripping. The working electrode was cleaned after each sample by rinsing with distilled water and thoroughly wiping the electrode surface with a Kimwipe tissue.

Procedure for graphite-furnace a.a.s. Standard or GSR sample (0.5 ml) prepared as described above was added directly to the graphite tube in 5—20 μl aliquots from the Gilson pipet. The 2176-nm line for antimony was used. The atomization cycle involved 40-s dry time with 20-s ramp at 100° C, 20-s char time with 10-s ramp at 600° C and a 5-s atomization time at 1900° C.

RESULTS AND DISCUSSION

Five 4.0-ml samples containing 10, 20, 30, 40, and 50 ng of antimony were used to establish standard and standard-addition calibration curves. The pooled standard deviations (3 runs for each of five samples in each case)

were 0.43 ng for the standard calibration curve and 0.85 ng for the standard-addition calibration curve. The least-squares equations of current (μA) vs. mass (m, ng) were $I = 0.101m - 0.261$ for the standard calibration data and $I = 0.0628m - 0.0090$ for the standard-addition data.

Results for <10 ng of antimony were difficult to reproduce and thus 10 ng represents a practical detection limit for the a.s.v. experiment as described. Linearity can be extended to about 120 ng of antimony, beyond which one loses both linearity and reproducibility because of the appearance of two peaks for antimony at —0.18 and —0.24 V. Thus, GSR samples containing large amounts of antimony must be diluted accordingly. Although the standard calibration technique showed a little higher sensitivity than the standard addition technique, the latter was chosen because of the simplicity and speed with which GSR samples could be analyzed. It was also observed that the presence of the cotton swab in the procedure was important for reproducibility, probably because it introduced some surfactant into the system. The influence of surfactants on a.s.v. peaks can involve both change in peak heights as well as peak potentials [12].

Figure 1 shows a typical voltammogram for the electrolyte control blank before and after the addition of 30 ng of antimony and a typical GSR sample containing approximately 50 ng of antimony. One observes the antimony peak at —0.18 V and the presence of small amounts of lead at —0.54 V and copper at —0.30 V in the control blank. The presence of large amounts of copper and lead in the GSR voltammogram provides the typical three-peak pattern giving immediate indication that the sample may indeed be GSR. The size of the antimony peak provides the approximate concentration which dictates how to proceed with the standard addition experiment for accurate determination of the antimony content in the sample.

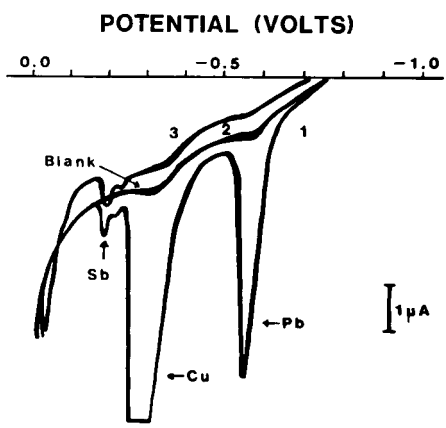

Fig. 1. Voltammograms of a sample, blank and standard: (1) gunshot residue showing Pb, Cu, and Sb; (2) blank electrolyte; (3) blank electrolyte spiked with 30 ng Sb.

Four samples containing 0.5, 1.0, 1.5, and 2.0 ng of antimony were used to evaluate the a.a.s. method at low concentrations. The pooled standard deviation (3 runs on each of 4 samples) was 0.05 ng. The least-squares equation of absorbance, A, vs. mass (m, ng) was $A = 1.98m + 0.182$. Linearity and reproducibility could be maintained up to 15 ng of antimony injected in the graphite furnace by using injection volumes of 5—20 μl; with volumes outside this range, data were difficult to reproduce. Because the procedure for collecting GSR samples involves placing the swab in 1.00 ml of 4 M hydrochloric acid, the smallest amount of antimony in a sample which can be determined with any degree of confidence is approximately 15 ng. Thus the a.a.s. procedure is only slightly less sensitive than the a.s.v. procedure. The graphite-furnace technique does have a considerably larger concentration range of linear response for real samples, 15—1500 ng for graphite-furnace a.a.s. and 10—120 ng for a.s.v.

Table 1 shows data for cotton swabs spiked with specified amounts of standard antimony taken through the GSR sample preparation procedure, split in half, and analyzed by both techniques. The results are similar and one observes the general trend of the a.s.v. results being slightly low and the a.a.s. results being slightly high. This trend will also be observed on real samples.

Table 2 lists assay results obtained on real samples which represent firing a hand gun under controlled laboratory procedures and actual samples submitted to the SEMO Regional Crime Laboratory as physical evidence by various law enforcement agencies. It should be noted that the standard addition technique on half the sample by a.s.v. does not allow for duplication after addition of antimony to the solution whereas the graphite-furnace a.a.s. results can be run in duplicate. Thus, this laboratory tends to favor the use of a calibration curve for quantitation of a.s.v. results. In general, the results by a.s.v. and the a.a.s. method agree fairly consistently. The a.a.s. results were obtained without using background correction. If one were depending only on graphite-furnace a.a.s. for information on GSR samples, background correction should always be used. In a recent article, Gustavsson and Hansson [13] compared the use of a.s.v. with flameless a.a.s. for the determination of

TABLE 1

Comparison of recovery data for antimony by a.s.v. and graphite-furnace a.a.s.

Cotton swab spike[a] (ng Sb)	Recovery (%)[b]	
	A.s.v.	A.a.s.
100 (N = 10)	92.00 ± 0.20	102.50 ± 0.58
50 (N = 5)	47.33 ± 11.20	55.83 ± 3.33
20 (N = 5)	22.00 ± 2.04	25.00 ± 3.61

[a]N = number of samples. [b]Mean and standard deviation.

TABLE 2

Determination of antiomony in GSR from test firings and actual cases

Case[a]	Conditions	Hand	Antimony found (ng)[b]	
			A.s.v.	A.a.s.
1	After shot[c]	RB	25	23 ± 12
		RP	32	23 ± 10
		LB	ND	ND
		LP	27	20 ± 13
2	Indoor range	RB	74	89 ± 13
		RP	65	55 ± 23
		LB	34	23 ± 13
		LP	280	223 ± 12
3	Indoor laboratory[d]	RP	138	82 ± 10
4	Suspected suicide	RB	ND	ND
		RP	18	22 ± 13
		LB	20	27 ± 8
		LP	14	27 ± 8
5	Accidental shooting	RB	ND	ND
		RP	ND	ND
		LB	24	21 ± 3
		LP	38	28 ± 7
6	Assault	RB	ND	NA
		RP	20	NA
		LB	30	NA
		LP	ND	NA

[a]Weapons used in the six cases: (1) 0.38 caliber Smith & Wesson, 2-in. barrel, 0.385 special ammunition; (2) 0.38 caliber Smith & Wesson, 2-in. barrel, RP ammunition; (3) 0.38 caliber Smith & Wesson, 1.5-in. barrel; (4) weapon unknown; (5) 0.357 Magnum, 0.38 special ammunition; (6) 0.357 Magnum, 0.38 special ammunition with indication of cross-over grip (left over right). [b]ND, none detected; NA, not analyzed; a control sample was run with each case. [c]Before the shot, no antimony was detected in RB, RP, LB or LP. [d]No antimony detected in RB, LB or LP.

trace metals in Baltic Sea water and concluded that a.s.v. is at least a viable alternative to a.a.s. as it requries less handling, less time, and less expensive instrumentation [13]. The ability to observe all three elements at one time allows for pattern recognition of GSR data which this laboratory has found to be very beneficial.

The initial purpose of this research was to determine if the use of a.s.v. for the detection of antimony in GSR would prove to be as reliable as graphite-furnace a.a.s. which has been used as admissible evidence in courts of law. The results obtained by the described methods on identical samples, both real and fabricated in this study, are generally in good agreement. Anodic stripping voltammetry does seem to offer several advantages. The most obvious is a rapid screening of samples for the relatively small antimony peak at −0.18 V and the very large signals produced for copper and lead at

−0.30 and −0.54 V, respectively, which give characteristic patterns for GSR. The presence of antimony with corresponding absence of copper and/or lead would suggest that the sample was not a GSR sample. After sample collection and preparation, a characteristic pattern is obtained in 13 min and the standard addition experiment to determine the exact amount of antimony can be completed in an additional 13 min. The procedure is rapid and simple and does not require a lot of operator expertise.

If quantitative information on additional elements such as Ba, Pb and Cu is warranted, a.s.v. could be applied to lead or copper and because a.s.v. is nondestructive, the sample is still available for graphite-furnace a.a.s. for barium.

Although the elemental profile described in this paper is not conclusive evidence that an individual has fired or handled a hangun, it suggests a strong possibility.

The authors thank Michael A. O'Connor, graduate student at Southeast, C. Robert Longwell, SEMO Regional Crime Laboratory, and Lowell Shank, Dept. of Chemistry, Western Kentucky State University, Bowling Green, KY, for valuable technical assistance.

REFERENCES

1 H. Harrison and R. Gilroy, J. Forensic Sci., 4 (1959) 184.
2 K. Bratin and R. Briner, Current Separations, Bioanalytical Systems, W. Lafayette, IN, 1980.
3 J. A. Goleb and C. R. Midkiff, Jr., Appl. Spectrosc., 29 (1975) 44.
4 M. L. Newbury, Can. Soc. Forensic Sci. J., 13 (1980) 19.
5 S. Krishnan, J. Forensic Sci., 22 (1977) 304.
6 G. Wolten and R. Nesbitt, J. Forencis Sci., 25 (1980) 533.
7 G. Wolten, R. Nesbitt, A. Calloway, G. Loper and P. Jones, J. Forensic Sci., 24 (1979) 409, 423.
8 J. H. Liu, W. Lin and J. D. Nicol, Forensic Sci. Int., 16 (1980) 53.
9 N. K. Knoanur and G. W. Van Loon, Talanta, 24 (1977) 184.
10 R. G. Candela, M. Colonna and L. Strada, Zacchia, 12 (1976) 44.
11 C. I. Brihaye, R. Machiroux and G. Gillian, Forensic Sci. Int., 20 (1982) 269.
12 A. Ciszewski and A. Lukaszewski, Anal. Chim. Acta, 146 (1983) 51.
13 I. Gustavsson and L. Hansson, Int. J. Environ. Anal. Chem., 17 (1984) 57.

Analytica Chimica Acta, 172 (1985) 39—47
Elsevier Science Publishers B.V., Amsterdam — Printed in The Netherlands

ANODIC STRIPPING VOLTAMMETRY AT A NICKEL-BASED MERCURY FILM ELECTRODE

ZENKO YOSHIDA*

Analytical Chemistry Laboratory, Japan Atomic Energy Research Institute, Tokai, Ibaraki 319-11 (Japan)

SORIN KIHARA

Institute for Chemical Research, Kyoto University, Uji-shi 611 (Japan)

(Received 2nd October 1984)

SUMMARY

The electrochemical properties of the nickel-based mercury film electrode (Ni-MFE) were investigated with respect to application of the electrode in the anodic stripping voltammetry (a.s.v.) of heavy metal ions. The hydrogen overpotential at the Ni-MFE is higher than those at MFEs based on other metals, and high enough to get quantitative a.s.v. peaks of lead and cadmium. The mercury film of the Ni-MFE is stable both mechanically and chemically; a.s.v. peaks at a Ni-MFE which had been used fifty times within 300 h after its preparation were identical with those at the freshly prepared electrode. With the Ni-MFE, 5×10^{-10}—10^{-7} M lead(II) and 2×10^{-10}—10^{-7} M cadmium(II) in the solution can be determined with relative standard deviations of 11 and 12%, respectively. These results are comparable to those obtained by a.s.v. at an in situ mercury-plated glassy carbon electrode.

The mercury film electrode (MFE) has received much attention [1—4] as the working electrode in anodic stripping voltammetry (a.s.v.) for determining traces of heavy metal ions in solution. For very low concentrations of metals, at which inter-element effects are insignificant, the metal atoms formed by the electrolytic reduction are concentrated within the mercury film, and the anodic dissolution of the concentrated metal proceeds rapidly and efficiently.

Platinum [5, 6] and silver [7, 8] have been most widely studied as supporting metals for the MFE. The hydrogen overpotential at the platinum- or silver-based MFE (Pt- or Ag-MFE), however, is less than that at a pure mercury electrode, reflecting the low hydrogen overpotential at the supporting metal, even when the mercury film thickness is more than 1 μm [6, 7]. The hydrogen overpotentials at these MFEs decrease further with passage of time after their preparation [7]. When metals such as platinum, silver, and gold [9], which easily form intermetallic compounds with mercury, are used as the supporting metal, the growth of intermetallic compounds at the interface between mercury and the supporting metal also produces lowering of the

0003-2670/85/$03.30

hydrogen overpotentials [6, 7, 9]. The growth of such intermetallic compounds also produces low, broad, and/or non-quantitative a.s.v. peaks, owing to permeation of the concentrated analyte into the intermetallic compounds [10].

Carbon is a suitable non-metallic supporting material for the MFE [1, 4, 11]. However, the chemical bond between carbon and mercury is rather weak, so that the mercury film is unstable mechanically [11, 12]. Hence, a mercury film deposited in situ is usually adopted in a.s.v. with a glassy carbon electrode [13].

It has been reported previously [9] that mercury forms a mechanically stable film on nickel, cobalt, and copper by electrodeposition and that these metals, especially nickel, hardly produce any intermetallic compound with mercury. Also the hydrogen overpotentials at the MFEs based on these metals are high enough for a.s.v. measurements of heavy metals.

In the present paper, a procedure is described for the preparation of nickel-based mercury film electrodes (Ni-MFE) and the voltammetric character of the Ni-MFE as well as results obtained in the a.s.v. of lead and cadmium are discussed. The a.s.v. results are compared with those obtained at MFEs based on other materials including glassy carbon.

EXPERIMENTAL

Preparation of mercury film electrodes

As the supporting materials for the MFE, nickel (>99.9% pure; Johnson Matthey Chemicals), platinum, gold (>99.99% pure; Tanaka Noble Metals Co.), and glassy carbon rods (GC-30S; Tokai Carbon Co.) were used. The carbon rods were 6 mm in diameter and 50—70 mm in length.

The rod was pushed into a teflon cylinder (9 mm i.d., 14 mm o.d., 30 mm long) interposing a silicone rubber tube (4.5 mm i.d., 8.5 mm o.d., 35 mm long) as a packing (Fig. 1). The bottom surface of the rod was used as the electrode disc. Infiltration of the solution into a gap between the casing and the rod was avoided by this technique. The surface of the nickel disc was polished by means of emery paper (No. 1200) to a mirror-like finish, and was washed with ethanol and then water under ultrasonic treatment. The disc electrode was then electrolyzed by cyclic potential scans between −0.1 V and −0.8 V at a scan rate of 20 mV s^{-1} in 0.2 M potassium nitrate/10^{-3} M nitric acid (usually 3—5 cycles).

The mercury film was deposited on the disc by electrolysis at −0.25 V for 30 min in the above nitrate/nitric acid solution containing 5×10^{-7}—10^{-3} M of mercury(II). At −0.25 V, there was neither hydrogen evolution nor anodic dissolution of the supporting material. The electrode was rotated at 1500 rpm during this deposition. The mercury-coated electrode obtained was electrolyzed in the 0.2 M potassium nitrate/10^{-3} M nitric acid solution by repeated cyclic potential scans between 0 V and −1.8 V at a rate of 20 mV s^{-1} until reproducible current/potential curves and the metallic lustre

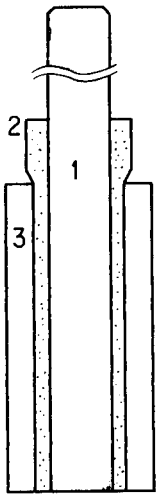

Fig. 1. Mercury film disc electrode: (1) supporting material; (2) silicone rubber packing; (3) teflon cylinder.

of mercury were obtained (usually 4—6 cycles). The prepared MFE was stored in the same nitrate/nitric acid electrolyte. If deaeration of the solution was insufficient during storage, an oxide film was formed at the surface of the MFE, which frequently resulted in the non-quantitative pre-concentration of the analyte in the a.s.v. measurement.

Apparatus

The electrolytic cell with a volume of 100 ml for the a.s.v. measurement was made of quartz. Voltammograms were recorded by using a potentiostat (Hokuto Denko Co.; Type HA-211), combined with a function wave generator (Hokuto Denko Co.; Type HB-104) and an X-Y recorder (Yokogawa Electrics Co.; Type 3036). The MFE was rotated at 1500 rpm by using a synchronous rotator (Yanagimoto Mfg. Co.; Type P10-RE). The electrode potential was referred to a saturated calomel electrode (SCE), and a platinum wire was used as the counter electrode.

Reagents

Water was deionized by passing through a mixed-bed ion-exchange column, and then distilled three times in quartz apparatus. The distillation rate was about 100 ml h^{-1}. The purified water was stored in the quartz vessel.

Mercury(II) solution. Triple-distilled mercury (2 g) was dissolved with 10 ml of hot 7 M nitric acid, and excess of acid was removed by evaporation. The residue was dissolved in water to give a 0.1 M mercury(II) solution. This mercury(II) solution was diluted to an appropriate concentration with 0.2 M potassium nitrate/10^{-3} M nitric acid, which had been electrolytically purified at −1.0 V for about 20 h at a mercury pool cathode.

Supporting electrolyte solution for a.s.v. A deaerated mixture of 1 M ammonium acetate and 0.2 M tartaric acid was electrolyzed at −1.0 V at a mercury pool electrode with stirring. The resulting solution was diluted with water to obtain the required 0.5 M ammonium acetate/0.1 M tartaric acid supporting electrolyte. Lead and cadmium remaining in the supporting electrolyte were found to be 5×10^{-10}—6×10^{-10} M and less than 10^{-10} M, respectively.

Lead(II) and cadmium(II) solutions. Acetate salts of these ions (99.99% pure) were dissolved in the supporting electrolyte solution.

Nitric acid, potassium nitrate, and other reagents used were of analytical-reagent grades.

Procedure for anodic stripping voltammetry

The electrolyte solution containing 10^{-10}—10^{-7} M of lead(II) and cadmium(II) was deaerated by passing argon of high purity for 20 min. After pre-concentration of the metals by electrolysis at −1.0 V for 10 min at the rotated electrode, the rotation of the electrode was stopped and the electrode potential was kept at −1.0 V for 30 s. Then the potential was scanned anodically to +0.1 V at a scan rate of 50 mV s^{-1} to record the anodic stripping voltammogram. Argon was passed over the solution in the cell throughout the procedure. All electrolytic measurements were made at 25 ± 1°C.

RESULTS AND DISCUSSION

Characteristics of the Ni-MFE

The thickness of the mercury film was calculated, on the assumption that the mercury film was uniform, from the amount of mercury determined by cold-vapour atomic absorption spectrometry (a.a.s.) after dissolution of the mercury layer in concentrated nitric acid. When the mercury was electrodeposited from a solution that was 2×10^{-5}, 2×10^{-4}, or 1×10^{-3} M in mercury(II), the thickness of the mercury film was 0.043, 0.45, or 2.3 μm, respectively. The amounts of mercury found by cold-vapour a.a.s. agreed well with those calculated from the quantity of electricity for the deposition of mercury, indicating that the mercury deposition on nickel proceeds quantitatively and that the MFEs with reproducible thickness can be prepared by electrolysis at −0.25 V.

The voltammogram at the rotated MFE in 0.2 M potassium nitrate/10^{-3} M nitric acid was recorded by a cathodic potential scan from −0.1 V at a rate of 20 mV s^{-1}. The relation between the mercury film thickness, l, of the MFE and the half-wave potential, $E^{H}_{1/2}$, of the diffusion-controlled wave for the reduction of 10^{-3} M hydrogen ion is given in Fig. 2. With increasing film thickness from 0.0001 to 0.04 μm, $E^{H}_{1/2}$ shifted to more negative potential from −0.68 V, which was the $E^{H}_{1/2}$ at the nickel electrode without mercury. With film thickness in the range 0.04—5 μm, $E^{H}_{1/2}$ was constant at −1.4 ± 0.2 V. Results at a MFE which had stood for 24 or 300 h after its preparation showed a positive shift in $E^{H}_{1/2}$ with lapse of time for film thicknesses of

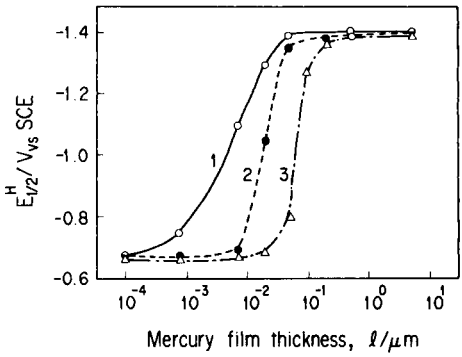

Fig. 2. Hydrogen overpotential at Ni-MFEs with various mercury film thicknesses. Electrode: (1) prepared and used within 2 h; (2) stood for 24 h; (3) stood for 300 h; Electrolyte solution: 0.2 M $KNO_3/10^{-3}$ M HNO_3.

$<0.2\ \mu m$; this may be attributable to a change in the electrode surface caused by the growth of the intermetallic compound between nickel and mercury. When the film thickness exceeded $0.2\ \mu m$, $E^H_{1/2}$ remained constant even when the electrode had been left for 300 h.

The residual voltammogram was recorded in the electrolyte solution without lead(II) and cadmium(II) as described in the above procedure for a.s.v. The residual currents, i_R, at −0.75, −0.50, and −0.25 V are given in Fig. 3. The large negative i_R at −0.75 V with film thicknesses of $<0.1\ \mu m$ is attributed to the reduction of hydrogen ion. The large positive i_R at −0.25 V with film thicknesses of $<0.01\ \mu m$ is due to the oxidation of nickel. Even when

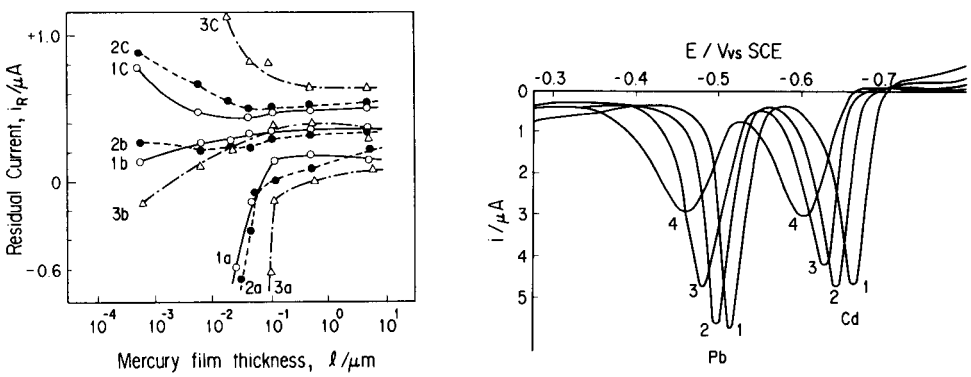

Fig. 3. Residual current at the Ni-MFE at different potentials: (a) −0.75 V; (b) −0.50 V; (c) −0.25 V. Electrode: (1) freshly prepared and used within 2 h; (2) stood for 24 h; (3) stood for 300 h. Electrolyte solution: 0.5 M ammonium acetate/0.1 M tartaric acid.

Fig. 4. Anodic stripping voltammograms of 5×10^{-8} M lead(II) and 5×10^{-8} M cadmium(II) at a freshly prepared Ni-MFE. Mercury film thickness (μm): (1) 0.05; (2) 0.5; (3) 2; (4) 5.

the MFE had been allowed to stand for 300 h after preparation, the i_R values at MFEs with film thickness >0.1 μm were little changed from those at the freshly prepared MFE.

Anodic stripping voltammetry of lead(II) and cadmium(II) at the Ni-MFE

The anodic stripping voltammograms shown in Fig. 4 were obtained at the freshly prepared Ni-MFE from a solution containing 5×10^{-8} M lead(II) and 5×10^{-8} M cadmium(II). The peak current, i_p, the peak width at half height ($b_{1/2}$), the peak potential, E_p, and the number of coulombs under the peak (Q) are summarized in Table 1. Regardless of the mercury film thickness over the range 0.05—0.5 μm, both i_p and $b_{1/2}$ are constant and are very close to those theoretically predicted for an ultra-thin mercury film electrode [14], 5.9 μA and 38 mV for lead(II), and 5.4 μA and 38 mV for cadmium(II), respectively. These results indicate that at the Ni-MFE (l = 0.05—0.5 μm) the diffusion process of lead and cadmium atoms in the mercury layer is not a rate-determining step in the anodic dissolution of the metals. When the film thickness exceeds 2 μm, although i_p decreases with increasing film thickness, Q is constant, indicating that the anodic dissolution process is controlled by diffusion of metals in the mercury layer. The shift of E_p with increasing film thickness from 0.05 to 0.5 μm also agrees with the expected

TABLE 1

Characteristics of a.s.v. peaks of lead and cadmium at various MFEs[a]

l (μm)	5×10^{-8} M lead(II)				5×10^{-8} M cadmium(II)			
	i_p (μA)	$b_{1/2}$ (mV)	$-E_p$ (V)	Q (μC)	i_p (μA)	$b_{1/2}$ (mV)	$-E_p$ (V)	Q (μC)
Ni-MFE								
0.05	5.4(0.6)	38(2)	0.514(0.007)	5.0(0.4)	4.8(0.5)	38(2)	0.663(0.007)	4.8(0.5)
0.5	5.3(0.4)	42(2)	0.496(0.005)	5.2(0.6)	4.7(0.4)	38(2)	0.641(0.007)	5.0(0.4)
2	4.4(0.4)	50(3)	0.482(0.005)	5.7(0.5)	4.1(0.3)	46(2)	0.627(0.008)	4.5(0.4)
5	2.3(0.2)	75(3)	0.457(0.005)	5.4(0.3)	2.6(0.3)	66(4)	0.600(0.003)	4.6(0.4)
Pt-MFE								
0.5	2.6(0.8)	50(5)	0.480(0.010)		1.8(0.3)	50(5)	0.630(0.005)	
0.5[b]	2.3(0.8)	55(5)	0.465(0.010)		0.8(0.8)	55(5)	0.602(0.008)	
Au-MFE								
0.5	2.5(0.3)	62(2)	0.486(0.003)		no peak			
0.5[b]	2.0(0.5)	61(3)	0.460(0.004)		no peak			
GC-MFE								
0.5	5.2(0.3)	39(2)	0.500(0.007)		4.7(0.3)	38(2)	0.641(0.007)	
0.5[b]	two peaks				two peaks			
GC-MFE prepared in situ[c]								
	5.4(0.3)	39(2)	0.496(0.009)		5.0(0.3)	38(2)	0.638(0.008)	

[a]The numbers in parentheses are the standard deviations for five repeated measurements. [b]MFE left for 24 h after preparation. [c]Analyte ions were codeposited with 1×10^{-4} M mercury(II).

value, 30 mV, for the ultra-thin film electrode [14]. Neither $b_{1/2}$ nor E_p obtained at the Ni-MFE (l = 0.05—2 μm) were changed when the amount of lead or cadmium was changed from 5×10^{-13} to 5×10^{-10} mol.

With a Ni-MFE (l = 0.2—5 μm) which had been used 50 times for a.s.v. measurements during 300 h after its preparation, i_p, $b_{1/2}$ and E_p were practically the same as those listed in Table 1. With a Ni-MFE (l = 0.05—0.1 μm) which had stood for more than 300 h, it was difficult to get reproducible a.s.v. curves and sometimes the a.s.v. peak had a shoulder. Roughly speaking, however, a.s.v. peaks of smaller i_p and larger $b_{1/2}$ values than those listed in Table 1 were obtained, although Q did not change significantly with standing time.

Calibration graphs for lead(II) and cadmium(II). The anodic stripping peak heights, i_p, for lead(II) and cadmium(II) measured at the Ni-MFE (l = 0.5 μm) were linearly proportional to the initial concentrations of these metal ions over the ranges 10^{-8}—10^{-7} M and 10^{-10}— 10^{-7} M, respectively. The relative standard deviations were 11, 8, 12 and 8% for the five repeated measurements of 5×10^{-9} M lead(II), 5×10^{-8} M lead(II), 5×10^{-9} M cadmium(II), and 5×10^{-8} M cadmium(II), respectively. When the concentration of lead(II) in the solution was less than 10^{-8} M, the calibration graph exhibited a positive Y-intercept corresponding to the background lead(II) in the supporting electrolyte solution.

Considering the residual current at the potential where the a.s.v. peak appears and the background quantity of metal ion in the electrolyte solution, the lower detection limits for lead(II) and cadmium(II) are concluded to be 5×10^{-10} and 2×10^{-10} M, respectively.

Comparison of the Ni-MFE with MFEs on other supporting materials

Data gathered in Table 2 are the hydrogen overpotentials and the residual currents at the platinum-, gold-, and glassy carbon-based MFEs (Pt-, Au- and GC-MFE) with mercury films 0.5 μm thick. The table also includes the results for the Ni-MFE (l = 0.5 μm) which are identical with those shown in Figs. 2 and 3.

TABLE 2

Hydrogen overpotential and residual current at different MFEs (l = 0.5 μm)

MFE	Standing time (h)	$-E^H_{1/2}$ (V vs. SCE)	i_R (μA)		
			at −0.75 V	at −0.50 V	at −0.25 V
Ni-MFE	<2	1.41	+0.20	+0.37	+0.51
	24	1.40	+0.11	+0.33	+0.53
Pt-MFE	<2	0.93	−0.15	−0.06	+0.82
	24	0.68	−0.66	+0.52	+0.80
Au-MFE	<2	1.22	−0.36	−0.08	+0.34
	24	1.05	−0.50	+0.12	+0.48
GC-MFE	<2	1.57	+0.72	+1.2	+2.8
	24	1.50	+0.34	+0.96	+3.2

The hydrogen overpotentials at the Pt-MFE and the Au-MFE, even at the freshly prepared electrodes, were significantly smaller than that at the Ni-MFE, and they decreased pronouncedly with standing time. The GC-MFE lost its mercury layer during repeated use because of the poor adhesion of the mercury to the glassy carbon, e.g., 30—45% of mercury was lost from a film thickness of 0.5 μm when the MFE was used for 3 or 7 repeated a.s.v. measurements, respectively. The GC-MFE, however, showed the highest hydrogen overpotential, as the hydrogen overpotential at GC without mercury is also high.

The residual currents at −0.75 V observed with the Pt- or Au-MFE were negative and large because of the low hydrogen overpotential. The large residual current at the GC-MFE might be due to non-uniform structure of the electrode surface, e.g., mercury-island formation.

The characteristics of the a.s.v. peaks for lead and cadmium observed at Pt-, Au-, and GC-MFEs (l = 0.5 μm) are summarized in Table 1. At the Pt- and Au-MFEs, it was difficult to get reproducible a.s.v. peaks. Similarly to the phenomena observed by Ostapczuk and Kublik [10] in the a.s.v. at the silver-based MFE, the peak current in the a.s.v. of cadmium at these MFEs was very low. The reason for the low i_p could be that the reversible anodic dissolution of cadmium is arrested by permeation of the cadmium into the intermetallic compound between the supporting metal and mercury. The a.s.v. curve obtained at a freshly prepared GC-MFE was almost identical to that at the Ni-MFE. At a GC-MFE which had been used more than 5 times for a.s.v. measurements and then left for 20 h, however, the a.s.v. peaks of lead and cadmium were split into two peaks; this again may be due to structural changes in the mercury layer.

Comparing the above-mentioned characteristics of these MFEs, it can be concluded that the Ni-MFE is superior to the others as the working electrode for a.s.v.

Comparison of a.s.v. at the Ni-MFE with that at the glassy carbon electrode with mercury film deposited in situ

The MFE with mercury deposited in situ [4, 13] involves the addition of mercury(II), usually 10^{-5}—10^{-4} M, to the sample solution and the codeposition of the heavy metals with the mercury on the GC electrode. This method has been widely used [2—4] in the a.s.v. determination of heavy metals because of its high sensitivity and reproducibility. The characteristics of the a.s.v. peak found with this codeposited film were very similar to those found with the Ni-MFE, as shown in Table 1. The detection limits for lead(II) and cadmium(II) were reported [1] as 6×10^{-10} and 3×10^{-10} M, respectively, with the in-situ GC-MFE method, and the relative standard deviations in determining lead(II) and cadmium(II) were ca. 10%, which were also very similar to those obtained with the Ni-MFE.

REFERENCES

1 G. E. Batley and T. M. Florence, J. Electroanal. Chem., 55 (1974) 23.
2 W. Davison and M. Whitfield, J. Electroanal. Chem., 75 (1977) 763.
3 L. Mart, H. W. Nurnberg and P. Valenta, Z. Anal. Chem., 300 (1980) 350.
4 T. M. Florence, J. Electroanal. Chem., 168 (1984) 207.
5 L. Ramaley, R. L. Brubaker and C. G. Enke, Anal. Chem., 35 (1963) 1088.
6 A. M. Hartley, A. G. Hiebert and J. A. Cox, J. Electroanal. Chem., 17 (1968) 81.
7 Z. Stojek and Z. Kublik, J. Electroanal. Chem., 60 (1975) 349.
8 J. P. Riley and H. Gu, Anal. Chim. Acta, 130 (1981) 199.
9 Z. Yoshida, Bull. Chem. Soc. Jpn., 54 (1981) 562.
10 P. Ostapczuk and Z. Kublik, J. Electroanal. Chem., 93 (1978) 195.
11 M. I. Abdullah, B. R. Berg and R. Klimek, Anal. Chim Acta, 84 (1976) 307.
12 Z. Yoshida and S. Kihara, J. Electroanal. Chem., 95 (1979) 159.
13 T. M. Florence, J. Electroanal. Chem., 27 (1970) 273.
14 W. T. de Vries and E. Van Dalen, J. Electroanal. Chem., 14 (1967) 315.

Analytica Chimica Acta, 172 (1985) 49—56
Elsevier Science Publishers B.V., Amsterdam — Printed in The Netherlands

PARAMETER EVALUATION FOR THE DETERMINATION OF SELENIUM BY CATHODIC STRIPPING VOLTAMMETRY AT THE HANGING MERCURY DROP ELECTRODE

U. BALTENSPERGER and J. HERTZ*

Institute for Inorganic Chemistry, University of Zurich Irchel, Winterthurerstr. 190, 8057 Zurich (Switzerland)

(Received 21st November 1984)

SUMMARY

The behaviour of selenium(IV) in cathodic stripping voltammetry is evaluated systematically. The effects of copper concentration, pH, deposition potential and complexing agents on the stripping peak are examined and criteria are given for the choice of suitable quantitative parameters. The detection limit was found to be 20 ng l^{-1} and the background contamination level was 35 ng l^{-1}. Zinc and lead do not affect the determination of selenium if EDTA is added to the solution whereas cadmium interferes badly; the corresponding mechanisms are discussed.

Selenium is essential for animals [1], and accumulating evidence suggests that it may also be required by humans [2]. Nevertheless, it is toxic in higher concentrations, and the safe and adequate range of daily intake recommended by the U.S. Food and Nutrition Board for adult humans is 50—200 μg [2]. Recognition of the biological role of selenium and of the critically narrow concentration range between deficiency and toxic levels has stimulated the development of new sensitive and accurate methods for the determination of this element. Spectrophotometry or fluorimetry after reaction with diaminonaphthalene or diaminobenzidine [3], x-ray fluorescence [4], neutron activation analysis [5], gas chromatography [6], atomic absorption spectrometry [7, 8] and electrochemical methods have been proposed.

Polarographic investigations of selenium in hydrochloric acid showed the presence of two waves at —0.01 V and —0.54 V (SCE) [9] which are attributed to the following reactions [10]

$$Se(IV) + 6e^- + 2H^+ = H_2Se$$

$$H_2Se + Hg^0 = HgSe + 2H^+ + 2e^-$$

with the net reaction

$$Se(IV) + 4e^- + Hg^0 = HgSe \quad (I)$$

$$HgSe + 2H^+ + 2e^- = H_2Se + Hg^0 \quad (II)$$

0003-2670/85/$03.30

More recently, cathodic stripping voltammetry (c.s.v.) has been used as a very sensitive method for the determination of selenium(IV) in aqueous solutions. Most of the authors proposed the use of an acidic electrolyte consisting of hydrochloric acid or ammonium sulphate and sulphuric acid, but the reported analytical conditions vary widely with regard to deposition potential, pH of the solution and addition of reagents such as copper or complexing agents [11—17].

In this work the influence of these parameters on the voltammograms in c.s.v. was investigated systematically in order to optimize experimental conditions.

EXPERIMENTAL

A V/A Processor (Metrohm 646) with a V/A Stand 647 was used with a multimode electrode. This newly developed system allows various kinds of voltammetric and polarographic methods to be done with the same instrumentation. The software provides systematic variation of parameters such as deposition potential, drop diameter or stirring speed automatically, thus leading to excellent reproducibility. The silver/silver chloride (3 M KCl) reference electrode was connected with the solution via a double junction filled with the buffer solution corresponding to the analyte solution. A glassy carbon rod served as counter electrode. For cathodic stripping voltammetry at a hanging mercury drop electrode, a simple program was normally used. First, the solution was deaerated by bubbling nitrogen for 10 min. The differential pulse method with a pulse amplitude of 50 mV every 600 ms was applied. After a deposition time of 60 s at —350 mV, the solution was allowed to come to rest over a period of 20 s. After that, the voltammogram was recorded from —350 to —900 mV with a sweep rate of 10 mV s^{-1}, and the peak height evaluated by a built-in mathematical model.

All reagents were of analytical grade. Deionized water, cleaned by additional ion exchange and filtration through activated carbon and a 0.45-μm filter (Millipore, MilliQ), was used throughout. Selenium standard solutions were prepared daily by diluting a 1000 mg l^{-1} stock solution (selenous acid in water). Handling of samples, and the voltammetric procedure were in a clean bench.

RESULTS

Role of copper

Some authors have suggested the addition of copper(II) ions in order to increase the sensitivity of the c.s.v. method [12, 16]. This enhancement seems to be due to the formation of copper selenide, which is more soluble in the mercury drop than mercury selenide. Figure 1 shows differential pulse polarograms of a solution containing selenium in an ammonium sulphate/sulphuric acid buffer with EDTA and varying copper concentra-

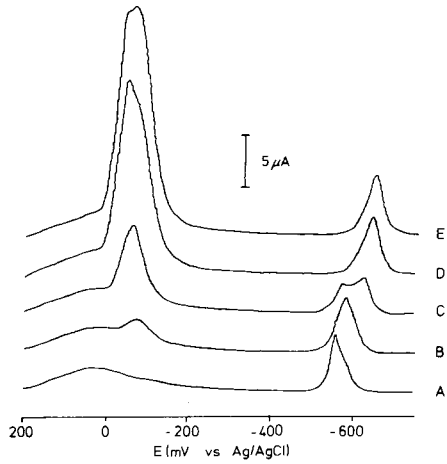

Fig. 1. Polarograms for selenium in the presence of copper: (A) without copper; (B) 4.4×10^{-5} M Cu; (C) 1.75×10^{-4} M Cu; (D) 5×10^{-4} M Cu; (E) 7×10^{-3} M Cu. Conditions: 10^{-4} Se(IV) in 0.5 M ammonium sulphate, with 8×10^{-3} M EDTA adjusted to pH 2.0 with sulphuric acid.

tions. Polarogram A exhibits two peaks; the first, an irreversible reaction at a potential of about +10 mV (Ag/AgCl), is due to the formation of HgSe according to reaction I. The second at −560 mV (Ag/AgCl) is due to the reductive dissolution of HgSe (reaction II). On the addition of a substoichiometric amount of copper(II), a new peak appears at −80 mV (Ag/AgCl) and the second peak is shifted towards more negative potentials. Increasing the copper concentration leads to the formation of a third peak at a potential of −630 mV (Ag/AgCl) which is assigned to the reaction

$$Cu_2Se + 2H^+ + 2e^- = H_2Se + 2Cu^0 \qquad \text{(III)}$$

At a molar ratio (Cu:Se) of about 2:1, the peak at −560 mV disappears. At even higher copper concentrations, the reduction of Cu^{2+} to Cu^0 can be observed at a slightly more negative potential than step I. To confirm the formation of copper(I) selenide at the electrode surface, one mercury drop was removed from the solution after the deposition step in c.s.v., placed on a copper grid (coated with a carbon film) and evaporated under vacuum at 170°C. High-resolution transmission electron micrographs and electron diffraction patterns of selected areas were taken from the residue (Fig. 2). Evaluation of the diffraction patterns gave evidence for the formation of not only Cu_2Se, but also Cu_3Se_2 and possibly one additional phase [18]. A Cu_6Se phase, however, as observed on graphite electrodes [19], could not be confirmed.

In order to find the optimum amount for the addition of copper, the height of the stripping peak in c.s.v. was plotted as a function of copper concentration. Figure 3 shows the increase in sensitivity when copper(II) is added to the solution. At a specific concentration (which depends on the

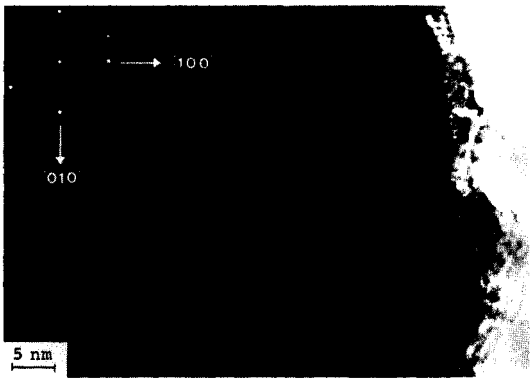

Fig. 2. Transmission electron micrograph of Cu_2Se deposited on a mercury electrode, with SAED pattern.

drop size), the peak height decreases rapidly. This decrease is accompanied by a sudden change in peak potential at the corresponding copper concentration. A change in selenium concentration does not alter the breakdown concentration; thus it is independent of the Cu/Se ratio. However, decreasing the diameter of the mercury drop from 0.71 to 0.53 mm (0.190 to 0.078 mm^3) leads to a decrease in the peak height at a lower copper concentration. According to Shain and Lewinson [20], the diffusion of metals within the mercury drop is so fast that virtually no concentration gradient within the drop can be detected after a few seconds. Because the amount of deposited copper is proportional to r^2 (radius) and the volume of the drop is $4/3\ \pi\ r^3$, this breakdown concentration should be proportional to r^{-1}, which

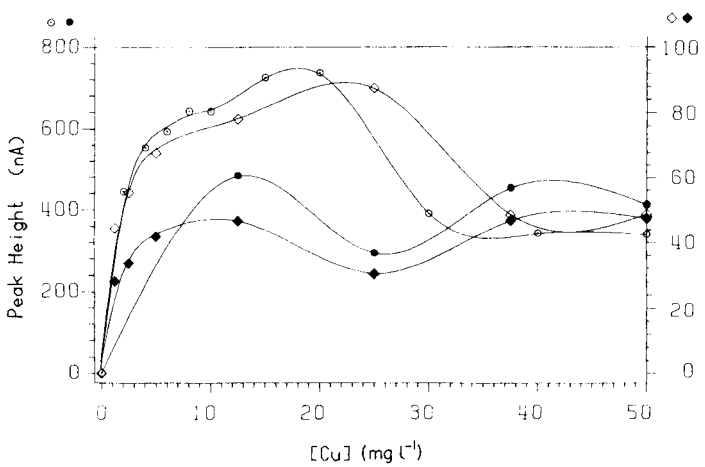

Fig. 3. Peak heights for d.p.c.s.v. of selenium as a function of Cu^{2+} concentration at pH 2.0 (8×10^{-3} M EDTA): (◇◆) 10 μg l^{-1} Se; (○●) 62.5 μg l^{-1} Se; (●◆) drop diameter 0.53 mm; (○◇) drop diameter 0.71 mm.

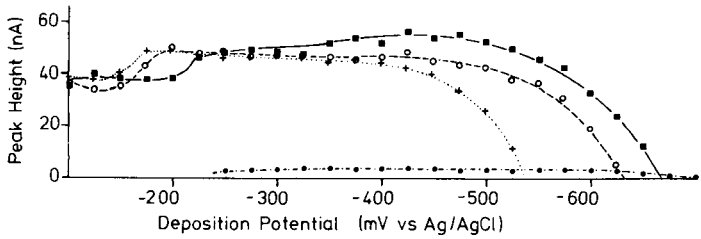

Fig. 4. Dependence of d.p.c.s.v. peak heights on deposition potential and pH: (•) pH 4.7; (▪) pH 3.0; (○) pH 2.4: (+) pH 2.0. Conditions: 10 $\mu g\ l^{-1}$ Se with 2 mg l^{-1} Cu in 8×10^{-3} M EDTA.

is in rough agreement with the experiment (Fig. 3). This leads to the suggestion that the sudden change in peak height and potential is due to saturation of the mercury drop with copper, thus changing the electrochemical behaviour of the electrode material. This is confirmed by the fact that the present results (calculated from the breakdown concentration) agree within a factor of 4 to 5 with the reported solubility of copper in mercury (0.002--0.003% w/w [21]).

Influence of pH and deposition potential

There are several possible choices of an appropriate electrolyte for the determination of selenium by c.s.v. Jarzabek and Kublik [15] examined different acids as supporting electrolytes and found perchloric acid and hydrochloric acid to be suitable. The latter was used by others [13, 16, 17], but still others selected ammonium sulphate buffer solutions [11, 12, 14]. The sulphate buffer was preferred here, because the pK_a values of the acids involved (H_2SeO_3 and H_2Se) lie within the accessible pH range. The influence of solution pH and deposition potential on peak height in c.s.v. is summarized in Fig. 4. Changing the deposition potential at a given pH shows a limited region where the peak potential and the height of the stripping peak are independent of deposition potential. At deposition potentials more positive than the formation of Cu_2Se, the stripping peak shifts to more positive potentials and the peak height decreases. A similar but even more pronounced effect can be seen at more negative deposition potentials. Both limiting deposition potentials are pH-dependent, because proton transfers are involved in reactions I and III. The optimum conditions for the quantitative procedure have to be chosen with respect to pH and deposition potential. In this study, a deposition potential of −350 mV (Ag/AgCl) at a pH of 2.0 proved to be favourable.

Interferences and role of complexing agents

In hydrochloric acid solutions, several elements were found to interfere seriously with the c.s.v. determination of selenium. The stripping peak height was decreased by Fe^{3+}, Pb^{2+}, Zn^{2+}, Cd^{2+} and Te(IV) but increased by As(III) [16, 17]. In the ammonium sulphate buffer, lead and cadmium

interfered [22]. The present investigations showed, that, in the presence of 2 mg l^{-1} copper(II), zinc(II) interferes slightly at 100-fold concentrations with respect to selenium only if no complexing agent is added to the solution. Addition of 8×10^{-3} M EDTA removes this interference completely. No interferences from lead could be detected, whereas there was serious interference from cadmium. Addition of cadmium(II) caused a decrease of the stripping peak of Cu_2Se, while two new peaks were formed. The first peak, at a slightly more positive potential was due to the reduction of Cd^{2+} ion. The second peak, slightly more negative, represented the cathodic dissolution of CdSe in a manner analogous to reaction III. As can be seen from Fig. 5, the original stripping peak disappeared almost completely on the addition of a twentyfold excess of cadmium, whereas the stripping peak for CdSe increased correspondingly. These effects can be reduced by the addition of a complexing agent such as EDTA. When the EDTA concentration is doubled, the CdSe peak is halved, accompanied by a corresponding growth of the Cu_2Se peak. The low stability constant of the Cd-EDTA complex explains why this cadmium interference cannot be eliminated completely by EDTA; log K = 16.5 [23], thus log K' at pH 2.0 is only 3.8, which means that an EDTA concentration of 8×10^{-3} M and 100 μg l^{-1} cadmium only CdSe forms if there is 10 μg l^{-1} selenium, whereas with 20 μg l^{-1} selenium, Cu_2Se is also formed (Fig. 6). No alteration of peak heights was observed when the deposition potential was changed from −350 mV to −250 mV (vs. Ag/AgCl). An additional advantage of using

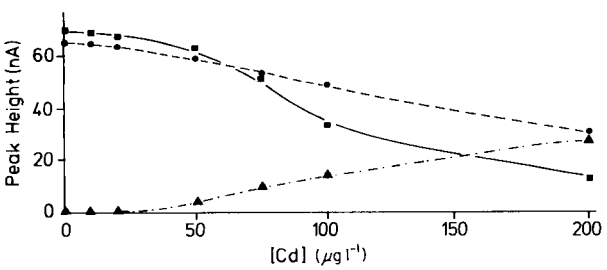

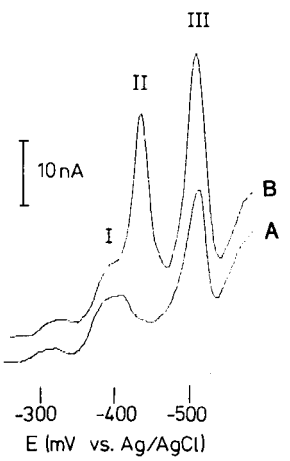

Fig. 5. D.p.c.s.v. peak heights as a function of cadmium concentration: (■) Cu_2Se without EDTA; (●) with EDTA; (▲) CdSe without EDTA. Conditions: 10 μg l^{-1} Se, pH 2.0, 2 mg l^{-1} Cu.

Fig. 6. Stripping voltammogram of selenium with 2 mg l^{-1} copper and 1 mg l^{-1} cadmium: (A) 10 μg l^{-1} Se; (B) 20 μg l^{-1} Se. Peaks: (I) $Cd^{2+} = Cd^0$; (II) $Cu_2Se = Cu^0 + H_2Se$; (III) $CdSe = Cd^0 + H_2Se$.

EDTA is that the reproducibility can be improved. The relative standard deviations for 10 measurements of 10 $\mu g\ l^{-1}$ selenium were 3.4% without EDTA and 0.9% with EDTA.

In order to elucidate the mechanisms of the different steps in the presence of interfering elements, differential pulse polarography and cyclic voltammetry were applied to the various systems. When cadmium was added to the system described in Fig. 1 (without copper), a new peak appeared at −360 mV (vs. Ag/AgCl). Addition of copper to the solution shifted this peak to about −470 mV. These peaks are assigned to substitution peaks, i.e., caused by formation of CdSe from HgSe or Cu_2Se, respectively [22]. Cyclic voltammetry showed that the mechanisms of these two substitutions are not identical; the former peak (HgSe) appears only in the first of a number of consecutive voltammograms at a single drop, whereas the latter (Cu_2Se) is also formed in the following scans. Further work is needed to understand the mechanisms more fully.

Quantitative performance

Calibration curves for two copper concentrations were nearly linear from 0—50 $\mu g\ l^{-1}$ selenium (Fig. 7), but they showed a slightly increasing slope with increasing selenium concentrations. This was also observed in similar c.s.v. determinations reported by other authors [15, 24, 25] and could be due to the manifold stoichiometry of Cu_xSe. This phenomenon could not be overcome and is a point of trouble when the standard addition method is used; nevertheless, standard addition is the method of choice for such systems. The detection limit, evaluated from three times the standard deviation of the baseline noise, was 20 ng l^{-1}, and the blank value reached 35 ng l^{-1} for a deposition time of 3 min.

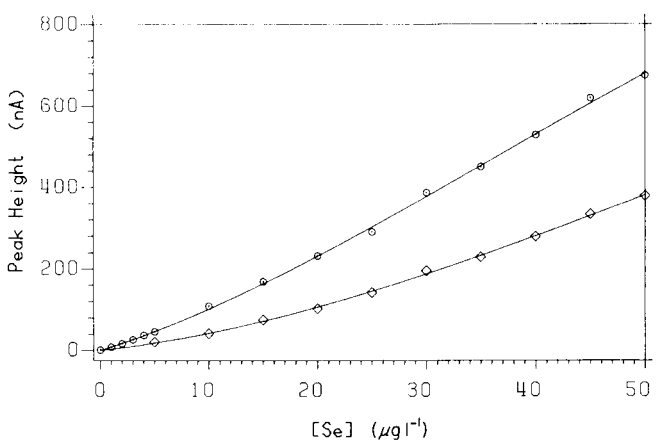

Fig. 7. Calibration curves for selenium: (◇) with 2 mg l^{-1} Cu; (○) with 15 mg l^{-1} Cu. Conditions: pH 2.0, 8×10^{-3} M EDTA, deposition potential −350 mV.

Conclusion

The procedures described above are well suited to determine selenium(IV) with high sensitivity and good precision. Interferences can be reduced by the addition of a strong complexing agent such as EDTA. Other approaches to the elimination of interferences would be possible; for example, a flow-through cell would allow the supporting electrolyte to be changed easily after the deposition step [24] or an extraction procedure could be used.

We thank Dr. A. Reller for the transmission electron microscope work and for helpful discussions.

REFERENCES

1 K. Schwarz and C. M. Foltz, J. Am. Chem. Soc., 79 (1957) 3292.
2 Subcommittee on Selenium, Committee on Animal Nutrition, Board on Agriculture, National Research Council, Selenium in Nutrition, revised edn., National Academy Press, Washington, DC, 1983.
3 P. A. Whetter and D. E. Ullrey, J. Assoc. Off. Anal. Chem., 61 (1978) 927.
4 K. I. Strausz, J. T. Purdham and O. P. Strausz, Anal. Chem., 47 (1975) 2032.
5 H. J. M. Bowen, Application of Activation Techniques to Biological Analysis, in CRC Crit. Rev. Anal. Chem., 10 (1981) 127.
6 T. P. McCarthy, B. Brodie, J. A. Milner and R. F. Bevill, J. Chromatogr., 225 (1981) 9.
7 J. A. Fiorino, J. W. Jones and S. G. Capar, Anal. Chem., 48 (1976) 120.
8 G. Horlick, Anal. Chem., 56 (1984) 278R.
9 G. D. Christian, E. C. Knoblock and W. C. Purdy, Anal. Chem., 35 (1963) 1128.
10 A. J. Bard, (Ed.), Encyclopedia of the Electrochemistry of the Elements, Vol. IV, M. Dekker, New York, 1975, p. 367ff.
11 K.-B. Ebhardt and F. Umland, Fresenius Z. Anal. Chem., 310 (1982) 406.
12 G. Henze, P. Monks, G. Tölg, F. Umland and E. Wessling, Fresenius Z. Anal. Chem., 295 (1979) 1.
13 S. Forbes, G. P. Bound and T. S. West, Talanta, 26 (1979) 473.
14 C. Arlt and R. Naumann, Fresenius Z. Anal. Chem., 282 (1976) 463.
15 G. Jarzabek and Z. Kublik, Anal. Chim. Acta, 143 (1982) 121.
16 S. B. Abdeloju and A. M. Bond, Anal. Chim. Acta, 148 (1983) 59.
17 R. bin Ahmad, J. O. Hill and R. J. Magee, Analyst (London), 108 (1983) 835.
18 Joint Committee on Powder Diffraction Standards, Powder Diffraction File Nr. 27-1131, Nr. 19-402, Swarthmore.
19 E. Ya. Neiman and G. B. Ponomarenko, J. Anal. Chem. USSR, 30 (1975) 952.
20 I. Shain and J. Lewinson, Anal. Chem., 33 (1961) 187.
21 M. Hansen, Constitution of Binary Alloys, 2nd edn., McGraw-Hill, NY, 1958, p. 588.
22 F. Umland and W. Wallmeier, J. Less Common Metals, 76 (1980) 245.
23 G. Schwarzenbach and H. Flaschka, Die komplexometrische Titration, Enke, Stuttgart, 1965.
24 H. Kavel and F. Umland, Fresenius Z. Anal. Chem., 316 (1983) 386.

Analytica Chimica Acta, 172 (1985) 57—64
Elsevier Science Publishers B.V., Amsterdam — Printed in The Netherlands

STRIPPING VOLTAMMETRY OF ALUMINUM BASED ON ADSORPTIVE ACCUMULATION OF ITS SOLOCHROME VIOLET RS COMPLEX AT THE STATIC MERCURY DROP ELECTRODE

JOSEPH WANG*, PERCIO A. M. FARIAS[a] and JAWAD S. MAHMOUD
Department of Chemistry, New Mexico State University, Las Cruces, NM 88003 (U.S.A.)
(Received 2nd January 1985)

SUMMARY

A very sensitive electrochemical stripping procedure for aluminum is reported. Accumulation is achieved by controlled adsorption of the aluminum/solochrome violet RS complex on the static mercury drop electrode. Optimal experimental parameters include an accumulation potential of −0.45 V, solochrome violet RS concentration of 1×10^{-6} M, and a linear-scan stripping mode. The detection limit is 0.15 $\mu g\ l^{-1}$, the response is linear over the 0—30 $\mu g\ l^{-1}$ concentration range, and the relative standard deviation (at the 10 $\mu g\ l^{-1}$ level) is 2%. Most cations do not interfere in the determination of aluminum. The interference of iron(III) is eliminated by addition of ascorbic acid. Results are reported for snow samples.

Considerable interest in the behavior of aluminum in environmental and biological systems has developed. The electrochemical behavior of aluminum makes its voltammetric quantitation difficult. Aluminum is reduced at −1.75 V, yielding an irreversible wave, distorted by the hydrogen evolution background current. In 1950, Willard and Dean [1] found that solochrome violet RS (SVRS) forms a discrete polarographic reduction wave in the presence of aluminum. The height of the complex wave, which was about 0.2 V more cathodic than the wave of the free dye, was shown to be proportional to the aluminum concentration. This wave was enhanced by the adsorption of the complex at the dropping mercury drop electrode, allowing polarographic quantitation at concentrations as low as 0.01—1 mg l^{-1} [1—3]. Similar detectability was obtained from the oxidation wave of the aluminum/SVRS complex at the pyrolytic graphite electrode [4]. With increasing needs to quantify lower ($\mu g\ l^{-1}$) levels of aluminum, more sensitive electrochemical procedures are needed.

This paper describes a sensitive electrochemical stripping procedure for trace measurements of aluminum based on its complex with SVRS. In a previous report of stripping voltammetry of aluminum, employing the adsorptive

[a]Present address: Department of Chemistry, Pontificia Universidade Catolica de Rio de Janeiro, Rio de Janeiro, Brazil.

0003-2670/85/$03.30

accumulation and oxidation of its SVRS complex at the carbon paste electrode, poor detectability (0.1 mg l^{-1}) was obtained [5]. As illustrated in the present study, sub-μg l^{-1} concentrations of aluminum can be measured by using the static mercury drop electrode and carefully optimizing the operating conditions.

EXPERIMENTAL

Apparatus and reagents

Stripping and cyclic voltammograms were obtained with an EG & G Princeton Applied Research Corp. (PAR) Model 264A stripping analyzer. The working electrode was a PAR Model 303A static mercury drop electrode. A medium-size drop (0.016 cm^2 surface area) was used. The sample cell (PAR Model 0057) was fitted with a Ag/AgCl (saturated KCl) reference electrode and a platinum wire auxiliary electrode. The cell was covered with aluminum foil. A magnetic stirrer (Troemner Model 500) and a stirring bar (1-cm long, 2-mm thick) provided the convective transport during the accumulation step. A PAR Model 0073 X-Y recorder was used for the collection of experimental data.

All solutions were prepared from double-distilled water. A 1000 mg l^{-1} aluminum stock solution was prepared by dissolving the chloride salt. The SVRS (Aldrich Chemical Co.) stock solution (1×10^{-4} M) was prepared daily. The supporting electrolyte was 0.2 M acetate buffer (pH 4.5) prepared by mixing ammonium acetate and perchloric acid. Snow samples, collected in a clean beaker, were melted at room temperature.

Procedure

Samples were prepared in 15-ml test tubes, containing 10 ml of supporting electrolyte, 1×10^{-6} M SVRS and various concentrations ($\mu g\, l^{-1}$) of aluminum. After heating for 10 min at 90°C in a block heater (Supelco), the solution was allowed to cool at room temperature for 15 min. Then it was transferred to the electrochemical cell and degassed with nitrogen for 8 min. The accumulation potential, —0.45 V, was applied to the working electrode, while the solution was stirred. The stirring was stopped, and after 15 s the voltammogram was recorded by applying a negative linear scan at 50 mV s^{-1}. The scan was terminated at —1.0 V and the adsorptive stripping cycle was repeated with a new mercury drop. The entire procedure was automated, as controlled by the PAR264A Stripping Analyzer. All data were obtained at room temperature.

RESULTS AND DISCUSSION

Parameters affecting the adsorptive stripping behavior

Figure 1 shows repetitive cyclic voltammograms for 50 $\mu g\, l^{-1}$ aluminum in an acetate buffer (pH 4.5) solution containing 1×10^{-6} M SVRS. Stirring the

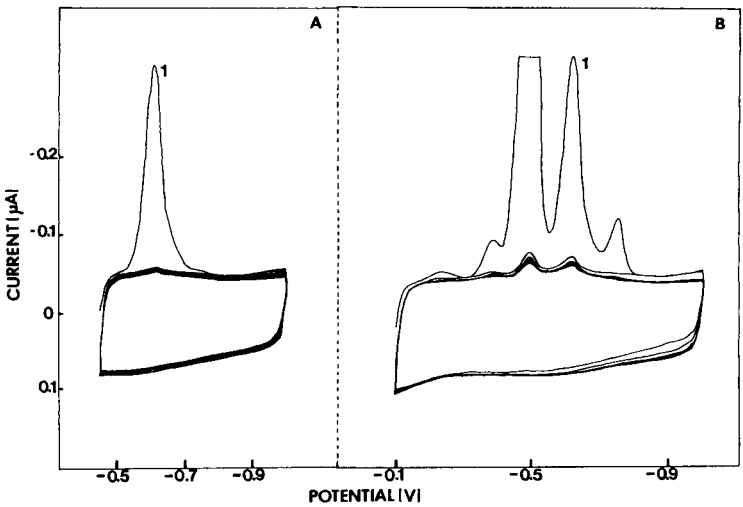

Fig. 1. Repetitive cyclic voltammograms for 50 μg l^{-1} aluminum in an acetate buffer (pH 4.5) solution, containing 1×10^{-6} M SVRS, after 1-min stirring at —0.45 V (A) and —0.10 V (B). Scan rate, 100 mV s^{-1}.

solution for 1 min at —0.10 V prior to the scan (B, scan 1), results in four cathodic peaks because of reduction of the adsorbed complex (at —0.61 V) and of the adsorbed dye (at —0.39, —0.49 and —0.75 V). The two large peaks at —0.49 and —0.61 V were reported in polarographic determinations of aluminum [1]. No peaks are observed in the anodic branch. Subsequent repetitive scans yield significantly smaller cathodic peaks, indicating rapid desorption of the complex and free dye from the surface. When the same experiment was repeated after accumulation at —0.45 V (A, scan 1), only a single cathodic peak, caused by the reduction of the adsorbed complex, was observed at —0.61 V. Again, the peak current with the adsorbed species was significantly larger than that of the dissolved complex alone (subsequent scans).

The surface coverage can be measured from the quantity of charge consumed by the surface process during the cyclic voltammetry. Division of the number of coulombs transferred, 0.185 μC, by the conversion quantity (nFA) yielded a coverage of 3×10^{-11} mol cm^{-2}. Each adsorbed complex molecule thus occupies an area of 5.5 nm^2. The peak current for the surface-adsorbed complex is directly proportional to the scan rate (v). A plot of log i_p vs. log v was linear, with a slope of 0.92, over the 10—200 mV s^{-1} range. A slope of 1.0 is expected for an ideal redox couple immobilized on an electrode surface.

The spontaneous adsorption of the Al/SVRS complex can be used as an effective accumulation step, prior to the voltammetric measurement. In this way, highly sensitive measurements of aluminum can be achieved by means of adsorptive stripping voltammetry. Figure 2 compares linear-scan (A) and

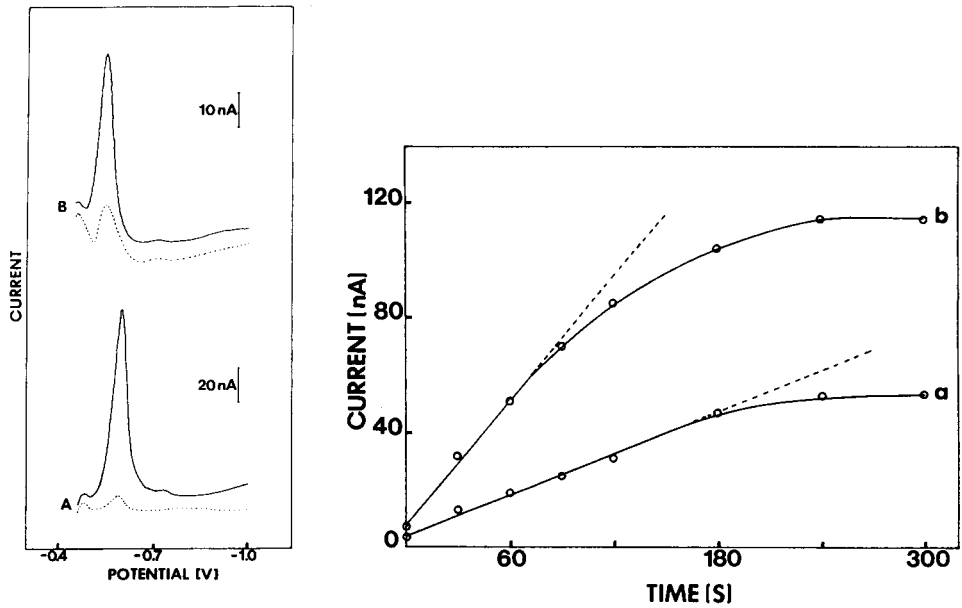

Fig. 2. Linear-scan (A) and differential-pulse (B) stripping voltammograms for 12 μg l^{-1} aluminum. Accumulation for 2 min at —0.45 V with 400 rpm stirring. Scan rate, 50 (A) and 5 (B) mV s^{-1}; pulse amplitude (B), 50 mV. Buffer and SVRS concentration as in Fig. 1. Dotted lines represent the response without accumulation.

Fig. 3. Dependence of the stripping peak current on the accumulation time for aluminum: (a) 4; (b) 12 μg l^{-1}. Other conditions as in Fig. 2A. Dotted lines correspond to the linear fit to the first portion of each curve.

differential-pulse (B) stripping voltammograms for 12 μg l^{-1} aluminum, following 2-min accumulation. Both stripping modes exhibit significant peak-current enhancements compared to direct voltammetric measurements. In particular, a 16-fold peak enhancement is obtained by the linear-scan mode. This mode offers better signal-to-background characteristics and greater speed, and is recommended for the determination of aluminum. Overall, the use of short accumulation periods allows convenient quantitation of aluminum at the μg l^{-1} level.

Figure 3 shows the dependence of the adsorptive stripping peak current on the accumulation time at two concentration levels. The longer the accumulation time, the more Al/SVRS complex adsorbed and the larger the peak current. At both concentrations, the peak increases linearly at first and then curves toward the time axis. Such time-dependent profiles represent the corresponding adsorption isotherms because the peak current depends on the amount adsorbed. This is in contrast to the linear dependence expected for metals deposited electrolytically. As in all types of stripping measurements, the choice of accumulation time requires a trade-off between sensitivity and

speed. Times of 4 and 0.5 min suffice for quantitation of aluminum at the 1 and 15 $\mu g\ l^{-1}$ levels, respectively.

Forced convection during the accumulation period affects the resulting stripping response by increasing the rate of transport of Al/SVRS molecules to the surface. For example, a 4.5-fold peak enhancement was obtained for a stirred (400 rpm) solution compared to a quiescent one (15 $\mu g\ l^{-1}$ Al; other conditions, as in Fig. 2A). Such mass-transport control indicates a fast rate of adsorption.

The effect of the accumulation potential on the stripping peak current was examined over the 0.0 to —0.45 V range (14 $\mu g\ l^{-1}$ Al, 1-min accumulation, other conditions as in Fig. 2A). The peak current remains essentially the same over the 0.0 to —0.3 V region; a 25% increase in the peak was observed with accumulations at —0.40 and —0.45 V. With accumulation potentials more positive than —0.40 V, the complex stripping peak was accompanied by current peaks associated with the reduction of the adsorbed free dye. Because of the similarity in peak potentials, the complex peak of interest was not adequately resolved from the free dye peaks. Similar resolution problems are common to analogous polarographic measurements of aluminum [4]. In contrast, stripping measurements after accumulation at a potential of —0.45 V yielded only the complex peak of interest. The improved resolution obtained by a proper choice of the accumulation potential is demonstrated in Fig. 4. Besides the improvement in resolution, accumulation at —0.45 V alleviates problems associated with competition on the surface sites by the free dye. This was evidenced by various experiments. For example, an accumulation potential of —0.1 V resulted in a gradual decrease in the complex stripping peak at high SVRS concentrations or long accumulation periods. The free dye displaced the complex from the surface, producing the above abnormalities. With an accumulation potential of —0.45 V, such effects were minimized. For example, the accumulation time profiles reflected the adsorption isotherms (Fig. 3). Similarly, Fig. 5 shows the dependence of the stripping peak current on the SVRS concentration. The peak increased linearly with the SVRS concentration, up to about 1×10^{-6} M, and then started to level off. At pH values around 4.5, used for electroanalytical measurements, the SVRS/Al ratio in the complex is 1:2 [6]. A SVRS concentration of 1×10^{-6} M was used in the stripping measurements reported here.

Quantitative utility

Figure 6 shows voltammograms for solutions of increasing aluminum concentration (2—12 $\mu g\ l^{-1}$) after 2-min accumulation. Well-defined stripping peaks were observed over this concentration range. In contrast, the corresponding solution-phase response was not useful for quantitative work at this level. The resulting calibration plots are also shown in Fig. 6. The stripping peak current increases linearly with the concentration. Least-squares analysis of these plots yielded slopes of 0.77, 5.32 and 8.07 $nA/10^{-8}$ M for the 0, 1 and 2-min experiments, respectively (correlation coefficients, 0.991, 0.999

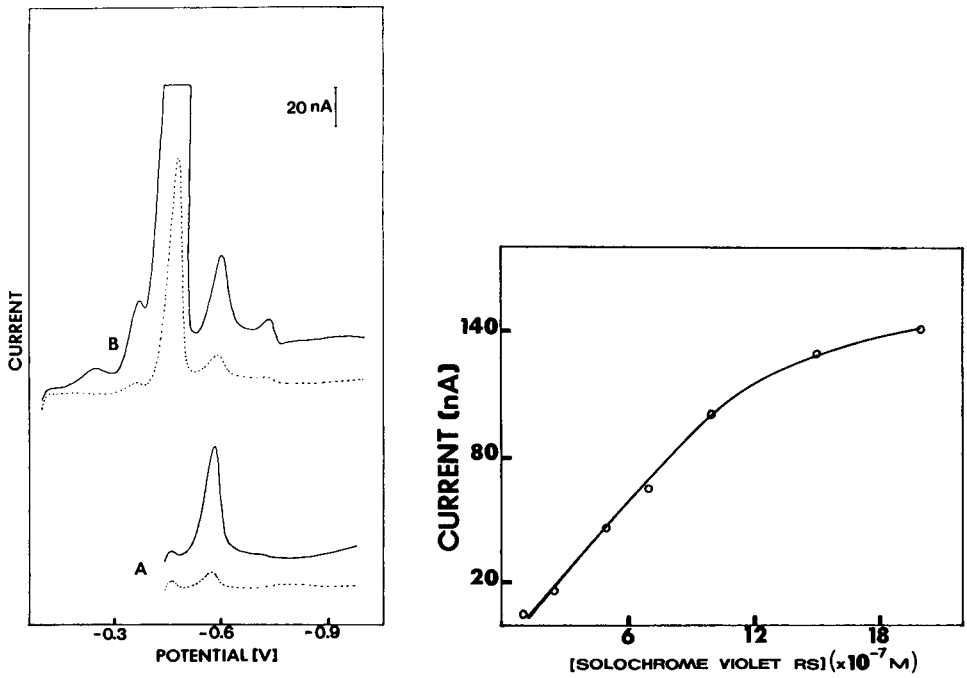

Fig. 4. Linear-scan voltammograms for 10 μg l^{-1} aluminum after 45-s accumulation at —0.45 V (A) and —0.10 V (B). Other conditions as in Fig. 2A. Dotted lines represent the corresponding response without accumulation.

Fig. 5. Dependence of the stripping peak current on the SVRS concentration, 10 μg l^{-1} aluminum. Other conditions as in Fig. 2A.

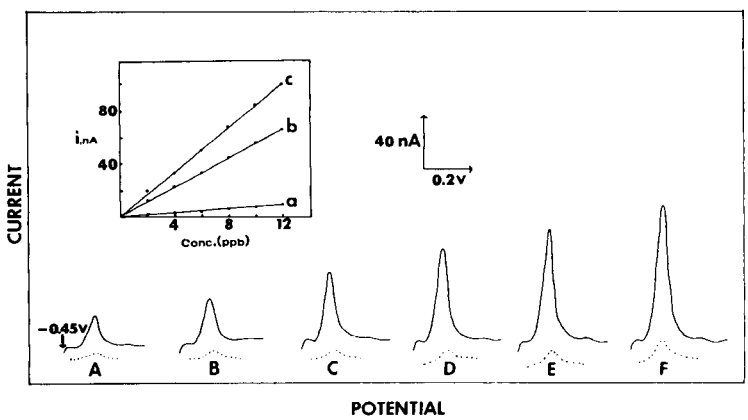

Fig. 6. Stripping voltammograms obtained for solutions of increasing aluminum concentration, 2—12 μg l^{-1} (A—F). Other conditions as in Fig. 2A. Dotted lines represent the solution-phase response at 0 min. Also shown are the resulting calibration plots, after different accumulation times: (a) 0 min; (b) 1 min; (c) 2 min.

and 0.999). In another experiment, solutions of increasing concentrations (5—30 $\mu g\ l^{-1}$), provided a linear response (1-min accumulation, other conditions as in Fig. 2A). Because of the nature of the complex formation and adsorption, quantitation may be better accomplished by a calibration curve than via standard additions.

The effective preconcentration associated with the adsorption process results in significant lowering of the detection limit compared to the corresponding solution measurements. A detection limit of 0.15 $\mu g\ l^{-1}$ (5.5×10^{-9} M) was estimated from quantitation of 2 $\mu g\ l^{-1}$ after a 10-min accumulation (S/N = 3). Thus, 1.5 ng could be detected in the 10 ml of solution used. In contrast, the detection limit of solution-phase measurements is around 2.2×10^{-7} M.

The adsorptive stripping response of aluminum is highly reproducible. Twelve successive measurements yielded a mean peak current of 179 nA, a range of 173—182 nA, and a relative standard deviation of 2.0%. Such behavior is attributed to the reproducibility of the adsorption process, and to the use of a new drop of reproducible area in each run.

Interference from coexisting metal ions capable of forming complexes with SVRS or depositing at the mercury electrode were evaluated. Ions tested at the 50 $\mu g\ l^{-1}$ level and found not to interfere in the determination of 10 $\mu g\ l^{-1}$ aluminum were Bi(III), Ca(II), Cd(II), Co(II), Eu(III), In(III), La(III), Mg(II), Ni(II), Pr(III), Se(IV), Sn(IV) and Zn(II); Na(I) and K(I) did not interfere at the 2000 $\mu g\ l^{-1}$ level. The addition of 50 $\mu g\ l^{-1}$ Cu(II) or Fe(III) resulted in severe depression of the Al(III) peak, and the appearance of new peaks at —0.65 V and —0.75 V, respectively. It was possible to eliminate the iron(III) interference by reduction to iron(II) with ascorbic acid. Humic acid was tested as an interfering organic surfactant. Measurements of 10 $\mu g\ l^{-1}$ aluminum were not affected by increased humic acid concentration up to 500 $\mu g\ l^{-1}$; higher concentrations caused a gradual decrease of the aluminum peak.

Because of its high sensitivity, the possibility of applying the adsorptive stripping procedure for the determination of aluminum in snow samples was tested. Unlike the direct measurement (without accumulation), the adsorptive stripping procedure allows convenient quantitation of aluminum in snow. Replicate samples yielded similar responses. The relatively high concentration of aluminum found in the snow sample (ca 1.7 $\mu g\ kg^{-1}$) may be related to emission associated with local smelting.

In conclusion, the present study describes an effective means for the determination of trace levels of aluminum. Among the reported electroanalytical methods for aluminum, the described procedure is distinguished by the lowest detection limit. The adsorptive accumulation provides an efficient and versatile alternative approach to electrolytic deposition, and can be extended to many other metal ions in stripping voltammetry. Work in this laboratory is continuing in this direction.

This work was supported by the National Institutes of Health under Grant No. GM30913-01A1. P. A. M. Farias acknowledges the financial support of the National Council for Scientific Development CNPq of the Brazilian government.

REFERENCES

1 H. H. Willard and J. A. Dean, Anal. Chem., 22 (1950) 1264.
2 M. Perkins and C. F. Reynolds, Anal. Chim. Acta, 19 (1958) 54.
3 T. M. Florence and D. B. Izard, Anal. Chim. Acta, 25 (1961) 386.
4 T. M. Florence, F. J. Miller and H. E. Zittel, Anal. Chem., 38 (1966) 1065.
5 H. Specker, H. Monien and B. Lendermann, Chem. Anal. (Warsaw), 17 (1971) 1003.
6 G. W. Latimer, Talanta, 15 (1968) 1.

Analytica Chimica Acta, 172 (1985) 65—72
Elsevier Science Publishers B.V., Amsterdam — Printed in The Netherlands

POLAROGRAPHIC DETERMINATION OF PICOLINALDEHYDE IN THE PRESENCE OF SOME RELATED COMPOUNDS

F. J. BARRAGÁN DE LA ROSA, M. CALLEJÓN MOCHÓN* and A. GUIRAÚM PÉREZ
Department of Analytical Chemistry, Faculty of Chemistry, University of Seville, Tramontana s/n, 41012 Seville (Spain)

(Received 27th July 1984)

SUMMARY

A d.c. polarographic method is described for the determination of picolinaldehyde (1.5×10^{-5}—2.9×10^{-4} M), based on the in situ formation of its Girard-P derivative in aqueous solution. A mechanism of reduction ($E_{1/2} = -0.71$ V at pH 3.5) is proposed. The applicability of this method is checked in synthetic samples containing pyridine, picoline and pyridine carboxylic acids.

Pyridine-2-carboxaldehyde (picolinaldehyde) is of use in the synthesis of other organic compounds. For example, simply by heating it in acetic acid 2,2′-pyridoin is produced [1]; by treatment with ethyl magnesium bromide [2] and reduction with sodium, the hemlock alkaloid coiine can be prepared; and numerous Schiff's bases used as analytical reagents can be obtained from it [3—5]. Picolinaldehyde occurs in the oxidation products of methylpyridines, and has been determined in these samples by polarographic reduction [6, 7] or identified by gas-liquid chromatography [8—10].

Volke [11] has described the polarographic reduction of pyridine carboxaldehydes and has reported their determination at pH 6—7 in the range 5×10^{-5}—3×10^{-3} M. In this paper a method is described for the determination of picolinaldehyde in the range 1.5×10^{-5}—2.9×10^{-4} M by d.c. polarography of its Girard-P derivative (PAHP) at pH 3.5. This procedure is superior to that of Volke, because there is a better definition of the single wave of PAHP than of the two waves of picolinaldehyde, the diffusion current measurement of which is critically affected by pH.

Girard-T hydrazones undergo polarographic reduction and have been used for polarographic identification of ketosteroids in urine or blood [12] and determination of aliphatic ketones [13]. However, Girard-P reagent and its derivatives have been little studied analytically [14].

EXPERIMENTAL

Apparatus and analytical conditions

A Beckman Model Φ-70 pH meter with a combined glass-calomel electrode was used. A Metrohm E-506 polarograph was used with an E-505

0003-2670/85/$03.30

polarographic stand, and a Metrohm VA-Scanner E-612 as signal generator, fitted with a Linseis LY 1800 X-Y recorder for cyclic voltammetry. A three-electrode combination was used, consisting of a SCE, a dropping mercury electrode and a platinum wire as auxiliary electrode. A Metrohm Model EA-87620 cell maintained at 21 ± 1°C, with high-purity nitrogen used to remove oxygen, were used throughout. When the effect of temperature was studied, the SCE was shielded with a Luggin's capillary. The working electrode used for single-sweep and cyclic voltammetry was a hanging mercury drop with a drop surface area of 2.20 ± 0.05 mm^2.

The main instrumental parameters were: height of mercury column h = 60 cm; flow rate of mercury m = 3.02 mg s^{-1}; drop time t = 2.13 s. The last two were measured at the potential of the SCE in the supporting electrolyte (0.2 M potassium chloride buffered with 0.1 M sodium hydroxide/phosphoric acid, pH 4.7). Separate values of m and t were measured at the potential of interest for the calculation of diffusion coefficients. The applied potential range was 0.00 to −2.00 V, and the scan rate 16 mV s^{-1}.

Controlled-potential coulometry was done with the Metrohm E-505 in the potentiostatic mode at a mercury pool cathode with continuous stirring. The electrolysis was done under a continuous stream of nitrogen. Before the addition of the reagent, a current was passed through the supporting electrolyte for 15 min to remove any electroactive traces. The concentration of the sample before and after 20-min electrolysis was measured polarographically and the area under the current/time (i/t) curve was evaluated by computer.

Reagents

The PAHP was synthesized as described previously [14]. An aqueous 1 × 10^{-2} M solution was prepared. Picolinaldehyde (Ega-Chemie) was prepared as a 1 × 10^{-2} M solution in aqueous 0.5% (v/v) ethanol. The purity of the standard solution of picolinaldehyde was checked by comparison with the waves of pure PAHP. Girard-P reagent [1-(2-hydrazino-2-oxoethyl)-pyridinium] chloride (Merck) was used as an aqueous 1 × 10^{-2} M solution. The supporting electrolyte (pH 3.5) was 0.5 M potassium chloride/0.250 M phosporic acid/0.215 M sodium hydroxide/0.01% Triton X-100. All solutions were prepared with distilled, de-ionized water from analytical-grade chemicals.

Procedure. Place an aliquot of sample solution at pH 2—9 containing 3.75 × 10^{-7}—7.25 × 10^{-6} mol of picolinaldehyde in a 25-ml volumetric flask. Add 5 ml of 1 × 10^{-2} M Girard-P reagent and 10 ml of supporting electrolyte (pH 3.5). Dilute to volume with water, and add the contents to a polarographic vessel thermostated at 21 ± 1°C. Record the polarogram (h = 60 cm) after deoxygenation for 10 min with oxygen-free nitrogen from 0.00 to −2.00 V vs. SCE. Measure the wave height at −1.00 V.

Use a calibration graph obtained with known concentrations of picolinaldehyde to convert wave height into concentrations in the sample. Alternatively, use a standard addition procedure.

RESULTS AND DISCUSSION

The aim of the present work was to study electroanalytically the behaviour of PAHP, and hence to follow its formation in situ from picolinaldehyde, and thereby determine the aldehyde polarographically as its Girard-P derivative, with PAHP for calibration. A comparison of several supporting electrolytes (Fig. 1) showed in all cases a well-defined wave, with $E_{1/2}$ = —0.76 V (vs. SCE) at pH 4.7. An adsorption wave is found at pH > 10, $E_{1/2}$ = —1.20 V. Of the supporting electrolytes studied, those that gave the first wave at most negative potentials were sodium acetate/acetic acid and potassium chloride/sodium hydroxide/phosphoric acid. Both were selected for a study of optimum conditions. No substantial differences were observed between the results obtained in either system. It was better to use the potassium chloride/sodium hydroxide/phosphoric acid system, because it permits a wider pH range and the current/potential (i/E) curves are steeper.

At pH 4.7 the wave height of 8×10^{-4} M PAHP was constant for 24 h, and the 1×10^{-2} M PAHP stock solution was stable for 1 month. In acidic (pH 1.7) and alkaline (pH 10.6) media, the current decreased markedly over a 4-h period, presumably because of hydrolysis. Picolinaldehyde in acidic medium produced two waves, $E_{1/2}$ = —0.74 V and —1.25 V; the Girard-P reagent was not reduced over the normal pH range.

The dependence of the limiting current on the height of the mercury column, temperature and PAHP concentration were investigated for a 1×10^{-3} M solution at pH 4.7. The plot of current vs. $h^{1/2}$ (corrected for back-pressure) was linear, proving that the wave height was diffusion-controlled. The temperature dependence of the current increase between 15 and 55°C (1.21% per degree), also supports diffusion control. Measurements over the

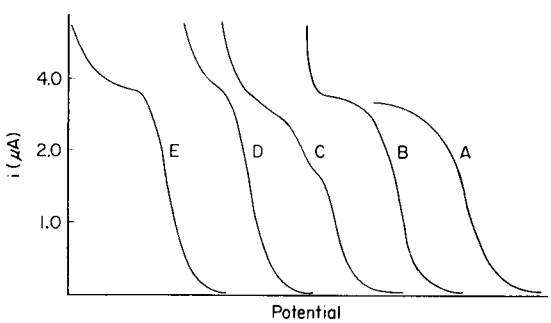

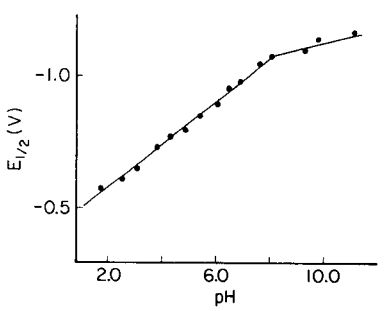

Fig. 1. Effect of supporting electrolyte on the polarographic waves of 1×10^{-3} M PAHP: (A) 1 M sodium acetate/acetic acid, pH 4.8, $E_{1/2}$ = —0.770 V; (B) 1 M ammonium acetate/acetic acid, pH 5.9, $E_{1/2}$ = —0.960 V; (C) 1 M ammonium chloride/ammonia, pH 9.6, $E_{1/2}$ = —1.168 V; (D) 1 M potassium chloride, pH 5.3, $E_{1/2}$ = —0.816 V; (E) 0.2 M potassium chloride in 0.1 M sodium hydroxide/phosphoric acid, pH 4.9, $E_{1/2}$ = —0.782 V.

Fig. 2. Dependence of half-wave potential on pH for 4×10^{-4} M PAHP.

concentration range normally used in polarography (4×10^{-5}—1×10^{-3} M) showed a linear dependence of wave height on concentration. In all cases $E_{1/2}$ (—0.740 and —0.820 V in pH 4.7 acetate and phosphate buffers, respectively) was independent of concentration. The diffusion coefficient D was 4.7×10^{-6} cm^2 s^{-1} (n = 2, m = 3.06 mg s^{-1}, t = 2.03 s). The transfer coefficient determined from the Tafel slope was 0.236.

Controlled-potential coulometry was used to determine n, the number of electrons involved in the reduction. Three replicate electrolyses of 5×10^{-6} mol of PAHP in 30 ml of solution at pH 4.7 or pH 6.5 gave values of 1.87 or 1.94, respectively.

The dependence of the half-wave potential on pH was studied to establish the number of hydrogen ions involved in the rate-determining step of the reduction of 4×10^{-4} M PAHP. Figure 2 shows that $E_{1/2}$ varies linearly with pH in the range 1.7—8.1 ($E_{1/2}$ (V) = —0.430—0.086 pH). Beyond pH 8.1 the wave is essentially pH independent; the variation probably reflects changes caused by the buffer composition. The limiting diffusion current (i_d) remained constant at 2.5 μA over the whole pH range. The transfer coefficient α was calculated [15] to be 0.3.

A logarithmic analysis of the i/E plots (based on the average current during the drop life) at three pH values showed that the plot of log $[i^2/(i_d - i)]$ vs. E was linear, which suggests [16] that the reduction is generally of a dimer. This possibility would be justified by hydrogen bonding over a wide pH range and/or ionic intermolecular bonds formed between the protonated pyridine nitrogen and the keto—enol oxygen.

Single-scan voltammetric curves obtained for PAHP at several pH values showed a linear dependence of log (peak current) vs. sweep rate (Fig. 3) with

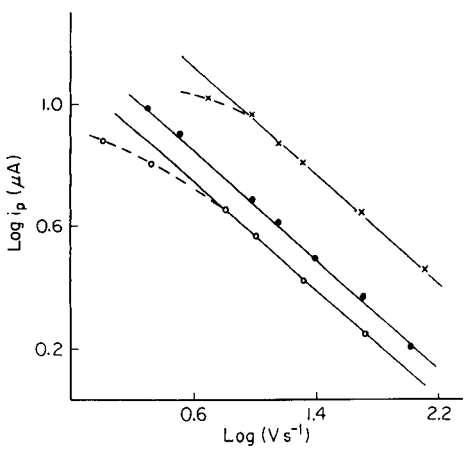

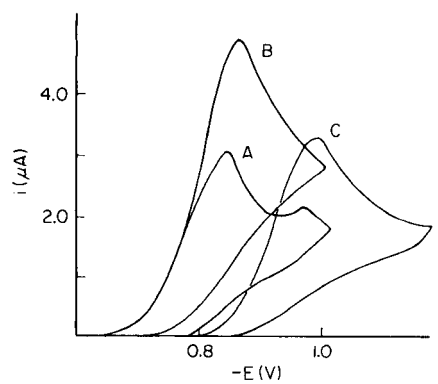

Fig. 3. Dependence of peak current on voltage scan rate at different pH: (○) 1.7; (●) 3.5; (×) 10.7.

Fig. 4. Cyclic voltammetric curves for 6.1×10^{-4} M PAHP at different pH: (A) 1.7; (B) 3.5; (C) 5.0.

an average slope of 0.450, which agrees with the theoretical value [17] for a reversible system. However, cyclic voltammetry (Fig. 4) at the hanging mercury drop electrode showed no reversible couple at any pH, even when the sweep rate was fast. At pH 1.7 both single-scan and cyclic voltammograms exhibited a supplementary peak (E_p = —0.96 V), corresponding to the reduction of the picolinaldehyde produced by PAHP hydrolysis. Thus the data suggest a two-electron, two-proton (one of these from the dimer molecule) reduction of PAHP, followed by rapid disproportionation [18].

From the above results, and on the basis of mechanisms proposed for similar compounds [19—22], the reduction of PAHP is suggested to be

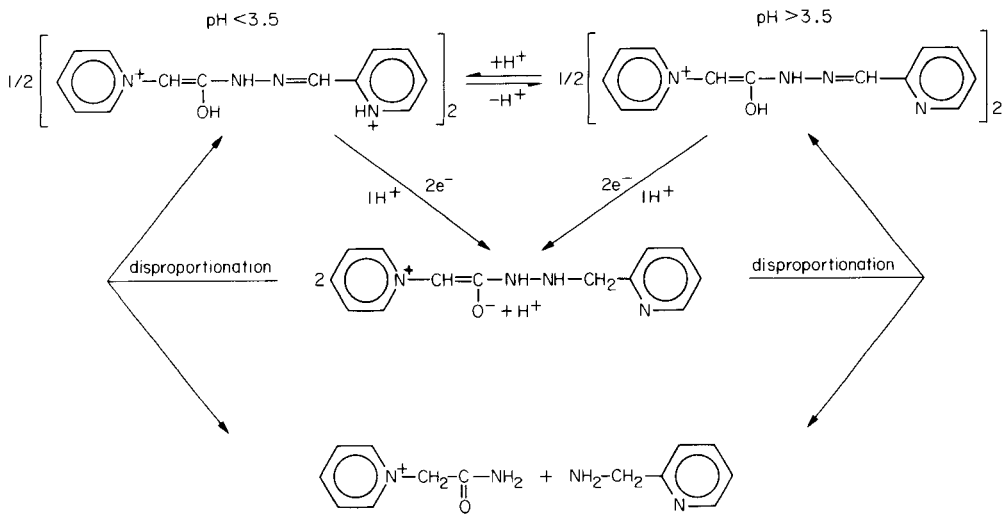

Optimum conditions for determination of picolinaldehyde

The optimum concentrations for determination of PAHP are given in the recommended procedure. Triton X-100 was used as a maximum suppressor and did not modify i_d, but $E_{1/2}$ moved towards more positive potentials when the PAHP concentration was >0.04%. Increasing the buffer concentration decreased i_d. The phosphate buffer gave good resolution of the wave from the background discharge.

A polarographic study of the effect of metal ions in a 1:1 mole ratio in a PAHP solution, showed cathodic shifts in the presence of Cr^{3+}, Al^{3+} and Ga^{3+} at pH 2.5, and Ni^{2+} at pH 6.5, indicating complex formation.

Girard-P itself is electroinactive. Picolinaldehyde exhibits two waves. As the pH increases, $(i_d)_1$ increases and $(E_{1/2})_1$ shifts in the cathodic direction, whilst $(i_d)_2$ = 0.35 μA and $(E_{1/2})_2$ = —1.25 V are constant, in agreement with Volke's report [11] that the wave height was decreased by acid-catalyzed dehydration of picolinaldehyde. The PAHP wave is 0.080 V more cathodic than that of picolinaldehyde and shows more sensitivity at pH $\leqslant$ 5.4.

The aim of this work was to determine picolinaldehyde via its condensation in situ with Girard-P reagent and subsequent polarographic determination of PAHP. Therefore optimum conditions for this reaction were established. To ensure the total reaction of picolinaldehyde with Girard-P reagent, a detailed study of pH dependence was made by mixing equimolar concentrations (5×10^{-4} M) of picolinaldehyde and Girard-P reagent, and leaving the mixture to react for 20 min. After this time, i_d could be correlated with that of a 5×10^{-4} M solution of PAHP in weakly acidic media, but i_d decreased at pH < 2.5, because of the hydrolysis of PAHP.

At several pH values, and a 1:5 picolinaldehyde/Girard-P mole ratio, the change in wave height with time was measured (Fig. 5). From this study, pH 3.5 was selected as optimum. In addition to this, the dependence of reaction rate on Girard-P reagent concentration at pH 3.5 showed that for a 1:4 mole ratio, reaction was complete and a constant current was obtained in <15 min. The effect of temperature (heating the samples for 10 min at 21—60° C and cooling for 20 min in a water-bath to ambient temperature), confirmed that the reaction was fairly complete at 21° C, so that no heating was needed.

Finally the order of addition of reagents was studied, the best being picolinaldehyde, Girard-P reagent and then supporting electrolyte solution.

Determination of picolinaldehyde. Picolinaldehyde was determined, based on a calibration graph for pure PAHP. The reaction was found to reach completion for samples prepared according to the recommended procedure, with 2×10^{-3} M Girard-P reagent and 1.5×10^{-5}—2.9×10^{-4} M picolinaldehyde. Standard addition methods were also used for samples containing 2.8×10^{-5} M of picolinaldehyde and increasing concentrations of PAHP, and also 3.0×10^{-5} M of PAHP and increasing concentrations of picolinaldehyde. In both cases the results were concordant. These graphs are shown in Fig. 6.

Precision data were obtained for seven determinations of 2.9×10^{-4} M picolinaldehyde. The relative standard deviation was 2.5%.

Interferences. The effect of some substances structurally related to picolinaldehyde (i.e., picolinic, isonicotinic and nicotinic acids, picoline and

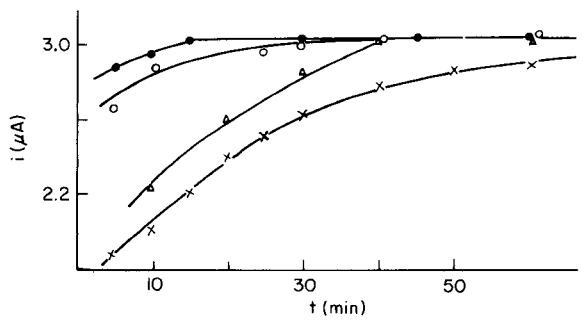

Fig. 5. Effect of time on the condensation of 5.0×10^{-4} M picolinaldehyde with Girard-P reagent: (×) pH 2.5, 2.5×10^{-3} M Girard-P; (•) pH 3.5, 2.5×10^{-3} M Girard-P; (△) pH 3.5, 1×10^{-3} M Girard-P; (○) pH 5.4, 2.5×10^{-3} M Girard-P.

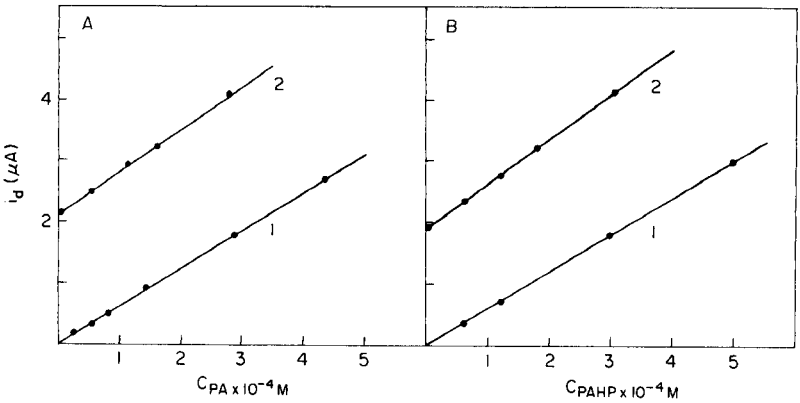

Fig. 6. Graphs of i_d against concentration. A: (1) Various concentrations of picolinaldehyde; (2) various concentrations of picolinaldehyde in the presence of 3.1×10^{-4} M PAHP. B: (1) Various concentrations of PAHP; (2) various concentrations of PAHP in the presence of 2.8×10^{-4} M picolinaldehyde. In all cases, the concentration of Girard-P reagent was 2.5×10^{-3} M.

pyridine) on the picolinaldehyde determination was studied. For all these compounds, the tolerance limit was at least 1000 times the molar concentration of picolinaldehyde. In the presence of pyridine and picoline, the pH must be adjusted with phosphoric acid to >2 before the supporting electrolyte solution is added.

Determination of picolinaldehyde in some synthetic samples

Picolines and pyridine occur in coal tar and bone oil, therefore it is of interest to study the determination of picolinaldehyde in the presence of large concentration of these compounds, and to determine it in picoline used as a raw material. The recommended procedure was applied to the determination of picolinaldehyde in three synthetic samples, by direct comparison with a calibration graph for PAHP, and by standard addition of PAHP. Sample 1 was 1.5×10^{-2} M in picolinaldehyde, with 1.5 M each of pyridine and picoline, and picolinic, nicotinic and isonicotinic acids. Sample 2 was 3.75 M in picoline and 3.75×10^{-3} M in picolinaldehyde. Sample 3 was 3.75 M in pyridine and 3.75×10^{-3} M in picolinaldehyde. Aliquots of 0.25 ml were taken for sample 1, and 1 ml for samples 2 and 3. The recoveries summarized in Table 1 show acceptable accuracy.

Conclusions

Picolinaldehyde exhibits a double polarographic wave so that its direct polarographic determination is possible, but it requires an inconveniently fine adjustment of pH in a relatively small range (pH 6—7), because the wave is displaced on changing the pH, and the wave height greatly decreases with increasing acidity because the picolinaldehyde is catalytically hydrolyzed.

TABLE 1

Determination of 1.50×10^{-4} M picolinaldehyde in various synthetic samples

Sample[a]	Picolinaldehyde found[b] ($\times 10^{-4}$ M)		Relative error (%)	
	A	B	A	B
1	1.41	1.47	−6.0	−2.0
2	1.43	1.50	−4.6	0.0
3	1.48	1.38	−1.0	−8.0

[a]For composition, see text. [b]Average of 4 determinations; A, calibration graph; B, standard addition.

With the present technique, the wave shifts in the cathodic direction on increasing the pH, but the wave height remains constant. Thus the recommended method is applicable in the pH range 3.0—8.0, and offers good precision and accuracy. The sensitivity of the method is sufficient to permit the determination of picolinaldehyde equivalent to 0.1% in pyridine, picoline or pyridine carboxylic acids.

REFERENCES

1 H. R. Hensel, Angew. Chem., 65 (1953) 491.
2 C. Engler and F. M. Bauer, Ber., 24 (1981) 2530.
3 R. B. Singh, P. Jain and R. P. Singh, Talanta, 29 (1982) 77.
4 M. Katyal and Y. Dutt, Talanta, 22 (1975) 151.
5 F. J. Barragan de la Rosa, J. L. Gómez Ariza and F. Pino, Talanta, 30 (1983) 555.
6 V. A. Seratzetdinova, L. S. Saltybaeva and B. V. Suvorov, Izv. Akad. Nauk. Kazakh. SSR, 5 (1972) 77.
7 H. Marciszewski, Chem. Anal. Warsaw, 8(5) (1963) 775.
8 M. Kalnins, G. Konstante, L. Leitis and M. V. Shimauskaya, Izv. Akad. Nauk. Latv. SSR, Ser. Khim., 4 (1971) 498.
9 L. Leitis, R. Skolmeistere, A. Petersone and M. V. Shimauskaya, Izv. Akad. Nauk. Latv. SSR, Ser. Khim., 5 (1973) 576.
10 L. Leitis, R. Skolmeistere, A. Petersone, M. Kalnins and M. V. Shimauskaya, Zh. Anal. Khim., 29(3) (1974) 567.
11 J. Volke, Chem. Listy, 52(1) (1958) 16.
12 E. B. Hersliberg, J. K. Wolfe and L. F. Fieser, J. Biol. Chem., 140 (1941) 215; J. Am. Chem. Soc., 62 (1940) 3516.
13 M. D. Booth and B. Fleet, Analyst (London), 95 (1970) 649.
14 M. Callejón Mochón and J. L. Gómez Ariza, Microchem. J., 26 (1981) 463.
15 L. Meites, Polarographic Techniques, 2nd edn., Interscience, New York, 1965, Ch. 4.
16 S. G. Streitweiser, Progress in Physical Organic Chemistry, Vol. 3, Wiley, New York, 1965, pp. 177—184.
17 R. Brdička, V. Hanus and J. Koutecky, Progress in Polarography, Interscience, New York, 1962.
18 R. H. Wopschall and I. Shain, Anal. Chem., 39 (1967) 1535.
19 B. Fleet, Anal. Chim. Acta, 36 (1966) 304.
20 M. D. Booth and B. Fleet, Analyst (London), 95 (1970) 649.
21 E. Garcia Gijón, Ph.D. Thesis, Granada, Spain, 1973.
22 J. M. Bosque Sendra, Ph.D. Thesis, Granada, Spain, 1983.

Analytica Chimica Acta, 172 (1985) 73—78
Elsevier Science Publishers B.V., Amsterdam — Printed in The Netherlands

THE PROPERTIES OF THE INTERFACIAL ANTIMONY CELL AND ITS APPLICATION IN POTENTIOMETRIC TITRATIONS OF ALKALOIDS IN NON-CONDUCTING SOLUTIONS

PATRYCJA DYNAROWICZ

Department of Physical Chemistry, Faculty of Pharmacy, Medical Academy, 34 Lubicz Street, 31-512 Kraków (Poland)

MARIA PALUCH*

Department of Physical Chemistry and Electrochemistry, Faculty of Chemistry, Jagellonian University, 3 Karasia Street, 30-060 Kraków (Poland)

(Received 23rd October 1984)

SUMMARY

The behaviour of an interfacial antimony device in potentiometric titrations in non-conducting solutions is described. In tests of the device, various alkaloids were titrated with organic acids, *p*-toluenesulphonic acid being the most satisfactory. The non-conducting media examined were chloroform, ligroin, benzene and carbon tetrachloride. In all cases, solutions of the titrant and the sample were prepared in the same organic solvent. Alkaloids in the range 10^{-3}—10^{-4} M could usually be titrated with a precision of about 2%.

Conventional methods of potentiometric titrations use various cells that work in conducting solutions. Electrical conductance of the media in which the electrodes are inserted is essential to the satisfactory behaviour of such devices. Therefore all conventional methods of potentiometric titrations are based on cells with conducting solutions, whether aqueous or nonaqueous. In the case of solvents which do not exhibit sufficient electrical conductance (e.g., hydrocarbons and their derivatives) these methods fail because the indicator electrode does not show the characteristic potential changes necessary for quantitative purposes. Yet, numerous organic substances (e.g., alkaloids) dissolve easily only in such solvents. This is the reason why methods of potentiometric titration would be valuable in organic solvents with low dielectric permittivity. Most papers concerning the problem of potentiometric titration of alkaloids are limited only to conducting organic media, e.g., anhydrous acetic acid, acetic acid anhydride [1—4] and mixtures such as acetic acid anhydride/chloroform and acetic acid anhydride/benzene [5—8]. Positive results for potentiometric titrations of alkaloids in non-conducting solvents have not been reported previously. It appeared recently that the problems of the determination of alkaloid content, both in non-aqueous and non-conducting media, by means of potentiometric titration could be solved with the aid of a new type of interfacial cell [9]. All the

0003-2670/85/$03.30

existing papers concerning the interfacial device lack full description of the properties of the cell. It is, therefore, the aim of this paper to fill this gap.

EXPERIMENTAL

The interfacial antimony cell

The construction of the cell used in this work was described in detail previously [9]. The essential part of the interfacial cell is a porous corundum disc which closes the outlet of a salt bridge filled with aqueous 0.1 M potassium chloride solution. The external surface of the disc is covered with metallic antimony scratches in order to extend the surface of the thin antimony electrode touching the disc. That porous corundum disc has a very important role in the interfacial cell because it lies exactly at the interface between the aqueous and organic phases and provides a mechanical barrier to prevent the mixing of phases that are in contact. Further, the porous disc covered with the antimony scratches acts as a conductor between the indicator and reference electrodes. The pointed end of the antimony electrode touches the external surface of the disc covered with the antimony scratch (wetted by a potassium chloride solution) and is connected with the calomel electrode through the potassium chloride solution in the salt bridge.

Preliminary treatment of the interfacial cell. In order to obtain the best reproducibility, the cell was both disconnected and cleaned before each titration. Special attention should be given to cleaning the corundum disc from the remains of the metallic scratch and the products of the titration and to cleaning the external tip of the antimony electrode (by rubbing it on a sheet of blotting paper). Afterwards, the potassium chloride solution in the salt bridge must be changed. Before each titration, the cleaned device is dipped for some time (15—30 min) in the 0.1 M potassium chloride solution for regeneration. After the cell has been rinsed in distilled water and dried very carefully, new antimony scratches are formed on the disc by scratching the whole surface of the disc with chemically pure antimony. The interfacial device is then ready for measurements.

Chemicals and solutions

All the chemicals used were of analytical-reagent grade.

The following alkaloids were used as samples: atropine (Merck), strychnine (British Drug Houses), papaverine (Polfa, Poland), narceine (Merck) and colchicine (Merck). The alkaloids were investigated in solutions with concentrations ranging from 10^{-5} to 10^{-2} mol l^{-1}.

The titration media tested were ligroin (boiling range 80—130° C), carbon tetrachloride, benzene and chloroform. All these solvents (POCh, Poland) were further purified by distillation. As titrants, the following acids were used: *p*-toluenesulphonic acid, picric acid, and trichloroacetic acid (all from POCh, Poland). The titrants were dissolved in the same solvent as that used for the samples and they were of the same concentration as the solution of the base to be titrated.

Procedures

The titrant was added from a burette in 0.2—0.5 ml portions. After each addition of the acid, the titrated solution was mixed for about 15 s with a magnetic stirrer. The e.m.f. of the interfacial cell was measured 45 s after each addition of the acid. In all experiments, 15 ml of a dilute solution of a particular alkaloid was titrated. An electrometer (Model 6350, Veb Stratron, RFT, East Germany) was used for measuring the changes of e.m.f. of the interfacial cell.

RESULTS AND DISCUSSION

The course of the potentiometric titration curves clearly indicates that useful results were obtained in each solvent used. These curves confirm the possibility of practical utilization of the interfacial device for determinations of weak bases in non-conducting liquid media (Figs. 1—3).

The distinct potential changes of the indicator electrode observed during the titrations are due to the fact that the chemical reaction is monitored not in the bulk of the solution but at the boundary of two phases with markedly

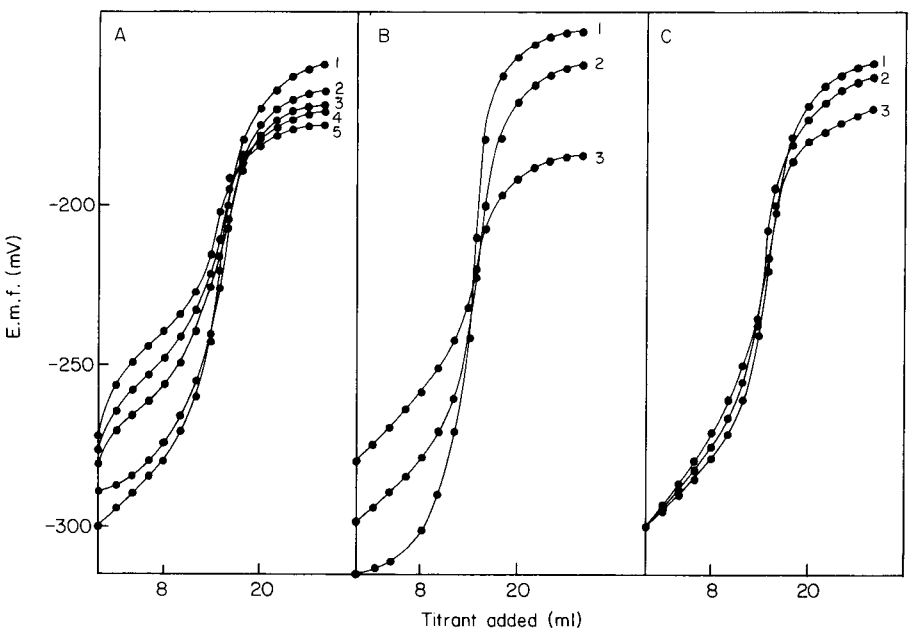

Fig. 1. Potentiometric titrations of alkaloids in chloroform. A, Titration curves for 0.0005 M solutions of atropine (1), strychnine (2), papaverine (3), narceine (4) and colchicine (5) titrated with *p*-toluenesulphonic acid. B, Titration curves for atropine solutions with *p*-toluenesulphonic acid: (1) 0.001 M; (2) 0.0005 M; (3) 0.0001 M. C, Titration curves for 0.0005 M atropine with different titrants: (1) *p*-toluenesulphonic acid; (2) picric acid; (3) trichloroacetic acid.

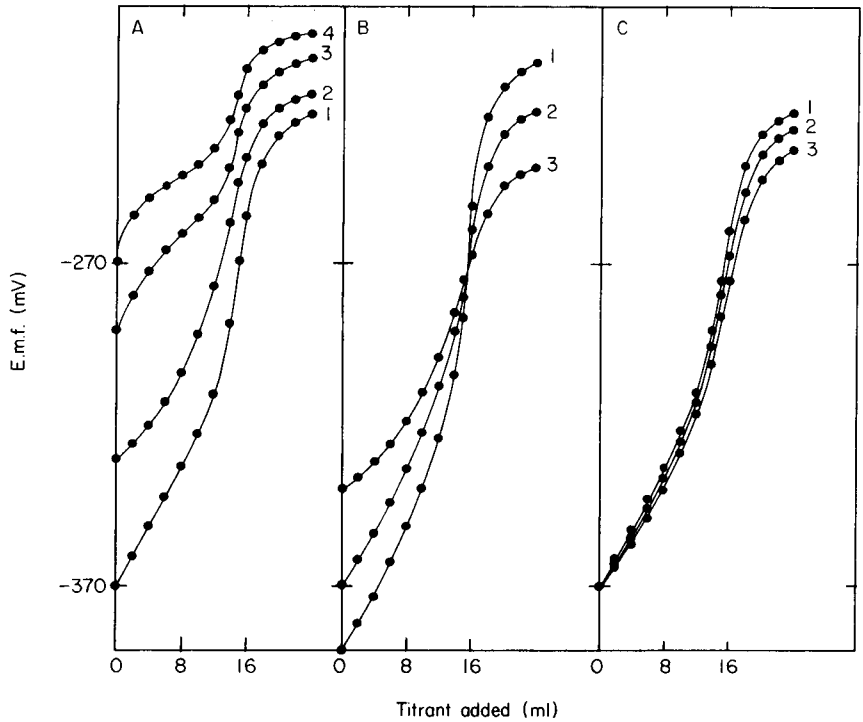

Fig. 2. Potentiometric titrations of alkaloids in benzene. A, Titration curves for 0.0005 M solutions of atropine (1), strychnine (2), papaverine (3), and colchicine (4) titrated with *p*-toluenesulphonic acid. B, Titration curves for atropine solutions with *p*-toluenesulphonic acid: (1) 0.001 M; (2) 0.0005 M; (3) 0.0001 M. C, Titration curves for 0.0005 M atropine with different titrants: (1) *p*-toluenesulphonic acid; (2) picric acid; (3) trichloroacetic acid.

different dielectric permittivities. The curves in Figs. 1—3 exhibit sharp inflections at the equivalence points, which allow the base to be determined even at the remarkably low concentration of 10^{-4} mol l^{-1} (Figs. 1B, 2B and 3B). The courses of the titration curves shown in Figs. 1—3 indicate that the strength of the base to be titrated and the kind of solvent used have very significant effects. The titration curves for strong bases such as atropine exhibit sharp changes at the equivalence point and the shapes of the potentiometric titration curves are quite normal. However, when the basic strength of the titrated alkaloid decreases, the courses of the titration curves undergo changes (Figs. 1A, 2A, 3A). In the case of weaker bases (e.g., narceine or colchicine), the potential jumps around the equivalence point are smaller and the titration curves are rather flat, which makes quantitative evaluation difficult by the classical method, though the inflections are obviously good enough for the application of derivative curves or Gran plots to provide satisfactory results, given appropriate calibration. It can be seen from Figs. 1—3 that the weaker the base, the more electropositive is the initial e.m.f. in the titration.

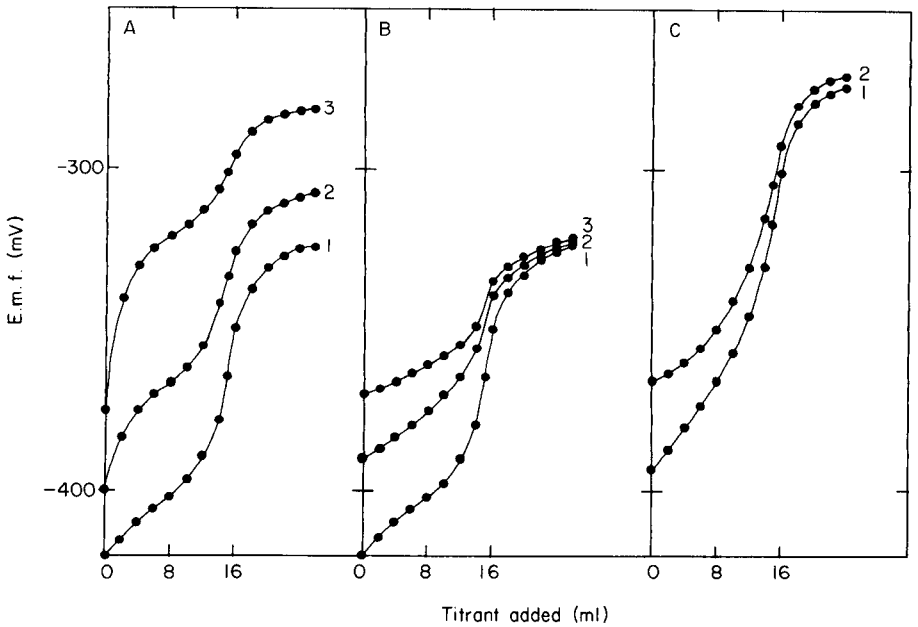

Fig. 3. Potentiometric titrations of alkaloids in carbon tetrachloride (A, B) and ligroin (C). A, Titration curves for 0.001 M solutions of atropine (1), papaverine (2) and colchicine (3) titrated with picric acid. B, titration curves for atropine solutions with picric acid: (1) 0.001 M; (2) 0.0005 M; (3) 0.0001 M. C, Titration curves for 0.0001 M solutions of atropine (1) and strychnine (2) with *p*-toluenesulphonic acid.

After the first small portion of titrant has been added to a solution of a strong base, the shapes of the titration curves change only slightly, but in solutions of weak bases, the changes are considerable. This is probably due to the chemical character of the solvent used (see Figs. 1A, 2A, 3A, C).

It is possible to determine some individual alkaloids in mixtures by using the interfacial cell when their basic strengths differ markedly. When the basic strengths differ by about two orders of magnitude, the potentiometric titration curve consists of two jumps, the first potential jump corresponding to the stronger base. Otherwise, the potential jump represents the sum of changes in e.m.f. for both alkaloids titrated.

The whole series of measurements showed that the best titrant for the determination of weak bases in non-conducting media is *p*-toluenesulphonic acid (Figs. 1C and 2C). With this titrant, the potentiometric titration curves are the best, the changes in potential around the equivalence point being sharper than those obtained with the other acidic titrants.

During these experiments, special attention was given to all the factors that can affect the behaviour of the interfacial device. These factors are connected both with the preparation of the cell for measurements and the procedure for the titrations. The optimal conditions for use of the interfacial cell can be outlined as follows. First, a time of 15 s is required for mixing the

solutions after the addition of each increment of titrant, and the time necessary for stabilization of the potential in all the solvents tested is about 30 s. To obtain the best results, the e.m.f. should be read 45 s after each addition of titrant. Secondly, after each titration (and cleaning of the device), the cell should be kept in 0.1 M potassium chloride for 15—30 min for regeneration. After this regeneration, the cell is rinsed in distilled water and dried, the antimony scratches are placed on the disc surface. Traces of water on the corundum hinder the scratching process. When non-aqueous but conducting solvents are used, the antimony scratches on the surface of the disc are not strictly necessary but their presence facilitates the evaluation of the equivalence point because the potential changes are bigger than those obtained without the antimony scratches. All the factors which modify the characteristics of an antimony electrode will also change the characteristics of the interfacial device.

The reproducibility of the initial potential of the indicator electrode in serial measurements was ±20 mV, depending on the thoroughness of the cleaning of the corundum disc and the antimony electrode.

It was found that the minimal amount of base which could be determined correctly by the interfacial cell was 1.45×10^{-5} g ml^{-1}. In serial experiments, the precision of the measurements was ±2%.

REFERENCES

1 A. P. Kreshkov, T. V. Maksimova and V. A. Drozdov, Farmatsiya (Moscow), 21 (1972) 96.
2 M. Ono, M. Shimamine and K. Takahashi, Eisei Shikenjo Hokoku, 89 (1971) 75.
3 W. L. Schertz and G. D. Christian, Anal. Chem., 44 (1972) 755.
4 E. Casassa and F. Garcia Montelongo, An. Quim., 67 (1971) 259.
5 A. L. Popov and J. A. Caruso, in I. M. Kotthoff and P. J. Elving (Eds.), Treatise on Analytical Chemistry, 2nd edn., Wiley-Interscience, New York, 1979.
6 E. Sell and J. Teodorczuk, Ann. Acad. Med. Gedanensis, 3 (1973) 67.
7 W. Wiśniewski and E. Klepaczewska-Saluda, Far. Pol., 25 (1969) 633.
8 E. Zoltaine-Maltoscy and E. Posgayne-Kovacs, Acta Pharm. Hung., 47 (1977) 217.
9 B. Waligóra and M. Paluch, Anal. Chim. Acta, 132 (1981) 229.

Analytica Chimica Acta, 172 (1985) 79—100
Elsevier Science Publishers B.V., Amsterdam — Printed in The Netherlands

MULTI-ELEMENT DETERMINATION OF DISSOLVED HEAVY METAL TRACES IN SEA WATER BY TOTAL-REFLECTION X-RAY FLUORESCENCE SPECTROMETRY

A. PRANGE*,[a] and A. KNÖCHEL

Institut für Anorganische und Angewandte Chemie, Martin-Luther-King-Platz 6, D-2000 Hamburg 13 (Federal Republic of Germany)

W. MICHAELIS

Institut für Physik, GKSS-Forschungszentrum Geesthacht GmbH, Postfach 1160, D-2054 Geesthacht (Federal Republic of Germany)

(Received 13th November 1984)

SUMMARY

Dissolved heavy metal traces in sea water are determined by a procedure based on total-reflection x-ray fluorescence spectrometry (t.x.r.f.). The trace elements are separated from the salt matrix by chelation with sodium dibenzyldithiocarbamate, selective chromatographic adsorption of the metal complexes onto a lipophilized silica-gel carrier, and subsequent elution of the metal chelates by a chloroform/methanol mixture. Aliquots of the eluate are then dispensed onto highly polished quartz sample carriers and evaporated to thin films for the t.x.r.f. measurements. The following elements can be determined: V, Mn, Fe, Co, Ni, Cu, Zn, Se, Mo, Cd, (Hg), Pb, and U. For 200-ml samples and a measuring time of 1000 s, detection limits of 5—20 ng kg^{-1} are achieved for most of these elements. The limits are slightly higher for iron, zinc and mercury because of fluctuations in the blank values. Systematic investigations of the yield in the separation and enrichment step are described, and the procedure is characterized with regard to blanks, detection limits, precision and accuracy. The accuracy was checked with the aid of the sea-water reference material NASS-1. Some applications to Baltic sea water and open ocean waters are reported and discussed in terms of their information content.

Dissolved heavy metals in sea water are normally present in the $\mu g\ kg^{-1}$ to ng kg^{-1} range and their determination makes high demands on the trace analytical procedures. These are usually based on atomic absorption spectrometry (a.a.s.) or stripping voltammetry and allow either single-element determination or simultaneous determination of four or five elements [1—7]. Owing to the growing need for information prompted by the large numbers of samples produced in monitoring systems and also because of favourable cost-benefit ratios, there is a need for efficient procedures which allow multi-element determination and are also applicable on board research vessels. In this respect, x-ray fluorescence spectrometry with total

[a]Present address: Institut für Physik, GKSS-Forschungszentrum Geesthacht GmbH, Postfach 1160, D-2054 Geesthacht, Federal Republic of Germany.

0003-2670/85/$03.30

reflection of the excitation beam on a highly polished quartz sample carrier, a special variant of energy-dispersive x.r.f. appears to be very promising [8—10]. Compared to more conventional x.r.f. variants, this principle offers the following advantages: detection limits are low, comparable with those of a.a.s.; data are easily quantified by use of one internal standard and the thin film technique; and the x-ray spectra are less complicated as a result of low background owing to the total reflection of the excitation beam on the sample carrier. Further, the instrumentation for total-reflection x-ray fluorescence spectrometry (t.x.r.f.) can be taken on board research vessels.

Direct application of t.x.r.f. to the determination of trace elements in sea water is usually impeded by the high salt matrix, which hinders the detection of extremely low traces. It is therefore imperative that the trace elements are separated from the matrix prior to measurement and if this is accompanied by an enrichment step, the detection limits are improved further. Such sample preparation steps, however, often conceal dangerous sources of systematic errors (e.g., contamination of the sample) and so may worsen the problems of determining extremely low concentrations in sea water. A comprehensive review of the various methods available for prior enrichment in connection with water analysis by conventional x.r.f. has recently been published [11]. First attempts to develop a preconcentration procedure for the determination of heavy metals by t.x.r.f. were reported in 1980 [12, 13].

In this paper, the recent development of a procedure for multi-element determination of dissolved heavy metals traces in sea water is described. High efficiency in terms of detection limits, accuracy, and precision is achieved by a combination of t.x.r.f. with an appropriate separation and enrichment procedure. Examples are presented to illustrate the applicability of the procedure to the very low traces of metals in sea water.

EXPERIMENTAL

Sampling and storage

In order to prevent contamination during sampling and storage, instrumentation and working conditions were selected carefully. Surface waters were sampled some few hundred meters away from the research vessels, from a rubber boat in slow forward motion. The purified polyethylene sampling bottles used were filled up about 30 cm under water in front of the boat. The personnel wore polyethylene gloves.

Sampling of deeper waters was done with Trans-Plastic-Nansen (TPN)-coc-samplers made from polycarbonate (Hydro-Bios, Kiel), specially modified for trace metal determination. These samples entered the water closed and were opened at a depth of about 10 m to prevent contamination from the surface microlayer and debris from the ship. They can be let down opened further to any desired depth before being closed by a messenger (coc-type: closed-open-closed). The samplers had a volume of 1.7 l.

Other items of equipment belonging to the sampling device were: 6-mm plastic-coated hydrowire and 6-mm Kevlar hydrowire; plastic-coated messengers each 500 g and two plastic-coated ground weights each 50 kg; and pulleys and reels having contacts with the hydrowire made of hard wood or plastic (Pertinax).

Especially for waters with a high content of suspended matter (e.g , in the Baltic Sea), filtration is necessary to differentiate the dissolved amount from the total content of heavy metals in the water. In the open sea, the amount of heavy metals carried by suspended particles is negligible, and filtration can be omitted to avoid contamination.

When filtration is inevitable, it is done in a clean bench, with purified nitrogen providing the necessary pressure (precleaned Nuclepore filter, 0.4 μm). First 50—100 ml of the sea water was prefiltered as a means of conditioning the filter and sample bottles. Aliquots (500 ml) of sea water were taken directly from the sampler with the help of polyethylene-covered PTFE tubing in the clean bench. The aliquots were transferred to purified polyethylene bottles, acidified to pH < 2, tightly closed and sealed in numbered polyethylene bags. These were then stored in a refrigerator.

The 500-ml polyethylene bottles were cleaned by first washing with acetone to remove grease and fat residues. After being rinsed with pure water, the bottles were filled with a few ml of concentrated hydrochloric acid (Suprapur, Merck) and shaken. They were then washed several times with pure water. Subsequently dilute (1:50) hydrochloric acid (Suprapur) was introduced into the bottles and left for some days at 60—70°C. The bottles were then washed thoroughly with water and, until needed, were filled with acidified water and sealed in polyethylene bags for storage.

The samplers were soaked in a detergent bath (RBS; Roth), then filled with dilute nitric acid and left for several days before being washed with pure water.

Separation and concentration

Heavy metal traces in the sea-water samples were separated from the salt matrix as dithiocarbamate complexes by using the reverse-phase technique [12—15].

The following procedure was used for the separation and enrichment. A portion (200 g) of an acidified sea-water sample was spiked with 50 μl of selenium standard solution (10 mg kg^{-1}). About 300 μl of a freshly prepared saturated solution of ammonia (Suprapur) and 1 ml of acetate buffer (Suprapur) were added to attain pH 4.5—5. Then 1 ml of a methanolic 4% (w/v) solution of sodium dibenzyldithiocarbamate (NaDBDTC; Fluka), to give a final concentration of 27 μmol kg^{-1}, was added and shaken to mix. After the reverse-phase column (see below) had been pretreated with a few ml of methanol and ultrapure water, the reaction mixture was sucked through the column within 10—15 min, the carbamate complexes being adsorbed. After the column had been sucked dry, the complexes were eluted with 3—4 ml of purified chloroform/methanol (1:1 v/v).

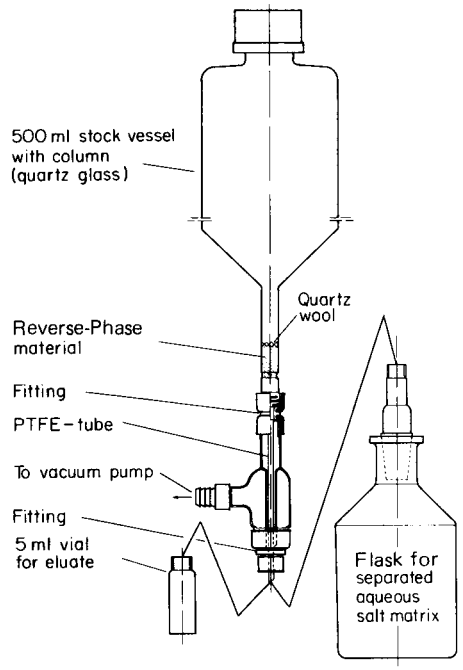

Fig. 1. Equipment for the separation and enrichment.

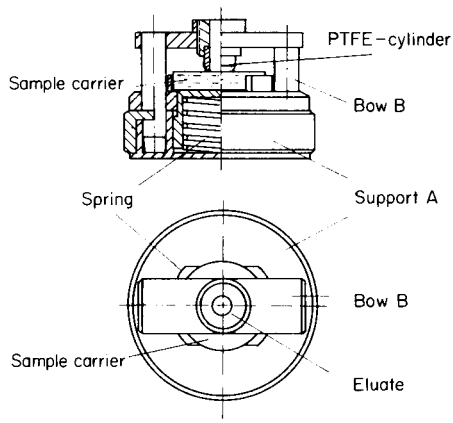

Fig. 2. Device for the preparation of the sample for t.x.r.f.

The separation and enrichment device made of quartz (Fig. 1) was also precleaned before use. This entailed boiling it in a detergent bath for 2 h, then heating for 3 days in a dilute nitric acid bath at 70°C, followed by rinsing with ultrapure water and sub-boiled methanol and drying in a clean bench. The column was then packed with 250 mg of Chromosorb AW-DMCS (Merck) using purified and siliconized quartz wool to cover it. The Chromosorb column was washed three times with hot (70°C) 0.1 M nitric acid, then with ultrapure water, sub-boiled chloroform and methanol. After a few blank separation steps with 200 g of ultrapure water instead of sea water, the Chromosorb column was ready for use.

Radiotracer studies

Detailed radiotracer studies for most of the elements under consideration were undertaken during the development of the method. The ultimate aim of these studies was to assay the yield of the various trace elements during the separation step and to optimize this step for use with t.x.r.f. Reaction parameters varied were the type of ligand, i.e., APDC (Merck) and NaDBDTC (Fluka), ligand concentration and pH. The results obtained with the optimized reaction conditions were then compared with those evaluated

by standard addition and succeeding t.x.r.f. measurements. The application of radiotracers and inactive standards might lead to possible discrepancies between the yields of their artificial composition and those for the species of the trace elements naturally present in sea water. Therefore, it was necessary to check the method further with a certified natural sea water reference material (see below).

The following radionuclides, obtainable as aqueous acidic solutions were considered: ^{48}V, ^{51}Cr, ^{54}Mn, ^{56}Mn, ^{59}Fe, ^{60}Co, ^{65}Ni, ^{64}Cu, ^{65}Zn, ^{74}As, ^{75}Se, ^{115}Cd and ^{203}Hg. Uranium cannot be traced under the given conditions. In the case of lead there was no suitable isotope available which could be measured simultaneously with the other elements. Single-tracing with ^{210}Pb and measurement with a Si(Li)-detector was discarded, as results of investigations with t.x.r.f. and standard additions proved to be positive. During the selection of the radionuclides for a multi-tracer mixture, it became necessary to operate with two groups: (a) V, Cr, Mn, Fe, Co, Zn, As, Se, Hg; and (b) Mn, Ni, Cu, Cd. The reasons are that the half-lives are very different, some being relatively short, and that the only practicable means to evaluate ^{64}Cu is to use its 511-keV line. Aliquots of solution containing 10^{-2} nmol—10^{-2} μmol of the radionuclide metal salts were added to 10 ml of water and reserved for the multi-tracer solution; 100 μl of this solution was added to 200 g of sea water, providing concentrations between 2×10^{-4} nmol and 2 nmol and specific activities from 1.8×10^{3} to 1.8×10^{5} Bq ml^{-1}.

The eluate from the Chromosorb column, the aqueous waste, and the Chromosorb itself were measured and compared with standard solutions and so the absolute or relative yields were calculated.

Preparation of the sample for t.x.r.f.

After the separation and concentration step, an aliquot of 100--300 μl of the organic extract was transferred to the top of the highly polished quartz sample carrier and evaporated to a thin film for the t.x.r.f. measurement. This was achieved with the help of a special device, shown in Fig. 2, designed optimally to adjust the sample spot to meet the excitation beam.

The sample carrier is fixed on a spring platform (A). A small PTFE cylinder with both ends open and one side bevelled is pressed against the sample carrier by means of the bow B, so that the bottom of a small cup is created. The aliquot is pipetted into this cup, in which the evaporation to the sample film is effected by careful heating. The quartz sample carrier is cleaned first by rinsing with chloroform and wiping with Kleenex tissue to remove the carbamate residues from previous measurements. Then the samples carrier is placed in a boiling detergent bath for 1—2 h and in boiling dilute nitric acid for 5 min. Finally, it is rinsed with ultrapure water and dried in a clean bench.

Total-reflection x-ray fluorescence spectrometry

Total-reflection x-ray fluorescence spectrometry (t.x.r.f.) is a modified version of conventional energy-dispersive x.r.f., with substantially improved

detection limits. In contrast to conventional x.r.f., the angle of incidence of the exciting radiation from the x-ray tube is only a few minutes of arc, such that the radiation is totally reflected from the highly polished quartz sample carrier. Prior to incidence, the x-ray is geometrically and spectrally formed within a simple optical arrangement comprising two quartz mirrors and some diaphragms. The sample is placed on the sample carrier as a thin amorphous film. Because of the small angle of incidence, the primary beam has virtually no interaction with the sample support, thus leading to a dramatic reduction of scattered radiation, a substantial improvement in the peak/background ratio, and so a reduction in detection limits to the lower picogram range [8]. The principle is outlined in Fig. 3. Compared to other variants of x.r.f., the t.x.r.f. method has a detection power which is better by 2—3 orders of magnitude.

The outstanding sensitivity of t.x.r.f. allows the unrestricted application of the thin-film technique with internal standardization. With this technique, a fixed calibration function is an inherent feature of the method. Unlike conventional x.r.f., there is no need for matrix corrections or for external standards. The calibration curve is established by repeated measurements of multi-element standard solutions. Once carefully established (normally at the installation phase), the calibration should never be altered or adapted, unless of course hardware is varied or a sensitive part of the software is changed. It maintains its validity for all matrices, for the entire concentration range, and for any element chosen as internal standard.

The spectrum-processing software plays an important role in terms of the capacity, the ease of operation, and the reliability of the method. Because of the complexity of x-ray spectra of real samples, deconvolution of overlapping peaks and automatic background subtraction are mandatory, e.g., for the

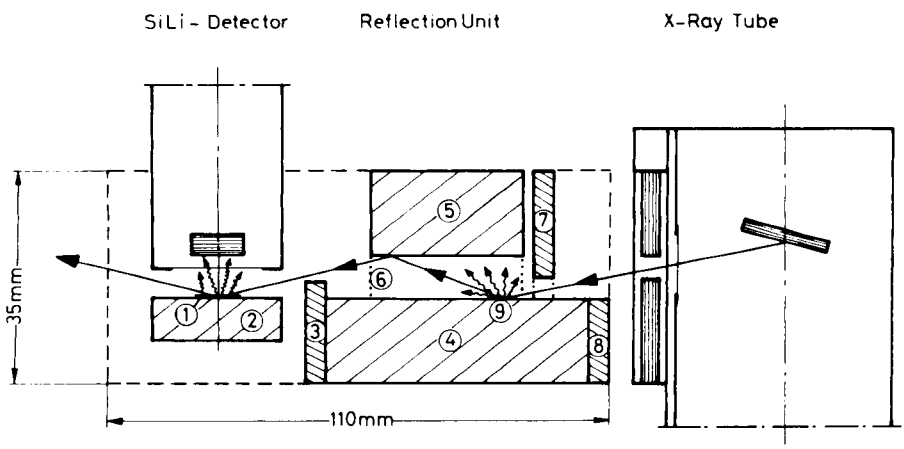

Fig. 3. Schematic design of the t.x.r.f. module: (1) sample; (2) sample support; (3) diaphragm; (4) reflector I; (5) reflector II; (6) spacer (20 μm); (7) diaphragm; (8) diaphragm; (9) first reflection zone (with low-pass filter effect).

determination of arsenic and lead in the presence of selenium and bromine. Past experience has shown that adequate programs are commercially available. Details of t.x.r.f. have been described elsewhere [8—10].

In the course of this work, t.x.r.f. systems with molybdenum-tube excitation as well as tungsten-tube excitation were used. The former variant is based on the prototype of the multi-reflection module for total-reflection of excitation x-ray fluorescence [16]. The electronic periphery was obtained from Northern Tracor (Nuclear Spectroscopy System TN 2000); the x-ray generator as well as the tubes were from Rich. Seifert & Co. The latter variant is based on the total-reflection x-ray fluorescence module of the commercial system EXTRA II (Rich. Seifert & Co.). The electronic periphery is supplied by LINK System (System 860/500). Usually the samples were measured for 1000 s at 59 kV and 13 mA.

RESULTS AND DISCUSSION

Optimization of the reaction parameters

Complexation of heavy metals with dithiocarbamates is known to be sensitive to pH and concentration. Hence, the reaction parameters for the separation and enrichment step were optimized by means of radiotracer studies and standard addition tests.

Tracer studies. Determination of the yield with radiotracers was conducted in two groups for technical reasons (see above). With respect to the employment of t.x.r.f., the absolute values of the yield were not as important as the relative yields related to a particular element which could later serve as internal standard for the t.x.r.f. (e.g., cobalt or selenium). After a suitable carbamate had been chosen, the tests were extended to other elements in which vanadium and a second group of short-lived radionuclides (Mn, Ni, Cu and Cd) were included. Figures 4 and 5 illustrate the results.

The study of ammonium pyrrolidinedithiocarbamate (APDC) showed that the relative yields based on cobalt, which has an absolute yield of

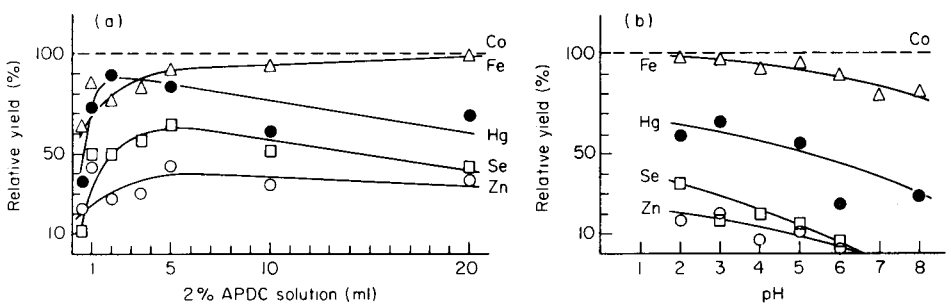

Fig. 4. Recovery of radiotracers added to sea water in relation to cobalt, with APDC: (a) as a function of APDC concentration; (b) as a function of pH. Symbols: (□) Se; (○) Zn; (●) Hg; (△) Fe; (---) Co = 100%.

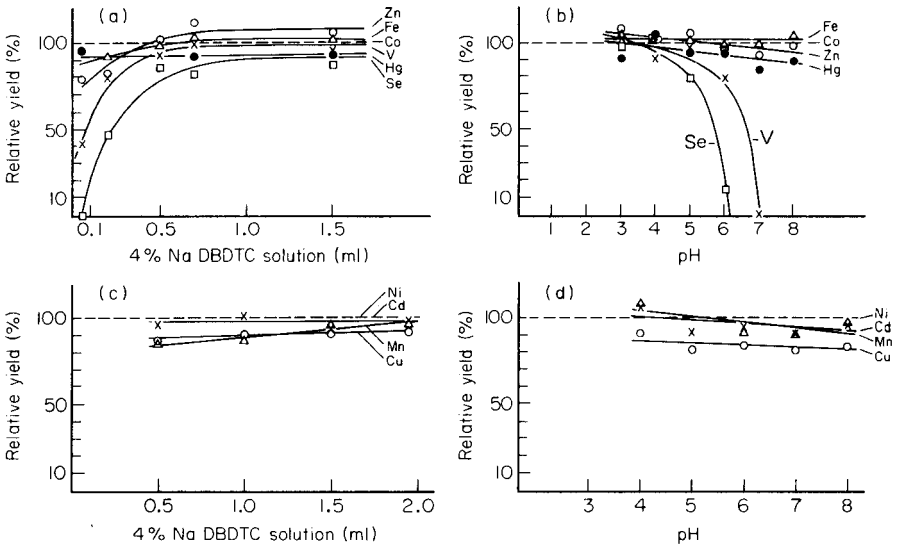

Fig. 5. Recovery of radiotracers added to sea water in relation to cobalt, with NaDBDTC: (a, c) as a function of NaDBDTC concentration; (b, d) as a function of pH. Symbols in (a) and (b): (□) Se; (○) Zn; (△) Fe; (●) Hg; (×) V; (- - -) Co = 100%. Symbols in (c) and (d): (▲) Mn; (×) Cd; (○) Cu; (- - -) Ni = 100%.

80—90%, are highly irregular (Fig. 4a). Only when the ligand concentration exceeds 122 μmol kg^{-1}, corresponding to the addition of 5 ml of a 2% carbamate solution to 200 g of sea water, can relative yields of over 90% for iron, and 60% for selenium and mercury be achieved. Zinc goes up to only about a third of the expected value; Cr, Mn and As are not found and remain quantitatively in the aqueous waste. With the exception of mercury, the Chromosorb is completely eluted. Investigations of pH variations (Fig. 4b), done with a ligand concentration of 122 μmol kg^{-1}, did not produce regular element yields in the pH range 2—8; chromium and manganese were not separated. Arsenic appeared in the eluate above pH 5 but only to a small extent. Above pH 6, selenium and zinc remain in the aqueous medium. It can be ascertained that favourable reaction conditions prevail at pH < 5. The yields for mercury and iron are within 50—70% and 90—100%, respectively, relative to cobalt.

With the addition of a collector cation (e.g., cobalt) at a ligand concentration of 244 μmol kg^{-1} and a pH value of 5, all element yields are increased. Relative to cobalt, yields of 100% and an adjustment of the yields for Fe, Se and Hg to 90—100% are achieved. Chromium and zinc reach about 50—60% yield when 100 μg of cobalt is added to 200 ml of sea water.

The use of sodium dibenzyldithiocarbamate (NaDBDTC) as chelating reagent, applied as a methanolic 4% (w/v) solution, leads to clearly improved yields. Investigations of the dependence of element yields on ligand concentration (Fig. 5a) at pH 4.5 indicate that the absolute yields of the

elements considered are functions of the ligand concentration. This is especially true for vanadium and selenium. At low ligand concentrations, a substantial part of the added tracer can be found in the aqueous medium as the Chromosorb is quantitatively eluted. It follows from the yields in the eluate that only above a ligand concentration of 14 μmol kg^{-1} do V, Fe, Zn, Se and Hg reach high relative yields of 90 ± 10%. The short-lived radionuclides Mn, Ni, Cu and Cd are nearly quantitatively eluted (Fig. 5c).

The effects of variations in pH between 3 and 8 were studied at a ligand concentration of 27 μmol kg^{-1} (corresponding to an addition of 1 ml of a 4% NaDBDTC solution to 200 g of sea water). From Fig. 5(b) it can be seen that regularly high yields for the elements V, Fe, Zn, Se and Hg can be expected below pH 5. In practice, separations operated below pH 4 are cumbersome, because precipitating carbamic acid tends to obstruct free flow. For manganese, copper, cadmium and nickel, no significant dependence of the yield could be found in the pH region investigated (pH 4—8). The radionuclides were quantitatively detected in the eluate (Fig. 5d).

Addition of standards. The determination of yield by standard addition was limited to the reaction conditions found to be optimal in the course of the radiotracer studies. These are ligand concentrations of 122 μmol kg^{-1} for APDC and 27 μmol kg^{-1} for NaDBDTC, both at pH 4.5. In addition to the elements which could be considered in the tracer studies, molybdenum, lead and uranium were included as standard elements. Table 1 illustrates the results.

In the case of APDC, V, Mn, Zn and U could practically not be detected whereas Ni, Cu, Se, Mo and Hg reached yields of 60—70%; iron recovery was over 90% (all related to cobalt as internal standard). These results are

TABLE 1

Recoveries determined by standard addition to sea water with APDC or NaDBDTC as the chelating agent

Element	Additional standard (ng kg^{-1})	Element found (ng kg^{-1}) with APDC[a]		Yield (%)	Element found (ng kg^{-1}) with NaDBDTC[a]		Yield (%)
		Before addition	After addition		Before addition	After addition	
V	2500	148 ± 61	188 ± 79	—	1540 ± 100	3920 ± 70	95.3 ± 5.2
Mn	1000	—	—	—	32 ± 6	917 ± 9	88.5 ± 1.2
Fe	1000	353 ± 51	1320 ± 43	96.3 ± 4.8	344 ± 17	1370 ± 20	102.3 ± 2.9
Co	1000	internal	standard	100	internal	standard	100
Ni	1000	165 ± 15	735 ± 21	57.0 ± 6.9	241 ± 12	1230 ± 20	99.2 ± 2.4
Cu	1000	93 ± 23	790 ± 17	69.7 ± 6.1	107 ± 2	1090 ± 20	98.2 ± 2.3
Zn	1000	64 ± 12	146 ± 18	8.2 ± 6.4	179 ± 3	1190 ± 23	100.8 ± 2.3
Se	2500	—	1970 ± 100	78.8 ± 5.1	—	2530 ± 30	101.0 ± 3.1
Mo	5000	5590 ± 240	9210 ± 170	72.3 ± 9.8	10200 ± 490	15200 ± 670	100.2 ± 5.5
Cd	1000	—	313 ± 23	31.3 ± 2.3	—	984 ± 25	98.4 ± 2.5
Hg	1000	196 ± 27	925 ± 44	72.9 ± 6.1	75 ± 10	1050 ± 30	97.6 ± 2.9
Pb	1000	35 ± 7	472 ± 31	43.7 ± 5.2	49 ± 4	1100 ± 40	105.2 ± 3.8
U	2500	557 ± 51	772 ± 65	8.6 ± 3.1	3100 ± 190	5650 ± 110	102.1 ± 8.6

[a] $n = 3$.

in good agreement with the relative yields obtained for the same elements under corresponding reaction conditions in the tracer studies. Application of NaDBDTC as chelating agent led to relative yields of 95 ± 10% for all the elements considered. There was again good agreement with the results of the corresponding tracer studies.

To determine the concentration range of validity of the separation and enrichment method, the concentrations of the elements were increased stepwise by addition of standards to the sea water. For this purpose, another surface water sample from the Pacific was used. The amounts of standards added gave final concentrations of 5, 10, 50 and 100 $\mu g\ kg^{-1}$. Table 2 describes the yields obtained. They are all constant over the concentration region investigated.

For practical purposes, it is important to note that considerable precipitation began at a total element concentration of over 1 mg kg^{-1}; this heavily overburdened the Chromosorb column, causing a delay in the separation of the carbamate complexes to such an extent that with the usual 3—4 ml of organic solvent, elution could not be done quantitatively. Additionally, the films for measurement obtained from the eluate were of poor quality and could not be excited with the x-ray tubes at full power. Hence, the total concentration should either be kept under 1 mg kg^{-1} (1 ppm) or the seawater sample should be diluted.

The results of yield investigations show that the use of sodium dibenzyldithiocarbamate (NaDBDTC) as chelating agent for heavy metal traces in sea water combined with the reverse-phase method leads to the acquisition of high and regular yields in the separation and concentration process. Compared to ammonium pyrrolidinedithiocarbamate (APDC), NaDBDTC has various advantages which are reflected especially in the all important regularity of the yields for the different elements, and the coverage of a greater number of elements as required by the multi-element method under development. The reasons for this difference are most probably related to the hydrophobic properties of DBTC originating from the benzyl substituents. The following effects are favourable: (1) lowering of the solubility products of the chelate complexes of the metals; (2) increase of co-precipitation effects, supported by the low solubility of the reagent in water [17]; (3) more favourable adsorption properties as required by the mechanism of the reverse-phase technique [18]. These criteria positively affect the coverage of extremely low trace element concentrations such as are encountered in sea water.

The improvement of the element yields with APDC as chelating agent by addition of a collector cation can be interpreted in a similar way. Through the co-precipitation effect induced by these added cation, the secondary chemical equilibria as postulated for the reverse-phase method is altered in such a way that the complexes adsorbed on the stationary phase achieve better distribution coefficients against water.

Apart from the hydrophobic properties, other effects are conceivable

TABLE 2

Recoveries determined by stepwise increase of standard element concentrations with NaDBDTC as chelating agent

Standard addition[a] (μg)	Resulting conc. (μg kg^{-1})	Yields (%) (n = 3)												
		V	Mn	Fe	Co	Ni	Cu	Zn	Se	Mo	Cd	Hg	Pb	U
1.0	5	96.3	91.6	100.9	100	104.4	102.8	95.0	103.9	92.1	101.9	106.5	96.3	100.7
		±2.7	±2.6	±2.8		±2.9	±2.8	±2.6	±2.8	±1.4	±4.3	±7.3	±2.7	±3.0
2.0	10	100.8	90.9	97.8	100	103.6	98.5	99.6	102.0	93.9	105.3	102.2	99.4	99.9
		±2.8	±2.6	±2.7		±2.9	±2.3	±2.8	±2.8	±7.9	±4.2	±2.8	±2.8	±3.0
10.0	50	102.9	97.3	99.5	100	101.9	99.9	99.1	96.0	101.5	102.2	103.8	100.2	102.8
		±3.0	±2.8	±2.9		±2.9	±2.9	±2.9	±2.8	±2.1	±1.1	±3.0	±2.9	±3.3
20.0	100	101.3	90.9	96.4	100	99.9	96.5	94.5	94.5	102.0	99.9	100.0	96.1	97.1
		±2.9	±2.6	±2.8		±2.9	±2.8	±2.7	±2.7	±1.6	±4.0	±2.8	±2.8	±3.0

[a]To 200 g of sea water.

which may contribute to the marked advantages of NaDBDTC. Hence, the increased π-acceptor properties of sulphur in the DBDTC complex can enhance the chances of π back-donation and consequently the strength of the metal-sulphur bond, as exemplified for iron by Albertson et al. [19] in their comparison of bond lengths in the iron complexes of APDC and DBDTC; the Fe-S distances measured were 243.5 pm and 232.7 pm, respectively.

When the optimized reaction parameters of the separation and concentration step were used, i.e., a ligand concentration of 27 μmol kg^{-1} and pH 4.5—5, the absolute yields of the metals in the eluate were around 80%. Their variations of 5—22% were higher than the 1—14% achieved for the relative yields (95%) by t.x.r.f. measurements. In the case of the relative yields based on an internal standard, variations in the absolute yields do not have any significant effect, as long as all the elements display uniform behaviour. Thus, incomplete precipitation, adsorption or elution are levelled out by the internal standard and no systematic error occurs, if all the metals behave in the same way. In such cases, the only disadvantage is a slight deterioration of the detection limit. Some improvement in relation to the amount of the absolute yield and its stability might be achieved by replacing the Chromosorb by some of the newer reverse-phase materials.

Characterization of the analytical procedure

To illustrate the efficiency of the proposed method, blank values, detection limits, reproducibilities and accuracy were investigated thoroughly with different sea-water samples.

Blank values. In order to determine the overall blank values of the analytical method (from weighing of the specimen to preparation of the measuring sample), a series of analyses with ultra pure water and sea water (previously extracted with dithiocarbamate) was conducted, in which two independent separation devices were used. Typical examples of the results are given in Table 3. It can be seen that, with the exception of vanadium and uranium, only small differences exist in the averages of the blank values and of their variations. The values for vanadium and uranium can be explained by assuming an incomplete extraction of the trace metals from sea water. They correspond to a 4% unextracted part when compared to the amounts of uranium and vanadium found in sea-water samples. These facts clearly indicate that determination of blank values using extracted sea water is only reasonable with sea-water samples of extremely low element concentration such as are found in the open seas. In general, such determinations should preferably be done with extracted pure water.

Table 3 also shows that the blank values of V, Mn, U, Co, Pb and Ni are generally near the detection limit or below it (see below) when extracted pure water is used. Practically, only the blank values of iron, copper and zinc need to be considered, and for copper only in surface-water samples from the open seas. The variations of the blank values are relatively small. It is clear that the blank values must originate from the reagents used because

TABLE 3

Blank values from extracted sea water and extracted ultrapure water

	Column	Element concentration (ng kg^{-1})[a]									
		V	Mn	Fe	Co	Ni	Cu	Zn	Hg	Pb	U
Extracted	A	62	—	49	—	7	8	69	27	—	110
sea water	B	64	—	73	—	19	15	55	24	—	137
	A	54	—	51	—	10	15	73	31	—	114
	B	62	—	68	—	19	21	64	31	—	149
Mean		61	—	60	—	14	15	65	31	—	128
S.d.		4		12		6	5	8	3		19
Extracted	A	—	—	44	—	—	15	43	34	—	—
ultrapure	B	—	—	89	—	14	23	53	32	—	—
water	A	—	—	50	—	7	36	63	26	—	—
	B	—	—	86	—	—	29	41	21	—	—
	A	—	—	57	—	8	19	81	18	—	—
Mean		—	—	65		10	24	56	26	—	—
S.d.				21		4	8	16	7		

[a]The dashes mean that the concentration was at or below the detection limit. Standard deviations are based on the 4 (or 5) runs.

there were no significant differences in the results from the two independent apparatus.

The main source of blank values is the carbamate solution which was used as the "purum" reagent in purified methanol. A steady increase in the carbamate concentration led to a rise in the blank values, especially for iron and zinc. Extra purification of the carbamate solution (e.g., by recrystallization) was, however, not considered because the blank values and especially their small variations were in general well below the element contents in the sea-water samples. The blank values for cadmium and molybdenum were also below the detection limit (with W-anode excitation).

Detection limits. In the literature, different formulae are recommended for calculating detection limits [20—24]. In this work, the formula recommended by Currie [22] is adopted.

In an attempt to characterize the efficiency of the method developed with respect to the detection limit, two cases must be differentiated. In one case, the detection limits are derived from the peak/background ratio in the x-ray fluorescence spectra of the sea-water samples. The detection limits define the measured value or concentration above which a signal of an element under stipulated borderline conditions (e.g., amount of sample, measuring time, nature of measuring sample, etc.) can be recognized. According to this definition $\sigma_B = 2^{1/2} N_B^{1/2}$, and the detection limit (L_D) can be calculated from

$$L_D = 4.65\,(I_B - I_N)^{1/2}\, I_N^{1}\, t^{-1/2}\, C \qquad (1)$$

where N_B is the count rate of the background, I_B is the gross pulse rate, I_N is the net pulse rate, t is the measuring time, and C is the calibration factor.

For t.x.r.f. spectra, the peak/background ratio is largely a function of the nature of the sample prepared for measurement. An unfavourably thick sample film would warrant an adjustment of the excitation current of the x-ray tubes to prevent a certain total count rate being exceeded. Normally, from the sea-water samples, samples for measurement can be prepared which yield detection limits around 10 ng kg^{-1} (for a measuring time of 1000 s). This is illustrated in Fig. 6. Larger sample volumes of sea water (e.g., 500 g instead of 200 g) and longer measuring times lead to improvements of the detection limits.

In the second case, the detection limits can be derived from the variations of the blank values produced, for instance, by reagents. The detection limits state the measured value or concentration at which a real value from the sample can just be differentiated from the blank value. Therefore the uncertainty in assessing values for samples rests entirely with the degree of fluctuation of the blank values. A constant blank value can easily be handled with a correction factor. Blank values were determined from eleven different separation operations by using extracted sea water or extracted pure water. From these, the average $\bar{x}_{Bl}$ and its standard deviation σ_{Bl} were calculated. With a 95% probability one obtains the detection limits, tabulated in Table 4, from $L_D = 3.29\ \sigma_{Bl}$ The detection limits presented here are better by 2–3 orders of magnitude than the 5 μg kg^{-1} obtained from 100 ml of water after enrichment and precipitation as the DBDTC complex on a filter by using conventional x.r.f. techniques for measurement [11].

Reproducibility

The reproducibilities of the results were determined by subjecting three sea-water samples independently to three, four and six sample separation

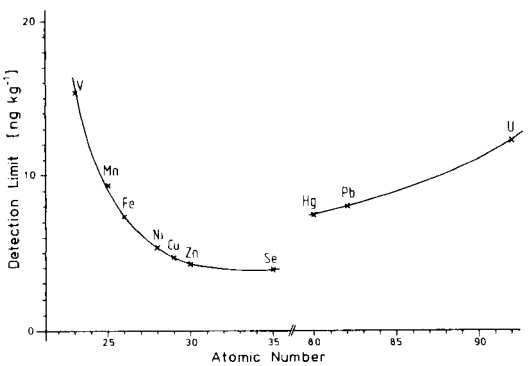

Fig. 6. Detection limits derived from peak-to-background ratios of sea-water spectra (200-ml sample volume and 1000-s counting time).

TABLE 4

Detection limits (L_D) derived from the standard deviation of blank values

	Element concentration (ng kg^{-1})[a]									
	V	Mn	Fe	Co	Ni	Cu	Zn	Hg	Pb	U
Mean $\bar{x}_{BL}$	$<L_D$	$<L_D$	72.3	$<L_D$	14.3	19.6	70.9	31.6	$<L_D$	$<L_D$
S.d. σ_{BL}	—	—	15.8	—	4.8	5.5	13.7	7.7	—	—
L_D (3.29 σ_{BL})	20	15	52.0	8	15.8	18.1	45.1	25.3	10	15

[a] $<L_D$ means that the blanks for these elements are below the detection limit derived from the peak/background ratio

TABLE 5

Reproducibilities of three distinct sea-water samples

	n	Element concentration (ng kg^{-1})									
		V	Mn	Fe	Co	Ni	Cu	Zn	(Hg)	Pb	U
Mean	3	1520	61	266		136	54	205	239	31	3070
S.d.		150	6	5		10	6	13	13	8	190
R.s.d. (%)		9.6	9.9	1.8		7.0	11.1	6.1	5.3	27.0	6.2
Mean	4	1420	67	326		139	53	162	132	43	3123
S.d.		136	12	23		7	3	23	7	7	54
R.s.d. (%)		9.5	17.7	7.0		4.7	5.4	14.0	5.1	17.3	1.7
Mean	6	1450	31	301	5	245	112	188	101	46	3170
S.d.		150	7	11	1	11	3	8	12	7	90
R.s.d. (%)		10.2	22.1	3.5	20	4.4	3.0	4.4	12.3	15.1	3.0

and preparation steps. The results are shown in Table 5. The relative standard deviations compared to selenium as internal standard are in the range of 2—20%. Reproducibilities of independently prepared samples for measurement from the same separation procedure are distinctly better with relative standard deviations ranging from 0.4 to 5%. Fluctuations in the absolute count rates for different samples for measurement obtained from a single separation step are smoothed out by the internal standard. The large standard deviations quoted in Table 5 result mainly from fluctuations in the yields of the trace metals during the separation. On the whole, the reproducibilities of the results achieved for these samples, relative to the internal standard, are satisfactory, bearing in mind that the results pertain to relatively low concentration regions.

Accuracy

The sea-water reference sample NASS-1, the composition of which has been verified by nine different methods was used to test the accuracy of the

proposed method. This reference sample was taken from the northwest Atlantic at a depth of 1300 m and stored in 2-l polyethylene bottles provided by Dr. Berman, Division of Chemistry of the National Research Council of Canada, Ottawa. Comparison of the results for NASS-1 is given in Table 6. It can be seen that for nine elements the deviations do not generally exceed 20% and are even under 10% in some cases. The errors quoted for the reference are averages of standard deviations of the various analytical methods, whereas the present values relate to the standard deviations of the averages from eight (for Co and Cd only four) separate analyses.

EXAMPLES OF APPLICATION

Application of the described analytical method to sea-water samples is demonstrated on selected examples. These samples were collected during a research trip to the Baltic Sea and the central Pacific.

Examples of results from the Baltic Sea

The trace elements in Baltic waters are expected to show a rather complicated geochemical behaviour [25—27]. Compiled in Table 7 are the results

TABLE 6

T.x.r.f. results compared to the sea-water reference sample NASS-1

Element	Method used for certification[a]	Concentration ($\mu g\ kg^{-1}$) reference values	T.x.r.f. (this work) $n = 8$
V	—	—	1.42 ± 0.14
Cr	g, m	0.184 ± 0.016	—
Mn	i, s	0.022 ± 0.007	0.023 ± 0.005
Fe	i, m, s	0.192 ± 0.036	0.235 ± 0.020
Co	i, m	0.004 ± 0.001	0.005 ± 0.002
Ni	e, i, m, s	0.257 ± 0.027	0.230 ± 0.010
Cu	a, c, i, m, s	0.099 ± 0.010	0.092 ± 0.005
Zn	a, i, m, s	0.159 ± 0.028	0.125 ± 0.020
As	a, h	1.65 ± 0.19	—
Mo	d, m	11.5 ± 1.9	10.5 ± 0.5
Cd	a, c, i, m, s	0.029 ± 0.004	0.038 ± 0.009
Hg	—	—	0.072 ± 0.011
Pb	a, i, m	0.039 ± 0.006	0.042 ± 0.006
U	—	—	3.16 ± 0.10

[a] a — Anodic stripping voltammetry. c — Coprecipitation separation/graphite-furnace atomic absorption spectrometry (g.f.a.a.s.). d — Direct determination by g.f.a.a.s. e — Chelation/hanging drop mercury electrode. g — Isotope dilution gas chromatography/mass spectrometry. h — Hydride-generation a.a.s. i — Immobilized ligand separation/g.f.a.a.s. m — Isotope dilution solid-source mass spectrometry. s — Chelation/liquid-liquid extraction/g.f.a.a.s.

TABLE 7

Concentration ranges of the trace elements above the halolines in different regions of the Baltic Sea

Element	Element concentration ($\mu g\ kg^{-1}$)[a]					
	Central Baltic		Gulf of Finland		Gulf of Bothnia	
	F2(A), BY5, BY15, BY20	Mean	BY22	Mean	US5, F2	Mean
V	0.10—0.25	0.16 ±0.05	0.04—0.14	0.08 ±0.04	<0.04—0.14	0.07 ±0.04
Mn	0.25—1.30	0.62 ±0.36	0.64—1.78 (3.0)	1.02 ±0.65	0.28—1.26	0.83 ±0.38
Fe	0.47—0.86 (1.5)	0.69 ±0.15	1.46—3.86	2.35 ±1.04	1.57—11.40	
Co	<0.015		0.02—0.05	0.03 ±0.01	0.01—0.08	
Ni	0.72—0.94	0.79 ±0.06	0.84—0.98	0.92 ±0.06	0.75—0.90	0.82 ±0.08
Cu	0.69—1.10	0.81 ±0.11	0.89—1.15	1.00 ±0.11	0.80—0.89	0.82 ±0.02
Zn	0.75—2.3	1.50 ±0.59	0.69—1.51	1.04 ±0.35	1.17—2.41	1.75 ±0.55
Mo	1.64—3.0	2.23 ±0.38	1.56—1.68	1.69 ±0.11	0.85—1.55	1.10 ±0.27
Pb	0.04—0.13	0.08 ±0.03	0.07—0.08	0.08 ±0.003	0.19—0.30	0.26 ±0.05
U	0.51—0.88	0.73 ±0.12	0.46—0.65	0.56 ±0.10	0.25—0.50	0.37 ±0.12

[a] F2(A), BY5, etc. refer to different sampling stations.

of analyses of surface water from the Baltic Sea, obtained by the method described. The results show good agreement with analogous data published recently [25]. Figure 7 shows vertical concentration profiles from a station in the Gotland basin (BY20), the hydrochemical behaviour of which is characterized by steep gradients of an O_2/H_2S interface in deep waters. The concentrations of many trace elements undergo definite changes around such oxygenated/anoxic interfaces. In these areas, Kremling [26] obtained the same concentration distribution for the elements Mn, Fe, Co, Ni, Cu, Zn and Cd; the increases of Mn, Fe and Co were rationalized as reductive remobilization from the sediments and those of Ni, Cu, Zn and Cd by the formation of hydrogen sulfide and/or polysulfide. In the case of molybdenum and uranium, conservative behaviour was established [27].

Examples of results from the Pacific

Table 8 compares the concentration ranges obtained here for surface and depth waters of the open ocean with those taken from recent literature [28—33]. Except for the values for iron and lead, which are too high, and

TABLE 8

Ranges of trace metal concentrations in ocean water

Element	Concentration (ng kg^{-1})	
	Literature values	This work
V	830—1570 [33]	960—1760
Mn	10—55 [29]	14—67
Fe	15—150 [32]	197—467
Co	1—5 [30]	<7—10
Ni	123—646 [28]	129—622
Cu	32—320 [28]	30—355
Zn	5—588 [28]	61—533
Pb	3—15 [31]	24—49
Conservative elements	(μg kg^{-1})	
Mo	10.1 ± 0.3 [33]	10.3 ± 0.5
U	3.08 ± 0.07 [33]	3.13 ± 0.12

are explained by contamination during sampling and storage, there is a fairly good agreement. The zinc value in the surface water is limited by the blank value of the sample preparation (see above).

As examples of vertical concentration profiles determined in the central Pacific, manganese and nickel are selected because they represent different types of vertical trace-element concentration profiles and demonstrate the capability of t.x.r.f. in ultra-trace determinations (Fig. 8). It can be seen that the manganese distribution differs distinctly from the vertical profile of the nutrient-type element nickel. While nickel shows evidence of surface depletion to values of about 160 ng kg^{-1}, with deep water maxima of about 620 ng kg^{-1} and a slight decrease in the bottom water, dissolved manganese shows evidence of a minor rise from a minimum of 15 ng kg^{-1} at 500-m depth to values of about 40 ng kg^{-1} at the surface. There is a steep gradient of the manganese profile through the upper pycnocline; it exhibits a slight maximum at about 750 m, corresponding to the well-known oxygen minimum at this depth, and decreases gradually below this depth. These results agree well with those obtained by other authors [34].

The significant correlation of the nickel concentrations with the nutrient components phosphate and silicate is obvious from Fig. 9. Because of this dual behaviour of nickel, multiple regression can be used with nickel being a function of both phosphate and silicate:

$$Ni = a + b\,[PO_4^{3-}] + c[Si(OH)_4] \qquad (2)$$

Table 9 gives the resulting correlation parameters, compared with those reported in the literature [28, 35]. The results show good agreement. From the slope values b and c in Eqn. 2, it could be verified that the role of phosphate in relation to nickel predominates over that of silicate in the biogeochemical cycle.

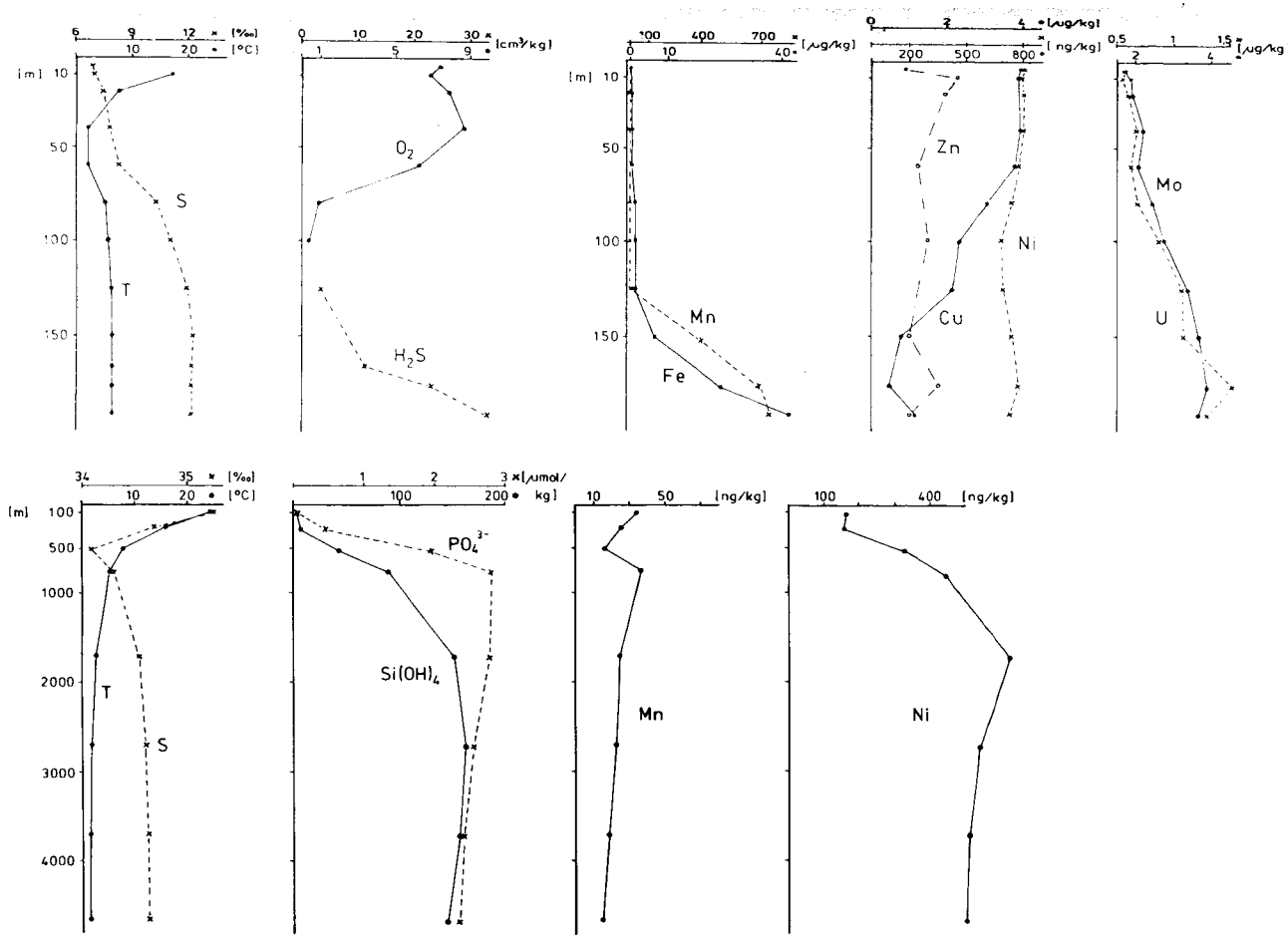

Fig. 7. (Top) Depth profiles for temperature (T), salinity (S), oxygen, hydrogen sulphide and dissolved metals at station BY20 in the central Baltic (Gotland basin).

Fig. 8. (Bottom) Depth profiles for temperature, salinity, nutrients and dissolved Mn and Ni in the central Pacific.

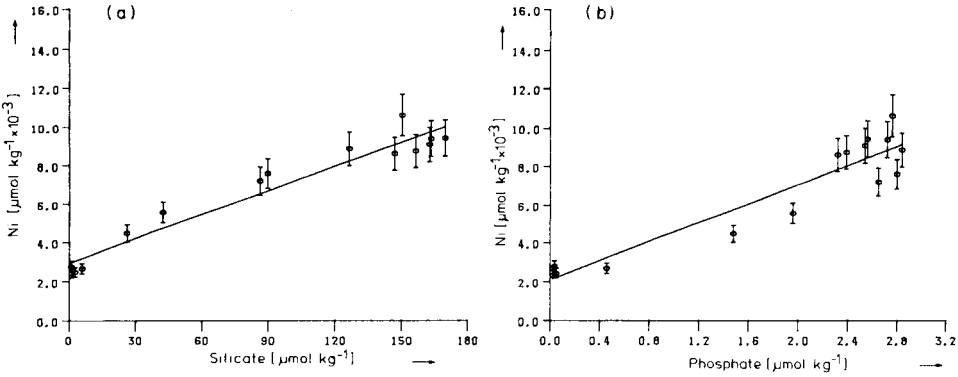

Fig. 9. Correlation of dissolved nickel versus silicate and phosphate. (a) Silicate: Ni, μmol kg^{-1} $\times$ 10^{-3} = 2.97 $\pm$ 0.32 + (0.04 $\pm$ 0.003) $Si(OH)_4$ μmol kg^{-1}; n = 15, r = 0.97. (b) Phosphate: Ni, μmol kg^{-1} $\times$ 10^{-3} = 2.10 $\pm$ 0.53 + (2.47 $\pm$ 0.25) PO_4^{3-} μmol kg^{-1}; n = 15, r = 0.94). Indicated bars refer to analytical precision.

TABLE 9

Correlation parameters for nickel as a function of phosphate and silicate

Authors	*a*	*b*	*c*	*r*
Bruland [28]	2.74	0.95	0.033	0.995
Sclater et al. [35]	3.5	1.07	0.033	0.93
This work	2.36	1.04	0.027	0.99

CONCLUSIONS

The analytical method developed, based on t.x.r.f., enables a large number of trace elements to be determined simultaneously. The range is suitable for different areas of the sea. The motivation to use t.x.r.f. resulted mainly from the characteristic features of the method: its high detection power, the universal calibration curve which eliminates the need for matrix-dependent standard samples or standard-addition procedures, the rather simple preparation of the sample films in comparison with other thin-film techniques, and, of course, the possibility of multi-element determination.

The essential features in the experimental procedure can be assessed as follows. The combination of the analytically efficient t.x.r.f. with the reverse-phase technique in conjunction with sodium dibenzyldithiocarbamate as chelating agent for the separation and enrichment of the heavy metal traces has proved to be very effective. This combination is new and emphasizes the suitability of energy-dispersive x-ray fluorescence spectrometry, in the form of t.x.r.f., as a general analytical principle for trace element determinations in sea water. Because of the relatively simple sample preparation, the danger of trace element loss or contamination can be controlled. Compared to

ammonium pyrrolidinedithiocarbamate (APDC), NaDBDTC is a far better chelating agent because of its hydrophobic properties. This is manifested especially by the greater number of elements covered and the regularity of the yields in the separation/concentration step. For t.x.r.f., which operates with an internal standard, this is of decisive importance.

The results obtained by this method represent the "dithiocarbamate-reactive" metals or metal concentrations in acidified sea water. Owing to the good general agreement of these results with those of other methods, such as were used for the certification of the NASS-1 sea water, each with their different sources of systematic errors, it can be safely assumed that in all cases the so-called "total dissolved" concentrations are obtained. For open ocean waters in which the salinity deviates practically only by 1—2‰, the "conservative" elements uranium or molybdenum could probably be used as natural internal standards.

The t.x.r.f. instrumentation has been tested successfully on board research ships. Experience gained during trips to the central Pacific Ocean and to the Baltic Sea has shown that the method is viable for use on ships. In situations where a rapid overview of the element pattern prevailing at selected sampling stations is required, the proposed method for multi-element determinations offers many advantages compared to other methods. Applications of the method in the context of known oceanographic relationships make it clear that the method provides meaningful information.

The authors express their gratitude to Mrs. R. Makhraban, R. Marten, and H. Schneider for their valuable support during the research trips to the Baltic Sea and the Middle Pacific. We also thank the crews of FS Poseidon and FS Sonne for their helpful assistance. Finally, we are indebted to the Bundesministerium für Forschung und Technologie (BMFT) for financial support.

REFERENCES

1 K. W. Bruland, R. P. Franks, G. A. Knauer and J. H. Martin, Anal. Chim. Acta, 105 (1979) 233.
2 L. G. Danielsson, B. Magnusson and S. Westerlund, Anal. Chim. Acta, 98 (1978) 47.
3 J. M. Bewers, J. Dalziel, P. A. Yeats and J. L. Barron, Mar. Chem., 10 (1981) 173.
4 K. Kremling, in K. Grasshoff, M. Ehrhardt and K. Kremling (Eds.), Methods of Seawater Analysis, Verlag Chemie, Weinheim, 1983.
5 L. Mart, H. W. Nürnberg, P. Valenta and M. Stoeppler, Thalassia Jugosl., 14 (1978) 1971.
6 L. Mart, H. W. Nürnberg and P. Valenta, Fresenius Z. Anal. Chem., 300 (1980) 350.
7 C. S. Wong, E. Boyle, K. W. Bruland, J. D. Burton and E. D. Goldberg (Eds.), Trace Metals in Sea Water, Plenum Press, New York, 1984.
8 J. Knoth and H. Schwenke, Fresenius Z. Anal. Chem., 301 (1980) 7.
9 K. Freitag, in Proc. Symp. Instrumental Multi-Element Analysis, Jülich, April, 1984, Verlag Chemie, Weinheim, in press.
10 W. Michaelis, J. Knoth, A. Prange and H. Schwenke, Adv. X-Ray Anal., 28 (1985) in press.

11 A. T. Ellis, D. E. Leyden, W. Wegscheider, B. B. Jablonski and W. B. Bodnar, Anal. Chim. Acta, 142 (1982) 73.
12 A. Knöchel and A. Prange, Microchim. Acta, (II) (1980) 395.
13 A. Knöchel and A. Prange, Fresenius Z. Anal. Chem., 306 (1981) 252.
14 G. Knapp, B. Schreiber and R. W. Frei, Anal. Chim. Acta, 77 (1975) 293.
15 A. Prange, Ph.D. Thesis, Hamburg University, Federal Republic of Germany, 1983.
16 German Patent Nr. 2736960; US-Patent No. 4426717.
17 H. R. Lindner, H. D. Seltner and B. Schreiber, Anal. Chem., 50 (1978) 896.
18 N. H. C. Cooke and K. Olsen, J. Chromatogr. Sci., 18 (1980) 512.
19 J. Albertson, I. Elding and A. Oskarsson, Acta Chem. Scand., A33 (1979) 703.
20 H. Kaiser and H. Specker, Z. Anal. Chem., 149 (1956) 46.
21 H. Kaiser, Z. Anal. Chem., 209 (1965) 1.
22 L. A. Currie, Anal. Chem., 40 (1968) 586.
23 ACS Committee on Environmental Improvement, Guidelines for Data Acquisition and Data Quality Evaluation in Environmental Chemistry, Anal. Chem., 52 (1980) 2242.
24 ACS Committee on Environmental Improvement, Principles of Environmental Analysis, Anal. Chem., 55 (1983) 2210.
25 K. Kremling and H. Petersen, Mar. Pollut. Bull., 15 (1984) 329.
26 K. Kremling, Mar. Chem., 13 (1983) 87.
27 A. Prange and K. Kremling, Mar. Chem., 16 (1985) 259.
28 K. W. Bruland, Earth Planet. Sci. Lett., 47 (1980) 176.
29 W. M. Landing and K. W. Bruland, Earth Planet. Sci. Lett., 49 (1980) 45.
30 G. A. Knauer, J. H. Martin and R. M. Gordon, Nature (London), 297 (1982) 49.
31 B. Schaule, Ph.D. Thesis, Heidelberg University, F.R.G., 1979.
32 R. M. Gordon, J. H. Martin and G. A. Knauer, Nature (London), 299 (1982) 611.
33 R. S. S. Murthy and D. E. Ryan, Anal. Chem., 55 (1983) 682.
34 M. L. Bender, G. P. Klinkhammer and D. W. Spencer, Deep Sea Res., 24 (1977) 799.
35 F. R. Sclater, E. Boyle and J. M. Edmond, Earth Planet. Sci. Lett., 31 (1976) 119.

Analytica Chimica Acta, 172 (1985) 101—110
Elsevier Science Publishers B.V., Amsterdam — Printed in The Netherlands

ROUTINE DETERMINATION OF THE ABSORPTION AND DISPERSION SPECTRA OF SOLIDS WITH A FOURIER-TRANSFORM INFRARED SPECTROMETER

JENNIFER A. BARDWELL and MICHAEL J. DIGNAM*
Department of Chemistry, University of Toronto, Toronto, Ontario M5S 1A1 (Canada)
(Received 29th November 1984)

SUMMARY

A method is given for the routine determination of the absorption and refractive index spectra of solids from their Fourier-transform infrared (F.t.i.r.) specular reflection spectra. The innovation responsible for making these determinations routine and rapid is the application of the fast Fourier-transform software of the F.t.i.r. spectrometer in the calculation of the optical constants. For strongly absorbing materials, accurate values of the resonance absorption frequencies and corresponding absorptivities cannot be obtained from either the reflectance or transmittance spectra. The absorption and refractive index spectra of fused silica are determined here by this method. Starting with a reflection spectrum, the entire procedure requires only 20 min at a resolution of 2 cm^{-1}. These calculations are impossible with the existing software of most small F.t.i.r. spectrometers; minor software modifications reduce the time required to a few minutes.

Spectrophotometric studies are normally done by measurement of transmission or absorption spectra. For qualitative purposes, such as identification of compounds, this approach is satisfactory; likewise, quantitative measurements can be made on dilute solutions. For concentrated, or strongly absorbing samples, however, relationships such as Beer's Law are frequently invalid, and the band shapes may be distorted so that the central frequencies are altered. In general, any measured optical quantity, such as reflectance or transmittance, is a complicated function of the refractive index, n, and the absorption index, k, of the material. It would be preferable, then, to obtain the values of n and k as a function of frequency, from which the quantitative optical properties of the sample could be calculated. The aim of this work is to introduce a technique for the routine determination of n and k.

To date, a commonly used method for solid samples has been the determination of the reflection spectrum, R, followed by application of a transformation to obtain the phase shift, θ [1]. From the quantities R and θ, n and k can then be calculated. The most commonly used mathematical expression of the transformation is the Kramers—Kronig (KK) relationship [2]. More recently, however, various Fourier-transform (F.t.) relationships, which are mathematically equivalent to the KK relationship, have been proposed

0003-2670/85/$03.30

[3—5]. Because of fast Fourier-transform techniques, the F.t. relationships are computationally more efficient. Despite this convenience, they are still much less widely exploited than the KK technique [6—8] and none is used on a routine basis.

In a recent review [9], it was noted that the F.t. relationship could be computed by using the software already provided with a F.t.i.r. spectrometer. This paper demonstrates the application of the software of a Nicolet F.t.i.r. spectrometer for the calculation of the n and k values of fused silica.

EXPERIMENTAL

The F.t.i.r. instrument used was the Nicolet 8000 series system. A Perkin-Elmer specular reflection accessory (mean angle of incidence 13°) was installed in the F.t.i.r. spectrometer with the KBr beam splitter, Hg/Cd/Te (cooled with liquid nitrogen) detector and Glowbar source. The spectral range was 400—4000 cm^{-1}. A wedge-shaped piece of suprasil fused quartz, polished to $\lambda/4$, was used as a sample. The reference surface was an evaporated gold film. The reflectance spectrum is calculated by ratioing the signal spectrum resulting from reflection from the sample to that resulting from reflection from the gold reference surface. No corrections were made for either the abnormal incidence or the reflection loss of the gold. At a resolution of 2 cm^{-1}, 300 scans were taken for the sample and reference surfaces. To avoid the artifact of negative reflectance, the Fourier-transformed spectra were phase-corrected by using the "power" algorithm, where all noise is positive.

THEORY

Transformation of the reflectance to obtain the phase

Both the refractive index, and its square, the dielectric constant, can be represented as complex quantities which are functions of frequency. From physical consideration of the properties of the dielectric constant, it is possible to derive mathematical relationships between its real and imaginary parts [10]. These relationships also apply to a generalized response function, such as the reflectance coefficient, the modulus of which represents the amplitude of the response to the periodic, harmonic stimulus, and the argument of which represents the delay or phase angle. A response function, $f(\omega)$, can then be considered that must satisfy the condition: $f(\omega) = f_r(\omega) - if_i(\omega)$, where $\lim_{\omega \to \infty} f_i(\omega) = 0$ and $\lim_{\omega \to \infty} f_r(\omega) = K$; where $i = (-1)^{1/2}$ and $f_r(\omega)$ and $f_i(\omega)$ are the real and imaginary parts of $f(\omega)$ respectively.

The most commonly used relations between $f_r(\omega)$ and $f_i(\omega)$ are the KK relations

$$f_i(\omega) = -(2\omega/\pi)P \int_0^\infty [f_r(\omega')/(\omega'^2 - \omega^2)]\,d\omega' \qquad (1)$$

$$f_r(\omega) - K = (2/\pi)P\int_0^\infty [\omega' f_i(\omega')/(\omega'^2 - \omega^2)]\,d\omega' \quad (2)$$

where P implies taking the Cauchy principal value. It may be noted that $P\int_0^\infty [K/(\omega'^2 - \omega^2)]\,d\omega' = 0$, where K is a constant. This implies that

$$f_i(\omega) = -(2\omega/\pi)P\int_0^\infty [(f_r(\omega') - K)/(\omega'^2 - \omega^2)]\,d\omega' \quad (3)$$

for any value of K, including $K = 0$, as written in Eqn. 1.

The conjugate Fourier-transform relations, which are mathematically equivalent to the KK relations, are [5]

$$f_i(\omega) = (2/\pi)\int_0^\infty dt \sin\omega t \int_0^\infty f_r(\omega')\cos\omega' t\,d\omega' \quad (4)$$

$$f_r(\omega) - K = (2/\pi)\int_0^\infty dt \cos\omega t \int_0^\infty f_i(\omega')\sin\omega' t\,d\omega' \quad (5)$$

In application to optical measurements, the function $f(\omega)$ may be the complex refractive index $\hat{n}(\omega) = n(\omega) - ik(\omega)$, or the complex dielectric constant, $\epsilon(\omega) = \epsilon_r(\omega) - i\epsilon_i(\omega)$, or the logarithm of the Fresnel reflection coefficient,

$$\ln\hat{r}(\omega) = \ln[R(\omega)]^{1/2} - i(-\theta),$$

where $\hat{r} = R^{1/2}\exp(i\theta)$, with R the reflectance and θ the phase shift.

At normal incidence, n and k can be calculated from R and θ by using the equations [2]

$$n = (1 - R)/[1 + R - 2R^{1/2}\cos\theta] \quad (6)$$

$$k = -2R^{1/2}\sin\theta/(1 + R - 2R^{1/2}\cos\theta) \quad (7)$$

The use of F.t.i.r. software to effect the phase calculation

What happens during the collection and Fourier transformation of an interferogram by an F.t.i.r. spectrometer is now considered. The following explanation has been culled from the Nicolet manuals and from Bell's monograph [11].

Normally, a single-sided interferogram is collected. It is not strictly single-sided, but starts some few points before the point of zero path difference ($\delta = 0$). A phase array, ϕ, is then calculated for a small region around $\delta = 0$, and this is used to correct the Fourier transform for instrumental imperfections. Fourier transformation is preceded by apodization, and the complex Fourier transform is calculated. The real and imaginary parts are stored separately. The single-sided Fourier transform is

$$B_I(\bar{\nu}) = 2C \int_0^\infty A(\delta)I(\delta)\exp(-i2\pi\bar{\nu}\delta)d\bar{\nu}$$

where $I(\delta)$ is the interferogram, δ the optical path difference, B_I the instrumental spectrum, A the apodization function, $\bar{\nu}$ the wavenumber, and C a constant which depends on instrumental settings. Normally, the instrumental spectrum is phase-corrected by using the following algorithm

$$B_c(\bar{\nu}) = \mathrm{Re}[B_r(\bar{\nu})]\cos\phi(\bar{\nu}) + \mathrm{Im}[B_r(\bar{\nu})]\sin\phi(\bar{\nu}) \quad (8)$$

where Re and Im denote the "real part of" and the "imaginary part of", respectively.

The Nicolet instrument has versatile software which allows one to process the interferogram in separate steps as follows: (1) collect an interferogram; (2) calculate the phase of an interferogram; (3) apodize an interferogram; (4) Fourier-transform an interferogram; (5) phase correct the single beam spectrum.

The algorithm for phase correction of the single-beam spectrum include that described by Eqn. 8 as well as

$$B_r(\bar{\nu}) = \mathrm{Re}[B_I(\bar{\nu})] \quad (9)$$

$$B_i(\bar{\nu}) = \mathrm{Im}[B_I(\bar{\nu})] \quad (10)$$

One can then see that if steps 2 and 3 are bypassed and the phase correction algorithms of Eqn. 9 is selected, the spectrometer software will perform the mathematical operation

$$B_r(\bar{\nu}) = 2C \int_0^\infty I(\delta)\cos 2\pi\bar{\nu}\delta d\delta \quad (11)$$

If steps 2 and 3 are omitted and the algorithm of Eqn. 10 is selected, the spectrometer software performs the operation

$$B_i(\bar{\nu}) = 2C \int_0^\infty I(\delta)\sin 2\pi\bar{\nu}\delta d\delta \quad (12)$$

Integrations in the fast Fourier transform are done in a pointwise manner. The interferogram data consist of N data points spaced at intervals of $\Delta\delta$, and $\Delta\delta$ can be calculated from the parameters under which the interferogram was collected. For the Nicolet, $\Delta\delta = SSP/(2\ (15\ 798))$ where SSP is the sample spacing and 15 798 is the He—Ne laser frequency. Likewise, the resulting spectra, $B(\bar{\nu})$, consist of N data points spaced at intervals of $\Delta\bar{\nu}$. For the Nicolet $\Delta\bar{\nu} = 15\ 798/(N \times SSP)$.

Subsequent discussions are greatly simplified by considering any data array as a function of the data point number, j or k. The spacing of the data points is solely determined by the settings of various flags in the file status block. For simplicity, we continue to write the relevant equations in integral

form, rather than in the more rigorous summation form. Making the substitutions $\bar{\nu} \rightarrow j\Delta\bar{\nu}$, $\delta \rightarrow k\Delta\delta$ in Eqns. 11 and 12 yields

$$B_r(j) = 2C \int_0^\infty I(k)\cos(2\pi\Delta\bar{\nu}\Delta\delta jk)\Delta\delta\,dk = F_r[I(k)] \tag{13}$$

$$B_i(j) = 2C \int_0^\infty I(k)\sin(2\pi\Delta\bar{\nu}\Delta\delta jk)\Delta\delta\,dk = F_i[I(k)] \tag{14}$$

Making the substitutions $\omega \rightarrow 2\pi\bar{\nu}$, $t \rightarrow \delta$ in Eqns. 4 and 5 yields

$$f_i(\bar{\nu}) = 4\int_0^\infty d\delta\sin(2\pi\bar{\nu}\delta)\int_0^\infty f_r(\bar{\nu}')\cos(2\pi\bar{\nu}'\delta)d\bar{\nu}' = 2\int_0^\infty d\delta\sin(2\pi\bar{\nu}\delta)A(\delta) \tag{15}$$

$$f_r(\bar{\nu}) - K = 4\int_0^\infty d\delta\cos(2\pi\bar{\nu}\delta)\int_0^\infty f_i(\bar{\nu}')\sin(2\pi\bar{\nu}'\delta)d\bar{\nu}' = 2\int_0^\infty d\delta\cos(2\pi\bar{\nu}\delta)B(\delta) \tag{16}$$

Making the substitutions $\bar{\nu} \rightarrow k\Delta\bar{\nu}$, $\delta \rightarrow j\Delta\delta$ in Eqn. 15 gives

$$A(j) = 2\int_0^\infty f_r(k)\cos(2\pi\Delta\bar{\nu}\Delta\delta jk)\Delta\bar{\nu}\,dk = (\Delta\bar{\nu}/C\Delta\delta)F_r[f_r(k)]$$

where F_r is the operation defined in Eqn. 13. Also:

$$f_i(k) = 2\int_0^\infty \Delta\delta\,dj\sin(2\pi\Delta\bar{\nu}\Delta\delta jk)A(j) = (1/C)F_i[A(j)] = (\Delta\bar{\nu}/C^2\Delta\delta)F_i\{F_r[f_r(k)]\}$$

Thus, the F.t. relationship in Eqn. 4 can be calculated as follows. First, in order to perform the Fourier transform, F_r, the software must recognise the F.t.i.r. file for $f_r(\bar{\nu})$ as an interferogram. Only some parameters in the file status block must be changed; the data array is not changed in any way. This operation of changing a non-interferogram file to an interferogram file by altering status block parameters is defined as I. Second, the data are Fourier-transformed and the real part is taken. The desired data array, A, is obtained by multiplying the resultant data by $\Delta\bar{\nu}/C\Delta\delta$. Third, the operation I is performed on the array, A. Fourth, the data are again Fourier-transformed, and the imaginary part is taken. The desired function, f_i, is obtained by multiplying the resultant data by $1/C$. In short form,

$$f_i(\bar{\nu}) = (\Delta\bar{\nu}/C^2\Delta\delta)F_i\{I\{F_r[I[f_r(\bar{\nu})]]\}\}$$

$$f_r(\bar{\nu}) - K = (\Delta\bar{\nu}/C^2\Delta\delta)F_r\{I\{F_i[I[f_i(\bar{\nu})]]\}\}$$

Correction for finite frequency range

The above development is only strictly correct for a case in which the data are available over the complete frequency range, 0 to ∞. Such is never the case in practice. The method of Roessler [2], originally developed to correct the KK relations, can also be applied to the F.t. method [3]. It is applicable only to the calculation of the phase shift, θ, from the reflectance, R. It requires that the value of θ be known at two frequencies within the measured range. If two points are chosen which have $\theta = 0$ then

$$\theta(\bar{\nu}) = A \ln|(a + \bar{\nu})/(a - \bar{\nu})| + \theta'(\bar{\nu}) + B \ln|(b + \bar{\nu})/(b - \bar{\nu})|$$

where a and b are the lower and upper limits of the measurement range, $\theta'(\bar{\nu})$ is the calculated phase shift over the limited range, and $\theta(\bar{\nu})$ is the corrected phase shift. A and B are calculated from the simultaneous equations

$$A \ln|(a + c)/(a - c)| + \theta'(c) + B \ln|(b + c)/(b - c)| = 0$$

$$A \ln|(a + d)/(a - d)| + \theta'(d) + B \ln|(b + d)/(b - d)| = 0$$

where $\theta(c) = 0 = \theta(d)$.

RESULTS

Synthetic spectrum

To determine the constant, C, as a function of the spectrometer collection parameters (the manual did not provide this information) the response function for a classical oscillator

$$f(\bar{\nu}) = f_r(\bar{\nu}) - if_i(\bar{\nu}) = S/[1 + (\bar{\nu}/\bar{\nu}_0)^2 + i\Gamma(\bar{\nu}/\bar{\nu}_0)] \tag{17}$$

was used. A synthetic spectrum of $f_i(\bar{\nu})$ was created as a single-beam spectrum, and is shown in Fig. 1. The operations corresponding to $F_r\{I\{F_i[I[f_i(\bar{\nu})]]\}\}$ were performed. The result is shown in Fig. 2 (curve a). Figure 2 (curve b) was calculated from the expression for $f_r(\bar{\nu})$. The agreement is excellent within a multiplicative constant $\Delta\nu/C^2\Delta\delta$. By varying the collection parameters, C was found to be 24.684/*SSP*. The reverse procedure was also used, again yielding C = 24.684/*SSP*, as expected.

Silica spectrum

The reflection spectrum (R vs. $\bar{\nu}$) of silica was measured as described in the experimental section; this spectrum is shown in Fig. 3. It was converted to

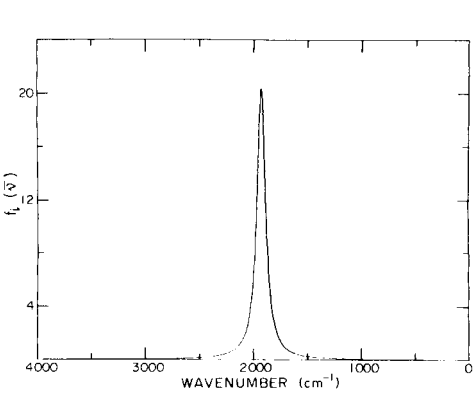

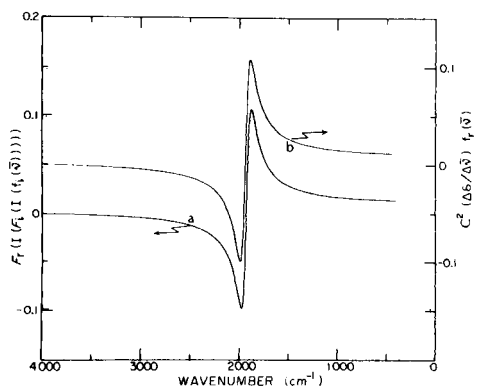

Fig. 1. A plot of the function $f_i(\bar{\nu})$ as defined by Eqn. 17, with S = 1, Γ = 0.05, $\bar{\nu}_0$ = 1928.6 cm^{-1}.

Fig. 2. (a) The result of the operations $F_r\{I\{F_i[I[f_i(\bar{\nu})]]\}\}$. (b) A plot of the function $C^2(\Delta\delta/\Delta\bar{\nu})f_r(\bar{\nu})$ where C = 24.684/SSP, SSP = 2. (b) has been displaced from (a) for clarity.

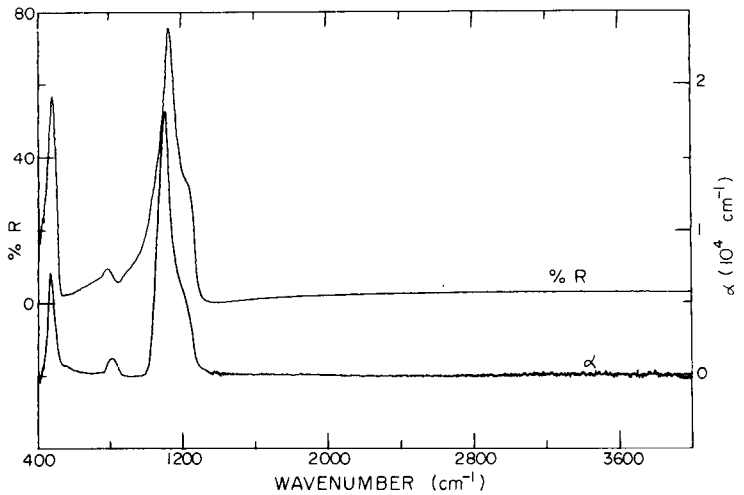

Fig. 3. The experimental reflection spectrum for the silica surface (%R, gold reference surface) and the base 10 absorptivity (α) calculated from k as shown in Fig. 4.

an "interferogram" containing the data $(1/2)\ln(R/R_\infty)$ where R_∞ was set to the value of R at the high frequency limit. The exact value of R_∞ did not change the resulting spectra of n and k except very close to the ends of the spectral range. Following the procedure outlined in the theoretical section, an effective spectrum of θ' was calculated. These data were corrected by using Roessler's method [2] where the true value of θ was assumed to be

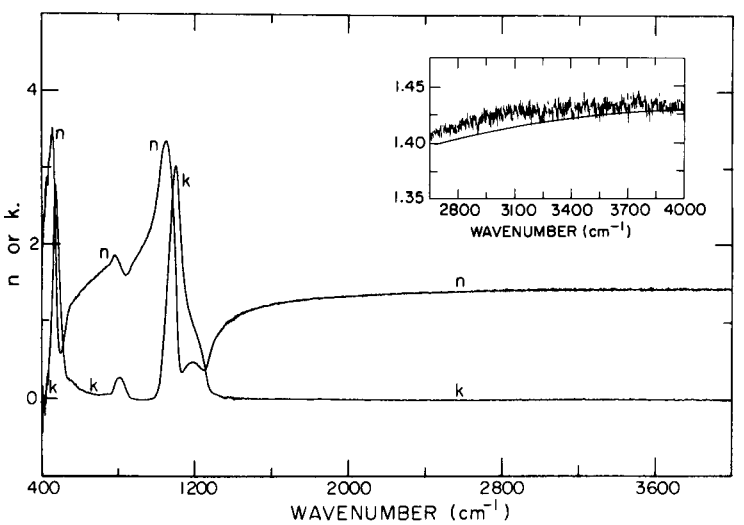

Fig. 4. Spectra of n and k. The inset shows a comparison of the refractive index data obtained at high frequency, with a smooth curve calculated from the dispersion relation [12].

zero at 900 and 3500 cm^{-1}. The optical constants, n and k, were then calculated from Eqns. 6 and 7 and were plotted, all by BASIC routines. The results are shown in Fig. 4. The spectra for n and k are qualitatively similar to those reported recently [12, 13]. In magnitude, the present results lie between those reported recently [12, 13] and those of Cleek [14]. In the region 2650—4000 cm^{-1}, a comparison can be made between the present results for n and those calculated from a dispersion relation [15]. The error is less than 1% over the whole frequency range (see Fig. 4).

A comparison of the reflection spectrum with the spectrum of the base 10 absorptivity, $\alpha = 4\pi k/2.303\ \lambda_0$, in Fig. 3 shows that significant errors would be made if the band positions were evaluated from the reflection spectrum.

APPENDIX

The program for operation I

The following is specific to the Nicolet instrument, and is only an outline of the complete program. A copy of this and other programs can be obtained by contacting the authors.

A Nicolet F.t.i.r. file consists of two parts, the file status block, which contains the parameters under which the data were collected, and a list of data, starting at $\delta = 0$ for single-beam or transmittance spectra and at $\bar{\nu} = 0$ for interferograms. All of the data are in integer form.

The BASIC routine, FLOAD, is used to read the entire F.t.i.r. file, including the status block, sequentially into a BASIC array. The command IAFLT is used to convert the entire array to floating point form.

In converting a reflectance or single-beam spectrum to interferogram form, a total of 18 parameters must be correctly set. These parameters can be located by using a map of the file status block, or by printing out the status blocks of a genuine interferogram, and comparing it to that of the file in question. The most important of the parameters to be changed are the interferogram and transmittance or single-beam flags and the parameter showing the peak location of the interferogram relative to start of scan. The latter parameter should be set to zero. This ensures that the integration in the Fourier transform will start at data point zero. Table 1 is a summary of the parameters which are altered.

Once the parameters have been correctly set, the reflectance data can be changed from R to $(1/2)\ln(R/R_\infty)$ for each data point. The integer values must first be converted back to the actual data values. In the case of the Nicolet, this is done by using an exponential scaling factor. When the data are changed, the exponential scaling factor must also be changed to insure that the new integer data leads to maximum sensitivity. The data and file status blocks are converted to integer form by the routine FAINT and are read back into the same F.t.i.r. file using the routine FSTORE. A branch in the program allows it to be used to handle both reflectance files and single-beam files (such as those obtained after the first Fourier transform).

Types of spectrometers

In principle, any F.t.i.r. software could be modified to run these calculations. However, the existing software must be accessible enough to allow the types of alterations described here. It is also necessary that the software stop execution after the Fourier-transform step, before performing the phase correction, so that the real and imaginary parts of the Fourier transform can be obtained. Of course, a modification by the manufacturer of the software routines would allow the spectra of the refractive index and absorptivity to be evaluated with almost no more effort than required for a conventional

TABLE 1

Decal location number	Contents	"Interferogram" value[a]
2	Number of scans	1
3	Gain	1
4	Gain for background	1
5	Exponential scaling factor	$1 + \mathrm{INT}[(\ln M - \ln 640)/\ln 2]$[b]
6	Single beam flag	−1
7	Interferogram flag	0
8	Transmittance flag	−1
13	Number of scans in background	1
14	Number of transform points/256	−1
19	Apodization function	−1
20	Low pass filter setting	1
21	High pass filter setting	1
22	Peak location of interferogram relative to start of scan	0
32	Phase correction algorithm	−1
33	Switched gain high	1
34	Switched gain low × gain	1
111	Number of transform points in phase correction	−1
112	Number of data points in phase correction	−1

[a] Value of −1 indicates that an operation has not occurred. [b] M is the maximum data value in the data file, and INT (x) is the greatest integer $\geqslant x$.

transmittance spectrum. The only restriction on the method is that two points exist where the absorption is zero. These could be determined from "first approximation" spectra which had not been corrected by Roessler's method [2]. However, failure to apply this correction leads to a distortion of the spectrum only near the ends of the spectral range. Often, this distortion is not large.

The authors thank the Natural Sciences and Engineering Research Council of Canada for supporting this work, and Dr. R. Nayler and D. W. Priddle for their kind assistance in operating the F.t.i.r. They are also grateful to Professor M. Thompson for reading this paper, and for his valuable suggestions.

REFERENCES

1 W. W. Wendlandt and H. G. Hecht, Reflectance Spectroscopy, Interscience, New York, 1966, pp.27—33.
2 D. M. Roessler, Br. J. Appl. Phys., 16 (1965) 1119; 16 (1965) 1359; 17 (1966) 1313.
3 M. G. Sceats and G. C. Morris, Phys. Status Solidi, 14 (1972) 643.
4 C. W. Peterson and B. W. Knight, J. Opt. Soc. Am., 63 (1973) 1238.
5 F. W. King, J. Opt. Soc. Am., 68 (1978) 994.
6 G. C. Morris and M. G. Sceats, J. Chem. Phys., 60 (1974) 375.
7 A. D. Annis and G. Simpson, Infrared Phys., 14 (1974) 199.
8 J. Roth, B. Rao and M. J. Dignam, J. Chem. Soc. Faraday Trans. 2, 71 (1975) 86.

9 J. A. Bardwell and M. J. Dignam, in H. Ishida (Ed.), FTIR Characterization of Polymers, Plenum, New York, 1985, in press.
10 L. D. Landau and E. M. Lifschitz, Electrodynamics of Continuous Media, Pergamon, London, 1960, pp. 247—263.
11 R. J. Bell, Introductory Fourier Transform Spectroscopy, Academic Press, New York, 1972.
12 A. Roseler and W. Molgedey, Infrared Phys., 24 (1984) 1.
13 M. L. Lang and W. L. Wolfe, Appl. Opt., 22 (1983) 1267.
14 G. W. Cleek, Appl. Opt., 5 (1966) 771.
15 I. H. Malitson, J. Opt. Soc. Am., 55 (1965) 1205.

Analytica Chimica Acta, 172 (1985) 111—118
Elsevier Science Publishers B.V., Amsterdam — Printed in The Netherlands

EFFECT OF THE DEGREE OF POLYNOMIALS IN THE SAVITZKY—GOLAY METHOD FOR CALCULATION OF SECOND-DERIVATIVE SPECTRA

KEISUKE KITAMURA* and KEIICHIRO HOZUMI

Laboratory of Analytical Chemistry, Kyoto Pharmaceutical University, 5 Nakauchi-cho, Misasagi, Yamashina-ku, Kyoto 607 (Japan)

(Received 24th May 1984)

SUMMARY

The second-derivative spectra of absorption curves simulated by a Gaussian function were obtained by using Savitzky—Golay cubic (CPC) and quintic polynomial convolutions (QPC), based on 17 points assumed to be at 0.25-nm intervals. For data obtained directly from the simulated curves (real-type data), the second derivatives agreed with the true values if the widths at half height of the peaks were > 15 nm for CPC and 5 nm for QPC. But when integer values obtained from the real-type data were used to simulate a 12-bit A/D conversion, considerable noise appeared on the second-derivative spectra of peaks wider than the above values, obtained by both CPC and QPC. This occurred because the rounding errors introduced by the A/D conversion formed small shoulders on the digitally reproduced absorption curves, which were enhanced by the differentiation to generate noise. The noise was more intense in QPC than in CPC, thus CPC is preferable for peaks that are not very narrow.

Smoothing and differentiation of spectral data can be executed by a desk-top computer by using the simplified least-squares procedure reported by Savitzky and Golay [1], if the data are stored in the computer memory. In the Savitzky—Golay method, the least-squares calculations were done by convolution of the data with a properly chosen set of integers. The integers and their normalizing factors were obtained by fitting sets of points to polynomials and for each objective (smoothing, first-order differentiation, etc.) two or three sets of integers obtained from polynomials of varied degree were described. However, differences in the processed results caused by the degree of the polynomial, have not been reported previously. Therefore, because second-derivative spectra seem to be most useful in derivative spectrophotometry, the influences of the degree of polynomials on the second-derivative spectra were investigated by simulating absorption spectra with a Gaussian function. Cubic and quintic polynomial convolutions were examined.

0003-2670/85/$03.30

MATHEMATICAL TREATMENT

Absorbance, A, at wavelength L nm is defined by a Gaussian function:

$$A = A_0 \exp(-2.77259(L - L_0)^2/W^2) \quad (1)$$

where A_0 is the maximum peak height at $L = L_0$, and W is the width at half height, i.e., the peak width at $A = A_0/2$. Subsequently, the second derivative of A, represented by A'', is given by

$$A'' = 5.54518/W^2(5.54518/W^2(L - L_0)^2 - 1)A \quad (2)$$

The value of W was varied from 2 to 50 nm and A_0 from 0 to 1 for each value of W to reproduce most of the peaks which would be found in ordinary ultraviolet (u.v.) or visible spectra of solutions. An example of a simulated absorption spectrum and its second-derivative spectrum is shown in Fig. 1.

The Savitzky–Golay method for calculation of second derivatives was examined by using 17 data points assumed to be at 0.25-nm intervals. The set of integers used for the cubic polynomial convolution was that originally reported by Savitzky and Golay [1], and for the quintic polynomial convolution was that corrected by Steiner et al. [2]. The second derivative calculated by the cubic polynomial convolution is denoted by D_c and by the quintic polynomial convolution by D_q.

The convolution results were evaluated by two kinds of parameters. One was a ratio of the trough depth (denoted by T in Fig. 1) obtained by the convolution method to the corresponding theoretical value obtained by Eqn. 2. The trough ratio for the cubic and quintic polynomial convolutions are denoted by R_c and R_q, respectively. The other parameters used are the relative mean deviations of D_c and D_q from A'' over the wavelength range

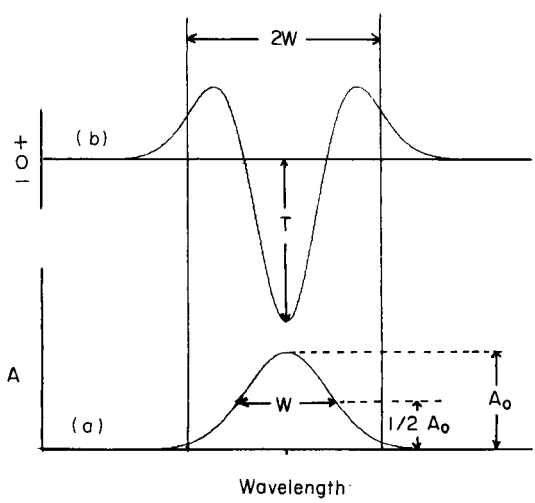

Fig. 1. (a) Absorption spectrum simulated by a Gaussian function; (b) its second-derivative. (For explanation of terms, see text.)

$L_0 - W$ to $L_0 + W$, which are denoted by S_c and S_q, and defined by $S_c = (\sum^n (D_c - A'')^2/n)^{1/2}/T$ and $S_q = (\sum^n (D_q - A'')^2/n)^{1/2}/T$, where $n = 2W/0.25$, i.e., the number of data points in the wavelength range $L_0 - W$ to $L_0 + W$ nm, and T is the true value of the trough depth.

A program of the calculation was written in BASIC and processed by an NEC PC-8001 desk-top computer.

RESULTS AND DISCUSSION

Real-type data

At first, convolutions were examined with the absorbance data given directly by Eqn. 1 (real-type data). Plots of R_c and R_q against peak width W are shown in Fig. 2. The peak heights did not affect the values of R_c and R_q at any peak width studied, and all plotted points in Fig. 2 were superimposed points calculated over a range of peak-height absorbances of 0.1—1.0. The results showed that the trough depth obtained by the cubic polynomial convolution decreased from the true value when the peak width was narrower than 15 nm but became nearly equal to the true value when the width exceeded 15 nm. By using the quintic polynomial convolution, the trough depth was almost equal to the true value when the peak width was wider than only 5 nm. The superiority of the quintic polynomial convolution for the narrow peaks can be accounted for by the fact that the higher the order of the polynomial, the more accurately will the fitting to the steepness of a narrow peak be attained.

The results for S_c and S_q are depicted in Fig. 3. Large values of S_c and S_q for the peaks narrower than 15 nm and 5 nm, respectively, are due to discrepancies in the trough depths as described above. But, for peaks wider than

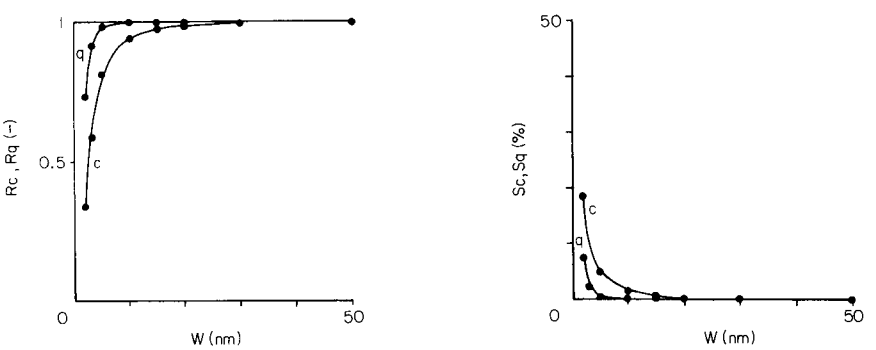

Fig. 2. Effect of width at half height (W) on trough depth for the second-derivative spectrum obtained by the convolution method with real-type data: (c) cubic; (q) quintic polynomial convolution.

Fig. 3. Effect of width at half height (W) on the relative mean deviations (S_c, S_q) of the second-derivative spectrum obtained by the convolution method with real-type data; (c, q) as in Fig. 2.

these dimensions, the values of S_c and S_q were almost zero, so it was apparent that both convolutions gave close to true second derivatives over the whole range of the spectra ($L_0 - W$ to $L_0 + W$).

In the calculations of second-derivative spectra with real-type data, the quintic polynomial convolution was somewhat superior to the cubic polynomial convolution for those peaks having a width at half height of less than 15 nm, but except for these very narrow peaks, both the cubic and quintic polynomial convolutions produced exactly true second-derivative spectra.

Integer-type data

When spectral data are acquired into computer memories from a spectrophotometer, the analog outputs from the spectrophotometer are converted to digital outputs by an analog/digital (A/D) converter and most available A/D converters will be 12-bit. Thus, spectral data are represented by integers between 0 and 4095, e.g., an absorbance of 1 may be converted to 2000 and 2 to 4000 for a normal 0—2 absorbance scale. Therefore, assuming the general case that spectral data are acquired into a computer through a 12-bit A/D converter, the absorbance values given by Eqn. 1 were multiplied by 2000 and their fractions below unity were rounded off so that fractions of 0.5 and over were counted as unity and the rest were neglected. With these simulated digital output data, the convolutions were examined again. The values of D_c and D_q were obtained by dividing the convolution results by 2000.

The results obtained from the integer-type data showed large differences from those obtained for the real-type data. Figure 4 shows the results for the trough depths calculated by the cubic and the quintic polynomial con-

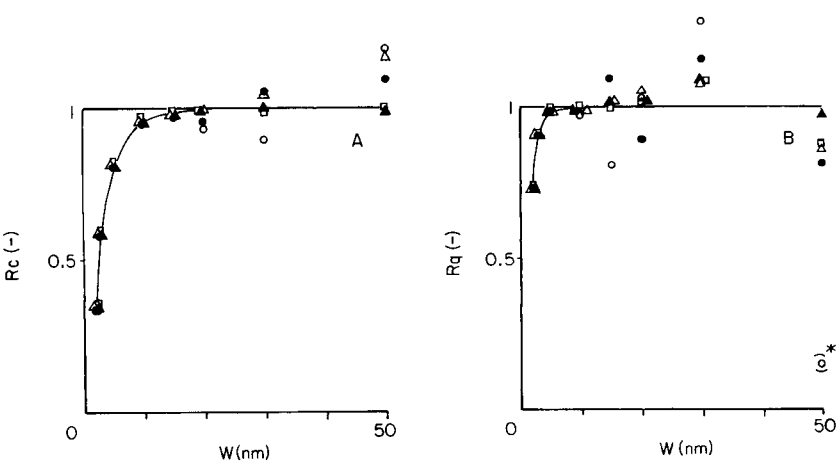

Fig. 4. Effect of width at half height (W) and peak height A_0 on trough depth of the second-derivative spectrum obtained by polynomial convolution with integer data. Peak heights: (○) 0.1; (●) 0.2; (△) 0.4; (▲) 0.7; (□) 1.0. (A) Cubic convolution; (B) quintic convolution ($*R_q = -0.49$).

volutions. As can be seen, the trough depths for peaks narrower than 15 nm (in the cubic polynomial convolution) or 5 nm (in the quintic polynomial convolution) were similar to the real-type data, but those for the wider peaks did not approach the true values, and were rather scattered as the peak height varied. The extent of disagreement with the true values was larger in the quintic polynomial convolution than in the cubic version.

The results for the relative mean deviations S_c and S_q showed similar tendencies in the trough depths. The values of S_c and S_q for peaks narrower than 15 nm and 5 nm, respectively, decreased with peak width and were not influenced by the peak height, as in the results for the real-type data. But for the wider peaks, the values of S_c and S_q increased according to the increase in peak width and the decrease in peak height, or both, as illustrated in Fig. 5. Comparing the results for identical peaks, the values for S_q were greater than those for S_c, i.e., the deviations were greater for the quintic polynomial convolution.

In order to clarify the cause of these unexpected results, an example of the second-derivative spectra obtained for integer data is shown in Fig. 6. It was apparent that when the integer data were used, the convolution methods generated considerable noise on the resulting second-derivative spectra and that the discrepancies in the trough depths and the large relative mean deviations were caused by this noise. The noise on spectrum (c) obtained by quintic polynomial convolution was greater than that on the spectrum (b) obtained by the cubic polynomial convolution, and this tendency was observed in all other spectra studied. This explained the fact that the convolution results for the integer data deteriorated more in the quintic polynomial convolution than in the cubic version.

The reason for the convolutions generating such noise when the integer data were used could be as follows. In the procedures for converting real-type data to integer data, after the former had been multiplied by 2000, the

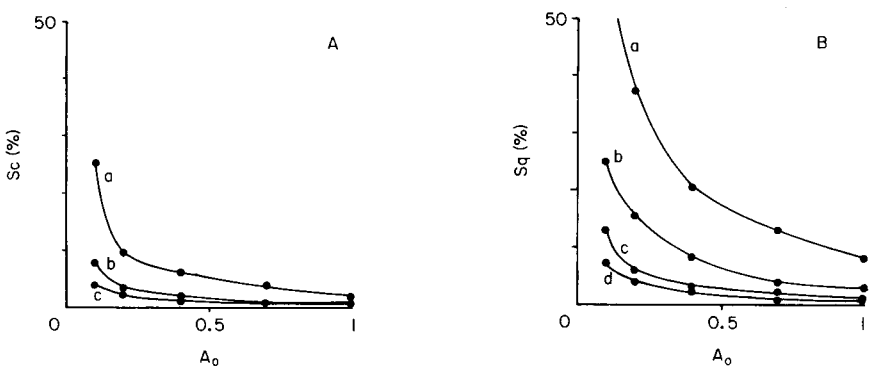

Fig. 5. Effect of width at half height (W) and peak height (A_0) on the relative mean deviation (S_c or S_q) on the second-derivative spectrum obtained by convolution with integer data. Widths at half height: (a) 50 nm; (b) 30 nm; (c) 20 nm; (d) 15 nm. (A) Cubic convolution; (B) quintic convolution.

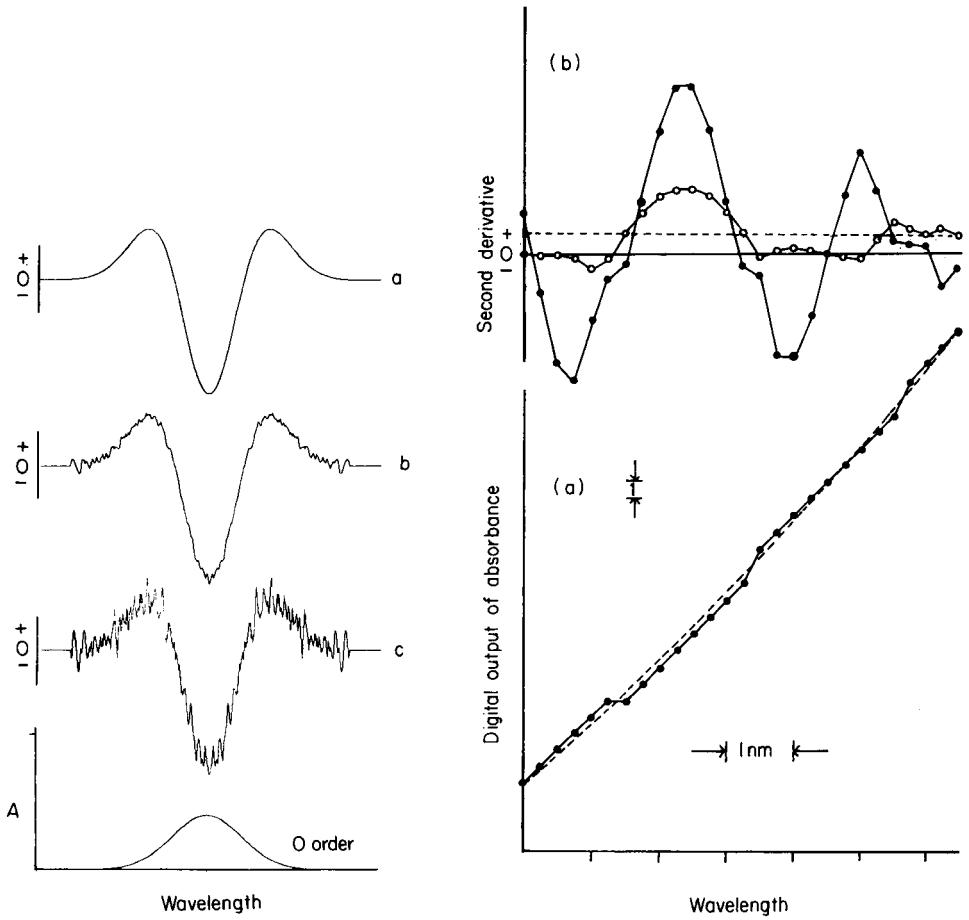

Fig. 6. Second-derivative spectra: (a) obtained by Eqn. 2 with real-type data; (b, c) with integer data by cubic (b) and quintic (c) polynomial convolutions. (A_0 = 0.4, W = 30 nm; the underivatized spectrum is shown beneath the others.)

Fig. 7. (a) Plot of integer data of the spectrum with A_0 = 0.1 and W = 50 nm. The dotted line is the true spectrum. (b) Plot of the second derivatives obtained by (○) cubic and (●) quintic polynomial convolutions, from the integer data in (a). The dotted line is the true second derivative of the true spectrum.

fractions below unity were rounded up or down. The rounding errors were equal to the residues between the integers and the corresponding true values, and so they increased or decreased consecutively between the values of −0.5 and 0.5 along the absorption curve. Therefore, they formed small shoulders having positive or negative deviations on the original smooth absorption curve, as shown in Fig. 7(a). The situation can be considered to be identical in the actual A/D conversion, i.e., when an analog output from a spectro-

photometer is digitized by an A/D converter, the increment of analog output smaller than that which can be represented by the least significant bit will be rounded, so that the absorption curve reproduced by these digitized outputs will also have small shoulders as shown in Fig. 7(a). It is known [3] and can be easily understood from Eqn. 2 that the trough depth is proportional to the reciprocal of the square of the width at half height (W) of the original absorption curve. Though the shoulders were not defined by Eqn. 1, the above rule would be effective to some extent. Therefore, as the widths of the shoulders were narrower than that of the absorption curve on which the shoulders existed, the heights of these shoulders were more enhanced by the differentiation processes than the absorption curve itself. This resulted in the formation of noise on the second derivative spectrum although the original absorption spectrum did not contain any noise.

As already seen, however, the trough depths of the narrow peaks (<15 nm) obtained by the cubic polynomial convolution were always smaller than those obtained by the quintic polynomial convolution. Therefore, the noise caused by the second derivatives of the shoulders was less in the cubic polynomial convolution than in the quintic convolution. These discussions are illustrated in Fig. 7, in which the second-derivative spectra obtained by the convolution methods clearly distinguished the shoulders on the digitally reproduced absorption curve and the spectrum obtained by the quintic polynomial convolution enhanced the small shoulders on the absorption curve more strongly.

The other feature for the integer data was that the convolution results deteriorated, i.e., the noise increased, according to the increase in peak width or decrease in peak height. This can be explained as follows. Because the rounding errors were within the range −0.5 to 0.5, this limited the heights of the shoulders, so that the intensities of the second derivatives of the shoulders, i.e., the intensities of the noise, could be considered to be roughly constant. Therefore, an increase in peak width or decrease in peak height decreased the intensities of the second derivative of an absorption spectrum, giving a relative increase in noise on the second-derivative spectrum.

In the Savitzky—Golay method, the ordinate distance between the adjacent points is always unity regardless of the actual wavelength interval. Therefore, if the interval between sample points is extended for a constant number of convolution points, the half width of the curve is treated as being decreased in the convolution process so that the signal-to-noise ratio in the second-derivative spectrum will be improved, though the resolution will be degraded by the coarse sampling.

In conclusion, it must be emphasized that even if an original absorption spectrum contains hardly any noise, the A/D conversion itself may generate small shoulders on the digitally reproduced absorption spectrum as a result of the rounding effect of digitization, which will produce significant noise on the second-derivative spectrum through the convolution method, unless the width of the original spectral peak is very small. Because the quintic

polynomial convolution enhances the shoulders causing more noise than the cubic polynomial convolution, the latter will be preferable even though it is inferior in principle for derivatizing very sharp peaks.

REFERENCES

1. A. Savitzky and M. J. E. Golay, Anal. Chem., 36 (1964) 1627.
2 J. Steiner, Y. Termonia and J. Deltour, Anal. Chem., 44 (1972) 1906.
3 J. E. Cahill, Am. Lab., 11 (1979) 79.

Analytica Chimica Acta, 172 (1985) 119—126
Elsevier Science Publishers B.V., Amsterdam — Printed in The Netherlands

THE DETERMINATION OF ANTIMONY IN NODULAR CAST IRON BY WAVELENGTH-DISPERSIVE X-RAY FLUORESCENCE SPECTROMETRY

F. ALLUYN, R. DAMS and J. HOSTE*

Institute of Nuclear Sciences, Rijksuniversiteit Gent, Proeftuinstraat 86, B-9000 Gent (Belgium)

(Received 13th November 1984)

SUMMARY

Antimony is determined in cast irons by wavelength-dispersive x-ray fluorescence spectrometry. Excitation and detection conditions are evaluated for the three most intense x-rays of antimony, i.e., the K_α, L_α and L_β lines. Standard samples were obtained by precise determination of the antimony content of some specimen cast irons by neutron activation analysis. Calibration graphs are linear from 0 to 200 mg kg^{-1}. The precision of the determination by means of the most sensitive Sb L_α line, using a chromium tube and a 5-min measuring time, ranges from 6% for samples containing 20 mg kg^{-1} antimony, to 1% for samples containing 200 mg kg^{-1}.

It is now well known that some elements, even at concentrations of a few parts per million, may be harmful to the structure and properties of ductile iron. Small amounts of antimony (100—500 mg kg^{-1}), for instance, have been reported by Morrogh [1], Donoho [2], Sawyer and Wallace [3] to cause nodule deterioration. In contrast, work by Campomanes [4] indicated that no nodule degeneration occurred when up to 50 mg kg^{-1} was added to a relatively pure ductile iron. The mechanical properties of fully nodular antimony-treated ductile iron may even be superior to the antimony-free iron. The presence of as little as 20 mg kg^{-1} antimony prevents the formation of chunky graphite, refines the microstructure and increases the number of nodules [4—6].

Because antimony tends to remain in recycled iron, its total amount from unknown scrap and additions may easily exceed 50 mg kg^{-1}. For this reason, a controlled amount of cerium or mischmetal is added to the melt. Yet, inexplicable variations in the structure and properties of the cast iron, because of unforeseen changes in the concentrations of trace elements in the raw materials used, make a precise determination of antimony at the mg kg^{-1} level necessary.

In an earlier paper, the determination of lanthanum and cerium in nodular cast iron by wavelength-dispersive x-ray fluorescence spectrometry (x.r.f.) was described [7]. In this work, the determination of antimony in nodular

0003-2670/85/$03.30

cast iron by the same technique is optimized. As x.r.f. combines a minimum of sample preparation with high sensitivity and good selectivity, it can be applied for routine production control. Because no standard nodular cast irons with certified antimony values are available, standard samples for the x.r.f. spectrometry were obtained by careful determination of the antimony content of a number of specimen cast iron samples by instrumental neutron activation analysis (i.n.a.a.).

EXPERIMENTAL

Preparation of the nodular cast iron samples

Charges consisting of S-100 grade Sorel pig iron, commercial Fe-Si alloy (70% Si), Fe-S alloy (33% S) and Fe-Mn alloy (75% Mn), were melted in a medium-frequency induction oven by the CRIF (Centre for Scientific and Technical Research of the Metalworking Industry in Belgium). Just before pouring, antimony was added to the melt as the pure metal at a temperature of ca. 1350°C. A set of seven 150 × 150 mm plates (6 mm thick) were cast in green sand moulds. The seven castings had a typical composition of 3.9% C, 2.1% Si, 0.7% Mn and a total of <0.3% of P, S, Cr and Ni, but contained increasing amounts of antimony.

For x.r.f., disks (40-mm diameter, 6 mm thick) were cut from the plates and polished with silicon carbide disks of decreasing particle size. The sample finish was not critical for the antimony determination; a nearly constant intensity was found after treatment with 100-mesh grinding disks.

From the rims of the cast disks, fine drillings were machined for neutron activation, because only an area with a diameter of 30 mm is irradiated in the x.r.f. spectrometer. The turnings were mixed with reagent-grade iron powder in a 1:1 ratio, and pressed at 10 000 psi into a circular pellet (12-mm diameter, 3 mm thick, ca. 2 g weight).

Neutron activation analysis

Standard pellets of the same size and the same weight as mentioned above, were prepared by spotting, on reagent-grade iron powder, known aliquots of an antimony (III)/hydrochloric acid solution. After being dried in a furnace and homogenized with a Turbula mixer, the mixture was pressed into a synthetic standard. The standards thus prepared were irradiated together with the specimens, four of each, for 7 h at a thermal neutron flux of 4.8×10^{11} n cm^{-2} s^{-1} in the Thetis reactor of the Institute of Nuclear Sciences.

The activities of the isotopes ^{122}Sb ($t_{1/2}$ = 2.72 d) and ^{124}Sb ($t_{1/2}$ = 60.2 d) were measured after decay for 4 and 30 days, respectively, on a Ge(Li) detector (relative efficiency 20%, resolution 1.9 keV at 1332.4 keV). The relevant parts of the γ-spectra are shown in Fig. 1. To correct for the neutron flux gradients in the irradiation container, the specific activity of the iron-59 isotope was used as internal standard.

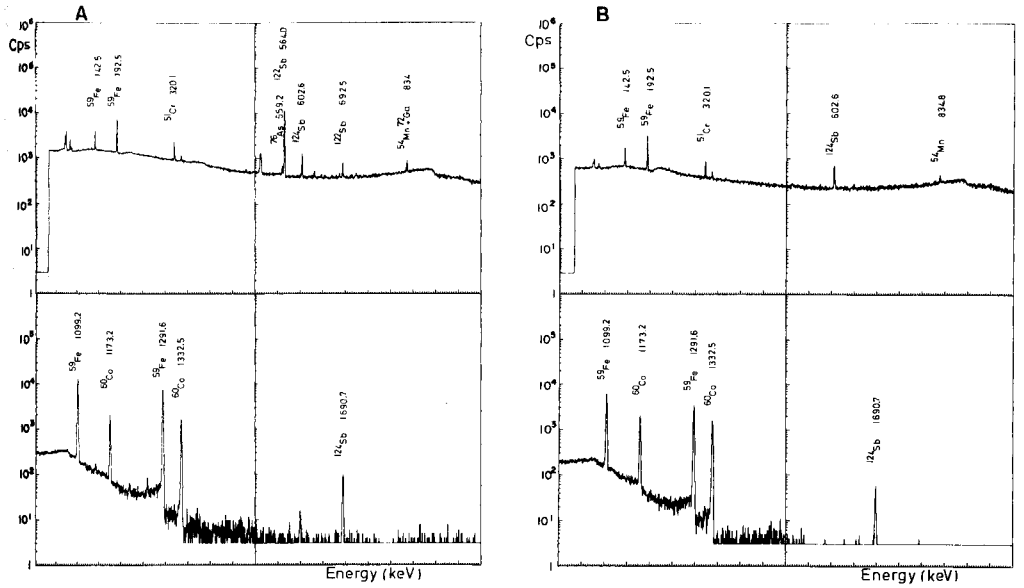

Fig. 1. Ge-Li γ-spectra of a grey cast iron (63 mg kg^{-1} Sb) after decay for 4 (A) and 30 (B) days.

X-ray fluorescence spectrometry

For the analysis of the cast iron samples by x.r.f., a PW-1400 spectrometer was connected with a Digital VT-132 video and a Digital LA 50 printer. All measurements were done under vacuum conditions. Rotation of the sample during measurement avoided errors from the grind marks introduced by the polishing treatment.

The x-rays of interest are Sb K_α, Sb L_α and Sb L_β, each with different excitation and detection parameters (Table 1). As no second-order peak interference occurs, a wide discriminator window can be applied in the pulse-height compensation circuit. The spectrometer is equipped with two

TABLE 1

Excitation and detection parameters for x.r.f.[a]

X-ray	Tube	Discr. window (%)	Diffraction crystal	Counter	Peak angle	Backgr. angle 1	Backgr. angle 2
Sb K_α	W	20—80	LiF(220)	Scintillation	19°10′	18°00′	20°50′
Sb L_α	Cr	30—70	LiF(200)	Flow	117°50′	116°00′	119°50′
Sb L_β	Cr	30—70	LiF(200)	Flow	106°60′	105°50′	108°00′

[a]In all cases the other parameters were as follows: tube voltage 60 kV; tube current 40 mA; P-10 flow counter; collimator at coarse.

primary collimator diaphragms of 28- and 35-mm diameter, respectively. The selection of the diaphragm with the smallest diameter is necessary when the sample holder and mask contribute to the antimony peaks. Comparison of the antimony blank intensities from an antimony-free cast iron, however, showed a negligible difference between the two diaphragms. Because Sb K_α, Sb L_α and Sb L_β can be detected about 10% more precisely with the 35-mm diaphragm, it was selected.

RESULTS AND DISCUSSION

Neutron activation analysis

The synthetic standards used for i.n.a.a. were checked for homogeneity, and the reproducibility of the entire procedure for the preparation of the standards was evaluated, as described previously [7]. The same homogeneity was obtained as for the lanthanum and cerium standard preparations, i.e., better than 2%.

A set of seven castings with antimony contents increasing from 20 to 150 mg kg^{-1} were irradiated for 7 h and analysed. The counting statistics on the measurement of the 564.0-keV peak of ^{122}Sb after 4 days are very favourable which results in a relative standard deviation of 2% for 20 mg kg^{-1} antimony and 0.5% for 200 mg kg^{-1}. The concentrations are summarized in Table 2, from which it can be seen that the antimony recovery in a cast iron melt is very high (>90%), in agreement with earlier reported recoveries [2, 8].

X-ray fluorescence spectrometry

Selection of diffraction crystal. For the diffraction of the Sb K_α peak, only LiF(220) is suitable. For the reflection of Sb L_α and Sb L_β, two crystals are applicable, namely PET (pentaerythritol) and LiF(200). The spectra of a blank cast iron and sample 6 (Fig. 2) illustrate that LiF(200) should be

TABLE 2

Determination of antimony in cast iron by i.n.a.a. and γ-spectrometry

Melt no.	Approx. Sb addition (mg kg^{-1})	Sb content of 4 samples (mg kg^{-1} ± s.d.[a])				Mean
		1	2	3	4	
1	20	19.5 ± 0.3	19.4 ± 0.3	20.5 ± 0.4	20.0 ± 0.4	19.9 ± 0.5
2	25	25.4 ± 0.5	24.2 ± 0.4	25.0 ± 0.5	23.8 ± 0.4	24.6 ± 0.7
3	35	34.4 ± 0.3	34.7 ± 0.3	35.0 ± 0.4	34.3 ± 0.3	34.6 ± 0.3
4	50	63.3 ± 0.4	63.1 ± 0.4	63.0 ± 0.5	63.8 ± 0.6	63.3 ± 0.4
5	70	66.0 ± 0.4	66.5 ± 0.4	65.9 ± 0.4	66.9 ± 0.4	66.3 ± 0.5
6	90	118.8 ± 1.4	118.2 ± 0.6	122.0 ± 0.8	122.6 ± 0.8	120.4 ± 2.2
7	150	187.6 ± 0.6	185.3 ± 0.6	186.5 ± 0.6	186.2 ± 0.6	186.4 ± 0.9

[a]The standard deviation on the weighted mean of the results obtained by using the ^{122}Sb (564 keV, 692.5 keV) and ^{124}Sb (603 keV, 1691 keV) peaks.

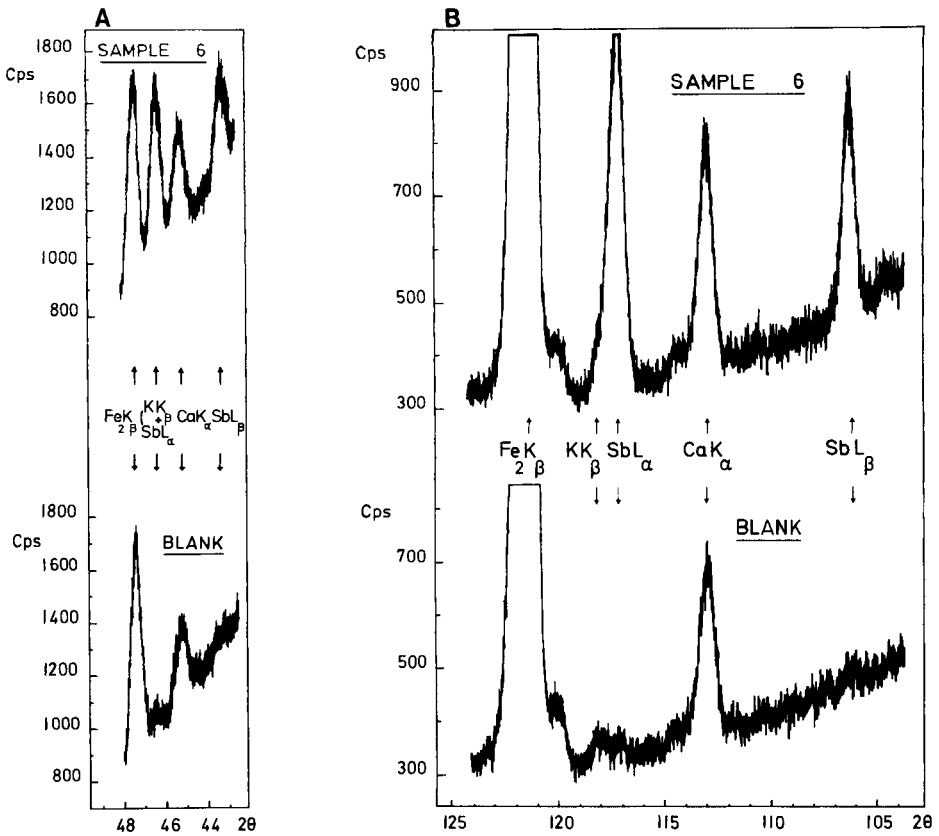

Fig. 2. The 2θ scan of the Sb L_α and Sb L_β lines on a blank and a grey cast iron sample (120 mg kg^{-1} Sb) recorded with (A) PET and (B) LiF(200) crystals (Cr-tube excitation).

preferred for the following three reasons: the background is lower, the reflections of Sb L_α and Sb L_β peaks are higher and thus allow a more precise detection of the net peak, and finally the dispersion is much better: $[\Delta(2\theta)/\Delta\lambda] \approx 140°$ nm^{-1} for PET, and $[\Delta(2\theta)/\Delta\lambda] \approx 510°$ nm^{-1} for LiF(200).

Selection of excitation tube. Two x-ray tubes were considered for the excitation of Sb K_α (E = 26.15 keV), Sb L_α (E = 3.59 keV) and Sb L_β (E = 3.83 keV). For the Sb K_α excitation, the chromium tube only contributes with its continuum. As the continuum intensity is linear with the atomic weight of the element, Sb K_α is poorly excited. The tungsten tube is 3.6 times more effective, resulting in doubled precision in spite of the high background (Fig. 3). For Sb L_α and Sb L_β excitation, the characteristic lines Cr K_α (E = 5.41 keV) and Cr K_β (E = 5.95 keV) are well suited, which is reflected in the higher efficiency of the chromium tube compared to the tungsten tube. In addition, the selection of the background angle for the Sb L_α detection is easy because the second-order iron K_{β_1} peak situated

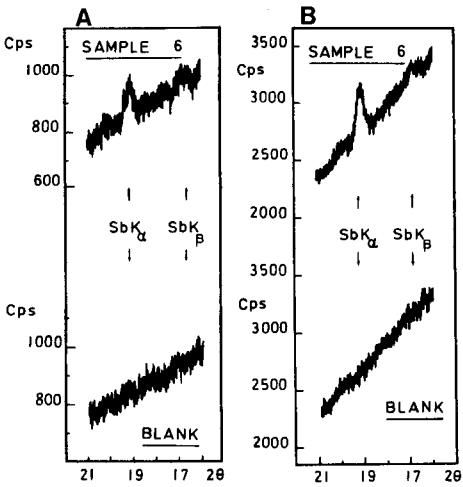

Fig. 3. The 2θ scan of the Sb K_α and Sb K_β lines on a blank and a grey cast iron sample (120 mg kg^{-1} Sb) after excitation with (A) a Cr-tube and (B) a W-tube.

TABLE 3

Comparison of the Sb K_α, Sb L_α, Sb L_β net intensities (cps) obtained with Cr-tube and W-tube excitation (measuring time 3 × 100 s) for the samples with lowest and highest antimony contents

Sample	Sb K_α			Sb L_α			Sb L_β	
	W-tube	Cr-tube	W/Cr	W-tube	Cr-tube	Cr/W	W-tube	Cr-tube
1	59.4 ± 8.2	16.9 ± 4.5	3.5	44.4 ± 4.7	107 ± 3	2.4	26.9 ± 4.7	53.7 ± 3.5
7	563 ± 8	154 ± 5	3.7	382 ± 5	1005 ± 4	2.6	214 ± 5	533 ± 4
Blank	13.0 ± 8.1	6.5 ± 4.5		7.4 ± 4.6	22.4 ± 2.9		5.9 ± 4.6	20.6 ± 3.4

around $2\theta = 121°60'$ (Fig. 2) is much less intense. A comparison of the excitation efficiencies for both tubes is given in Table 3. Obviously, the Sb L_α peak is the most sensitive for antimony. Because of the low potassium content of cast iron, the interference of the potassium K_β line ($2\theta = 118°20'$) is very low. If, as a result of unforeseen changes in the concentrations of minor elements in the scrap iron, a significant interference problem arose, the use of a fine collimator would help. In the case of very high potassium concentrations, the interference-free Sb K_α or Sb L_β lines must be selected. Table 3 also indicates that for each series of analyses, a blank value must be determined by means of a blank sample. This signal must originate from the excitation or detection equipment; no contribution comes from the sample holder or blank sample.

Calibration graphs

In order to investigate the homogeneous distribution of antimony in the samples, both sides of each plate casting were subjected to x.r.f. No gradient

could be detected. This allowed the construction of calibration graphs by using the concentrations found by i.n.a.a. and the Sb K_α/Sb L_α/Sb L_β intensities of the seven samples under the conditions of maximum precision (Table 1). The background intensity at the antimony peak position was obtained by linear interpolation of the background values before and after the peak. The variance s^2_{net} on the antimony net intensity was calculated as follows

$$s^2_{net}(t_m) = a + b_1 + (\Delta p/\Delta)^2 \ (b_1 + b_2)$$

where a is the measured intensity at the antimony peak position; b_1 and b_2 are the background intensities before and after the peak; t_m is the measuring time, Δp the 2θ difference between peak position and b_1 angle, and Δ the 2θ difference between the b_1 and b_2 angle. The variance may be improved by increasing the counting time.

For cast iron, the precision is largely determined by the high background originating from scattering of the continuum radiation from the tubes on the iron. The calibration graphs obtained from the data for the seven reference samples by means of the weighted least-squares method correspond to

Sb K_α $y = (3.004 \pm 0.042)\,x + (3.0 \pm 2.5)$
Sb L_α $y = (5.402 \pm 0.040)\,x + (4.1 \pm 2.4)$
Sb L_β $y = (2.849 \pm 0.046)\,x + (1.6 \pm 2.7)$

where x (mg kg^{-1}) is the concentration of the element found by i.n.a.a. and y is cps (Fig. 4). The high precision on the slopes illustrates the good linearity of the graphs, and the absence of self-absorption for concentrations up to

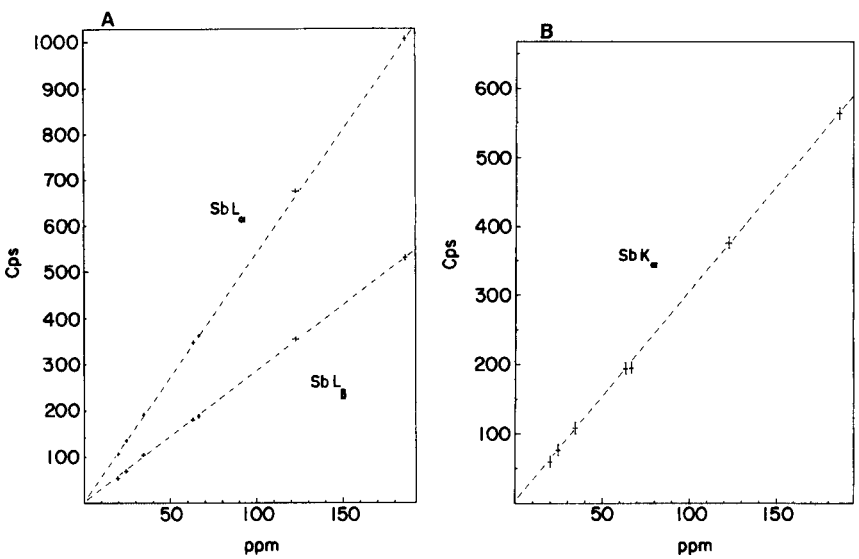

Fig. 4. Calibration graphs for the antimony determination: (A) Sb L_α/Sb L_β (Cr-tube); (B) Sb K_α (W-tube).

200 mg kg^{-1} antimony. The validity of the fits is also proven by the insignificant intercept of all lines.

With the help of these calibration graphs and by using the most sensitive Sb L_α peak, antimony can be determined in nodular cast iron with a relative standard deviation of 6% for samples containing 20 mg kg^{-1} and 1% for a concentration of 200 mg kg^{-1} antimony with a counting time of 3 × 100 s. Detection limits were calculated based on Currie's definition [9] as described earlier [7]. For measuring times of 3 × 100 s, the antimony detection limits are 1.7 mg kg^{-1} via Sb L_α, 4.8 mg kg^{-1} via Sb L_β, and 9.1 mg kg^{-1} via Sb K_α. These can be reduced to 0.7 mg kg^{-1}, 2.5 mg kg^{-1} and 3.9 mg kg^{-1} if counting times of 20-min (3 × 400 s) are used.

The authors gratefully acknowledge Ir. Lietaert and Dr. Ir. Defrancq of the CRIF (Centre for Scientific and Technical Research of the Metalworking Industry in Belgium) for preparing the specimen cast iron samples and for useful discussions. Financial support for this work was obtained from the Instituut voor Wetenschappelijk Onderzoek in de Nijverheid en de Landbouw and the CRIF-gieterijcentrum.

REFERENCES

1 H. Morrogh, A.F.S. Trans., 60 (1952) 439.
2 C. K. Donoho, Modern Castings, 46 (1964) 608.
3 J. C. Sawyer and J. F. Wallace, A.F.S. Trans., 76 (1968) 386.
4 E. Campomanes, A.F.S. Trans., 79 (1971) 57.
5 R. H. Aborn, A.F.S. Trans., 84 (1976) 503.
6 E. Campomanes, Giesserei, 65 (1978) 535.
7 F. Alluyn, J. Billiet, R. Dams and J. Hoste, Anal. Chim. Acta, 155 (1983) 209.
8 B. V. Kovacs, Giesserei-Praxis, No. 3 (1982) 37.
9 L. A. Currie, Anal. Chem., 40 (1968) 586.

Analytica Chimica Acta, 172 (1985) 127—138
Elsevier Science Publishers B.V., Amsterdam — Printed in The Netherlands

DETERMINATION OF TRACE CONCENTRATIONS OF ANTIMONY BY THE INTRODUCTION OF STIBINE INTO AN INDUCTIVELY-COUPLED PLASMA FOR ATOMIC EMISSION SPECTROMETRY

TAKETOSHI NAKAHARA* and NORIAKI KIKUI

Department of Applied Chemistry, College of Engineering, University of Osaka Prefecture, Sakai, Osaka 591 (Japan)

(Received 3rd October, 1984)

SUMMARY

A simple, rapid and sensitive method is described for the determination of trace concentrations of antimony by inductively-coupled plasma atomic emission spectrometry with hydride generation. Hydrochloric acid (1 M) is the best medium for stibine generation, but antimony(III) is also effectively reduced to stibine in 1 M malic acid or 0.5 M tartaric acid, whereas antimony(V) gives no significant signal in either of these acids. This permits the differential determination of Sb(III) and Sb(V). Most of the inter-element interference effects can be minimized by thiourea, but standard additions are recommended for accurate determinations. Thiourea is also effective in prereducing Sb(V) to Sb(III). The detection limit is 0.19 ng Sb ml^{-1} and the calibration graph is linear up to 100 μg ml^{-1}. The r.s.d. at 1 and 100 ng Sb ml^{-1} are 3.8 and 2.1%, respectively. The method is applied to copper metal and to speciation of antimony in waste water.

When inductively-coupled plasma/atomic emission spectrometry (i.c.p./a.e.s.) is used with conventional pneumatic nebulization, the detection limit for antimony is typically 32 [1] or 21 [2] ng ml^{-1}. The extreme inefficiency of liquid sample introduction to the i.c.p. by pneumatic nebulization (only 0.5—2% efficiency for most systems) has long been recognized as a weak link in the process, and several studies have been undertaken in order to enhance the sample introduction efficiency [3]. Among many types of more efficient sample introduction methods, an extensively documented technique is the generation of volatile hydrides, with subsequent single- or multi-element spectroscopic determination. Hydride generation techniques have been used widely in atomic absorption spectrometry (a.a.s.) for many years [4]. Thompson et al. [5, 6] first reported the successful combination of hydride generation with an i.c.p.

In the experiments described below, a flow-through hydride generation system is coupled with an argon plasma for the i.c.p./a.e.s. determination of trace concentrations of antimony. Its application to the determination of total concentrations of antimony in several copper samples and to the differential determination of antimony(III) and antimony(V) in waste waters is also reported.

0003-2670/85/$03.30

EXPERIMENTAL

Instrumentation

The experimental set-up and its components used in this study were as previously described [7, 8] except that the i.c.p./a.e.s. system was modified with an autotuning capability. Such an automatic impedance matching network was incorporated at the torch box to ensure that the impedance at the load coil is matched to that of the r.f. generator output. The impedance matching was done by using servo-driven vacuum capacitors, the performance of which was controlled by phase and magnitude detectors in the r.f. transmission line. A Nippon Jarrell-Ash Model ICAP-50SM inductively-coupled argon plasma emission spectrometer of a single-channel type was used in conjunction with a Nippon Jarrell-Ash Model HYD-1 continuous hydride generator which is an automated mixing-coil double stripping type, similar in concept to that of Thompson et al. [5], and with a Rikadenki Model R-21 chart recorder. The instrumentation used is described in Table 1.

The i.c.p. was initiated in the normal fashion with a Tesla discharge. On initiation, the impedance matching network automatically compensated for the change in impedance under running conditions. Thus, the automatic impedance matching network was undoubtedly indispensable for this hydride/i.c.p./a.e.s. system to overcome the primary difficulty encountered with interfacing the hydride generator to the i.c.p. caused by the inherent sensitivity of the plasma to any dramatic change in the nature or pressure of the gases flowing into the plasma.

When some emission lines of antimony were observed in the vacuum u.v. spectral region, the optical system between the i.c.p. and the monochromator

TABLE 1

Instrumentation

Component	Description
R.f. generator	Crystal-controlled type; 27.12 MHz; automatic power control; automatic impedance matching network; maximum output power, 2.0 kW
Plasma torch	All quartz; Fassel type
Gas for i.c.p.	Argon for coolant, plasma and carrier gases
Nebulizer	Pneumatic cross-flow type
Hydride generator	Continuous generation type with a peristaltic pump
Spectrometer	Ebert 0.5-m mounting; 1180 grooves mm^{-1} grating blazed at 240 nm; reciprocal linear dispersion (1st order), 1.6 nm mm^{-1}
Optics	Plasma source focussed as 1:1 image onto entrance slit with a 6-cm focal length quartz lens
Photomultiplier	Hamamatsu Photonics R-106UH
Signal measurement	D.c. amplification with 10-s integration, digital voltmeter readout; chart recorder

was enclosed so that nitrogen could be passed through the optical system including the monochromator in order to exclude air from the optical path. The detailed description of this modification will be given elsewhere [9].

Reagents

Unless otherwise stated, all reagents were of analytical-reagent grade or the highest purity available (Wako Pure Chemicals Co.). Stock solutions (1000 μg ml^{-1}) of antimony(III) and antimony(V) were prepared from antimony(III) potassium tartrate and antimony(V) chloride, respectively, and were assayed for antimony by conventional i.c.p./a.e.s. with solution nebulization, against a standard solution prepared from antimony (99.999%; Mitsuwa Chemical Co.). Solutions of lower concentrations were prepared by appropriate dilution of the stock solutions immediately before use. Laboratory-reagent grade sodium tetrahydroborate ($NaBH_4$) was used to prepare a stabilized solution in 1.0% (w/v) sodium hydroxide to decrease its rate of decomposition, which could be pumped without outgassing and could be used for at least several days.

Procedure

The operating conditions are summarized in Table 2. The wavelength was set, the plasma ignited, an antimony standard solution (10 μg Sb ml^{-1}) was aspirated into the plasma in a conventional manner, and the wavelength of

TABLE 2

Optimized operating conditions

	Hydride generation	Solution nebulization
Plasma		
R.f. power forward	1.6 kW	1.2 kW
Coolant gas flow rate	17.0 l min^{-1}	14.0 l min^{-1}
Plasma gas flow rate	1.0 l min^{-1}	1.0 l min^{-1}
Carrier gas flow rate	1.8 l min^{-1}	0.48 l min^{-1}
Wavelength	206.833 nm	206.833 nm
Observation height (above load coil)	18 mm	18 mm
Slit width	25 μm	25 μm
Slit height	2 mm	2 mm
Integration time	10 s	10 s
Hydride generation		
Sample solution acidity	1.0 M HCl	
Sample solution flow rate	17.0 ml min^{-1} (tube, 3.12 mm i.d.)	
$NaBH_4$ concentration	1.5% (w/v) in 1.0% (w/v) NaOH	
$NaBH_4$ solution flow rate	5.0 ml min^{-1} (tube, 1.56 mm i.d.)	
Carrier gas (I) flow rate	0.2 l min^{-1}	
Carrier gas (II) flow rate	1.6 l min^{-1}	

antimony was scanned manually until the peak was located. The argon carrier gas flow for solution nebulization was stopped and previously acidified working standard or sample solutions and the alkaline sodium tetrahydroborate solution were continuously introduced into the hydride generator by using two channels of a four-channel peristaltic pump and Tygon tubing. The generated stibine and excess of hydrogen were fed into the i.c.p. by a continuous flow of argon carrier gas via the drain outlet of the conventional nebulizer chamber. (The carrier gas flow system to the plasma torch was modified to allow either a conventional nebulizer or the hydride generator to be used for sample introduction. In this manner, it becomes easy to interchange the system from the conventional pneumatic nebulizer to the hydride generator and vice versa.) All emission intensities, when stabilized, were integrated at least in triplicate over 10 s. For off-line background correction at the same wavelength as the analyte, background emission (including that from the reagent blank) integrated over the same period (10 s) was subtracted from all line emission data. Under the operating conditions shown in Table 2, the antimony emission signal began to rise from the baseline within 10 s of an antimony solution being pumped and reached a plateau after ca. 15 s. The tail of the signal returned to the baseline within 20 s of the solution being exchanged for a blank solution (hydrochloric acid).

RESULTS AND DISCUSSION

Optimization of operating conditions

In order to obtain a maximum line-to-background intensity ratio, I_n/I_b (I_n, net analyte emission intensity; I_b, background emission intensity) for antimony, various operating parameters were optimized individually while the other parameters were kept at their optimum values. The parameters investigated were r.f. forward power to the plasma, analytical wavelength, observation height, flow rates of argon coolant, plasma and carrier gases, concentration and flow rate of the tetrahydroborate solution, and the acidity and flow rate of the sample solution. Solutions with 0.1 μg ml^{-1} antimony(III) were, unless otherwise stated, used in optimizing the operating parameters and in the following study.

Table 3 lists the background-corrected line intensities (I_n), line-to-background intensity ratios (I_n/I_b) and background equivalent concentrations obtained at the major emission lines of antimony after hydride generation or conventional solution nebulization. The antimony line in the vacuum u.v. region was observed with the nitrogen-purged optical system. The Sb(I) 259.809- and 259.805-nm doublets could not be separated by the monochromator used. The 206.833-nm line was throughout used as the analytical line except where noted.

The effects of several inorganic acids in the reaction medium on the reduction of antimony to stibine were investigated. The line-to-background intensity ratios for antimony were first studied in reaction media of 0.2—5 M

TABLE 3

Emission characteristics of major antimony lines

Wavelength (nm)	Hydride generation (0.1 μg Sb ml^{-1})			Solution nebulization (10 μg Sb ml^{-1})		
	I_n[a]	I_n/I_b[a]	b.e.c.[b]	I_n	I_n/I_b	b.e.c.
Sb(I) 259.809 Sb(I) 259.805	1.56	0.44	0.014	1.72	0.32	3.12
Sb(I) 252.852	1.49	0.45	0.014	1.54	0.33	2.97
Sb(I) 231.147	1.58	0.89	0.070	1.79	0.70	1.14
Sb(I) 217.919	0.35	0.34	0.019	0.35	0.21	4.67
Sb(I) 217.581	1.47	0.19	0.007	1.55	0.92	1.07
Sb(I) 206.833	1.00	1.00	0.006	1.00	1.00	0.99
Sb(I) 187.115[c]	0.14	0.43	0.015	0.14	0.33	2.96

[a] I_n = antimony intensity, I_b = background intensity, relative to the intensity or intensity ratio of the 206.833-nm line taken as 1.00. [b] Background equivalent concentration (μg Sb ml^{-1}). [c] Nitrogen-purged optical system [9].

hydrochloric, nitric, perchloric or sulfuric acids. The results obtained are shown in Fig. 1. As a result, an acidic reaction medium of 1 M hydrochloric acid was chosen for further work, if not noted otherwise. The antimony signal increased continuously with increasing concentration of phosphoric acid. This proved to result from the presence of a significant amount (μg ml^{-1} range) of antimony as an impurity in the phosphoric acid used [10]. In further tests on reduction efficiency, organic acids, including 0.2—5 M acetic and 0.2—2.5 M malic and tartaric acids were used. The results obtained are shown in Fig. 2. It should be noted that the line-to-background intensity

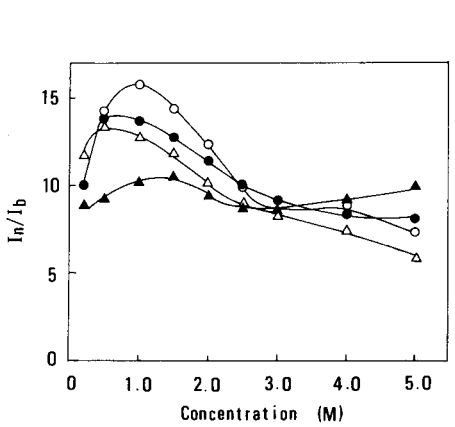

Fig. 1. Effects of acid concentration in the reaction medium: (○) hydrochloric; (●) perchloric; (△) sulfuric; (▲) nitric acid.

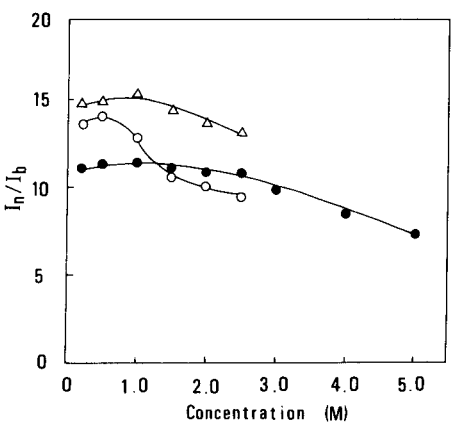

Fig. 2. Effects of concentration of organic acids in the reaction medium: (△) malic; (○) tartaric; (●) acetic acid.

ratio for antimony from the malic acid reaction medium is almost the same as from hydrochloric acid (Figs. 1 and 2). Therefore, malic acid is a possible substitute for hydrochloric acid as a reaction medium for stibine generation. It was also found that in a malic or tartaric acid medium, antimony(V) gave little or no signal compared with equal concentrations of antimony(III). This may be due to too low an acidity for stibine generation from antimony(V); the solutions of 1 M malic acid and 0.5 M tartaric acid had pH values of 1.70 and 1.71, respectively.

Prereduction step

Hydride generation in a.a.s. is often dependent on the oxidation state of the element to be reduced [4, 11, 12], and the combined hydride/i.c.p/a.e.s. method was expected to exhibit such effects [5, 7, 13]. As shown in Fig. 3, antimony(III) gave a higher sensitivity than antimony(V). It can be seen that both the Sb(V):Sb(III) intensity ratio, $I_n(V)/I_n(III)$, and the emission intensity from antimony(V), $I_n(V)$, reach a maximum in ca. 0.2 M hydrochloric acid, while the optimum acidity for stibine generation from antimony(III) is 1 M hydrochloric acid, as shown in Fig. 1. An Sb(V):Sb(III) intensity ratio of 0.24 was found at 1 M hydrochloric acid (Fig. 3), whereas a value of 0.12 was reported earlier [5]. Therefore, antimony(V) must be reduced to antimony(III) prior to hydride generation for the determination of total antimony.

Prereduction of antimony(V) to antimony(III) has been achieved by the addition of various reagents. In the present work, the use of potassium iodide ($\leqslant$5% w/v) was evaluated. In the presence of $\geqslant$1% potassium iodide, antimony in both oxidation states gave the same emission intensity. Prereduction by thiourea (1×10^{-4}—1 M) was also examined. The results

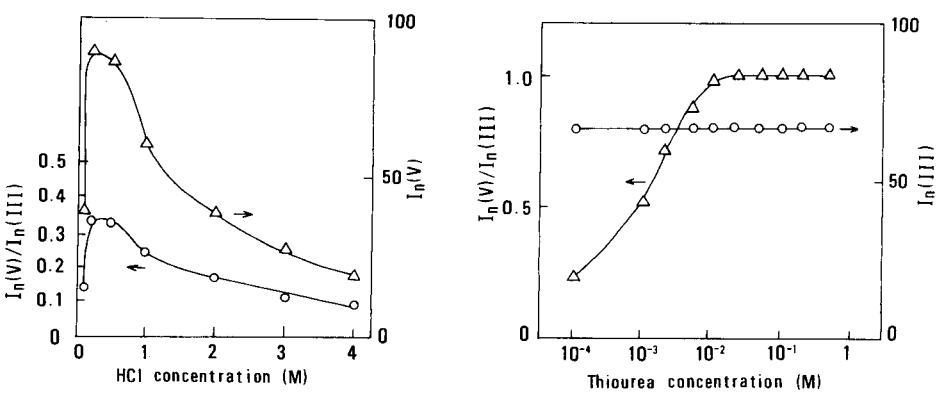

Fig. 3. Effects of hydrochloric acid concentration: (○) on Sb(V):Sb(III) emission intensity ratio; (△) on Sb(V) emission intensity. (Sb(III) = Sb(V) = 0.1 μg ml^{-1}.)

Fig. 4. Effect of thiourea concentration: (△) on Sb(V):Sb(III) emission intensity ratio; (○) on Sb(III) emission intensity. (1 M hydrochloric acid reaction medium; Sb(III) = Sb(V) = 0.1 μg ml^{-1}.)

obtained (Fig. 4) show that the addition of $>2 \times 10^{-2}$ M thiourea is also effective for prereducing antimony(V) to antimony(III). Little has been reported previously on the use of thiourea for this prereduction, so in the following study, 0.1 M thiourea was added as a prereductant for the determination of total antimony. As will be described below, both 1% potassium iodide and 0.1 M thiourea also appear to be effective in eliminating or minimizing some depressing interferences.

Calibration, detection limit and precision

Under the optimized conditions given in Table 2, calibration graphs were obtained at 206.833 and 217.581 nm by using freshly prepared antimony standard solutions. Typical graphs are shown in Fig. 5. For comparison, the corresponding graphs obtained by solution nebulization under the operating conditions given in Table 2 are shown also in Fig. 5. The lowest point of each corresponds to the smallest concentration of the analyte that can realistically be determined.

The detection limits, calculated using the 3σ recommendation [14], at the 206.833-nm line were 0.19 and 25 ng Sb ml^{-1} by hydride generation and solution nebulization, respectively. Detection limits of 0.07 [15] and 0.08 ng ml^{-1} [16] are the lowest reported by hydride generation i.c.p./a.e.s.; they were obtained by preconcentration procedures with use of a poly-(dithiocarbamate) resin and a liquid nitrogen condensation trap for the collection of stibine, respectively. Otherwise, the lowest value previously reported was 0.7 ng ml^{-1} [17, 18]. The relative standard deviations (r.s.d.) for 10 replicate measurements were 3.8, 2.5, 2.1 and 1.2% for 1, 10, 100 and 500 ng Sb ml^{-1}, respectively.

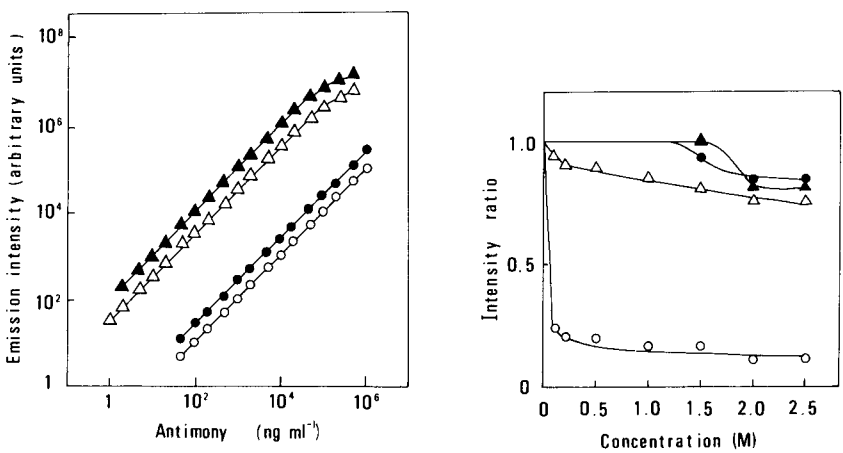

Fig. 5. Calibration graphs for antimony. Wavelengths: (○, △) 206.833; (●, ▲) 217.581 nm. Method: (△, ▲) hydride generation; (○, ●) solution nebulization.

Fig. 6. Effect of concentration of mineral acids in 1 M hydrochloric acid: (●) perchloric; (▲) phosphoric; (△) sulfuric; (○) nitric acid (0.1 μg Sb ml^{-1}).

Differential determination of antimony(III) and antimony(V)

As shown in Fig. 2, antimony(III) was reduced to stibine in 1 M malic acid or 0.5 M tartaric acid, whereas in either of these media antimony(V) gave little or no signal. This permits the selective determination of antimony-(III) and antimony(V). Antimony(III) is determined by using a reaction medium of 1 M malic acid (or 0.5 M tartaric acid) and total antimony is separately determined in the presence of 0.1 M thiourea as prereductant. Thus, antimony(V) can be determined by difference. This technique was applied to waste-water analysis (see below).

Possible interferences

Effect of mineral acids. As mineral acids other than hydrochloric acid are often used for sample decomposition, their effects were examined in the presence of 1 M hydrochloric acid. The results obtained are shown in Fig. 6. The intensity ratio in Fig. 6 is relative to 1.00 for the net intensity given by a 0.1 μg Sb ml^{-1} solution acidified with 1 M hydrochloric acid only. The pronounced depressing effect of nitric acid is probably due to oxidation of antimony(III) to (V) before stibine generation. The intensity ratio in the presence of nitric acid is very close to the Sb(V):Sb(III) intensity ratio of 0.24 described above. The presence of 0.1 M thiourea was found almost completely to eliminate the depressing interferences from $\leqslant$2.5 M mineral acids.

Effect of diverse elements. The determination of antimony by hydride generation/a.a.s. is well known to be susceptible to interferences from various elements [4, 11, 12], in particular, those which react with sodium tetrahydroborate in acidic media to form a volatile hydride or precipitate as the element. Elements that form volatile hydrides are those of Periodic groups IVA, VA and VIA; ions which are reduced to the elements belong to Groups IB, IIB and VIII. It was expected that similar interferences were likely to take place in the present procedure. Under the experimental conditions listed in Table 2, the effects of various species at concentrations 1000-fold greater than antimony were first investigated, added as the same compounds as described previously [19], unless otherwise noted.

The results, showing many depressing interferences, are shown in Table 4. Interference was considered to have occurred when the intensity changed by $>$5% from that for antimony alone. The following did not interfere: As, Ba, Be, Ca, Cd, Ce, Cs, Cr(III), Ga, Ge, In, K, La, Li, Mg, Mn, Mo, Na, P, Pb, Rb, Si, Sn, Sr, Tl, Th, Y and Zn. No element was found to cause an enhancing effect. The emission intensity for antimony was measured at 217.581 nm when germanium was present; its hydride (GeH_4) was generated and was introduced into the i.c.p. together with stibine. It gave a large enhancement at 206.833 nm owing to spectral overlap of Ge(I) 206.866-nm line [1]. These lines could not be separated with the monochromator used here. Most of the interferences shown in Table 4 are very similar to those in a.a.s. [4, 11, 12] and i.c.p./a.e.s. [6] studies. The tolerance limits for the inter-

TABLE 4

Interferences from diverse elements

Element[a]	Added as	1 M HCl		With 1% (w/v) KI present		With 0.1 M thiourea present	
		RI[b]	Limit[c]	RI	Limit	RI	Limit
Ag	$AgNO_3$	0.05	0.2	—[d]	—	—	—
Al	Al in HCl	0.64	40	—	—	—	—
Au	$HAuCl_4$	0.03	0.02	0.13	0.05	0.65	5
B	H_3BO_3	0.30	20	—	—	—	—
Bi	$Bi(NO_3)_3$	0.24	0.5	—	—	0.93	85
Co	$CoCl_2$	0.19	4	0.34	4	0.88	50
Cr	K_2CrO_4	0.23	0.005	—	—	—	—
Cu	$CuSO_4$	0.51	1	—	—	—	—
Fe	$FeCl_3$	0.27	0.1	0.75	5	—	—
Hg	$Hg_2(NO_3)_2$	0.48	50	—	—	0.84	55
Ni	$NiCl_2$	0.04	0.2	0.06	0.2	0.74	20
Pd	$PdCl_2$	0.02	0.02	0.04	0.01	0.25	10
Pt	H_2PtCl_6	0.03	0.1	0.06	0.02	—	—
Se	SeO_2	0.58	10	—	—	—	—
Te	Na_2TeO_3	0.42	5	0.38	1	0.87	65
Ti	Ti in HCl	0.87	70	—	—	—	—
V	NH_4VO_3	0.30	1	—	—	—	—
W	Na_2WO_4	0.55	10	0.83	10	—	—
Zr	$ZrCl_4$	0.48	10	—	—	—	—

[a]Added at 1000-fold ratio to 0.1 μg Sb(III) ml^{-1}. [b]Relative intensity compared to 1.00 for antimony alone. [c]Tolerance limit, i.e., maximum concentration (μg ml^{-1}) found to have no interference. [d]No interference up to 1000-fold ratio over Sb(III).

ferences, expressed as maximum concentrations found to have no significant effect, were determined; these are also given in Table 4.

Effect of thiourea on the interferences. The usefulness of thiourea for reduction of antimony(V) to antimony(III) prior to stibine generation was shown above. In order to minimize or eliminate depressing interferences in hydride generation/a.a.s. of antimony, several workers [4, 11, 12] have added masking agents, such as thiosemicarbazide, 1,10-phenanthroline, EDTA, pyridine-2-aldoxime, cyanide and iodide, or have separated the analyte from interferents by coprecipitation, liquid-liquid extraction or chromatography. Recently, the addition of thiourea as a masking agent was found to be effective in the determination of arsenic [20] and selenium [21] by hydride generation/a.a.s.

In addition to their use for prereduction of antimony(V), potassium iodide and thiourea were investigated as potential masking agents and added to the acidified sample solution at concentrations of 1% or 0.1 M, respectively. The results obtained are shown in Table 4. The tolerance limits for interferences in the presence of potassium iodide or thiourea are also shown in Table 4. It should be noted that thiourea is more effective in eliminating

or minimizing the interferences than potassium iodide. No further attempt was made to minimize or eliminate the depressing interferences from the remaining seven elements (Table 4).

Determination of antimony in copper samples and waste waters

To demonstrate the accuracy and precision of the present method, the following procedures were used for the determination of antimony in copper samples from the Mitsubishi Metal Corporation, Tokyo and in waste waters taken at the inlet of the Wastewater Treatment Facility, University of Osaka Prefecture.

A 0.5-g copper sample was dissolved in 2 ml of concentrated nitric acid by heating slowly on a hot plate. After complete dissolution, the solution was diluted exactly to 50 ml with distilled water. It was expected that copper at >1000-fold weight ratio to antimony was likely to interfere even in the presence of 0.1 M thiourea. A recovery test, therefore, was done by adding known amounts of antimony to the sample solutions and applying the recommended procedure, in a reaction medium of 1 M hydrochloric acid. The recovery of the added antimony was almost quantitative (96 ± 3%, n = 5), so that the method of standard additions was used for antimony determinations. The results for copper samples are shown in Table 5. They are in good agreement with the certified values.

The presence of some components of waste waters would be expected to cause low results in the determination of antimony. Recovery studies, therefore, were made by adding known amounts of antimony(III) and (V) to the samples and applying the recommended procedure, with a reaction medium of 1 M malic acid for the determination of antimony(III) and with 1 M hydrochloric acid and 0.1 M thiourea for the determination of total antimony. The mean recoveries of added antimony were in the range 94–104%, depending on samples of waste water. For accurate determination of antimony, therefore, a standard addition method was essential. A sample taken at the inlet of the Wastewater Treatment Facility was immediately filtered through a No. 2 filter paper (Toyo Filter Paper Co. Ltd., Tokyo),

TABLE 5

Determination of antimony in copper metal

Sample	Antimony ($\mu g\ g^{-1}$)	
	Certified value	This work[a]
A	11	10.8 ± 0.2 (n = 8)
B	25	25.4 ± 1.2 (n = 7)
C	53	53.1 ± 3.0 (n = 6)
D	360	356 ± 15 (n = 5)

[a]Mean ± standard deviation.

TABLE 6

Determination of antimony in waste waters

Sample (1984)	Antimony (ng ml^{-1})		
	This work[a]		Hydride generation/ nondispersive a.f.s.[b]
	Sb(III)	Sb(V)	Total Sb
Feb. 27	13.4 ± 0.9	3.2 ± 0.2	16.2
Feb. 28	4.0 ± 0.3	n.d.[c]	4.4
Mar. 16	9.9 ± 0.4	1.5 ± 0.1	12.1
Mar. 17	7.8 ± 0.4	n.d.	7.6
Mar. 19	7.0 ± 0.5	n.d.	7.2

[a]Mean ± standard deviation of 5 replicate determinations. [b]Average of triplicate determinations. [c]Not determinable.

and the filtrate was analyzed for antimony(III) and antimony(V) after spiking with antimony(III) and (V) in the range 5—50 ng ml^{-1}. The results for several samples of waste water are given in Table 6 and show good agreement between the proposed method and hydride generation/nondispersive atomic fluorescence spectrometry (a.f.s.) applied as described previously [10, 22].

Conclusions

The method described proved to be a useful and rapid approach to improving the sensitivity of antimony determinations. The detection limit of this hydride generation/i.c.p./a.e.s. system for antimony is improved by a factor of about 10^3 over the conventional solution nebulization technique. This dramatic decrease in detection limit could make the determination of traces of antimony by i.c.p./a.e.s. practical for a wide range of samples. In addition, thiourea appears to be effective in reducing antimony(V) to antimony(III) before hydride generation and in eliminating or minimizing serious interferences from several elements. Although the masking mechanism of thiourea is not known in detail, its effect on copper, for example, may arise from complex formation of copper(I) with thiourea after its reduction of copper(II) [23].

With the use of malic acid or tartaric acid as an acidic medium for stibine generation, solutions of antimony(V) give almost no response compared to antimony(III). This permits a differential determination of antimony(III) and (V). The present method was successfully applied to the determination of antimony in some samples of copper and waste water. The use of purer reagents such as sodium tetrahydroborate should make it possible to decrease the background emission including the antimony blank, resulting in some improvement in the lowest determinable concentration of antimony as well as in the linear calibration range. The application of this technique

looks promising and its extension to other hydride-forming elements is being investigated.

The authors are grateful to The Mitsubishi Metal Corporation, Tokyo, for providing samples of copper. The present work was partially supported by a Grant-in-Aid for Scientific Research (No. 59550515) from the Ministry of Education, Science and Culture, Japan.

REFERENCES

1 R. K. Winge, V. J. Peterson and V. A. Fassel, Appl. Spectrosc., 33 (1979) 206.
2 P. W. J. M. Boumans, Line Coincidence Tables for Inductively Coupled Plasma Atomic Emission Spectrometry, Pergamon Press, Oxford, 1980, Table 588.
3 R. F. Browner and A. W. Boorn, Anal. Chem., 56 (1984) 786A, 875A.
4 T. Nakahara, Prog. Anal. Atom. Spectrosc., 6 (1983) 163.
5 M. Thompson, B. Pahlavanpour, S. J. Walton and G. F. Kirkbright, Analyst (London), 103 (1978) 568.
6 M. Thompson, B. Pahlavanpour, S. J. Walton and G. F. Kirkbright, Analyst (London), 103 (1978) 705.
7 T. Nakahara, Anal. Chim. Acta, 131 (1981) 73.
8 T. Nakahara, Appl. Spectrosc., 37 (1983) 539.
9 T. Nakahara, Spectrochim. Acta, Part B, 40 (1985) 293.
10 T. Nakahara, S. Kobayashi and S. Musha, Anal. Chem., 51 (1979) 1589.
11 R. G. Godden and D. R. Thomerson, Analyst (London), 105 (1980) 1137.
12 W. B. Robbins and J. A. Caruso, Anal. Chem., 51 (1979) 889A.
13 D. D. Nygaad and J. H. Lowry, Anal. Chem., 54 (1982) 803.
14 I.U.P.A.C., Pure Appl. Chem., 45 (1976) 99.
15 P. Fodor and R. M. Barnes, Spectrochim. Acta, Part B, 38 (1983) 229.
16 M. H. Hahn, K. A. Wolnik, F. L. Fricke and J. A. Caruso, Anal. Chem., 54 (1982) 1048.
17 K. A. Wolnik, F. L. Fricke, M. H. Hahn and J. A. Caruso, Anal. Chem., 53 (1981) 1030.
18 D. A. Rose, Anal. Proc., 20 (1983) 436.
19 T. Nakahara and S. Musha, Anal. Chim. Acta, 75 (1975) 305; 80 (1975) 47.
20 C. J. Peacock and S. C. Singh, Analyst (London), 106 (1981) 931.
21 R. Bye, L. Engvik and W. Lund, Anal. Chem., 55 (1983) 2457.
22 T. Nakahara, S. Kobayashi and S. Musha, Anal. Chim. Acta, 101 (1978) 375.
23 E. I. Onstott and H. A. Laitinen, J. Am. Chem. Soc., 72 (1950) 4724.

Analytica Chimica Acta, 172 (1985) 139—145
Elsevier Science Publishers B.V., Amsterdam — Printed in The Netherlands

MICROWAVE-INDUCED PLASMA EMISSION SPECTROMETRIC DETERMINATION OF BROMIDE

M. M. ABDILLAHI, W. TSCHANEN[a] and R. D. SNOOK*
Department of Chemistry, Imperial College, London SW7 2AY (Great Britain)
(Received 21st August 1984)

SUMMARY

An argon microwave-induced plasma is used for the determination of traces of bromide in 10 μl of solution. Bromine is generated by using potassium dichromate in concentrated sulphuric acid, and bromine molecular emission is measured at 291 nm. The detection limit is 50 ng of bromide and log-log calibrations are linear (slope 2.0) in the range 0.05—50 μg. There are no major interferences.

There are few satisfactory emission spectroscopic methods for the determination of bromide in solutions. McCormack et al. [1] used gas chromatography (argon) coupled with a microwave-induced plasma (m.i.p.) as detector, and reported a detection limit for bromine of 2×10^{-7} g s^{-1}, using the Br(I) 298.5-nm emission. This detector is applicable to the gaseous effluent, but no application to solutions was reported. Bache and Lisk [2] reported a 2×10^{-11} g s^{-1} detection limit by using a gas chromatograph (helium) microwave-induced plasma combination. McLean et al. [3] also used a similar system and reported a detection limit of 9×10^{-11} g s^{-1}. Both used low-pressure helium plasmas for determining bromine, at Br(II) 478.55 nm and Br(II) 470.486 nm, respectively. Beenakker [4] reported a better detection limit (5×10^{-12} g s^{-1}) with the Br(II) line at 470.5 nm, by using a gas chromatograph coupled with a TM_{010} cavity operated at atmospheric pressure. Carnahan and Caruso [5] reported a detection limit of 8 ng at the 478.6-nm emission line by using electrothermal vaporization into a helium m.i.p. in a successful attempt to determine high-molecular weight organic halogen compounds. Inductively-coupled plasma atomic emission spectrometry has been used for the determination of bromine [6] but a poor detection limit of 200 μg was reported.

This paper describes a spectrometric method for the determination of bromide in solution. Bromine is generated by using potassium dichromate in concentrated sulphuric acid, and passed into a m.i.p. where the molecular emission of bromine is observed at 291 nm.

---

[a]Present address: ETH, Zurich, Switzerland.

0003-2670/85/$03.30

EXPERIMENTAL

Instrumentation and reagents

Similar equipment to that reported by Alder et al. [7] for the determination of chlorine was used for determining bromine. A resistively heated coil was added between the generating cell and the microwave plasma to prevent condensation of bromine. A reflected power meter placed between the generator and cavity was used to ensure optimum tuning of the cavity. Vapour phase analyte generation was as reported earlier [7]. The dispersed radiation was detected by a photomultiplier (EMI 9601B) mounted behind the exit slit of the monochromator, and recorded by a potentiometric chart recorder (JJ Lloyd Model CR450). Specifications of the other equipment used are given in Table 1.

Stock solutions (1000 μg ml^{-1}) of bromide were prepared freshly by dissolving sodium bromide in Milli-Q water. The generating solution was prepared from 0.05 g of potassium dichromate and 10 ml of concentrated sulphuric acid. This generating solution can be prepared immediately before use, or as a stock solution which is stable for weeks. All reagents were of analytical-reagent grade.

Procedure

A 4-ml portion of the generating solution was placed in the cell with the taps appropriately adjusted to keep the plasma alight [7]. A 10-μl aliquot of sample was added through a Suba-seal septum in the side arm. After 1 min, the generated bromine was swept into the m.i.p. by suitable tap switching [7]. Bromine molecular emission at 291 nm was measured, under the optimum conditions given in Table 2.

RESULTS AND DISCUSSION

Wavelength selection

The molecular emission spectrum of bromine in argon has been reported to consist of a short discrete band system in the region 297—315 nm, an extensive discrete band system in the region 267—295 nm and a short, weak

TABLE 1

Specification of equipment

Microwave generator	Microtron 200 (EMS, Wantage, Berks.)
Cavity	Broida 3/4 wave; silica tube (2 mm i.d., 4 mm o.d.)
Monochromator	Optica Model CF2768, 0.75 m: practical resolution of 0.06 nm at 100-μm slit width
Optics	M.i.p. imaged in 1:1 ratio on the entrance slit with a 7.5-cm focal length silica lens
Sample injector	100-μl BCL micropipette with disposable tips

TABLE 2

Operating conditions for m.i.p. determination of bromine

Generator forward power	30 W	Generating solution volume	4 ml
Reflected power	minimum	Sample solution volume	10 μl
Photomultiplier e.h.t.	800 V	Entrance and exit slit widths	100 μm
Argon flow rate	2 l min^{-1}	Wavelength	291 nm
Generating cell volume	25 ml		

discrete system at 259—260 nm [8]. Pearse and Gaydon [9] listed bromine molecular emission bands from a discharge tube containing bromine in argon, the strongest of which is at 311.07 nm. This band, however, is subject to spectral overlap by emissions from molecular impurities (OH, NH, CO and H_2O) in the argon m.i.p. Venkateswarlu and Verma [8] found that when bromine is excited in the presence of argon the spectrum obtained is different from that in the absence of argon.

In the present investigation, the band system between 267 and 295 nm was investigated in the m.i.p., with bromine continuously introduced from the generating apparatus. It was found that the molecular bromine emission had three maxima, at 290.4, 291.3 and 292.4 nm. The 291.3-nm head was the most intense, as shown in Fig. 1.

Methods of bromine generation

Three methods for bromine generation were investigated

$$MnO_2 + 4H^+ + 2Br^- \rightarrow Mn^{2+} + 2H_2O + Br_2 \quad (1)$$

$$ClO_3^- + 6H^+ + 6Br^- \rightarrow Cl^- + 3H_2O + 3Br_2 \quad (2)$$

$$IO_3^- + 6H^+ + 6Br^- \rightarrow I^- + 3H_2O + 3Br_2 \quad (3)$$

None of these reactions is suitable, however. Reaction (1) requires heating, and even at 60°C the efficiency of bromine generation was poor. Reactions (2) and (3) were used successfully but the ability to generate from successive injections of solution soon deteriorated. Potassium permanganate in concentrated sulphuric acid, which was used for chlorine generation [7], was also tried for the generation of bromine but did not generate bromine at low bromide levels (<0.5 μg).

The most suitable reaction found for generating bromine was that with potassium dichromate in concentrated sulphuric acid

$$Cr_2O_7^{2-} + 14H^+ + 6Br^- \rightarrow 2Cr^{3+} + 7H_2O + 3Br_2 \quad (4)$$

The green colour which appears after the addition of a total of 5 ml of sample solution to 4 ml of the generating solution, indicates that the chromium(VI) has finally been reduced to chromium(III).

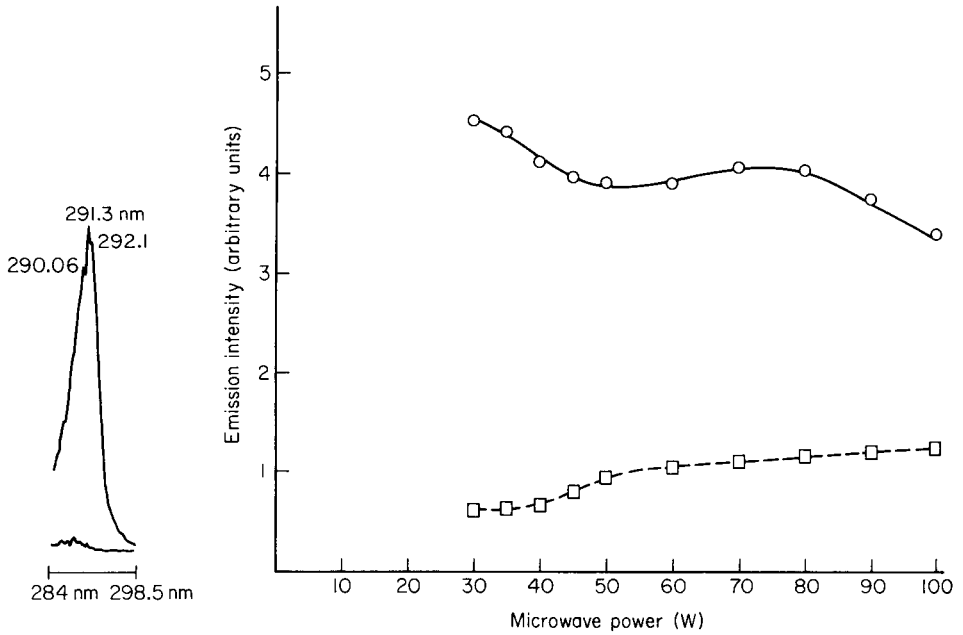

Fig. 1. Bromine band emission from the m.i.p. Lower spectrum: argon alone. Upper spectrum: argon with bromine generated continuously through the scan.

Fig. 2. Emission intensities as a function of microwave power: (○) bromine band; (□) background.

Optimization

The best sensitivity and precision were achieved by optimizing the instrumental system through the univariate search method [10]. For this procedure, bromine was generated from 10-μl injections of 500 μg ml^{-1} bromide solution and swept into the m.i.p. to give a Br_2 emission peak. The cavity was tuned for minimum reflected power for these experiments. The parameters optimized were photomultiplier voltage, slit widths, microwave forward power and argon plasma gas flow rate. The best attainable signal-to-noise ratio for the photomultiplier was found to be at 800 V and the slit-width optimum was 100 μm which yields a practical resolution of 0.06 nm (measured between the Mn 259.373-nm line and the Mn(II) 260.569-nm line). This apparently wide optimum slit width arises because a relatively wide band system is being measured (Fig. 1), rather than a narrow atomic line.

The effect of changing forward power on the Br_2 emission signal at the optimum slit widths and photomultiplier voltage is shown in Fig. 2. As the forward power is increased from the minimum attainable value of 30 W, there is a gradual decrease in the emission signal and a gradual increase in background. For all subsequent experiments, therefore, the forward power used was 30 W. It is possible that further improvements could be obtained

below 30 W, but this was the minimum output of the generator used. For routine work, where long-term source stability is important, there may be an advantage in using the plateau region between 40 and 80 W forward power, where the emission signal and background are insensitive to changes in microwave power.

The argon flow rate for the plasma was also optimized. The results are shown in Fig. 3. Between 0.5 and 2.5 l min^{-1}, there is only a slight improvement in signal-to-background ratio. Below 0.5 l min^{-1}, the gas flow rate is insufficient to sweep the bromine into the plasma for an accurate peak height measurement to be made. Above 2.5 l min^{-1}, the plasma becomes unstable. A flow rate of 2.0 l min^{-1} was chosen for all subsequent experiments. Repeated optimization of the system gave the same results. These conditions are summarized in Table 2.

Calibration, detection limit and interferences

Double logarithmic calibration graphs, as shown in Fig. 4, were obtained under the optimal operating conditions. They are linear with a slope of 2.0 over the range 0.05—50 μg bromide injected as 10-μl samples. The detection limit, defined as the mass of bromide required to produce a signal twice the standard deviation of the blank, was 50 ng. This limit depended mainly on the condition of the generating solution and was difficult to obtain after ca. 2 ml of sample solution (ca. 200 × 10-μl injections) had been added owing to the reduction of chromium(VI) to an intermediate oxidation state.

When a single bromide sample was introduced, the responses obtained

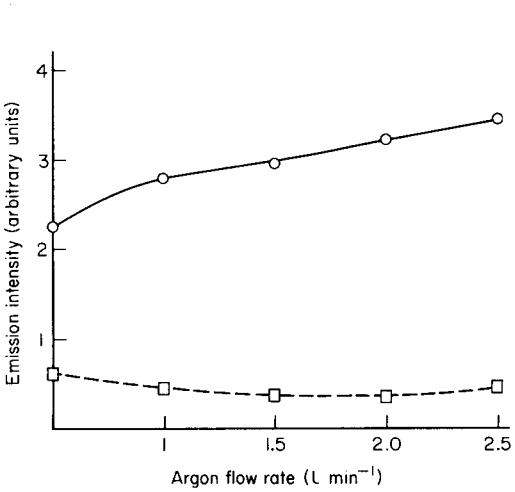

Fig. 3. Emission intensities as a function of argon flow rate: (○) bromine band; (□) background.

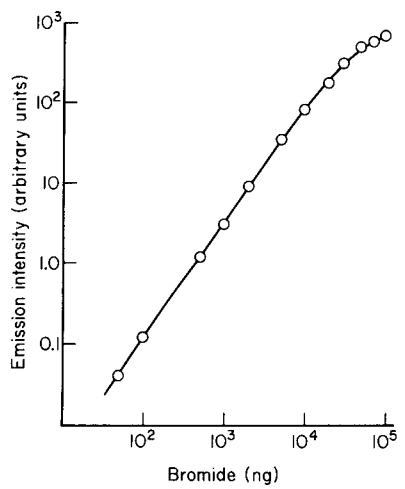

Fig. 4. Bromine calibration graph derived from first peak-height measurements (plasma held perpendicular to monochromator).

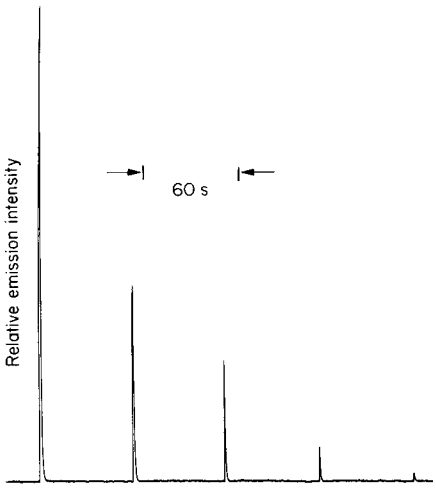

Fig. 5. Bromine emission peaks recorded at 1-min generation intervals for a single bromide sample.

were as given in Fig. 5, for successive 1-min degassing periods. The first peak height is representative of the cumulative peak heights, because each peak fits a geometric series [7], so that only the first needs to be recorded. After the recording of the first peak heights, the system is flushed with argon for 3 min before the next injection is made, to eliminate remaining bromine.

Interferences

The 291-nm bromine molecular emission band is free from spectral interferences from argon lines or impurities in the plasma gas. There is no interference from the silica plasma tube or other materials used in the construction of the generation cell/plasma assembly.

Several potentially interfering elements and anions were studied. A 1000-fold weight excess of Na^+, Fe^{2+}, Hg^{2+}, nitrate and sulphate in a solution of 1 μg Br^- ml^{-1} had no effect on the magnitude of the signals obtained. At such high concentrations of chloride or fluoride, however, an enhancement was observed which was directly proportional to the amount of chloride or fluoride added to the bromide solution. It is assumed, therefore, that this enhancement is attributable to bromide in these reagents (0.1% in the potassium chloride and 0.25% in the sodium fluoride used). These levels are higher by an order of magnitude for those quoted for the AnalaR reagent which suggests that there is a further source of bromine. No bromine blank was observed when excess of iodide was added to the generating solution, nor when fluoride or chloride was present in <50-fold amount.

We thank the Laboratory of the Government Chemist for support of this work.

REFERENCES

1 A. J. McCormack, S. S. C. Tong and W. D. Cooke, Anal. Chem., 37 (1965) 1470.
2 C. A. Bache and D. J. Lisk, Anal. Chem., 39 (1967) 786.
3 W. R. McLean, D. L. Stanton and G. E. Penketh, Analyst (London), 38 (1973) 432.
4 C. I. M. Beenakker, Spectrochim. Acta, 32B (1977) 173.
5 J. W. Carnahan and J. A. Caruso, Anal. Chim. Acta, 136 (1982) 261.
6 D. L. Windsor and M. B. Denton, J. Chromatogr. Sci., 17 (1979) 492.
7 J. F. Alder, Q. Jin and R. D. Snook, Anal. Chim. Acta, 120 (1980) 147.
8 P. Venkateswarlu and R. D. Verma, Proc. Indian Acad. Sci., 46 (1957) 251.
9 R. E. B. Pearse and A. G. Gaydon, The Identification of Molecular Spectra, 3rd edn., Chapman and Hall, London, 1965.
10 M. J. Box. D. Davis and W. H. Swann, Non-linear Optimization Techniques, Oliver & Boyd, Edinburgh, 1969.

Analytica Chimica Acta, 172 (1985) 147—156
Elsevier Science Publishers B.V., Amsterdam — Printed in The Netherlands

DIRECT DETERMINATION OF ARSENIC IN BLOOD SERUM BY ELECTROTHERMAL ATOMIC ABSORPTION SPECTROMETRY

Y. PEGON

Laboratoire de Biochimie D, Hôpital Edouard Herriot, Place d'Arsonval, 69374 Lyon Cedex 2 (France)

(Received 17th July 1984)

SUMMARY

A method for the direct determination of arsenic in human blood serum is described. To suppress loss of arsenic by volatilization and to remove chemical interferences in graphite-furnace atomic absorption spectrometry, the formation of involatile compounds with graphite, or with a matrix modifier is tested. With aqueous solutions, two sorts of interactions between graphite and arsenic are shown. But, in presence of serum, these interactions do not occur. Among 18 matrix modifiers tested, nickel gives the best sensitivity when used at high concentrations in the presence of Triton X-100. The proposed method allows direct arsenic determination, based on calibration with aqueous solutions. The method is applied to the serum of 20 normal subjects. The limit of detection is 0.4 $\mu g\ l^{-1}$ arsenic.

Arsenic in biological materials is determined mainly for toxicological purposes. Arsenic is usually measured in urine or hair, but arsenic is also a trace element which must be studied in blood serum. Recently, an increase of serum arsenic has been reported in a case of chronic liver disease [1]. The measurement of arsenic by atomic absorption spectrometry (a.a.s.) is usually done after conversion to arsine, but this method is slow and subject to interferences [2, 3]. Preliminary digestion of the biological materials followed by an extraction may be necessary [4].

Although the direct determination of arsenic by graphite-furnace a.a.s. is fast and suitable for routine purposes, several workers have described difficulties resulting from the volatilization of arsenic, the interaction of arsenic with carbon [5—10], spectral interferences from phosphates [11] and aluminium [12], and chemical interferences from a number of cations, anions or acids [13—17]. To suppress volatilization losses of arsenic during charring, several matrix modifiers have been proposed. The most widely used is nickel [7, 18—20]. No method for the direct determination of serum arsenic by graphite-furnace a.a.s. seems to have been described. Such a method would be very useful, and is described in this paper.

0003-2670/85/$03.30

EXPERIMENTAL

Apparatus

The Perkin-Elmer model 5000 spectrometer used was equipped with a Zeeman HGA-500 graphite furnace atomizer, a model AS-40 autosampler, a model 56 strip-chart recorder and a PRS-10 printer. All determinations were done with Zeeman background correction. The data given in the text were achieved with peak-area measurement and expansion 5. The radiation source was an arsenic electrodeless-discharge lamp operated at 8 W. The 193.7-nm arsenic line was used, at a 0.7-nm spectral slitwidth. The furnace was flushed with argon (L'air liquide argon U). The sample volume dispensed by the autosampler was 20 μl. Standard carbon tubes (Perkin-Elmer No. 02901633), pyrolytically coated graphite tubes (Perkin-Elmer No. B-0091504) and pyrolytically coated graphite tubes with an inserted L'vov platform (Perkin-Elmer No. P-0121091) made of solid pyrolytic graphite were tested. The furnace conditions are summarized in Table 1. A new tube and a new platform were used for each matrix and each change of matrix modifier.

Reagents and samples

All reagents used were of analytical grade. The arsenic(III) stock solution (1 g l^{-1}) was prepared by dissolving 0.132 g of arsenic(III) oxide in 5 ml of 1 M sodium hydroxide, acidifying the solution with 20 ml of 10% (v/v) hydrochloric acid, and diluting to 100 ml with water. The arsenic(V) stock solution (1 g l^{-1}) was prepared by dissolving $Na_2HAsO_4 \cdot 7\,H_2O$ in water. Standard solutions (1 mg l^{-1}) were prepared daily by dilution of the stock solutions with water. They were used to spike the appropriate solutions before injection into the furnace. The solutions of matrix modifiers tested were of nitrate salts, except for ammonium molybdate ($(NH_4)_6Mo_7O_{24} \cdot 7\,H_2O$) and sodium tungstate dihydrate.

Serum samples were obtained from the venous blood of twenty healthy subjects. Blood collection and serum conservation were done in pre-cleaned polyethylene tubes, avoiding contamination as much as possible.

TABLE 1

Furnace conditions
(In all cases, the recorder was switched on 5 s before atomization; integration time was 6 s and read time 0 s)

	Dry		Char	Atomize	Clean	Cool
	a	b	a and b	a and b	a and b	b
Temperature (°C)	110	130	—[c]	2600	2700	20
Ramp time (s)	10	10	1 or 5[d]	1[e]	1	1
Hold time (s)	15	20	20	5	2	10
Argon flow (ml min^{-1})	300	300	300	0	300	300

[a]Without platform. [b]With platform. [c]Charring temperatures are given in the text. [d]5-s ramp time used for sera. [e]See text for experiments at 0 ramp time.

RESULTS AND DISCUSSION

In order to achieve successful determinations of arsenic in serum by graphite-furnace a.a.s., the problems posed by spectral interferences from phosphates, by volatilization of arsenic during the charring step and by chemical interferences especially of chlorides, need to be solved. Zeeman background correction effectively eliminates spectral interferences. In order to suppress arsenic volatilization and chemical interferences, it is necessary to form non-volatile compounds of arsenic with the graphite of the atomizer or with an added matrix modifier.

Formation of stable compounds with graphite

Possible interactions between carbon and arsenic were reported by Robinson et al. [6]. The existence of a compound of general formula AsC_n was proposed by L'vov [8]. This hypothesis seems to be confirmed by the improvement in precision and sensitivity gained by coating the graphite tube with tantalum [5] or niobium [20]. Korečková et al. [7] found that graphite forms interstitial compounds with arsenate, arsenite being easily oxidized by oxygen absorbed on graphite. Nitric acid and hydrogen peroxide stabilize arsenic by making the formation of interstitial compounds easier.

In this work, three different atomizers (a standard carbon tube, a pyrolytically coated graphite tube and a L'vov platform) were used to study interactions between carbon and arsenic. The effects of charring temperature on the sensitivity for 20 $\mu g\ l^{-1}$ solutions of arsenic(III) or arsenic(V) in water and arsenic(III) in 2.5% (v/v) nitric acid were examined. The signals obtained for the three solutions and the three atomizers are shown in Fig. 1. As can be seen, with a standard tube, all three solutions show a decrease in sensitivity starting at 600°C, but between 1000°C and 1300°C, the signal is almost constant. This latter effect must indicate the formation of stable interstitial arsenic compounds. The signal is not changed when an arsenic(V) or arsenic(III) solution in water is used. This means that arsenic(III) is quantitatively converted to arsenic(V) by oxygen in the graphite. The sensitivity varied significantly from one tube to another when standard tubes were used, on account of the change in the graphite structure [21]. With a pyrolytically coated tube or a platform, there is no region of constant signal between 1000 and 1300°C because the coating prevents arsenic compounds from penetrating into the graphite.

With the three different atomizers and at all charring temperatures, the sensitivity is increased if a nitric acid solution of arsenic is injected. However, with the three different atomizers, if, after a series of measurements has been made on a 20 $\mu g\ l^{-1}$ arsenic(III) or arsenic(V) solution in water, 2.5% nitric acid is pipetted into the atomizer, a very high signal is obtained for the first injection. This signal diminishes when further quantities of the nitric acid solution are injected into the furnace (Table 2). No signal was observed if the nitric acid was replaced by water or if no solution was injected.

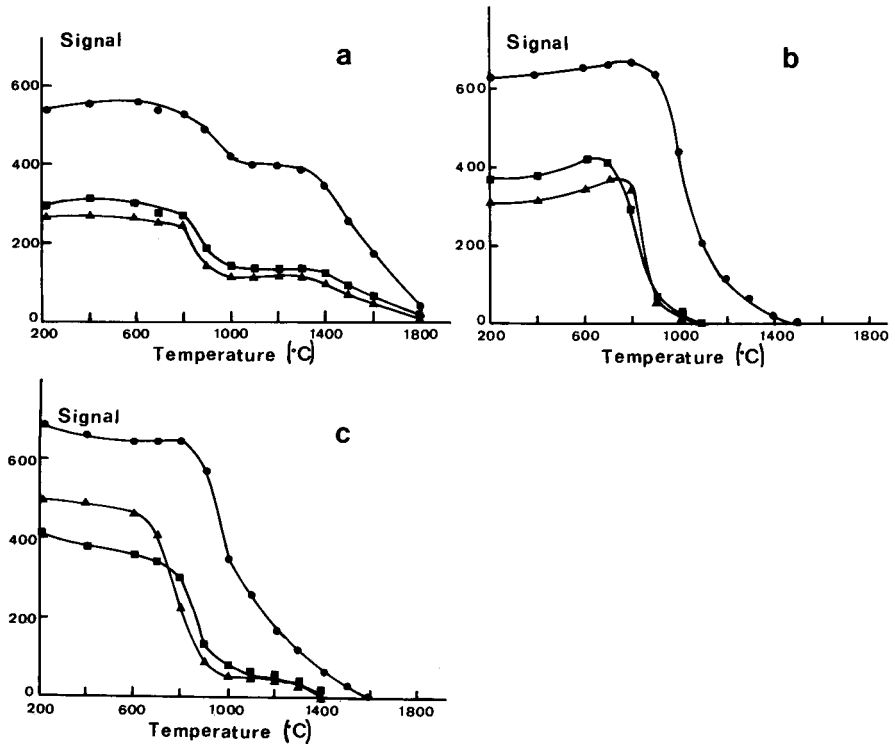

Fig. 1. Effect of charring temperature on signals for: (■) As(III); (▲) As(V); (●) As(III) in 2.5% HNO_3. (a) Standard tube; (b) pyrolytically coated tube; (c) a L'vov platform. (Atomization temperature, 2600°C.)

TABLE 2

Arsenic signals (arbitrary scale) obtained by injection of 2.5% nitric acid after 18 measurement cycles on 20 $\mu g\ l^{-1}$ arsenic solutions in water or in 2.5% nitric acid

HNO_3 injection no.	1	2	3	4
As(III) in H_2O	974	389	260	198
As(III) in HNO_3	134	101	83	71

Therefore a very stable compound is formed between carbon and arsenic, which is decomposed by the nitric acid. This compound is not dissociated at 2700°C (cleaning temperature). It is not an interstitial compound because it is also generated when a pyrolytically coated graphite tube is used.

In the presence of nitric acid, the sensitivity decreases only at charring temperatures above 800°C. It seems that the compound formed between carbon and arsenic is obtained more easily when the tube temperature increases. These findings lead us to believe that the decrease in sensitivity above 600°C for arsenic solutions without nitric acid is due both to volatilization losses and to the formation of this stable compound. Because the

injection of nitric acid into the tube destroys the arsenic—graphite bonds, the influence of nitric acid concentration on the signal was studied for the three different atomizers at two charring temperatures (Fig. 2). All the curves obtained are constant at >2% nitric acid. But, as shown in Table 2, after a series of determinations made on a 20 $\mu g\ l^{-1}$ arsenic(III) solution in 2.5% nitric acid, a small quantity of arsenic is bound to the atomizer in spite of the presence of nitric acid.

The addition of a surfactant to the solution injected into the atomizer makes the sample spread over the tube wall and soak more easily into the graphite. As shown in Table 3, the addition of Triton X-100 to a 20 $\mu g\ l^{-1}$ arsenic(III) solution decreases the sensitivity. The depression of the signal increases with increasing Triton concentration but the shape of the curves showing the signal as a function of the charring temperature is not modified, so interstitial compounds are still formed when a standard tube is used. If Triton is added to an arsenic(III) solution in 2.5% nitric acid, the arsenic signals are nearly the same as those given with additions of Triton in the

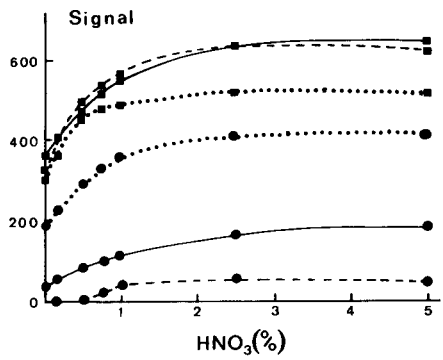

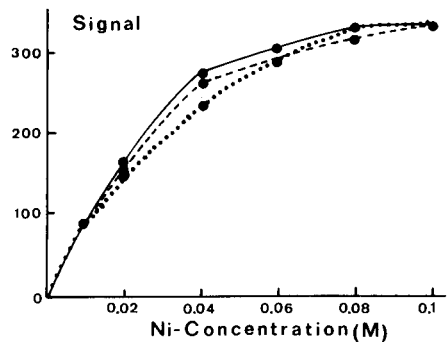

Fig. 2. Effect of nitric acid concentration on the signal from arsenic (20 μl^{-1}) at different charring temperatures: (▪) 500°C; (•) 1300°C. (...) Standard tube; (--) pyrolytically coated tube; (—) a L'vov platform.

Fig. 3. Signal from a 20 $\mu g\ l^{-1}$ arsenic addition to a serum as a function of nickel concentration. (...) Standard tube; (--) a pyrolytically coated tube; (—) L'vov platform.

TABLE 3

Arsenic signal as a function of Triton X-100(TX) concentration for a 20 $\mu g\ l^{-1}$ arsenic(III) solution in water, with different atomizers and charring temperatures

Atomizer	Arsenic signal (arbitrary units)					
	0.0% TX		0.2% TX		2.0% TX	
	500°C	1300°C	500°C	1300°C	500°C	1300°C
Standard tube	330	98	149	50	76	30
Pyrocoated tube	320	0	186	0	128	0
L'vov platform	402	40	194	27	141	18

absence of the acid (Table 3). This means that arsenic—carbon bonds are not formed in the presence of Triton X-100.

Arsenic determination in serum without matrix modification

Attempts were first made to determine arsenic in serum without addition of metal ions as matrix modifiers. Because serum arsenic concentrations are low, serum was diluted only (1 + 1). The diluent must contain a wetting agent so that the solution injected into the atomizer can spread over the wall, to facilitate the drying and charring steps. As Triton X-100 decreased the signal, the minimum Triton concentration necessary to make the sample spread on the wall was established. This was 0.2% (v/v). To decrease the volatilization losses of arsenic as far as possible, the lowest charring temperature for which the background absorbance (peak height) during atomization was less than 2 (Table 4) was established. The charring time and temperature were the same when serum was diluted (1 + 1) with a 0.4% Triton X-100 solution in water or 2.5% nitric acid. But in no case was any signal for serum arsenic obtained. Clearly, interstitial compounds and carbon—arsenic bonds were not formed in the presence of such a matrix. Therefore, it was necessary to stabilize arsenic by adding metal ions in the sample.

Determination of arsenic in serum with stabilization by matrix modifiers

Nickel ions are the most used matrix modifier, typically at a concentration of 1 g l^{-1}, but Chakraborti et al. [12] recommended 0.1 g l^{-1}. Preliminary studies on serum arsenic determination in the presence of 1 g l^{-1} nickel were unsuccessful with each atomizer. Therefore, the serum arsenic signal was investigated as a function of the nickel concentration by diluting a serum (1 + 1) with a 2% Triton X-100 solution containing various amounts of nickel. The maximum final concentration of nickel was 0.1 M because at higher concentrations, serum proteins precipitated after a few minutes. The charring temperature was 1600°C. For each nickel concentration, the signals were measured on the diluted serum solution with and without addition of 20 μg l^{-1} arsenic(III). The difference between the two signals, corresponding to the 20 μg l^{-1} addition, is shown in Fig. 3 as a function of the nickel concentration. The highest sensitivity is achieved with a final nickel concentration of 0.1 M, at which the sensitivity is the same for the three atomizers. Thus it appears that, in the presence of a considerable amount of serum, the

TABLE 4

Mildest charring conditions which gave background peak-height absorbance <2

	Temperature (°C)	Time (s)
Standard tube	900	60
Pyrocoated tube	900	60
L'vov platform	1000	20

TABLE 5

Signals corresponding to a 20 $\mu g\ l^{-1}$ arsenic addition to a serum in the presence of different matrix modifiers (signals are given as a percentage of that obtained with nickel as matrix modifier under the same experimental conditions)

Modifier	Signal	Modifier	Signal	Modifier	Signal
Ag	12.1	Cu	44	NH_4^+	3.1
Ba	22.4	Fe(III)	81.5	Pt(IV)	43.5
Ca	10.7	La	67.5	Sr	24.3
Cd	14.7	Mg	9.1	W(VI)	63.0
Co(II)	81.3	Mn	7.5	Zn	31
Cr(III)	11.4	Mo(VI)	50.7	Zr	67.6

nickel(II) concentration necessary to stabilize arsenic is high but the signal is practically independent of the type of atomizer.

The effects of other metal ions as arsenic stabilizers were also established (Table 5). Measurements were made at a final concentration of 0.1 M metal ion or ammonium ion and 1% Triton X-100, in standard tubes. The serum was diluted immediately before injection into the atomizer because serum proteins precipitate after a few minutes in the presence of some metal ions. The best sensitivity was obtained with nickel(II). Among the other ions which it would be possible to use, cobalt(II) and iron(III) rapidly caused the precipitation of serum proteins; this was not observed with lanthanum, zirconium and tungstate, which can be used in place of nickel, but with a decrease in sensitivity.

According to Korečková et al. [7], lanthanum stabilizes the oxidizing sites on graphite and, therefore, the interstitial compounds. But since it is proved that in the presence of serum these interstitial compounds are not formed, it is more than probable that lanthanum, like nickel, forms stable compounds with arsenic. According to Sanzolone et al. [19], silver can be used instead of nickel but this was not confirmed in the present study.

Arsenic content of normal sera

On the basis of these findings, the procedure to determine serum arsenic involves diluting the serum (1 + 1) with a matrix modifier solution of 0.2 M nickel/2% Triton X-100. The charring temperature should be 1600°C. Because the results are the same with the three atomizers, a standard tube may be used to decrease the cost of the determinations.

This method was applied to the analysis of sera from twenty normal subjects. Initially two calibration plots were drawn. The first corresponded to pooled sera diluted (1 + 1) with the matrix modifier solution, the second to water diluted (1 + 1) with that solution. To the two series, arsenic at concentrations of 0, 5, 10, 15, 25 and 50 $\mu g\ l^{-1}$ was added. Six determinations were made at each concentration. The variances of each series of six determinations were computed. Comparison of the six variances from the

same series with a Barlett's χ^2 test showed that they did not differ significantly. It was concluded that the variance was uniform for the standard addition graph for a serum and for the direct calibration graph. Thus it was possible to compute the linear regression equations for the two graphs and the variance of each regression. The two variances being equal (F-test), a common estimate of the variances was calculated and then an estimate was made of the variances of their slopes in order to compare them by a t-test. This test showed that the slopes had the same value. The limit of detection (2σ) was also calculated. The results are given in Table 6.

After the carbon tube had been replaced, arsenic was determined in 20 sera by the standard addition method; 0, 10 and 20 $\mu g\ l^{-1}$ arsenic(III) were added to aliquots of each serum. Direct calibration in water diluted (1 + 1) with the matrix modifier solution was also tested for 10, 20 and 30 $\mu g\ l^{-1}$ of arsenic(III). Three replicate measurements were made on each solution. The slope of each regression for a serum addition graph was compared with the slope of the regression for the direct calibration graph by a t-test, as previously described. The slopes were the same ($P > 0.05$), thus the serum arsenic concentration could be read from the direct calibration graph, without the need for the standard addition procedure. This also means that the sensitivity does not vary over a long series of measurements with the same carbon tube. To confirm these findings, the arsenic concentration in each serum was obtained by the direct and standard addition methods. There was no statistical difference between the data from the two methods (paired t-test).

A histogram of the serum arsenic content in 20 sera is shown in Fig. 4. The mean value is somewhat higher than that determined by Heydorn [22] (2.5 $\mu g\ l^{-1}$) for a Danish population by means of neutron activation analysis. But it must be noted that the serum arsenic level of a healthy population depends of the level of dietary arsenic.

Choice of ramp time for atomization

All the results reported above were obtained with a ramp time of 1 s ($1000°C\ s^{-1}$) at the beginning of the atomization step. The same experiments

TABLE 6

Statistical data for the direct calibration graph and the standard addition graph

	Direct calibration		Standard addition
Barlett's χ^2 test[a]	1.52		2.24
Linear regression slope	15.9		16.2
t-test for comparison of slopes[b]		1.12	
Limit of detection ($\mu g\ As\ l^{-1}$)	0.4		0.4

[a] χ^2 ($P = 0.05$), 5 d.f. = 11.1.
[b] t ($P = 0.05$), 68 d.f. = 1.67.

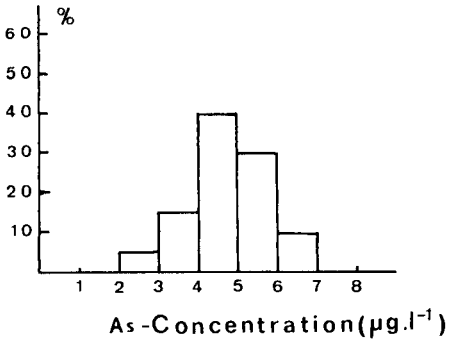

Fig. 4. Histogram showing the relative frequencies for 20 normal sera. (Mean = 4.7, s.d. = 1.02, range = 2.18—6.71 $\mu g\ l^{-1}$).

were run with the "maximum power" feature of the furnace (2000°C s^{-1}) and with peak-height measurement or signal integration. Under such conditions, the same conclusions were drawn about the formation of compounds with graphite and about the impossibility of determining arsenic in serum without stabilization by matrix modification. But when serum arsenic was determined in the presence of nickel(II) by the standard addition method or by direct calibration, the result was dependent on the atomizer. With a standard or pyrolytically coated tube, the arsenic concentration found was 3—4 times higher than when a 1-s ramp time was used whereas the concentration was unchanged when a platform was used. With the 'maximum power" mode, the vaporization of the sample deposited on a platform is delayed until the furnace tube and the gas within it are at nearly constant temperature [23], thus the heating rate of the platform is slower than that of the furnace. These experiments show that the signal is much higher when the heating rate of the sample is very fast. As quoted by Slavin et al. [23], the quality of the Zeeman background correction depends on the rate at which the background is evolved. When the "maximum power" mode is used in conjunction with a standard or a pyrolytically coated tube for the arsenic determination with nickel(II) as the matrix modifier, the background peak is too fast for the sampling rate of the photometer and an apparent signal is added to the analyte signal. No advantage was found, for using a platform with the "maximum power" mode instead of the standard tube with a 1-s ramp time.

Conclusions

It has been demonstrated that when arsenic is determined by graphite-furnace a.a.s., there are two sorts of interaction between arsenic and graphite. First, arsenate forms intercalation compounds with graphite as far as it can penetrate into the graphite. Second, arsenic bonds with carbon on the graphite surface of a platform or a tube, whether it is pyrolytically coated or not. As these bonds are not destroyed at high temperatures, they are probably covalent.

In the presence of such a matrix as serum, arsenic cannot react with graphite and it is not necessary to use a tube coated with pyrolytic graphite or with molybdenum or tantalum. It is absolutely necessary, however, to form stable compounds with arsenic by adding a matrix modifier. Of the metal ions tested, nickel(II) is the most effective. The results show that the concentration of the matrix modifier must be adjusted to the matrix concentration. To obtain the best sensitivity, a high nickel concentration is used. Under these conditions, arsenic determination in serum is very straightforward. The arsenic concentration is read directly from a calibration graph prepared for aqueous reference solutions; the equation for this line is readily calculated by standard linear regression because the variance is uniform. The sensitivity did not vary during the life of the standard carbon tube used. Arsenic in urine is commonly determined here by the same technique, for toxicological purposes.

REFERENCES

1 Y. Calmus, R. Poupon, M. B. Brijnen, C. Renaudeau and F. Darnis, Gastroenterocol. Clin. Biol., 6 (1982) 910.
2 H. W. Sinemus, M. Melcher and B. Welz, At. Spectrosc., 2 (1981) 81.
3 B. Welz and M. Melcher, Anal. Chim. Acta, 131 (1981) 17.
4 I. Mutsuo and K. Fujio, Sangyo Igaku, 19 (1977) 136.
5 R. R. Brooks, D. E. Ryan and H. F. Zhang, At. Spectrosc., 2 (1981) 161.
6 J. W. Robinson, R. Garcia, G. Hindman and P. Slevin, Anal. Chim. Acta, 69 (1974) 203.
7 J. Korečková, W. Frech, E. Lundberg, J. A. Persson and A. Cedergren, Anal. Chim. Acta, 130 (1981) 267.
8 B. V. L'vov, Spectrochim. Acta, Part B, 33 (1978) 153.
9 G. R. Henning, in F. A. Cotton (Ed), Progress in Inorganic Chemistry, Vol. 1, Interscience, New York, 1959, p. 125.
10 K. Kamegawa, H. Joshida and S. Arita, Chem. Abstr., 92 (1979) 217370j.
11 K. Saeed and Y. Thomassen, Anal. Chim. Acta, 130 (1981) 281.
12 D. Chakraborti, W. De Jonghe and F. Adams, Anal. Chim. Acta, 119 (1980) 331.
13 D. B. Ratcliffe, C. S. Byford and P. B. Osman, Anal. Chim. Acta, 75 (1975) 457.
14 G. C. Kunselman and E. A. Huff, At. Absorpt. Newsl., 15 (1976) 29.
15 F. D. Pierce and H. R. Brown, Anal. Chem., 49 (1977) 1417.
16 P. R. Walsh, J. L. Fasching and R. A. Duce, Anal. Chem., 48 (1976) 1014.
17 V. B. Stein, E. Canelli and A. H. Richards, At. Spectrosc., 1 (1980) 133.
18 R. M. Hamner, D. L. Lechak and Greenberg, At. Absorpt. Newsl., 15 (1976) 122.
19 R. F. Sanzolone and T. T. Chao, Anal. Chim. Acta, 128 (1981) 225.
20 P. Hocquellet, Analusis, 6 (1978) 426.
21 K. R. Sperling and B. Bahr, Fresenius. Z. Anal. Chem., 314 (1983) 760.
22 K. Heydorn, Clin. Chim. Acta, 28 (1969) 349.
23 W. Slavin, G. R. Carnrick, D. C. Manning and E. Pruszkowska, At. Spectrosc., 4 (1983) 69.

Analytica Chimica Acta, 172 (1985) 157—166
Elsevier Science Publishers B.V., Amsterdam — Printed in The Netherlands

DETERMINATION DE MICROQUANTITES DE LITHIUM SERIQUE PAR SPECTROMETRIE D'ABSORPTION ATOMIQUE SANS FLAMME
Optimisation des Conditions Expérimentales

E. BOURRET, I. MOYNIER et L. BARDET*

Laboratoire de Physique Industrielle Pharmaceutique, Faculté de Pharmacie, Av. Charles Flahault, 34060 Montpellier Cedex (France)

M. FUSSELLIER

Laboratoire AGUETTANT, 1 avenue Jules Carteret, 69007 Lyon (France)

(Reçu le 22 octobre 1984)

SUMMARY

(*Determination of traces of lithium in blood serum by electrothermal atomic absorption spectrometry. Optimization of experimental parameters*)

Electrothermal atomic absorption spectrometry is used to determine traces of lithium in blood serum; the limit of detection had to be decreased by optimizing the experimental conditions. Signal intensity and reproducibility were improved by the addition of Triton X-100 (0.1%). Other additives examined were less effective. The validity of the final method was checked by statistical tests for linearity of response and precision. The method is suitable for the determination of lithium in sera of normal subjects who have not had lithium therapy; the limits of the normal range are 2—17 $\mu g\ l^{-1}$ with a mean value of 8 $\mu g\ l^{-1}$.

RESUME

La spectrometrie d'absorption atomique sans flamme a été choisie pour la détermination de microquantités de lithium dans le sérum ce qui a nécessité d'abaisser la limite de détection de cette méthode. L'influence des différents paramètres et de divers adjuvants est discutée en termes d'amélioration de l'intensité du signal et de la reproductibilité des mesures. L'agent mouillant choisi est le Triton X-100 (0.1%). La validité de la méthode est contrôlée par vérification statistique de la linéarité et de l'exactitude. La méthode proposée permet de doser le lithium dans des sérums de sujets normaux non soumis à une lithiothérapie; le taux moyen normal est de 8 $\mu g\ l^{-1}$ avec des valeurs extrêmes de 2 et 17 $\mu g\ l^{-1}$.

La thérapeutique psychiatrique par le lithium nécessite la surveillance des taux sanguins de ce médicament. Actuellement ce dosage est de pratique courante et de très nombreux travaux sont consacrés à la détermination du lithium sérique à des taux thérapeutiques. Par contre peu d'auteurs se soucient de la lithiémie chez des sujets à l'état normal. Fournis et Chazot [1] évoquent pourtant l'intérêt de cette détermination par la mise en

0003-2670/85/$03.30

évidence d'un déficit sérique. Malgré l'absence d'une étude particulière, quelques auteurs citent le taux moyen trouvé chez des sujets normaux non soumis à un traitement au lithium et les teneurs publiées sont très variables allant de 10 $\mu g \cdot l^{-1}$ à 70 $\mu g\ l^{-1}$ [2—8]. Ces déterminations ont été effectuées selon l'une ou l'autre des deux techniques physiques largement répandues: la spectrométrie d'émission et d'absorption atomique. Aux taux thérapeutiques de lithium, une excellente corrélation a été rapportée [9, 10]. L'expérience a montré que l'absorption atomique bien que moins sensible que la technique en émission, reste la méthode de choix car sélective et d'une grande simplicité [11, 12].

Il semble possible de repousser la limite de détection de cette technique en augmentant sa sensibilité par l'optimisation de la méthode de dosage dont aucune étude approfondie n'a été publiée. Seul Woods [13] a publié une étude succinte sur la détermination du lithium à des taux avoisinant la limite de détection. Cette étude a donc pour but la mise au point d'une technique de dosage du lithium par spectrophotométrie d'absorption atomique sans flamme suffisamment sensible pour nous permettre de déterminer la lithiémie chez des sujets exempts de lithiothérapie.

L'addition d'adjuvants au milieu d'analyse a été préconisée afin d'éliminer soit les interférences physiques par l'ajout d'un agent mouillant soit les interférences chimiques par l'addition d'acides ou de bases diluées qui modifient l'environnement ionique [14]. L'étude de l'influence de plusieurs adjuvants sur la sensibilité et la reproductibilité du dosage nous permettra de définir les conditions optimales qui seront recherchées en solution aqueuse puis adaptées en milieu sérique. Enfin, en raison de la sélectivité et de la sensibilité recherchées, l'étude d'une corrélation avec une autre méthode s'avère impossible; aussi nous nous attacherons à apporter la preuve de la validité de la méthode en déterminant, outre la linéarité et la limite de détection, sa justesse et sa fiabilité.

PARTIE EXPERIMENTALE

Appareillage

L'appareil utilisé est un spectromètre d'absorption atomique Perkin-Elmer modèle 2380 équipé d'un four graphite HGA-76. Plusieurs paramètres instrumentaux ont été testés notamment trois longueurs d'onde du lithium (670,8; 610,4; 323,2 nm) et trois largeurs de fente (0,2; 0,7; 2 nm). Les essais montrent que les meilleurs résultats sont obtenus dans les conditions: longueur d'onde 670,8 nm, largeur de fente 0,7 nm, courant d'alimentation de la lampe 20 mA, avec un arrêt de débit de gaz durant l'étape d'atomisation. Des essais effectués avec des tubes pyrolytiques et non pyrolytiques dans des conditions optimales propres à chacun d'eux ont montré une meilleure reproductibilité des mesures avec les tubes pyrolytiques que nous choisissons.

Perturbations d'absorption

L'absorption non spécifique a été corrigée à 323,2 nm par l'emploi du correcteur de fond par lampe au deutérium. Aux longueurs d'onde 670,8 et 610,4 nm où le correcteur à arc à deutérium est inefficace, les perturbations d'absorption ont été controlées en mettant en oeuvre plusieurs méthodes indiquées par Pinta [15]: (a) par exécution d'essais à blanc, en milieu aqueux et en milieu d'analyse, comprenant toutes les opérations analytiques sans addition de lithium, en opérant à la longueur d'onde d'analyse; (b) par le test de recouvrement ou taux de récupération, de différentes additions de lithium au milieu d'analyse qui présente l'avantage de contrôler l'erreur de justesse ou exactitude de la méthode (ce procédé correspond à la méthode des ajouts dosés utilisée dans le même but [8]); (c) la perturbation spectrale par émissions parasites à partir du tube graphite, qui pourrait se produire à ces longueurs d'onde, est éliminée, comme l'ont montré les essais mentionnés ci-dessus, par l'emploi de tubes pyrolytiques dans des conditions thermiques optimisées.

Nous travaillons en lecture de hauteur de pic avec un temps d'intégration de 10 s. La reproductibilité de mesures est évaluée par leur coefficient de variation (c.v., %).

Reactifs et solutions

Solutions étalons. Considérant les travaux antérieurs [2, 4], les solutions étalons de lithium sont préparées par dilution d'une solution standard de chlorure de lithium à 1 g l^{-1} (solution Titrisol, Merck) de façon à obtenir trois solutions de concentrations finales 20, 50 et 100 μg l^{-1}, 3—5 injections étant pratiquées pour chacune d'elles.

Solutions d'adjuvants. Les adjuvants, choisis en fonction des travaux publiés, sont des réactifs Merck. Certains ont été testés à plusieurs concentrations et leurs concentrations finales dans la solution sont respectivement: acide chlorhydrique [14] et nitrique 0,03 M, hydroxide de sodium 0,03 M, ammoniaque 0,375 M; Brij-35 0,5; 0,8 ou 1%; Teepol 50 μl à 200 μl de sérum; ethylène glycol [16] 5; 10 ou 15%; Triton X-100 [14, 17, 18] 0.1—1%; ethanol [19] 2,5; 5; 7,5; 10 ou 15%; isopropanol [4].

Les serums. Les donneurs sont choisis exempts de traitement au lithium ou de tout apport exogène non négligeable de lithium. Le sang est prélevé par voie veineuse sur tube sec. Après exsudation, une centrifugation (4 min à 4000 trs min^{-1}) permet de séparer le sérum. Les essais ont été effectués avec trois dilutions de la matrice sérique 1/2, 1/5 ou 1/10.

RESULTATS ET DISCUSSION

Conditions analytiques

Volume d'injection. La reproductibilité des mesures pour deux volumes d'injection 10 et 20 μl, déterminée à partir de dix injections, a donné respectivement une valeur moyenne calculée sur huit évaluations de 11,75% et 4,9%, résultats en faveur d'une injection de 20 μl.

La température de carbonisation et d'atomisation. A chaque étape nous choisissons comme l'indique Pegon [14] la température qui, tout en étant la plus élevée possible pour faciliter la destruction de la matrice sérique ou l'atomisation du lithium, donne l'absorbance la plus forte. Ces résultats ont été acquis avec une solution aqueuse de lithium puis vérifiés avec une matrice sérique. La Fig. 1 révèle une zone de réponse optimale pour une température de carbonisation comprise entre 800°C et 1000°C et la plus forte réponse est atteinte à la température d'atomisation de 2700°C (Fig. 2). Cette température étant la température maximale d'utilisation de l'appareil, le signal subit souvent des variations non négligeables; aussi sera-t-elle limitée à 2650°C.

Recherche du programme. Nous avons testé plusieurs températures de séchage, la vitesse de montée (rate 1, 2...) et la durée de maintien à la température de séchage et de carbonisation, le nombre d'étapes pour atteindre la température de séchage ou de carbonisation. Après un nombre de tests suffisants [15], trois programmes ont été retenus (Tableau 1) et par la suite comparés en présence de l'adjuvant sélectionné dans le paragraphe suivant, le Triton X-100.

Lorsque la température de carbonisation est atteinte en deux paliers, l'amélioration de l'intensité du signal ou la reproductibilité des résultats ne compense pas le manque de rapidité de ce protocole que nous abandonnons. Par ailleurs les programmes 1 et 3 sont comparés par le coefficient de variation des mesures (c.v.) obtenues au cours des dosages de dix sérums: les valeurs moyennes sont respectivement 8,55% (range 2,2—16%) et 3,82

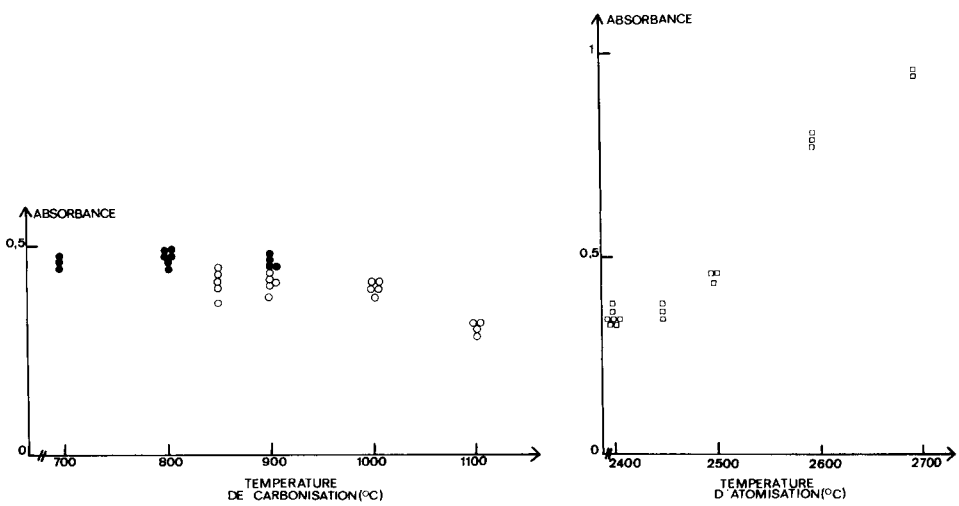

Fig. 1. La température de carbonisation en solution aqueuse (lithium 200 $\mu g\ l^{-1}$). Température d'atomisation: (•) 2700°C; (○) 2500°C.

Fig. 2. La température d'atomisation en solution aqueuse (dose lithium 200 $\mu g\ l^{-1}$, température de carbonisation 900°C).

TABLEAU 1

Programmes retenus

Programme	Température et temps		
	Séchage	Carbonisation	Atomisation
1	100°C, 40 s	1000°C, 50 s, rate 2	2650°C, 8 s
2	120°C, 50 s	300°C, 20 s, rate 2 975°C, 20 s, rate 2	2650°C, 10 s
3	100°C, 15 s, rate 1 150°C, 15 s, rate 2	1000°C, 25 s, rate 1	2650°C, 5 s

(range 1,2—8,1%) ce qui montre l'avantage de 2 étapes de séchage qui diminuent la dispersion des lectures. C'est donc le programme 3 qui est retenu pour la suite de cette étude.

Etude d'adjuvants

Leur influence a été effectuée dans une matrice sérique diluée (1 + 1) et leur choix est guidé par des observations qualitatives et/ou quantitatives. Le Tableau 2 regroupe les paramètres des droites absorbance/teneur en lithium pour chaque adjuvant envisagé. Lors de l'addition d'acide ou de base, les droites de régression sont correctes en ce qui concerne les ordonnées à

TABLEAU 2

Influence d'adjuvants sur les droites de régression

Adjuvant	Nombre de mesures	Coeff. de régression ($\times 10^{-3}$)	Ordonnée à l'origine Moyenne ± s.d.
—	23	0,94	−0,032 ± 0,002
HCl	14	0,96	0,012 ± 0,002
HNO_3	18	1,21	0,014 ± 0,001
NaOH	14	1,69	0,030 ± 0,002
NH_3	15	1,42	0,007 ± 0,001
NH_3 + Teepol	13	0,38	0,007 ± 0,007
Brij-35 0,5%	16	0,64	0,041 ± 0,005
0,8%	16	0,29	0,037 ± 0,004
1%	16	0,38	0,026 ± 0,003
Teepol	15	0,51	0,036 ± 0,005
Triton (0.1%)	15	3,29	0,048 ± 0,004
Eth. glycol 5%	14	0,79	−0,006 ± 0,002
10%	15	0,62	−0,006 ± 0,001
15%	20	0,72	−0,007 ± 0,001
Ethanol 2,5%	18	1,28	0,005 ± 0,001
5%	15	1,30	0,005 ± 0,001
7,5%	14	1,28	−0,003 ± 0,004
10%	19	0,86	0,006 ± 0,003
15%	16	1,12	−0,005 ± 0,002

l'origine mais la valeur des pentes reste généralement faible. En outre, un grand nombre de difficultés techniques apparaissent responsables d'un manque total de reproductibilité. Pour cette raison majeure, ces adjuvants sont rejetés d'emblée.

Les agents mouillants facilitent l'injection dans le four; la reproductibilité est ainsi améliorée et l'intensité du signal augmentée. Cependant la valeur négative de l'ordonnée à l'origine de la droite dose/réponse obtenue en présence de l'éthylène glycol et la faible valeur des coefficients de régression obtenus en présence du Brij-35 et du Teepol, nous amène à rejeter l'emploi de ces deux adjuvants. De même, le mélange Teepol-ammoniaque préconisé par Pegon [14] n'apporte pas de résultats valables. Pour l'addition de Triton X-100, seule la concentration à 0.1% a été retenue; son signal est beaucoup plus élevé que pour les adjuvants précédents, comme le montre le coefficient de régression.

Avec l'éthanol les ordonnées à l'origine sont positives ou non significativement différentes de zéro, sauf pour la plus forte teneur en éthanol (15%). En outre à 10 et 15% les lectures sont très variables notamment pour la dose la plus élevée en lithium (100 $\mu g\ l^{-1}$). L'avantage de ce diluant est donc confirmé à faible dose, 2,5 ou 5%. Quant à l'isopropanol, les mesures sont beaucoup trop dispersées pour envisager son emploi ce qui est en contradiction avec l'observation de Pybus et Bowers [4]. A partir de ces essais, deux diluants peuvent être sélectionnés: l'éthanol et le Triton X-100.

Etude comparée éthanol—Triton X-100. Les expériences obéissent à des conditions strictes: réalisées le même jour en utilisant la même matrice sérique à différentes dilutions constituée d'un pool de six sérums. Le Tableau 3 regroupe les résultats obtenus sans adjuvant et avec éthanol ou

TABLEAU 3

Comparaison des droites de régression en présence d'éthanol et de Triton X-100

Adjuvant	Nombre de mesures	Coeff. de régression ($\times 10^{-3}$)	Ordonnée à origine ($\times 10^{-3}$)	C.v.(%)
Dilution sérum, 1 + 1				
—	17	3,54	4,2	35,5
Ethanol (5%)	15	3,33	33,1	24,2
Triton (0.1%)	15	3,29	48,6	9,6
Dilution sérum, 1 + 4				
—	16	4,32	26,5	28,2
Ethanol (5%)	13	5,99	−7,6	23,8
Triton (0.1%)	16	6,72	16,7	6,7
Dilution sérum, 1 + 9				
—	16	5,64	5,2	13,5
Ethanol (5%)	13	6,41	−14,3	17,2
Triton (0.1%)	14	5,65	11,2	9,1

Triton X-100. De ces données ressortent deux points essentiels: les différences d'intensité du signal ne sont pas significatives d'un adjuvant à l'autre mais les ordonnées à l'origine sont souvent négatives pour l'éthanol alors qu'elles sont positives pour le Triton et d'autant plus élevées que la dilution du sérum est faible ce qui peut traduire la présence de lithium à l'état de traces dans le sérum utilisé; l'ajout d'éthanol ou de Triton réduit de façon notable les erreurs expérimentales qui sont considérablement amoindries avec le Triton ce que reflètent les coefficients de variation. L'évaluation de la dispersion des mesures au cours de plusieurs essais à différentes concentrations de ces deux adjuvants avec une matrice sérique diluée 1 + 1 et 1 + 4 confirme l'avantage du Triton X-100 (Tableau 4).

Controle de la validité de la méthode

Dans les conditions optimales décrites ci-dessus, l'écart à la linéarité contrôlé statistiquement s'est toujours révélé non significatif et la linéarité est correcte jusqu'à 140 $\mu g\ l^{-1}$ lithium. La limite de détection dans nos conditions du dosage est de 2 $\mu g\ l^{-1}$.

En vue de vérifier l'exactitude de la méthode, des dosages sériques ont été effectués par la méthode des ajouts dosés en présence de surcharges en lithium variant de 2,5 à 70 $\mu g\ l^{-1}$ avec une dilution (1 + 4) du sérum. La teneur expérimentale en lithium est déterminée à partir de l'équation des droites de régression. L'exactitude est alors exprimée par le taux de récupération de la surcharge en lithium (Tableau 5). L'écart entre quantité de lithium ajoutée et quantité retrouvée reste faible.

L'erreur systématique de la méthode peut être chiffrée [20] par l'équation de la droite de régression calculée à partir de 17 déterminations: (taux Li retrouvé, $\mu g\ l^{-1}$) = 2,25 + 0,927 (surcharges en Li, $\mu g\ l^{-1}$). La comparaison statistique par un test de Student du coefficient de régression de cette droite

TABLEAU 4

Influence de la nature et de la concentration des adjuvants

Adjuvant	Dilution sérum	Concentration adjuvant (%)	Coefficient de variation[a] (%)
Ethanol	1 + 1	2,5	12(18)
		5	12(16); 19(14); 24(18)
		7,5	65(14); 40(15); 43(16)
		10	42(13)
		15	18(12); 23(16)
	1 + 4	2,5	65(17)
		5	24(15)
		7,5	28(19)
Triton	1 + 1	0,1	10(13)
	1 + 4	0,1	2(17); 6(12); 5(16) 6(12); 7(16); 15(13)

[a](Nombre d'injections).

TABLEAU 5

Contrôle de l'éxactitude de la méthode

Surcharges ($\mu g\ l^{-1}$)	1 sérum (15.3.1984)			1 pool de 3 sérums (13.3.84)			1 sérum (19.7.84)		
	n^a	Taux retrouvé (%)	C.v.(%)	n^a	Taux retrouvé (%)	C.v.(%)	n^a	Taux retrouvé (%)	C.v.(%)
10	13	121	1,5	9	124	2,1	15	129	7,7
20	15	103	3,2				16	101	9,9
30	17	90	3,5	14	94	3,1	17	87	7,8
40	13	89	5,7	11	103	6,05	14	101	6,8
—[b]	15	—	4,1	9	—	2,6	15	—	6,2

[a]Nombre de mesures. [b]Sans ajouts.

expérimentale à la valeur théorique 1 caractérisant la méthode exacte n'indique pas de différence significative (t = 1,78).

Pour des surcharges inférieures ou égales à 40 $\mu g\ l^{-1}$, les droites expérimentales présentent un bon parallélisme. Pour des surcharges supérieures à 40 $\mu g\ l^{-1}$, un parallélisme insuffisant est mis en évidence entre les différentes droites ce qui définit la limite supérieure d'application.

Le Tableau 5 regroupe à côté des taux de récupération, les coefficients de variation des mesures. Comme le souligne Massmann [21] on peut difficilement s'attendre à ce qu'une méthode aussi sensible donne des résultats très précis. Cependant les résultats restent très corrects.

Le taux sérique de lithium a été déterminé chez 16 individus adultes présumés sains. La lithiémie moyenne est de 8 $\mu g\ l^{-1}$ avec une valeur minimale de 2 et maximale de 17. Ces résultats apportent la preuve que les conditions expérimentales décrites permettent de doser le lithium dans les sérums de sujets exempts de traitement au lithium.

CONCLUSION

Les très faibles teneurs de lithium rencontrées dans les sérums de sujets non soumis à une lithiothérapie nécessitaient d'améliorer la sensibilité de la technique choisie. L'étude de l'influence sur l'intensité du signal et la reproductibilité des résultats, des conditions techniques, et de l'addition d'adjuvants au milieu d'analyse ont permis de fixer les conditions optimales du dosage.

Les études antérieures [16, 22, 23] ont montré que la qualité des tubes influence la reproductibilité des résultats. Les tubes pyrolytiques offrent une très faible variabilité des réponses.

Au cours de la recherche des conditions analytiques, la complexité de la matrice sérique nécessite l'accès à la température de traitement choisie à des vitesses lentes ou comme le préconise certains auteurs en plusieurs paliers

successifs [16]. Dans notre cas, la montée à la température de carbonisation de 1000°C en deux paliers successifs ne présente pas d'avantage particulier. Par contre la phase de séchage en deux étapes améliore considérablement la reproductibilité des mesures. Au niveau des adjuvants, exception faite de l'isopropanol, les résultats acquis sont en accord avec ceux déjà rapportés savoir que tous les acides diminuent le signal alors que l'addition d'éthanol l'augmente [4, 19]. Seul Lehmann [24] trouve un intérêt à l'addition d'acide chlorhydrique (0,1 M). Comme l'ont montré Favier [16] et Pegon [14], l'intérêt d'un tensio-actif s'avère réel; cependant dans le cas du dosage du lithium, seul le Triton X-100 mérite d'être retenu compte tenu de son influence positive sur la précision des résultats.

Nous avons pu ainsi atteindre une limite de détection du lithium de 2 $\mu g\ l^{-1}$, valeur voisine de celle publiée par d'autres auteurs. Zettner [2] et Cooper [25] trouvent une limite de détection de 5 $\mu g\ l^{-1}$ et Pinta [15] indique également qu'il est possible dans de bonnes conditions de détecter 5 $\mu g\ l^{-1}$. Enfin dans une étude sur le microdosage de lithium dans les milieux biologiques, le plus petit ajout de lithium dosé était de 2,5 $\mu g\ l^{-1}$ [13] donc de l'ordre de celui obtenu par nos soins.

Soulignons que la valeur trouvée n'est pas aussi faible que la limite déterminée en spectrophotométrie d'émission [6, 8, 25] mais elle n'en est pas moins suffisante pour doser la lithiémie aux très faibles taux rencontrés chez les sujets normaux; le contrôle de la validité de la méthode en apporte la preuve.

En effet, les tests statistiques du contrôle de linéarité ont toujours été satisfaisants et la vérification du défaut de justesse de la méthode prouve sa validité. L'écart observé entre la droite expérimentale des taux de lithium retrouvé et la droite théorique ne révèle pas d'erreur systématique significative. Enfin le coefficient de variation des mesures est correct.

Les limites de la lithiémie normale définies dans un groupe de sujets sains soit 2—17 $\mu g\ l^{-1}$, sont en amélioration par rapport aux résultats publiés par ailleurs. Seul Stafford et Saharovici [12] fonit référence à une technique de spectrométrie en flamme donnant des valeurs comparables 2,8—42 $\mu g\ l^{-1}$. Dans les techniques en émission, le taux moyen le plus faible relevé est de 14 $\mu g\ l^{-1}$ [8]. En absorption, Zettner [2] indique que la lithiémie dans les sérums normaux est inférieure à la limite de détection de la méthode employée soit inférieure à 10 $\mu g\ l^{-1}$. Ainsi la méthode proposée ici en abaissant la limite de détection permet de définir précisément les limites normales de la lithiémie. Il faut souligner que l'influence de la dilution du sérum sur le dosage ainsi que les interférences ioniques n'ont pas été abordées dans ce travail. Compte tenu de l'importance que leur attribue divers auteurs, ces paramètres seront envisagés dans une prochaine publication.

Nous remercions les laboratoires Aguettant qui ont contribué à l'élaboration de ces recherches.

BIBLIOGRAPHIE

1 Y. Fournis et G. Chazot, Pathol. Biol., 19 (1971) 787.
2 A. Zettner, At. Absorpt. Newsl., 7 (1968) 32.
3 G. Mahuzier, Pathol. Biol., 25 (1977) 629.
4 J. Pybus et G. N. Bowers, Clin. Chem., 16 (1970) 139.
5 B. F. Rocks, Clin. Chem., 28 (1982) 440.
6 R. Robertson, Clin. Chim. Acta, 45 (1973) 25.
7 S. Long et J. Hermann, Z. Ges. Exp. Med., 139 (1965) 200.
8 J. Di Costanzo, Feuill. Biol., 22 (1981) 53.
9 S. Lippmann, Am. J. Psychiatry, 138 (1981) 1375.
10 M. Levy et R. Katz, Clin. Chem., 15 (1969) 787.
11 J. P. Godard, Le Concours Médical, 1—12 (1973) 7345.
12 D. T. Stafford et F. Saharovici, Spectrochimica Acta, Part B, 29B (1974) 277.
13 A. E. Woods, At. Absorpt. Newsl., 7 (1968) 85.
14 Y. Pegon, Anal. Chim. Acta, 101 (1978) 385.
15 M. Pinta, Spectrophotometrie d'Absorption Atomique, Tome 1, Ed. Masson, Paris, 1979.
16 A. Favier, Clin. Chim. Acta, 124 (1982) 239.
17 J. P. Buchet, Clin. Chim. Acta, 73 (1976) 481.
18 P. A. Pleban, Clin. Chem., 25 (1979) 1915.
19 B. G. Blijenberg, Clin. Chim. Acta, 19 (1968) 97.
20 C.E.A. Statistiques Appliquées à l'Exploitation des Mesures, Ed. Masson, Paris, 1978.
21 H. Massmann, Méthodes Physiques d'Analyse (GAMS), Juin, 1968, 193.
22 S. Hoenig, Analusis, 8 (1980) 16.
23 H. Massmann, Proc. Anal. Div. Chem. Soc., (1976) 258.
24 V. Lehmann, Clin. Chim. Acta, 20 (1968) 523.
25 T. B. Cooper, J. Clin. Psychopharmacol., 1 (1981) 53.

Analytica Chimica Acta, 172 (1985) 167—173
Elsevier Science Publishers B.V., Amsterdam — Printed in The Netherlands

FLUORIMETRIC DETERMINATION OF α-KETO ACIDS WITH 4,5-DIMETHOXY-1,2-DIAMINOBENZENE AND ITS APPLICATION TO HIGH-PERFORMANCE LIQUID CHROMATOGRAPHY

SHUUJI HARA, YASUYO TAKEMORI, TETSUHARU IWATA, MASATOSHI YAMAGUCHI and MASARU NAKAMURA

Faculty of Pharmaceutical Sciences, Fukuoka University, Nanakuma, Jonan-ku, Fukuoka 814-01 (Japan)

YOSUKE OHKURA*

Faculty of Pharmaceutical Sciences, Kyushu University 62, Maidashi, Higashi-ku, Fukuoka 812 (Japan)

(Received 29th October 1984)

SUMMARY

A highly sensitive fluorimetric method for the determination of α-keto acids of biological importance is described. The α-keto acids react in dilute hydrochloric acid with 4,5-dimethoxy-1,2-diaminobenzene to give a compound which fluoresces in neutral solution. The method is selective for α-keto acids and the limits of detection are 30—750 pmol ml^{-1} of test solution. The fluorescent compounds in a reaction mixture of ten α-keto acids are separated within 18 min by high-performance liquid chromatography on a reversed-phase column with isocratic elution. The limits of detection for the acids are in the range 9—780 fmol in a 10-μl injection volume.

Several methods have been reported for the determination of α-keto acids of biological importance. The colorimetric method based on 2,4-dinitrophenylhydrazine [1], which has been used most widely, is neither selective nor sensitive [1]. A fluorimetric method based on the reaction with *o*-phenylenediamine (OPD) is fairly sensitive and selective for α-keto acids [2]. The reaction has been applied in the determination of the acids by high-performance liquid chromatography (h.p.l.c.) with fluorescence detection [3, 4]. The methods, however, are not sensitive enough for quantifying the acids at femtomole level and do not permit the determination of *p*-hydroxyphenylpyruvic acid. In addition, the fluorescent products formed require gradient elution for separation.

In previous work [5—7], 4,5-dimethoxy-1,2-diaminobenzene (DDB) monohydrochloride has been developed as a fluorogenic reagent for aromatic aldehydes [5—7]. Recently, it was found that α-keto acids also react in an acidic solution with DDB to produce compounds which fluoresce intensely in neutral solution, whereas the fluorescent products from aromatic aldehydes fluoresce in alkaline solution. Pyruvic acid, α-ketoglutaric acid and

0003-2670/85/$03.30

phenylpyruvic acid were used as model compounds to establish reaction conditions suitable for a more general method. The reaction was then applied to precolumn derivatization of ten kinds of α-keto acids of biological importance and the derivatives were separated by h.p.l.c. with isocratic elution.

EXPERIMENTAL

Reagents, solutions and equipment

All chemicals and solvents were of analytical-reagent grade, unless otherwise noted. Deionized-distilled water was used. Sodium salts of the acids listed in Table 1 were purchased from Sigma Chemical Company. The DDB monohydrochloride was prepared as described previously [5]; it is now available from Dojindo Laboratories (Kumamoto, Japan).

The DDB solution (0.25 mM) was prepared by dissolving 5.1 mg of DDB monohydrochloride in 100 ml of 0.5 M hydrochloric acid containing 0.21 M β-mercaptoethanol. The solution was used within 3 h.

Uncorrected fluorescence spectra and intensities were measured with a Hitachi 650-60 spectrofluorimeter in 10 × 10 mm quartz cells; spectral bandwidths of 10 nm were used in both the excitation and emission monochromators. A Hitachi 635A high-performance liquid chromatograph equipped with a sample injector (10-μl loop) was used. A Shimadzu RF-530 fluorescence spectromonitor was equipped with a 12-μl flow cell operated at an excitation wavelength of 362 nm and an emission wavelength of 450 nm. The column was a Radial Pak cartridge C_{18} (100 × 8 mm i.d.; particle size, 5 μm; Waters Assoc.). The column can be used for more than 1000 injections

TABLE 1

Excitation and emission maxima of the fluorescence from α-keto acids and their limits of detection in the manual assay method and the h.p.l.c. method

Compound	Excitation maximum[a] (nm)	Emission maximum[a] (nm)	Limit of detection[b]	
			Manual assay (pmol ml^{-1})	H.p.l.c. (fmol/10 μl^{-1})
Pyruvic acid	361	448	30	300
α-Ketobutyric acid	361	448	60	33
α-Ketovaleric acid	363	448	40	23
α-Ketoisovaleric acid	361	448	110	95
α-Ketocaproic acid	363	446	40	43
α-Ketoisocaproic acid	364	448	30	20
α-Keto-β-methylvaleric acid	363	448	95	67
α-Ketoglutaric acid	361	450	35	9
Phenylpyruvic acid	366	451	90	43
p-Hydroxyphenylpyruvic acid	365	448	750	780

[a]Portions (1.0 ml) of 5 nmol ml^{-1} α-keto acid solutions were treated by the manual procedure. [b]Defined as the concentration which gave a fluorescence intensity twice the blank.

with only a small decrease in the number of theoretical plates, provided that it is washed with aqueous methanol (1:1, v/v) at a flow rate of 1.0 ml min^{-1} for about 30 min after the daily use is complete. A Hitachi-Horiba M-7 pH meter was used at 25° C as required.

Procedures

Manual procedure (procedure for fluorescent derivatization). To 1.0 ml of the DDB solution placed in a teflon-lined screw-capped test tube was added 1.0 ml of aqueous test solution. The tube was tightly closed and heated at 100° C for 2.5 h. The reaction mixture was cooled in ice-water to stop the reaction, and then adjusted to pH 6.6—7.4 by adding 1.0 ml of 0.4 M phosphate buffer (pH 7.0) and 0.5 ml of 1.0 M sodium hydroxide. A reagent blank was prepared by treating 1.0 ml of water in the same manner. The fluorescence intensities of the test and blank were measured at the emission maximum wavelength with irradiation at the excitation maximum (see Table 1). The concentration of α-keto acid was read from a calibration graph prepared in the usual manner.

Procedure for the separation of the DDB derivatives of α-keto acids by h.p.l.c. A mixture (1.0 ml) of α-keto acids was treated as in the manual procedure except that the neutralization with phosphate buffer and sodium hydroxide solution was omitted. The reaction mixture (10 μl) was directly injected into the chromatograph. The mobile phase was a mixture of methanol, acetonitrile and 40 mM phosphate buffer, pH 7.0 (65:40:95, v/v). The flow rate was 1.2 ml min^{-1} (approximately 100 kg cm^{-2}). The column temperature was ambient (ca. 25° C).

RESULTS AND DISCUSSION

Manual assay conditions

The optimal conditions for derivatization were examined by using the conventional fluorimetric method. The excitation and emission maxima of the fluorescence from pyruvic acid occurred at 361 and 448 nm, respectively (Fig. 1). On irradiation at 361 nm, the reagent blank fluoresced weakly (Fig. 1); the intensity was only 0.6% of that given by 5 nmol ml^{-1} solution of pyruvic acid. The fluorescence spectra of other model compounds were almost identical in shapes and maxima to those of pyruvic acid. Raman scattering of the solvent water was not observed under the recommended conditions.

α-Keto acids reacted with DDB in dilute hydrochloric acid solution, but not in neutral and alkaline solutions. Although sulfuric acid also allowed the same fluorescence to develop, DDB was only slightly soluble in sulfuric acid. Thus, DDB was dissolved in dilute hydrochloric acid. An acid concentration in the DDB solution in the range 0.4—0.6 M gave almost maximum fluorescence intensities; a 0.5 M solution was selected as optimum (Fig. 2). For all the model compounds, the DDB solutions giving the most intense fluorescences were greater than ca. 0.2 mM. The fluorescence intensity of the blank

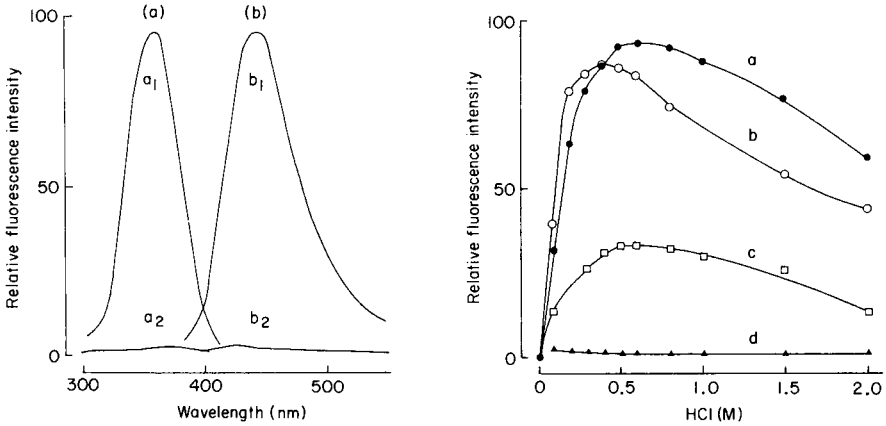

Fig. 1. Excitation (a) and emission (b) spectra of the reaction mixture from pyruvic acid (a_1, b_1) and from the reagent blank (a_2, b_2). A portion (1.0 ml) of 5 nmol ml^{-1} pyruvic acid was treated as in the manual procedure.

Fig. 2. Effect of the concentration of hydrochloric acid on the fluorescence development. Portions (1.0 ml of 1 nmol ml^{-1} solutions) of pyruvic acid (a), α-ketoglutaric acid (b), phenylpyruvic acid (c) and water (d, blank) were treated as recommended with various concentrations of hydrochloric acid in the reaction mixture.

increased slightly in proportion to the DDB concentration. Therefore, 0.25 mM DDB was used as a suitable concentration. β-Mercaptoethanol in the DDB solution stabilized DDB during the reaction. In its absence, the reaction mixture became red, which interfered with the assay of the acids. The fluorescence from the model compounds reached maximum and constant values at concentrations of β-mercaptoethanol greater than 0.2 M in the DDB solution; 0.21 M was used in the procedure.

The fluorescence reaction occurred at temperatures above ca. 37° C; higher temperatures allowed the fluorescence to develop more rapidly. At 100° C, which was selected for convenience, the intensities of the fluorescences from the model compounds became almost maximal after heating for 2.5 h (Fig. 3). When 0.4 M phosphate buffer (pH 7.0) and variously concentrated sodium hydroxide solutions (0.1—2.5 M) were added to the reaction mixture to adjust the pH to 6.0—8.0, the fluorescence from the model compounds became at least 30 times more intense than that in the acidic reaction mixture (Fig. 4). Thus, the pH of the reaction mixture was adjusted to 6.6—7.4 by adding 1.0 ml of 0.4 M phosphate buffer (pH 7.0) and 0.5 ml of 1.0 M sodium hydroxide. The fluorescence in the final mixtures was stable for at least 5 h in daylight at room temperature.

The calibration graphs for the model compounds were linear over the concentration range 0.01—100 nmol ml^{-1} and passed through the origin; these ranges are unusually wide. The precision was established by repeated determinations of 0.5 and 5.0 nmol ml^{-1} solutions of the model compounds. The

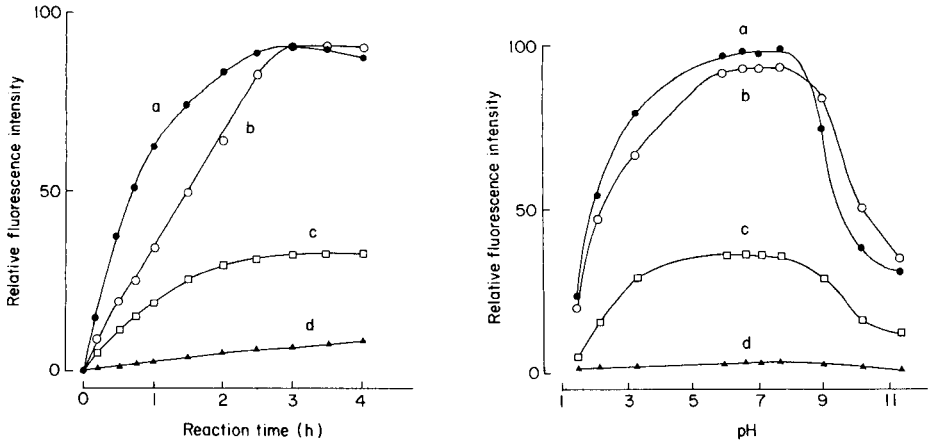

Fig. 3. Effect of reaction time on the fluorescence development: (a—d) as in Fig. 2. Conditions: 0.5 M hydrochloric acid in the DDB solution; reaction temperature 100° C.

Fig. 4. Effect of the pH on fluorescence intensities: (a—d) as in Fig. 2. Conditions: manual procedure except for pH adjustment (see text).

relative standard deviations were 1.5 and 1.4% for pyruvic acid, 1.8 and 2.0% for α-ketoglutaric acid, and 1.2 and 1.9% for phenylpyruvic acid, respectively (n = 10 in each case).

Fluorescence from other α-keto acids

Many α-keto acids fluoresced under the conditions recommended. The excitation and emission maxima, and the limits of detection by the manual assay are shown in Table 1. The excitation and emission wavelengths changed only slightly, if at all, for the individual acids. The fluorescence intensity obtained by the proposed method was 20—50 times that obtained by the method with OPD for all the acids. The limits of detection for most of the compounds were in the range 30—100 pmol ml^{-1}. *p*-Hydroxyphenylpyruvic acid could be detected at a concentration of 1.5 nmol ml^{-1}; however, the acid did not fluoresce appreciably even at a concentration of 10 nmol ml^{-1} in the reaction with OPD [4].

Reaction of other substances

Alloxan, diacetyl and ascorbic acid gave weak responses with the reagent at concentrations of 5 nmol ml^{-1}; the intensities were about double that of the reagent blank. None of the other biologically important substances examined fluoresced under the recommended conditions at a concentration of 10 nmol ml^{-1}. The compounds tested were benzaldehyde, 3-tolualdehyde, 2-hydroxybenzaldehyde, 3- and 4-hydroxybenzaldehyde, 2,4- and 3,4-dihydroxybenzaldehyde, 2-, 3- and 4-methoxybenzaldehyde, 2-chlorobenzaldehyde, glycine, 17 different L-α-amino acids, glutathione, creatine,

creatinine, histamine, tyramine, octopamine, dopamine, thiamine, citrulline, allantoin, uric acid, bilirubin, urea, *N,N*-dimethylurea, acetone, cyclohexane, 4-methylcyclohexane, acetylacetone, acetophenone, benzil, lactic acid, 3-hydroxybutyric acid, acetoacetic acid, homogentisic acid, inositol, D-xylose, D-glucose, D-fructose, D-galactose, D-mannose, D-maltose, D-lactose, epiandrosterone, dehydroepiandrosterone, cortisone and cholesterol. This suggested that the proposed method is usefully selective for α-keto acids.

Separation of DDB derivatives of α-keto acids by h.p.l.c.

Figure 5 shows typical chromatograms obtained with a standard mixture of ten α-keto acids of biological importance, and with water for the reagent blank. The individual α-keto acids gave single peaks in the chromatogram. This indicates that DDB can be used as a precolumn derivatization reagent for α-keto acids. The DDB derivatives of the acids could be separated within 18 min by isocratic elution.

A small peak in the chromatogram of the blank (peak 11 in Fig. 5, b) had exactly the same retention time as that of the peak for pyruvic acid (peak 2 in Fig. 5, a), and increased in height in proportion to increasing concentration of DDB. The peak could not be separated from the peak for pyruvic acid by

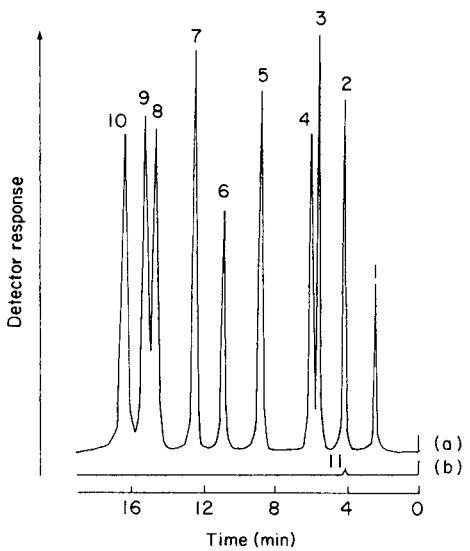

Fig. 5. Chromatograms of the DDB derivatives of α-keto acids (a) and the reagent blank (b). A portion (1.0 ml) of a mixture of ten α-keto acids or water was treated as in the recommended h.p.l.c. procedure. Peaks: (1) α-ketoglutaric acid, 5 nmol ml^{-1}; (2) pyruvic acid, 10 nmol ml^{-1}; (3) *p*-hydroxyphenylpyruvic acid, 700 nmol ml^{-1}; (4) α-ketobutyric acid, 20 nmol ml^{-1}; (5) α-ketovaleric acid, 20 nmol ml^{-1}; (6) α-ketoisovaleric acid, 40 nmol ml^{-1}; (7) α-ketoisocaproic acid, 20 nmol ml^{-1}; (8) phenylpyruvic acid, 60 nmol ml^{-1}; (9) α-ketocaproic acid, 30 nmol ml^{-1}; (10) α-keto-β-methylvaleric acid, 40 nmol ml^{-1}; (11) the reagent blank.

any changes in h.p.l.c. conditions. Thus, the peak caused an increase in the limit of detection for pyruvic acid. The eluates from peaks 1—10 in Fig. 5 had almost the same fluorescence excitation and emission spectra as those from the corresponding α-keto acids described in Table 1.

Aqueous methanol, aqueous acetonitrile and their mixtures were examined as mobile phase for reversed-phase h.p.l.c. on a Radial Pak Cartridge C_{18} column. With aqueous methanol, α-ketocaproic acid and α-keto-β-methylvaleric acid remained unseparated. When aqueous acetonitrile was used, the peaks for phenylpyruvic acid and α-ketocaproic acid could not be completely separated. All the DDB derivatives of the α-keto acids were most favourably separated with methanol/acetonitrile/water (65:40:95, v/v). The DDB derivatives fluoresced most intensely at pH 6.0—8.0 as described above. Thus, a phosphate buffer (pH 7.0) was used in place of water to give maximum peak heights. The concentration of the buffer had no effect on either the retention times or the peak heights in the range 10—50 mM; 40 mM phosphate buffer was used in the mobile phase.

Linear relationships were observed between the peak heights and the amounts of α-keto acids up to at least 300 pmol per injection volume (10 μl). The limits of detection are listed in Table 1. The sensitivity was at least 30 times better than those of the h.p.l.c. method with OPD [4].

The present h.p.l.c. method is very sensitive and selective for α-keto acids, and may be applicable to the determination of the acids in small amounts of serum and urine. The method, particularly, should be useful for the assay of phenylpyruvic acid, which is present in only minute amounts in normal urine. Work is in progress on these aspects.

REFERENCES

1 D. Cavallini, N. Frontali and G. Toschi, Nature (London), 163 (1949) 568.
2 J. E. Spikner and J. C. Towne, Anal. Chem., 34 (1962) 1468.
3 J. C. Liano, N. E. Hoffman, J. J. Barboriak and D. A. Roth, Clin. Chem., 23 (1977) 802.
4 T. Hayashi, H. Tsuchiya and H. Naruse, J. Chromatogr., 273 (1983) 245.
5 M. Nakamura, M. Toda, H. Saito and Y. Ohkura, Anal. Chim. Acta, 134 (1982) 39.
6 M. Nakamura, M. Toda, K. Mihashi, M. Yamaguchi and Y. Ohkura, Chem. Pharm. Bull., 31 (1983) 2910.
7 J. Ishida, M. Yamaguchi, M. Kai, Y. Ohkura and M. Nakamura, J. Chromatogr., 305 (1984) 381.

Analytica Chimica Acta, 172 (1985) 175—182
Elsevier Science Publishers B.V., Amsterdam — Printed in The Netherlands

SIMULTANEOUS DETERMINATION OF IRON(III) AND VANADIUM(V) WITH *N*-PHENYLCINNAMOHYDROXAMIC ACID AND THIOCYANATE BY EXTRACTION-SPECTROPHOTOMETRY

B. S. CHANDRAVANSHI*, ABIY YENESEW and ZERIHUN KEBEDE

Analytical Services and Research Unit, Department of Chemistry, Addis Ababa University, P.O. Box 1176, Addis Ababa (Ethiopia)

(Received 30th July 1984)

SUMMARY

N-Phenylcinnamohydroxamic acid (PCHA) reacts with iron(III) and vanadium(V) in the presence of thiocyanate to form water-insoluble orange and green complexes, respectively. The iron(III)-PCHA and vanadium(V)-PCHA-thiocyanate complexes can be quantitatively extracted into toluene and other common organic solvents at pH 1.5—2.0. The absorption spectra and composition of both complexes are described. The effects of foreign ions and of experimental variables on the extraction and determination of the two metal ions are studied. A simple, selective method is described for the simultaneous determination of iron(III) and vanadium(V) by extraction-spectrophotometry; absorbances are measured at 440 and 580 nm. Mixtures can be determined over the range 10^{-4}—10^{-5} M in each metal. The method was applied successfully to the analysis of standard steels for iron and vanadium.

N-Phenylcinnamohydroxamic acid (PCHA) has been used for the determination of several metal ions [1—11], including the extraction-spectrophotometric determination of iron(III) [8,9] and vanadium(V) [1,10]. Successive extraction and spectrophotometric determination of these two metal ions have been reported [8, 9], but not their simultaneous determination, probably because of the very different conditions needed for the extraction of iron(III) and vanadium(V). Further study of the reactions of PCHA with these two metal ions under different conditions has led to the method for their simultaneous determination described below. In this procedure, *N*-phenylcinnamohydroxamic acid is used with thiocyanate for extraction and spectrophotometry. The method is simple, sensitive and selective, and does not need rigid control of experimental variables. The method compares well with earlier procedures for this purpose [12—14] and can be applied to the determination of iron and vanadium in alloy steels and complex mixtures.

EXPERIMENTAL

Apparatus and reagents

A Beckman Model 24 u.v.-visible spectrophotometer with 1-cm quartz cells and a Beckman Chem Mate pH meter were used. Analytical-grade reagents were used unless otherwise specified. Distilled water was used throughout.

0003-2670/85/$03.30

Standard solutions of iron(III) and vanadium(V) were prepared from iron(III) nitrate nonahydrate and ammonium metavanadate, respectively, in water acidified with nitric acid; the solutions were standardized conventionally. An aqueous 0.50 M solution of ammonium thiocyanate was standardized by Volhard's method. Solutions of foreign ions (10 mg ml^{-1}) were acidified if necessary to prevent hydrolysis. The pH of solutions was adjusted with hydrochloric acid or ammonia (Spectrosol). Toluene and other solvents were redistilled.

The *N*-phenylcinnamohydroxamic acid (PCHA) was prepared as described previously [7]. A 0.005 M solution of PCHA in toluene was used.

Procedures

Preparation of sample solution. The steel sample (0.1 g) was heated gently in a 400-ml beaker with 10 ml of concentrated nitric acid until brisk reaction ceased, 5—10 ml of aqua regia was added, and the solution was evaporated to near dryness to expel nitrogen oxides. The residue was dissolved in 50 ml of slightly acidified (hydrochloric acid) water by heating. The solution was filtered through Whatman No. 42 filter paper to remove silicic acid and hydrated tungstic acid, the precipitate being washed several times with hot water. The filtrate and washings were diluted to volume in a 500-ml volumetric flask with water. Suitable aliquots of this solution were used.

Extraction of iron and vanadium. A solution containing 25—175 μg of iron(III) or vanadium(V) or both was mixed with 5 ml of 0.50 M ammonium thiocyanate and diluted to 25 ml with water, and the pH was adjusted to 1.5—2.0 with 1 M hydrochloric acid or 1 M ammonia solution. After quantitative transference to a 100-ml separatory funnel, the solution was extracted with 10 ml of the 0.005 M PCHA solution in toluene by vigorous shaking for 2—3 min. After phase separation, the organic phase was dried over anhydrous sodium sulphate (2 g), transferred quantitatively with toluene to a 25-ml volumetric flask and diluted to volume with toluene. The absorbance was measured after 40 min at 440 nm for iron(III), at 580 nm for vanadium(V), and at 440 and 580 nm for the simultaneous determination of the two metal ions, against the reagent blank.

For calibration, 0—2.5 ml of standard solutions of each metal ion (50 μg ml^{-1}) were taken through the procedure.

RESULTS AND DISCUSSION

Solvent for extraction and absorption spectra

Benzene, toluene, *o*-xylene, chlorobenzene, *o*-dichlorobenzene, chloroform, and carbon tetrachloride were found to extract both the complexes from the aqueous phase. Toluene was the most suitable solvent, giving quantitative extraction readily, and providing higher sensitivities for the colour reactions than the other solvents. The absorption spectra of the individual complexes were similar in all the nonpolar organic solvents but there were some variations in absorbances.

The absorption spectra are shown in Fig. 1. The reagent, PCHA, showed strong absorption only below 400 nm, with an absorbance maximum at 365 nm (π-π* transition). Thus a reagent blank is necessary for precise measurements at <500 nm. The iron(III)-PCHA complex showed strong absorption bands at 440 and 375 nm; the spectrum was identical regardless of the presence or absence of thiocyanate, which proves that thiocyanate is not involved in the complex formation with iron(III). The vanadium(V)-PCHA complex showed strong absorbance at 380 nm and weak broad absorbance band around 475 nm in the absence of thiocyanate. In the presence of ethanol, a clearer absorption band appeared at 450 nm, possibly because of esterification [15]. When thiocyanate was added, the absorption bands at 380 and 450 nm were shifted to 373 and 430 nm, respectively, with an increase in intensity, and a new intense band appeared at 580 nm, indicating the formation of a mixed ligand complex. This spectrum was not affected by ethanol, suggesting the absence of a hydroxyl group in this complex. Probably the hydroxyl group in the vanadium(V)-PCHA complex is replaced by thiocyanate.

Composition of complexes

The compositions of iron(III)-PCHA and vanadium(V)-SCN-PCHA complexes were examined by the mole ratio [16] and continuous variations [17] methods and by a simple spectrophotometric method [18]. Both the mole ratio and Job's methods showed that the stoichiometric ratio of iron(III) to PCHA was 1:3 and the ratio of vanadium(V) to PCHA was 1:2 in the complexes; thiocyanate was kept at a constant concentration throughout these tests. To determine the stoichiometric ratio of vanadium(V) to thiocyanate in the mixed ligand complex, a series of solutions was prepared in which the

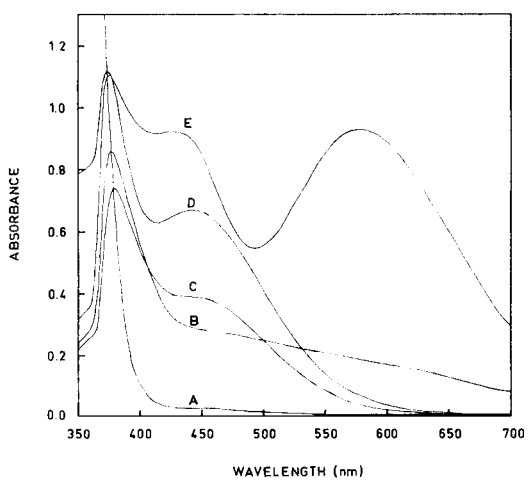

Fig. 1. Absorption spectra in toluene: (A) 2×10^{-3} M PCHA; (B) 8×10^{-5} M V(V)-PCHA; (C) 8×10^{-5} M V(V)-PCHA-ethanol; (D) 8×10^{-5} M Fe(III)-PCHA; (E) 1.2×10^{-4} M V(V)-SCN-PCHA (measured against reagent blank).

concentrations of vanadium(V) and PCHA, the pH, and ionic strength were kept constant, and the concentration of thiocyanate was varied; the complex was extracted (see Experimental) and the absorbance was measured at 580 nm against the reagent blank. A plot of $\log(A - A_{min})/(A_{max} - A)$ against $\log[SCN^-]$ (where A_{min} is the absorbance without thiocyanate, A_{max} is the maximum absorbance with excess of thiocyanate, and A is the equilibrium absorbance at a particular concentration of thiocyanate) had unit slope. This indicates that the stoichiometric ratio of vanadium(V) to thiocyanate is 1:1 in the mixed ligand complex.

To summarize, the composition of iron(III)-PCHA complex in the presence of thiocyanate is 1:3; this is the same as in the absence of thiocyanate [9]. The stoichiometric ratio of vanadium(V) to PCHA is 1:2 and the ratio of vanadium(V) to thiocyanate is 1:1; thus, the overall composition of the mixed ligand complex is 1:2:1 ($V:PCHA:SCN^-$). A 1:2 vanadium(V)-PCHA complex is formed in the absence of thiocyanate.

Effects of experimental variables

The optimum pH ranges of the aqueous phase for the complete extraction of iron(III) and vanadium(V) were found to be 1.1—2.5 and 1.3—2.1, respectively. At lower pH, the percentage extraction of both metal ions decreases because of protonation of PCHA and the formation of stable thiocyanate complexes; at higher pH, hydrated iron(III) oxide starts to precipitate.

Minimally, 4- and 8-fold molar excesses of PCHA were needed for complete extraction of vanadium(V) and iron(III), respectively, under the conditions described. Up to 100-fold excesses had no adverse effect on the extractions. The optimum concentration ranges of thiocyanate in the aqueous phase for the complete extraction of iron(III) and vanadium(V) were found to be 0.02—0.80 M and 0.03—0.15 M, respectively. At higher concentrations, formation of the vanadium(V) complex was incomplete while a large excess of PCHA was necessary for complete extraction of the iron(III) complex. At higher concentrations the water-soluble thiocyanate complexes became more stable, resulting in incomplete extraction of both metal ions. The order of addition of reagents had no effect on the characteristics of the coloured systems.

The wavelengths of maximum absorption and the absorbances of the coloured extracts of both the complexes were not affected by changes in ionic strength between 0.10 and 1.00 M, with respect to ammonium thiocyanate, potassium nitrate, and potassium chloride. Variations in temperature between 20 and 40°C did not affect the final absorbance values. The volume of the aqueous phase could be varied from 10 to 100 ml, with a 10-ml organic phase, without any adverse effect on extraction efficiency. The iron(III)-PCHA complex was completely extracted into toluene within 2 min, and the vanadium(V) mixed ligand complex in 2—3 min. Maximum absorbance in the toluene extract of the vanadium(V) complex was attained within 40 min and remained constant for 2 days at 20 ± 2°C. The toluene extract of the iron(III)-PCHA complex remained stable for 15 days at 20 ± 2°C.

Molar absorptivity, optimum concentration range and precision

The molar absorptivity (ϵ) and photometric sensitivity [19] for the complexes at different wavelengths are summarized in Table 1. The systems obeyed Beer's law in the concentration ranges 0.6—7.2 mg l^{-1} iron and 0.6—8.0 mg l^{-1} vanadium (referred to the final solution) at 440 and 580 nm, respectively. The reason for the choice of these wavelengths is obvious from Fig. 1. The optimum concentration ranges for determination evaluated from Ringbom plots [20] were 1.5—6.0 mg l^{-1} iron and 1.8—6.2 mg l^{-1} vanadium.

The precision of the method was evaluated from ten separate evaluations on samples containing 5 mg l^{-1} iron or 1 mg l^{-1} vanadium. The relative standard deviations were 0.4% for iron and 0.6% for vanadium.

Effect of foreign ions

The effects of foreign ions on the extraction and determination of iron(III) and vanadium(V) with PCHA in the presence of thiocyanate were studied by adding known quantities of the species to solutions containing 150 μg of iron(III) and 25 μg of vanadium(V) either separately or together. The pH of the solutions was adjusted to 1.5 ± 0.1 and the procedure described earlier given under Experimental was followed. The tolerance limits, taken as the concentration (mg l^{-1}) which caused an error less than 2%, are listed in Table 2.

Titanium(IV), zirconium(IV) and tungsten(VI) react with the reagents to form coloured complexes extractable into toluene and so interfere. The interferences from titanium(IV) and zirconium(IV) were eliminated by extraction of these metal ions with PCHA from 6—8 M hydrochloric acid solutions in the presence of thiocyanate [3, 5]; iron(III) and vanadium(V) remain in the aqueous phase under these conditions and can be determined as described above after the pH has been adjusted to 1.5. The interference from tungsten(VI) was eliminated by precipitation as tungstic acid with nitric acid and filtration or centrifugation. The results given in Table 2 prove that few ions normally associated with iron and vanadium in ores, alloys, steels, etc., will interfere in the simultaneous determination of iron(III) and vanadium(V) with PCHA and thiocyanate.

TABLE 1

Spectral characteristics of iron(III)-PCHA and vanadium(V)-SCN-PCHA complexes

Iron(III)-PCHA complex			Vanadium(V)-SCN-PCHA complex		
λ (nm)	ϵ (l mol^{-1} cm^{-1})	Sensitivity (μg Fe cm^{-2})	λ (nm)	ϵ (l mol^{-1} cm^{-1})	Sensitivity (μg V cm^{-2})
580	800	0.07	580[a]	7750	0.007
440[a]	8200	0.007	440	7720	0.007
375	12800	0.004	430	7780	0.007
—	—	—	373	9240	0.005

[a] Selected for simultaneous determination.

TABLE 2

Tolerance limit of foreign ions in the determination of iron(III) and vanadium(V) determined separately and together

Ion	Tolerance limit (mg l^{-1})
NO_3^-	2000
Na^+, K^+, Cl^-, SO_4^{2-}, acetate, phthalate	1000
Li^+, Be^{2+}, Mg^{2+}, Ca^{2+}, Sr^{2+}, Ba^{2+}, Zn^{2+}, Cd^{2+}, Hg^{2+}, Al^{3+}, La^{3+}, Tl^{3+}, Pb^{2+}, AsO_4^{3-}, Sb^{3+}, Ce^{4+}, UO_2^{2+}, Ni^{2+}, Co^{2+}, Mn^{2+}, citrate, tartrate, borate, phosphate	800
Cu^{2+}	400
Bi^{3+}, Cr^{3+} [a], Th^{4+} [b], Sn^{2+}	200
F^- [c]	100
Ti^{4+} [d], Zr^{4+} [d], MoO_4^{2-}, WO_4^{2-} [d]	50
Oxalate	10

[a] 400 mg l^{-1} in the vanadium determination. [b] 400 mg l^{-1} in the iron determination. [c] 200 mg l^{-1} in the vanadium determination. [d] See text.

Simultaneous determination of iron(III) and vanadium(V)

It has been found that iron(III) and vanadium(V) are completely extracted together into toluene from aqueous phase under identical conditions and the absorption spectra of the two metal complexes do not overlap considerably. Although the two spectra overlap in the regions 500—460 nm and 420—350 nm, they overlap very little in the region 600—550 nm. The iron(III)-PCHA complex absorbs strongly at 440 nm and weakly at 580 nm whereas vanadium(V)-SCN-PCHA complex absorbs strongly at 580 nm but less strongly at 440 nm. Thus by measuring the absorbance of the toluene extract (1 cm pathlength) at 440 and 580 nm, the concentration of the two metal ions can be determined in the original solution by solving the simultaneous equations

$$A_{440} = 8200\,[\text{Fe(III)}] + 7720\,[\text{V(V)}] \quad (1)$$

$$A_{580} = 800\,[\text{Fe(III)}] + 7750\,[\text{V(V)}] \quad (2)$$

Thus, a series of solutions was prepared by mixing the varying amounts of iron(III) and vanadium(V), the two metal ions being extracted together by the general procedure described above. The absorbances of the coloured extracts at 440 and 580 nm were measured against the reagent blank, and the concentrations of the two metal ions in the original solutions were calculated by solving the simultaneous equations. The results of several determinations (Table 3) indicate that the two metal ions present in different weight ratios can be determined precisely in given samples by the proposed method.

TABLE 3

Simultaneous determination of iron(III) and vanadium(V) in artificial mixtures

Iron(III) conc. ($\times 10^5$ M)		Vanadium(V) conc. ($\times 10^5$ M)	
Added	Found	Added	Found
12.00	12.16	0.24	0.23
12.00	12.18	0.60	0.58
12.00	12.15	1.20	1.18
7.20	7.04	7.20	7.21
1.20	1.22	12.00	12.03
0.40	0.39	8.00	7.76
0.24	0.24	12.00	12.02

TABLE 4

Determination of iron and vanadium in steels

B.C.S. Steel No.	Iron certified (%)	Iron found[a] (%)	Vanadium certified (%)	Vanadium found[a] (%)
64a	83.45	83.40	1.57	1.55
241/1	65.87	65.83	1.57	1.54

[a] Average of 6 determinations.

Application of the method

In order to check the reliability of the proposed method, it was applied for the simultaneous determination of iron and vanadium in British Chemical Standard Steels 64a and 241/1. The steel samples were decomposed as described above and iron(III) and vanadium(V) were extracted from suitable aliquots of the sample solutions. The absorbances of the coloured extracts were measured at 440 and 580 nm against the reagent blank and the concentrations of the two metal ions were calculated as above. The results are given in Table 4; they are in good agreement with the certified values, indicating that the accuracy of the method is satisfactory.

The authors are grateful to the Chairman, Department of Chemistry, Addis Ababa University, for providing the facilities.

REFERENCES

1 U. Priyadarshini and S. G. Tandon, Analyst (London), 86 (1961) 544.
2 A. K. Majumdar and A. K. Mukherjee, Anal. Chim. Acta, 22 (1960) 514.
3 N. K. Dutt and T. Seshadri, Ind. J. Chem., 6 (1968) 741.
4 N. K. Dutt and T. Seshadri, J. Inorg. Nucl. Chem., 31 (1969) 2153.
5 K. F. Fouche, H. J. LeRoux and F. Philips, J. Inorg. Nucl. Chem., 32 (1970) 1949.

6 E. A. Ostroumov and V. A. Kulumbegashvili, Zh. Anal. Khim., 26 (1971) 1111; Chem. Abstr., 75 (1971) 94377b.
7 A. K. Majumdar, *N*-Benzoylphenylhydroxylamine and its Analogues, Pergamon, Oxford, 1972.
8 F. G. Zharovskii and R. I. Sukhomlin, Zh. Anal. Khim., 21 (1966) 59; Chem. Abstr., 64 (1966) 14950f.
9 B. S. Chandravanshi and Alemayehu Amsalu, Mikrochim. Acta, II (1984) 7.
10 Mulugeta Assefa and B. S. Chandravanshi, Mikrochim. Acta, I (1983) 255.
11 Mulugeta Assefa and B. S. Chandravanshi, Ann. Chim. (Rome), 73 (1983) 421.
12 Z. Holzbecher, L. Divis, M. Kral, L. Sucha and F. Vlacil, Handbook of Organic Reagents in Inorganic Analysis, Ellis Horwood, Sussex, 1976.
13 A. K. Majumdar and D. Chakraborti, Anal. Chim. Acta, 53 (1971) 127.
14 R. S. Kharsan, K. S. Patel and R. K. Mishra, Mikrochim. Acta, I (1979) 353.
15 I. Kojima and Y. Miwa, Anal. Chim. Acta, 83 (1976) 329.
16 J. H. Yoe and A. L. Jones, Ind. Eng. Chem., Anal. Ed., 16 (1944) 111.
17 P. Job, Ann. Chim. (Paris), 9 (1928) 113.
18 J. Inczedy, Analytical Applications of Complex Equilibria, Ellis Horwood, Sussex, 1976.
19 E. B. Sandell, Colorimetric Determination of Traces of Metals, 3rd edn., Interscience, New York, 1959.
20 A. Ringbom, Z. Anal. Chem., 115 (1939) 332.

Analytica Chimica Acta, 172 (1985) 183—192
Elsevier Science Publishers B.V., Amsterdam — Printed in The Netherlands

INDIRECT SPECTROPHOTOMETRIC DETERMINATION OF TRACES OF ANTIMONY(III) BASED ON ITS OXIDATION BY CHROMIUM(VI) AND REACTION OF CHROMIUM(VI) WITH DIPHENYLCARBAZIDE

NORINOBU YONEHARA*, YASUYUKI NISHIMOTO and MASAAKIRA KAMADA

Department of Chemistry, Faculty of Science, Kagoshima University, Korimoto, Kagoshima 890 (Japan)

(Received 11th September 1984)

SUMMARY

An indirect method for the determination of antimony(III) is described. Antimony(III) is oxidized to antimony(V) by chromium(VI) and the excess of chromium(VI) is then determined spectrophotometrically with diphenylcarbazide. Optimal conditions were established for both the determination of antimony(III) and the elimination or reduction of interferences. Antimony(III) can be determined quickly and easily in the range 0.05—5 mg l^{-1}; the relative standard deviation is 2% for 1.0 mg l^{-1} antimony(III). The method is applicable to marine sediments and geothermal waters.

The determination of antimony, like arsenic, is of considerable current interest because of the influence of volcanic activity and the development of geothermal energy on the environment. A variety of instrumental methods has been developed for the determination of antimony; atomic absorption spectrometry [1—4] has recently been used in various samples. However, most of these methods require fairly sophisticated instrumentation and there is still a need for reasonably simple chemical methods. Spectrophotometric methods have been widely used and are usually based on ion-pair formation of an antimony(V) anion with a large dye cation followed by extraction for the absorbance measurement; the rhodamine-B method [5] is a standard procedure but many such methods have been described [6].

A kinetic method for the determination of antimony(III) based on induced oxidation of tris(1,10-phenanthroline)iron(II) by chromium(VI) has recently been reported [7]. Antimony(III) reacts rapidly and quantitatively with chromium(VI) in acidic solutions. The present paper describes an investigation on the indirect spectrophotometric determination of antimony(III). Antimony(III) is oxidized to antimony(V) by chromium(VI) and the excess of chromium(VI) is then determined with diphenylcarbazide (DPC) which is a fairly sensitive spectrophotometric reagent for chromium(VI). The resulting method is rapid, simple and reasonably sensitive without extraction.

003-2670/85/$03.30

EXPERIMENTAL

Apparatus and reagents

A Hirama Model 6B spectrophotometer was used for procedures A and B. A Hitachi Model-200-20 double-beam spectrophotometer was used with a thermostated (±0.1°C) cell holder coupled with a Hitachi Model-200 recorder for procedure C. Temperature was controlled with a Taiyo Model CL-15 circulating thermostated bath.

Deionized, distilled water and analytical-reagent grade chemicals were used throughout.

Antimony(III) stock solution (100 mg l^{-1}) was prepared by dissolving 100 mg of pure antimony in 25 ml of concentrated sulfuric acid with heating, and diluting the solution to exactly 1 l with 2.6 M sulfuric acid. The concentration of acid in this solution was determined titrimetrically with sodium carbonate. A 20 mg l^{-1} working solution of antimony(III) was prepared by taking 20 ml of the stock solution, adding just sufficient sodium carbonate to neutralize the acid and diluting to 100 ml with water. More dilute working solutions were prepared by simple dilution.

Potassium dichromate solution (4.8×10^{-3} M) was prepared by dissolving 0.353 g of potassium dichromate in water and diluting to 250 ml with water. More dilute solutions were prepared by simple dilution. The DPC solution (4.1×10^{-2} M) was prepared by dissolving 0.50 g of diphenylcarbazide in 25 ml of acetone and diluted to 50 ml with water.

Procedures

Procedure A. To 8.0 ml of sample solution containing up to 50 μg of antimony(III) in a glass-stoppered tube, 1.0 ml of 1.0 M sulfuric acid and 0.80 ml of 1.8×10^{-4} M potassium dichromate solution were added. Then 0.20 ml of the above DPC solution was added as quickly as possible (about 20 s) and mixed thoroughly. The absorbance of the solution was measured at 540 nm in 1-cm glass cells against a distilled water reference. When measurements were made with 2-cm glass cells, 0.80 ml of 9.0×10^{-5} M dichromate solution was used.

Procedure B. This procedure is the same as procedure A, except that the order of addition of the reagents was changed. The sulfuric acid and DPC solutions were added to the sample, and then the dichromate solution was added.

Procedure C (for following the chromium(VI)/DPC reaction). To a standard solution of antimony(III) in a 1-cm glass cell, 0.20 ml of sulfuric acid and 0.10 ml of DPC solution were added. The final volume was adjusted to 2.10 ml with water. The reaction was initiated by injection of 0.10 ml of dichromate solution. Equipment and technique to record absorbance vs. time plots have been described [7]. The chromium(VI)/DPC reaction was followed by absorbance measurements.

RESULTS AND DISCUSSION

Development of the method

The determination of antimony(III) is achieved indirectly through its reaction with an excess of chromium(VI)

$$3Sb(III) + 2Cr(VI) = 3Sb(V) + 2Cr(III) \quad (1)$$

followed by reaction of the excess of chromium(VI) with DPC and measurement of the resulting absorbance at 540 nm.

Calibration graphs by procedure A. A series of standard solutions of antimony(III) were treated as in procedure A. The resulting graphs (Fig. 1) show a good linear relationship. A series of solutions containing various amounts of dichromate and no antimony(III) were also treated as in procedure A; the absorbances obtained were plotted against the molar concentrations of the excess of chromium(VI) for an initial concentration of chromium(VI) of 2.9×10^{-5} M according to Eqn. (1). The calibration

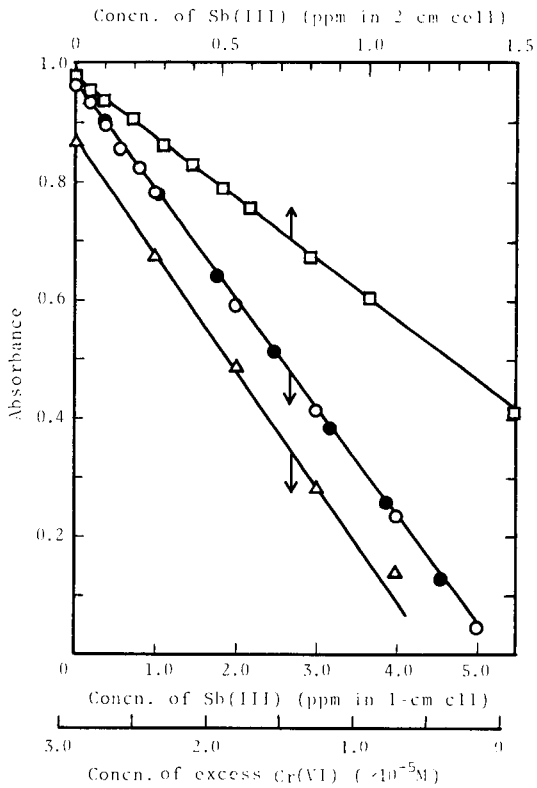

Fig. 1. Calibration graphs by procedure A: (○, □) antimony(III) at 27°C; (●) excess of chromium(VI) at 27°C; (△) antimony(III) in the presence of 0.25 M fluoride at 30°C. (○, △, ●) 1-cm cells; (□) 2-cm cells.

graph for antimony(III) coincided exactly with that for chromium(VI). This shows that antimony(III) reacts quantitatively with chromium(VI) according to Eqn. (1).

The sensitivity of the method obtained by use of 2-cm cell is twice that with the 1-cm cell, as expected. The smallest concentration that could be determined was 0.05 mg l^{-1} (ppm). The relative standard deviation for 11 replicate determinations of 1.0 mg l^{-1} antimony(III) with the 1-cm cell was 2.0%; that of 0.20 mg l^{-1} antimony(III) with the 2-cm cell was 3.5%.

Effect of reaction variables. The reaction of antimony(III) with chromium(VI) proceeds fairly rapidly even at 1° C. No significant changes in the sensitivity of the method were observed when the temperature was changed in the range 5—35° C, the concentration of sulfuric acid in the range 0.02—0.5 M or the DPC concentration in the range 4.1×10^{-4}—2.1×10^{-3} M. The conditions recommended for chromium(VI) determination [8] were used as a starting point in investigating this method. With increasing chromium(VI) concentrations, the calibration graphs rose in parallel and hence a wide quantitative range was obtainable. Given the absorbance value of the blank, an initial concentration of chromium(VI) of 2.9×10^{-5} M was selected in the case of 1-cm cells.

Interferences and their elimination

The effects of diverse ions on the determination of 1.0 mg l^{-1} antimony(III) were examined for procedure A. No interferences were found up to at least the following concentrations: 10 000 mg l^{-1} Cl^-, NO_3^-, PO_4^{3-}; 5000 mg l^{-1} Na, ClO_4^-; 3000 mg l^{-1} NH_4^+; 2000 mg l^{-1} K, SO_4^{2-}; 1000 mg l^{-1} F^-, Br^-; 100 mg l^{-1} Ag, Mg, Ca, Pb, Co(II), Ni, Al, Cr(III), Ti(IV), As(V) or acetic acid. Interfering ions are listed in Table 1. The interferences of Mo(VI), V(V), Fe(III) and Hg(II) are due to their reactions with DPC; most other ions seem to interfere by affecting the chromium(VI)/antimony(III) reaction.

The proposed method is based on the reaction of antimony(III) with an excess of chromium(VI). Therefore, arsenic(III) and vanadium(IV), which can reduce chromium(VI), interfere seriously with the determination of antimony(III). However, antimony(III) reacts rapidly with chromium(VI), while the other ions react fairly slowly. An attempt was made to eliminate their interferences by using the difference in reaction rates. The absorbance of a chromium(VI)/DPC solution remained unaltered by the addition of antimony(III), arsenic(III) and vanadium(IV). Accordingly, if DPC is added to the sample solution as rapidly as possible after the addition of chromium(VI), thus preventing the reduction of chromium(VI) by arsenic(III) or vanadium(IV), the interferences of these ions can be eliminated or significantly reduced.

Effects of standing times, temperature and concentration of sulfuric acid on the interferences of arsenic(III) and vanadium(IV). Solutions containing 10 mg l^{-1} arsenic(III) or 5 mg l^{-1} vanadium(IV) and sulfuric acid with and without 1.0 mg l^{-1} antimony(III) were treated with DPC solution at various

TABLE 1

Effect of interfering ions on the determination of 1.0 mg l^{-1} antimony(III) by procedures A and B

Species added	Concn. added (mg l^{-1})	Sb(III) found (mg l^{-1})		Species added	Concn. added (mg l^{-1})	Sb(III) found (mg l^{-1})	
		A[a]	B[b]			A[a]	B[b]
Mo(VI)	100	1.4	1.3	Fe(II)	1	1.8 (2.1)	1.3
	100[c]	(0.8)	0.8	Cu(II)	1	1.2	1.2
W(VI)	100	0.4	0.2	Ce(III)	1	1.3	1.1
	100[c]	(1.0)	1.1	Ce(IV)	1	1.3	1.1
V(V)	100	2.7		As(III)	100	2.2	1.3
	10	1.0	2.2		10	1.1 (2.0)	1.0
Fe(III)	100	(2.0)	7.5	V(IV)	20	3.3	1.4
	100[c]	(1.1)	2.0		10	2.3 (4.0)	1.2
	10	(1.6)	1.6	I^-	100	1.4	1.1
Hg(II)	10	0.2 (0.0)	0.1	S^{2-}	1	1.9 (2.5)	1.1
	1	0.7 (0.9)	1.0	F^-	1000	(1.0)	1.2
Sn(IV)	10	0.8	0.6	Cl^-	10000	(1.0)	1.5
Mn(II)	100		1.1	Oxalate	100	1.6 (1.8)	1.4
	10	1.5		Ethanol	37000	1.5 (1.8)	1.0

[a] 27° C with a standing time of 20 s; the values in parentheses are for a standing time of 2 min. [b] 30° C. [c] In the presence of 0.25 M fluoride.

reaction times after the addition of chromium(VI); the conditions were otherwise as in procedure A. As shown in Fig. 2, the difference between the absorbance of the antimony(III) solution and that of the solution without antimony(III), which corresponds to the stoichiometric reduction of chromium(VI) by antimony(III), indicates that antimony(III) has reacted completely with chromium(VI) after 10 s even at 1° C. As the standing time is increased, the absorbance decreases, thus it is preferable to add the DPC solution as rapidly as possible after the addition of chromium(VI); the shortest time feasible in a routine procedure was 20 s. Lower temperatures are also desirable for elimination of interferences in procedure A. The reactions of arsenic(III) and vanadium(IV) went to completion in 5 and 2 h, respectively, at 27° C. The higher the concentration of sulfuric acid, the lower the absorbance (Fig. 3). With <0.03 M sulfuric acid, the color was unstable in the presence of vanadium(IV) and the lower the sulfuric acid concentration, the longer the time for color development. The range 0.05—0.10 M was favorable.

In the determination of 1.0 mg l^{-1} antimony(III) in the presence of 5 mg l^{-1} vanadium(IV) or 10 mg l^{-1} arsenic(III), high values of 1.8 and 1.7 mg l^{-1}, respectively, were obtained for a standing time of 2 min at 27° C with 0.10 M sulfuric acid, whereas normal values of 1.0 and 1.1 mg l^{-1}, respectively, were obtained for a time of 20 s at 1° C with 0.10 M sulfuric acid. The effect of other species after a standing time of 2 min are also shown in Table 1. The effects of ions for which data at 2 min are not given were independent of standing time.

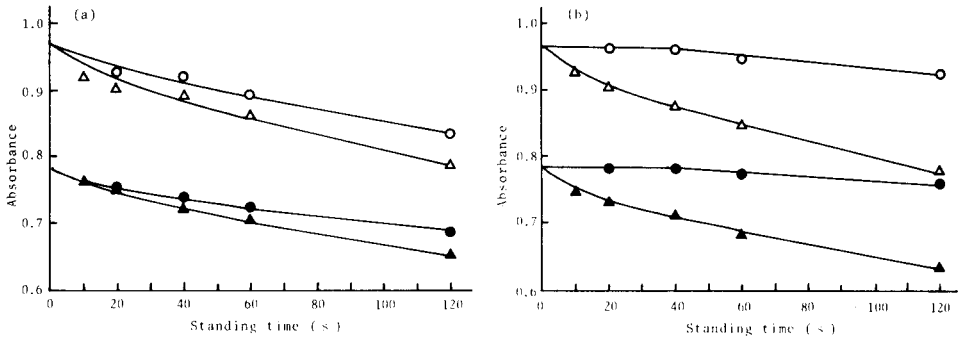

Fig. 2. Effect of standing time on the interferences of (a) arsenic(III) and (b) vanadium(IV). Curves: (○, △) 10 mg l^{-1} arsenic(III) or 5 mg l^{-1} vanadium(IV); (●, ▲) 1 mg l^{-1} antimony(III) in the presence of 10 mg l^{-1} arsenic(III) or 5 mg l^{-1} vanadium(IV). Temperature: (○, ●) 1°C; (△, ▲) 27°C. Other conditions: 2.9×10^{-5} M chromium(VI), 8.2×10^{-4} M DPC, 0.10 M sulfuric acid.

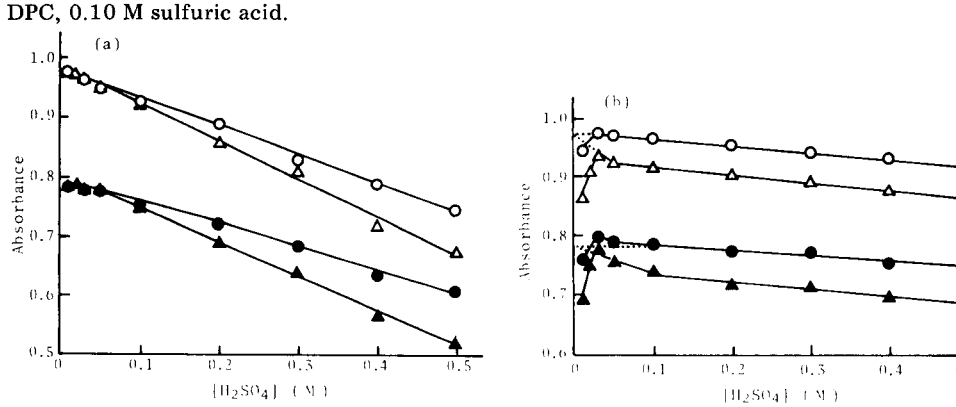

Fig. 3. Effect of sulfuric acid concentration on the interferences of (a) arsenic(III) and (b) vanadium(IV) for a standing time of 20 s. All symbols and conditions (except sulfuric acid concentration) as in Fig. 2.

Reactions in procedure B

When the reactions of antimony(III), arsenic(III) or vanadium(IV), and DPC with chromium(VI) were initiated by adding chromium(VI) as in procedure B, the three species present competed for the chromium(VI). If the rate of reaction between DPC and chromium(VI) were sufficiently smaller than that of the antimony(III)/chromium(VI) reaction, but larger than those of the interfering reactions, the interferences could be eliminated or decreased. The reaction conditions for minimizing the interferences were therefore examined.

Calibration graphs by procedure B. A series of standard solutions of antimony(III) were treated as in procedure B; the resulting graphs are shown in Fig. 4. The graphs deviate from a stoichiometric relationship at higher concentrations of antimony(III); the higher the temperature, the larger the deviation. Probably an increase in temperature has a greater effect on the

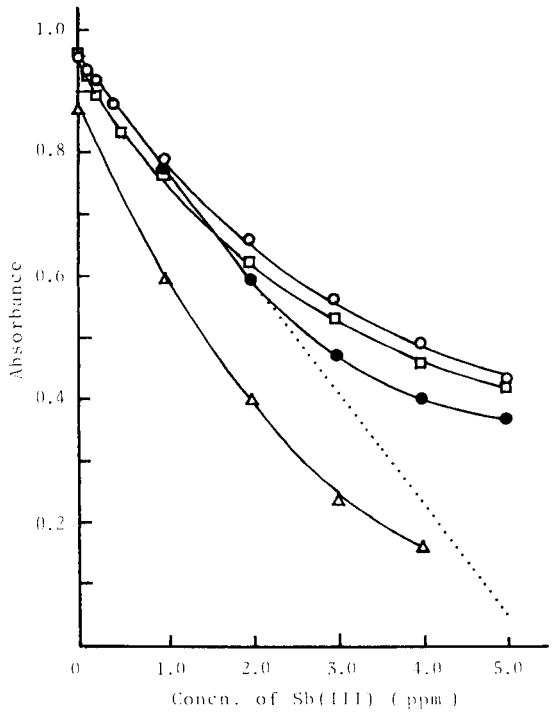

Fig. 4. Calibration graphs by procedure B: (○, ●, △) 1-cm cell; (□) 2-cm cell (see text); (○, △, □) 30°C; (●) 1°C; (△) in the presence of 0.25 M fluoride.

rate of the DPC/chromium(VI) reaction than on that of the antimony(III)/chromium(VI) reaction, thus reducing the chromium(VI) concentration available to antimony(III). The limit of determination was 0.1 mg l^{-1} and the relative standard deviation for 11 determinations of 1.0 mg l^{-1} antimony(III) with 1-cm cells was 2.0%. For the calibration graph obtained by the use of 2-cm cells, the concentration of chromium(VI) used was half of that used with the 1-cm cells, thus the absorbances were similar.

Effect of reaction variables on the effects of interfering species. The reactions were studied by procedure C. The reaction of DPC with chromium(VI) was followed by measuring the increase in absorbance as a function of time. The times required for the absorbance to reach a maximal constant value in the absence of antimony(III) are given in Table 2. The time decreased with increasing temperature and the concentrations of sulfuric acid and DPC, but was independent of chromium(VI) concentration.

The effects of the concentrations of sulfuric acid and DPC on the interferences of arsenic(III) or vanadium(IV) were examined further by procedure C; the maximal constant absorbances obtained are shown in Figs. 5 and 6. As can be seen, the effects of arsenic(III) and vanadium(IV) decrease with increasing DPC concentration, because of the increased rate of the

TABLE 2

Times required for absorbance to reach a maximal constant value in the absence of antimony(III)

H_2SO_4		DPC		Cr(VI)		Temp.	
M	s	$\times 10^{-3}$ M	s	$\times 10^{-5}$ M	s	°C	s
0.027	76	0.38	69	1.3	34	15	58
0.09[a]	35	0.75[a]	35	2.6[a]	35	20	45
0.27	18	1.30	24	5.2	35	27[a]	35
0.45	13	1.90	17			35	28
						40	25

[a]Conditions except that specified at the column head were maintained at the values asterisked in the various tests.

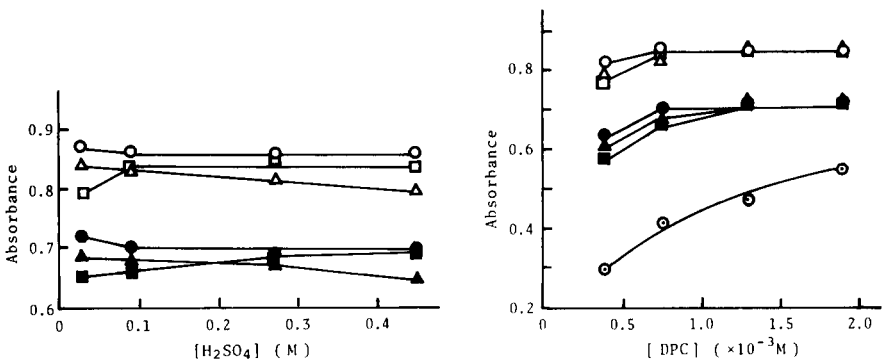

Fig. 5. Effect of sulfuric acid concentration on the interferences of arsenic(III) and vanadium(IV): (○) blank; (△) 20 μg As(III); (□) 10 μg V(IV); (●) 2 μg Sb(III); (▲) 2 μg Sb(III) with 20 μg As(III); (■) 2 μg Sb(III) with 10 μg V(IV). Conditions: 7.5 × 10^{-4} M DPC, 2.6 × 10^{-5} M chromium(VI); reaction temperature, 27° C; reaction volume, 2.2 ml.

Fig. 6. Effect of DPC concentration on the interferences of arsenic(III) and vanadium(IV): (⊙) 8 μg Sb(III); all other symbols as in Fig. 5. Conditions: 0.09 M sulfuric acid; otherwise as for Fig. 5, except DPC.

chromium(VI)/DPC reaction. However, the reaction of antimony(III) is also depressed, producing the large deviation from linearity in the calibration graph and thus the narrow determination range. Thus 0.10 M sulfuric acid and 8.2 × 10^{-4} M DPC were selected for the general procedure.

Although the interferences of arsenic(III) and vanadium(IV) decreased at lower chromium(VI) concentrations, the slope of the calibration graph also decreased. Taking into account the magnitude of the interferences, the sensitivity and the absorbance value of the blank, 2.9 × 10^{-5} M in the case of 1-cm cells and 1.4 × 10^{-5} M for 2-cm cells were suitable as the initial chromium concentrations.

TABLE 3

Determination of antimony in samples

Sample	Proc.	Aliquot (ml)	Sb added (μg)	Calibration graph		Standard addition		Other method
				Sb found (μg)	Recovery (%)	Sb found (μg)	Sb in sample (μg mg^{-1})	Sb in sample (μg mg^{-1})
I[a]	A	0.25	0	3.7	—	3.3	12	14[e]
			2.0	6.0	115			
			4.0	8.4	118			
	B	0.25	0	3.7	—	2.8	10	
			2.0	6.8	155			
			4.0	8.5	120			
II[b]	A	0.50	0	1.9	—	1.9	1.9	1.1[e]
			2.0	4.4	125			
			4.0	6.3	110			
	B	0.50	0	1.8	—	1.3	1.3	
			2.0	4.9	155			
			4.0	7.3	138			
III[c]	A	5.0	0	2.1	—	2.3	0.46	0.15[f]
			1.0	3.0	90			
			2.0	3.8	85			
	B	5.0	0	0.5	—	1.0	0.20	
			2.0	1.1	30			
			4.0	2.6	53			
IV[d]	A	4.0	0	0.7	—	0.6	0.15	0.074[f]
			1.0	2.1	140			
			2.0	2.8	105			
	B	4.0	0	0.7	—	0.5	0.13	
			1.0	1.8	110			
			2.0	2.9	110			

[a]Prepared by treating 109 mg of marine sediment I. [b]Prepared by treating 205 mg of marine sediment II. [c]Geothermal water taken at Kirishima. [d]Geothermal water taken at Yamakawa. [e]Rhodamine-B method [5]. [f]Atomic absorption method [4].

Changing temperature in the range 15—40° C made little difference to the effects of arsenic(III) and vanadium(IV). However, when 1 mg l^{-1} antimony-(III) was determined in the presence of 10 mg l^{-1} arsenic(III), 5 mg l^{-1} vanadium(IV), 100 mg l^{-1} oxalate or 0.8 M ethanol by procedure B, the results obtained were, respectively, 1.3, 1.0, 1.6 or 1.2 mg l^{-1} at 1° C, but 1.0, 1.0, 1.4 or 1.0 mg l^{-1}, respectively, at 30° C. The higher temperature is thus suitable for procedure B.

Effect of diverse ions on procedure B. The effects of the interfering ions listed in Table 1 were also examined for procedure B. Most ions, except Fe(III) and V(V), showed less interferences than on procedure A.

Sodium fluoride was tested as a masking agent for iron(III). Fluoride up to 0.05 M had no effect on procedure A and only a slight effect on procedure

B, but it did not effectively eliminate the iron interference. A fluoride concentration of 0.25 M was used; 5 min was then needed to attain maximal absorbance, and the calibration graphs were affected, especially for procedure B (see Figs. 1 and 4). The influence of 100 mg l^{-1} iron(III) was eliminated in procedure A and reduced in procedure B; the interferences of 100 mg l^{-1} Mo(VI) or W(VI) were also reduced (Table 1).

Application to marine sediments and geothermal water

In order to check the applicability of this method, procedures A and B were applied to the determination of antimony in samples which may contain various interfering ions. Marine sediments were taken at the sea bottom quite near the submarine fumaroles of the Sakurajima volcano in Japan and were first treated by the procedure described previously [7]. Geothermal waters were taken from deep geothermal drill holes at Kirishima and Yamakawa in Japan. These samples were also analyzed by the rhodamine-B extraction method [5] or the atomic absorption method [4]. The results are shown in Table 3, together with those obtained by standard additions with the present method. The values obtained directly from a calibration graph show excessive or deficient recoveries of added antimony. The results obtained by the standard addition method according to procedure B, however, agree approximately with those obtained by the other methods.

Procedure B is recommended as the general procedure; it is easier and suffers from fewer interferences. The interferences may be further reduced by using less chromium(VI) and more DPC with 2-cm cells, but the determination range then becomes narrower. The effects of changing acid concentration and temperature may be beneficial in some cases, as shown in Figs. 2, 3 and 5.

REFERENCES

1 T. Kamada and Y. Yamamoto, Talanta, 24 (1977) 330.
2 S. Nakashima, Analyst (London), 105 (1980) 732.
3 M. Yamamoto, K. Urata and Y. Yamamoto, Anal. Lett., 14 (1981) 21.
4 M. Yamamoto, K. Urata, K. Murashige and Y. Yamamoto, Spectrochim. Acta, Part B, 36 (1981) 671.
5 Japanese Industrial Standard Method (JIS)K-0102-1981, Japanese Standards Association, Tokyo, p. 182.
6 See, e.g., Z. Marczenko, Spectrophotometric Determination of Elements, Horwood, Chichester, 1976.
7 N. Yonehara, Y. Nishimoto and M. Kamada, Anal. Chim. Acta, 143 (1982) 277.
8 Japanese Industrial Standard Method (JIS)K-1020-1981, Japanese Standards Association, Tokyo, p. 187.

Analytica Chimica Acta, 172 (1985) 193—205
Elsevier Science Publishers B.V., Amsterdam — Printed in The Netherlands

EXTENSION OF MULTICOMPONENT SELF-MODELING CURVE RESOLUTION BASED ON A LIBRARY OF REFERENCE SPECTRA

MICHAEL F. DELANEY* and DAVID M. MAURO
Department of Chemistry, Boston University, Boston, MA 02215 (U.S.A.)
(Received 31st January 1985)

SUMMARY

The recently proposed linear programming algorithm for estimating component spectra by using self-modeling curve resolution is shown to be inadequate in cases for which some of the components have similar, nondescript spectra and when the data are noisy. The extension of this technique reported is based on the use of a library of representative reference spectra. In this technique, the spectral library is searched for spectra reconstructed by using the significant principal eigenvectors of the second moment matrix. Similarity between the reconstructed spectra and the best match in the library is used as the objective function to yield estimates of the component spectra. This approach can be used to obtain better estimates of the component spectra. The approach can be used with noisy data, and is shown to perform well when the actual pure components are not members of the reference library.

The technique of self-modeling curve resolution (SMCR) was developed by Lawton and Sylvestre [1] in 1971 to address the experimental situation in which the samples consist of mixtures of unknown amounts of an unknown number of unknown compounds. This can be considered to be the most difficult and general of a type of problem referred to in chemometrics review articles [2—4] as "resolution". The SMCR method has been applied by Kowalski and co-workers to two of the major combinations of spectrometry and chromatography: gas chromatography with mass spectrometry [5, 6] and liquid chromatography with multichannel ultraviolet absorption detection [7]. These efforts, and a recent chromatographic application of SMCR [8], show the resolution of only two component peaks. Vandeginste [9] briefly presented results of three-component SMCR; however, it is not clear whether this implementation can be generalized to a higher dimensionality.

In an effort to extend SMCR to a general solution, Meister [10] recently reported an extension of SMCR, using a linear programming algorithm to estimate the pure component spectra. This seemingly efficient approach, which functions under the assumption of maximally dissimilar component spectra, uses an optimization strategy to position the largest simplex within the boundary constraints imposed by the requirement of non-negative spectral intensities. This paper demonstrates two inadequacies in Meister's heur-

0003-2670/85/$03.30

istic approach, and further extends SMCR by using a library of reference spectra. Meister's approach assumes that the pure spectra should be most dissimilar. This new method assumes that a library of reasonably representative reference spectra is available. It has been found that this approach is more immune to the problems caused by noisy data and nondescript pure spectra than is Meister's approach. The success of the new method is demonstrated by examples of vapor-phase Fourier-transform infrared spectra.

THEORY

No attempt will be made to repeat the mathematical development of SMCR; the original references [1, 5, 6] are easily available.

For SMCR applied to spectrometric/chromatographic combinations, the experimental data consist of a set of spectra obtained during the elution of the chromatographic peak. Each spectrum can be regarded as a different mixture of the pure components which comprise the peak. This raw data matrix is first normalized so that the intensities for each spectrum sum to one, and then the spectra are centered about the mean by subtracting the average value from each wavelength channel. This decreases the number of significant eigenvectors by one [7], thus reducing the dimensionality of the resulting eigenspace.

Next, the correlation matrix (second moment matrix) is formed by premultiplying the normalized, centered data matrix by its transpose. Principal components analysis (eigenanalysis) is then performed on the correlation matrix to produce the characteristic eigenvectors and their corresponding eigenvalues. A suitable stopping rule is used to determine the number of significant eigenvectors, which should be one less than the number of pure components in the chromatographic peak. The significant eigenvectors can be considered to form a reduced Cartesian coordinate system in which each normalized, centered mixture spectrum can be represented as a single point. The spectrum of each pure component in the sample mixtures can also be similarly projected onto a single point in this space.

Because the chemical concentration of each component in each mixture is constrained to be positive, all the mixture points must lie within the convex polygon (simplex) formed by connecting together each of the pure points. An example of this for a three-component situation is shown in Fig. 1. As mathematically derived by Sharaf and Kowalski [5, 6], this simplex can also be used to describe the relative concentrations of the pure components in any mixture which can be formed; the vertices correspond to pure solutions, the edges of the simplex would be two-component mixtures, and the internal points correspond to mixtures formed from all three components with their positions indicating the composition of the mixture. From any of the points in this eigenspace, a spectrum can be calculated, because each spectrum is a weighted sum of the eigenvectors which define the eigenspace, with the coordinates of each point being the weights for its respective spectrum.

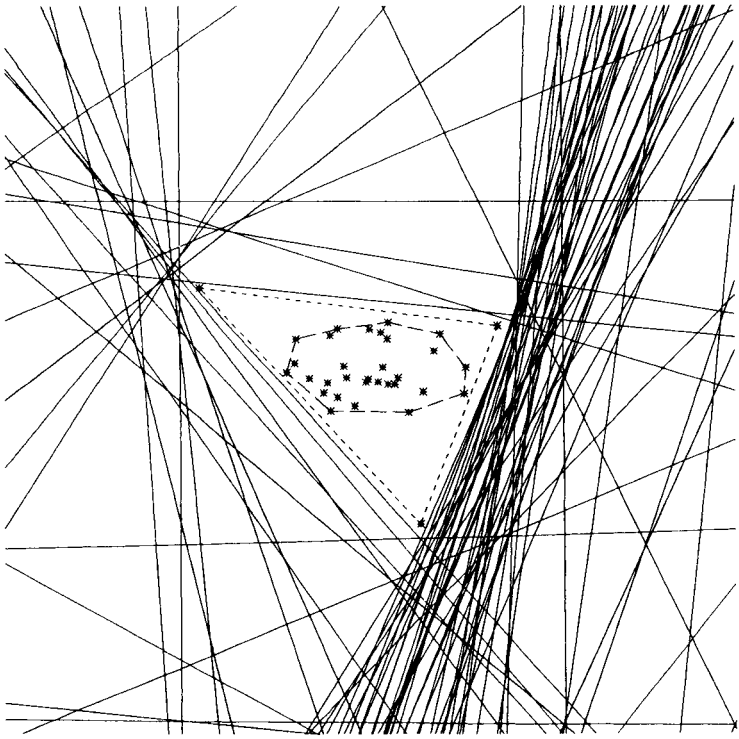

Fig. 1. Example of a 3-component SMCR solution (for mixture 2) which includes projections of the mixture spectra, projections of the pure components (connected by a dotted line), inner boundary (dashed line), and outer boundaries (solid lines). The horizontal axis is the projection onto the first eigenvector and the vertical axis is the projection onto the second eigenvector. The range of both axes is from −0.2 to +0.2. The same axes are used in Figs. 3, 4, 6, 8, 9, 10 and 11.

At this point in SMCR, one has deduced the dimensionality of the data, and (at least ideally) the number of pure components in the mixtures. The goal of SMCR is to locate the pure points, from which one can obtain the spectra of the pure components and the composition of each of the mixtures. The problem is constrained in two ways. The limitation that no concentration of any component in a mixture can be negative constrains a pure point to lie outside of an inner boundary, which contains all of the measured mixture points. The second constraint is that the spectral intensity in each channel (wavelength) must be positive. This gives rise to an outer boundary inside which a pure point must lie in order to have positive intensities in each spectral channel (Fig. 1).

Meister's method [10] produces estimates of the locations of the pure points by making the assumption that the pure spectra are as different as possible. This effectively ignores the inner boundary, and locates the largest possible simplex of the desired dimensionality which lies within the outer

boundary. This method works well in cases such as that in Fig. 1; however, as will be shown later, this method can fail when either the pure spectra are reasonably similar or when the measurement noise is large enough to distort the location of the outer boundary.

Because a spectrum can be generated from any point in the eigenspace, it was reasoned that these spectra could be used as the unknowns for library searching (LS) against a collection of reference spectra [11]. In the ideal case, a spectrum for each of the pure components is present in the library. When a spectrum is generated from a point near one of the pure points, that spectrum should match well with its corresponding spectrum in the library. For this reason, the proposal was to use the similarity between the generated spectrum and its best match in the reference library as an objective function by which to locate the pure points in the eigenspace.

In practice, there can be no guarantee that the correct spectra will be in the reference library; however, the library search will always find the spectrum which is most similar to the one being sought. As will be seen later, even in this case, the best-match objective function can still find restricted regions of eigenspace which contain the pure points.

EXPERIMENTAL

In this study the same 2000 vapor-phase Fourier-transform infrared (F.t.i.r.) spectra were used as in previous studies [11—13]. Each original full-intensity spectrum consisted of 1842 data points, sampled at 2 cm^{-1} from 4000 cm^{-1} to 450 cm^{-1}. Each of the 2000 library spectra was reduced to a 231-dimensional spectrum by a combination of moving and boxcar averaging [12], which corresponds to a sampling interval of about 15 cm^{-1}. The signals, linear in absorbance units, were normalized to fall between 0 and 1000 at unit resolution.

To simulate a chromatographic experiment consisting of an unresolved peak of three components, library spectra were selected and combined in various randomly selected proportions to generate spectra for thirty random mixtures. In some experiments, normally (Gaussian) distributed noise was added to the mixture spectra to produce noisy spectra with a preselected signal/noise ratio (S/N). These thirty 231-dimensional spectra were carried through the entire SMCR process, to yield the significant eigenvectors, the mixture points projected into the reduced eigenspace, and the information necessary to represent the inner and outer boundaries. All matrix manipulations, including principle components analysis (p.c.a.), were performed in double-precision arithmetic by using subroutines from the IMSL package (IMSL, 7500 Bellaire Blvd., Houston, TX 77036-1927).

Two sets of random mixtures were used. The first (mixture 1) was composed of the relatively similar spectra of tricosane, 3-decyne, and 3,5-dimethyl-4-heptanol (Fig. 2a—c). The results of calculations with this group of three compounds were compared to results with mixtures of three rather

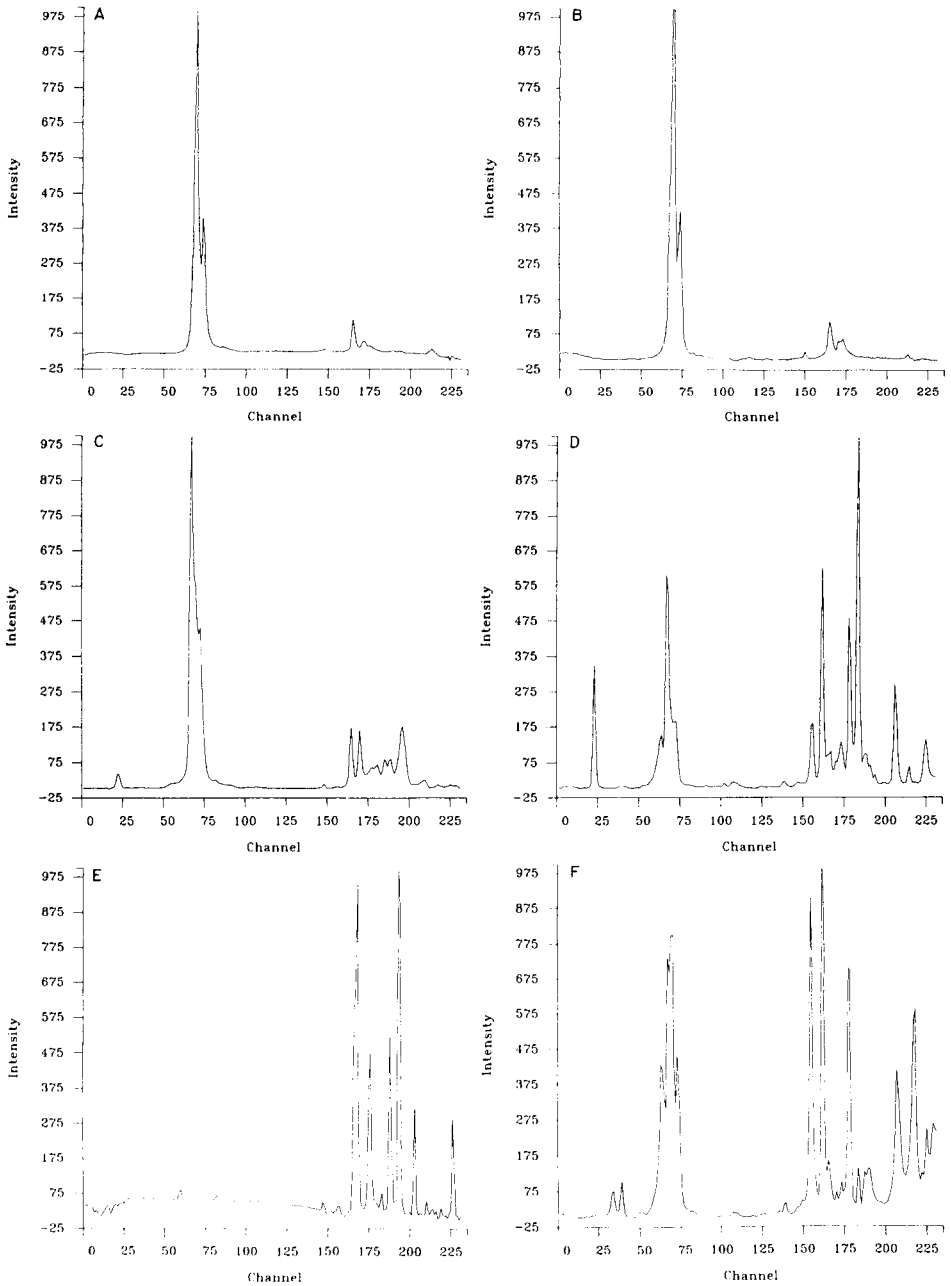

Fig. 2. Spectra of compounds used in this study. Spectra were sampled at approximately 15 cm^{-1} resolution, from 4000 cm^{-1} to 450 cm^{-1}. (a) Tricosane; (b) 3-decyne; (c) 3,5-dimethyl-4-heptanol; (d) *p*-cumenol; (e) 1,2,4,5-tetrabromobenzene; (f) *p*-propylaniline.

different compounds (mixture 2) having complex spectra, i.e., *p*-cumenol, 1,2,4,5-tetrabromobenzene, and *p*-propylaniline (Fig. 2d—f).

In the second phase of each experiment, an evenly spaced 25 × 25 point grid spanning the interesting region of the solution eigenplane was located. Using the eigenvectors, a 231-point spectrum was reconstructed from each point. The spectra were normalized from 1 to 1000 and converted to integer values. These spectra were then matched against the library of 2000 F.t.i.r. spectra and the closest two matches were saved. The distances to the best match for these 625 spectra were used to generate a contour plot and a three-dimensional surface plot, in order to show how the success of matching these reconstructed spectra varies with the location on the solution eigenplane. Because the distances obtained by library searching span a wide range (about 10^8 in this study), before the contour or surface plots are generated, the distances were normalized by multiplying the logarithm of the distance by ten. This gave distances which typically ranged from 10 to 100. Contour-line intervals were chosen to emphasize the surface minima by plotting contours from 1 to 100 in increments of 1 or 2 depending on the steepness of minima and maxima.

In each of the SMCR diagrams (Figs. 1, 3, and 8), and the accompanying SMCR-LS contour plots (Figs. 4, 6, 9, and 11), the axes correspond to the projection onto the two significant eigenvectors. The horizontal axis is the projection onto the first eigenvector and the vertical axis is the projection onto the second eigenvector. The range of both axes is from −0.25 to +0.25. The three-dimensional surface plots (Figs. 5, 6, 10, and 12) have been inverted because the human vision system seems to have more acuity for viewing peaks than valleys. Also, these plots have been rotated about the coordinate origin (as described in the figure captions) to afford the best direction for viewing the peaks. These plots, and the underlying interpolations were constructed by using the DI-3000 graphics package (Precision Visuals, 6060 Lookout Road, Boulder, CO 80301-9989).

RESULTS AND DISCUSSION

Even two-component SMCR can at best determine regions of the solution eigenspace where the pure components should be found. As the dimensionality of the problem increases, the magnitude and complexity of the solution zone increases. Meister's approach [10] attempts to overcome this uncertainty by finding estimates of the pure spectra, using the assumption that spectra should be as different as possible. The spirit of the SMCR approach is to avoid making limiting assumptions. Specifically, no assumptions are made about the number of sample components, spectral band shapes, or relationships between the mixtures (chromatographic peak shapes). However, there is still a need either to reduce the size of the resulting solution zones, so that the pure points can be found, or to estimate acceptable pure spectra from the solution zone. Meister's approach does this by making a constraining

assumption. The present approach of combining library searching with self-modeling curve resolution (SMCR/LS) avoids making assumptions, yet still is able to find better estimates of the pure spectra, even when one or more of the mixture components do not have a spectrum in the library.

The first of the two cases in which Meister's method is unsatisfactory occurs when the pure component spectra are rather similar and do not contain very many peaks. In mixture 1, even though the 30 mixture points represent the three components quite well (there are mixtures relatively pure in each component), the outer boundaries are significantly larger than the pure component triangle (Fig. 3). This should be compared to mixture 2, where it is seen that the outer boundaries closely approximate the pure component simplex (Fig. 1). It can be seen in Fig. 3 that while Meister's simplex triangle solution to this problem would estimate the two upper pure components reasonably well, the third vertex of the triangle would be very far from its corresponding pure point. This situation is even observed in the simulated example used in the original paper (Fig. 1 [10]).

The use of LS to find the locations of the pure points gives the results shown in Fig. 4 for mixture 1 and Fig. 6 for mixture 2. There are three well-defined valleys which indicate close matches in the SMCR/LS process. Also these valleys are seen to contain the pure points near the bottom. It can be seen that for this example the analysis results in a much better estimate of the location of all three of the pure points. The 3-dimensional surface plots for these examples are shown in Figs. 5 and 7. It should be noted that in practice it would not be necessary to generate and search all 625 reconstructed spectra and to produce the surface contouring. A more efficient approach

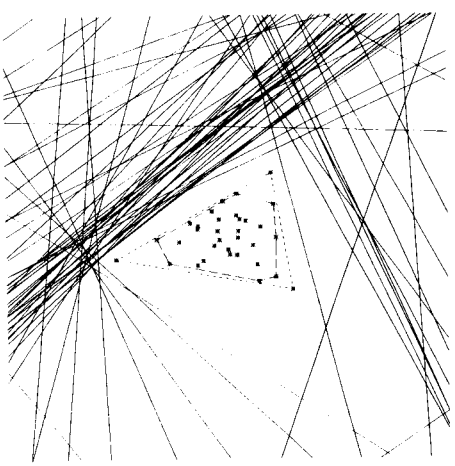

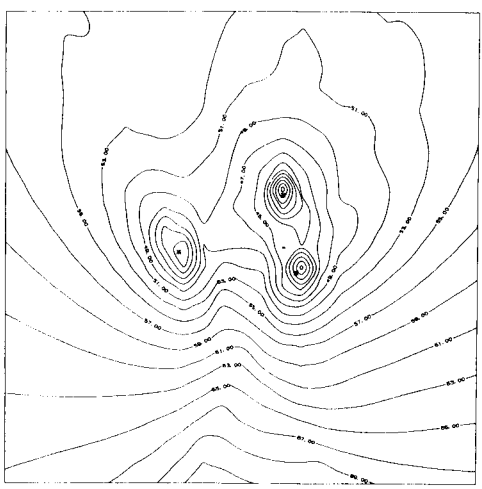

Fig. 3. The 3-component solution for mixture 1. The pure component projections are connected by dotted lines; the inner boundary is a dashed line; the outer boundary is the solid line.

Fig. 4. Contour diagram generated by SMCR/LS from the data for mixture 1.

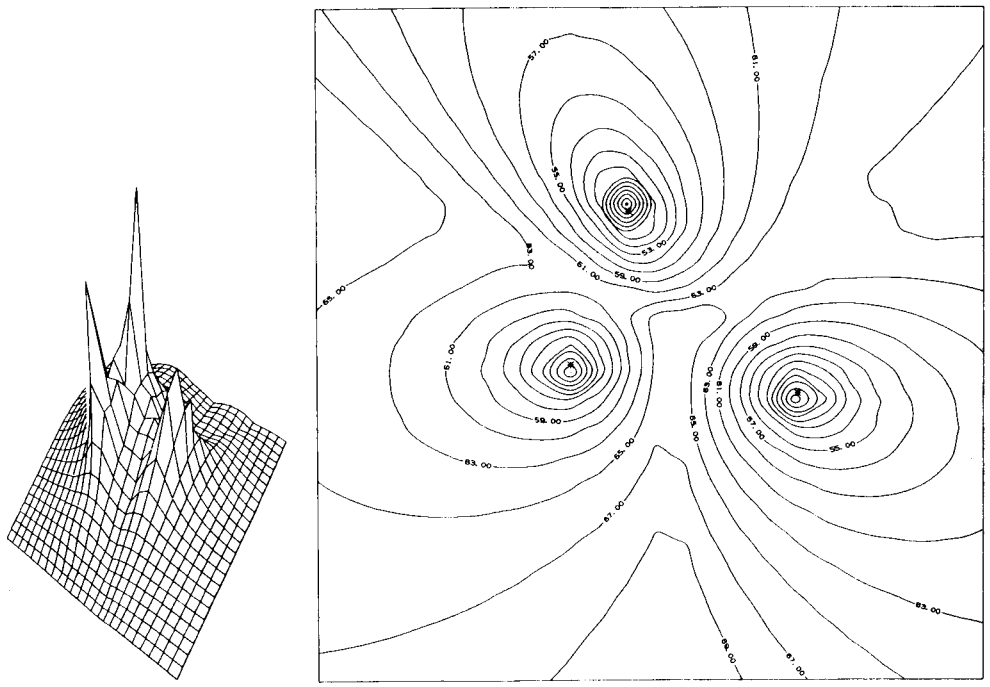

Fig. 5. Surface plot corresponding to the contour diagram in Fig. 4. The plot has been inverted for clarity; peaks correspond to valleys observed in the contour plot. Also the plot has been pivoted about the origin so that the axis corresponding to the first eigenvector is on the right-side rear edge of the plot and the second eigenvector is on the right-side front edge of the plot.

Fig. 6. Contour diagram generated by SMCR/LS from the data for mixture 2.

would be to start several simplices just outside of the inner boundaries, and let them find the pure points using the simplex optimization strategy [14]. Because the p.c.a. results in significant noise reduction, these optimizations should not be greatly troubled by noise, and it should be possible to find the solution points quite accurately.

The second case in which Meister's method has trouble occurs when the mixture spectra are noisy. As discussed in his paper [10], wavelengths with low signal intensity can result in outer boundary lines which arbitrarily cross the mixture zone. Figure 8 shows the SMCR for the same compounds used in Figs. 3—5, but in this case the mixture spectra have been degraded with normally distributed random noise to give a S/N of about 20. In this situation, several outer boundary constraint lines are seen to cut across the mixture region. This would cause Meister's triangle to be placed incorrectly, and severely distort the estimates for two of the pure spectra. The SMCR/LS contour diagram for the same data is shown in Fig. 9 in which the minima corresponding to the three pure components can still be seen clearly. The

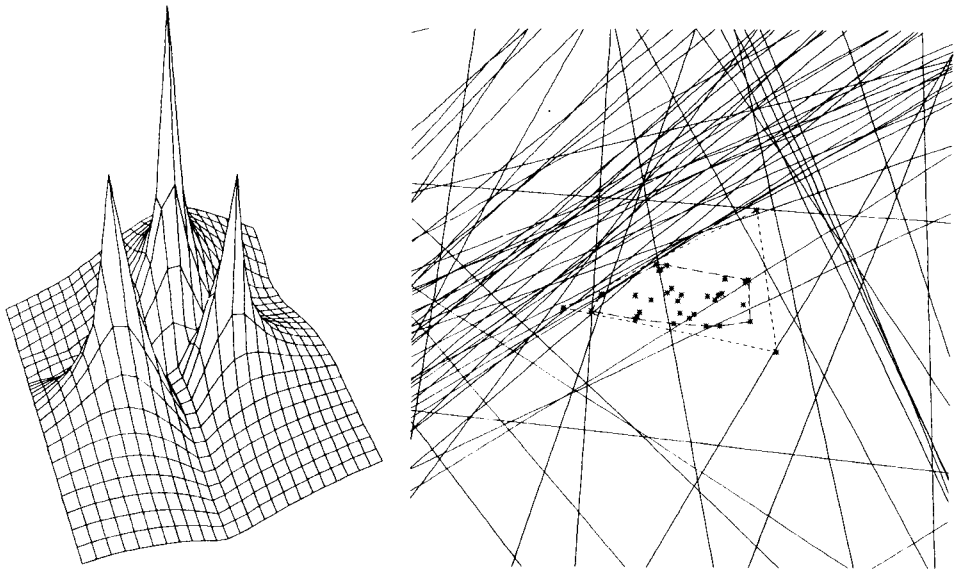

Fig. 7. Surface plot corresponding to the contour diagram in Fig. 6. The plot has been inverted for clarity and pivoted about the origin so that the axis corresponding to the first eigenvector is on the front edge of the plot and the second eigenvector is on the left edge of the plot.

Fig. 8. The 3-component solution for mixture 1, after addition of random noise to the raw data (S/N = 20).

corresponding 3-dimensional surface plot is shown in Fig. 10. Even in this case of noisy spectra, simplex optimization could be used to find the minima, and from these locations the spectra for each pure component could be obtained.

Meister [10] presented an extension to his heuristic approach which deals with spectral noise by considering the amount of noise in the spectral intensities in each wavelength channel. This is done by weighting the eigenvector elements by their corresponding eigenvalues, eliminating those weighted eigenvector elements which are found to be smaller than the measurement uncertainty, and finally modifying the outer boundary constraints to allow small negative spectral intensities which are within experimental error of zero. While this does appear to keep outer boundary restriction lines from crossing the mixture zone, it is not clear from Meister's paper how well this approach actually works, either in terms of the location of the pure component points in eigenspace relative to the outer boundaries, or in the correctness of the estimated pure component spectra. Our major concern with this approach is that information is being eliminated and the outer boundary restrictions are being pushed outward, increasing the size of the region where the pure points can be found. The SMCR/LS approach does not suffer from these limitations.

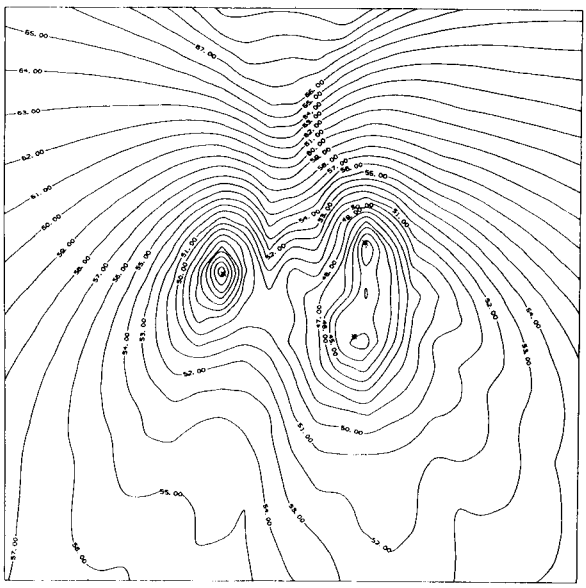

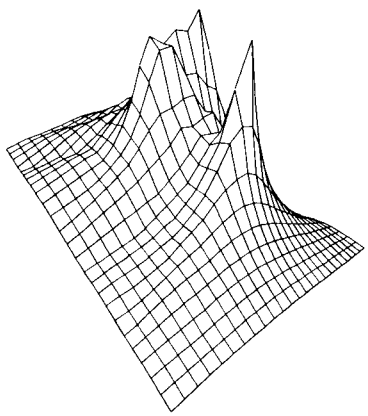

Fig. 9. Contour diagram generated by SMCR/LS using the noisy data of mixture 1, and corresponding to the solution shown in Fig. 8.

Fig. 10. Surface plot corresponding to the contour diagram in Fig. 9. The plot has been inverted for clarity and pivoted about the origin so that the axis corresponding to the first eigenvector is on the right-side rear edge of the plot and the second eigenvector is on the right-side front edge of the plot.

One possible criticism of the SMCR/LS approach concerns the situation when the pure component spectra are not present in the reference library. This situation was examined with succesful results. The same mixture spectra as are shown in Figs. 8—10, which have a S/N of 20 were used, the reference spectrum for one of the pure components was eliminated from the library, and the SMCR/LS was repeated. The resulting contour plot is shown in Fig. 11. Three minima are still clearly present, with a pure point in each. The only significant difference is that the minimum corresponding to the compound which was removed from the library is not as deep as the other two minima, or its corresponding depth in Fig. 9. With the spectrum for 3,5-dimethyl-4-heptanol in the library, SMCR/LS produces a normalized minimum of less than 42 for that compound (Fig. 9). After removal of that spectrum from the library, SMCR/LS results in a normalized minimum of about 45 (Fig. 11). The shallow minimum is still well-defined enough (Fig. 12) for the pure point to be located accurately by using simplex optimization.

This general trend was followed in each of the several examples examined. The success of the SMCR/LS when the correct spectrum is not present in the library is presumably the result of the existence of a library spectrum which is somewhat similar to the missing spectrum, and to the severe distortion of

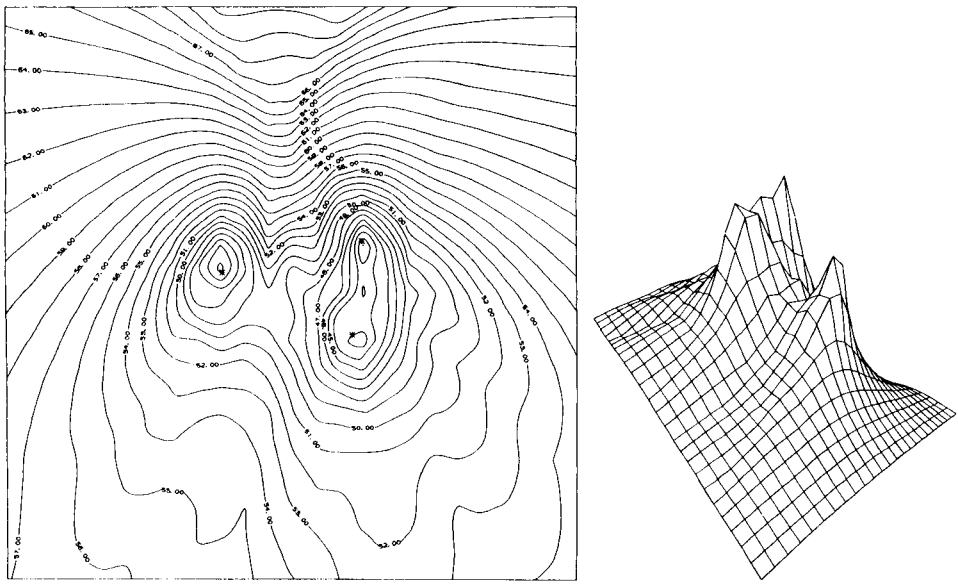

Fig. 11. Contour plot corresponding to the same mixture data as used for Figs. 8—10 but with the SMCR/LS done using a library of spectra which did not contain one of the correct mixture components (3,5-dimethyl-4-heptanol). The minimum on the left-hand side of the figure is not as deep as the other two minima.

Fig. 12. Surface plot corresponding to the contour diagram in Fig. 11. The plot has been inverted and pivoted as for Fig. 10.

spectra reconstructed from points beyond the outer boundaries. Figure 13A is a spectrum reconstructed from the point (0.0, —0.125) on Fig. 4, corresponding to the center of the bottom edge of the figure. Large negative peaks result from the subtraction of intensity values of key frequencies in a region which violates the non-negative concentration constraint. Comparing this spectrum with any spectrum in the library, using the sum of squared differences as the measure, will invariably result in a large calculated distance. This would be true whether the correct spectrum is in the library or not. Thus the presence or absence of the correct spectrum in the library does not greatly affect the region beyond the outer boundaries.

The observed minimum around a solution point when that spectrum is absent from the library is the result of a similar spectrum being present in the library. These spectra would be the normally observed second and third best matches in a common library search. Because the spectra of these next best matches are similar to the spectrum of the true component, the search distances will be small compared to the majority of spectra in the library. Figures 2(c) and 13B illustrate this point. Figure 2(c) is the spectrum for 3,5-dimethyl-4-heptanol (DMH), which was used to generate mixture 1. When DMH was removed from the library, searching produced Fig. 11. The

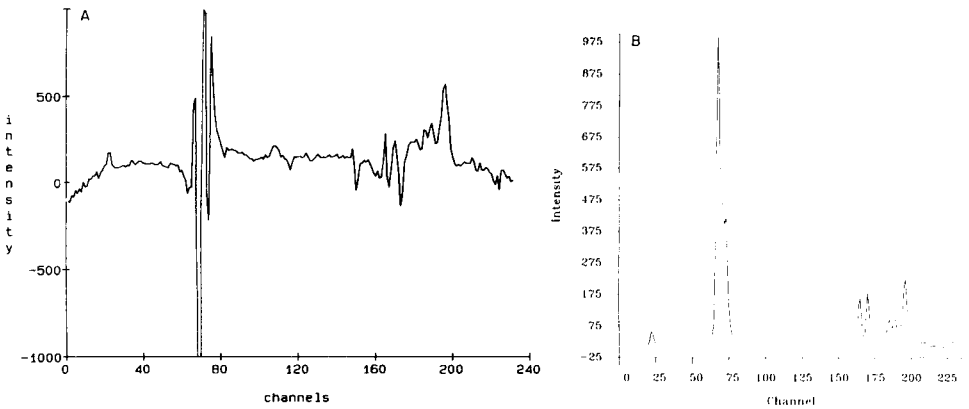

Fig. 13. (A) A spectrum reconstructed from the point (0.0, —0.125) on Fig. 4, corresponding to the center of the bottom edge of the figure. (B) The spectrum for 2,4-dimethyl-3-hexanol which corresponds to the reduced minimum in Fig. 11 and which very closely resembles the spectrum of 3,5-dimethyl-4-heptanol (Fig. 2c).

spectrum which corresponds to the reduced minimum in Fig. 11 is that for 2,4-dimethyl-3-hexanol (Fig. 13B), which very closely resembles the spectrum for DMH. When a library is used which is larger than the 2000-spectrum library presently in use, the SMCR/LS should work even better.

Conclusion

The self-modeling curve resolution technique has been demonstrated recently to be useful in determining the underlying components in complex mixtures or unresolved chromatographic peaks. The need to generalize the method to any dimensionality, and to characterize its limitations more fully is obvious. The method presented above utilizes the information present in a library of reference spectra, to locate accurately the solution points in a SMCR experiment in any dimensionality, and thus reduce the uncertainty of the results. The method is shown to produce useful results in the presence or absence of random noise, and in the case when the spectra of an underlying component is not present in the reference library. Work is proceeding in this laboratory to characterize the method more thoroughly, to develop a more efficient algorithm, and to apply the method to several experimental situations.

We thank John R. Hallowell Jr. for providing the library search programs used in this study, and F. Vincent Warren Jr. for stimulating discussion. Acknowledgement is gratefully made to the National Science Foundation's Information Science and Chemical Analysis Divisions (Grant No. IST-8120255) for the financial support.

REFERENCES

1 W. H. Lawton and E. A. Sylvestre, Technometrics, 14 (1971) 617.
2 M. F. Delaney, Anal. Chem., 56 (1984) 261R.
3 B. R. Kowalski, Anal. Chem., 52 (1980) 112R.
4 I. E. Frank and B. R. Kowalski, Anal. Chem., 54 (1982) 232R.
5 M. A. Sharaf and B. R. Kowalski, Anal. Chem., 53 (1981) 518.
6 M. A. Sharaf and B. R. Kowalski, Anal. Chem., 54 (1982) 1291.
7 D. W. Osten and B. R. Kowalski, Anal. Chem., 56 (1984) 991.
8 J. C. Nicholson, J. J. Meister, D. R. Patil and L. R. Field, Anal. Chem., 56 (1984) 2447.
9 B. G. M. Vandeginste, Pure Appl. Chem., 55 (1983) 2007.
10 A. Meister, Anal. Chim. Acta, 161 (1984) 149.
11 M. F. Delaney, F. V. Warren and J. R. Hallowell, Anal. Chem., 55 (1983) 1925.
12 F. V. Warren and M. F. Delaney, Appl. Spectrosc., 37 (1983) 172.
13 M. F. Delaney, J. R. Hallowell and F. V. Warren, J. Chem. Inf. Comput. Sci., 25 (1985) 27.
14 S. N. Deming and S. L. Morgan, Anal. Chem., 45 (1973) 278A.

Analytica Chimica Acta, 172 (1985) 207—214
Elsevier Science Publishers B.V., Amsterdam — Printed in The Netherlands

EVALUATION OF THE EQUIVALENCE POINT IN POTENTIOMETRIC TITRATIONS WITH APPLICATION TO TRACES OF CHLORIDE

TADEUSZ MICHAŁOWSKI* and RYSZARD STĘPAK
Faculty of Chemistry, Jagiellonian University, 30-060 Kraków (Poland)
(Received 22nd October 1984)

SUMMARY

A mathematical model applicable to the determination of the equivalence point (V_{eq}) is described. The regression equation is $(1 + V/V_0)^3 E = \Sigma_{i=0}^{3} A_i V^i$, where E is the e.m.f. corresponding to volume V of titrant added, V_0 is the initial volume of titrand, and A_i are the regression coefficients. On the basis of A_i values obtained by the least-squares method, the algorithm for V_{eq} and the criterion of correctness of results obtained from measurements are presented. The method is applied to titrations of chloride with silver nitrate solutions.

Most mathematical methods of evaluating the equivalence point of potentiometric titrations (V_{eq}), e.g., Fortuin's method [1], Yan's method [2, 3], and Gran's method [3, 4], are not applicable to titrations of traces of halide and thiocyanate with silver ions. The method proposed below is applicable for very dilute solutions of both titrand and titrant. Computational algorithms are presented that enable V_{eq} to be calculated in such systems and the results obtained to be verified. The applicability of the method in potentiometric titrations of sodium chloride with silver nitrate is checked, and correlations between the systematic error (e%) of measurements of the equivalence points, the solubility product (K_{so}) of the precipitate formed and the standard redox potential (E_0) are examined. The method can also be applied for obtaining an accurate K_{so} value for the given precipitate.

THE PROPOSED METHOD

The titration of V_0 ml of c_0 M NaX with V ml of c M silver nitrate is considered. From the concentration balances, the relation obtained is

$$c(V_{eq} - V)/(V_0 + V) = [X] - [Ag] \quad (1)$$

where $cV_{eq} = c_0 V_0$ and X = Cl, Br, I, SCN (charges are omitted for simplicity). At low c_0 and c values, the concentrations of AgX_i (i = 2, 3, 4) and $Ag(OH)_i$ (i = 1, 2, 3) complexes can be neglected in comparison with [X] and [Ag]. From Eqn. 1

0003-2670/85/$03.30

$$pX = \frac{1}{2} pK_{so} - \log e \sinh^{-1} y \tag{2}$$

where $\sinh^{-1}y$ = arcsinh y, K_{so} = [Ag] [X] and

$$y = cx/2K_{so}^{1/2} \tag{3a}$$

$$x = (V_{eq} - V)/(V_0 + V) \tag{3b}$$

The function $z = \sinh^{-1}y$ can be expanded into the Maclaurin series [5]

$$\sinh^{-1} y = y + \sum_{m=1}^{\infty} [(-1)^m/(2m + 1)] \{[(2m - 1)!!/(2m)!!]\} y^{2m+1} \tag{4}$$

If only the first two terms of Eqn. 4 are used and are substituted into Eqn. 2, and given

$$E = E_0 - (RT/F) \ln 10 \, pX \tag{5}$$

then

$$E = a_0 + a_1 x + a_3 x^3 \tag{6}$$

where $a_0 = E_0 - (RT/2F) \ln 10 \, pK_{so}$, $a_1 = (RT/2F)(c/K_{so}^{1/2})$, and $a_3 = -(RT/48F)c^3/K_{so}^{3/2}$. From Eqn. 6, a regression equation is obtained

$$(1 + V/V_0)^3 E = A_0 + A_1 V + A_2 V^2 + A_3 V^3 \tag{7}$$

and (see Appendix)

$$(1 - 2b)V_{eq}^3 + (2 - 3b)V_0 V_{eq}^2 + V_0^2 V_{eq} + bV_0^3 = 0 \tag{8}$$

$$b = 1/3(3A_0 - 2V_0 A_1 + V_0^2 A_2)/(2A_0 - V_0 A_1 + V_0^3 A_3) \tag{9}$$

$$a_3 = (V_0^3/3V_{eq})(3A_0 - 2V_0 A_1 + V_0^2 A_2)/(V_0 + V_{eq})^2 \tag{10a}$$

$$a_1 = (3A_0 - A_1 V_0)V_0/(V_0 + V_{eq}) - 3a_3 V_{eq}^2/V_0^2 \tag{10b}$$

$$a_0 = V_0^3 A_3 + a_1 + a_3 \tag{10c}$$

The A_i coefficients in Eqn. 7 can be calculated by the least-square method, by solving the set of four equations

$$\sum_{i=0}^{3} A_i \sum_{j=1}^{n} V_j^{h+i} = \sum_{j=1}^{n} (1 + V_j/V_0)^3 E_j V_j^h \quad (h = 0, 1, 2, 3)$$

where $n \geqslant 5$ is the number of individual measurements, and E_j is the e.m.f. corresponding to volume V_j of titrant added. Then V_{eq}, a_0, a_1 and a_3 are calculated from Eqns. 8 and 10; V_{eq} is the real positive root of the third-degree Eqn. 8. From the definitions of a_0, a_1 and a_3 for Eqn. 6,

$$K_{so} = K_{so(1)} = (RTc/2Fa_1)^2 \tag{11}$$

$$K_{so} = K_{so(3)} = (-RTc^3/48Fa_3)^{2/3} \tag{12}$$

$$E_0 = a_0 + (RT/2F) \ln 10 \, pK_{so} \tag{13}$$

In order to obtain accurate results, it is necessary to define the V interval for which the above calculations will be valid. Then the accurate Eqn. 4 must be compared with its simplified form. The inequality

$$|\sinh^{-1} y - (y - y^3/6)| < \Delta pX \ln 10 = 0.0115$$

(where $\Delta pX = 0.005$, relating to $\Delta E = 0.3$ mV, is an admissible pX difference between the pX values calculated from the corresponding equations) is fulfilled for $|y| < y_{max} = 0.725$. Setting $cV = \phi c_0 V_0$ and $q = c_0/c$ yields (see Eqn. 3) $|(1-\phi)/(1+q\phi)| < (2K_{so}^{1/2}/c_0)y_{max} = \delta/q$, where $\delta = 1.45\, K_{so}^{1/2}/c$. For $pK_{so} = 9.75$ (X=Cl), the lower (ϕ_1) and upper (ϕ_2) limits of the admissible ϕ values are obtained: $\phi_1 = (1-\delta/q)/(1+\delta) < V/V_{eq} < (1+\delta/q)/(1-\delta) = \phi_2$, where $\delta = 1.93 \times 10^{-5}/c$.

Evaluation of V_{eq}

The E vs. V dependence in the immediate vicinity of the equivalence point is practically linear. In fact, from Eqns. 5 and 2

$$dE/dV = -(RTc/2FK_{so}^{1/2})(y^2+1)^{-1/2}(V_0 + V_{eq})/(V_0 + V)^2$$

$$= -(RTc/2FK_{so}^{1/2})(V_0 + V_{eq})^{-1}\{1 - [2(V - V_{eq})/(V_0 + V_{eq})]$$

$$- [(c^2/8K_{so}) - 3][(V - V_{eq})^2/(V_0 + V_{eq})^2] + \ldots\}$$

$$|dE/dV|_{V=V_{eq}} = (RTc/2FK_{so}^{1/2})(V_0 + V_{eq})^{-1} = w$$

Then the approximation can be given as $w = |\Delta E/\Delta V|$.

If $E_{obs,j}$ and $E_{cal,j}$ denote, respectively, the e.m.f. observed at the jth experimental point and the e.m.f. calculated on the basis of the regression function (Eqn. 7) at this point, then the standard deviation

$$s_E = \{[\sum_{j=1}^{n} (E_{cal,j} - E_{obs,j})^2]/(n-4)\}^{1/2} \qquad (14)$$

is the basis for calculation of the value $\Delta E = (s_E/n^{1/2})t(0.95, f)$, where $f = n - 4$ and $\alpha = 0.95$ is the probability level in the Student t-test. From these equations given for w, s_E and ΔE, $|\Delta V| = |\Delta E|w$ and the estimated V_{eq} value is equal to $V_{eq} \pm |\Delta V|$.

Application to the method based on cells in series

A potentiometric procedure based on cells connected in series was described previously [6, 7]. For application of the proposed algorithms to this variation, $\epsilon = kE$, $\epsilon_0 = kE_0$, $A_1' = kA_i$ ($i = 0, 1, 2, 3$) and $a_i' = ka_i$ ($i = 0, 1, 3$) are set into the corresponding equations; thus

$$(1 + V/V_0)^3\epsilon = \sum_{i=0}^{3} A_i' V^i,\quad b' = 1/3(3A_0' - 2V_0A_1' + V_0^2A_2')/(2A_0' - V_0A_1'$$

$$+ V_0^3A_3') = b,\quad K_{so} = K'_{so(1)} = \left(\frac{kRTc}{2Fa_1'}\right)^2,\quad K_{so} = K'_{so(3)} = \left(\frac{-kRTc^3}{48Fa_3'}\right)^{2/3}$$

(where the definitions of a'_3, a'_1 and a'_0 are identical with those given in Eqns. 10 except that a and A are replaced by a' and A' with the same subscripts.) Similarly, $w' = kw$, w being defined as above.

In order to illustrate the above V_{eq} evaluation, 1.00×10^{-4} M sodium chloride was titrated with 1.00×10^{-3} M silver nitrate.

EXPERIMENTAL

Stock solutions of sodium chloride and silver nitrate were prepared from analytical-grade reagents and water triple-distilled from quartz.

The titration assembly consisted of a 250-ml beaker with $V_0 = 100$ ml of sodium chloride solution. The burette tip and the silver indicator electrode were inserted into this solution. A silver reference electrode was placed into the titrant stream. When the method based on cells in series [6, 7] was applied, four such cells were connected in series. The e.m.f. was measured with a digital voltmeter (Type V540; Mera-Tronik, Poland).

All titrations were done at room temperature.

RESULTS AND DISCUSSION

The results of the titrations are shown in Table 1. From the results in columns 8 and 9, $k = 4.16 \pm 0.02$ and $\kappa = 4.1 \pm 0.4$, respectively. The regression function obtained on the basis of the cells in series (Table 1) is

$$(1 + V/100)^3 \epsilon = -0.0015 + 249.1\ V - 28.677\ V^2 + 0.91382\ V^3$$

and $V_{eq} = 10.078 \pm 0.024$ (the relative systematic error, +0.78%, is significant at the 0.95 probability level), $pK_{so(3)} = 9.745$, $pK_{so(1)} = 10.007$ ($k = 4.16$).

TABLE 1

Results of titration of V_0 ml of 1.00×10^{-4} M NaCl (c_0) with 1.00×10^{-3} M $AgNO_3$ (c)

No.	1	2	3	4	5	6	7	8	9
	V ml[a]	One cell (e.m.f., mV)			Four cells (e.m.f., mV)			$k = \frac{\epsilon}{E}$	$\kappa = \frac{\Delta\epsilon}{\Delta E}$
		E_{obs}	E_{cal}	ΔE_{obs}	ϵ_{obs}	ϵ_{cal}	$\Delta\epsilon_{obs}$		
	—	—			—				
1	8.50	114.7	115.0		474.5	474.9		4.14	
				5.5			22.2		4.03
2	9.00	109.2	108.8		452.3	451.9		4.14	
				6.0			24.0		4.00
3	9.50	103.2	102.8		428.3	428.9		4.15	
				6.5			24.5		3.77
4	10.00	96.7	96.7		403.8	403.6		4.18	
				6.6			25.2		3.82
5	10.50	90.1	90.7		378.6	379.3		4.20	
				4.8			23.0		4.79
6	11.00	85.3	85.1		355.6	355.7		4.17	
				5.3			22.1		4.17
7	11.50	80.0	79.9		333.5	333.2		4.17	
	—	—			—				

[a] 10^{-3} M $AgNO_3$ added.

Analogously, the regression function obtained from the single-cell potentiometric titration (Table 1) is

$$(1 + V/100)^3 E = -0.001 + 64.595\ V - 7.7964\ V^2 + 0.262364\ V^3$$

and $V_{eq} = 9.572 \pm 0.050$ (the relative systematic error, −4.28%, is significant at the 0.95 probability level), $pK_{so(3)} = 9.795$, $pK_{so(1)} = 10.045$.

The results leading to construction of the corresponding pK_{so} vs. $e\%$ plots (Figs. 1–3) are presented in Table 2.

Consideration of the results obtained leads to the following conclusions. First, the corresponding regression lines fit the experimental points (V_j, E_j) very well. The values of the standard deviations s_E (Eqn. 14) are then small. Second, there is a correlation between $e\%$ and $pK_{so(3)}$. The plot of $pK_{so(3)}$ vs. $e\%$, obtained from points characterized by relatively small s_E values, is linear. The equation related to the classical titration (Fig. 1, line a) is $e\% = 115\ (9.761 - pK_{so(3)})$. The relative error $e\%$ can then be evaluated on the basis of $pK_{so(3)}$ value calculated from Eqn. 12. The corresponding line (b) obtained from the cells-in-series method, plotted for $k = 4.15$, is shifted by the value $\log (4.15/4) = 0.014$ in comparison with the line plotted on the assumption

TABLE 2

Results for the determination of chloride by the classical and cells-in-series methods ($V_0 = 100$, $c_0 = 10^{-4}$, $c = 10^{-3}$)

No.	$-A_0$	A_1	$-A_2$	A_3	V_{eq}	a_0	a_1	$-a_3$	$pK_{so(13)}$
1	0.001	64.595	7.7964	0.26236	9.572	101.916	1350.49	263612	9.6706
2	0.001	64.569	7.7785	0.26102	9.597	101.773	1355.01	262275	9.6671
3	0.001	62.802	7.3741	0.23875	9.919	98.199	1371.78	240027	9.6229
4	0.001	62.616	7.3513	0.23792	9.923	97.843	1369.09	239192	9.6224
5	0.001	61.877	7.2088	0.23131	10.004	97.022	1357.69	232575	9.6139
6	0.002	60.593	6.9407	0.21747	10.225	94.372	1364.18	218743	9.5851
7	0.002	60.651	6.9027	0.21342	10.346	93.015	1399.70	214730	9.5660
No.	$-A'_0$	A'_1	$-A'_2$	A'_3	V_{eq}	a'_0	a'_1	$-a'_3$	$pK'_{so(13)}$
1	0.000	253.450	29.5830	0.96104	9.900	408.479	5341.97	965974	9.6374
2	0.001	253.540	29.5781	0.96007	9.908	408.432	5350.74	965009	9.6364
3	0.002	253.077	29.5459	0.95838	9.914	408.067	5351.97	963328	9.6355
4	0.001	252.483	29.3650	0.94895	9.948	406.190	5357.31	953902	9.6308
5	0.001	250.533	29.0409	0.93574	9.977	404.571	5307.51	940649	9.6287
6	0.001	250.041	28.9525	0.93172	9.989	403.924	5300.88	936620	9.6274
7	0.002	251.041	29.1186	0.93653	9.992	404.642	5351.16	941481	9.6254
8	0.001	250.029	28.9709	0.93162	9.995	403.382	5319.45	936534	9.6258
9	0.001	250.902	29.0234	0.93106	10.016	403.233	5364.09	936018	9.6219
10	0.000	250.001	28.8542	0.92307	10.042	401.909	5355.87	928022	9.6189
11	0.002	249.588	28.7530	0.91701	10.070	400.476	5372.26	921977	9.6147
12	0.002	248.369	28.5627	0.91051	10.076	400.461	5320.22	915430	9.6159
13	0.002	250.031	28.8273	0.91834	10.079	400.256	5409.31	923353	9.6118
14	0.002	251.928	29.0528	0.92513	10.081	401.004	5476.25	930205	9.6105

that $k = 4$ (number of cells connected in series). The value $pK_{so} = 9.761$ (obtained at $e\% = 0$ and for Nernstian slope of the E vs. pCl plot at 293 K) is very close to the value 9.75 found in the literature [8]. The accuracy of results obtained by the cells-in-series method is influenced by accidental error to a lesser degree than in the classical method (see Fig. 1).

The dependence of $pK_{so(1)}$ on $e\%$ is not monotonic (Fig. 2) for either the classical or the cells-in-series titration method applied (cf. a_1' values in Table 2). The $pK_{so(3)}$ values are higher than the corresponding $pK_{so(3)}$ values by 0.2—0.3.

When the definitions for a_3 and a_1 (see Eqn. 6) are compared with the definitions for a_3' and a_1', then, for $c = 10^{-3}$,

$$pK_{so} = pK_{so(13)} = 7.3802 + \log(-a_3/a_1)$$

$$pK_{so} = pK'_{so(13)} = 7.3802 + \log(-a_3'/a_1')$$

respectively. The plots are shown on Fig. 3. The plots are linear despite the nonlinear $pK_{so(1)}$ and $pK'_{so(1)}$ vs. $e\%$ dependences (see Table 2). The equation of line a in Fig. 2 is $e\% = 74(9.614 - pK_{so(13)})$. The $pK_{so(13)}$ value is independent of the real slope of the E vs. pCl plot for the given electrode.

The possibility of verifying the results obtained is useful with respect to low reaction rates in dilute solutions. The linear dependence E_0 vs. $e\%$ for the classical method is shown in Fig. 4; a Nernstian calibration slope was assumed.

The deviations between the corresponding pK_{so} vs. $e\%$ lines where pK_{so} corresponds to $pK_{so(3)}$ and $pK'_{so(3)}$ or $pK_{so(13)}$ and $pK'_{so(13)}$, respectively (Figs. 1 and 3) is caused by different slopes of the E vs. pCl plots for individual electrodes.

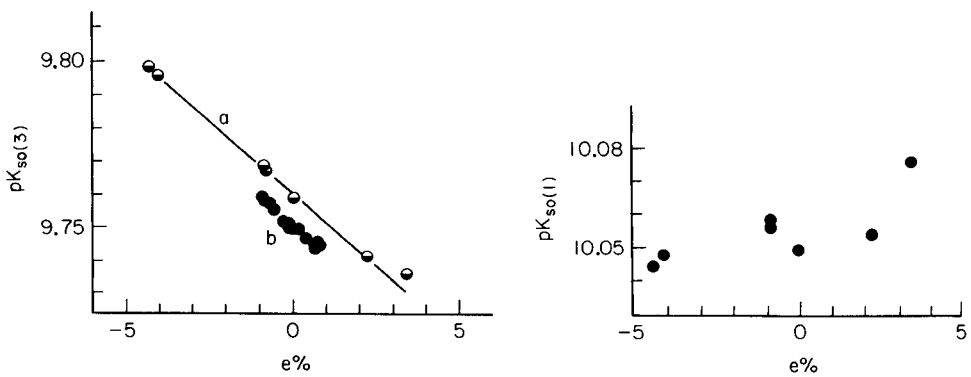

Fig. 1. The dependence of $pK_{so(3)}$ (line a, classical method) and $pK'_{so(3)}$ (line b, cells-in-series method) vs. relative systematic error ($e\%$) of V_{eq} determination.

Fig. 2. Points ($e\%$, $pK_{so(1)}$) obtained from the results of classical titrations.

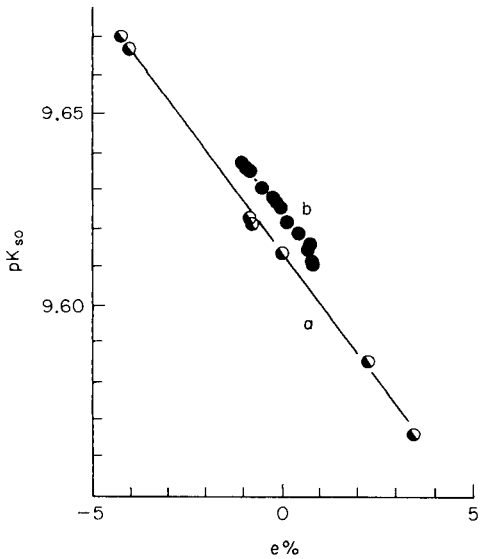

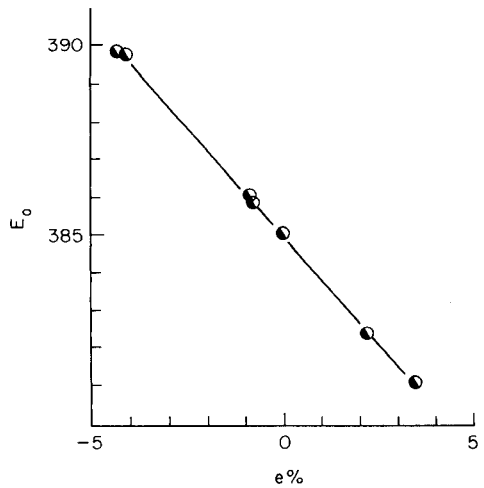

Fig. 3. The dependence of $pK_{so(13)}$ and $pK'_{so(13)}$ vs. relative systematic error ($e\%$) of V_{eq} determination. (a, b) as in Fig. 1.

Fig. 4. The dependence of E_0 (in mV) vs. $e\%$ for the classical method.

Comparison of the regression equation (Eqn. 8) with the one given for the Fenwick—Yan method, $E = \Sigma_{i=0}^{3} A_i V^i$ (see [3]), leads to the conclusion that the latter method should be applied in the V interval where the factor $(1 + V/V_0)^3$ in Eqn. 8 becomes practically constant; this factor changes distinctly, however, in the V interval presented in Table 1, from 1.2772 at V = 8.5 to 1.3861 at V = 11.5 (V_0 = 100). From the E values for V = 9, 9.5, 10, 10.5 (Table 1), V_{eq} = 10.125 for the classical method and V_{eq} = 8.250 for the cells-in-series method. For the E values at V = 9.5, 10, 10.5, 11 (Table 1), V_{eq} = 9.974 and V_{eq} = 10.121. Thus, although the equation is incorrect, the Fenwick—Yan method gives accurate results for the classical method; this accuracy is accidental, however. The method is based on the assumption that the inflection point (V_{inf}) on the titration curves coincides with V_{eq}, whereas the difference [3]

$$V_{eq} - V_{inf} = x_{inf} V_0 (c_0/c + 1)/(1 + x_{inf})$$

where $x_{inf} = 8K_{so}/c^2 + (8K_{so}/c^2)^2 + \ldots$, becomes significant for low c values; at $c_0 = 10^{-4}$, $c = 10^{-3}$, V_0 = 100 and pK_{so} = 9.75, $V_{eq} - V_{inf}$ = 0.16.

Relatively high levels of white gaussian noise mean that the Gran I method and the Fortuin nomogram cannot be applied generally for systems with dilute solutions.

The general form of the nonlinear equation obtained from Eqns. 2, 3 and 6 is

$$E = a_0 + \delta \sinh^{-1}[a(V_{eq} - V)/(V_0 + V)]$$

This can be also applied for the determination of V_{eq}. The V_{eq} value obtained is then verified on the basis of formula $K_{so} = (c/2a)^2$.

APPENDIX

Deduction of Eqns. 8—10

From Eqns. 6 and 3b, Eqn. 8 is obtained. The A_i coefficients are related to a_i coefficients in a set of four equations:

$$V_0^3 A_0 = a_0 V_0^3 + a_1 V_0^2 V_{eq} + a_3 V_{eq}^3 \quad (1')$$

$$V_0^3 A_1 = 3a_0 V_0^2 + 2a_1 V_0 V_{eq} - a_1 V_0^2 - 3a_3 V_{eq}^2 \quad (2')$$

$$V_0^3 A_2 = 3a_0 V_0 + a_1 V_{eq} - 2a_1 V_0 + 3a_3 V_{eq} \quad (3')$$

$$V_0^3 A_3 = a_0 - a_1 - a_3 \quad (4')$$

From Eqns. 1′ and 2′,

$$3V_0^3 A_0 - V_0^4 A_1 = a_1 V_0^2 V_{eq} + 3a_3 V_{eq}^3 + a_1 V_0^3 + 3a_3 V_0 V_{eq}^2 \quad (5')$$

From Eqns. 1′ and 3′,

$$3V_0^3 A_0 - V_0^5 A_2 = 2a_1 V_0^2 V_{eq} + 3a_3 V_{eq}^3 + 2a_1 V_0^3 - 3a_3 V_0^2 V_{eq} \quad (6')$$

From Eqns. 1′ and 4′,

$$V_0^3 A_0 - V_0^6 A_3 = a_1 V_0^2 V_{eq} + a_1 V_0^3 + a_3 V_{eq}^3 + a_3 V_0^3 \quad (7')$$

From Eqns. 5′ and 6′,

$$3V_0^3 A_0 - 2V_0^4 A_1 + V_0^5 A_2 = 3a_3 V_{eq}^3 + 6a_3 V_0 V_{eq}^2 + 3a_3 V_0^2 V_{eq} \quad (8')$$

From Eqns. 5′ and 7′,

$$2V_0^3 A_0 - V_0^4 A_1 + V_0^6 A_3 = 2a_3 V_{eq}^3 + 3a_3 V_0 V_{eq}^2 - a_3 V_0^3 \quad (9')$$

Dividing the last two equations gives

$$(V_{eq}^3 + 2V_0 V_{eq}^2 + V_0^2 V_{eq})/(2V_{eq}^3 + 3V_0 V_{eq}^2 - V_0^3) = b$$

leading to Eqn. 8. Equations for a_3, a_1 and a_0 are obtained from Eqns. 8′, 5′ and 4′, respectively.

REFERENCES

1 J. M. H. Fortuin, Anal. Chim. Acta, 24 (1961) 175.
2 J. F. Yan, Anal. Chem., 37 (1965) 1588.
3 T. Michałowski, Chem. Anal. (Warsaw), 26 (1981) 799; Proceedings of Conference of PTCh and SITPChem., Lublin, Book A, III-36, 1982.
4 G. Gran, Acta Chem. Scand., 4 (1950) 559.
5 I. N. Bronstein and K. A. Semendyaev, Guide-Book on Mathematics (in Russian), Nauka, Moscow, 1964, p. 329.
6 R. Stępak, Z. Anal. Chem., 315 (1983) 629.
7 A. Parczewski and R. Stępak, Z. Anal. Chem., 316 (1983) 29.
8 I. Inczedy, Analytical Applications of Complex Equilibria, Akad. Kiadó, Budapest, 1976.

Analytica Chimica Acta, 172 (1985) 215—221
Elsevier Science Publishers B.V., Amsterdam — Printed in The Netherlands

SEPARATION AND DETERMINATION OF TRACES OF HEAVY METALS COMPLEXED WITH HUMIC SUBSTANCES IN FRESH WATERS BY SORPTION ON DIETHYLAMINOETHYL-SEPHADEX A-25

MASATAKA HIRAIDE, SUJITH PRASAN TILLEKERATNE, KOJI OTSUKA and ATSUSHI MIZUIKE*

Faculty of Engineering, Nagoya University, Chikusa-ku, Nagoya 464 (Japan)

(Received 22nd November 1984)

SUMMARY

Copper(II), lead and cadmium complexed with humic and fulvic acids in filtered 1-l samples of fresh water are sorbed on a column containing 0.5 ml of the macroreticular weak-base anion exchanger, diethylaminoethyl-Sephadex A-25 at a flow rate of 20 ml min^{-1}. Simple metal cations are not sorbed at all. The sorbed trace metals are quantitatively desorbed with 4 M nitric acid batchwise and determined by graphite-furnace atomic absorption spectrometry. For synthetic aqueous solutions containing traces of heavy metals and humic acid, the results are in conformity with those obtained by cation-exchange separation. About 80% of the sorbed humic substances are eluted with 0.5 M sodium hydroxide solution from the A-25 column and its quantity is estimated spectrophotometrically at 400 nm.

Part of the traces of heavy metals in natural waters are complexed with humic substances (humic and fulvic acids) and their behavior in the environment and their biological effects, such as toxicity to algae, may differ greatly from those of simple ions of the same elements [1]. Therefore, methods for the separation and determination of heavy metals in these chemical states are required in environmental studies. Humic substances in natural waters have been separated by sorption on macroreticular polystyrene resins (Amberlite XAD-2, etc.) [2—4] and the weak-base anion exchanger, diethylaminoethylcellulose [5]. It was found here that sorption on the XAD-2 did not give satisfactory results for the separation of humic substance from inorganic species in fresh waters, because significant amounts of simple metal cations were also sorbed. Similar results were reported by Mackey [6].

In the present work, negatively-charged humic substances in a 1-l water sample are selectively and quantitatively sorbed on a small column of the macroreticular weak-base anion exchanger, diethylaminoethyl-Sephadex A-25 (cross-linked dextran gel with diethylaminoethyl groups), and the heavy metals complexed with it are quantitatively desorbed with a small volume of 4 M nitric acid for graphite-furnace atomic absorption spectrometry. The proposed method is simple and rapid in procedure and gives reproducible and reliable results.

0003-2670/85/$03.30

EXPERIMENTAL

Apparatus

Figure 1 shows the separation column consisting of ion-exchanger bed, vitreous-silica wool and two Pyrex glass parts connected by a ground joint. For the determination of trace metals, a Nippon Jarrell-Ash AA-1 Mark II atomic absorption spectrometer with an FLA-10 graphite-furnace atomizer was employed under the following conditions: wavelengths (nm) copper 324.8, lead 283.3 and cadmium 228.8; drying at 160°C for 15 s, decomposition at 500°C for 20 s; and atomization at 2500°C (copper), 2000°C (lead) and 1500°C (cadmium). A Shimadzu UV-180 spectrophotometer with matched 1-cm vitreous-silica cells was used for the determination of humic substances at 400 nm. Other apparatus used were a Kaijo-Denki ultrasonic generator (29 kHz) with a type-4335 ferrite transducer, a Kubota KH-180 centrifuge (eight 50-ml tubes) and a Hitachi ECV-841BN clean bench.

Reagents

Diethylaminoethyl-Sephadex A-25 and sulphopropyl-Sephadex C-25 (50—100-μm diameter; Pharmacia Fine Chemicals) were washed in 0.1 M hydrochloric acid by ultrasound for 1 min and stored in water.

A humic acid solution (0.4 g l^{-1}) was prepared by dissolving humic acid powder (Wako Pure Chemical Industries) in 0.1 M potassium hydroxide solution and filtering the solution through 0.4-μm pore size Nuclepore filters. The concentration was obtained by subtracting the filtration residue.

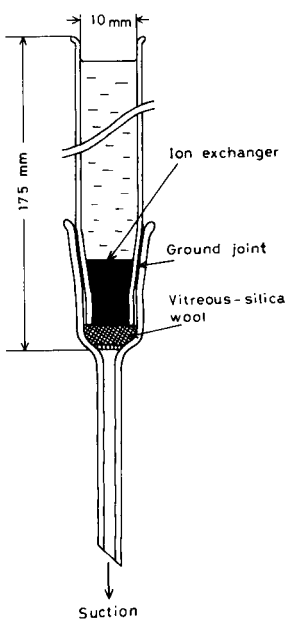

Fig. 1. Separation column.

The molecular weight distribution of the humic acid after the filtration was obtained by ultrafiltration as follows: >200 000, 5%; 200 000—20 000, 35%; 20 000—10 000, 30%; 10 000—1000, 30%; <1000, 0%. A fulvic acid solution (1 g l^{-1}) was prepared by dissolving fulvic acid powder (extracted from soil and purified by Arai and Kumada [7]) in water.

Water was purified by distillation and ion exchange. All reagents were of reagent grade unless otherwise stated.

Procedure

Trace heavy metals complexed with humic substances. Centrifuge a water sample at 10 000 rpm for 10 min. Filter the supernatant solution through 0.4-μm pore size Nuclepore filters (47 mm diameter, purified by ultrasonic washing in 1 M hydrochloric acid followed by water) with a Millipore Pyrex glass vacuum filter unit. Pass the filtrate through the separation column containing 0.5 ml of A-25 at a flow rate of 20 ml min^{-1}. Reserve the effluent for the determination of inorganic cations. Remove the upper part of the column and add 2 ml of 4 M nitric acid to transfer the anion exchanger to a test tube (13 mm internal diameter, 80 mm long, 1 mm thick). Apply ultrasound for 1 min to desorb the trace heavy metals. Centrifuge the solution at 5000 rpm for 5 min and collect the supernatant solution. Add 2 ml of 4 M nitric acid to the anion exchanger and repeat the desorption and centrifugation once more. Combine the two 4 M nitric acid solutions and transfer a 40-μl aliquot to the graphite furnace to quantify the heavy metals by atomic absorption spectrometry. Repeat each measurement three times and average the absorbances. Construct calibration curves by using standard solutions in 4 M nitric acid.

Humic substances. Collect the humic substances from a water sample on the A-25 column as described above. Elute the humic substances (ca. 80%) with 10 ml of 0.5 M sodium hydroxide solution at a flow rate of 0.5 ml min^{-1}. Determine the concentration of the humic substances by measuring the absorbance at 400 nm. At this wavelength, the absorbance from decomposition products of A-25 was negligible.

Inorganic cations in effluents from the A-25 column. Pass the reserved effluent through a column containing 0.5 ml of the strong-acid cation exchanger C-25 at a flow rate of 20 ml min^{-1}. Desorb the sorbed heavy metals with 4 M nitric acid and determine as described above. When the concentrations of copper, lead and cadmium exceed ca. 5, 5 and 1 μg l^{-1}, respectively, use 40-μl aliquots of the reserved effluent directly for the determination.

RESULTS AND DISCUSSION

Retention of humic and fulvic acids on the A-25 column was examined at various concentrations, solution volumes, and pH values by measuring the absorbance of the effluent at 400 nm (after concentration by evaporation for 1 mg l^{-1} solutions). As shown in Table 1, humic and fulvic acids were

TABLE 1

Retention of humic substances on the A-25 column

Concentration ($mg\ l^{-1}$)	Solution passed (ml)	pH	Humic substances in effluent (%)	Concentration ($mg\ l^{-1}$)	Solution passed (ml)	pH	Humic substances in effluent (%)
Humic acid				*Fulvic acid*			
1	1000	7	0	1	1000	7	0
5	300	7	4	50	100	3	0
10	100	3	0	50	100	6	0
10	100	6	0	50	100	7	0
10	100	7	1	50	100	9	0
10	100	9	0				
10	200	7	13				

quantitatively collected between pH 3 and 9, up to 1.5 mg and at least 5 mg, respectively. Microscopic observations showed that the shape and diameter of the anion exchanger were not changed even after the 1-l treatment. In order to confirm that metal/humic acid complexes behave similarly to humic acid, 100 ml of aqueous solution (pH 7) containing 1000 μg each of humic acid and lead was passed through the column and the effluent was analyzed. More than 95% of humic acid and about 28% of lead (as humic acid complexes) were retained on the A-25 column. Copper(II), lead and cadmium ions at low $\mu g\ l^{-1}$ levels and colloidal hydrated oxides of aluminum and iron(III) were not retained on the A-25 column at all.

Synthetic aqueous solutions (pH 7) containing humic acid and trace heavy metals were passed through the A-25 or C-25 column and their concentrations in the effluents were measured directly. Because the anion and cation exchangers collect metal/humic acid complexes and metal cations, respectively, the sum of the percentages of metals in the effluent from each column should be 100%. This was confirmed as shown in Table 2.

In each separation, however, positive or negative errors may occur and compensate each other in the summation. Therefore, positive errors for both separations were estimated by the following two experiments. First, 100 ml of aqueous solution (pH 7) containing 10 μg each of copper(II) and lead, 1 μg of cadmium and 1000 μg of humic acid, was passed through the A-25 column to sorb the humic substance including 5 μg of copper and 4 μg of lead. Then 100 ml of pure water (pH 7) was introduced into the column to see if the metals were desorbed. No metal was eluted. This result shows that, in the anion exchange, the most probable positive error, arising from release of metal ions from the sorbed metal/humic acid complexes, is negligible. Next, 100 ml of aqueous solution (pH 7) containing 10 μg each of copper(II) and lead and 1 μg of cadmium was passed through the C-25 column to sorb the heavy metals quantitatively, and then 100 ml of metal-free humic acid

TABLE 2

Effluents from anion- and cation-exchange columns

Solution volume (ml)	Added	Amount (μg)	Found (%)[a] in effluent from a column containing		Sum (%)
			A-25	C-25	
100	Cu(II)	10	49	47	96
			(39)	(57)	(96)
	Pb	10	58	38	96
			(65)	(34)	(99)
	Cd	1	97	5	102
			(100)	(0)	(100)
	Humic acid	1000	0	95	95
			(0)	(94)	(94)
25	Cu(II)	2.5	5	88	93
	Pb	2.5	19	84	103
	Cd	0.25	72	28	100
	Humic acid	1500	0	96	96

[a]Second run in parentheses.

solution (10 mg l^{-1}, pH 7) was passed. The metals in the latter effluent were negligible, i.e., less than detection limits for lead (<0.2 μg) and cadmium (<0.05 μg) and 0.3 μg for copper(II). This result shows that, in the cation exchange, the most probable positive error, from elution of the sorbed metals with humic acid, is negligible. From the above results as well as the data in Table 2, it can be concluded that negative errors are also negligible in both separations.

Further, the metal concentrations in effluent fractions from the A-25 column were measured at intervals. The concentrations may change if the separation step contains positive or negative errors. Figure 2 shows that the metal concentrations were constant for copper(II), lead and cadmium.

Metal/humic acid complexes in synthetic aqueous solutions (pH 7) were collected on the A-25 column, desorbed with 4 M nitric acid and determined by the proposed procedure. As shown in Table 3, the metals were quantitatively desorbed, while most of the humic acid remained on the exchanger. Metal contamination from the anion and cation exchangers and humic acid was not detected for copper, lead and cadmium. Decomposition products of the A-25 had absorption at 400 nm; this was subtracted in the determination of humic acid, but the products did not interfere with the atomic absorption spectrometry.

The proposed method was applied to the analysis of pond water. Direct filtration of only 30 ml of the sample with a 0.4-μm pore Nuclepore filter caused serious clogging. Centrifugation prior to the filtration increased the filterable volume to ca. 300 ml. The results are shown in Table 4. The concentrations of humic substance were estimated to be ca. 100 μg l^{-1} for

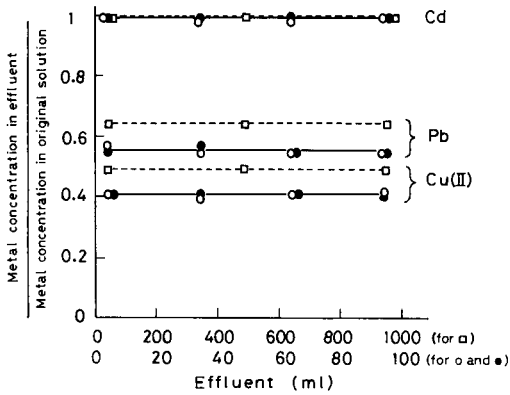

Fig. 2. Effluents from A-25 column. (□) Aqueous 1000-ml solution containing 1 μg each of Cu(II) and Pb, 0.5 μg of Cd and 500 μg of humic acid (effluent fraction taken, 100 ml) at 20 ml min^{-1}. (○, ●) Aqueous 100-ml solution containing 10 μg each of Cu(II) and Pb, 1 μg of Cd and 1000 μg of humic acid (effluent fraction taken, 10 ml) at a flow rate of 20 ml min^{-1} (○) or 2 ml min^{-1} (●).

TABLE 3

Separation of metal/humic acid complexes from cations on the A-25 column

Solution volume (ml)	Added	Amount (μg)	Sorbed and then desorbed (μg)[a]	Found in effluent (μg)[a]	Total
1000	Cu(II)	1.0	0.6	0.5	1.1
	Pb	1.0	0.4	0.6	1.0
	Cd	0.50	0.01	0.51	0.52
	Humic acid	500	—	—	—
100	Cu(II)	10.0	5.8	3.9	9.7
			(5.8)	(3.9)	(9.7)
	Pb	10.0	3.4	5.7	9.1
			(3.6)	(5.5)	(9.1)
	Cd	1.0	0.03	1.0	1.0
			(0.04)	(1.0)	(1.0)
	Humic acid	1000	46	0	46
			(54)	(0)	(54)
25	Cu(II)	2.5	2.3	0.1	2.4
	Pb	2.5	2.1	0.5	2.6
	Cd	0.25	0.05	0.2	0.25
	Humic acid	1500	—	0	—

[a] Second run in parentheses.

sample I (molecular weight distribution: >20 000, 10%; 20 000—10 000, 10%; 10 000—1000, 0%; <1000, 80%) and ca. 140 μg l^{-1} for sample II. More than half of the total cadmium was retained on the A-25 column, which cannot be interpreted because cadmium was only slightly complexed with humic

TABLE 4

Analysis of pond water

Sample[a]	Aliquot taken (l)		Complexed with humic substance (μg metal l^{-1})	Inorganic cation (μg metal l^{-1})
I	1	Cu	0.61	0.16
		Pb	0.14	0.32
		Cd	0.01	0.00
	1	Cu	0.58	0.17
		Pb	0.14	0.31
		Cd	0.01	0.00
II	1	Cu	1.10	0.49
		Pb	0.17	0.43
		Cd	0.01	0.004
	2	Cu	1.15	0.45
		Pb	0.16	0.43
		Cd	0.01	0.004

[a] Sampled on separate days.

acid in synthetic aqueous solutions. Although other anionic species such as metal/EDTA complexes can also be collected on the A-25 column, it seems to be acceptable that the fraction retained on the column is mainly complexed with humic substances.

The authors thank Prof. Kumada and Dr. Arai of Nagoya University for providing fulvic acid.

REFERENCES

1 T. M. Florence, Trends Anal. Chem., 2 (1983) 162.
2 R. F. C. Mantoura and J. P. Riley, Anal. Chim. Acta, 76 (1975) 97.
3 K. L. Cheng, Mikrochim. Acta (Wien), 1977 II (1977) 389.
4 Y. Sugimura, Y. Suzuki and Y. Miyake, J. Oceanogr. Soc. Jpn., 34 (1978) 93.
5 C. J. Miles, J. R. Tuschall, Jr. and P. L. Brezonik, Anal. Chem., 55 (1983) 410.
6 D. J. Mackey, J. Chromatogr., 236 (1982) 81.
7 S. Arai and K. Kumada, Soil Sci. Plant Nutr., 29 (1983) 543.

Analytica Chimica Acta, 172 (1985) 223—239
Elsevier Science Publishers B.V., Amsterdam — Printed in The Netherlands

ION-EXCHANGE RESINS CONTAINING S-BONDED DITHIZONE AND DEHYDRODITHIZONE AS FUNCTIONAL GROUPS

Part 1. Preparation of the Resins and Investigation of the Sorption of Noble Metals and Base Metals

M. GROTE and A. KETTRUP*

Angewandte Chemie, Universität-GH Paderborn, Warburger Straße 100, D-4790 Paderborn (Federal Republic of Germany)

(Received 6th December 1984)

SUMMARY

The one-step reaction of dehydrodithizone with chloromethylated polystyrene yields the anion-exchanger P-TD. Reduction of the immobilized tetrazolium groups of P-TD produces a chelating resin, P-D, containing S-bonded dithizone as the functional group. Distribution coefficients as a function of acidity are presented for 27 metal ions, to establish the selectivity of these sorbents for noble metals. For gold and platinum group metals, the ion-exchangers show marked differences in loading capacities, rates of simultaneous sorption in static conditions and efficiencies in column tests. The P-TD anion exchanger seems to be more profitable than the P-D chelating resin for most purposes.

In a continuation of earlier work in the field of selective separation procedures for noble metals, solid as well as liquid extractants based on formazans were synthesized as metal chelating groups [1—3]. Satisfactory separations of palladium from larger amounts of platinum in weak acid medium and of silver from copper in alkaline medium were achieved. The regenerated extractants could be used again for extraction, which is promising for the development of cyclic separation processes.

The application of ion exchangers to the removal of platinum group metals and gold from aqueous solutions of hydrometallurgical processes requires stability in strongly acidic media. Because of the low stability of strong base resins containing ionically immobilized formazans [2], attempts were made to produce polymers with covalently bonded functional groups containing donor nitrogen and especially sulfur atoms. Resins with such functional groups are promising ion exchangers for the selective sorption of noble metals, e.g., isothiouronium resins [4—6], dithiocarbamate resins [7, 8] and polymers with bonded thiol groups [9—13]. Difficulties in the recovery of metals by elution and the tendency to decompose in neutral or acidic media, however, may limit the applicability of these resins.

The well known thiol-substituted formazan dithizone exhibits remarkable chelating abilities [14]. In chromatographic applications, the reagent was

0003-2670/85/$03.30

used for separations in gel columns [15, 16] and its disulphonic acid derivative was immobilized onto anion-exchange resins [17]. Chemical attachment of dithizone to cellulose [18] and polystyrene [19] was achieved by diazo coupling, but the multistep procedure of diazotation and coupling may produce a multifunctional sorbent. In the interaction of dithizone with aryldiazonium salts, the formation of S-aryl derivatives was observed [20]. The selectivity of either the free or immobilized dithizone is, of course, not very good. Replacement of the thiol proton by alkyl groups reduces the reactivity of dithizone towards various metal ions; thus S-methyldithizone does not form extractable metal complexes under conditions where dithizone itself is effective [21, 22]. These results reported by Irving and coworkers confirmed the intention of the present study: polystyrene should be attached to dithizone via the S-atom of the thiol group, in order to yield a sorbent with suitably selective behaviour.

Preparation of the resins

Nucleophilic displacement of halogens from alkyl- and benzyl-halides by thiol groups offers a convenient method for incorporating functional groups into styrene/divinylbenzene copolymers [4, 5, 23]. Thus, chloromethylated polystyrene (1, Fig. 1) was first treated with solutions of dithizone (2) under various reaction conditions. But the chelating agent, dissolved in methanol, ethanol, dimethylformamide or chloroform, formed no well-defined products with the resin; even in the presence of inorganic (potassium hydroxide, barium oxide) and organic bases (triethylamine), black or brown polymers were isolated with different non-stoichiometric contents of sulfur and nitrogen.

These observations may be due to the tendency of dithizone to undergo cyclization with alkylhalides to yield, for example, 1,3,4-thiadiazolines and verdazyles [24].

The use of dehydrodithizone (3), an oxidation product of dithizone, enabled an improved reaction path to be developed. Because of the enhanced nucleophilic properties of the meso-ionic compound [25], displacement

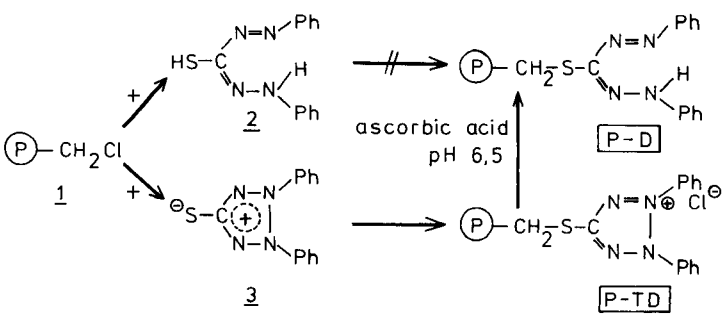

Fig. 1. Reaction of chloromethylated polystyrene (1) with dithizone (2) and dehydrodithizone (3).

reactions on the chloromethylene group of the reactive polymer proceed successfully, resulting in a support carrying sulfur-bonded tetrazolium groups, denoted as P-TD in Fig. 1. Reductive opening of the heterocycle can be achieved by treatment of the orange resin with a neutralized solution of ascorbic acid. The P-TD becomes black, indicating the formation of S-bonded dithizone, the functional group of the desired polymer P-D (Fig. 1). In this report, it will be shown that the two polymers, the intermediate P-TD and the final product P-D, exhibit quite different sorption properties.

Though the reactions described are successful, an apparent problem is that a long reaction time (14 days) is necessary to achieve quantitative conversion of the chloromethylated polystyrene by dehydrodithizone without side-reactions. Shorter times were tested with use of higher temperatures, addition of bases and variation of the solvent (ethanol, chloroform), but in all these cases, even under a nitrogen atmosphere, the reaction failed. The best results were obtained simply by suspending the reactive resin in a solution of dehydrodithizone in dimethylformamide at room temperature. The reaction vessel must be protected from light, to prevent change of P-TD to a red product. The colour shading indicates a side-reaction, which can be monitored by i.r. spectroscopy. The spectrum of the original orange resin exhibits no significant absorption around 1525 cm^{-1}, whereas a reddish P-TD shows more or less intense absorptions in this region, depending on the amount of the by-product. Model reactions with benzylchloride and dehydrodithizone in the presence of alkalies and under the influence of light produce the colourless, free tetrazolium salt, 2,3-diphenyl-5-phenylmethylthio-2H-tetrazolium chloride (Fig. 2, 4) as the main product, but promote a secondary reaction, yielding 2,3-diphenyl-5-phenylazo-1,3,4-thiadiazolines (5) [26]. The red compound, which has been already synthesized by Irving and Mahnot [27] using another reaction path, is characterized by a marked infrared band at 1525 cm^{-1}, which may be assigned to ν(C=N).

From these experimental data, it is suggested that an analogous side-reaction may proceed in the case of the immobilization of dehydrodithizone onto polystyrene. As expected, the reduction of the free tetrazolium salt (4),

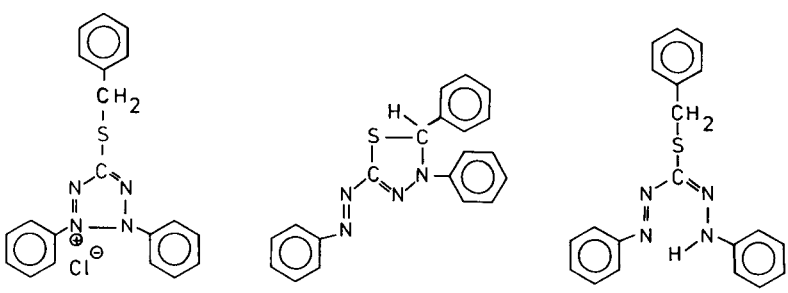

4 5 6

Fig. 2. Formulae of model compounds.

with ascorbic acid results in S-benzyldithizone (6) as a black-brown solid. Comparative i.r. spectroscopic studies support the proposed conversion of the polymer P-TD to P-D (Fig. 1).

EXPERIMENTAL

Model reactions

Dehydrodithizone (2,3-diphenyl-2H-tetrazolium-5-thiolate, Fig. 1, 3) was prepared by the method of Irving et al. [28], using dithizone and potassium hexacyanoferrate(III) as oxidizing agent. (Yield 65%, m.p. 173°C decomp., lit. [28] 172°C.)

Reaction of dehydrodithizone with benzylchloride. Dehydrodithizone (1.07 g, 0.004 mol) was suspended in 60 ml of chloroform under nitrogen and with protection from light. After addition of 500 μl of benzylchloride, the mixture was stirred and refluxed for 3 h. Then the solvent was distilled off and the reddish crude product was recrystallized from (3 + 1) ethanol/diethyl ether, producing colourless crystals of 2,3-diphenyl-5-phenylmethylthio-2H-tetrazolium chloride (4), which tends to decompose rapidly, whether as solid or in solution, in light and air. [Yield 80%, m.p. 161°C (decomp.); λ_{max} (H_2O) 249 and 324 nm; ν_{max} (KBr) 1600, 1484 and 1450 cm^{-1}; $\delta(CDCl_3)$ 7.5 ppm (ArH); *m/z* 344 ($M^+ - 1$) fragments of decomposition products.]

Evaporation of the filtrate of the tetrazolium salt produced about 200 mg of 2,3-diphenyl-5-phenylazo-1,3,4-thiadiazoline (5). The red product was purified by recrystallization from (2 + 8) chloroform/n-hexane. [M.p. 144–145°C, lit. [28] 144–145°C; λ_{max} (ethanol) 492 nm; ν_{max} (KBr) 1597, 1525, 1497 cm^{-1}; $\delta(CDCl_3)$ 6.9 ppm (Ph—$C^{(2)}$—H); *m/z* 344 ($M^{+\cdot}$).]

The reaction of dehydrodithizone with benzylchloride in DMF in presence of stoichiometric amounts of triethylamine increased the yield of the thiadiazoline up to 60% and thus decreased the amount of tetrazolium salt.

Conversion of the tetrazolium salt (4) to S-benzyldithizone (6). Compound 4 (2 g) was dissolved in 50 ml of chloroform under nitrogen, then 50 ml of aqueous 1 M ascorbic acid adjusted to pH 10 with sodium hydroxide was added and the whole mixture was shaken for 30 min. From the dark violet organic phase, a black-brown solid was separated after evaporation of the solvent. Recrystallization from methanol gave 1.8 g (87%) of S-benzyldithizone. This compound is identical with the product obtained by the method of Neugebauer and Fischer [24], using benzylbromide and dithizone as parent compounds. [M.p. 109–110°C, lit. [24] 109–110°C; λ_{max} ($CHCl_3$) 416 nm (violet isomer) and 534 nm (yellow isomer); ν_{max} (KBr) 3342, 1599, 1522, 1501 cm^{-1}; *m/z* 346 ($M^{+\cdot}$); $\delta(CDCl_3)$ (a) 4.06 and 4.34 (s, S—CH_2—Ph), 10.25 and 9.29 (s, —NH), 7.2 ppm (m, ArH); ^1H decoupled (b) 37 and 38 (s, S—$^{13}CH_2$—Ph), 126 (m, $^{13}C_6H_5$—), 138 ppm (s, $^{13}C^{(3)}$)].

The u.v. and n.m.r. spectroscopic results gave evidence for two isomers in tautomeric equilibrium. Their structures may be similar to those of S-methyldithizone, characterized by different intramolecular N—H··N and N—H··S

hydrogen bonds [29]. The structures of the products were also confirmed by elemental analysis (Mikroanalytisches Laboratorium Beller, Göttingen). A Perkin-Elmer 554 spectrophotometer, a Bruker WP 80 and WP 250 Fourier-transform n.m.r. spectrometer and a Varian MAT (CH-5) mass spectrometer were used.

Preparation of the sorbents

Chloromethylated polystyrene (1.3 mmol g^{-1} chlorine, 2% DVB) was purchased from Bio-Rad (200—400 mesh).

Synthesis of P-TD. Weigh 5 g of chloromethylated polystyrene in a 250-ml Erlenmeyer flask and swell the resin in 50 ml of freshly distilled dimethylformamide (DMF) for 30 min. Add 2 g of dehydrodithizone, dissolved in 50 ml of DMF, cover the flask with aluminium foil, and shake the mixture mechanically at room temperature. After 14 days, filter the orange resin and wash with 500 ml of each of DMF, a (1 + 1) mixture of DMF and water, water, 1 M hydrochloric acid and finally water. Store the ion exchanger under 0.01 M hydrochloric acid in a brown glass bottle. Calculated from its sulfur content (3.1%), the dry P-TD resin carries about 1.1 mmol tetrazolium groups per gram, so that the reaction is nearly quantitative. The product, transformed to the chloride form, contains about 55% of water.

If a reactive resin with a threefold content of chlorine is used, the theoretical capacity of P-TD can be increased to 1.9 mmol g^{-1}.

Synthesis of P-D. Mix 100 ml of 0.5 M ascorbic acid and 50 ml of 1 M sodium hydroxide in an Erlenmeyer flask, so that the pH of the solution is adjusted to 6.5. Add a 5-g portion of wet P-TD and shake the reaction mixture for 30 min protected from light. Filter the black resin beads and wash successively with 500 ml of each of water, 0.01 M sodium hydroxide, water, 0.1 M hydrochloric acid and finally with water. Transfer the product to a brown glass bottle and store in 0.01 M hydrochloric acid.

The conversion of P-TD to the chelating sorbent P-D occurs without decrease in the sulfur content. Because the functional groups of P-D are less hydrophilic than those of P-TD, the content of water diminishes to 40% after complete conversion. Both ion exchangers are stable in highly concentrated, non-oxidizing mineral acids, whereas in alkaline media (pH $\geqslant$ 9) decomposition reactions were observed.

Determination of the sorption properties of P-TD and P-D

Solutions. Stock solutions of platinum group metals and gold were prepared from the sodium salts of the individual chloro complexes, which were kindly donated by Degussa, Hanau. Solutions of base metals were normally obtained from their metal chlorides, nitrates were used for Ag(I) and Pb(II) and the appropriate oxyanions for Cr(VI), As(III), and Se(IV). The metal content of each solution was determined by direct-current plasma (d.c.p.) emission spectrometry (see below) with use of commercially available standards (Spex Industries).

Determination of distribution coefficients. Air-dried resin samples (200 mg) were equilibrated by mechanically shaking with 10 ml of 0.001 M solutions of the individual metal salts, containing dilute mineral acid (usually hydrochloric or nitric acid). After a shaking time of 24 h at 20 ± 2°C, aliquots were taken from the aqueous solutions and analysed. The distribution data, D_g, were calculated in the usual way. Practical specific capacities Q_A were determined by a similar method, with 0.01 M solutions of the platinum metals and gold in 1 M hydrochloric acid.

Determination of the rate of simultaneous loading of precious metals. These experiments were done with different synthetic mixtures, containing the same concentration (0.001 mol l^{-1}) of each platinum group metal and gold in 20 ml of 1 M hydrochloric acid and 400 mg of resin. After reaction times of 5, 15, 30 min and 1, 2, 4 and 24 h, the shaking machine was stopped and an aliquot (500 μl) was taken for analysis with the multi-element equipment of the d.c.p. spectrometer.

Simultaneous loading of precious metals and base metals. A portion (200 mg) of resin was shaken in 30 ml of 1 M hydrochloric acid, containing 500 μg (16.6 mg l^{-1}) of each platinum metal and gold and also of copper(II), nickel(II) and iron(III). After 1 h, aliquots were taken for multi-element determination.

Spectrometric procedure. A Beckman Spectraspan III d.c. argon-plasma emission spectrometer with a three-electrode plasma jet was used as described elsewhere [30, 31]. The instrument contained, in addition, a dynamic background compensator (DBC-33). Usually, the spectral background was compensated by matrix matching of samples and standards.

Simultaneous multi-element determinations were done by using a 10-element cassette and detector. Details of elements and wavelengths are listed in Table 1. All other elements were determined in the sequential mode.

Combination of d.c.p. emission spectrometry and liquid chromatography (d.c.p./l.c. system)

The sorption properties were tested under dynamic conditions with a combined technique of liquid chromatography and d.c.p. emission spectrometry as shown in Fig. 3.

A small column (0.7 cm i.d. with 2-cm bed height, or 0.5 cm i.d. with 4-cm bed height) usually filled with 750 mg of resin, was coupled via a three-way valve and a peristaltic pump with the nebulizer of the d.c.p. spectrometer. Flow rates can be adjusted between 0.5 and 2 ml min^{-1}. When a solution containing the combined precious metals passes through the column, the concentrations of the individual metals can be followed simultaneously in the effluent by the d.c.p. multi-element detector, using an integration time of 10 s and an interval of 30 s between measurements. This d.c.p./l.c. system offers a convenient and economical method of obtaining a survey of the order of breakthrough or elution of various metals.

TABLE 1

Wavelengths (λ) of the atomic emission lines used, and detection limits (c_L) of the d.c.p. multi-element equipment

Element	λ (nm)	Order no.	c_L (μg l^{-1})[a]
Au	242.795	93	10
Pt	265.945	85	40
Os	290.906	78	80
Ni	305.082	74	8
Ir	322.078	70	40
Cu	324.754	69	4
Pd	340.458	66	3
Ag[b]	338.289	66	not determined
Ru	349.894	64	18
Rh	369.236	61	3

[a] c_L values were determined simultaneously from ten repeated recordings of 1 M hydrochloric acid solutions. The c_L were taken as three times the standard deviation of the background noise beneath the analyte lines. [b] Element determined in the sequential mode.

RESULTS AND DISCUSSION

Distribution data

The distribution data for noble metals and base metals with the sorbents P-TD and P-D are summarized in Tables 2–5. From the results in Table 2 it is evident that especially Au(III) and Os(IV) are sorbed markedly by the P-TD ion exchanger even at high acidities whereas the D_g values for Pt(II/IV), Pd(II) and Ir(IV) are relatively high at low acidities. The sorption of Ir(III), Rh(III), Ru(III) and Ag(I) (in nitric acid) is not very pronounced, whereas a medium affinity for Hg(II) was observed up to 4 M hydrochloric acid. The

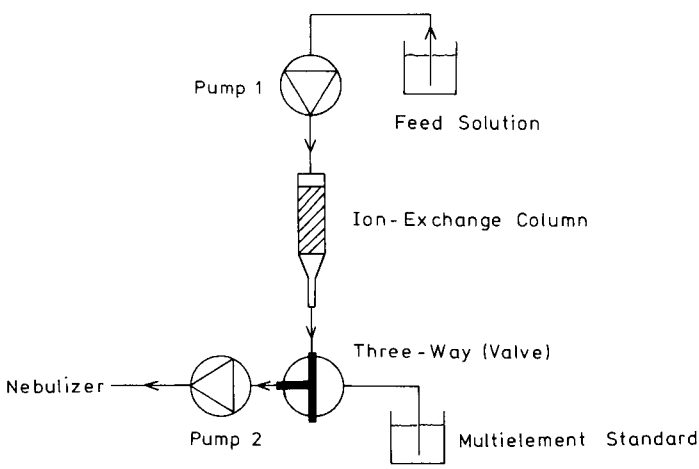

Fig. 3. Schematic diagram of the d.c.p./l.c. system.

TABLE 2

Distribution coefficients of noble metals with P-TD in hydrochloric acid solutions of various concentrations

Metal	Distribution coefficients in HCl solutions					
	0.01 M	0.1 M	1 M	2 M	4 M	6 M
Au(III)	2.1×10^5	2.8×10^5	2.8×10^5	4.2×10^5	3.2×10^5	1.9×10^5
Os(IV)	1×10^6	4.7×10^5	28900	11200	3180	1030
Pt(IV)	1.9×10^5	67200	11900	2710	864	320
Pt(II)	3.4×10^5	1.8×10^5	14500	2570	663	237
Pd(II)	7.7×10^5	1.8×10^5	4320	502	182	67.6
Ir(IV)	25700	20700	2800	355	261	179
Ir(III)[a]	4340	3140	379	64.4	16	3.3
Rh(III)	107	75.5	42.3	16.4	8.8	0.1
Ru(III)	10.9	26.7	90.4	81.7	47	15.3
Ag(I)	—	—	—	p[b]	28.5	4.7
	[3.5	6.5	7.2	—	—	—][c]
Hg(II)	—	6220	6280	2940	1480	520
	[10.4	15.2	14.3	—	—	—][c]

[a]Partly oxidized to Ir(IV). [b]Precipitation. [c]Data obtained with nitric acid solutions.

following order of affinities was found in 1 M hydrochloric acid, considering gold and platinum metals: Au(III) $\gg$ Os(IV) > Pt(II/IV) > Pd(II) > Ir(IV) $\gg$ Ir(III) $\approx$ Rh(III) $\approx$ Ru(III). This order is similar to that for isothiouronium resins [4—6] and the weakly basic amino-polystyrol [32], but differs from that for strongly basic resins, their affinities being higher for Ir(IV) [33, 34]. In general, the uptake of noble metal ions decreases with increasing molarity of hydrochloric acid, thus the behaviour of the resin P-TD is similar to that of polymers which bind noble metal ions predominantly by anion-exchange mechanisms.

Typical anion-exchange properties of the immobilized tetrazolium salt were observed also in the case of base metals (Table 3). Elements which form stronger chloride complexes [Cd(II), Sn(II), Zn(II), Fe(III)] are sorbed to some extent, but usually their distribution coefficients are much lower in medium acid strength than those of some important noble metals. The enhanced uptake of bismuth(III) at intermediate acidities may be caused by its tendency to hydrolysis.

The sorption behaviour of the resin P-D is quite different from that of its intermediate P-TD. Very high distribution coefficients ($D_g \approx 10^4$—10^6) were observed for Pd(II), Pt(II) and Au(III) in the whole range of hydrochloric acid concentration. It is noteworthy that a change in the oxidation state of platinum greatly affects its distribution; sorption of Pt(IV) is not appreciable at higher hydrochloric acid concentrations. The other platinum group metals were taken up only to a small extent. In contrast to the P-TD polymer, interactions between the functional groups of P-D and Ir(IV) and Ru(III) are accompanied by redox reactions, indicated by a colour change of the individual solutions during the contact with the resin. However, the formation

TABLE 3

Distribution coefficients of base metals with P-TD in hydrochloric acid solutions of various concentrations

Metal	Distribution coefficients in HCl solutions						
	0.01 M	0.1 M	0.5 M	1 M	2 M	4 M	6 M
Bi(III)	—	—	2330	1120	—	106	22.6
Cd(II)	39.0	227	386	839	—	633	261
Sb(III)	—	—	412	793	—	899	297
Sn(II)	—	—	208	492	—	1920	1930
Zn(II)	0	4.9	78.8	180	—	208	103
Cr(VI)	—	—	106	105	—	34.3	8.4
Fe(III)	4.0	9.3	10.1	12.7	35.6	450	3570
Pb(II)	—	—	11.6	17.9	—	11.3	3.3
Cu(II)	0	2.4	3.0	3.3	5.5	8.9	13.6
Se(IV)	—	—	3.0	3.3	—	3.9	3.4
As(III)	—	—	0.8	3.2	—	5.1	15.7
Ni(II)	0	0	0	0	—	0	1.9
Co(II)	—	—	0	0	—	0	0
Mn(II)	—	—	0	0	—	0	0
Cr(III)	—	—	0	0	—	0	0
Al(III)	—	—	0	0	—	0	0

of gold metal on the resin, as has been reported for isothiouronium resins [4], could not be observed.

Silver(I) and mercury(II) were also retained favourably by the sorbent in weak nitric acid medium, whereas in hydrochloric acid the uptake of mer-

TABLE 4

Distribution coefficients of noble metals with P-D in hydrochloric acid solutions of various concentrations

Metal	Distribution coefficients in HCl solutions					
	0.01 M	0.1 M	1 M	2 M	4 M	6 M
Pd(II)	5×10^6	5×10^6	4.8×10^6	4.5×10^5	3.6×10^5	1.1×10^5
Pt(II)	8.9×10^5	4.3×10^5	5.1×10^5	73 000	14 900	5710
Au(III)	33 700	20 800	27 100	1.5×10^5	62 400	4610
Pt(IV)	1.7×10^5	60 400	926	234	104	31.8
Ru(III)	63.7	58.5	66.1	68.7	143	63.7
Rh(III)	32.4	31.6	64.9	69.1	71.2	26.7
Os(IV)	49.3	38.4	36.4	35.4	39.4	43.4
Ir(IV)	69.2	38.4	18.6	3.9	0.4	0.2
Ir(III)	28.7	19.0	6.2	2.3	3.4	0.3
Ag(I)	—	—	—	p[a]	0.4	1.3
	[1100	1600	3200[b]	—	—	—]c
Hg(II)	—	568	57.4	47.3	44	47
	[58 000	82 000	55 000[b]	—	—	—]c

[a]Precipitation. [b]Decomposition of the resin. [c]Data obtained with nitric acid solutions.

cury(II) was reduced by its competing complexation with chloride. Unfortunately, the polymer started to decompose even in 1 M nitric acid. It can reasonably be assumed from these observations that the metal ions bind to to S-bonded dithizone by chelation.

The results obtained with base metals (Table 5) show that generally the retention of these metals by P-D is negligible in comparison to some noble metals. Though the sorbent extracts Cu(II) to a greater extent than P-TD does, the distribution coefficients are very low ($\leqslant 36.6$) over the whole range of acidity. These results provide particular support for the prediction that dithizone, covalently bonded to polystyrene via its sulfur atom, would exhibit remarkable selectivity in its sorption properties. The dependence of the values of D_g on molarity of hydrochloric acid is in some cases, e.g., Bi(III), Sn(II), Fe(III), similar to that with P-TD, but the effects are considerably diminished.

These results indicate that in strong acid medium immobilized dithizone may act also as an anion exchanger. Protonation of the ligand and partial conversion of functional groups to tetrazolium groups or other different products by interaction of oxidizing metal ions may promote such behaviour. Further experiments are in progress to clarify the mechanism of ion binding of both polymers.

The presentation of the basic sorption properties is completed by summarizing the maximum loading capacities (Q_A) for platinum group metals and gold of the two resins in 1 M hydrochloric acid (Table 6). In this report,

TABLE 5

Distribution coefficients of base metals with P-D in hydrochloric acid solutions of various concentrations

Metal	Distribution coefficients in HCl solutions						
	0.01 M	0.1 M	0.5 M	1 M	2 M	4 M	6 M
Cu(II)	13.9	36.6	35.0	18.9	17.9	15.9	3.1
Sb(III)	—	—	6.1	16.0	—	34.8	27.4
Sn(II)	—	—	5.1	14.2	—	41.5	61.5
Bi(III)	—	—	9.6	7.9	—	5.3	4.3
Cd(II)	0	0.4	4.7	6.2	—	13.1	19.7
Se(IV)	—	—	2.9	5.4	—	10.2	13.6
Pb(II)	—	—	2.1	2.5	—	3.8	2.1
Zn(II)	—	—	0	1.6	—	2.1	1.8
Ni(II)	0	0	0	0.3	1.9	1.5	1.5
Fe(III)	0	0	0	0	0.8	11.3	120
Cr(VI)	—	—	0	0	—	3.9	1.4
Co(II)	—	—	0	0	—	0	0
Mn(II)	—	—	0	0	—	0	0
Cr(III)	—	—	0	0	—	0	0
Al(III)	—	—	0	0	—	0	0
As(III)	—	—	0	0	—	0	0

TABLE 6

Practical specific capacities Q_A from 1 M hydrochloric acid solutions

Resin	Q_A (mmol g^{-1})								
	Au(III)	Pd(II)	Pt(II)	Pt(IV)	Os(IV)	Ir(IV)	Ir(III)	Ru(III)	Rh(III)
P-TD	0.95	0.49	0.58	0.48	0.53	0.52	0.27	0.21	0.12
P-D	0.74	0.68	0.39	0.31	0.12	0.14	0.02	0.14	0.16

further investigations will be restricted to these metals. It is obvious that the loading capacities of the P-TD resin reach approximately the theoretical capacity of 1.1 mmol g^{-1} only for the monovalent chloro complexes of gold(III). Metal complex ions with a higher charge were bonded to a lower extent. As expected by their distribution coefficients (Table 4), particularly gold, palladium and platinum are sorbed by the P-D chelating sorbent with maximum values of capacities. In general, the sorption of rhodium and ruthenium on the two exchangers is not pronounced enough to be useful for separation procedures.

Sorption rates

The rate of simultaneous loading of the exchangers by precious metals was determined in solutions containing 10^{-3} mol l^{-1} of each platinum metal and gold in 1 M hydrochloric acid. To study the influence of the various oxidation states of some metals, two different synthetic mixtures were prepared.

In the first stock solution, the elements were present in their commonest oxidation states, as denoted in Fig. 4; it must be emphasized that platinum and iridium were maintained in their tetravalent state. As is typical for

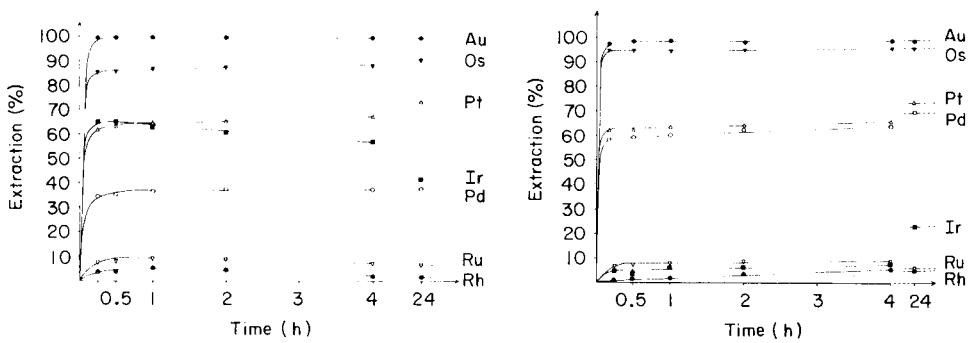

Fig. 4. Simultaneous sorption of precious metals by P-TD showing extraction yield (%) as a function of time (1×10^{-3} mol l^{-1}, 1 M HCl): (+) Au(III); (▾) Os(IV); (△) Pt(IV); (▪) Ir(IV); (○) Pd(II); (▽) Ru(III); (×) Rh(III).

Fig. 5. Simultaneous sorption of precious metals by P-TD showing extraction yield (%) as a function of time. Conditions as for Fig. 4 but with Pt(II) and Ir(III) instead of the higher oxidation states.

anion-exchange reactions, the time necessary to reach half the maximum uptake by P-TD is of the order of a few minutes. However, it is striking that the uptake of iridium(IV) decreases with increasing shaking time. This could be due to reduction of the adsorbed metal complex and subsequent desorption.

Another experiment was done by shaking the immobilized tetrazolium salt with a second sample mixture in which the chloro complexes of platinum(II) and iridium(III) were used along with the other noble metal ions. An adjustment of the appropriate oxidation states can be utilized for improved separation conditions [35]. As shown in Fig. 5, the behaviour of Ir(III) was quite different from that of iridium(IV). The slight increase in the extraction yield of iridium after a reaction time of 24 h may be caused by slow oxidation of the trivalent ion.

Figures 6 and 7 elucidate the different characteristics of the P-D chelating resin. Comparatively high sorption rates were found only in the case of gold and palladium, whereas the extraction of the other metal ions was retarded, indicating a more complicated mechanism of metal binding (formation of ion pairs, chelation by N- and S-atoms of the ligand, ligand exchange) by the formazan functional groups. As is known [36], complexes of platinum(IV) are subject to slow rates of ligand substitution, thus differing from Pd(II) and Pt(II). Therefore, replacing of Pt(IV) by Pt(II) causes an enhanced uptake of this metal, owing to faster substitution of ligands (Fig. 7). This knowledge of the effect of shaking time on the efficiency of resins is important for interpretation of the results of sorption studies under dynamic conditions (see below).

Simultaneous loading of precious metals and base metals

Sorption studies under static conditions with mixtures of precious metals and base metals were selected with regard to potential applications of the ion

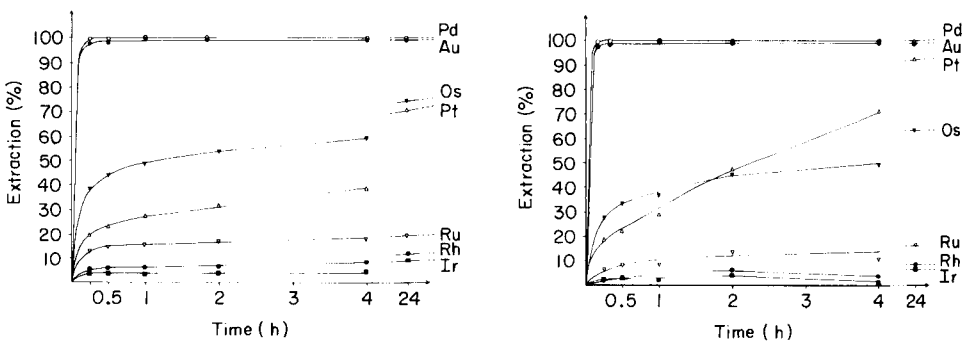

Fig. 6. Simultaneous sorption of precious metals by P-D showing extraction yield (%) as a function of time. Conditions as for Fig. 4, with Pt(IV) and Ir(IV).

Fig. 7. Simultaneous sorption of precious metals by P-D. Conditions as for Fig. 5, with Pt-(II) and Ir(III).

exchangers in hydrometallurgy. For this purpose, 500 μg of each of Fe(III), Ni(II) and Cu(II) as representative base metals were combined with equal amounts of platinum group metals and gold in hydrochloric acid of various concentrations. The individual synthetic mixtures were treated for 1 h with a slight excess of P-TD or P-D and then the solutions were analyzed. The results of these studies are presented graphically in Fig. 8A and B. Every black column represents the amount of an individual metal taken up by the resin from 0.3, 1.0, 3.5 or 6 M hydrochloric acid. It is evident that only traces of copper and nickel were retained by both sorbents; in contrast, iron(III) was co-extracted nearly quantitatively by P-TD but less well by P-D from strongly acidic medium. Similar observations were reported by Warshawsky in the case of isothiouronium resins [5]. Lowering of the selectivity by iron(III) may limit

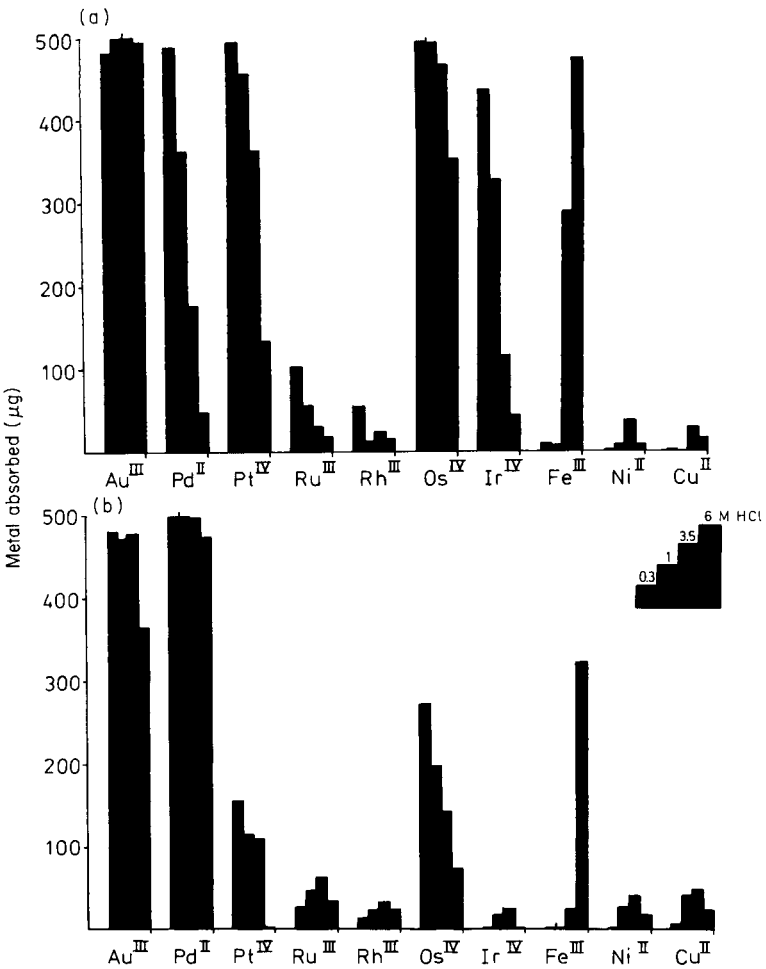

Fig. 8. Loading of P-TD (A) and P-D (B) with a mixture of precious metals and base metals from hydrochloric acid (0.2 g of resin, shaking time 1 h, 500 μg of each metal).

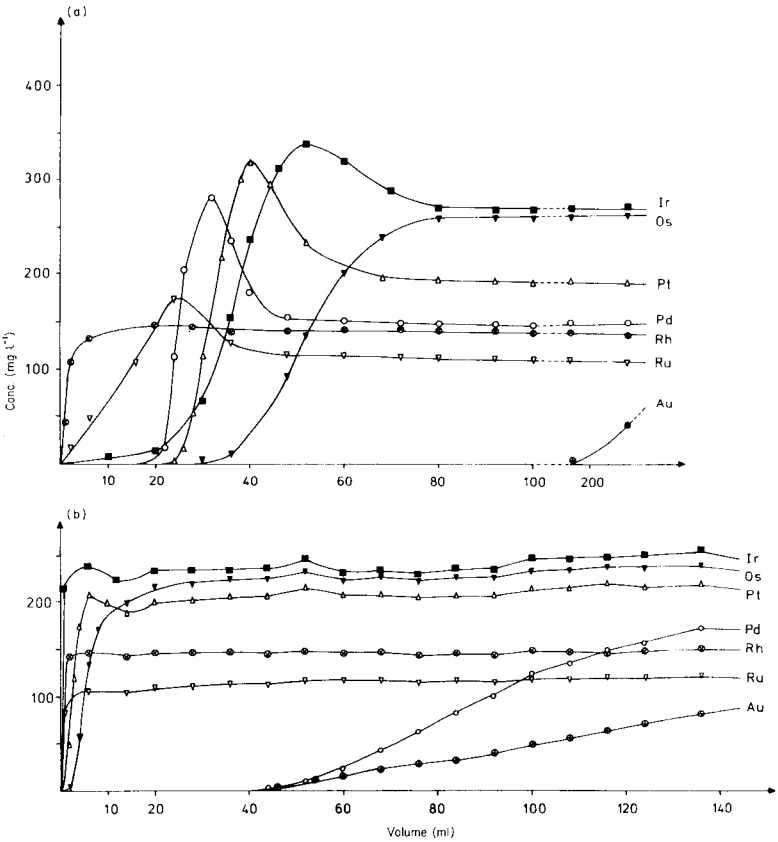

Fig. 9. Breakthrough volumes for a mixture of precious metals on P-TD (A) and P-D (B) (0.7 × 2 cm resin bed; Pt(IV) and Ir(IV) in both cases). Symbols as for Fig. 4.

the applicability of the sorbents. However, this base metal is stripped easily by dilute hydrochloric acid in contrast to co-extracted noble metals, so that a separation can be carried out successfully [39].

Depending on the acidity of the sample solution, the extraction yields of the combined platinum group metals and gold obtained for the P-TD anion exchanger coincide with the values of the individual distribution coefficients (Table 2). Thus, complete sorption of Au(III), Pd(II), Pt(IV) and Os(IV) was achieved in weak hydrochloric acid medium, whereas iridium(IV) was not taken up quantitatively. In contrast, the results for simultaneous loading of P-D (Fig. 8B) cannot be predicted correctly by the order of the D_g values (Table 4). Redox reactions between the immobilized dithizone and noble-metal ions, as well as comparatively lower rates of loading, may cause the extraction yields for osmium to be higher and yields for platinum to be lower than expected. High efficiency over the whole range of acidity was obtained only for gold and palladium. Similarly to P-TD, the P-D polymer takes up ruthenium and rhodium only negligibly.

Simultaneous loading in column techniques

Ion-exchange resins are normally utilized in chromatographic columns. Therefore attempts were made to study the sorption behaviour of the synthesized sorbents under dynamic conditions. These tests were conducted with the combination of liquid chromatography and d.c. plasma spectrometry (d.c.p./l.c. system) described under Experimental. Small columns were usually filled with 750 mg of the appropriate resin. Feed solutions, containing the platinum group metals and gold (≈ 100—260 mg l^{-1}) were passed continuously through the resin bed at a flow rate of 2 ml min^{-1}. During the loading, the concentration of the individual noble metals in the effluent was measured simultaneously.

Figure 9A presents the results of such an experiment with P-TD. In terms of increasing breakthrough volumes, the adsorption order corresponds with the order of distribution coefficients in 1 M hydrochloric acid. The high affinity for gold is especially well demonstrated by the very late appearance of its chloro complexes. Under these chromatographic conditions, the practical specific capacity for gold is about 0.9 mmol g^{-1}. It is striking that the shapes of the individual breakthrough curves differ significantly. Beside the usual breakthrough of some ions (e.g., Os and Au, which is not plotted completely in Fig. 9A), some curves are characterized by a marked maximum, e.g., Pd(II), Pt(IV) and Ir(IV). In the case of platinum(IV), similar observations were described by Knothe [34] who used a strong base anion exchanger; Knothe noticed those maxima during the sorption of hydroxo complexes of Pt(IV). One can assume that the variety of assorted complex noble-metal ions in the feed solution, and their different tendencies to be adsorbed by the P-TD resin and to be replaced by competing ions [37, 38], causes the behaviour described.

In the case of the formazan-type P-D polystyrene resin, quite different courses of loading were observed, as is shown in Fig. 9B.

The data obtained make it clear that the flow rate of 2 ml min^{-1} is permissible only for the maximum retention of palladium and gold. The low breakthrough volumes of the other platinum group metals, and the run of the simultaneous loading of palladium and gold, provide evidence that individual kinetic behaviour, e.g., with Pt(IV), and the oxidizing power of some metal ions, e.g., Ir(IV), can have serious effects on the utilization of P-D in column techniques. Especially, the influence of the oxidation of functional groups is indicated by the fact that a feed solution containing iridium(III) and platinum(II) resulted in an inverted order of breakthrough of gold and palladium compared to the Ir(IV) and Pt(IV) mixture as illustrated in Fig. 9B.

In conclusion, the P-TD anion exchanger with incorporated sulfur-bonded tetrazolium groups seems to be more profitable than the chelating P-D resin containing sulfur-bonded formazan; its selectivity for palladium and gold is remarkable. The basic properties of the ion exchangers, as presented in this report, may offer some useful applications in separation procedures for noble metals. Finally, the ability of a sorbent to be regenerated is a very

important characteristic. Detailed desorption and separation studies, including stability tests in cyclic processes with use of both polymers, will be reported shortly.

Financial support from Fonds der Chemischen Industrie and Deutsche Forschungsgemeinschaft is gratefully acknowledged. The authors thank Degussa, Hanau, for donating noble metal salts. The contribution of Mrs. R. Knaup in running many emission spectroscopic measurements is also acknowledged. This work was presented in part at the International Conference on Ion Exchange, July, 1984, Cambridge, England.

REFERENCES

1 M. Grote, A. Schwalk, U. Hüppe and A. Kettrup, Fresenius Z. Anal. Chem., 316 (1983) 247.
2 M. Grote, P. Wigge and A. Kettrup, Fresenius Z. Anal. Chem., 310 (1982) 369.
3 M. Grote, U. Hüppe and A. Kettrup, Talanta, 31 (1984) 755.
4 G. Koster and G. Schmuckler, Anal. Chim. Acta, 38 (1967) 179.
5 A. Warshawsky, M. M. B. Fieberg and Y. B. Ras, Natl. Inst. Metall. Repub. S. Afr. Rep., 1364 (1979).
6 A. Warshawsky, M. M. B. Fieberg, P. Mihalik, T. G. Murphy and Y. B. Ras, Sep. Purif. Methods, 9 (1980) 209.
7 J. F. Dingman, K. M. Gloss, E. A. Milano and S. Siggia, Anal. Chem., 46 (1974) 774.
8 K. Hiratani, Y. Onishi and T. Nakagawa, J. Appl. Polym. Sci., 26 (1981) 1475.
9 M. J. Hudson and J. F. Thorns, Hydrometallurgy, 11 (1983) 289.
10 Z. Slovák, M. Smrž, B. Dočekal and S. Slováková, Anal. Chim. Acta, 111 (1979) 243.
11 E. M. Moyers and J. S. Fritz, Anal. Chem., 48 (1976) 1117.
12 A. Deratani and B. Sebille, Anal. Chem., 53 (1981) 1742; Reactive Polymers, 1 (1983) 261.
13 H. Gruber, Monatsh. Chem., 112 (1981) 747.
14 G. Iwantscheff, Das Dithizon und seine Anwendung in der Mikro- und Spurenanalyse, Verlag Chemie, Weinheim, 1972.
15 Y. K. Lee, K. J. Whang and K. Ueno, Talanta, 22 (1975) 535.
16 K. Lorber and K. Müller, Mikrochim. Acta, I (1976) 375.
17 H. Tanaka, M. Chikuma, A. Harada, T. Ueda and S. Yube, Talanta, 23 (1976) 489.
18 A. J. Bauman, H. H. Weetall and N. Weliky, Anal. Chem., 39 (1967) 932.
19 M. Griesbach and K. H. Lieser, Fresenius Z. Anal. Chem., 302 (1980) 109.
20 E. P. Nesynov and P. S. Pel'kis, Zh. Org. Khim., 4 (1968) 1425.
21 H. M. N. H. Irving and C. F. Bell, J. Chem. Soc., (1954) 4253.
22 H. M. N. H. Irving, A. H. Nabilsi and S. S. Sahota, Anal. Chim. Acta, 67 (1973) 135.
23 M. Stern, M. Fridkin and A. Warshawsky, J. Polym. Sci., Polym. Chem. Ed., 20 (1982) 1469.
24 F. A. Neugebauer and H. Fischer, Chem. Ber., 107 (1974) 717.
25 J. W. Ogilvie and A. H. Corwin, J. Am. Chem. Soc., 83 (1961) 5023.
26 A. Schwalk, Dissertation, University of Paderborn, 1983.
27 H. M. N. H. Irving and U. S. Mahnot, Talanta, 15 (1968) 811.
28 H. M. N. H. Irving, A. M. Kiwan, D. C. Rupainwar and S. S. Sahota, Anal. Chim. Acta, 56 (1971) 205.
29 A. T. Hutton and H. M. N. H. Irving, J. Chem. Soc. Perkin Trans. II, (1982) 1118.
30 R. J. Decker, Spectrochim. Acta, 35B (1980) 19.
31 M. W. Blades and N. Lee, Spectrochim. Acta, 39B (1984) 879.

32 V. Sykora, F. Dubsky, O. Vyskočilova and J. Chladńa, Sb. Vys. Sk. Chem.-Technol. Praze, Anal. Chem., H 13 (1978) 171.
33 S. S. Berman and W. A. E. McBryde, Can. J. Chem., 36 (1958) 835.
34 M. Knothe, Z. Anorg. Allg. Chem., 463 (1980) 204.
35 K. Brajter and K. Slonawska, Chem. Anal. (Warsaw), 24 (1979) 273.
36 L. F. Elding and L. Gustafson, Inorg. Chim. Acta, 19 (1976) 31.
37 M. Knothe and S. Ziegenbalg, Z. Chem., 22 (1982) 295.
38 G. Gebhardt, Z. Phys. Chemie, Leipzig, 259 (1978) 399.
39 M. Grote and A. Kettrup, Anal. Chim. Acta, in press.

Analytica Chimica Acta, 172 (1985) 241—248
Elsevier Science Publishers B.V., Amsterdam — Printed in The Netherlands

A COMPARISON OF VARIOUS COMMERCIALLY-AVAILABLE LIQUID CHROMATOGRAPHIC SUPPORTS FOR IMMOBILIZATION OF ENZYMES AND IMMUNOGLOBULINS

RICHARD F. TAYLOR

Biomedical Research and Technology Section, Arthur D. Little, Inc., Acorn Park, Cambridge, MA 02140 (U.S.A.)

(Received 22nd October 1984)

SUMMARY

A number of commercially-available, activated supports were evaluated and compared for the immobilization of enzymes (alkaline phosphatase, glucose oxidase and peroxidase) and human immunoglobulin G (IgG). The supports studied included pressure-stable, epoxy-activated acrylate-based supports (Separon HEMA 1000 and Eupergit C); agarose-based, epoxy-, cyanogen bromide-, glutaraldehyde- or *N*-hydroxysuccimide-activated supports (epoxy-activated or cyanogen bromide-activated Sepharose, ACT-Ultrogel AcA 22, Reacti-Gel 6X and Affi-Gel 10); and glass bead-based, activated supports (CDI- and NHS-Glycophase). As expected, the pH required for maximum protein immobilization and retention of activity varied with both protein and support. For example, the amount of alkaline phosphatase coupled was maximum at pH 3 or 5 for most supports, but retention of activity was greatest for immobilization at pH 7, 9 or 11. Glucose oxidase and peroxidase coupling and activity retention in general showed less variation in optimal coupling pH. Coupling of IgG and retention of anti-IgG binding activity were both optimal at a coupling pH of 9 or 11. The Separon HEMA-IgG support made in these studies was also utilized for rapid h.p.l.c. purification of anti-IgG from serum.

The immobilization of proteins onto inert carriers remains of primary interest for achieving stability with retention of activity during continuous use of the immobilized proteins in assays, reactors, industrial processes, etc. Such preparations also allow the use of the proteins under widely varying conditions of pH, temperature and medium composition and for recovery of the protein from the reaction end product(s).

Protein immobilization on a carrier may be accomplished by using a number of methods including adsorption, entrapment (e.g., encapsulation), copolymerization or covalent linkage [1, 2]. Of these, covalent linkage is favored for long-term stability and use of the immobilized protein. Such linkage can be accomplished by utilizing a coupling agent (e.g., carbodiimide), an activated protein (e.g., activation of the carbohydrate residues in glycoproteins) [3], or an activated support. Of these, activated supports, which can react directly with protein reactive groups (e.g., amino, carboxyl, sulfhydryl and hydroxyl groups) provide a convenient and rapid means for protein immobilization.

0003-2670/85/$03.30

The present study is directed at the use of commercially-available activated supports for protein immobilization. The primary aim of this study was to compare, under identical conditions, the immobilization and retention of activity of a number of enzymes and human immunoglobulin (IgG) on these supports. It was found that such supports can vary greatly in their immobilization characteristics.

EXPERIMENTAL

Materials

The activated supports used and their source are reported in Table 1. Glucose oxidase (GOD, EC. 1.1.3.4., Type VII, 16 400 U g^{-1}), peroxidase (POD, EC. 1.11.1.7., Type VI, 265 U mg^{-1}), alkaline phosphatase (AP, EC. 3.1.3.1., Type I-S, ca. 7 U mg^{-1}), human IgG, anti-human IgG (αIgG), αIgG-AP conjugate, *p*-nitrophenyl phosphate (*p*-NPP), 4-aminoantipyrine (4-AAP), bovine serum albumin (BSA) and ethanolamine were all purchased from Sigma Chemical Co.

TABLE 1

Properties of the activated supports used for protein immobilization

Support	Activating agent	Bead composition	Active (coupling) group and concentration	Coupling time (h)[a]	Supplier
Acrylate-based					
Eupergit C	Epichlorohydrin(?)	100—200 μm acrylate copolymers	800—1000 μmol epoxy groups g^{-1}	16—72	Rohm Pharma, Weiterstadt (F.R.G.)
Separon HEMA 1000 Emax	Epichlorohydrin	100—200 μm acrylate copolymers	1500—1800 μmol epoxy groups g^{-1}	12—48	Laboratory Instruments Works, Prague
Agarose-based					
ACT Ultrogel	Glutaraldehyde	60—140 μm agarose acrylamide (2%/2%)	50—80 μmol active aldehyde groups ml^{-1}	12—18	LKB, Stockholm
Affi-Gel 10	*N*-Hydroxysuccinimide	80—180 μm agarose (6%)	15 μmol active ester groups ml^{-1}	1—4	Bio-Rad Laboratories Richmond, CA
CNBr-Sepharose 4B	Cyanogen bromide	60—140 μm agarose (4%)	>12 μmol active groups g^{-1} [b]	2—18	Pharmacia-PL Biochemicals, Piscataway, NJ
Epoxy-Sepharose 6B	1,4-Bis-(2,3-epoxypropoxy)-butane	45—165 μm agarose (6%)	>300 μmol epoxy groups g^{-1}	12—24	Pharmacia-PL Biochemicals
Reacti-Gel 6X	1,1′-Carbonyldiimidazole	40—210 μm agarose (6%)	20—25 μmol imidazoyl carbamate groups ml^{-1}	36—72	Pierce Chemical Co., Rockford, IL
Glass beads					
CDI-Activated Glycophase	1,1′-Carbonyldiimidazole	74—125 μm CPG	50 μmol imidazoyl carbamate groups g^{-1}	16—24	Pierce Chemical Co.
NHS-Activated Glycophase	*N*-Hydroxysuccinimide	125—177 μm CPG[c]	100 μmol active ester groups g^{-1}	16—24	Pierce Chemical Co.

[a] For proteins. [b] Based on chymotrypsinogen binding. [c] Hydrophilic controlled-pore glass.

Immobilization method

Prior to immobilization, each support was washed (if necessary) and preconditioned according to the supplier's instructions. Each support (0.2—0.5 g) was reacted at pH 3, 5, 7, 9 or 11 with GOD (18 mg), POD (16 mg), AP (30 mg) or IgG (6 mg) in 5 ml of the appropriate buffer for the maximum time (up to 72 h) recommended by the supplier (Table 1). The buffers used were 0.1 M sodium acetate/acetic acid (pH 3 and 5), 0.1 M sodium dihydrogenphosphate/disodium hydrogenphosphate (pH 7), and 0.1 M sodium carbonate/sodium hydrogencarbonate (pH 9 and 11). After reaction, the supports were washed three times with 5 ml each of reaction buffer, the 0.1 M acetate buffer pH 5, water, 0.5 M sodium chloride, water, the 0.1 M carbonate buffer pH 9, and water. The washed supports were resuspended in 5 ml of 0.1 M ethanolamine in the 0.1 M phosphate buffer pH 7 for 18 h to block any remaining active groups. The supports were then washed five times with 10 ml each of water, 0.5 M sodium chloride and water, and suspended in a total volume of 6 ml of the buffer required for activity determinations.

Activity assays

The amounts of protein in the reaction solutions before and after immobilization were determined by the bromophenol blue method [4]. The AP activity was determined by reacting 0.2 ml of support (from a total volume of 6 ml in 0.1 M diethanolamine buffer, pH 9.8, 5×10^{-4} M in magnesium chloride) with 1 ml of substrate solution (3×10^{-3} M *p*-NPP in diethanolamine buffer) for 10 min. After addition of 0.1 ml of 6 M sodium hydroxide to stop the reaction, the reaction mixture was centrifuged (1000*g* for 5 min) and the absorbance of the supernatant solution was measured at 405 nm. The GOD activity was determined by reacting 0.1 ml of support (from a total volume of 6 ml in 0.05 M acetate buffer pH 5) with 1 ml of substrate solution (0.18 M phenol, 0.15 M β-D-glucose, 2×10^{-3} M 4-APP and 1 mg of POD in 0.05 M acetate buffer pH 5) for 10 min. After centrifugation, the absorbance of the supernatant solution was measured at 490 nm. The POD activity was determined by reacting 0.05—0.1 ml of support (from a total volume of 6 ml in the 0.1 M phosphate buffer, pH 7) with 1 ml of substrate solution (0.18 M phenol and 0.002 M 4-APP in the 0.1 M phosphate buffer, pH 7) and 0.2 ml of 0.5% (v/v) hydrogen peroxide for 10 min. After centrifugation, the absorbance of the supernatant solution was measured at 490 nm.

The IgG antibody binding activity was determined by reacting 3 ml of support (from a total volume of 6 ml in phosphate-buffered saline/Tween buffer: 0.01 M phosphate buffer, pH 7.4 which was 0.14 M in sodium chloride, 3×10^{-3} M in potassium chloride and contained 0.05% Tween-20) with 1 ml of αIgG-AP solution (9 μg of αIgG-AP, 2 mg of αIgG and 5 mg of BSA in phosphate-buffered saline/Tween buffer) for 18 h at 25°C. After centrifugation, 0.1 ml of the supernatant solution was reacted with 1 ml of *p*-NPP and the (immobilized) AP activity was determined as described above.

RESULTS AND DISCUSSION

The advantage of utilizing a specific activated support for protein immobilization depends on its ease of handling, the conditions required for protein coupling and the amount or activity of protein coupled to the support. Of the nine supports tested, the easiest to handle throughout the immobilization process were Separon HEMA, Sepharose, Reacti-Gel and the glass bead products. These supports formed uniform suspensions without clumping and were not prone to formation of fines. Of these, the Separon HEMA and glass bead products were stored dry at room temperature without loss of activity, the Sepharose products at 2—8°C and the Reacti-Gel product in an acetone slurry at 2—8°C. Of the remaining supports, the Eupergit C product (stored dry at −20°C), while forming uniform suspensions, was prone to formation of fines which made centrifugation and filtration (during washing) difficult. The ACT Ultrogel (supplied as an aqueous suspension and stored at 2—8°C) was especially difficult to work with because of clumping and, at acidic pH, a tendency to undergo apparent polymerization. The Affi-Gel product (supplied in an aqueous suspension and stored at −20°C) also showed clumping problems at acidic pH.

The primary purpose of this study was to evaluate protein binding to each support at various pH values. As shown in Table 2, and as expected, the optimal pH for coupling varied with the protein and the support. The activity recovered after immobilization was calculated from the actual activity of the immobilized protein in comparison to the activity expected on the support had all the protein which was immobilized retained the original activity (per mg) of the soluble protein. In comparing the amount of protein coupled to a support to retention of activity, it was found that the optimal pH for coupling did not necessarily correlate with the optimal pH for retention of activity. For example, the largest amounts of AP coupled to the supports occurred at pH 3 or 5, but retention of activity was greatest if the enzyme was coupled at pH 7, 9 or 11 (exceptions to this generalization occurred with Affi-Gel and CDI-Glycophase). GOD and POD coupling also showed some variation between the optimal pH for coupling and for retention of activity but it was not as great as was seen with AP. These results show that coupling conditions with an activated support must be considered carefully to balance the amount of protein coupled with maximum retention of activity. On the basis of activity retention only, the best supports for binding AP were Eupergit C and CNBr-Sepharose; for GOD, Separon HEMA, ACT Ultrogel and CNBr-Sepharose; and for POD, Affi-Gel and CNBr-Sepharose. In general, however, all the supports coupled significant amounts of each enzyme with retention of activity provided that the proper coupling pH (for each enzyme) was used.

Table 3 reports the amount of IgG coupled to each support, and the amount of αIgG bound to the immobilized IgG. The latter assay method to

TABLE 2

Enzyme immobilization onto activated supports

Support[a]	Enzyme	mg Protein bound/g support[b] at pH					Activity (%) recovered after immobilization at pH[c]				
		3	5	7	9	11	3	5	7	9	11
Acrylate-based											
Eupergit C	AP	6.4	4.6	4.2	4.0	0	60	37	81	95	—
	GOD	0	0	0	1.4	10.2	—	—	—	65	41
	POD	0	0	1.2	3.8	5.4	—	—	33	21	15
HEMA 1000	AP	18.8	8.8	5.9	1.2	0	40	55	26	79	—
	GOD	0	0	3.5	7.4	12.7	—	—	45	68	23
	POD	0	3.5	7.1	5.9	7.8	—	33	31	29	7
Agarose-based											
ACT Ultrogel	AP	3.9	7.7	2.8	3.9	0	42	72	76	71	—
	GOD	0	6.2	0	0	0	—	73	—	—	—
	POD	0	3.7	7.1	2.3	0	—	23	45	31	—
Affi-Gel 10	AP	10.0	8.6	0	8.6	0	72	54	—	9	—
	GOD	0	9.5	2.5	0	0	—	42	66	—	—
	POD	0	6.7	8.6	5.0	6.1	—	32	53	48	19
CNBr-Sepharose	AP	13.0	23.0	7.0	3.6	0	14	45	66	92	—
	GOD	0	2.8	4.2	10.6	8.8	—	51	67	73	55
	POD	0.9	3.6	5.9	7.6	2.4	20	43	59	50	51
Epoxy-Sepharose	AP	8.8	10.0	12.4	9.4	3.0	25	20	15	20	39
	GOD	0	0	0	4.2	8.4	—	—	—	35	21
	POD	0	1.7	2.6	1.7	5.9	—	16	21	30	9
Reacti-Gel 6X	AP	13.4	18.8	9.0	5.4	0	11	40	79	83	—
	GOD	0	2.9	5.4	7.6	10.9	—	39	57	60	42
	POD	0	1.2	1.9	3.5	4.9	—	21	32	29	15
Glass beads											
CDI-Glycophase	AP	15.2	15.2	0	0	0	13	31	—	—	—
	GOD	0	0	4.2	7.8	8.0	—	—	32	43	21
	POD	0	2.8	1.4	1.8	3.6	—	14	21	19	9
NHS-Glycophase	AP	16.4	17.6	9.4	3.0	0.6	19	22	10	16	44
	GOD	0.7	2.8	3.2	7.8	8.8	33	41	50	42	22
	POD	0	3.6	2.4	4.2	4.8	—	19	27	29	11

[a]See Table 1 for support descriptions. [b]Each value is the mean of those obtained for two separate immobilization reactions, with no single value deviating from the mean by more than ±11.2%; a zero value indicates <0.5. [c]Calculated using: U/G support/(U/G protein prior to immobilization) (MG protein/G support) × 100.

determine retention of immobilized IgG binding to αIgG utilized a ca. 5-fold excess of αIgG over bound IgG to ensure saturation of all available (immobilized) IgG sites. Thus, the relative antibody binding is a direct measure of available specific binding sites on the immobilized IgG, i.e., the higher the value, the greater the retained αIgG binding activity of the IgG after immobilization. As shown by the data in Table 3, maximum coupling of IgG to the supports was achieved at pH 11, except for CNBr-Sepharose (pH 7—9), and maximum retention of antibody binding occurred at pH 9 or

TABLE 3

Human IgG immobilization onto activated supports

Support	mg Protein bound/g support[a] at pH					mg αIgG bound/g support[b] at pH					Relative antibody binding[c] at pH				
	3	5	7	9	11	3	5	7	9	11	3	5	7	9	11
Acrylate-based															
Eupergit C	0	0	0	0.6	1.8	0	0	0	0.2	0.5	—	—	—	0.33	0.28
HEMA 1000	0	0	1.2	1.8	2.4	0	0	1.3	2.2	2.4	—	—	0.40	0.91	0.78
Agarose-based															
ACT Ultrogel	0	0	1.1	1.2	1.9	0	0	0.3	0.4	0.5	—	—	0.27	0.33	0.94
Affi-Gel 10	0	0	0.7	1.2	2.3	0	0	0.2	0.5	0.7	—	—	0.29	0.42	0.30
CNBr-Sepharose	0.5	1.3	2.2	2.2	1.4	0.4	0.4	0.6	0.6	0.6	0.80	0.31	0.27	0.27	0.43
Epoxy-Sepharose	0	0	1.0	1.2	2.4	0	0	0.2	0.2	0.4	—	—	0.20	0.17	0.17
Reacti-Gel 6X	0	0.6	1.3	2.3	3.0	0	0.2	0.5	0.9	1.1	—	0.33	0.38	0.39	0.37
Glass beads															
CDI-Glycophase	0	0	0.8	0.9	2.4	0	0	0.1	0.2	0.4	—	—	0.13	0.22	0.17
NHS-Glycophase	0	0.5	1.3	1.8	2.4	0	0.1	0.1	0.2	0.3	—	0.2	0.08	0.11	0.13

[a] Each value is the mean of those obtained for two separate immobilization reactions, with no single value deviating from the mean by more than ±12.3%; a zero value indicates <0.5. [b] Determined by bound AP activity; each value is the average of determinations on two separate IgG supports with no single value deviating from the mean by more than ±12.1%. [c] mg protein bound per g support/mg αIgG bound per g support.

11, again with the exception of CNBr-Sepharose (pH 3). Based on retention of antibody binding, the best supports for IgG coupling were found to be Separon HEMA and ACT Ultrogel. The most inefficient supports for IgG coupling were those based on glass beads and the epoxy-Sepharose product.

The results reported concerning the amounts of proteins coupled to the various supports and the pH dependence of coupling and activity retention are in agreement with those of other workers [5—11]. In all cases, the immobilization of any protein requires careful pilot studies to establish optimal reaction conditions. In addition, the selection of the immobilization support must consider not only protein-coupling efficiency, but also the chemical and mechanical stability of the support both before and after immobilization. This becomes especially important in large-scale industrial processes or in long-term, recycling operational use. For example, in such applications, a pressure- and mechanically-stable acrylate-based support such as the Separon HEMA product would prove superior to the use of a soft agarose-based gel without the associated problems of loss of enzyme activity on glass bead supports.

As an example of such an application, the Separon HEMA-IgG support was dried after washing with methanol and packed into an 8 × 250 mm high-performance liquid chromatography (h.p.l.c.) column. The column was equilibrated with the 0.01 M phosphate buffer pH 7, and 25 mg (protein

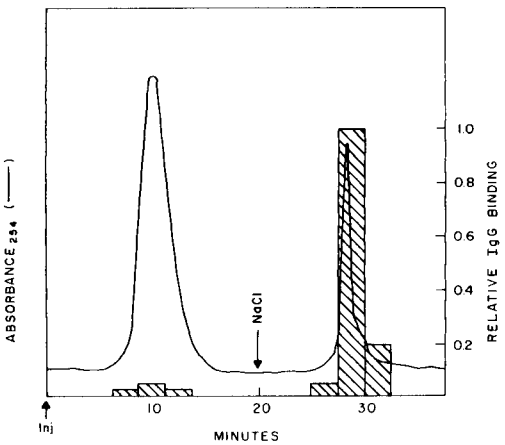

Fig. 1. Purification of human IgG antibody (αIgG) by h.p.l.c. on a column packed with Separon HEMA containing immobilized human IgG. Hatched portions indicate αIgG concentrations.

content) of αIgG serum was injected onto the column. Figure 1 illustrates a typical chromatographic run. After elution with the equilibration buffer for 20 min at 1 ml min^{-1} (ca. 700 psi) to remove non-αIgG, purified IgG was recovered from the column by elution for 15 min with 1 M sodium chloride in the equilibration buffer. The IgG binding activity of the column fractions was determined by an enzyme-linked immunoassay. Comparison of the relative titers (i.e., titer per mg protein) of the IgG serum and the purified IgG showed that from 15- to 25-fold purification could be achieved in this single (30—40 min) step. This is in contrast to the traditional means for antibody purification which requires ammonium sulfate precipitation, desalting and ion-exchange chromatography to achieve similar purification [12]. Reuse of such columns over six months (about 12 times per month) showed no degradation in performance, thus indicating that the IgG-immobilized supports are stable. The supports have also been reanalyzed after multiple affinity chromatography runs and less than 10% losses in antibody-binding ability were found. This illustrates a potential use of pressure-stable protein immobilization supports for widespread biotechnology applications on both laboratory and industrial scales.

REFERENCES

1 K. Mosbach, Methods Enzymol., 44 (1976) 1.
2 T. Godfrey, in T. Godfrey and J. Reichelt (Eds.), Industrial Enzymology, The Nature Press, New York, 1983, p. 437.
3 O. R. Zaborsky, Methods Enzymol., 44 (1976) 317.
4 C. S. Greenberg and P. R. Craddock, Clin. Chem., 28 (1982) 1725.
5 O. Hannibal-Friedrich, M. Chun and M. Sernetz, Biotechnol. Bioeng., 22 (1980) 157.

6 J. Turkova, K. Blana, M. Malanikova, D. Vancurova, F. Suec and J. Kalal, Biochim. Biophys. Acta, 524 (1978) 162.
7 I. Zemanova, J. Turkova, M. Capka, L. A. Nakhapetyan, F. Suec and J. Kalal, Enzyme Microb. Technol., 2 (1981) 229.
8 T. Ternynck and S. Aurameas, FEBS Lett., 23 (1972) 24.
9 J. P. Chen and H. M. Shurley, Thrombosis Res., 7 (1975) 425.
10 M. Landt, S. C. Boltz and L. G. Butler, Biochemistry, 17 (1978) 915.
11 M. T. W. Hearn, E. L. Harris, G. S. Bethell, W. S. Hancock and J. A. Ayers, J. Chromatogr., 218 (1981) 509.
12 B. A. L. Hurn and S. M. Chantler, Methods Enzymol., 70 (1980) 104.

Analytica Chimica Acta, 172 (1985) 249—255
Elsevier Science Publishers B.V., Amsterdam — Printed in The Netherlands

DETERMINATION OF PROTEIN-FREE AND PROTEIN-BOUND CALCIUM AND MAGNESIUM IN BIOLOGICAL SAMPLES BY USE OF ULTRAFILTRATION AND ION CHROMATOGRAPHY

SUSUMU MATSUSHITA

Central Research Laboratories, Toyo Soda Manufacturing Company, Shinnanyo, Yamaguchi (Japan)

(Received 5th June 1984)

SUMMARY

Protein-free and protein-bound calcium and magnesium are determined selectively in biological samples by use of ultrafiltration followed by ion chromatography. A commercial ultrafiltration kit is used to remove proteins of molecular weight >10 000. The content of protein-bound cation is calculated by subtracting the value of protein-free from that of total cation. A protein-free cation filtrate is prepared by ultrafiltration of a diluted sample; a total cation filtrate is prepared by adding EDTA to the sample and filtering. Calcium and magnesium are determined in each filtrate by single-column ion chromatography with 1 mM EDTA (pH 6.5) as eluent and a conductivity detector. The use of a u.v. detector, in series with the conductivity detector, is useful for monitoring small molecules in the filtrates. The proposed method has been successfully applied to the determination of calcium and magnesium in blood serum, milk and egg white.

Several workers have reported the use of ion chromatography for the determination of alkaline earth metal ions [1—4]. A single-column method for anion chromatography with EDTA solution as eluent that uses a conductivity detector has been reported [5], but its scope is limited because the presence of proteins in a sample would foul the separator column [6]. The problem can be solved by ultrafiltration of the sample and the injection of the filtrate into the chromatograph.

There are three distinct forms of serum calcium and magnesium: a free or ionized form, a complexed form associated with anions such as phosphate, hydrogen carbonate and citrate, and a protein-bound unfilterable form.

Some methods [7, 8] have been proposed for measuring ultrafilterable calcium (ionized plus complexed) by ultrafiltration through a permeable membrane, but they have not been applied to the determination of protein-bound calcium. Titration with EDTA for the determination of calcium [9] and magnesium [10] needs a large sample of blood serum. However, addition of EDTA should be capable of liberating these metal ions from proteins, thus making them available for ultrafiltration:

$$\text{Protein} \cdot M^{2+} + H_2EDTA^{2-} \rightarrow \text{Protein} \cdot 2H^+ + MEDTA^{2-}$$

0003-2670/85/$03.30

Ion chromatography is reasonably precise and requires only small samples (<100 μl). When modified, with use of ultrafiltration, this method is effective for the determination of protein-free and protein-bound calcium and magnesium in biological samples. Simultaneously, the proposed method is suitable for determining anions such as chloride, nitrate, sulfate, thiocyanate and iodide.

EXPERIMENTAL

Equipment

Size-exclusion chromatography. A Toyo Soda HLC-803B solvent-delivery system and a Toyo Soda RI-8 refractometer were used with a G3000SW column (300 × 7.6 mm; Toyo Soda, Tokyo). The eluent was 0.2 M phosphate buffer pH 6.9 at a flow rate of 0.5 ml min^{-1}.

Ion chromatography. The ion-chromatographic system (Toyo Soda Model HLC-601) was described previously [11]. The sample loop volume was 100 μl and the flow rate was 1.0 ml min^{-1}. Separations were done on a TSK-gel IC-Anion-SW anion-exchange column (50 × 4.6 mm; Toyo Soda, Tokyo) with 1 mM EDTA (pH 6.5) as eluent.

A Toyo Soda UV-8 variable wavelength detector was connected in series with the conductivity detector.

Ultrafiltration. The UFO-P kit (10 000 cut-off membrane; Toyo Soda) is all-plastic, consisting of a narrow reservoir capped with a back-stopper valve of silicone rubber, an appropriate membrane support and a receiving cap.

In the procedure, 1 ml of sample solution was placed in the reservoir and compressed air was applied from a 2-ml airtight syringe. After 20 min, when 200—400 μl of the ultrafiltrate had accumulated in the receiving cup, the ultrafiltrate was removed and subjected to ion chromatography. Protein retention in the ultrafiltration was determined by size-exclusion chromatography [12].

Atomic absorption spectrometry. A portion (1 ml) of sample was completely decomposed with a mixture of nitric acid and perchloric acid (5 + 1) in a beaker at 130—150°C. The solution was diluted and used for the determination of calcium and magnesium at 422.7 nm and at 202.6 nm, respectively, with a Perkin-Elmer Model 2000 atomic absorption spectrometer.

Materials

Reagents were of the highest grade available commercially. Size-exclusion columns were calibrated with a protein kit (Sigma, St. Louis, MO) covering the molecular weight range 12 500—450 000. Metal stock solutions for ion chromatography were standardized with EDTA titrations. Calf serum was purchased from Nakarai Kagaku (Kyoto, Japan). Human serum was obtained from healthy adult blood by centrifugation. Milk and egg white were commercial products.

Assay

In order to adjust the calcium and magnesium concentrations to within the calibration ranges for the measurement of the protein-free cations, serum and egg white samples were diluted (1 + 9) with water and milk was diluted (1 + 19). Aliquots (1 ml) of these sample solutions were filtered with the UFO-P kit and the filtrate was injected into the ion chromatograph.

In the measurement of total cations, a portion (50 or 100 μl) sample was mixed with 2 mM disodium-EDTA (at pH 7.9) and the volume was adjusted to 1 ml. The mixed solution was filtered with the UFO-P kit and the filtrate was injected into the ion chromatograph. The concentrations of calcium and magnesium were calculated from peak-height measurements.

The value of protein-bound cation was calculated by subtracting the value of protein-free cation from that of total cation.

RESULTS AND DISCUSSION

Protein retention

Protein retention was tested by the UFO-P ultrafiltration kit with standard solutions of calf serum albumin for total protein before and after ultrafiltration. Less than 0.4% of the albumin appeared in the filtrates when more than 50 kits were tested. Total protein in the filtrate was determined by size-exclusion chromatography. Figure 1 shows the chromatograms of the various biological samples before and after ultrafiltration. Of the major proteins (albumin in blood serum, casein in milk, and ovoalbumin in egg white), less than 0.4% appeared in the filtrates.

Elution behavior of ions

EDTA is a favorable eluent for anion separation, because of its high eluting power and low equivalent conductance. Control of the pH of the eluent can be very useful in adjusting the retention time of calcium and magnesium ions relative to most other ions. The retention times decreased with increasing pH, accompanying the increase of concentration of $HEDTA^{3-}$. Eluent adjusted to pH 4.8 was not suitable because the separation was time-consuming. For rapid satisfactory separations of calcium and magnesium, the eluent proposed is 1 mM EDTA at pH 6.5; this can be prepared by pH adjustment or by mixing equal volumes of 1 mM disodium-EDTA and trisodium-EDTA (Dojindo).

The retention times of typical ions encountered in physiological solutions are summarized in Table 1. The retention times observed for metals injected as the metal ions and those injected as their EDTA chelates were not significantly different. It appears that a divalent metal ion forms the EDTA chelate anion immediately on contact with the EDTA eluent and so is separated on the anion-exchange column.

The elution order on the silica-based TSK gel IC-Anion-SW is somewhat different from that observed with conventional anion-exchangers based on

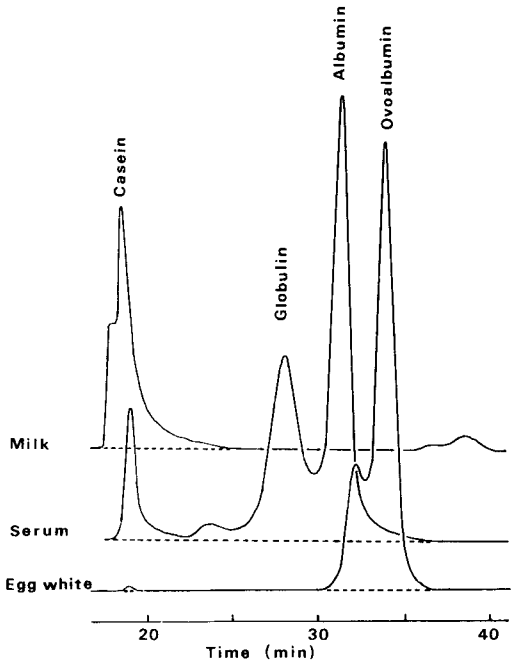

Fig. 1. Separation of proteins before (——) and after (----) ultrafiltration for diluted milk (10 μl), serum (5 μl) and egg white (2 μl). Conditions: column, G3000SW; eluent, 0.2 M phosphate buffer (pH 6.9); flow rate, 0.5 ml min^{-1}; detector, refractometer.

TABLE 1

Retention times (t_R) and detection limits with u.v. (at 210 nm) and conductivity detectors for fifteen ions
Column, TSK gel IC-Anion-SW; eluent, 1 mM EDTA at pH 6.5; flow rate, 1.0 ml min^{-1}

Ion	t_R (min)	Detection limit (ng)[a]		Ion	t_R (min)	Detection limit (ng)[a]	
		U.v.	Cond.			U.v.	Cond.
$H_2PO_4^-$	2.6	30.0[b]	15.0[b]	Oxalate	12.8	3.0	6.0
Cl^-	3.0	6.6	1.3	Citrate	37.0	18.0	35.0[b]
NO_3^-	3.4	0.4	2.7	Ca^{2+}	5.8	8.0	3.0[b]
I^-	5.8	1.4	3.3	Zn^{2+}	6.4	19.0	30.0[b]
SCN^-	7.6	2.2	4.4	Mg^{2+}	6.8	4.0	4.0[b]
SO_4^{2-}	9.0	26.0[b]	2.0	Cu^{2+}	9.4	2.0	50.0[b]
Hippurate	4.7	2.5	4.6[b]	Fe^{2+}	17.0	12.0	13.0[b]
Succinate	10.5	2.8	18.0[b]				

[a]Calculated as twice the random baseline noise. Based on three 100-μl injections of a 5 μg ml^{-1} solution of each ion. [b]Negative peak.

polystyrene/divinylbenzene. For example, iodide and thiocyanate are eluted quickly on the TSK gel (Table 1). Table 1 also shows the detection limits of eluted ions with the dual conductivity/u.v. detectors.

All the metal-EDTA anions appeared as negative peaks with the conductivity detector, i.e., these anions with large ionic radii have lower mobilities and thus lower equivalent conductances than the EDTA eluent at pH 6.5. The calibration graphs for calcium and magnesium based on peak-height measurements were linear up to 20 μg ml^{-1}. The u.v. detector offers lower detection limits for some species. The dual u.v./conductivity detection system is very useful for identifying the constituents in a sample.

Ultrafiltration

In this study, ultrafiltrations were done at room temperature; this is convenient both in terms of time and operation. The effect of the EDTA concentration on chelate formation in the UFO-P kit was studied. Calcium and magnesium in 1 ml of calf serum (diluted 1 + 9 with water) were liberated and ionized with varying concentrations of EDTA (at pH 7.9). The maximum and constant formation of chelate was attained by the addition of more than 0.2 mM EDTA (at pH 7.9). The sulfate peak was completely unaffected by the amount of EDTA present (up to 0.8 mM at least).

The effect of the EDTA concentration was also tested for milk and egg white. A 2 mM EDTA solution (at pH 7.9) was enough to liberate calcium and magnesium from protein in each sample. Thus, it was confirmed that the total cation filtrate was obtained when the sample contained 2 mM EDTA (at pH 7.9) whereas the protein-free cation filtrate was obtained without EDTA. The metal-EDTA chelates in the filtrate are stable in the separator column owing to the EDTA eluent.

Applications

Results obtained for calcium, magnesium and sulfate in serum, milk and egg white are summarized in Table 2. No interferences from other ions were

TABLE 2

Results obtained for calcium, magnesium and sulfate in serum, milk and egg white (in μg ml^{-1})
(Values represent the average and standard deviation of n determinations on the same day)

Sample	n	Method[a]	Ultrafiltrate without EDTA			Ultrafiltrate with EDTA		
			Ca^{2+}	Mg^{2+}	SO_4^{2-}	Ca^{2+}	Mg^{2+}	SO_4^{2-}
Serum	6	I.c.	70 ± 2	17 ± 2	31 ± 2	103 ± 2	25 ± 3	31 ± 2
		A.a.s.	(69 ± 3)	(16 ± 1)		(98 ± 2)	(24 ± 2)	
Milk	8	I.c.	541 ± 5	74 ± 3	85 ± 2	918 ± 5	123 ± 3	85 ± 2
		A.a.s.	(538 ± 4)	(72 ± 2)		(912 ± 5)	(120 ± 2)	
Egg white	4	I.c.	25 ± 2	34 ± 2	9 ± 2	65 ± 2	131 ± 3	9 ± 2
		A.a.s.	(24 ± 2)	(33 ± 1)		(64 ± 2)	(129 ± 2)	

[a]Ion chromatography (i.c.) with 1 mM EDTA (pH 6.5) is based on peak-height measurements. For a.a.s. the Perkin-Elmer Model 2000 spectrometer was used.

observed with the dual u.v./conductivity detector. The total concentrations of calcium and magnesium in each sample obtained by ion chromatography are in good agreement with those found by atomic absorption spectrometry.

Typical chromatographic profiles obtained from diluted serum and milk

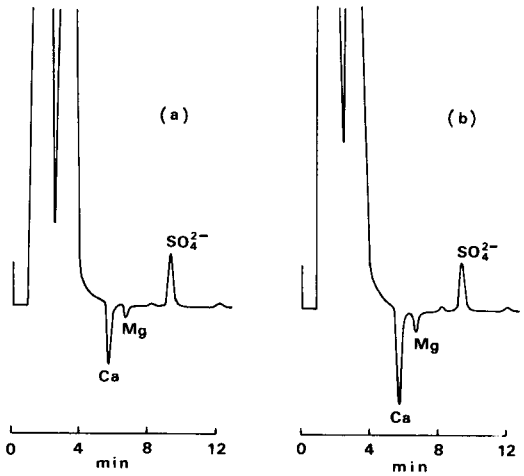

Fig. 2. Chromatograms showing calcium, magnesium and sulfate in diluted human serum: (a) ultrafiltration without EDTA; (b) ultrafiltration after addition of EDTA. Conditions: conductivity detector set at 2.5 μS cm^{-1} full scale, TSK gel column, 1 mM EDTA (pH 6.5) at 1.0 ml min^{-1} as eluent.

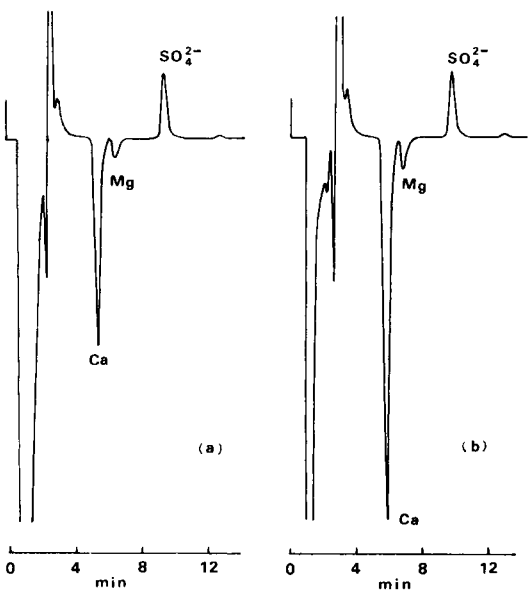

Fig. 3. Chromatograms showing calcium, magnesium and sulfate in diluted milk: (a) ultrafiltration without EDTA; (b) ultrafiltration after addition of EDTA. Conditions as for Fig. 2 except that the detector was set at 5-μS cm^{-1} full scale.

are shown in Figs. 2 and 3, respectively. The peaks for calcium and magnesium are easily distinguished by their characteristic elution times. For the serum, protein-bound calcium and magnesium were each 32% of the total for that metal. From the values for total and protein-free cations shown in Table 2, the calculated values of protein-bound calcium and magnesium were 41% and 40%, respectively, of the totals in milk and 62% and 74%, respectively, in egg white.

Conclusions

Ion chromatography provides a useful assay of alkaline earth metals in biological samples. Proteins foul the separator column owing to the precipitation of protein on the surface of the ion-exchange gels [6], but this problem can be avoided by using ultrafiltration before ion chromatography. The addition of EDTA easily liberates these metals from proteins and filtrates as the anionic metal chelates. The amount of biological sample required is about an order of magnitude less than for flame atomic absorption spectrometry.

I am very grateful to Y. Yamamoto and M. Yamamoto of Hiroshima University, Hiroshima, Japan for helpful consultation and advice; to N. Nakamura, Y. Tada and T. Tabata for assistance in some experimental work; and to K. Fukano and S. Ohno for supplying the ultrafiltration kits.

REFERENCES

1 H. Small, T. S. Stevens and W. C. Bauman, Anal. Chem., 47 (1975) 1801.
2 F. R. Nordmeyer, L. D. Hansen, D. J. Batough, D. K. Rollins and J. D. Lamb, Anal. Chem., 52 (1980) 852.
3 J. W. Wimberley, Anal. Chem., 53 (1980) 2137.
4 J. S. Fritz, D. T. Gjerde and R. M. Becker, Anal. Chem., 52 (1980) 1519.
5 M. Yamamoto, H. Yamamoto, Y. Yamamoto, S. Matsushita, N. Baba and T. Ikushige, Anal. Chem., 56 (1984) 832.
6 F. R. Nordmeyer and L. D. Hansen, Anal. Chem., 54 (1982) 2605.
7 J. Toffaletti and D. Tompkins and G. Hoff, Clin. Chem., 27 (1981) 466.
8 M. D. Costa and P. Cheng, Clin. Chem., 29 (1983) 519.
9 B. Fingerhut and H. Miller, Clin. Chem., 9 (1963) 360.
10 H. A. Frank and M. A. Carr, J. Lab. Clin. Med., 49 (1957) 24.
11 S. Matsushita, Y. Tada, N. Baba and K. Hosako, J. Chromatogr., 259 (1983) 562.
12 K. Fukano, K. Komiya, H. Sasaki and T. Hashimoto, J. Chromatogr., 166 (1978) 47.

Analytica Chimica Acta, 172 (1985) 257—263
Elsevier Science Publishers B.V., Amsterdam — Printed in The Netherlands

THE APPLICATION OF 5,5,7,12,12,14-HEXAMETHYL-1,4,8,11-TETRAAZACYCLOTETRADECANE TO THE EXTRACTION OF METAL IONS

Z. BRZÓZKA and Z. TRYBUŁOWA*

Department of Analytical Chemistry, Technical University, ul. Noakowskiego 3, 00-664 Warsaw (Poland)

(Received 16th October 1984)

SUMMARY

The use of 5,5,7,12,12,14-hexamethyl-1,4,8,11-tetraazacyclotetradecane (Tet) in chloroform solutions provides quantitative extraction of lead(II), cadmium(II), copper(II) and zinc(II) at different pH values from solutions containing perchlorate and cyclohexanecarboxylic acid. Nickel(II) and cobalt(II) ions are not extracted quantitatively. Single extractions of mixtures of copper with transition metals gave the best separations for the copper/nickel system. Separations of copper from cobalt, lead, manganese and iron were less satisfactory.

Macrocyclic amines constitute a new and interesting group of analytical reagents. Because of their structure and their ability to form complexes with different transition metal ions, according to ring size, they are suitable extractants for the separation of metals, and reagents for spectrophotometric determination of metals [1, 2]. The influence of the ring size on the complexation rate is interesting. According to Riedo and Kaden [3], increase in the ring size is accompanied by decrease in the reaction rate constant, whereas the ring size does not influence the stability constant. It appears that complex formation occurs at different rates for different protonated forms of macrocyclic compounds. It was found that rate constants for the complexation of ions with the same protonated form decreased in the order Cu > Zn > Co > Ni.

Regardless of the ring size, the rate constants for complexation with the monoprotonated form do not change for the same ion, but with the double protonated form of the macrocyclic compound, they increase with ring size. Complexation with the unprotonated macrocyclic amine proceeds at a rate similar to that of the open chain amine.

Experiments on the extraction of metal cations were preceded by potentiometric investigation of the complexing power of Tet in aqueous solutions. In the present paper, extractions of some transition metal ions and separations by Tet solution in chloroform are reported. Copper(II), Ni(II), Co(II), Pb(II), Zn(II), Cd(II), Mn(II) and Fe(III) ions were examined and the copper extraction was investigated more closely.

0003-2670/85/$03.30

EXPERIMENTAL

Reagents and apparatus

Stock solutions (0.1 M) and working (10^{-3} M, 10^{-5} M) solutions of metal cations were prepared from analytical-grade salts. The 5,7,7,12,12,14-hexamethyl-1,4,8,11-tetraazacyclotetradecane was used as a solution in chloroform (5×10^{-3} M). (The reagent was synthesized at the Organic Chemistry Institute, Polish Academy of Science, Warsaw, under the supervision of Dr. R. Koliński.) Other chemicals were cyclohexanecarboxylic acid (Aldrich) and analytical-grade sodium perchlorate, sodium hydroxide and sulphuric acid.

A Radelkis OP-208 pH meter was used with a combined glass-calomel electrode. The atomic absorption spectrometer was a Pye-Unicam 90A model and the equipment for automatic titrations was from Radiometer.

Procedure

A portion (5 ml) of the metal ion solution, 5 ml of electrolyte (sodium perchlorate) solution and 10 ml of an aqueous solution of cyclohexanecarboxylic acid were placed in a 50-ml beaker and diluted to 45 ml. The pH was adjusted as required with 4 M sodium hydroxide; then, the solution was diluted with water to the mark in a 50-ml volumetric flask. (For the extractions at $pH_{init.} > 6$, the working solution was prepared directly in a volumetric flask and prior measurements were made on aliquots to estimate the amounts of sodium hydroxide necessary to establish the appropriate pH; these amounts were then added by micropipette directly into the separatory funnel.) Next, 10 ml of the prepared solution and 5 ml of the Tet solution in chloroform were pipetted into a 50-ml separatory funnel and shaken for 60 or 20 min. The phases were separated and the pH of the aqueous phase was measured. The organic phase was back-extracted with 10 ml of aqueous 0.1 M sulphuric acid for 20 min. The metal ion content in the aqueous phase and in the back-extract was determined by atomic absorption spectrometry.

RESULTS AND DISCUSSION

The results of the experiments are given in the following form: (1) plots of percentage extraction vs. initial pH, which are important for analytical purposes; and (2) plots of percentage extraction vs. equilibrium pH. The $pH_{0.5}$ values of the extracted metal ions and the percentage extraction of metal ions from Cu/Me mixtures are collected in Tables 1 and 2. The evaluation of potentiometric titration curves indicated that the complexation of copper(II) and lead ions was stronger than that of the other elements. This creates possibilities for the separation of these metal ions. Detailed extraction investigations were then conducted.

TABLE 1

Comparison of the $pH_{0.5}$ (equilibrium) values of extraction by Tet solution in chloroform (10^{-3} M metal ion in 0.1 M $NaClO_4$ with 8×10^{-3} M CHCA)

Metal	Cu(II)	Zn(II)	Cd(II)	Pb(II)	Co(II)	Ni(II)
$pH_{0.5}$ (Me)	5.0	7.9	7.4	6.2	8.55	9.3
$pH_{0.5}$ (Cu/Me)	—	8.0	7.0	6.3	8.4	8.8

TABLE 2

Comparison of the percentage extraction (%E) of metal ions from copper/metal mixtures ($C_{Cu,Me} = 10^{-3}$ M in 0.1 M $NaClO_4$ with 8×10^{-3} M CHCA; 5×10^{-3} M Tet solution in chloroform)

%E (Cu)	Mn(II)		Pb(II)		Zn(II)		Cd(II)		Co(II)		Ni(II)	
	%E	pH_{in}	%E	pH_{in}	%E	pH_{in}	%E	pH_{in}	%E	pH_{in}	%E	pH_{in}
80	11	4.3	4	3.7	5	4.9	5	4.3	6	4.2	4	4.8
96[a]	12	5.1	10	4.4	17	5.6	26	5.2	8	4.7	4	5.3

[a]The maximum obtained.

Extraction of copper(II)

Quantitative extraction of copper(II) by Tet solution in chloroform from 0.1 M sodium perchlorate was impossible (Fig. 1). For comparison, on the basis of the extraction results of these metals by carboxylic acids [4], copper was extracted by a 0.1 M solution of cyclohexanecarboxylic acid (CHCA) in chloroform. Almost quantitative (100%E) extraction of copper(II) was obtained for equilibrium pH values of 6.0—6.5; however, it was necessary to

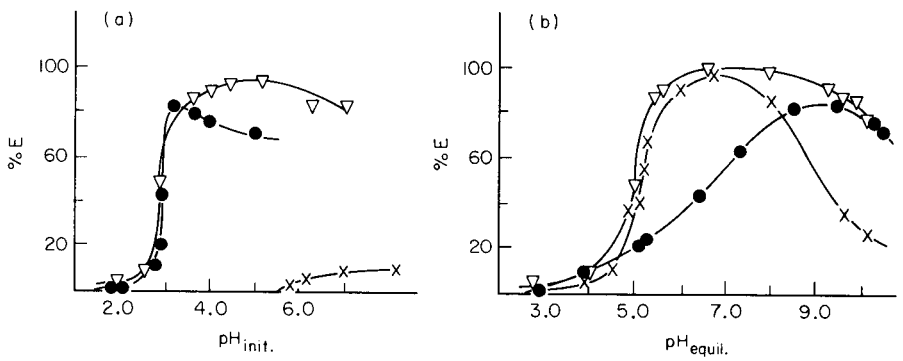

Fig. 1. The extraction of copper(II) from 0.1 M sodium perchlorate: (a) Initial pH; (b) equilibrium pH. (10^{-3} M Cu^{2+}, 5×10^{-3} M Tet in chloroform, 8×10^{-3} M CHCA in water or 0.1 M CHCA in chloroform; $V_w/V_o = 2$, shaking time 60 min.) (×) CHCA in chloroform; (•) Tet in chloroform; (▽) CHCA in water and Tet in chloroform.

use an alkaline initial pH of the aqueous phase (>11.5). This created difficulties during the preparation of extractions; because of the occurrence of precipitates at the interface, it would be more correct to call this a quantitative "isolation" of copper from the aqueous phase rather than extraction. In order to improve the extractions, Tet solution in chloroform was used as the extractant while CHCA was added in the form of a saturated aqueous solution to the prepared aqueous phase. These extraction results are also shown in Fig. 1. Quantitative extraction of copper(II) was then obtained from solutions with initial pH values of 5.0—5.5, and it was found that, in contrast to the extraction by the carboxylic acid in chloroform, the equilibrium pH range for the quantitative extraction of copper was considerably wider.

In order to establish the influence of the macrocyclic amine, pure chloroform was used to extract copper(II) from an aqueous phase containing perchlorate and cyclohexanecarboxylic acid. Only about 70% of copper ($pH_{init.}$ = 5.5) was extracted; the extraction curve had a narrow maximum for $pH_{equil.}$ = 7.5. The influence of shaking time on the percentage extraction of copper(II) ions and on equilibrium pH values was examined. Maximum extraction was reached after 60 min of shaking and this time was applied in further investigations of metal extractions.

Extraction of other metals

The extraction of Ni(II), Co(II), Pb(II), Cd(II), Zn(II), and Fe(III) ions by a Tet solution in chloroform was studied for aqueous 0.1 M sodium perchlorate solutions containing cyclohexanecarboxylic acid (Fig. 2). Quantitative extractions were obtained for zinc(II) and cadmium(II) for $pH_{init.}$ = 6.0—8.0 and of lead(II) for $pH_{init.}$ = 5.5—8.0. Only 80% of cobalt(II) ($pH_{init.} \approx 6.0$) and 60% of nickel(II) ($pH_{init.} \approx 6.5$) were extracted. The lower percentage extraction of these cations may be caused by hydrolysis of the metal ions in

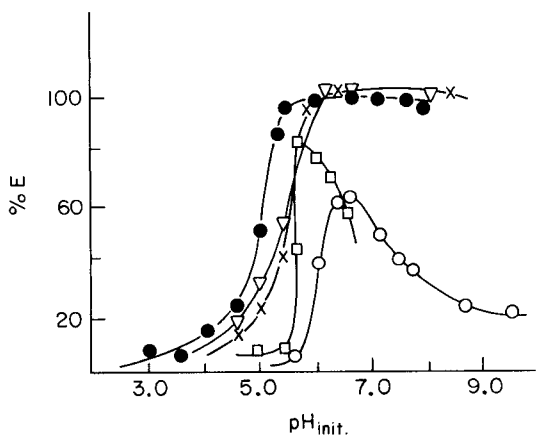

Fig. 2. Extraction from 0.1 M sodium perchlorate in the presence of CHCA: (•) Pb(II), (×) Zn(II), (▽) Cd(II), (□) Co(II), (○) Ni(II). (10^{-3} M Me^{2+}, 10^{-3} M CHCA, 5×10^{-3} M Tet in chloroform, 4×10^{-2} M CHCA in water; shaking time 20 min.)

the alkaline aqueous phase before extraction, because of the formation of precipitates at the interface. Further, cobalt(II) in the complexes underwent oxidation to cobalt(III) readily and remained at the interface. The extraction of iron(III) was tested, but poor (ca. 80%) "isolation" of this cation was obtained because of precipitation at the interface.

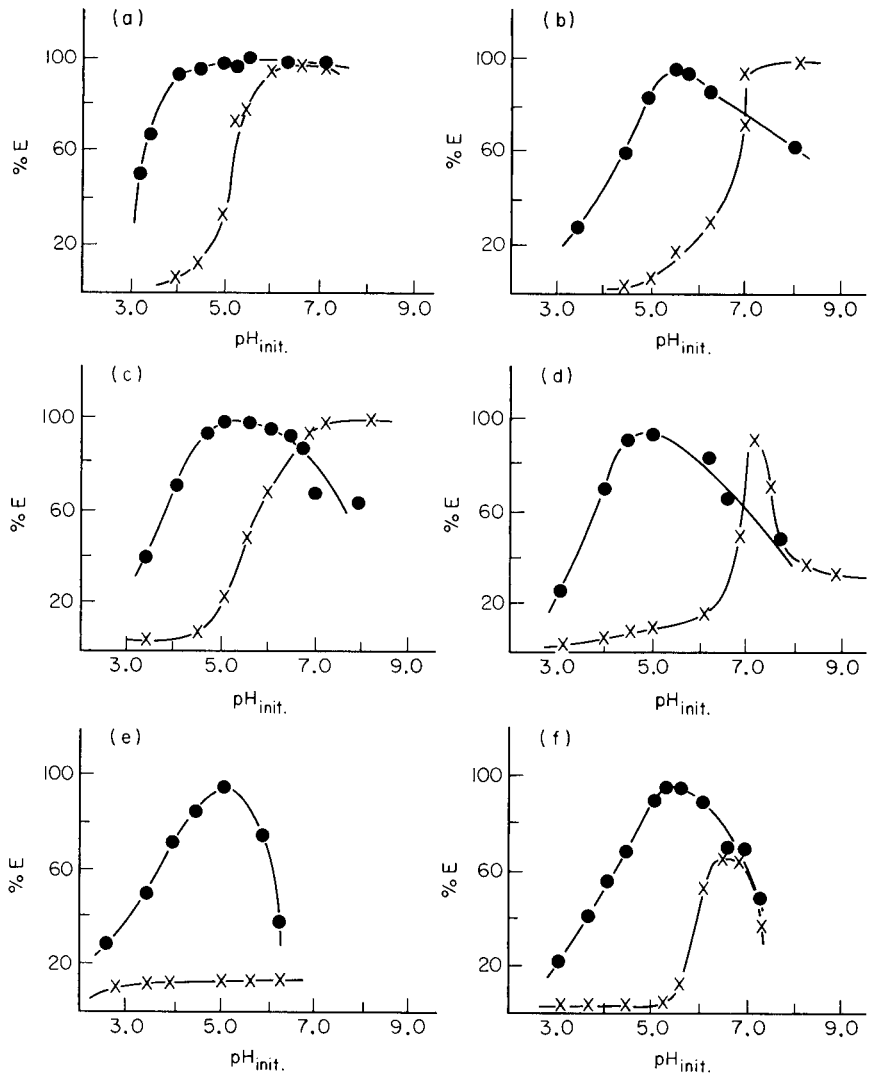

Fig. 3. Extraction of mixtures of copper with another metal: (a) Cu/Pb; (b) Cu/Zn; (c) Cu/Cd; (d) Cu/Co; (e) Cu/Mn; (f) Cu/Ni. In all cases: (•) copper; (×) other metal. (10^{-3} M metal ion, 5×10^{-3} M Tet in chloroform, 8×10^{-3} M CHCA in water; shaking time 60 min, $V_w/V_o = 2$.)

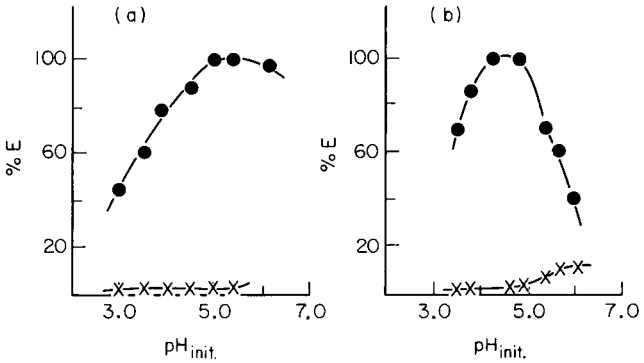

Fig. 4. Extraction of Cu/Ni mixtures: (a) 10^{-5} M Cu^{2+}, 10^{-2} M Ni^{2+}; (b) 10^{-5} M Cu^{2+}, 10^{-1} M Ni^{2+}. (•) Copper; (×) nickel.

Extraction of mixtures of copper with other metals

Extractions of equimolar solutions (10^{-3} M) of Cu/Pb, Cu/Zn, Cu/Ni, Cu/Cd, Cu/Co and Cu/Mn mixtures were examined with Tet solution in chloroform in the presence of cyclohexanecarboxylic acid. The results are shown in Fig. 3 and Table 2. The best separations were obtained for the copper/nickel mixture; at 96% copper extraction for an initial pH of 5.3, only 4% nickel was extracted. The results were less satisfactory for cobalt(II), lead(II) and manganese(II). In the separation of the copper/manganese mixture under the conditions suitable for copper extraction, manganese ions remain in the aqueous phase in the hydrolyzed form, partly oxidized to Mn(III). Despite the poorer results for the Cu/Zn and Cu/Cd separations by single extraction, the described extractive system would be applicable with multiple extractions.

Separation of copper/nickel mixtures

The extraction of Cu/Ni mixtures was investigated with respect to different amounts of nickel ions. The results are shown in Fig. 4. Quantitative copper extraction was obtained for all of the separated mixtures while nickel was extracted in minimum amounts (below 3%). The optimum initial pH value of the mixture depended on the amount of nickel, fluctuating from 4.25 to 5.25. For comparison, the extractive separation of copper and nickel was done with a 0.1 M solution of CHCA in chloroform [5]. Although the single extraction gave good results, the necessity of using a high pH of the initial solution (>11.0) and the formation of precipitates at the interface mean that the CHCA extraction is less attractive than the method used in the present work.

This work was financed by the Third Department of the Polish Academy of Sciences.

REFERENCES

1 W. Szczepaniak and B. Juskowiak, Anal. Chim. Acta, 140 (1982) 261.
2 W. Szczepaniak, B. Juskowiak and W. Ciszewska, Anal. Chim. Acta, 156 (1984) 235.
3 T. J. Riedó and T. A. Kaden, Helv. Chim. Acta, 62 (1979) 1089.
4 Z. Brzózka and C. Różycki, Chem. Anal., 28(5) (1983) 585.
5 Z. Brzózka and C. Różycki, Chem. Anal., 28(4) (1983) 453.

Analytica Chimica Acta, 172 (1985) 265—271
Elsevier Science Publishers B.V., Amsterdam — Printed in The Netherlands

A SHORT SURVEY OF SEMIQUANTITATIVE METHODS OF ANALYSIS AND SOME NEW CONTRIBUTIONS

HERBERT WEISZ* and HERBERT LEPPER

Institut für Anorganische und Analytische Chemie der Universität, D-7800 Freiburg i. Br. (Federal Republic of Germany)

(Received 31 August 1984)

SUMMARY

The definition and use of non-sophisticated semiquantitative methods in analytical chemistry are described. The most important principles for such techniques are discussed: colorimetry, comparison of time, counting of portions, identification limit, area, temperature, volume of precipitate. Some new methods are proposed: strip methods with three different volumes or with three different reagents, an 8-channel colour comparator, titrations with and on impregnated paper, and an evaporation method. Examples are given for the estimation of various ions in the microgram or nanogram range.

Simple methods which need only a little equipment and have a higher range of error than the usual quantitative methods are generally named semiquantitative. The term is appropriate [1] if the relative standard deviation, s_r, of the method is greater than 0.2 ($s_r = s/\bar{x}$; s = standard deviation, $\bar{x}$ = average of test values). Even the differentiation between major, minor and trace components of a sample during qualitative analysis represents a very coarse semiquantitative analysis. Sometimes a qualitative analysis is regarded as a "special case" of quantitative analysis [1]. Semiquantitative methods are often termed non-sophisticated and indeed the simplicity of such techniques can serve as a criterion for definition. The enormous development of technology has led to the automation of many quantitative methods, primarily for routine purposes. Simultaneously with the mechanization of analysis, however, the need for simple, cheap and quick methods has also been recognized in recent years.

The interest in semiquantitative methods is apparent in the steadily increasing number of publications about such methods; a detailed bibliography is available [2]. The commercial side of semiquantitative methods is also gaining more importance; several companies have realized that there is a need for non-sophisticated methods. Consequently, various test sets, mainly for clinical analysis, production control and environmental protection but also for other applications, have been offered commercially for several years. Especially in clinical chemistry, semiquantitative methods can often replace more complicated and time-consuming techniques. The growing interest in

0003-2670/85/$03.30

environmental protection has catalysed the development of simple methods that can provide useful results not only in the laboratory but also in the field, even by untrained personnel.

Principles of measurement

In order to provide information about the quantity of a substance or a mixture of substances, it is necessary to measure the size of a phenomenon that depends in one way or another on the mass or concentration of that substance. Whenever there is a defined relationship between the measured size of an effect and the amount of substance causing that effect, it can be used as a measure for quantifying the substance.

For quantitative purposes, many effects can be used, e.g., weight, length, volume, time, absorption and emission of light, fluorescence, temperature, conductivity, potential, amount of electrical current and many more. To fulfil one of the conditions for semiquantitative methods, namely, the use of simple equipment, only a few of these measurable phenomena can be applied. In this paper, the most important principles of measurement for semiquantitative determinations are discussed. Some newer methods developed in this laboratory [2] are described.

APPLICATION OF COLORIMETRIC PRINCIPLES

In the simplest kind of colorimetry, the colour intensity of the sample solution is compared with that of a series of standard solutions. If the coloured reaction product is not stable enough, a standard scale can also be prepared from more stable materials having a similar colour (e.g., coloured glass). Some variations of such simple colorimetry are spot colorimetry [3], spot nephelometry [4], confined spot colorimetry [5] and ring colorimetry [6]. The well known methods for semiquantitative determinations in thin-layer and paper chromatography should be mentioned, based on comparisons of sample and standard spots. New examples include the following two methods.

Strip method with three different volumes

The lower end (about 0.5 cm) of a narrow paper strip is dipped into the sample solution. The sample solution ascends and passes through a narrow (ca. 0.1 mm) reagent zone (prepared, for example, with the aid of a heat barrier). The substance to be quantified forms an insoluble coloured reaction product. The sample solution can rise to three different marks; this means that three different sample volumes which are in the volume ratio 1:2:3 can be applied (see Fig. 1). The colours formed are compared with standard scales.

For each of the three volumes, a separate standard scale can be prepared and used, but it is also possible to compare sample strips made from one volume with standard strips made from another volume; in the latter case,

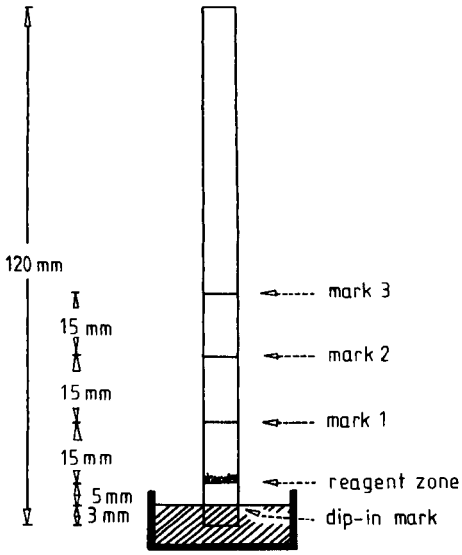

Fig. 1. Strip with a reagent zone.

the different volumes must be taken into account. In this way, 5—50 μg ml^{-1} mercury(II) have been estimated with cadmium sulphide as reagent, and 1—10 μg ml^{-1} nickel(II) with dimethylglyoxime as reagent.

Strip method with three different reagents

Three different reagents are placed on a strip of filter paper in a suitable way (as an alcoholic solution or a precipitate). The strip is dipped for a given time (e.g., 15 s) into a sample solution (in contrast to the above method). The three reagents form coloured products with the ion to be estimated. The time of dipping must be chosen so that the reagent remains in excess, otherwise one would always get the same colour intensity regardless of the concentration of the sample. After the strips have been dried, the intensities of the spots are compared with those of a standard scale, prepared in the same way (see Fig. 2). Thus 3—30 μg Ni^{2+} ml^{-1} can be estimated with dimethylglyoxime, rubeanic acid, and quinolin-8-ol/rubeanic acid and 5—50 μg Cu^{2+} ml^{-1} with rubeanic acid, zinc sulphide and $K_2Zn_3[Fe(CN)_6]_2$.

METHODS BASED ON COMPARISON OF TIME

Measurement of time is mostly applied in catalysed reactions for the determination of catalysts, inhibitors or reactivators. Usually the time is measured until a colour appears or disappears after sample and reagent solutions have been mixed. The measurement of time is sometimes replaced by a simultaneous comparison: standard and sample systems are started at the same moment and the standard selected is the one which reacts more or less

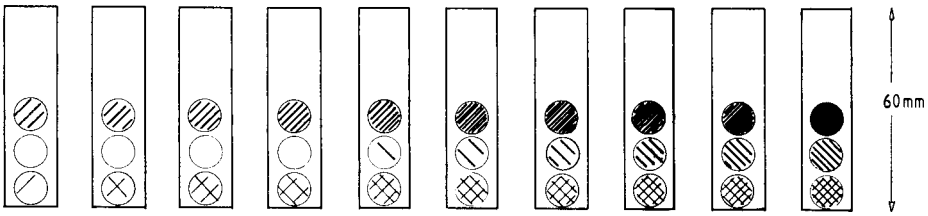

Fig. 2. Standard scale for strips with three reagents.

simultaneously with the sample. An advantage of such techniques is that there is no need to thermostat the solutions.

As a new example of the application of such a "dynamic standard scale", the following method illustrates the estimation of catalytically active substances.

A comparator with eight chambers

In a plexiglas vessel (40 × 70 × 40 mm), the solutions for a suitable indicator reaction are mixed; then seven partition walls are inserted in position to form eight chambers which contain identical volumes of reagent solutions. With the use of an 8-channel pipette (Titerpek, Flow Laboratories) providing simultaneous additions, 50 μl each of different standard solutions are added into seven of the chambers while the sample solution is introduced into the eighth chamber. The change in the colour intensities is observed. This is a simplified type of simultaneous comparison, because there is no need to prepare eight sets of reagent solutions separately. With this simple method, it is possible to complete an estimation within 5 min. Thus 10—100 μg Cu^{2+} ml^{-1} can be estimated by means of the iron(III) thiocyanate/thiosulphate indicator reaction, 10—100 μg Mn^{2+} ml^{-1} by means of the periodate/malachite green indicator reaction, 1—10 μg Co^{2+} ml^{-1} by means of the hydrogen peroxide/tiron indicator reaction, and 10—100 μg V ml^{-1} (as VO^{2+}) by means of the iodide/bromate indicator reaction in the presence of ascorbic acid.

METHODS BASED ON OTHER PRINCIPLES

Counting of portions

Counting the number of small portions of reagent which have to be added to a sample until a colour change appears can be used for semiquantitative determinations. These portions can be added either as solids, e.g. ion-exchanger beads loaded with a reagent, as portions of sodium hydroxide or peroxide [7], or as drops of solutions. The latter type of addition is reminiscent of Home's titrations with teaspoonfuls of an acid solution until effervescence from potassium carbonate ceased [8]. In the two methods described below, counting portions is again applied in a simple type of titration.

Titration with impregnated paper. A filter paper is impregnated with a known amount of EDTA. Portions (1 cm^2) are cut from the paper and added to a sample solution, containing a suitable indicator (eriochrome black T) and buffer until the colour changes. Thus, for example, the hardness of water can be estimated very quickly.

Titration on impregnated paper. A circle is drawn on a paper impregnated with a suitable reagent. To the centre of this circle, sample solution is added dropwise until the area within the circle has just changed colour. The necessary number of drops is counted and evaluated by using a standard graph. In this way, $1—50 \times 10^{-3}$ M hydrochloric acid can be estimated with methyl orange indicator, and $1—10\ \mu g\ Fe^{3+}\ ml^{-1}$ with $K_2Zn_3[Fe(CN)_6]_2$.

Dilution to the identification limit

As another principle for the semiquantitative determination of substances, the identification limit of a known reaction can be applied. Once the identification limit has been established, the sample can be diluted stepwise until just no positive reaction is observed. From the necessary dilution and the known identification limit, the concentration of a sample can be found [9, 10]. A modified application of this principle is described below.

Evaporation method. A number of standard solutions of the ion to be estimated is prepared. Into these standards and into the unknown solution itself, paper strips are introduced as shown in Fig. 3. The upper ends of these strips are impregnated with a suitable colour-forming reagent for the ion to be estimated. The required substance is thus concentrated. Depending on the concentration of the solution, coloured reaction products appear at various time intervals. The succession of colour change on the sample strip is compared with that of the standards, and so the sample concentration can be

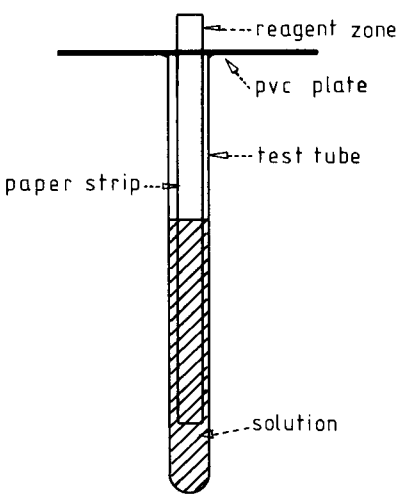

Fig. 3. Evaporation method.

found. For example, 50—500 ng Fe^{3+} ml^{-1} have been estimated with potassium hexacyanoferrate(II) and 2—20 μg Ni^{2+} ml^{-1} with dimethylglyoxime.

Measurement of area or length

The size of the area which results when a sample drop is placed on an impregnated filter paper is measured; either a coloured or a bleached spot may be visible. Logically, the size of the spot depends on the sample concentration. For many years, sample components have been estimated in paper chromatography by comparing the size of sample spots with spots of equally treated standard solutions. In the so-called "retention analysis", measurement of area was likewise used [11].

The measurement of length is just a special case of measurement of an area; it is applied if the sample (solution or gas) is passed through a reagent-loaded support (e.g., a narrow paper strip or a narrow glass tube filled with an impregnated support). The sample forms a coloured zone with the reagent. The length of this zone is a measure of the sample concentration, because the width and thickness of the paper strip, or the inner diameter of the glass tube are known. Well known examples of this technique are the Dräger—Röhrchen [12] for determining many gases in air.

Measurement of temperature or volume

The measurement of temperature is a simple and quick method applicable for semiquantitative determinations. The calorific effect depends on the concentration of the reactants. Thermistors can be used with only simple equipment.

Substances can also be estimated by measurement of volumes, not only of gases (e.g., from carbonates) but also of precipitates. The latter can be collected by sedimentation or centrifugation in a small graduated glass tube [13].

Conclusions

As stated above, there is no really well-defined borderline between semiquantitative and quantitative methods. If a relative standard deviation exceeding 0.2 serves as the definition [1], the new methods described above are not really semiquantitative, because their relative standard deviation is always less than 0.2. The "practical" error of the methods discussed is less than 10% in most examples. Because of their simplicity, they should nevertheless be called "semiquantitative". There are, of course, other principles to be found which have been or could be applied for such non-sophisticated methods in analytical chemistry.

REFERENCES

1 K. Danzer, E. Than and D. Molch, Analytik — Systematischer Überblick, Wissenschaftliche Verlagsgesellschaft, Stuttgart, 1977, pp. 237, 242.
2 H. Lepper, Dissertation, Freiburg, 1983.

3 F. Feigl, Tüpfelanalyse — Anorganischer Teil, 4. Aufl., Akademische Verlagsgesellschaft, Frankfurt am Main, 1960.
4 P. A. Kober, Ind. Eng. Chem., 10 (1918) 556.
5 H. Yagoda, Mikrochemie, 24 (1938) 117.
6 H. Weisz, Microanalysis by the Ring-Oven Technique, 2nd edn., Pergamon Press, Oxford, 1970.
7 B. Sansoni, Neue chemische Arbeitsmethoden durch heterogene Reaktionen, UNI-Druck, München, 1968.
8 F. Home, Experiments on Bleaching, 1756, cited in E. Rancke Madsen (Ed.), The Development of Titrimetric Analysis till 1806, G. E. C. Gad Publishers, Copenhagen, 1958.
9 M. Dennstedt, Ber. Dtsch. Chem. Ges., 44 (1911) 5.
10 P. E. Wenger, D. Monnier and Y. Rusconi, Helv. Chim. Acta, 29 (1946) 1698; 30 (1947) 1636; 31 (1948) 290; 32 (1949) 1865; Anal. Chim. Acta, 1 (1947) 190; Bull. Soc. Chim. Fr., 15 (1948) 517.
11 T. Wieland and L. Wirth, Angew. Chem., 62 (1950) 473; 63 (1951) 171.
12 Dräger; Prüfröhrchentaschenbuch, 5. Aufl., Drägerwerk AG, Lübeck, 1982.
13 A. Benedetti-Pichler, Introduction to Microtechniques of Inorganic Analysis, Douglaston, 1935, cited in I. P. Alimarin and M. N. Petrikova (Eds.), Anorganische Ultramikroanalyse, VEB Deutscher Verlag der Wissenschaften, Berlin, 1962, p. 60.

Analytica Chimica Acta, 172 (1985) 273—283
Elsevier Science Publishers B.V., Amsterdam — Printed in The Netherlands

SEMI-AUTOMATIC CATALYTIC TITRATION OF METAL ION MIXTURES AND ITS APPLICATION TO METALLURGICAL SAMPLES

T. RAYA SARO and D. PÉREZ-BENDITO*

Department of Analytical Chemistry, Faculty of Sciences, University of Córdoba, Córdoba (Spain)

(Received 20th November 1984)

SUMMARY

The semi-automatic catalytic titration of several metal ions and binary mixtures of iron(III) with copper(II), nickel or manganese(II) is described. The 4,4'-dihydroxybenzophenone thiosemicarbazone/hydrogen peroxide system was used in the presence of EDTA or EGTA as inhibitors with copper(II) as catalytic titrant. Two sample aliquots are necessary for the analysis of binary mixtures. In one, both metals are titrated in the presence of EDTA; in the other, only copper, nickel or manganese is titrated with EGTA or EDTA if a masking agent for iron(III) (triethanolamine or fluoride) is added. The iron/metal ratios tolerated range from 1:14 to 13:1 for the 0.2—3.0 μmol range, the relative standard deviation being 1—2%. The method was applied to metallurgical samples with good results.

The indirect titration of metal ions by catalytic end-point indication has been extensively discussed [1, 2] whilst the analysis of metal ion mixtures has received little attention. Although catalytic titrations can be simple, fast, sensitive and accurate, few applications have been reported. The present paper describes a semi-automatic method for the catalytic titration of metal ions and their mixtures with copper(II) as titrant; the oxidation of 4,4'-dihydroxybenzophenone thiosemicarbazone (DBPT) by hydrogen peroxide is used as the indicator reaction in the presence of an aminopolycarboxylic acid (EDTA or EGTA) as inhibitor. The semi-automatic catalytic titration of these ligands and metal ions such as copper(II), nickel and manganese(II) with this system was reported earlier [3]. In this work, cobalt(II), zinc(II), cadmium(II) and iron(III) are indirectly titrated in order to allow the resolution of binary mixtures with iron(III) by use of masking agents, in a similar way. Mixtures of copper, nickel and manganese with iron were selected because of their analytical interest. Only the catalytic titration of binary mixtures of mercury(II) with zinc, copper or cadmium, with cyanide for masking mercury, and of cobalt/nickel mixtures has been reported previously [4]. This method, which has found no practical application, was used for a narrower concentration ratio range of metal ions at a similar concentration level as the one proposed herein.

0003-2670/85/$03.30

The poor selectivity of the titration reactions previously used for this purpose may be responsible for their lack of application. The use of a masking agent for one component of the mixture permits the resolution of that component, although it is not easy to find a suitably selective masking agent. In this work the use of triethanolamine and sodium hydroxide or fluoride is proposed as a masking agent for iron. The method which is free from chromium, aluminium and iron interferences when EGTA is used, is applied to the analysis of several components of some metallurgical samples.

EXPERIMENTAL

Reagents

All solvents and reagents used were of analytical-reagent grade. 4,4'-Dihydroxybenzophenone thiosemicarbazone was synthesized by condensation of 4,4'-dihydroxybenzophenone with thiosemicarbazide [5]. A 0.1% (w/v) solution of the reagent in ethanol was used. A 1.0 g l^{-1} solution of copper(II) was standardized iodimetrically. Solutions of lower concentration were prepared by appropriate dilution. Standard solutions of EDTA and EGTA (0.1 M) were standardized potentiometrically [6]. The EDTA solution was prepared from the disodium salt dihydrate in distilled water. The EGTA solution was prepared in distilled water, adding sodium hydroxide to form the disodium salt. More dilute solutions (1×10^{-3} M) were prepared immediately before use. Standard solutions of nickel, manganese(II), cobalt(II), zinc, cadmium and iron(III) (1.0 g l^{-1}) were also prepared. The buffer solution (pH 10.2) was 0.45 M in ammonium chloride and 1.5 M in ammonia.

Apparatus

A block diagram of the apparatus for the semi-automatic catalytic photometric titration is presented in Fig. 1. A scanning phototitrator (Mettler DK-18) with a dual-channel detector and a continuous circular interference filter as monochromator, furnished with an immersion probe (Mettler DK-181) consisting of a double bundle of glass fibres, was used. The remain-

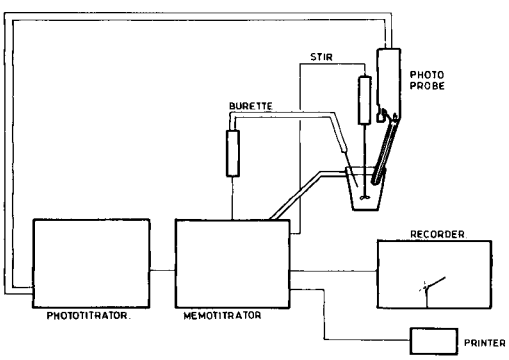

Fig. 1. Equipment for photometric titrations.

ing units of the titration equipment were as described earlier [7]. As shown in Fig. 1, the Memotitrator controls the whole system.

Procedures

General procedure for determination of metal ions by back-titration. To a solution containing between 0.2 and 3.0 μmol of an ion (Cu^{2+}, Ni^{2+}, Mn^{2+}, Co^{2+}, Zn^{2+}, Cd^{2+} or Fe^{3+}) in a 100-ml titration vessel, add 3.5 ml of 1×10^{-3} M EDTA (or EGTA, except for iron(III) samples), 1 ml of 0.1% (w/v) DBPT in ethanol, 5 ml of 0.36% (v/v) hydrogen peroxide, and 5 ml of pH 10.2 buffer solution and dilute to ca. 60 ml with distilled water. Stir for 5—10 s and start the titration with standard 25 μg ml^{-1} copper(II) solution at an addition rate of 6 ml min^{-1}. Previously, set the stirring speed at 120 rpm, the slow factor at position 1, the chart width at 10 mm ml^{-1} and the initial absorbance at 0.2 (200 mV). From the titration curve recorded (absorbance at 415 nm as a function of titrant volume), determine the end-point of the titration graphically from the intercept of the straight segments. The metal ion content is calculated by applying either of the methods indicated below.

Determination of the sum of iron(III) and another metal ion. Use the procedure above, but with an aliquot containing a total amount of metal of 0.2—3.0 μmol at an iron/metal molar ratio in the range 1:14—13:1, and add EDTA as inhibitor.

Determination of another metal ion in the presence of iron(III). Three experimental procedures are proposed. (1) To an aliquot containing 0.2—2.8 μmol of copper(II) or nickel and up to 2.6 μmol of iron(III), add 5 ml of 1.7×10^{-2} M triethanolamine and 1 ml of 0.1 M sodium hydroxide, and continue as in the general procedure from the stage of inhibitor addition (with EGTA).

(2) To an aliquot containing 0.2—2.8 μmol of copper(II), nickel or manganese(II) and up to 2.6 μmol of iron(III), add 10 ml of 12 g l^{-1} sodium fluoride solution and continue as in procedure 1 (using EGTA).

(3) To an aliquot containing 0.2—2.8 μmol of copper(II) or nickel and up to 2.6 μmol of iron(III), add 5 ml of 1.7×10^{-2} M triethanolamine and 2 ml of 0.1 M sodium hydroxide, and continue as in the general procedure from the stage of inhibitor addition (with EDTA).

The iron(III) concentration is calculated by difference.

Determination of copper in aluminium alloys. Place an accurately weighed amount of alloy (100 mg) and 5 ml of concentrated hydrochloric acid in a beaker. Warm the solution and add several drops of hydrogen peroxide to complete dissolution. Cool, and dilute to 100 ml with distilled water in a volumetric flask. Use 1-ml aliquots for the titration following the general procedure, with EGTA as inhibitor.

Determination of iron and nickel in steel. To an accurately weighed steel sample (ca. 50 mg) in a beaker, add 5 ml of concentrated hydrochloric acid, a few drops of concentrated nitric acid, and distilled water. Heat until dis-

solution is complete. Cool, transfer the solution to a 250-ml volumetric flask and dilute to the mark with distilled water. Use 2-ml aliquots for the determination of nickel (by procedure 2) and 0.8-ml aliquots for the determination of the sum of nickel and iron.

Determination of copper, nickel, iron and manganese in an aluminium alloy. Place an accurately weighed amount of alloy (ca. 500 mg) in a beaker, add 10 ml of 6 M hydrochloric acid and a few drops of concentrated nitric acid. Heat until dissolution is complete. Cool, and dilute to the mark with 6 M hydrochloric acid in a 50 ml volumetric flask. In order to separate copper and iron from the other metal ions, percolate the solution through a Dowex 1-X8 anion-exchange column (2 cm diameter, 10 cm high). Elute nickel, manganese and the other metal ions with 6 M hydrochloric acid (eluate 1), and elute iron and copper with distilled water (eluate 2). Evaporate both eluates down to ca. 5 ml and dilute each to volume with distilled water in 100-ml volumetric flasks. Dilute both solutions (1 + 9) with distilled water. Use 2.5-ml aliquots from the resulting solution of eluate 1 for the determination of the sum of nickel and manganese by the general procedure, with EGTA as inhibitor. Use similar aliquots for determining nickel alone, masking manganese as described in procedure 1 for masking iron. Use 5-ml aliquots from the resulting solution of eluate 2 solution for the determination of the sum of iron and copper by the procedure indicated above and similar aliquots for the determination of copper alone by applying any of the three procedures given above.

RESULTS AND DISCUSSION

Fundamentals

The semi-automatic catalytic titration of metal ions based on the copper(II)-catalyzed oxidation of the 4,4′-dihydroxybenzophenone thiosemicarbazone (DBPT) by hydrogen peroxide as the indicator reaction is done via an easy and fast back-titration. The sample containing a metal ion M^{n+} (e.g., Cu^{2+}, Ni^{2+}, Co^{2+}, Fe^{3+}) and a known excess of EDTA or EGTA (both inhibit the catalytic reaction) together with the ingredients of the indicator reaction, is titrated with a standard copper(II) solution. The inhibitor in excess of that needed to complex with the metal ion to be determined reacts with the titrant. Once all the free inhibitor has been complexed by copper, two types of reactions may occur when more copper is added. One is a displacement reaction, in which copper displaces the metal ion being determined from its EDTA or EGTA complex. The other is catalysis of the indicator reaction. The determination of the metal ion is only feasible in the absence of the displacement reaction. The titration end-point is marked by the initiation of the indicator reaction. The amount of metal ion present in the sample is then calculated by difference between the amount of inhibitor added and that not bound to the metal (determined by back-titration).

The method can be applied to the determination of several metal ions

without the need for them to form much stronger complexes with the inhibitor than the titrant. This is probably due to the high sensitivity of the indicator reaction and to the relatively slow displacement reaction between copper and the metal ion/EDTA (or EGTA) complex. Consequently, the amount of copper necessary to start the catalytic cycle is smaller than that required for making the substitution reaction feasible. However, those metal ions forming labile complexes with the inhibitor or giving rise to side-reactions with some reactants of the indicator system, or both, cannot be determined. This last effect is observed for mercury(II) and bismuth(III), which react with the substrate of the indicator reaction (DBPT).

Semi-automatic catalytic titration of individual metal ions

The shape of the catalytic titration curves and the sharpness of the endpoints were affected by the concentrations of copper, DBPT, ammonia and other chemical and instrumental variables. However, when all these factors are kept constant, the results obtained are reproducible. The optimum chemical and instrumental conditions were as selected earlier [3] and are described in the general procedure. Figure 2 shows the curves recorded at constant reaction conditions for different metal ion concentrations. Similar titration curves were obtained for all the metal ions tested.

For a constant amount of inhibiting ligand added to all the samples, the volume of titrant required decreased as the metal ion concentration increased. This provides the basis of three different methods. In the first (proportional method), the amount of unbound EDTA or EGTA is obtained numerically from a simple equivalence relation, and the amount of metal ion/EDTA (or EGTA) complex is found subsequently by difference between the concentration of ligand added and that back-titrated. In the second (numerical-graphical method), the metal content in the sample is also found by difference, but the amount of free inhibitor (which is back-titrated) is obtained from the EDTA (or EGTA) calibration graph obtained in the absence of metal ion. In the third (calibration graph method), the metal con-

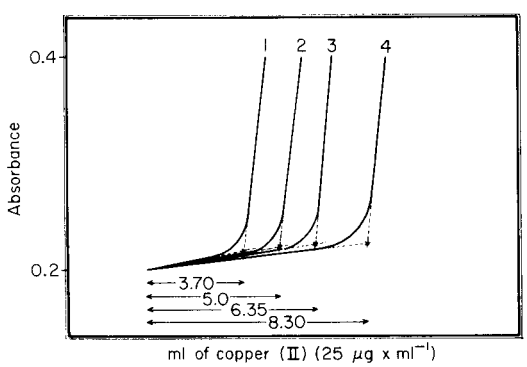

Fig. 2. Titration curves for different amounts of cobalt(II): (1) 2.0; (2) 1.5; (3) 1.0; (4) 0.2 μmol.

centration is obtained directly from a calibration graph by plotting end-point volumes against the amount of metal ion added.

The proportional method can be applied with satisfactory results only when the empirical end-points coincide with the equivalence points. This requires the inhibitor to react fully with both the titrant and the metal to be determined before the indicator reaction has started and for titration curves not to show pseudo-induction periods in the absence of inhibitor. The numerical-graphical method avoids errors resulting from the occurrence of a blank and from an incomplete titration reaction. However, the errors are magnified when the degree of dissociation of the complexes involved is different. The calibration graph method avoids all these errors and is therefore the most practical, although a calibration graph is needed for each metal ion to be determined.

Some of the results found for cobalt, cadmium, zinc and iron(III) in aqueous solutions of known concentration are shown in Table 1. The calibration graph method yields the best results in all the instances (average relative error less than 1%), although the precision is similar for the two methods and for the four cations tested (relative standard deviation of 1.0—1.5%). Analogous results were obtained for cobalt by using EGTA as inhibitor. Whilst it is advisable to use EDTA for the determination of zinc or cadmium, only EDTA is suitable in determining iron.

The equations for the calibration graphs obtained by the numerical graphical method for each metal ion with each inhibitor, as well as those corresponding to the inhibitors themselves, are shown in Table 2. The equations for copper, nickel and manganese are also included because these ions occur

TABLE 1

Semi-automatic catalytic titration of metal ions (Titrant, 25 μg ml^{-1} copper(II) solution; inhibitor, 3.5 ml of 1 × 10^{-3} M EDTA)

Metal ion	Added (μg)	Found (μg)[a]		Relative error (%)[b]	
		A	B	A	B
Cobalt(II)	11.60	12.13	11.62	4.56	0.17
	58.00	58.24	58.03	0.41 (±1.4)	0.05 (±1.4)
	139.20	138.80	139.07	−0.28	−0.09
Zinc(II)	12.85	13.45	12.81	4.66	−0.03
	64.25	65.82	64.32	2.44 (±1.3)	0.10 (±1.3)
	128.50	131.38	128.39	2.24	−0.08
Cadmium(II)	22.10	23.14	21.74	4.57	−1.62
	110.50	113.50	110.87	2.71 (±1.5)	0.33 (±1.5)
	265.20	269.98	265.23	1.80	0.01
Iron(III)	11.00	11.49	10.83	4.45	−1.54
	55.00	55.50	54.90	0.90 (±1.5)	−0.18 (±1.5)
	143.00	144.00	143.50	0.70	0.35

[a]Average of three separate determinations. A, Numerical-graphical method; B, calibration graph method. [b]With r.s.d. (%) for n = 11 in parentheses.

TABLE 2

Calibration equations for various metal ions and ligands (titrant, 25 μg ml^{-1} copper(II) solution)

Inhibitor[a]	Equations[b]	Linear range (μmol/60 ml)	r^2
EDTA	$V = 2.550[EDTA] - 0.10$	0.5—3.5	0.9999
	$V = -2.535[Cu^{2+}] + 8.80$	0.2—3.1	0.9997
	$V = -2.524[Ni^{2+}] + 8.82$	0.2—2.8	0.9999
	$V = -2.554[Mn^{2+}] + 8.79$	0.2—2.8	0.9996
	$V = -2.534[Co^{2+}] + 8.80$	0.2—2.4	0.9998
	$V = -2.602[Zn^{2+}] + 8.81$	0.2—2.0	0.9998
	$V = -2.585[Cd^{2+}] + 8.80$	0.2—2.8	0.9999
	$V = -2.549[Fe^{3+}] + 8.79$	0.2—2.6	0.9998
EGTA	$V = 2.549[EGTA] - 0.03$	0.5—3.5	0.9998
	$V = -2.541[Cu^{2+}] + 8.89$	0.2—2.8	0.9997
	$V = -2.518[Ni^{2+}] + 8.86$	0.2—2.8	0.9999
	$V = -2.543[Mn^{2+}] + 8.87$	0.2—2.8	0.9998
	$V = -2.534[Co^{2+}] + 8.90$	0.2—2.4	0.9994
	$V = -2.400[Zn^{2+}] + 8.86$	0.2—1.6	0.9999
	$V = -2.518[Cd^{2+}] + 8.89$	0.2—2.8	0.9999

[a] 3.5 μmol of inhibitor used for the determination of M^{n+} in all cases; [b] V is the volume of titrant at end-point (ml); $[M^{n+}]$ is given as μmol/60 ml.

in the metal mixtures examined. The slopes of the calibration graphs (i.e., the sensitivities) are roughly indicative of the degree of dissociation of the metal ion/inhibitor complexes.

The empirical limits of determination (X_2) are in agreement with those calculated from $X_L = \bar{X}_B + 10s_B$ where $\bar{X}_B$ represents the mean value of the signal corresponding to the blank (end-point volume of titrant for the inhibitor consumed in the absence of metal ion) and s_B is the standard deviation of X_B. Generally, X_L denotes the minimum analytical signal that can be measured but, because this is an indirect method, X_L should be interpreted as the closest analytical signal to $\bar{X}_B$ that can be distinguished. Eleven titrations with 3.5 μmol of EDTA (or EGTA) gave the following values: $\bar{X}_B$ = 8.795 ml and s_B = 0.048 ml for EDTA, and $\bar{X}_B$ = 8.895 ml and s_B = 0.051 ml for EGTA. These gave X_L values of 8.315 ml and 8.385 ml for EDTA and EGTA, respectively. The limit of determination of the metal ions can be found by substituting these values into the calibration equations in Table 2. The limits thus calculated are in the range 0.186—0.203 μmol of metal ion, which coincide with those obtained empirically (0.2 μmol).

Larger amounts than those indicated in Table 2 can be determined by using higher inhibitor concentrations or more concentrated copper(II) solution as titrant. However, insofar as the method does not allow the use of more dilute titrant solutions, <0.2 μmol of metal ion cannot be determined.

Selectivity. The influence of several anions on all the determinations described above is the same as that exerted on the direct titration of EDTA and

EGTA, for which results were reported earlier [3]. With regard to the influence of metal ions, it is obvious that all those forming stable complexes with the inhibitors must be absent, although it is worth noting the high levels of some common metals such as chromium, aluminium, magnesium and iron can be tolerated in some instances. Thus, chromium(III) can be tolerated in all the determinations at a molar ratio to the metal determined of about 50:1. Molar ratios of aluminium and magnesium of 100:1 and 10:1, respectively, can also be tolerated when EGTA is used as the inhibitor. When triethanolamine and sodium hydroxide are used, aluminium does not interfere with the determination of zinc, cadmium and copper by back-titration of an excess of EDTA. Cobalt cannot be determined in the presence of sodium hydroxide because of the precipitation of hydrated cobalt(III) oxide. Iron(III) and aluminium are also masked. The determination of nickel is subject to interferences under these conditions.

Semi-automatic catalytic titration of metal ions in mixtures

Only binary mixtures containing iron(III) with copper(II), nickel or manganese(II) were studied here, although the methods should be applicable to the other metal ions tested. Thus, the sum of iron(III) and a second metal ion is first determined in a sample aliquot by the proposed procedure, and iron(III) is masked and the other metal ion determined by any of the proposed procedures in another aliquot. The iron(III) concentration is found by difference. The volume of each aliquot taken depends on the molar ratio between the two metal ions in the sample.

Copper/iron mixtures. The sum of iron and copper can be determined over the range 0.2—3.0 μmol. The amount of iron in the aliquot taken should not exceed 2.6 μmol (to prevent precipitation of hydrated iron(III) oxide). Although the three methods of determination were used, the numerical-graphical procedure is advisable because the proportional method yields large errors and the calibration graph method is laborious.

Copper in the presence of iron can be determined in the range 0.2—2.8 μmol of copper by one of the three proposed procedures. The maximum iron(III) concentration in the aliquot depends on the procedure employed. An iron/copper molar ratio of up to 90:1, 25:1 and 35:1 can be tolerated in procedures 1, 2 and 3, respectively. Several synthetic samples containing iron and copper in different molar ratios (13:1—1:14) were analyzed. The results are shown in Table 3. The relative errors encountered were generally less than 2.5% and the relative standard deviation was about 1.5% in every case.

Nickel/iron mixtures. Samples containing iron and nickel in mole ratios from 13:1 to 1:14 were analyzed in a similar way to the copper/iron mixtures. Table 4 shows some of the results obtained with several synthetic samples. The maximum amount of iron(III) in the aliquot taken for the determination of nickel is 0.4, 0.3 and 0.4 mg when procedure 1, 2 or 3, respectively, is used. Consequently, mole ratios (Fe/Ni) of up to 35:1

TABLE 3

Analysis of synthetic copper/iron mixtures

Added (μmol)		Found (μmol)[a]						
Cu(II)	Fe(III)	(Cu + Fe)[b]	Cu[b]			Fe		
			1[c]	2	3	1	2	3
2.80	0.20	2.99	2.78	2.78	2.79	0.21	0.21	0.20
2.40	0.60	3.01	2.38	2.41	2.39	0.63	0.60	0.62
2.00	1.00	3.01	1.96	1.99	2.00	1.05	1.02	1.01
1.60	1.40	3.03	1.59	1.62	1.59	1.44	1.41	1.44
1.20	1.80	3.01	1.21	1.23	1.22	1.80	1.78	1.79
0.80	2.20	3.03	0.81	0.82	0.81	2.22	2.21	2.22
0.40	2.60	3.03	0.40	0.41	0.41	2.63	2.62	2.62
0.20	2.60	2.79	0.21	0.21	0.20	2.58	2.58	2.59

[a]Average of three separate determinations. [b]Numerical-graphical method. [c]Procedure number.

TABLE 4

Analysis of synthetic nickel/iron mixtures

Added (μmol)		Found (μmol)[a]						
Ni	Fe(III)	(Ni + Fe)[b]	Ni[b]			Fe		
			1[c]	2	3	1	2	3
2.80	0.20	2.96	2.73	2.75	2.78	0.23	0.21	0.17
2.40	0.60	3.00	2.39	2.39	2.36	0.61	0.61	0.63
2.00	1.00	2.98	1.99	1.99	1.97	0.98	0.99	1.01
1.50	1.50	3.00	1.47	1.46	1.47	1.52	1.54	1.53
1.20	1.80	2.98	1.18	1.20	1.19	1.80	1.78	1.78
0.80	2.20	3.00	0.80	0.78	0.79	2.20	2.21	2.20
0.40	2.60	3.02	0.40	0.40	0.40	2.61	2.61	2.61
0.20	2.60	2.80	0.20	0.21	0.21	2.60	2.59	2.59

[a–c]See Table 3.

(procedures 1 and 3) and 25:1 (procedure 2) can be determined by making appropriate volume corrections.

Manganese/iron mixtures. Manganese(II) is oxidized in a triethanolamine/sodium hydroxide medium to form a green manganese(III) complex, which is capable of oxidizing the reagent. Hence, this cation cannot be determined in the presence of iron by procedures 1 and 3. Table 5 shows some of the results obtained in the resolution of several mixtures of iron and manganese by procedure 2. Mole ratios (Fe/Mn) higher than 13:1 and lower than 25:1 can also be accommodated provided that the aliquot used for determining the sum of manganese and iron contains a total amount of these metals in the range 0.2—3.0 μmol, and that the aliquot taken for determining manganese contains manganese in the range 0.2—2.0 μmol.

TABLE 5

Analysis of synthetic manganese/iron mixtures

Added (μmol)		Found (μmol)[a]		
Mn(II)	Fe(III)	(Mn + Fe)[b]	Mn[b]	Fe
2.80	0.20	2.97	2.77	0.20
2.00	1.00	3.00	2.00	1.00
1.00	1.00	2.00[c]	1.00[d]	1.00[e]
0.60	2.40	2.97	0.61	2.36
0.40	2.60	3.00	0.41	2.59
0.20	2.60	2.80	0.20	2.60

[a]Average of three separate determinations. [b]Numerical-graphical method. [c–e]Relative standard deviations (n = 8): [c]0.75%; [d]1.7%; [e]1.5%.

TABLE 6

Analysis of metal samples

Sample		Composition (%)				Composition found[a] (%)			
		Fe	Cu	Ni	Mn	Fe	Cu	Ni	Mn
Al alloy	1[b]	—	4.90[c]	—	—	—	5.00 ± 0.02	—	—
	2[b]	—	4.54[c]	—	—	—	4.59 ± 0.02	—	—
	3[b]	—	4.33[c]	—	—	—	4.38 ± 0.02	—	—
Al alloy (B.A.S. 20 b)	4[d]	0.43[e]	4.10[e]	1.93[e]	0.19[e]	0.45 ± 0.04	4.10 ± 0.03	1.88 ± 0.03	0.17 ± 0.06
Stainless steel[f] (B.A.S. 69b)			—	9.35[e]	—	71.90 ± 0.10	—	9.30 ± 0.06	—

[a]Mean ± standard deviation for 8 determinations. [b]Supplied by Westinghouse S.A., also containing >90% Al, <0.2% Mg and 0.2% Ti. [c]By atomic absorption. [d]Also containing 0.29% Si and 1.61% Mg. [e]Certificate values. [f]Also containing 18.60% Cr.

Application to the analysis of steel and other alloys. In order to test the reliability of the proposed methods, they were applied to the determination of some metals in several samples of alloys and steel. Table 6 shows the results obtained, which were compared either with results found by atomic absorption spectrometry or with certificate values. These data demonstrate the reliability of the proposed methods for these types of samples.

Conclusions

The use of a catalyzed reaction for end-point indication in titrimetry provides rapid determinations of traces of a variety of metal ions, which may or may not catalyze the indicator system, over wide concentration and concentration-ratio ranges in metal ion mixtures, with accurate results. These are major advantages in contrast to kinetic methods based on counter-inhibition effects [8], although the latter generally result in more sensitive determinations. Compared with conventional titrimetric methods, catalytic titrations are suitable for determinations of small amounts of substances, generally at the μmol level.

This work, as part of Project No. 0248, was supported by a grant from the C.A.I.C.Y.T.

REFERENCES

1 H. A. Mottola, Talanta, 16 (1969) 1265.
2 T. P. Hadjiioannou, Rev. Anal. Chem., 3 (1976) 82.
3 T. Raya and D. Pérez-Bendito, Analyst (London), 108 (1983) 857.
4 E. A. Piperaki and T. P. Hadjiioannou, Chimica Chronica, 6 (1977) 375.
5 F. Toribio, J. M. Fernández, D. Pérez-Bendito and M. Valcárcel, Quim. Anal., I (1982) 21.
6 J. Veselý, D. Weiss and K. Štulík, Analysis with Ion-selective Electrode, Ellis Horwood, 1978, pp. 194.
7 A. Moreno, M. Silva, D. Pérez-Bendito and M. Valcárcel, Analyst (London), 109 (1984) 249.
8 T. Raya and D. Péres-Bendito, Mikrochim. Acta, 1 (1984) 467.

Analytica Chimica Acta, 172 (1985) 285—287
Elsevier Science Publishers B.V., Amsterdam — Printed in The Netherlands

Short Communication

DETERMINATION OF HYDROGEN PEROXIDE BY USE OF AN ANION-EXCHANGE RESIN MODIFIED WITH MANGANESE TETRAKIS (SULFOPHENYL) PORPHINE AS A MIMESIS OF PEROXIDASE

YUTAKA SAITO*, SUZUYO NAKASHIMA, MASAKI MIFUNE, JUNICHI ODO and YOSHIMASA TANAKA

Faculty of Pharmaceutical Sciences, Okayama University, Okayama (Japan)

MASAHIKO CHIKUMA

Chest Disease Research Institute, Kyoto University, Sakyo-ku, Kyoto (Japan)

HISASHI TANAKA

Faculty of Pharmaceutical Sciences, Kyoto University, Sakyo-ku, Kyoto (Japan)

(Received 4th January 1985)

Summary. The peroxidase-like activity of the modified resin is demonstrated in its use for the determination of hydrogen peroxide by means of the chromogenic reaction with 4-aminoantipyrine and phenol. The sensitivity achieved is 80% of that obtained with peroxidase; the r.s.d. is 1.1%, and the catalyst can be reused without deterioration for up to 10 assays.

In an attempt to develop new methods of analysis by mimesis of enzyme systems, the enzyme-like activity of an anion-exchange resin modified with metalloporphines has been studied. Recently, it was demonstrated that an anion-exchange resin was easily converted to a functional resin bearing catalase-like activity by modification with manganese tetrakis(sulfophenyl)-porphine (MnTPPS) [1]. This communication deals with the peroxidase-like activity of the modified resin and the applicability of the resin to the determination of hydrogen peroxide by its catalysis of the chromogenic reaction

$$\text{4-Aminoantipyrine} + \text{phenol} + 2\,H_2O_2 \rightarrow \text{quinone dye} + 4\,H_2O$$

In clinical analysis, glucose and cholesterol, for example, are routinely determined by measurement of the hydrogen peroxide produced by these substances in the presence of their oxidases by using peroxidase to catalyze this reaction [2, 3].

Experimental

Preparation of MnTPPS and the modified resin. For the preparation of aqueous MnTPPS solution, reagent-grade manganese(II) chloride (30 mg) was added to 10 ml of an aqueous solution containing 100 mg (1×10^{-4} mol) of H_2TPPS (Tokyo Kasei Ltd.) and the mixture was refluxed until the Soret

0003-2670/85/$03.30

band of H_2TPPS disappeared. The excess of manganese was removed by a cation-exchange resin (Amberlite IR-120B) from the resulting MnTPPS solution. The absorption spectrum of the solution obtained coincided with that of MnTPPS reported by Harriman and Porter [4]. Amberlite IRA-900 (4.0 g, 24—42 mesh, nitrate form) was added to a MnTPPS solution (200 ml, 1×10^{-4} mol) in a 1:1 mixture of acetone and water, and the mixture was shaken at 35° C until the supernatant liquid became colorless (ca. 6 h). The resin was filtered off, washed with water and acetone, and air-dried.

Peroxidase was purchased from Sigma Chemical Co.

The chromogenic reagent solution was a 1:1:3 (by volume) mixture of 4-aminoantipyrine (500 μg ml^{-1}), phenol (7.0 mg ml^{-1}) and pH 7.8 (0.05 M) borate buffer.

Procedure. The chromogenic reagent solution (5.0 ml) and the modified resin (50 mg) were added to a sample solution (1.0 ml) containing 10—40 μg of hydrogen peroxide, and the mixture was incubated at 35° C for 10 min. The absorbance of the supernatant liquid was measured at 505 nm against the reagent blank. The latter was negligible.

Results and discussion

Conditions for hydrogen peroxide determination. The reaction conditions described above gave satisfactory results. The amount of phenol necessary for the reaction was more than 10 times that of 4-aminoantipyrine, probably because the resin adsorbs some of the phenol. No elution of MnTPPS from the resin was detectable under these conditions.

Repeated use. The effect of repeated use of the resin on the absorbance from sample solutions which contained 20 μg of hydrogen peroxide was examined. As shown in Fig. 1, the absorbance becomes almost constant after the second use of the resin. The lower absorbance value on initial use may be caused by adsorption of the quinone dye onto the resin.

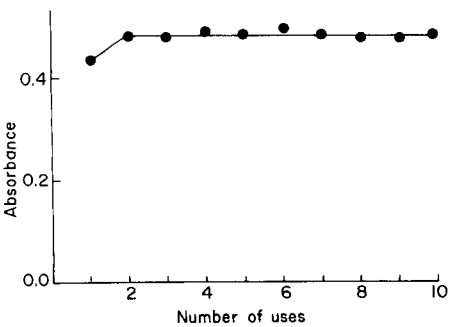

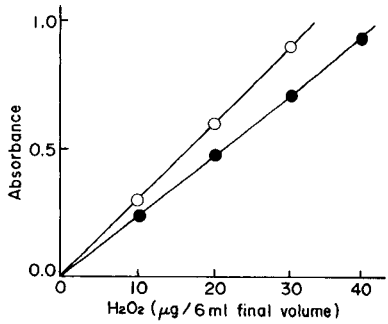

Fig. 1. Effect of repeated use with 20 μg of hydrogen peroxide.

Fig. 2. Calibration graphs obtained: (•) with the MnTTPS resin; (○) with peroxidase.

Calibration. A calibration graph obtained by the new procedure is shown in Fig. 2, together with that obtained by the use of peroxidase. Both are linear upto an absorbance of 1.0. The relative standard deviation was 1.1% for the determination of 40 μg of hydrogen peroxide (n = 6). The apparent molar absorptivity obtained with the MnTTPS resin was 4.8×10^3 l mol^{-1} cm^{-1} under the conditions described above, whilst that for the use of peroxidase was 6.0×10^3 l mol^{-1} cm^{-1}. This efficiency (ca. 80%) of the artificial material compared to peroxidase is remarkable.

Interferences. In the new procedure, the differences in the absorbance for 30 μg of hydrogen peroxide caused by the presence of 30 μg of K^+, NH_4^+, Ca^{2+}, Fe^{3+}, F^-, Br^-, I^-, CO_3^{2-}, PO_4^{3-}, EDTA, glycine or citric acid, or 1.5 mg of albumin or 30 μl of serum were less than 2.5%. The increase in absorbance caused by the presence of 30 μg of ascorbic acid was 12.7%, whereas it was negligible when the amount of ascorbic acid was less than 15 μg.

In conclusion, $MnTPPS_r$ can be regarded as an excellent mimesis of peroxidase, with some advantageous features, namely ease of preparation and high stability. The results indicate that the modified resin could probably be used to determine hydrogen peroxide in place of peroxidase or immobilized peroxidase in many routine clinical analyses.

REFERENCES

1 Y. Saito, M. Mifune, J. Odo, Y. Tanaka, M. Chikuma and H. Tanaka, Reactive Polymers, 2 (1984) in press.
2 P. Sharp, Clin. Chim. Acta, 40 (1972) 115.
3 C. C. Allain, L. S. Poon, C. G. S. Chan, W. Richmond and P. C. Fu, Clin. Chem., 20 (1974) 470.
4 A. Harriman and G. Porter, J. Chem. Soc, Faraday Trans. 1, 75 (1979) 1532.

Analytica Chimica Acta, 172 (1985) 289—290
Elsevier Science Publishers B.V., Amsterdam — Printed in The Netherlands

Short Communication

A REINVESTIGATION OF THE "DETERMINATION" OF URANIUM(VI) AND THORIUM(IV) WITH DITHIZONE

H. M. N. H. IRVING* and C. J. FOOT

Department of Analytical Science, University of Cape Town, Rondebosch 7700, Cape Province (South Africa)

(Received 26th November 1984)

Summary. It has not been possible to repeat any of the observations in a paper describing the determination of traces of uranium(VI) and thorium(IV) via coloured 1:2 complexes with dithizone.

Malik and Sharma [1] have described "a colorimetric determination of micro amounts of uranium(VI) and thorium(IV) with dithizone", for which they stated that pink and orange complexes with maximum absorbance at 480 and 500 nm, respectively, are formed in a monophase prepared from dithizone in 1 M ammonia (concentration of reagent unspecified) diluted (to an unspecified extent) with aqueous alcohol (1:1). It was further stated that in each case the existence of 1 (metal):2 (dithizone) complexes was shown by Job's method of continuous variations.

We have completely failed to repeat any of these observations which are so completely at variance with the substantial corpus of previous work [2]. With purified materials (i.e., analytical-grade reagents, redistilled water and ethanol, purified dithizone [2], isopiestic ammonia solution [3] and scrupulously cleaned glassware), the maximum absorbance of the yellow dithizonate ion in the monophase at pH 6.7—9.7 was at 470—475 nm and no change in absorption spectra occurred even when the concentration of added uranyl or thorium(IV) ions was made five times greater than that of the dithizone. The absence of any reaction was confirmed by running the spectra of the yellow dithizonate solution containing uranium (or thorium) ions in the sample cell against the same basic dithizone solution (appropriately diluted) in the reference cell. The difference spectra did not deviate from the baseline.

With these negative results, it is difficult to understand how Job's method of continuous variations could have been used or how the Beer—Lambert law was confirmed "up to a concentration of 5 ppm (uranium) or 3.5 ppm (thorium)"; at these concentrations, no coloured metal complexes whatsoever are formed. We have also confirmed the findings of previous workers [2] that neither thorium(IV) nor uranium(VI) can be extracted as dithizone complexes into carbon tetrachloride or chloroform. It is also

0003-2670/85/$03.30

interesting to note that the alleged 1:2 thorium complex would carry a double positive charge unless its coordination sphere was completed by appropriate anions.

Malik and Sharma [1] did not record the concentration of their dithizone solutions (although they gave λ_{max} = 460 nm and do not appear to have purified the dithizone or any other reagents) and they did not report on the molar absorptivities of the alleged uranyl and thorium complexes which gave the pink and orange complexes at 480 nm and 500 nm, respectively. It is possible that these colourations could have been due to samples of uranyl acetate and thorium chloride grossly contaminated by (different) metals.

Malik and Sharma's Table 1 deals with "the effect of diverse ions on the microdetermination of uranium(VI) and thorium(IV)". While copper(II) and cobalt(II) not unexpectedly interfered at all concentrations, the tolerance limits for zinc (20 mg l^{-1}) and thallium (150 mg l^{-1}) seem remarkably high for elements commonly determined as dithizonates [2]. What is at first sight surprising is that Be(II), Al(III), Ti(IV) are said to interfere at all concentrations and the tolerance for Mg, Ca, Ba and Ce(IV) is 50—100 mg l^{-1}. Yet none of these metals is known to react with dithizone. It is unfortunate that Malik and Sharma did not particularise the effects of these interfering ions. In the present experiments, hydrolysis at the pH used gave rise to broad absorbance changes or even turbidity. In view of the well-established complexing ability of fluoride towards uranium(VI) and thorium(IV), the statement [1] that "large excesses of fluoride (...) have no effect on the sensitivity" is surprising.

In aqueous 50% (v/v) ethanol, dithizone (pK_a = 5.60) has been reported [4] to give 1:1 complexes with all the lanthanons, with low stability constants ranging from $10^{1.40}$ (lanthanum) to $10^{2.30}$ (lutetium). Manku [4] stated that the formation of 1:2 complexes "which is accompanied by the precipitation of the metal was not observed". It would be interesting to know more about the composition and spectra of these lanthanon complexes and the possibility of using them in trace metal determinations.

REFERENCES

1 W. V. Malik and T. C. Sharma, Fresenius Z. Anal. Chem., 258(2) (1972) 124.
2 H. M. N. H. Irving, Dithizone, Analytical Science Monographs, No. 6, Chemical Society, London, 1977, and refs. therein.
3 H. M. N. H. Irving and J. J. Cox, Analyst (London), 83 (1958) 526.
4 G. C. S. Manku, J. Inorg. Nucl. Chem., 33 (1971) 3173.

Analytica Chimica Acta, 172 (1985) 291—296
Elsevier Science Publishers B.V., Amsterdam — Printed in The Netherlands

Short Communication

SPECTROPHOTOMETRIC DETERMINATION OF COPPER BY FLOW INJECTION ANALYSIS WITH AN ON-LINE REDUCTION COLUMN

AZAD T. FAIZULLAH and ALAN TOWNSHEND*
Chemistry Department, University of Hull, Hull HU6 7RX (Great Britain)
(Received 11th November 1984)

Summary. A silver reductor minicolumn is used in a flow-injection system for reduction of copper(II) to copper(I), which is detected spectrophotometrically using bathocuproine disulphonic acid. The reductor functions very well at flow rates up to 4 ml min^{-1}; this allows sample injection at rates up to 120 h^{-1}. Linear calibration is achieved for 5×10^{-7}—1×10^{-4} M copper. The detection limit is 3.4 ng and the midrange precision is 1%.

In a previous paper [1], the determination of iron(III) by flow injection analysis (f.i.a.) was described. A Jones reductor minicolumn in the flow system was used to reduce iron(III) to iron(II), which was measured spectrophotometrically with 1,10-phenanthroline. This provided a simple and reliable system which eliminated the need for addition of a soluble reductant. This communication describes a similar procedure in which copper(II) is reduced in a silver minicolumn to copper(I), which is determined spectrophotometrically with bathocuproine disulphonic acid (2,9-dimethyl-4,7-diphenyl-1,10-phenanthroline-3,8-disulphonic acid). Reduction of copper(II) by a silver reductor is quantitative under appropriate conditions [2].

In recent years, other flow-injection procedures have been developed for copper. These include atomic absorption spectrometry [3—6], potentiometry [7—9], chemiluminescence measurements [10] and u.v.-visible spectrophotometry based on various chromogenic reagents [11—14]. The present method is very simple and has high sensitivity, selectivity and reproducibility.

Experimental

All chemicals were of analytical-reagent grade, and deionized water was used throughout. A 0.25% solution of bathocuproine disulphonic acid, disodium salt (Koch-Light) was prepared by dissolving 0.625 g in 250 ml of water. This solution was prepared every 3 days. Acetate buffers of different pH values were prepared by mixing appropriate volumes of 0.2 M acetic acid and 0.2 M sodium acetate [15], and diluting to 100 ml with water. Citrate buffers were prepared as described previously [1]. Stock 0.100 M copper solutions were prepared by dissolving 4.2622 g of copper(II) chloride dihydrate (BDH) in 250 ml of 0.1 M hydrochloric acid. Other copper(II)

0003-2670/85/$03.30

standards were prepared by appropriate dilution. Hydrochloric or sulphuric acids used as carriers were prepared by dilution from their concentrated solutions (BDH).

Preparation of the silver reductor minicolumn. Silver for the reductor was prepared [16] by suspending a piece of electrolytic copper sheet (BDH), about 15 cm long and 10 cm wide, in 300 ml of 0.4 M silver nitrate. The reaction was allowed to proceed with continuous vigorous mechanical stirring until tests (with chloride or *p*-dimethylaminobenzalrhodanine in acidic media) showed the absence of silver ions in the solution. The precipitated silver was washed by decantation with dilute sulphuric acid until almost all of the copper was removed (tested with ammonia). About 15 g of silver was produced. Some of the silver was added slowly to a glass tube (3.0 cm long, 2.0 mm i.d.) until the required packing was achieved. An electronic vibrator (Pifco, 50 Hz) was used to settle the particles uniformly in the column. Water was passed through the column until no copper blank signal was obtained when used in the flow-injection system, and the reductor was stored in this condition until required for use.

Flow system. A flow injection system similar to that described previously [1] was used for the determination of copper. It was modified by incorporating a silver reductor minicolumn in place of the Jones reductor, and inserting some glass bead columns. The manifold is shown in Fig. 1, together with the optimal conditions and concentrations.

Copper(II) solutions were added by means of a Rheodyne RH-5020 injection valve (Anachem) with a 40-μl sample loop. A 4-channel peristaltic pump (Gilson Minipuls 2) was used to propel the solutions. Glass bead columns (2 cm long, 2 mm i.d.) filled with glass beads (0.25 mm diameter) were used to provide adequate mixing [17]. Figure 2 shows the consequence of utilizing such columns in the manifold. Teflon tubing (0.5 mm i.d.) was used for the rest of the manifold.

The complex formed between copper(I) and bathocuproine disulphonate was measured at 483 nm by using a Cecil CE-373 single-beam, linear readout spectrophotometer (provided with a 18-μl flow-through cell) connected to a Tekman Labwriter model TE200 recorder.

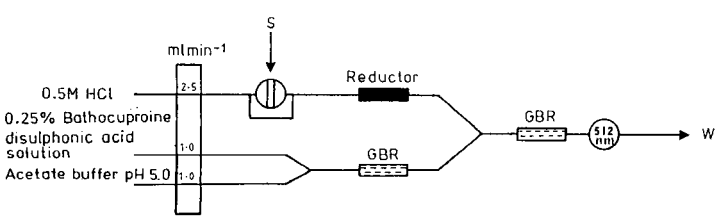

Fig. 1. Manifold used for the determination of copper: (S) sample injected; (GBR) column containing glass beads, (W) waste.

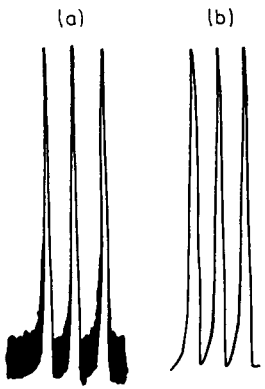

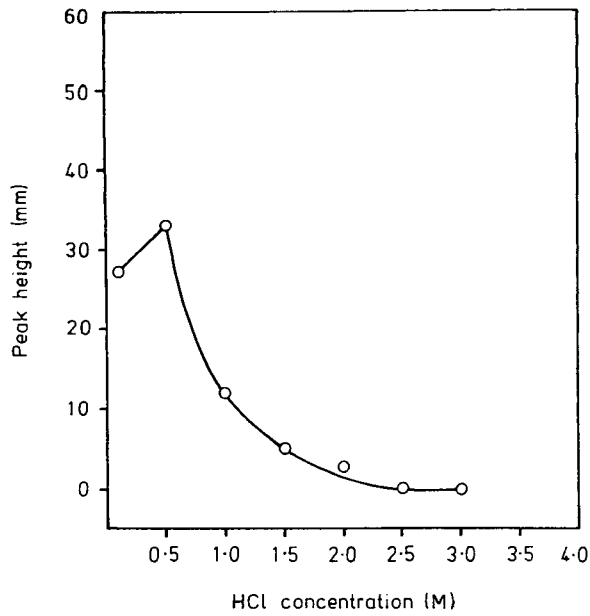

Fig. 2. Effect of using columns containing glass beads on the signals obtained from 1×10^{-5} M copper: (a) without columns; (b) with columns.

Fig. 3. Effect of hydrochloric acid concentration on the peak height from 2.5×10^{-5} M copper.

Results and discussion

Optimization of conditions. When a silver reductor column is used for reduction of copper(II), hydrochloric acid at concentrations up to 1 or 2 M is essential for quantitative reduction [2, 16, 19]. The electrode potential varies with the chloride concentration, therefore the concentration of hydrochloric acid is more critical than with the zinc reductor [1]. The effects of different hydrochloric acid concentrations on the copper peak height were therefore investigated. The results (Fig. 3) show an increase in peak height as the hydrochloric acid concentration increases from 0.1 to 0.5 M and then a decrease to 2.5 M hydrochloric acid. For copper, a high chloride concentration favours formation of soluble $CuCl_2^-$ ($\beta_2 = 6.5 \times 10^{-7}$ M) rather than insoluble CuCl, which is produced at lower chloride concentrations. Therefore, low hydrochloric acid concentrations favour the formation of copper(I) chloride, which deposits on the silver particles, leading to small signals. Hydrochloric acid at >0.5 M gives greater production of $CuCl_2^-$ [2], but the peak heights obtained are smaller because the high acidity decreases the extent of the chromogenic reaction between copper(I) and bathocuproine disulphonic acid. Therefore 0.5 M hydrochloric acid was chosen as optimal for this system. Almost no response was obtained when

0.01—2 M sulphuric acid was used in place of hydrochloric acid, probably because the copper(I) produced deposits on the column, being unable to form a soluble complex under these conditions.

The copper/bathocuproine disulphonate complex is reported to show constant absorbance at 483 nm between pH 4 and 8 [19, 20], therefore acetate and citrate buffers (of pH 3—6) were examined for their suitability. Both buffers gave similar results, and the peak heights were the same over the pH range examined. Therefore, as citrate buffer did not seem to have any advantage, acetate buffer, pH 5.0, was used in all further experiments.

The effect of flow rate was studied for a reductor column 3 cm long and 2 mm i.d. Figure 4 shows that the minicolumn performs efficiently even at high flow rates (4 ml min^{-1}), unlike the Jones reductor, which required a low flow rate (1 ml min^{-1}) for greatest sensitivity [1]. Thus, rapid flow can be used, greatly decreasing the time needed for one analysis, and increasing sample throughput. For example, at 1.5 ml min^{-1} through the reductor, analysis of 60 samples h^{-1} is possible compared with 120 samples h^{-1} at 2.5 ml min^{-1}. The effect of different concentrations of bathocuproine disulphonic acid solutions was investigated for two copper concentrations. Figure 5 shows that a significant increase in absorbance is obtained up to 0.25% reagent, which was used in subsequent experiments.

Interferences. There are few metal ion interferences when copper is determined by using bathocuproine disulphonic acid in conventional spectrophotometry [19]. For the flow-injection procedure, two groups of metal ions were tested for possible interfering effects; they were those metal ions in a higher oxidation state (Fe^{3+}, Cr^{3+}, V(V), Mo(VI)) which might be reduced by the reductor, and those metals normally present in copper samples (Co^{2+}, Zn^{2+}, Ni^{2+}, Pb^{2+}, Hg^{2+}). For each potential interferent, a series of solutions was prepared that contained a fixed concentration of

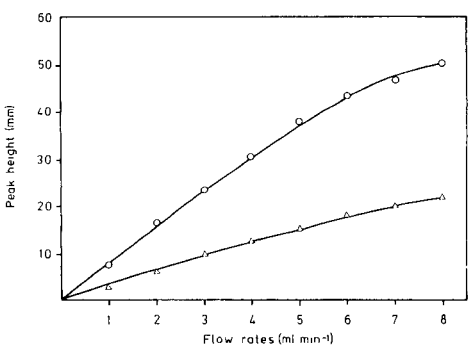

Fig. 4. Effect of flow rates on the peak height from: (△) 2 × 10^{-5} M; (○) 4 × 10^{-5} M copper (0.15% bathocuproine disulphonic acid).

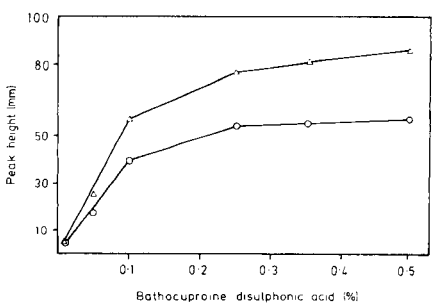

Fig. 5. Effect of bathocuproine disulphonic acid concentration on the peak height from: (○) 5 × 10^{-5} M; (△) 8 × 10^{-5} M copper.

copper(II) (6×10^{-5} M) and different concentrations (1—150 mg ml^{-1}) of the other ions. None of these ions interfered at any concentration up to 150 mg ml^{-1}.

Calibration. Typical calibration peaks for copper obtained under the optimized conditions are shown in Fig. 6. The linear relation between peak height absorbance and copper concentration is expressed by the least-squares equation $A = -6.65 \times 10^{-4} + 3190$ [Cu] where the copper concentration is in mol l^{-1} ($r = 0.9999$, 5 points). The graph was linear up to 1×10^{-4} M. The limit of detection (2× noise) was 5×10^{-7} M (3.4 ng). The precision of 12 replicate injections of 6×10^{-5} M copper was 0.83%. Sample injection rates of 120 h^{-1} were achievable when a flow rate of 2.5 ml min^{-1} was used through the reductor.

Conclusion

The use of standard flow-injection systems as a means of modifying classical assays has been remarkably successful. Reduction of copper by a silver column is efficient and reproducible, and its use with bathocuproine disulphonic acid provides an effective means of determining copper with great selectivity and sensitivity. The use of the reductor minicolumn eliminates the need for use of a soluble reductant.

Azad T. Faizullah is grateful to the University of Salahaddin, Iraq, for a scholarship.

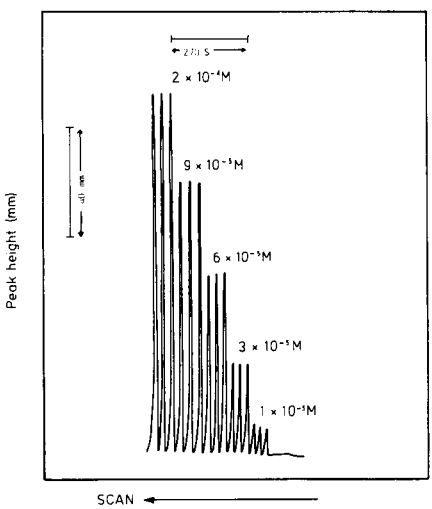

Fig. 6. Peaks obtained by injecting triplicate copper(II) standards at the concentrations shown, using the manifold in Fig. 1. (sampling rate 120 h^{-1}).

REFERENCES

1 A. T. Faizullah and A. Townshend, Anal. Chim. Acta, 167 (1985) 225.
2 N. Birnbaum and S. M. Edmonds, Ind. Eng. Chem., Anal. Ed., 12 (1940) 155.
3 W. R. Wolf and K. K. Stewart, Anal. Chem., 51 (1979) 1201.
4 L. Nord and B. Karlberg, Anal. Chim. Acta, 125 (1981) 129.
5 B. F. Rocks, R. A. Sherwood, L. M. Bayford and C. Riley, Ann. Clin. Biochem., 19 (1982) 338.
6 F. Fukamachi and N. Ishibashi, Anal. Chim. Acta, 119 (1980) 383.
7 W. E. van der Linden and R. Oostervink, Anal. Chim. Acta, 101 (1978) 419.
8 A. Hu, R. E. Dessy and A. Graneli, Anal. Chem., 55 (1983) 320.
9 T. E. Hu, Diss. Abstr. Int. B., 42 (1981) 1874.
10 M. Yamada and S. Suzuki, Chem. Lett., 11 (1982) 1747.
11 S. Baban, Anal. Proc., 17 (1980) 535.
12 R. Kuroda and T. Mochizuki, Talanta, 28 (1981) 389.
13 D. Betteridge, E. L. Dagless, B. Fields and N. F. Graves, Analyst (London), 103 (1978) 897.
14 D. Betteridge, E. L. Dagless, B. Fields, P. Sweet and D. R. Deans, Anal. Proc., 18 (1981) 20.
15 D. D. Perrin and B. Dempsey, Buffers for pH and Metal Ion Control, Chapman and Hall, London, 1974, p. 134.
16 H. Walden, L. P. Hammett and S. M. Edmonds, J. Am. Chem. Soc., 56 (1934) 350.
17 R. C. Schothorst, M. van Son and G. den Boef, Anal. Chim. Acta, 162 (1984) 1.
18 S. M. Edmonds and N. Birnbaum, Ind. Eng. Chem., 12 (1940) 60.
19 Z. Marczenko, Spectrophotometric Determination of Elements, Horwood, Chichester, 1976, p. 245.
20 D. Blair and H. Diehl, Talanta, 7 (1961) 163.

Analytica Chimica Acta, 172 (1985) 297—302
Elsevier Science Publishers B.V., Amsterdam — Printed in The Netherlands

Short Communication

SPECTROPHOTOMETRIC DETERMINATION OF FLUORIDE WITH LANTHANUM/ALIZARIN COMPLEXONE BY FLOW INJECTION ANALYSIS

H. WADA*, H. MORI and G. NAKAGAWA

Laboratory of Analytical Chemistry, Nagoya Institute of Technology, Showa-ku, Nagoya (Japan)

(Received 10th August 1984)

Summary. Lanthanum/alizarin complexone (1:1) in 70% acetone is used in conjunction with a 500-cm reaction coil at 60°C to determine 0.03—1.2 mg l^{-1} fluoride at 24 samples per h. The method is applied to tap-water samples.

The fluoride ion-selective electrode has been widely used for monitoring fluoride, but its application in flow-injection systems is limited because of its memory effect [1, 2]. Recently, Van Oort and Van Eerd [3] obtained a fast response from a fluoride ion-selective electrode in a flow injection system by using a mixture of methanol and total ionic-strength adjusting buffer containing 10^{-6} M fluoride in the carrier and by polishing the electrode surface with fine wet alumina powder. However, no application to real samples was presented.

The spectrophotometric determination of fluoride with cerium or lanthanum/alizarin complexone (La-AC) [4] is well known. The sensitivity is very high, but the rate of reaction between La/AC and fluoride is slow, and the reagent blank is relatively large. Therefore, experimental conditions such as pH, acetone concentration and standing time are critical.

This communication describes a spectrophotometric method for fluoride with La/AC by flow injection analysis (f.i.a.). By heating at 60°C the drawback of the slow reaction can be overcome, and about 24 samples (0.03—1.2 mg l^{-1}) can be determined in 1 h.

Experimental

Reagents. A standard solution of fluoride was prepared from analytical-grade sodium fluoride. The chromogenic reagent solution was prepared from 0.52 g of Dotite Alfusone (2.5% La/AC (1:1), hexamethylenetetramine and potassium phthalate, pH 5.1—5.3; Dojindo Laboratories, Kumamoto) dissolved in 20 ml of redistilled water, to which 70 ml of acetone was added and the solution was diluted to 100 ml with redistilled water. This solution was freshly prepared every 3 h. All water used was redistilled in a hard glass

0003-2670/85/$03.30

vessel, and was boiled to deaerate just before use. All other chemicals used were of analytical grade.

Apparatus. A diagram of the flow-injection manifold is shown in Fig. 1. The chromogenic reagent solution (protected from light) and redistilled water were each delivered at 0.40 ml min^{-1} with a double-plunger reciprocal pump (Kyowa Seimitsu Model KHU-W-52, Tokyo). The sample was injected into the water stream by using a rotary valve (Oyo—Bunko Kiki, Tokyo) to which a sample loop of appropriate volume was attached. Sample and reagent solutions were mixed in a 500-cm coil fixed in a water bath thermostatted at 60°C. A flow-cell (10 mm light path, 8 μl) situated in a Jasco Uvidec 100 II-W spectrophotometer (Japan Spectroscopic, Tokyo), and a chart recorder (Yokokawa, Tokyo) were used. A back-pressure coil (0.25 mm i.d., 100 cm long) was attached to the outlet of the flow cell.

Recommended procedure. Aliquots of sample solution containing 0.03—1.2 mg l^{-1} fluoride were injected into the carrier stream at 2.5-min intervals. The peak-height absorbance at 620 nm was measured in each instance.

Results and discussion

Optimal reaction conditions. Several chromogenic reagents, La/AC (1:1), i.e., Alfusone, described above [5], La-AC (2:1) [6, 7] and Ce/AC (1:1) [8] were examined in aqueous and aqueous acetone solutions by a batch method. Alfusone in 40% acetone solution gave the best sensitivity and calibration linearity. Dotite Alfusone is also recommended because of the simple preparation of the reagent solution.

When acetone was added to be 40% in both the reagent and carrier solutions, large ghost peaks were observed. When it was added only to the reagent solution to give 70% acetone, the ghost peaks disappeared. A 2.5×10^{-4} M Alfusone solution in 70% acetone was found to be most suitable as the chromogenic reagent. More concentrated Alfusone in more than 70% acetone solution formed precipitates. If a more dilute Alfusone solution was used, the calibration graph curved at >0.8 mg l^{-1} fluoride. The reagent gradually decomposed, but the peak heights were almost constant for a reagent prepared within 3 h, if the reagent was protected from light. Because the Alfusone

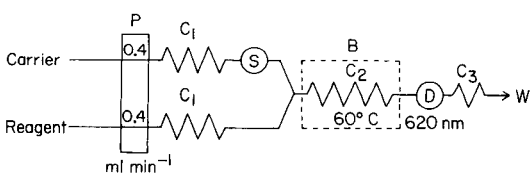

Fig. 1. Manifold for fluoride determination: P, pump with flow rate in ml min^{-1}; S, sample injector with a 40-μl loop; C_1, damping coils (1 mm i.d., 500 cm long); C_2, reaction coil (0.5 mm i.d., 500 cm long); B, water bath at 60°C; D, spectrophotometer with flow cell (12.5 mm peak height ≡ 0.01 absorbance); C_3, back-pressure coil (0.25 mm i.d., 100 cm long); W, waste.

solution is stable for several days in the dark and in a cool place, unless it contains acetone, an attempt was made to mix acetone with Alfusone solution in coil C_1, but mixing was incomplete. Therefore, the reagent solution was freshly prepared every 3 h. Under such conditions, the relative standard deviation for the determination of 0.8 mg l^{-1} fluoride was 1.12% (n = 72). For accurate work, it is recommended that a standard solution of fluoride is injected every ten sample injections.

Heating accelerated the reaction and, as described by Hashitani et al. [5], the absorbance was decreased by heating at 70° C. The effect of reaction temperature was examined by a batch method (Fig. 2). The absorbance increased with an increase in temperature. In the flow-injection system, the reaction coil was heated at 60° C, because the reproducibility was better than that at 70° C. The length of the reaction coil was varied between 3 and 7 m. When the 7-m coil was used, the peak height was the largest, but a 5-m coil was preferred because of the better reproducibility. The flow rate was varied between 0.25 and 0.50 ml min^{-1}. At 0.25 and 0.50 ml min^{-1} for each line, the reproducibility was less than at intermediate values, although the peak height increased with decreasing flow rates. For a reasonable sampling rate, 0.40 ml min^{-1} is recommended.

Calibration graphs are shown in Fig. 3; they illustrate the effects of sample volume and the deterioration of the chromogenic reagent solution. When a

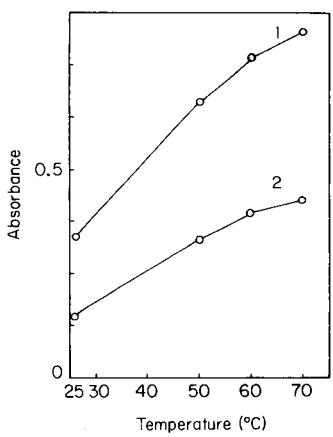

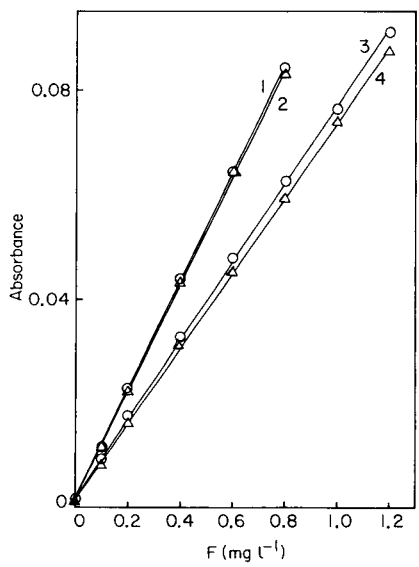

Fig. 2. Effect of temperature on peak heights for different fluoride concentrations: (1) 0.8; (2) 0.4 mg l^{-1}.

Fig. 3. Calibration graphs for different sample volumes: (1, 2) 60 µl; (3, 4) 40 µl. Time after preparation of the chromogenic reagent solution: (1) 30; (2) 90; (3) 40; (4) 210 min.

60-μl sample was injected, the reproducibility was inferior to that with a 40-μl sample. The injection interval was fixed at 2.5 min because it gave good reproducibility for any sample concentration tested.

The maximum tolerable amounts of diverse ions were established. They are given in Table 1. Only aluminum seriously interfered with this method, as well as with the batch method [5, 6].

Applications to potable water. Fluoride in tap waters was determined by a standard addition method. Aliquots of a 10 mg ml^{-1} fluoride solution (0.5 ml for 0.2 mg l^{-1} fluoride and 1.0 ml for 0.4 mg l^{-1} fluoride) were added to a 25-ml volumetric flask and the water sample was added to the mark. The peaks obtained are shown in Fig. 4 together with calibration standards. The results for some tap waters are given in Table 2.

TABLE 1

Effect of diverse ions on the determination of 0.40 mg l^{-1} fluoride

Ion	Added as	Concentration		F^- found (mg l^{-1})
		(M)	(mg l^{-1})	
Cl^-	NaCl	4.0×10^{-3}	142	0.39
		1.0×10^{-2}	355	0.36
NO_3^-	$NaNO_3$	5.0×10^{-3}	310	0.38
		1.0×10^{-2}	620	0.37
NO_2^-	$NaNO_2$	2.5×10^{-3}	115	0.39
		1.0×10^{-2}	460	0.37
ClO_4^-	$NaClO_4$	2.1×10^{-3}	209	0.39
		2.1×10^{-2}	2090	0.34
SO_4^{2-}	Na_2SO_4	1.2×10^{-2}	1150	0.40
		2.4×10^{-2}	2310	0.42
SO_3^{2-}	Na_2SO_3	1.6×10^{-3}	128	0.41
		2.0×10^{-3}	256	0.42
SiO_3^{2-}	Na_2SiO_3	8.0×10^{-4}	61	0.39
		2.0×10^{-3}	152	0.36
BO_3^{3-}	H_3BO_3	2.0×10^{-3}	54	0.40
		2.0×10^{-2}	536	0.39
PO_4^{3-}	NaH_2PO_4	1.0×10^{-5}	0.95	0.39
		1.2×10^{-4}	11.4	0.25
Fe^{3+}	$NH_4Fe(SO_4)_2 \cdot 12H_2O$	2.1×10^{-5}	1.17	0.40
		1.0×10^{-4}	5.58	0.50
Al^{3+}	$K_2Al_2(SO_4)_4 \cdot 24H_2O$	2.0×10^{-6}	0.05	0.40
		1.0×10^{-5}	0.27	0.28[a]
Ca^{2+}	$CaCl_2$	4.0×10^{-5}	1.60	0.39
		4.0×10^{-4}	16.0	0.34
Mg^{2+}	$MgCl_2$	1.0×10^{-4}	2.43	0.39
		1.0×10^{-3}	24.3	0.35

[a]The interference of Al^{3+} increased quickly; with 0.14 and 0.24 mg l^{-1} Al^{3+}, the fluoride concentrations found were 0.37 and 0.35 mg l^{-1}, respectively.

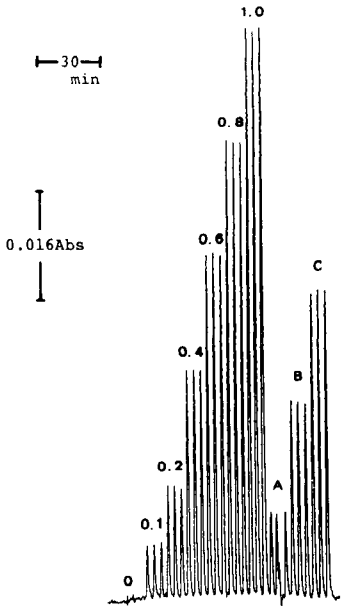

Fig. 4. Responses obtained with fluoride standards and tap water 1 (see Table 2). The numbers on the peaks correspond to mg l^{-1} fluoride. (A) Sample; (B) sample + 0.2 mg l^{-1} fluoride; (C) sample + 0.4 mg l^{-1} fluoride.

TABLE 2

Determination of fluoride in tap waters

Sample	Fluoride conc. (mg l^{-1})		Sample	Fluoride conc. (mg l^{-1})	
	Added	Found		Added	Found
Tap water 1	0.00	0.15	Tap water 3	0.00	0.04
	0.20	0.35		0.20	0.24
	0.40	0.55		0.40	0.44
Tap water 2	0.00	0.08		0.60	0.635
	0.20	0.28			
	0.40	0.47			

The authors acknowledge a Grant-in-Aid for Scientific Research (No. 59540364) from the Ministry of Education, Science and Culture, Japan.

REFERENCES

1 J. Slanina, W. A. Lingerak and F. B. Bakker, Anal. Chim. Acta, 177 (1980) 91.
2 M. Trojanowicz and W. Matuszewski, Anal. Chim. Acta, 138 (1982) 71.
3 W. J. Van Oort and E. J. J. M. Van Eerd, Anal. Chim. Acta, 155 (1983) 21.
4 See, e.g., R. Belcher and T. S. West, Talanta, 8 (1961) 853, 863.

5 H. Hashitani, H. Yoshida and H. Muto, Bunseki Kagaku (Japan Analyst), 16 (1967) 44.
6 R. Greenhalgh and J. P. Riley, Anal. Chim. Acta, 25 (1961) 179.
7 H. Hashitani and H. Muto, Bunseki Kagaku (Japan Analyst), 14 (1965) 1114.
8 S. S. Yamamura, M. A. Wade and J. H. Sikes, Anal. Chem., 34 (1962) 1308.

Analytica Chimica Acta, 172 (1985) 303—306
Elsevier Science Publishers B.V., Amsterdam — Printed in The Netherlands

Short Communication

SPECTROPHOTOMETRIC DETERMINATION OF COBALT(II) BASED ON THE ION-PAIR OF TETRATHIOCYANATOCOBALTATE(II) WITH NEOTETRAZOLIUM CHLORIDE

A. K. SINGH*, D. KUMAR and M. KATYAL[a]
Department of Chemistry, Indian Institute of Technology, New Delhi 110 016 (India)
(Received 26th July 1984)

Summary. The ion-pair formed between tetrathiocyanatocobaltate(II) and [3,3'-(4,4'-biphenylene)bis(2,5-diphenyl)]-2H-tetrazolium chloride (neotetrazolium chloride) can be extracted into 4-methylpentan-2-one and used for the spectrophotometric determination of cobalt (2.5—9.8 μg ml^{-1}) at pH 3.5—5.0. The Sandell sensitivity of the method is 0.02 μg Co cm^{-2}. With suitable masking, the method is quite selective and is applicable to nickel wire alloys.

Thiocyanate is commonly used as a spectrophotometric reagent for cobalt [1—3]. Tetrathiocyanatocobaltate(II) and its ion-pairs with various large cations have been used to determine the metal [2, 3], but Sandell sensitivities less than 0.04 μg cm^{-2} (for 0.001 absorbance) are rare. In a study of tetrazolium salts, it was observed that the ion-pair formed between neotetrazolium chloride (NTC) and $[Co(SCN)_4]^{2-}$ absorbs strongly in 4-methylpentan-2-one, providing a sensitive procedure for cobalt. The ion-pair formed with malachite green in carbon tetrachloride/cyclohexanone provides a greater absorptivity [4] but the coloured complex is not very stable.

An aqueous solution of tetrathiocyanatocobaltate(II) on mixing with NTC solution forms a greenish-blue precipitate which can be extracted into organic solvents. The absorbance of this ion-pair is greatest in cyclohexane ($\epsilon = 6.4 \times 10^4$ mol^{-1} cm^{-1}) but the colour is unstable. In 4-methylpentan-2-one (MIBK), the absorbance remains stable for about 12 h, thus MIBK was chosen for extraction. The tolerance to other anions is improved in this system compared to other thiocyanate systems for cobalt. Thus this spectrophotometric method provides reasonable selectivity as well as sensitivity.

Experimental

Apparatus. Unicam SP-500 and SP-700 spectrophotometers and an Elico pH meter model LI-10 were used.

Reagents. A stock solution (0.01 M) of cobalt(II) was prepared by dissolv-

[a]Present address: St. Stephens College, Delhi 110007, India.

0003-2670/85/$03.30

ing cobalt(II) sulphate heptahydrate (BDH Chemicals) in doubly distilled water; it was standardized by titration with EDTA before use. The solution (0.4% w/v) of NTC (Aldrich Chemical Co.) was prepared in 50% (v/v) ethanol. Acetate buffers (pH 3—6) were used for pH adjustment. Ammonium thiocyanate solution (10% w/v) was prepared in doubly distilled water. All solutions, including those for the interference study, were prepared by dissolving analytical-grade chemicals in doubly distilled water.

Recommended procedure. To a suitable aliquot (2—3 ml) containing 20—70 μg of cobalt, add acetate buffer (pH 4.5), 4 ml of the thiocyanate solution and 4 ml of the NTC solution. Then add 2 ml of water and 5 ml of dimethylformamide to dissolve the precipitate. Extract the complex with 7 ml of MIBK and measure the absorbance of the organic layer after centrifugation at 620 nm against a water blank. Calculate the metal content from a calibration graph prepared from data obtained with standard solutions.

Results and discussion

The ion-pair absorbs maximally at 620 nm. The absorbance remains constant and maximal in pH range 3.5—5.0. Variations in pH do not affect the wavelength of maximum absorbance of the complex. The reagent blank does not absorb at 620 nm.

For 1 ml of 1 mM cobalt(II) solution, maximum absorbance is attained in the presence of $\geqslant$3.7 ml of NTC solution (0.4%). At least 3 ml of 10% thiocyanate solution is needed for full colour development. Excess of either reagent does not affect the absorbance. Samples up to 10 ml in volume (containing 20—70 μg of cobalt) can be successfully treated by the recommended procedure if the concentration of dimethylformamide (DMF) in the aqueous phase is maintained around 30%. At least 4.5 ml of DMF must be added in the determination of 1 ml of 1 mM cobalt(II) (with a final volume of aqueous phase around 20 ml); up to 8 ml does not have any effect but more than that makes the extraction erratic because of slow and irreproducible phase separation. The colour in the extract is stable for 12 h.

Characteristics of the complex. Beer's law is obeyed up to 13 μg ml^{-1} of cobalt in the extract at pH 4.5. The optimum concentration, evaluated by a Ringbom plot, is 2.5—9.8 μg ml^{-1}. The Sandell sensitivity is 0.02 μg Co cm^{-2}. The molar absorptivity is 3.0×10^3 l mol^{-1} cm^{-1}. The metal/NTC ratio, as found by Job's method of continuous variations, is 1:1. Thus NTC[$Co(SCN)_4$] is probably responsible for the absorption. The standard deviation for a mean absorbance of 0.345 corresponding to 6.5 μg ml^{-1} of cobalt was found to be 0.006.

Effect of diverse ions. Synthetic solutions containing known amounts of cobalt(II) and varying amounts of diverse ions were prepared and the recommended procedure was followed. An error of 2% in the absorbance reading was considered tolerable. In the determination of 8.4 μg ml^{-1} cobalt, the anions tolerated (in μg ml^{-1} given in parentheses) were as follows: fluoride, chloride, iodide, nitrate (1000 each); bromide (625); phosphate (1250);

thiosulphate (600); nitrite (1200); oxalate (1280); citrate or tartrate (1800); and thiourea (150). The metal ions tolerated were: Ca(II), Sr(II), Ba(II), Ni(II), Cd(II), Mn(II), Al(III), Ti(IV) (250 μg ml^{-1} each); Zn(II) or Fe(II) (50 μg ml^{-1}); and Cu(II) (10 μg ml^{-1}). EDTA interfered seriously. All other metal ions which form coloured complexes [1] with thiocyanate also interfere. However, iron(III) (400 μg ml^{-1}) can be masked with fluoride. The tolerance for copper can be improved to 50 μg ml^{-1} by using thiourea as masking agent. Similarly, a mixture of citrate and tartrate improves the tolerance for nickel to 1000 μg ml^{-1}.

Determination of cobalt in alloys. Weighed samples (0.1 g) of "K" Monel wire and Nilo "K" wire were dissolved in concentrated nitric acid. Excess of acid was boiled out and the residues were dissolved in 1000 and 50 ml of doubly distilled water, respectively, for the Nilo and Monel wires. The recommended procedure was applied to 3—4 ml of these solutions to quantify the cobalt content. To mask copper, nickel and iron in these alloys, the requisite amounts of thiourea, citrate/tartrate (3 mg each) and fluoride (15 mg) were added. The results are reported in Table 1.

TABLE 1

Determination of cobalt in alloys

Alloy	Cobalt (%)		R.s.d. (%)
	Reported	Found[a]	
"K" Monel wire	0.51	0.50	4.8
Nilo "K" wire	17.4	17.6	2.1

[a]Mean of 6 determinations with relative standard deviation (r.s.d.).

TABLE 2

Sensitivities of thiocyanate methods for the spectrophotometric determination of cobalt(II)

Other reactant	Wavelength (nm)	Sandell sensitivity (μg Co cm^{-2})	Ref.
(Isoamyl alcohol)	620	0.055	1, 5
Tetraphenylarsonium (chloroform)	620	0.034	1, 5
Methyldiantipyrylmethane	625	0.075	5
Tri-*n*-butylammonium	615	0.045	5
2,3,5-Triphenyltetrazolium	625	0.055	1, 6
Malachite green	630	0.0007	4
Neotetrazolium chloride	620	0.02	This work

Comparison with other methods based on thiocyanates. The present method is better in sensitivity than most thiocyanate methods. Sandell sensitivities are compared in Table 2. The high molecular weight of NTC is responsible for better sensitivity. However for malachite green the higher values are reported in CCl_4 + cyclohexanone medium but the colour fades too quickly. The Co-SCN-NTC ion association complex formed in the presence of less amounts of SCN^- also has ϵ value 6.4×10^4 l mol^{-1} cm^{-1} in cyclohexane medium but suffers from the poor stability.

REFERENCES

1 E. B. Sandell, Colorimetric Determination of Traces of Metals, 3rd edn., Interscience, New York, 1959, p. 414.
2 F. D. Snell, Photometric and Fluorimetric Methods of Analysis (Metal), Part I, Wiley, New York, 1978.
3 E. B. Sandell and H. Onishi, Photometric Determination of Traces of Metals, 4th edn., Wiley, New York, 1979, p. 536.
4 L. I. Kotelyanskaya and P. P. Kish, Zh. Anal. Khim., 28 (1973) 1999.
5 I. V. Pyatnitskii, Analytical Chemistry of Cobalt, Israel Programme for Scientific Translations, Jerusalem, 1966, p. 104.
6 M. C. Mehra and D. LeBlanc, Microchem. J., 24 (1979) 435.

Analytica Chimica Acta, 172 (1985) 307—311
Elsevier Science Publishers B.V., Amsterdam — Printed in The Netherlands

Short Communication

AN IMPROVED SPECTROPHOTOMETRIC DETERMINATION OF SILICATE IN WATER BASED ON MOLYBDENUM BLUE

R. RAMACHANDRAN* and P. K. GUPTA
Analytical Chemistry Division, National Physical Laboratory, New Delhi-110 012 (India)
(Received 29th October 1984)

Summary. Silicate in water is determined by a heteropoly blue method with ascorbic acid and antimony as reducing agents; antimony does not participate in the complex but enhances the absorbance. The method is comparatively fast and sensitive. Beer's law is obeyed for 0.02—1.2 μg ml^{-1} silica. Interferences are discussed.

Thermal power stations require high-purity water for generation of steam. Chemical control of water plays an important role in their efficient operation. Silica is one of the major impurities, the concentration of which has to be carefully controlled; an upper limit of only 20 μg l^{-1} of silica is prescribed for high-pressure boilers.

Many reductants have been used for the selective reduction of molybdosilicic acid to molybdenum blue and a limit of detection of about 0.1 μg ml^{-1} silicon has been achieved. Murphy and Riley [1] introduced antimony and ascorbic acid as a mixed reagent for the reduction of molybdophosphate, which has several advantages. This method has been applied successfully to the determination of phosphorus in steel [2]. Addition of antimony results in the formation of an antimonylmolybdophosphate complex which is reduced selectively and quickly without heating. It has been reported that antimony does not form a similar complex with molybdosilicate [3]. In the work reported here, the effect of antimony on the reduction of molybdosilicate and on the stability of the blue complex formed was studied again. A comparative study of the effects of different reducing agents showed that there was considerable improvement in the sensitivity and rate of formation when antimony was added to the solution (Table 1). The absorption spectra of the molybdenum blue formed with 1-amino-2-naphthol-4-sulphonic acid, ascorbic acid and ascorbic acid/antimony(III) are shown in Fig. 1; the wavelength of maximum absorption is the same, but maximum absorbance is observed for ascorbic acid/antimony reductant.

Experimental

Solutions. Twice-distilled water was used for all solution preparation. Analytical-grade chemicals were used where possible. All solutions were stored in polythene bottles.

0003-2670/85/$03.30

TABLE 1

Comparison of different reagents for the reduction of molybdosilicic acid to molybdenum blue

Reductant	λ_{max} (mm)	Absorbance for 0.9 μg ml^{-1} SiO_2[a]	Time for max. absorbance (min)	Stability of colour (h)
Tin(II) chloride[b]	810	0.362	15	0.5
Metol[b]	812	0.350	120	24
Hydroquinone[b]	810	0.346	120	24
1-Amino-2-naphthol-4-sulphonic acid[b]	810	0.300	20	24
Ascorbic acid[c]	810	0.340	20	>6
Ascorbic acid/antimony(III)[c]	810	0.390	10	>6

[a]In 1-cm cell. [b]Conditions as reported by Mullen and Riley [4]. [c]As in the recommended procedure (see below).

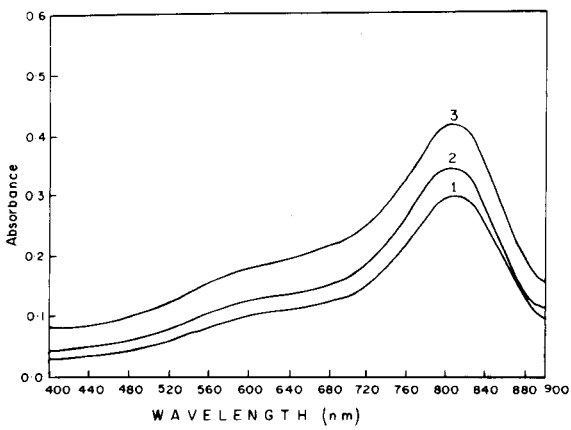

Fig. 1. Absorption spectra for heteropoly molybdenum blue from 0.9 μg ml^{-1} silica solution with different reductants: (1) 1-amino-2-naphthol-4-sulphonic acid; (2) ascorbic acid; (3) ascorbic acid/antimony(III).

Pure silica prepared in the laboratory was fused with sodium carbonate. A stock solution of ca. 1000 μg ml^{-1} silica was prepared and standardized [5]. Appropriate dilutions were made as required.

Apparatus. A Hilger-Watt H-700 u.v. spectrophotometer and an Elico digital pH meter were used.

Volumetric flasks were filled with concentrated sulphuric acid, left overnight and washed well with tap water and then with distilled water just before use.

Recommended procedure. To a sample containing 1—60 μg of silica in a 50-ml volumetric flask add 10—12 drops of 2.5 M sulphuric acid and 1—1.5 ml of aqueous 10% (w/v) ammonium molybdate solution. Dilute the solution to about 25 ml so that the pH is between 1 and 1.4. Leave the solution for 10 min to allow complete formation of yellow molybdosilicic acid. Increase the acidity by adding 15 ml of 2.5 M sulphuric acid and add 4 ml of 10% (w/v) tartaric acid solution. Immediately after addition of tartaric acid, add 0.5 ml of aqueous potassium antimonyl tartrate solution (1 mg ml^{-1} antimony) and 5 ml of aqueous 1% (w/v) ascorbic acid solution (prepared daily), and dilute to 50 ml. Measure the absorbance at 810 nm against a reagent blank prepared in the same way, 15 min after mixing the solutions. Calibrate the method with known amounts of silica from the standard solution. For 1—4 μg of silica, use 4-cm cells; otherwise, use 1-cm cells.

Results and discussion

Under the recommended conditions, 1—60 μg of silica in distilled water could be determined reproducibly and with close adherence to Beer's law. The molar absorptivity was 26 000 l mol^{-1} cm^{-1}. The average result of six determinations of 1 μg ml^{-1} silica (1-cm cells) showed a standard deviation of 0.002. Absorbances at the 1—4 μg of silica level were measured in 4-cm cells. Water samples containing silica below this level can be measured by concentrating the solution, so that the method is suitable for boiler feed water.

It was found that for complete formation and stability of the molybdenum blue produced, it was necessary carefully to control various experimental parameters. An acidity range of 0.5—0.75 M with respect to sulphuric acid was optimum for the formation of the heteropoly blue with minimum blank. The most suitable molybdate concentration for the silica range studied was provided by 1—1.5 ml of 10% (w/v) ammonium molybdate solution. After the addition of the reductants, 10 min was sufficient for full development of the blue colour at room temperature (25—30°C), but as a precautionary measure 15 min was allowed. The colour did not improve on longer reaction times or on heating. The colour was stable for more than 6 h at room temperature. Concentrations of ascorbic acid in the range 0.025—0.1 g/50 ml did not affect the results; 0.05 g was chosen as optimum. The concentration of antimony was not critical in the range 0.1—3 mg; more antimony caused turbidity, and 0.5 mg was chosen as optimum.

Effect of antimony. An attempt was made to establish if antimony reacts with unreduced molybdosilicic acid to form a mixed heteropoly acid. The absorption spectra were identical for molybdosilicic acid with and without antimony and also antimony did not enhance the yellow colour of unreduced molybdosilicic acid. The absorption maximum occurred at 810 nm for the heteropoly blue as with ascorbic acid alone. Isomolar series were also used to examine the possible formation of a mixed heteropoly acid. A study of the change in absorbance with time (up to 20 min), with different molar ratios of silicon and antimony but a constant total concentration (5.1×10^{-4} M),

showed that antimony does not form a part of the complex as in the case of phosphorus but rather acts only to enhance the absorbance of the blue complex.

Interference of diverse ions. Phosphate, arsenate and vanadate, which also form heteropoly acids, interfere. Phosphate interference can be reduced to some extent by adding tartaric acid and increasing the amount of molybdate. Vanadate interference can be neglected as it is not encountered in the water samples dealt with. Interference from more than 5 μg ml^{-1} arsenate cannot be avoided but this is again not critical when boiler-feed water is analyzed. The results obtained with diverse ions are listed in Table 2. Calcium interference can be eliminated by addition of citric acid; up to 500 μg ml^{-1} calcium can be tolerated. Fluoride in large amounts (>50 μg ml^{-1}) decreases the molybdenum blue absorbance; its interference can be decreased by adding 0.1 ml of 0.1 M boric acid prior to the addition of the molybdate reagent. Copper(II) and iron(III) ions are coloured and absorb at 810 nm. Less than 10 μg ml^{-1} copper causes negligible errors; higher concentrations up to 100 μg ml^{-1} cause positive interference. Interference of iron(III) can be overcome by reducing iron(III) to iron(II) with 10% (w/v) hydroxylammonium chloride solution before the formation of the molybdosilicic acid; up to 100 μg ml^{-1} iron(III) can then be tolerated.

Conclusion

Ascorbic acid in the presence of antimony is a useful reductant in determining traces of silicate by the heteropoly molybdenum blue method. The molybdosilicic acid is reduced rapidly at room temperature. Antimony is not a constituent of the complex but serves to improve the sensitivity of the

TABLE 2

Effect of diverse ions on the determination of silica (0.9 μg ml^{-1})

Ions	Added as	Conc. of element (μg ml^{-1})	Absorbance at 810 nm (1-cm cell)		
			Blank	0.9 μg ml^{-1} SiO_2	Difference
—	—	—	0.008	0.400	0.392
Arsenate	$Na_2HAsO_4 \cdot 7H_2O$	5	0.010	0.400	0.390
Arsenite	As_2O_3/NaOH	5	0.008	0.395	0.387
Phosphate	KH_2PO_4	5	0.010	0.396	0.386
Chloride	KCl	1000	0.012	0.398	0.386
Fluoride	NaF	10	0.032	0.422	0.390
Sulphate	K_2SO_4	500	0.006	0.393	0.387
Calcium	$CaCl_2$	500	0.008	0.395	0.387
Sodium	NaCl	1000	0.010	0.396	0.386
Copper	$CuSO_4 \cdot 5H_2O$	10	0.012	0.399	0.387
Iron(III)	$FeCl_3$	30	0.028	0.417	0.389
Iron(II)	$FeSO_4 \cdot 7H_2O$	500	0.028	0.416	0.388

method. A comparison with other reducing agents shows that the method developed gives maximum sensitivity in the aqueous medium.

REFERENCES

1 J. Murphy and J. P. Riley, Anal. Chim. Acta, 27 (1962) 153.
2 P. K. Gupta and R. Ramachandran, Microchem J., 26 (1981) 32.
3 L. V. Tumurova, L. A. Lyalyulina, S. A. Morosanova and I. P. Alimarin, Zh. Anal. Khim., 26 (1971) 2155.
4 J. B. Mullen and J. P. Riley, Anal. Chim. Acta, 12 (1955) 162.
5 D. F. Boltz, Colorimetric determination of nonmetals, Interscience, New York, 1958.

Analytica Chimica Acta, 172 (1985) 313—316
Elsevier Science Publishers B.V., Amsterdam — Printed in The Netherlands

Short Communication

DETERMINATION OF CADMIUM, COPPER AND LEAD IN URINE BY FLAME ATOMIC ABSORPTION SPECTROMETRY AFTER EXTRACTION OF THE IODIDE COMPLEXES AS ION-PAIRS WITH TRI-n-OCTYLAMINE

JOHANN FLANJAK* and ALLAN HODDA

Division of Analytical Laboratories, Department of Health, N.S.W., P.O. Box 162, Lidcombe, New South Wales 2141 (Australia)

(Received 7th August 1984)

Summary. A simple, rapid and sensitive atomic absorption spectrometric method is described for the determination of cadmium, copper and lead in urine. The metals are extracted as their iodide complexes with tri-n-octylamine in n-butyl acetate, without elaborate pretreatment, and measured by direct nebulization of the extract into an air/acetylene flame. Detection limits for cadmium, copper and lead in urine were 0.008, 0.05 and 0.02 × 10^{-6} mol l^{-1}, respectively.

The determination of cadmium, copper and lead in urine is an important clinical screening procedure. Urine is easily sampled and often provides a useful indicator of exposure and disease. Copper is biologically essential for the metabolism of iron in the synthesis of haemoglobin and as a component of several amine oxidases. Copper toxicity is manifested in Wilson's disease where the metal accumulates in tissue such as brain, kidney, liver and cornea to produce neurological, hepatic and corneal lesions [1], and also results in high concentrations of copper in urine. Cadmium and lead are cumulative poisons. Exposure to cadmium and lead is common in industry where the metals are used in a wide range of manufacturing processes, but the general population is also exposed to these metals in food, water and air.

Atomic absorption spectrometry (a.a.s.), when used in conjunction with liquid-liquid extraction, gives increased sensitivity, and interferences from matrix elements may be avoided. Since their introduction by Smith and Page [2] for extraction of acids, long-chain amines have been utilized extensively as extractants for various metals in geological or metallurgical applications [3—10]. Extraction by a tertiary amine [11] may be represented most simply by

$$(nR_3NH^+X^-)_o + (MX_p^{n-})_w \rightleftharpoons [(R_3NH^+)_n MX_p^{n-}]_o + nX_w^-$$

where subscripts o and w indicate the organic and aqueous phases, respectively, and X is an appropriate anion.

0003-2670/85/$03.30

Cadmium, copper and lead give iodo complexes [4, 6, 8] which form easily extracted ion-pairs with tertiary ammonium ions [4]. Such procedures were investigated here for isolating cadmium, copper and lead as iodo complexes from acidified urine. The tertiary amine used was tri-n-octylamine (TOA), diluted with n-butyl acetate. The extraction was quantitative. The method is simple, sensitive, accurate and rapid compared to other extraction procedures which require accurate pH control.

Experimental

Apparatus. A Varian 775 atomic absorption spectrometer with a standard air/acetylene burner was used. Hollow-cathode lamps were used under the following operating conditions: cadmium (228.8 nm, 0.5 nm slit width, 3.5 mA), copper (324.8 nm, 0.5 nm, 3.5 mA), lead (283.3 nm, 1.0 nm, 5 mA). An air/acetylene flame was used with oxidizing flame conditions. Burner and flame conditions were optimized; the scale expansion was 2 for lead determination. All laboratory ware was soaked in 7 M nitric acid for 24 h and was thoroughly rinsed with distilled water.

Reagents. Analytical-grade reagents and glass-distilled water were used throughout. A tri-n-octylamine solution (1% v/v) was prepared just before use by dissolving 1 ml of tri-n-octylamine (Sigma Chemical Co.) in 100 ml of n-butyl acetate. The potassium iodide/ascorbic acid solution consisted of 75 g of potassium iodide and 4 g of ascorbic acid dissolved in water and diluted to 100 ml. A stock cadmium solution (5×10^{-3} mol l^{-1}) was prepared by dissolving 0.562 g of cadmium metal in the minimum volume of (1+1) nitric acid and diluting to 1 l with water. A working solution (5×10^{-6} mol l^{-1}) was obtained by diluting 1 ml of stock solution into 1 l in a volumetric flask. A stock copper solution (1.0×10^{-2} mol l^{-1}) was prepared by dissolving 0.635 g of copper metal in a minimum volume of (1+1) nitric acid and diluting to exactly 1 l with water. A 1×10^{-4} mol l^{-1} working solution was obtained by diluting 1 ml of the stock solution to 100 ml with water. A stock lead solution (5×10^{-3} mol l^{-1}) was prepared by dissolving 1.036 g of lead metal in the minimum volume of (1+1) nitric acid and diluting to 1 l with water. A 5×10^{-6} mol l^{-1} working solution was obtained by dilution with water.

Preparation of calibration standards. Transfer 0.0, 0.1, 0.2, 0.3 and 0.4 ml (cadmium, copper) or 0.0, 0.5, 1.0, 2.0 and 2.5 ml (lead) of working solution to a 25-ml calibrated test tube. Add water to bring the volume to 25 ml. For 25-ml urine samples, these solutions correspond to $0—0.08 \times 10^{-6}$ mol l^{-1} for cadmium, $0—1.6 \times 10^{-6}$ mol l^{-1} for copper and $0—0.5 \times 10^{-6}$ mol l^{-1} for lead, with corresponding absorbances of 0—0.063, 0—0.228 and 0—0.064 when the following procedure is applied.

General procedure. Transfer a 25-ml aliquot of acidified urine (1% v/v acetic acid) or standard to a 25-ml calibrated test tube. Add 0.5 ml of (1+1) sulfuric acid and 1 ml of the potassium iodide/ascorbic acid solution. Mix and let stand for 1 min. Add 2.5 ml of the TOA solution and mix by rapid

inversion for 1 min (violent shaking results in the formation of an emulsion, with less extraction efficiency). Allow the phases to separate. If an emulsion forms, remove the organic layer and emulsion by Pasteur pipette and centrifuge it to complete the phase separation. Aspirate the organic layer into the flame, and measure the absorbance. From the readings obtained from the calibration standards, construct the calibration graphs, which should be linear. Calibration standards containing the three metals may be extracted in one operation, and should be run with each batch of samples.

Results and discussion

The extraction of cadmium, copper and lead from acidified urine depends mainly on the capacity of these metals to form anionic metal iodide complexes, which form ion-pairs with TOA for extraction into n-butyl acetate. Not all trace elements are excreted in urine in a readily extractable form. It was necessary to verify that cadmium, copper and lead were not excreted in urine to any significant degree as acid-stable organometallic compounds, as this would affect the accuracy of the proposed determination.

The accuracy of the method was verified, therefore, by analyzing fresh urine samples known to contain slightly elevated concentrations of cadmium, copper and lead, by two basically different methods. The other method chosen was graphite-furnace atomic absorption spectrometry with direct injections [12, 13]. From Table 1, it can be seen that agreement between the two methods is good, indicating that there is probably no significant inaccuracy in the extraction method, and that any organometallic species that may be present are broken down on acidification of the urine.

The precision of the method is shown in Table 1. The relative standard deviations for cadmium, copper and lead were 4.4, 0.9 and 2.2%, respectively. Table 2 shows the recovery of known amounts of cadmium, copper and lead added to urine samples at low and elevated clinical levels. Recoveries of ca. 90% were obtained at "normal" concentrations. At slightly elevated concentrations, the recovery rose to ca. 95%. Sensitivity and detection limits of cadmium, copper and lead in urine are: 0.007, 0.008; 0.03, 0.05; 0.03, 0.02 $\times 10^{-6}$ mol l^{-1}, respectively.

TABLE 1

Comparison of results obtained for cadmium, copper and lead in urine by the proposed flame a.a.s. method and a graphite-furnace method

Element	Concentration found[a] (10^{-6} mol l^{-1})	
	Proposed method	Graphite furnace
Cadmium	0.113 ± 0.005	0.12 ± 0.01
Copper	1.09 ± 0.01	1.05 ± 0.04
Lead	0.45 ± 0.01	0.48 ± 0.03

[a]Mean ± standard deviation (n = 10).

TABLE 2

Recoveries of cadmium, copper and lead added to urine

Element	Amount added (10^{-6} mol l^{-1})	Mean recovery (%)[a]
Cadmium	0.02	90.0
	0.10	94.4
Copper	0.10	90.0
	0.70	94.5
Lead	0.10	88.0
	0.50	94.2

[a] $n = 10$.

This method has been used successfully in these laboratories as a routine screening procedure for the above metals in urine for several years. Accurate results have consistently been obtained for various proprietary urine control samples.

The authors thank Dr. E. P. Crematy, Director & Government Analyst, Division of Analytical Laboratories, Department of Health, N.S.W., for permission to publish this paper.

REFERENCES

1 B. L. O'Dell, Med. Clin. North Am., 60 (1976) 687.
2 E. L. Smith and J. E. Page, J. Soc. Chem. Ind., 67 (1948) 48.
3 T. Honjo, S. Ushijima and T. Kiba, Bull. Chem. Soc. Jpn., 46 (1973) 3764.
4 C. W. McDonald and F. L. Moore, Anal. Chem., 45 (1973) 983.
5 T. Groenewald, Anal. Chem., 41 (1969) 1012.
6 J. R. Clark and J. G. Viets, Anal. Chem., 53 (1981) 61.
7 S. de Moraes and A. Abrão, Anal. Chem., 46 (1974) 1812.
8 J. G. Viets, Anal. Chem., 50 (1978) 1097.
9 I. Tsukahara, M. Sakahibara and T. Yamamoto, Anal. Chim. Acta, 83 (1976) 251.
10 I. Tsukahara and T. Yamamoto, Anal. Chim. Acta, 61 (1972) 33.
11 U. A. Th. Brinkman and G. de Vries, J. Chem. Educ., 49 (1972) 244.
12 K. S. Subramanian and J. C. Meranger, Clin. Chem., 27 (1981) 1866.
13 O. Wawschinek and H. Hofler, At. Absorpt. Newsl., 18 (1979) 97.

Analytica Chimica Acta, 172 (1985) 317—321
Elsevier Science Publishers B.V., Amsterdam — Printed in The Netherlands

Short Communication

PRECISE DETERMINATION OF LOW ISOTOPIC NITROGEN-15 ABUNDANCES BY EMISSION SPECTROMETRY

Y. FUKUTOKU*, M. YOSHIDA, M. IKEDA and Y. YAMADA

Faculty of Agriculture, Kyushu University, 6-10-1 Hakozaki, Higashi-ku, Fukuoka 812 (Japan)

(Received 6th November 1984)

Summary. Improvements in the determination of low nitrogen-15 abundances by emission spectrometry are described. Stronger emission is observed if a capillary constriction is formed at the centre of the discharge tube, and the background under the $^{14}N^{15}N$ peak is greatly reduced. The relative error normally caused by problems in estimating the background is thus decreased. The overall precision is better than 1% in the range from natural abundance to 1.0 atom-% nitrogen-15.

Emission spectrometry is being used increasingly in biochemical studies, as an alternative to mass spectrometry, for determining isotopic nitrogen-15 because microgram amounts of nitrogen suffice for the measurements. However, the precision and accuracy are not very good. Overall precision for the method, including sample preparation, exceeds 1% in the range from natural abundance to 1.0 atom-% ^{15}N, which is higher than that for mass spectrometry [1—8]. The main source of error in the determination of nitrogen-15 in low abundances by emission spectrometry lies in the ill-defined background under the $^{14}N^{15}N$ bandhead; several procedures have been evolved to estimate the background [1—3, 6]. Further, in the Dumas method, errors caused by impurities in the calcium oxide and copper oxide reagents cannot be neglected [2, 4].

Yamamuro [9] observed a reduction in the background emission under the $^{14}N^{15}N$ bandhead, which allowed a precise determination of low abundances of nitrogen-15, when the conversion to nitrogen gas was done by excitation with a high-frequency generator instead of combustion in a furnace. However, the method is somewhat tedious. Improved procedures for obtaining precise results for nitrogen-15 in low abundance by emission spectrometry are reported here.

Experimental

The electrodeless discharge tubes were prepared by the modified Dumas method [4]. Calcium oxide granules (1.5—2.0 mm) was preheated to 950° C for 2 h and copper oxide wires to 550° C for 30 min, in order to eliminate impurities and absorbed water; they were stored in a desiccator. Solutions of

0003-2670/85/$03.30

samples containing about 5 μg of nitrogen as ammonium chloride, proline or albumin were taken up by capillary action into Pyrex tubes (10 mm long, 1.5 mm o.d., 1 mm i.d.) and dried at 70° C under an infrared lamp in a box through which clean air passed. The sample tubes were inserted into the Pyrex discharge tubes (150 mm long, 4 mm o.d., 2 mm i.d.) together with the calcium oxide and copper oxide. The discharge tubes were cleaned by heating with a hand torch under high vacuum (10^{-5} mm Hg). The copper oxide and calcium oxide in the tubes were reheated simultaneously. While one end of the tubes was baked, the sample-containing capillaries were moved to the cool end. After the tubes had cooled and been carefully sealed off at 10 cm from one end with a hand torch, the ammonium chloride was converted to nitrogen by heating at 550° C for 30 min; albumin and proline required heating for 3 h. After the tubes had cooled, a capillary constriction was formed at the middle of the tubes by applying the flame of a hand torch at one side of the tube (see Fig. 1A). When Pyrex glass is used, this constriction is easily made because of the low pressure in the tube.

The nitrogen-15 content was quantified with a ^{15}N-analyzer (JASCO Model NIA-1). The electrodeless discharge tube was placed in position at the electrodes of the high-frequency generator with the capillary constriction at the middle of the electrodes. The power was switched on and the maximum intensity of the $^{14}N^{14}N$ emission was found on a recorder chart by rotating the tube while the photomultiplier high voltage was held constant. The emission spectrum of N_2 molecules at the constricted portion of the tube was then scanned.

Results and discussion

The amount of the nitrogen needed was only 2—8 μg. The photomultiplier voltage was adjusted so that the $^{14}N^{14}N$ peak height was 60—90% of full-scale deflection on the chart to minimize recording errors.

As Pyrex glass absorbs radiation strongly around 300 nm, its transmittance depends on the thickness of the tube [4]. In the proposed method, the thickness of the glass at the constriction is not changed, and the mechanical strength of the tube is not affected. Thus, the enhanced light intensity is not caused simply by an increase in the transmittance (Table 1). Possibly, excitation of nitrogen molecules is enhanced by a steep increase in the current density in the constricted portion of the tube.

Figure 2 shows the emission spectra of a sample with natural abundance at the capillary constriction and at the main part of the tube. The latter spectra have a high noisy background under the $^{14}N^{15}N$ peak. When the constricted

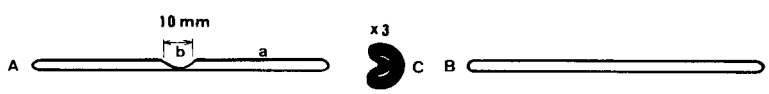

Fig. 1. Different forms of electrodeless discharge tubes (4 mm o.d., 10 cm long): (A) proposed type; (B) ordinary tube; (C) cross-section at the capillary constriction.

TABLE 1

Enhancement of light intensity by the capillary constriction[a]

Tube No.	1	2	3	4	5	6	7	8	Mean	SD
I_c/I_o	9.6	9.2	6.4	10.4	8.6	7.9	11.5	9.8	9.2	1.6

[a] I_c and I_o are the relative intensities of the emission from $^{14}N^{14}N$ molecules at positions (b) and (a) (Fig. 1) with the same discharge tube at a constant photomultiplier voltage. SD is the standard deviation.

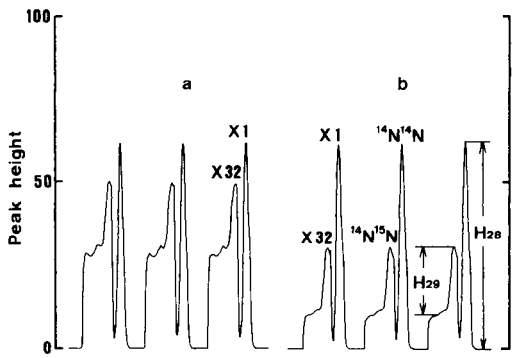

Fig. 2. Typical recorder tracings for optical ^{15}N measurement of ammonium chloride: (a) and (b) are the emission scans for the main part of the tube and at the constricted portion, respectively; X 1 and X 32 are the amplifier gain settings; H_{28} and H_{29} are peak heights.

portion is used, the background is much lower and the noise is greatly reduced, possibly because a lower photomultiplier voltage can be used. The relative error in the estimation of the background under the $^{14}N^{15}N$ peak is thus decreased.

The precision of results can be affected in several ways. Short-term variations in the observed values of many scans for one tube can be caused by changes in the light intensity during the time needed for the scans. When repeated analyses are done with several different tubes of one sample, a more likely source of error is variation in the background emission. Day-to-day variations in the observed values may also be due to changing environmental conditions, electronic instabilities, etc. These three factors were tested here. In the range from natural abundance to 1.0 atom-% ^{15}N, short-term variation in the observed values of ten scans gave a relative standard deviation of 1.3% and the overall method (including sample preparation) gave relative standard deviations within 1% (Table 2). These precisions are better than those obtained by earlier workers [5] using the same instrument. Day-to-day variations over a week indicated a precision of about 1.5%; this error can be

TABLE 2

Precision of the nitrogen-15 values for ammonium chloride standards, albumin and proline by emission spectrometry (e.s.) and comparison with mass spectrometric values (m.s.)

M.s. values	Observed e.s. values (atom-%)[a]										Mean	SD	RSD
	1[b]	2	3	4	5	6	7	8	9	10			
0.365	0.530	0.528	0.528	0.528	0.527	0.526	0.526	0.526			0.527	0.001	0.3
0.603	0.791	0.792	0.777	0.778	0.780	0.782	0.783	0.774	0.779		0.782	0.006	0.8
0.694	0.882	0.881	0.885	0.870	0.884	0.879	0.883	0.887	0.875		0.881	0.005	0.6
0.795	0.996	0.986	0.988	1.002	0.985	1.000	0.989	1.003	0.985	0.990	0.992	0.007	0.7
0.889	1.083	1.080	1.092	1.089	1.085	1.082	1.091	1.083	1.076	1.085	1.085	0.005	0.5
0.991	1.153	1.161	1.156	1.156	1.155	1.155	1.172	1.163			1.159	0.006	0.5
Albumin	0.540	0.534	0.535	0.533	0.532	0.538	0.540	0.535	0.532	0.535	0.535	0.003	0.6
Proline	0.540	0.538	0.538	0.542	0.537	0.537	0.544	0.536	0.538	0.541	0.539	0.003	0.5

[a]The data given are the means of 10 scans on each tube. SD, standard deviation; RSD, relative standard deviation (%). [b]Tube nos. 1—10.

TABLE 3

Accuracy of the atom-% ^{15}N values by emission spectrometry

M.s. values	Gain	Observed e.s. values	Corrected values[a]	Deviation	Relative error (%)
0.365	x 32	0.530	0.363	—0.002	0.5
0.603		0.775	0.604	+0.001	0.2
0.694		0.874	0.701	+0.007	1.0
0.795		0.970	0.796	+0.001	0.1
0.889		1.07	0.894	+0.005	0.6
0.991		1.16	0.983	—0.008	0.8
1.19		1.37	1.19	0	0
1.39		1.56	1.38	—0.01	0.7
1.58		1.77	1.58	0	0
1.78		1.97	1.78	0	0
1.98		2.18	1.99	+0.01	0.5
0.991	x 8	1.23	0.998	+0.007	0.7
1.39		1.65	1.39	0	0
1.98		2.27	1.97	—0.01	0.5
2.95		3.29	2.95	0	0
3.93		4.28	3.92	—0.01	0.3
4.91		5.28	4.91	0	0
6.87		7.21	6.88	+0.01	0.1
8.86		9.08	8.86	0	0
9.85		9.99	9.85	0	0

[a]The observed e.s. values were corrected by the calibration equations given in the text.

eliminated by running samples with an appropriate series of calibration standards.

The observed values shown in Table 2 are obviously inaccurate compared to the mass spectrometric values. They were corrected to the true values by

means of calibration equations (Table 3). For an amplifier gain of × 32, a linear regression equation was fitted to the range from natural abundance to 2 atom-% ^{15}N; the equation $y = 0.9836x - 0.1581$ ($r = 0.9999$) gave the true nitrogen-15 values. For an amplifier gain of × 8, a second-degree polynomial was needed to fit the range from 1.0 to 10 atom-% ^{15}N; the equation $y = 9.266 \times 10^{-3}x^2 + 0.9059x - 0.1299$ ($r = 0.9998$) gave the true values. The values from emission spectrometry corrected in this way agreed with the mass spectrometric values within 0.01 atom-% ^{15}N (Table 3).

REFERENCES

1 J. P. Leicknam, V. Middelboe and G. Proksch, Anal. Chim. Acta, 40 (1968) 487.
2 H. Perschke, G. Proksch, E. A. Keroe and A. Muehl, Anal. Chim. Acta, 53 (1971) 459.
3 K. Kumazawa, Bunseki, 9 (1975) 43.
4 R. Fiedler and G. Proksch, Anal. Chim. Acta, 78 (1975) 1.
5 G. Guiraud and L. A. Buscarlet, Int. J. Appl. Radiat. Isotopes, 26 (1975) 187.
6 J. D. S. Goulden and D. N. Salter, Analyst (London), 104 (1979) 756.
7 F. Martin, B. Maudinas, M. Chemardin and P. Gadal, Int. J. Appl. Radiat. Isotopes, 32 (1981) 215.
8 D. N. Salter, Proc. Nutr. Soc., 40 (1981) 335.
9 S. Yamamuro, Soil Sci. Plant Nutr., 27 (1981) 405.

Analytica Chimica Acta, 172 (1985) 323—327
Elsevier Science Publishers B.V., Amsterdam — Printed in The Netherlands

Short Communication

DETERMINATION OF NANOGRAM AMOUNTS OF BROMIDE AND CHLORIDE BY MOLECULAR EMISSION CAVITY ANALYSIS BASED ON GALLIUM HALIDE EMISSION

Z. M. KASSIR*, A. A. H. TA'OBI and A. T. AL-SAMARAIE
Department of Chemistry, College of Science, University of Basrah, Basrah (Iraq)
T. A. K. NASSER
Department of Chemistry, College of Education, University of Basrah, Basrah (Iraq)
(Received 9th April 1984)

Summary. By measuring the GaBr emission enhanced by iodide at 350 nm in a carbon cavity heated by a hydrogen/argon flame, 0—60 ng of bromide is determined with a detection limit of 0.5 ng μl^{-1}. In a similar way, gallium (0—20 ng) can be determined with a detection limit of 0.15 ng μl^{-1}. Interferences are reported. Chloride (0—1200 ng) is determined by means of GaCl emission; the detection limit is 50 ng μl^{-1}.

Halogens have previously been determined by molecular emission cavity analysis (m.e.c.a.) by measuring MX emission, where M is Cu, In, Ga, etc. [1, 2] and X is Cl, Br or I. Various sensitive procedures were described for the determination of bromide and chloride ions [1—4]. Bromide was determined as gallium bromide by using iodide as enhancing agent; as little as 50 ng of bromide could be detected [1, 4]. An emission of gallium chloride was not detected [1].

In the present communication, the emission of gallium chloride in a m.e.c.a. cavity is reported, as well as the parameters affecting the emission from gallium bromide and gallium chloride. Linear calibration graphs for bromide and chloride were obtained, with an improvement in the detection limit for bromide. Gallium is also determined by measuring its bromide or chloride emission.

Experimental

Instruments. A molecular emission cavity analyzer (Model 22; Anacon, Burlington, MA) was used. The instrument has been described [1, 5]. A Beckman DU-2 spectrophotometer with appropriate attachments was used for recording spectra as described previously [6]. Carbon, stainless steel and silica-coated stainless steel cavities (Anacon) were used.

Chemicals. The chemicals were of high purity. Deionized-distilled water was used for the preparation of all solutions. Hydrochloric, hydrobromic and hydroiodic acid solutions were standardized by conventional titration and

0003-2670/85/$03.30

diluted to give 1000 mg l^{-1} stock solutions of the halides. A 1000 mg l^{-1} gallium solution was prepared from gallium nitrate octahydrate. High-purity gases were used for the cool flame.

General procedure. Place 1—10 μl of the test solution, pretreated with gallium ion (see below), in the cavity and insert it into the flame under the optimum conditions (see below). Use one cavity for a set of measurements. Take at least 5 readings for each sample and use the average. Frequently check the blank and residual emissions. On changing from one type of sample to another, wash the cavity with dilute nitric acid followed by distilled water, and place the cavity in the flame for a few seconds to clean it.

Results and discussion

Spectra. The emission spectra of gallium chloride and bromide were recorded by a point-to-point method with the m.e.c.a. instrument and by scanning with the Beckman DU-2 (where the cavity replaces the rod in the published set-up [6]). Reasonable agreement was obtained with the spectra reported in the literature [1, 7]. Gallium bromide showed a strong peak at 355 nm and a broad peak at 350 nm. When the gallium bromide peak was enhanced by adding hydroiodic acid, the peak at 350 nm became stronger. Gallium chloride gave two peaks, at 334 and 338 nm, the latter being more intense. Therefore, the peak at 350 nm was chosen to measure GaBr and that at 338 nm for GaCl in all subsequent measurements.

Cavity type. Several cavities normally used in m.e.c.a. were tested. The results (Table 1) show that the carbon cavity gave the greatest emission from GaCl and GaBr. Stainless steel and silica-coated cavities gave lower intensities, owing to their high thermal conductivity which caused them to heat up faster, and thus decreased the enhancing effect of the Salet phenomenon [1].

Flame gases. The flame composition was examined, in order to find the optimum flow rates and the best diluent gas (argon or nitrogen) for hydrogen. The hydrogen flow rate was fixed, the flow of nitrogen or argon was changed and the emission from a fixed amount of gallium halide was measured. This procedure was repeated for other hydrogen flow rates. Figure 1 shows the effects on the GaBr emission and the GaCl emission. It is clear that argon gave more intense emissions than did nitrogen. Therefore, argon

TABLE 1

Effect of cavity type on gallium halide emissions

Cavity	Relative emission intensity	
	GaBr	GaCl
Carbon	31	19
Stainless steel	11	5
Silica-coated steel	14	7

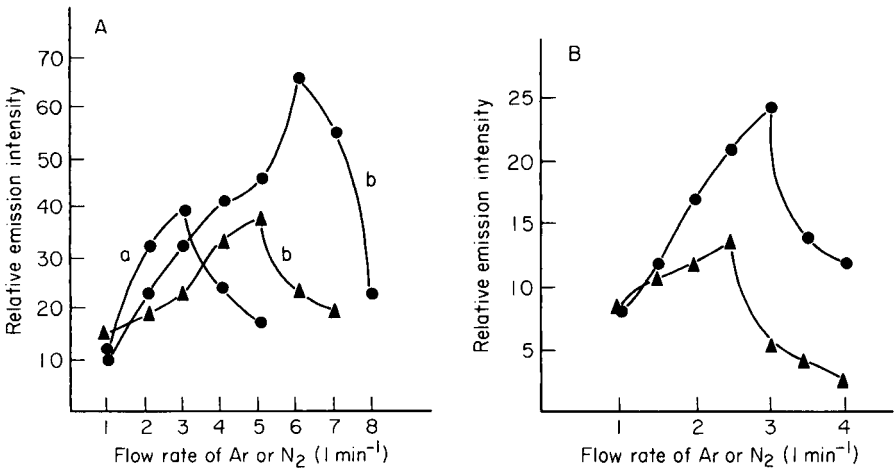

Fig. 1. Effect of diluent flow rate: (A) on GaBr emission; (B) on GaCl emission (▲) N_2; (●) Ar. Hydrogen: (a) 1.5; (b) 2.0 l min^{-1}; 1.5 l min^{-1} in all cases in B.

was used with hydrogen in the remainder of this study. The optimum hydrogen and argon flows for GaBr were 2.0 and 6.0 l min^{-1}, respectively. Those for GaCl were 1.5 and 2.0 l min^{-1}, respectively.

Gallium/halide ratio. In order to establish the gallium/halide ratio that gave the maximum emission intensity, a fixed concentration of bromide or chloride was mixed with various amounts of gallium. A constant volume from the mixture was injected into the cavity and the emission was measured. The results showed that the best ratio for bromide and chloride was 1:3 (w/w). Therefore, this ratio was used to study most of the other parameters.

Sample volume. A series of solutions was prepared in which the halide concentration was decreased so that increasing volumes of these solutions provided the same amount of halide. The gallium/halide ratio was kept constant. The results (Fig. 2) show that the emission from GaBr and GaCl is a maximum when 4 μl of sample is injected.

Iodide as an enhancing agent. Iodide enhances the emission of gallium bromide [1]. This was studied further by preparing a number of solutions containing a constant concentration of gallium bromide and an increasing concentration of hydroiodic acid. The emissions from 4-μl aliquots were measured. Figure 3 shows the relation between the relative emission intensity and the hydroiodic acid concentration. Greatest intensity was achieved in 0.05 M hydroiodic acid. No spectral interference from gallium iodide at 350 nm was noticed. The enhancing effect of iodide on the emission from gallium bromide has been explained [1] on the basis of the formation of a mixed halide (e.g., GaI_2Br) which is more volatile than $GaBr_3$, but which gives rise to GaBr emission. It has also been suggested that a complex salt containing nitrate (e.g., $Ga(NO_3)IBr$) is formed [7].

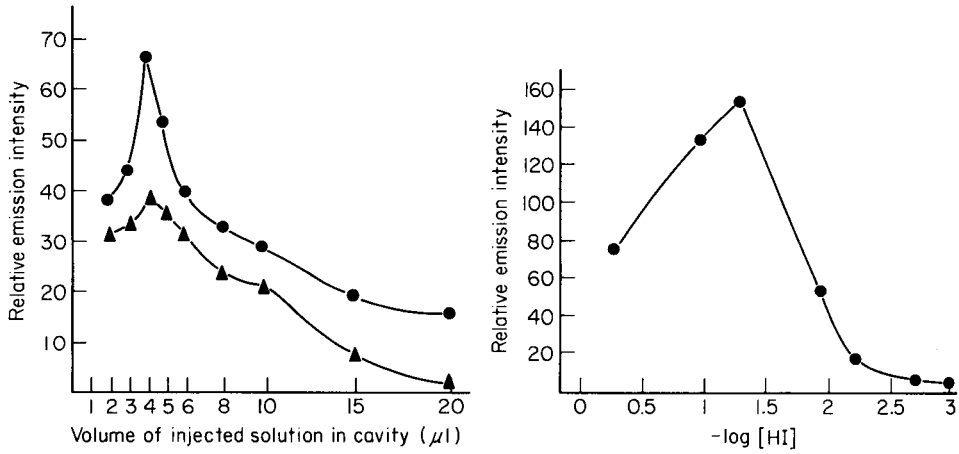

Fig. 2. Effect of injected volume on the emission intensity: (•) GaBr; (▲) GaCl.

Fig. 3. Effect of hydroiodic acid on the GaBr emission intensity.

Calibration graphs. The GaBr emission from solutions containing various concentrations of bromide ion in 0.05 M hydroiodic acid with constant ratio of gallium to bromide was measured at 350 nm under the established optimal conditions. A linear relation was obtained between 0 and 60 ng of bromide. The detection limit was 0.5 ng μl^{-1} with a 6.9% relative standard deviation (r.s.d.). In the same way, gallium can be determined over the range 0—20 ng, with a detection limit of 0.16 ng μl^{-1}; the r.s.d. was the same as for bromide. A fixed ratio of gallium to bromide could not be used for measurements on samples, therefore an excess of gallium ion was added to a set of bromide solutions and the GaBr emission was measured. A linear graph was again obtained for 0—360 ng of bromide, but with a higher detection limit (40 ng μl^{-1}). The relative emission intensity for bromide was lower than at the constant ratio to gallium. The excess of gallium used (200 ng) showed no detrimental effects to subsequent samples, as checked by successive measurements on the same solution. When gallium was determined in the presence of a constant, excess amount of bromide, the calibration graph was linear for 0—60 ng of gallium, with a detection limit of 2 ng μl^{-1}.

Chloride was similarly determined by measuring GaCl emission at 338 nm under the established optimum conditions in the presence of an excess of gallium (200 ng). A linear calibration graph was obtained for 0—1200 ng of chloride with a detection limit of 50 ng μl^{-1} and the r.s.d. was 5.5%. Gallium could similarly be determined in the range 0—400 ng with a detection limit of 16 ng μl^{-1}.

Interferences. The effect of a number of cations and anions on the emission of gallium bromide was studied. The results are summarized in Table 2. All the cations examined, except indium, decreased the intensity, mainly because

TABLE 2

Effect of various ions on GaBr emission

Ion	Change in intensity (%)			Ion	Change in intensity (%)		
	1 x[a]	2 x[a]	5 x[a]		1 x[a]	2 x[a]	5 x[a]
Na^+	−78	−90	−92	Fe^{3+}	−35	−64	−70
K^+	−53	−64	−73	Al^{3+}	−46	−50	−55
Mn^{2+}	−85	−91	−94	In^{3+}	+>100	+>100	+>100
Cu^{2+}	−82	−87	−94	F^-	−3	−10	−58
Cd^{2+}	−53	−70	−32	Cl^-	−27	−62	−63
Ni^{2+}	−67	−80	−86	NO_3^-	+1	+2	+3
Co^{2+}	−74	−87	−93	SO_4^{2-}	+12	+>100	+>100
Zn^{2+}	−45	−83	−93	PO_4^{3-}	−43	−78	−86
Mg^{2+}	−8	−22	−44				

[a]Weight excess.

of the formation of less volatile metal bromides, but possibly because of the emission of a metal bromide at a different wavelength. Indium greatly enhanced the emission by indium bromide emission [1]. Most of the anions examined decreased the intensity. Nitrate enhanced the emission slightly, possibly because of the formation of the mixed gallium salt [7]. Sulphate showed excessive interference because of the strong S_2 emission.

REFERENCES

1 M. Burguera, S. L. Bogdanski and A. Townshend, CRC Crit. Rev. Anal. Chem., 10 (1980) 185.
2 R. Belcher, S. L. Bogdanski, I. H. B. Rix and A. Townshend, Anal. Chim. Acta, 81 (1976) 325.
3 R. Belcher, S. L. Bogdanski, Z. M. Kassir, D. A. Stiles and A. Townshend, Anal. Lett., 7 (1974) 751.
4 S. A. Al-Tamrah, Ph. D. Thesis, Birmingham University, England, 1978.
5 R. Belcher, S. L. Bogdanski, D. J. Knowles and A. Townshend, Anal. Chim. Acta, 77 (1975) 53.
6 S. M. Dhaher and Z. M. Kassir, Anal. Chem., 52 (1980) 459.
7 R. M. Dagnall, K. C. Thompson and T. S. West, Analyst (London), 94 (1969) 643.

Analytica Chimica Acta, 172 (1985) 329—333
Elsevier Science Publishers B.V., Amsterdam — Printed in The Netherlands

Short Communication

ATOM CELL FOR USE IN HYDRIDE-GENERATION ATOMIC FLUORESCENCE SPECTROMETRY

A. A. BROWN* and J. M. OTTAWAY

Department of Pure and Applied Chemistry, University of Strathclyde, Cathedral Street, Glasgow G1 1XL (Great Britain)

G. S. FELL

Department of Clinical Biochemistry, Royal Infirmary, Glasgow, G4 0SF (Great Britain)

(Received 11th June 1984)

Summary. An electrically-heated silica tube atom cell is described for the determination of selenium in blood serum. The detection limit was 1.4 ng in 10 ml of aqueous solution. The r.s.d. at 10, 50 and 200 ng of selenium was 6.8% (n = 5), 4.3% (n = 6) and 4.7% (n = 10) respectively. Calibration was linear up to 600 ng.

The use of atomic fluorescence spectrometry (a.f.s.) has mainly been restricted to research laboratories, primarily because high-intensity light sources and instrumentation are not commercially available. The recent introduction of a commercially available a.f.s. instrument may stimulate greater interest [1]. To achieve low detection limits in a.f.s., high-intensity light sources are needed. The light source most favoured in recent years has been the microwave electrodeless discharge lamp (EDL). The elements which produce a stable, high-intensity lamp are those which are relatively volatile (e.g., lead, arsenic, selenium and mercury). Many of these elements also form gaseous hydrides. Various reports have been published on hydride-generation a.f.s. [2—7]. In each case, the instrumentation used was unique to those workers. The atom cell most favoured, however, was an argon/hydrogen diffusion flame (or cold-vapour cells for mercury).

This communication reports the development of a silica tube atom cell for hydride-generation a.f.s. In preliminary experiments, the gaseous hydride was introduced into the auxiliary oxidant port of a conventional nebuliser/spray chamber, with atomisation in an argon/hydrogen diffusion flame. Results obtained from this system were not encouraging. It was thought that if the flow rate of the gas passing through the measurement zone were decreased, a significant improvement in response would occur. A simple glass atomiser was constructed with this aim in mind. It can be considered as an atom cell designed to support an argon/hydrogen diffusion flame at low flow rates. A simple, electrically-heated silica tube atomiser was also constructed, in order to achieve atomisation efficiencies at least as good as

*Present address: Pye Unicam Ltd., York Street, Cambridge CB1 2PX, Great Britain.

0003-2670/85/$03.30

that of a conventional flame system but with significantly decreased background (noise). This would improve the detection limit of the complete system. Both of the atomisers were evaluated.

Experimental

Instrumentation. A schematic diagram of the instrumentation is shown in Fig. 1. The main components include the monochromator (1670, Spex Industries), photomultiplier tube (R431S, Hamamatsu), lock-in amplifier (9503D, Ortec Brookdeal), Broida ¾-wave cavity (210L, Electromedical Supplies) and a microwave generator (MK.1, Electromedical Supplies). The optimized conditions for the selenium EDL were 60 W with an air temperature of 140°C. The monochromator was centred at the 204.0-nm atomic line with an optimized bandpass of 20 nm. The photomultiplier tube voltage was 0.8 kV.

Figure 2 shows the two atom cells investigated. The glass cell was a soda-glass tube (10 cm long, 1.2 cm o.d.) with an insert (0.4 cm o.d.) for hydride introduction. The electrically-heated atomiser was a silica tube (16 cm long,

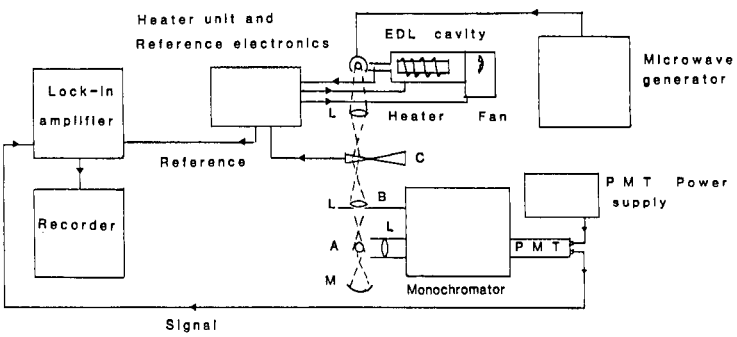

Fig. 1. Schematic diagram of the atomic fluorescence instrument: A, atomiser; B, baffle; C, chopper; M, mirror; L, lens.

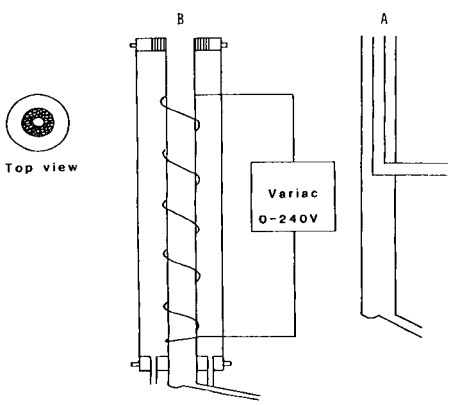

Fig. 2. (A) Glass atomiser; (B) electrically-heated silica tube atomiser.

1.2 cm o.d.) wound with nichrome wire and heated resistively via a Variac (0—240 V) transformer. A setting of 120 V produced a white hot glow inside the silica tube. The flow of argon, acting as a sheathing gas, was controlled by a flowmeter (0—15 l min^{-1}). The hydride generation unit was the Perkin Elmer MHS-10 system. The T-shaped flame-heated atom cell was replaced by the cells shown in Fig. 2.

Reagents. AristaR acids (BDH Chemicals) were used. All other reagents were of analytical reagent grade. Deionized-distilled water was used throughout. Glassware was soaked overnight in 1—5% (v/v) nitric acid and rinsed with water before use. Stock solutions (1000 μg ml^{-1}) of selenium were prepared by dissolution of selenium dioxide in 1×10^{-2} M hydrochloric acid. The reductant solution used for hydride generation was 3% (w/v) sodium tetrahydroborate stabilised with 1% (w/v) sodium hydroxide solution. The solution was filtered (Whatman 541) before use. For the initial evaluation of each atom cell, the hydrochloric acid concentration of samples was 2% (v/v).

The dissolution procedure for blood serum was as previously described [8].

Results

The lowest detection limits were obtained with a bandpass of 20 nm centred at the 204.0-nm selenium atom line. This is due, in part, to the use of a solar-blind photomultiplier tube; the fluorescence emitted at the 196.0, 204.0, 206.0 and 207.5-nm selenium atom lines was detected by the photomultiplier. The signal-to-noise increased as the slit of the monochromator was opened, up to a 20-nm bandpass. A further increase in slit width degraded the signal-to-noise ratio. In contrast, when a simple photomultiplier tube (E.M.I. 9789QB) was used, the best ratio was obtained with a bandpass of 1.0 nm centred at the 204.0-nm line.

Glass atomiser. This was designed to support an argon/hydrogen diffusion flame at low flow rate. The flame conditions were adjusted by varying the flow rates of argon and hydrogen to produce an almost cylindrical flame which neither lifted off the burner head nor was unstable during a determination. The optimised flame conditions were 6 l min^{-1} argon and 1.5 l min^{-1} hydrogen. The fuel-lean flame produced better signal-to-noise ratios, which was attributed to a decrease in flame noise.

The apparatus was tested for 10-ml samples in 2% (v/v) hydrochloric acid. The best observation height above the burner head was found to be 3.0 cm. The detection limit (signal/noise of 2) was 2.4 ng of selenium. The relative standard deviation (r.s.d.) for 50 ng of selenium was 8.6% (n = 10). The calibration graph was linear up to 400 ng of selenium.

Electrically-heated silica tube atomiser. Preliminary experiments were conducted with a Perkin-Elmer r.f. EDL as the radiation source. The silica tube was heated to 800°C and the argon sheathing gas was set at 8 l min^{-1}. Figure 3A shows the recorder tracings of signals produced by selenium and

a blank. The signals were erratic and the detection limit was 0.8 μg of selenium. A low argon flow rate (< 1 l min^{-1}) enabled oxygen from the surrounding atmosphere to penetrate the argon sheath and produce a small hydrogen diffusion flame at the atomiser head. The hydrogen is produced from the decomposition of the tetrahydroborate. The effect of the presence of the small flame on the atomisation efficiency of the hydride is shown in Fig. 3B. This signal, which is over twice as high as the signal obtained from 2 μg of selenium at 8 l min^{-1} argon, was obtained from only 0.1 μg of selenium. The background also increased somewhat, however. A flow rate of 0.5 l min^{-1} argon was low enough to allow a small hydrogen diffusion flame to burn at the atomiser head and also gave the extra advantage of protecting the nichrome wire from burning away too quickly. The detection limit was then 1.4 ng of selenium (microwave EDL) and the r.s.d. for 10, 50 and 200 ng of selenium was 6.8% (n = 5), 4.3% (n = 6) and 4.7% (n = 10), respectively. The calibration graph was linear up to at least 600 ng of selenium.

From previous experiments, it was known that a fuel-rich argon/hydrogen flame produced poorer signal-to-noise (S/N) ratios than a fuel-lean flame. Because most real samples require some pretreatment, it was necessary to

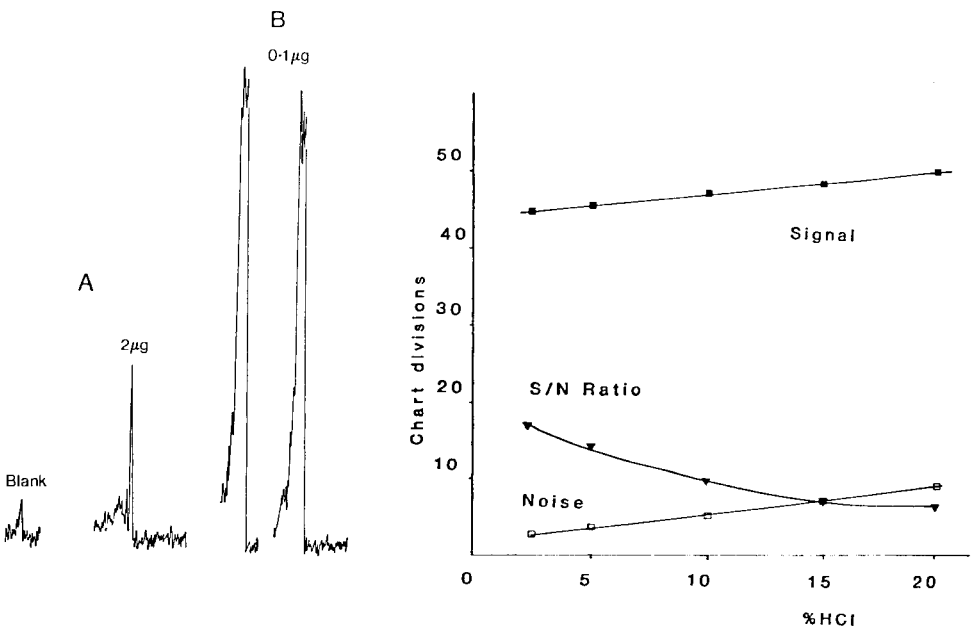

Fig. 3. Effect of argon sheath gas flow rate: (A) 8 l min^{-1} argon, 0 and 2.0 μg of selenium; (B) 0.5 l min^{-1} argon, 0.1 μg of selenium (25-ml samples, in 2% HCl, commercial r.f. EDL used).

Fig. 4. Effect of hydrochloric acid concentration on signal (S) and noise (N) measurements for the electrically-heated silica tube atomiser (50 ng of selenium).

TABLE 1

Comparison of the results obtained for the determination of selenium in blood sera by hydride-generation a.a.s. and hydride-generation a.f.s.

Sample	1	2	3	4	5	6	7	8	9	10
Se found (ng ml^{-1})										
a.a.s.	86	90	98	151	132	98	124	126	120	110
a.f.s.	82	89	104	149	130	104	124	123	124	114

evaluate the use of the atomiser with increasingly acidic samples. Figure 4 shows the signal, noise and S/N ratios at increasing acidities. The net effect is a decrease in S/N ratio with increasing acidity. To test the accuracy of the complete system, ten blood serum samples, which had previously been analysed by hydride-generation atomic absorption spectrometry (a.a.s.) [8] were analysed by the silica-tube a.f.s. method. The results are presented in Table 1. Statistical analysis on all the results indicated that the observed differences are not significant (paired t-test, $P = 0.73$).

Discussion

Of the two atom cells evaluated, the electrically-heated atomiser is preferred for hydride-generation a.f.s. It needed only low flow rates of gases through the optical path of the spectrometer. No additional diluting gases such as argon are added. The hydrogen ignites instantaneously at the atomiser head because it is preheated. When the addition of tetrahydroborate is stopped, this flame is extinguished. This atomiser also gave improved precision, a lower detection limit and an extended linear calibration range. In contrast, the glass atomiser gave relatively poor precision, although the detection limit was only 1.7 times worse than that for the electrically-heated atomiser. The detection limit obtained during this study was 1.4 ng of selenium. This compares with 0.06 ng [5], 0.4 ng [2] and 10 ng ml^{-1} [7] obtained by previous workers.

Work is now in progress to decrease the detection limit by improving the spectrometer and by making use of continuous-flow hydride generation and collection of the hydride in a liquid nitrogen trap prior to re-evaporation by rapid heating.

REFERENCES

1 D.R. Demers and C. D. Allemand, Anal. Chem., 53 (1981) 1915.
2 T. Nakahara, S. Kobayashi, T. Wakisaka and S. Musha, Appl. Spectrosc., 34 (1980) 194.
3 L. Ebdon, J.R. Wilkinson and K. W. Jackson, Anal. Chim. Acta, 128 (1981) 45.
4 R. Ferrara, A. Seritti, C. Barghigiani and A. Petrosino, Anal. Chim. Acta, 117 (1980) 391.
5 K. C. Thompson, Analyst (London), 100 (1975) 307.
6 K. Tsujii and K. Kuga, Anal. Chim. Acta, 97 (1978) 51.
7 J. Azad, G. F. Kirkbright and R. D. Snook, Analyst (London), 104 (1979) 232.
8 A. A. Brown, J. M. Ottaway and G. S. Fell, Anal. Proc., 19 (1982) 321.

Analytica Chimica Acta, 172 (1985) 335—340
Elsevier Science Publishers B.V., Amsterdam — Printed in The Netherlands

Short Communication

THE ISOLATION OF SOME POLYNUCLEAR AROMATIC HYDROCARBONS FROM AQUEOUS SAMPLES BY MEANS OF REVERSED-PHASE CONCENTRATOR COLUMNS

PAUL C. M. VAN NOORT* and ERIK WONDERGEM

National Institute for Public Health and Environmental Hygiene, Laboratory for Ecology, Water, and Drinking Water, P.O. Box 150, 2260 AD Leidschendam (The Netherlands)

(Received 8th November 1984)

Summary. The results for some polynuclear aromatic hydrocarbons (PAH) in canal water and rain water differ depending on whether the PAH are concentrated directly on Sep-Pak C-18 cartridges or concentrated after filtration with further analysis of the particulate matter. For canal waters, higher total PAH concentrations are obtained when the suspended material is also analyzed.

Polynuclear aromatic hydrocarbons (PAH) in the environment have been the subject of considerable attention in recent years [1]. Methods for the determination of PAH in aquatic environments have recently been reviewed [2]; they are mainly based on high-performance liquid chromatography (h.p.l.c.) and gas chromatography (g.c.) after isolation by liquid-liquid partition or the use of solid adsorbents. A procedure involving an enrichment on Sep-Pak C-18 cartridges followed by quantitative reversed-phase h.p.l.c. with fluorescence detection has been used in this laboratory. Recently, it has been reported that recoveries of PAH from water on Sep-Pak C-18 cartridges can be substantially enhanced by the addition of methanol [3] or 2-propanol [4] to the sample. It has been reported that suspended material in samples may significantly affect the recovery of PAH on liquid-liquid extraction [2]. It does not seem to have been established whether the Sep-Pak C-18 cartridges function as efficient filters for suspended materials and, if so, whether the elution of the cartridges with organic solvents would result in efficient desorption of the PAH. Therefore, in this communication, the results of a comparison of two isolation procedures for PAH in turbid water samples on Sep-Pak C-18 cartridges are reported. The procedures compared are direct concentration, and isolation of suspended matter by filtration prior to the concentration. In addition, comparison with a calibration graph and the standard additions method are evaluated for quantifying the data. Measurements were done on: (i) a standard solution of PAH in an organic solvent, (ii) a standard solution of PAH in deionized water, (iii) canal water with and without suspended material, (iv) canal water spiked with PAH with and without suspended material, (v) suspended material from canal water, and (vi) suspended material from canal water spiked with PAH.

0003-2670/85/$03.30

Experimental

Materials. Acetonitrile, tetrahydrofuran (THF) and water were of h.p.l.c. grade. The PAH investigated [fluoranthene, benzo(a)anthracene, benzo(b)-fluoranthene, benzo(k)fluoranthene, benzo(a)pyrene, benzo(ghi)perylene, and indeno(1,2,3-cd)pyrene] were obtained as the NBS Standard Reference Material 1647. The usual procedure for cleaning glassware (with detergent, followed by rinsing with deionized water and drying at 200°C) did not cause interference with the determination of PAH. Glass-fibre filters were obtained from Schleicher & Schull (No. 14).

H.p.l.c. A Waters Rad-Pak C-18 PAH column was used in a Waters radial compression module at 30°C. Isocratic elution with 50% acetonitrile/water for 2 min was followed by gradient elution linear to 100% acetonitrile in 30 min. The PAH in the effluent were detected with a fluorescence detector (λ_{ex} = 280 nm, $\lambda_{em} \geqslant$ 389 nm).

Sampling and sample treatment. Samples were collected from a canal near the laboratory by immersing a 20-l glass bottle, and were transported immediately to the laboratory, where 2-propanol was added to give a 15% (v/v) solution. Then the sample was divided into subsamples of 1100 ml under turbulent mechanical stirring. Samples were stored in the dark at 4°C. Suspended material was isolated from subsamples by filtration with suction on a glass-fibre filter.

Glass-fibre filters containing suspended material were extracted with 10 ml of THF by ultrasonication for 30 min. Repeated ultrasonication with THF proved this extraction to be complete.

Aqueous samples (1100 ml) were passed with suction through Sep-Pak C-18 cartridges, which were activated by elution with 5 ml of methanol and 5 ml of water. The compounds sorbed on the cartridge were eluted with 4 ml of THF. Prior to h.p.l.c., the THF solutions were evaporated almost to dryness under a gentle nitrogen stream. The residue was taken up in 300 µl of THF. The volume of the final solution was measured by weighing.

Results and discussion

Four subsamples of canal water were passed through Sep-Pak C-18 cartridges without additional filtration. The PAH were quantified by comparing the h.p.l.c. peak areas obtained with those from a solution of 10 µl of a PAH standard solution in 1100 ml of deionized water containing 15% (v/v) of 2-propanol taken through the same procedure. Another four subsamples were filtered on glass-fibre filters and then passed through Sep-Pak C-18 cartridges. The PAH desorbed from the filters were quantified by comparison with a standard PAH solution in acetonitrile. The PAH from the cartridges were quantified by the same procedure as for the unfiltered samples. The results are given in Table 1. It appears that, apart from fluoranthene, the PAH are recovered predominantly from the filter, with reasonable reproducibility. The data demonstrate that the concentrations of PAH found by separate analysis of filtrates and filters are about double those

TABLE 1

Concentrations of PAH in unfiltered canal water, in filtered canal water and in suspended material on the filter

Compound[a]	Concentration of PAH (ng l^{-1})[b]													
	Unfiltered				Average	Filtrate				Suspended material				Average total[c]
F	27	31	31	22	28 ± 18	30	9	23	30	23	24	21	16	44 ± 19
B(a)A	6	8	7	1	6 ± 27	2	1	3	7	10	10	9	6	12 ± 7
B(b)F	7	9	8	1	7 ± 31	2	nd	3	8	15	14	13	10	16 ± 11
B(k)F	4	6	5	2	4 ± 40	1	nd	1	5	9	9	8	6	10 ± 10
B(a)P	8	9	9	4	7 ± 32	1	nd	2	8	16	17	14	10	17 ± 5
B(ghi)P	9	nd	13	1	8 ± 79	nd	nd	2	12	18	20	18	14	21 ± 16
I(1,2,3-cd)P	12	10	15	6	11 ± 35	nd	nd	2	16	29	30	26	22	31 ± 15

[a] F = fluoranthene, B(a)A = benzo(a)anthracene, B(b)F = benzo(b)fluoranthene, B(k)F = benzo(k)fluoranthene, B(a)P = benzo(a)pyrene, B(ghi)P = benzo(ghi)perylene, I(1,2,3-cd)P = indeno(1,2,3-cd)pyrene.
[b] Average is the mean of four results with relative standard deviation (%), obtained from a calibration graph; nd indicates not detected, i.e., <1 ng l^{-1}. [c] Total PAH found in filtrate and suspended material.

found for the unfiltered sample. Furthermore, the standard deviations for the direct measurements (18—79%) are much higher than those obtained after initial filtration (5—19%). On the basis of these findings, it is concluded that filtration, prior to Sep-Pak C-18 concentration, with separate analysis of the filter and the filtrate yields higher and more reproducible values for concentrations of PAH in water.

However, this approach gives no definite conclusion on absolute recoveries of PAH. In order to investigate the effects of possible incomplete filtration on the accuracy of the data in Table 1, the data were also quantified by comparison with canal water samples spiked with PAH. To each of eight subsamples of canal water taken from the same bulk samples as those for the data in Table 1, 10 μl of a PAH standard solution was added. The mixtures were equilibrated overnight. The standard addition increases by ca. 500% the concentrations of the PAH as obtained by direct measurements. The results for the direct measurements on four spiked subsamples compared with the four unspiked samples are given in Table 2. The concentrations in the other four subsamples with additional filtration were calculated in the same way as for the unspiked samples. The results are given in Table 3.

Comparison of the calculated PAH concentrations in Table 2 with those in Table 1 for the concentration without additional filtration reveals reasonable agreement (within ca. 15%). This suggests high accuracy for the PAH concentrations obtained from measurements without additional filtration (Table 1). However, this conclusion is at odds with the higher PAH concentrations found on additional filtration (Table 1). The reason for this disparity can be found by comparison of the data for filtered samples. The ratios of the

TABLE 2

Peak areas for the calculation of PAH concentrations obtained by the procedure without filtration in spiked and unspiked samples

Compound[a]	Peak area (arbitrary units)[b]		PAH added (ng l^{-1})	Average conc.[c] (ng l^{-1})
	Unspiked	Spiked		
F	33.5 ± 18	167 ± 3	101	25 ± 2
B(a)A	15.7 ± 27	127 ± 6	50	7 ± 3
B(b)F	14.7 ± 31	98 ± 6	51	9 ± 4
B(k)F	16.7 ± 40	185 ± 5	50	5 ± 4
B(a)P	15.2 ± 32	100 ± 10	53	9 ± 4
B(ghi)P	2.1 ± 79	12.0 ± 16	40	8 ± 1
I(1,2,3-cd)P	5.15 ± 35	18.0 ± 15	41	16 ± 7

[a]See footnote to Table 1. [b]Mean and relative standard deviation of four results. [c]In unspiked sample.

TABLE 3

Concentrations of PAH in spiked canal water obtained on additional filtration

Compound[a]	Concentration of PAH (ng l^{-1})											
	Filtrate				Suspended material				Average total[b]	Added	Corrected total[c]	Difference[d]
F	121	132	124	133	29	27	37	26	157 ± 3	101	177 ± 4	76 ± 9
B(a)A	26	35	31	39	18	15	19	16	50 ± 9	50	61 ± 7	11 ± 39
B(b)F	17	25	21	30	31	27	33	29	53 ± 9	51	73 ± 6	22 ± 20
B(k)F	16	24	19	29	29	25	30	27	50 ± 9	50	68 ± 6	18 ± 23
B(a)P	14	23	18	26	35	30	33	32	53 ± 7	53	74 ± 4	21 ± 14
B(ghi)P	nd	nd	nd	nd	38	35	39	34	36 ± 7	40	60 ± 7	20 ± 21
I(1,2,3-cd)P	nd	nd	nd	nd	51	72	57	50	57 ± 18	41	95 ± 18	54 ± 32

[a]See footnote to Table 1. [b]Total PAH found in filtrate and suspended material with relative standard deviation. [c]Assuming 60% recovery from the filter. [d]Corrected total minus amount added.

amounts of PAH in the filtrates and on the filters for the unspiked samples (Table 1) differ substantially from those for the spiked samples (Table 3), e.g., for fluoranthene the ratios are about 1 and 4, respectively. Clearly, the behaviour of added PAH differs from that of PAH already present, and the similarity between the concentrations obtained from spiked samples and from a calibration graph does not necessarily mean that the direct measurement is accurate. In fact, the additional filtration measurements show that the direct measurement is inaccurate. The recovery of PAH from the suspended matter cannot be derived from the spiking experiments because of the partition differences. But this recovery can be estimated in the following way.

Close inspection of the data for the filtrates and the suspended material in Table 1 shows, for most of them, that above average values for the total of filtrate and filter are found for samples which gave below average values for the filters. For benzo(ghi)perylene for instance, the average total value from filtrate and filter is 21 and that for the suspended material is 17.5. This strongly suggests that the recovery from the filters is <100% which is in line with the data in Table 3 that demonstrate incomplete recovery of PAH (both added and already present) from the filters. Linear regression of the data for the filters and those for the total for filter and filtrate in Table 1 indicated, though with very poor correlation, recoveries from the filters of 40—80% for the PAH already present in the samples. The recoveries for the added PAH can be estimated, because of the good agreement between the data for the unfiltered measurements in Tables 1 and 2, to be the same as those for the isolation from the standard solution in deionized water, which were found to be 60—75% (Table 4). Accordingly, the recoveries from the filters for all PAH, both added and already present, are estimated to be approximately 60%. Recalculation of the data in Table 3 based on 60% recovery from the filters yields the data given as "corrected total". The difference between these data and those for the amount of PAH added affords an estimate of the actual average PAH concentrations in the samples (Table 3, last column). These concentrations agree reasonably well with those for the additional filtration measurements in Table 1 if a recovery of 60% is taken into account for the data on the filters in Table 1.

In order to investigate the influence of a less turbid water matrix on the differences between the two concentration methods, rain waters from three different locations were analyzed for PAH by the two methods. The results (Table 5) show that the additional filtration of samples 2 and 3 did not lead to additional recovery of PAH. In the case of sample 1, the filtration produced an additional recovery of ca. 50%, on the assumption of 100% recovery from the filters.

Conclusion

Filtration of water samples prior to Sep-Pak C-18 concentration with separate analysis of the filters usually results in higher PAH concentrations

TABLE 4

Percentage recoveries for PAH from deionized water containing 15% (v/v) 2-propanol

Compound[a]	Conc. (ng l^{-1})	Recovery (%)[b]	Compound[a]	Conc. (ng l^{-1})	Recovery (%)[b]
F	1010	74 ± 8	B(a)P	400	65 ± 3
B(a)A	505	73 ± 10	D(a,h)A	400	61 ± 8
B(b)F	511	67 ± 6	B(ghi)P	370	62 ± 10
B(k)F	500	66 ± 8	I(1,2,3-cd)P	405	59 ± 8

[a]See footnote to Table 1; D(a,h)A is dibenzo(a,h)anthracene. [b]Average of three determinations with standard deviation.

TABLE 5

Concentrations of PAH in rain water obtained with and without additional filtration

Compound[a]	Concentration (ng l^{-1})[b]					
	Sample 1		Sample 2		Sample 3	
	NF	F	NF	F	NF	F
F	175	219	88	87	156	162
B(a)A	33	47	21	23	20	23
B(b)F	55	84	51	55	39	46
B(k)F	29	41	27	20	21	24
B(a)P	27	38	21	22	21	23
D(a,h)A	5	11	7	7	5	5
I(1,2,3-cd)P	87	116	84	90	70	76
B(ghi)P	52	71	52	51	37	37

[a]See footnote to Table 4. [b]NF, without additional filtration; F, with additional filtration, sum of PAH in filtrate and suspended material.

relative to those from concentration without additional filtration. These differences are greater for surface water than for rain water. An additional advantage of filtration prior to Sep-Pak concentration is that clogging of the cartridges is prevented. It should be stressed that, although additional filtration leads to additional recovery of PAH, it cannot be concluded that direct concentration on Sep-Pak is inferior to additional filtration in all cases. In view of the different partition ratios in water-suspended material for PAH added and PAH already present, it may well be that the additionally recovered PAH are not available for the exchange between water and suspended material. Therefore, direct Sep-Pak concentration may afford information about the PAH available for water-suspended material exchange, where additional filtration may afford information about the total PAH content. The present results do not allow strict conclusions. Availability studies are needed to assess the true meaning of the results from the two different techniques.

This work was done within the framework of the Dutch National Coal Research Programme, managed by the Project Office for Energy Research, Netherlands Energy Research Foundation, and financed by the Ministry of Economic Affairs. The comments of Drs. Dik van de Meent, Ad Minderhoud and Jan Luijten were of great help.

REFERENCES

1 J. M. Neff, Polycyclic Aromatic Hydrocarbons in the Aquatic Environment, Applied Science Publishers, London, 1980.
2 A. E. McIntyre and J. N. Lester, Sci. Total Environ., 27 (1983) 201.
3 R. K. Symons and I. Crick, Anal. Chim. Acta, 151 (1983) 237.
4 N. v.d. Hoed, M. T. H. Halmans and J. S. Dits, in A. Bjørseth and G. Angeletti, (Eds.), Analysis of Organic Micropollutants in Water, D. Reidel, Dordrecht, 1982, p. 188.

Analytica Chimica Acta, 172 (1985) 341—346
Elsevier Science Publishers B.V., Amsterdam — Printed in The Netherlands

Short Communication

ION CHROMATOGRAPHIC DETERMINATION OF ALKALINE EARTH METALS AND SOME HEAVY METALS

O. A. SPIGUN, O. D. CHOPOROVA and YU. A. ZOLOTOV*

Institute of Analytical Chemistry, M. V. Lomonosov Moscow State University, Moscow (U.S.S.R.)

(Received 31st October 1984)

Summary. The method is described for ion chromatographic determination of Ba, Ca, Cd, Cu, Mn, Ni, Sr, Pb and Zn. Ethylenediammonium chloride or tartrate solutions are used as eluents with a suppressor column. The detection limits for the listed elements are (in $\mu g\ l^{-1}$): Ba 1.4, Ca 0.045, Cd 0.6, Cu 0.3, Mn 0.8, Ni 0.5, Pb 6.3, Sr 0.3, Zn 1.2. Relative standard deviations are 0.015—0.050 at the 20 mg l^{-1} level ($n = 5, p = 0.95$). Interferences are considered.

Ion chromatography [1] can be used for determining many organic and inorganic anions with high sensitivity [2—4]. With regard to metal cations, the method is mainly applicable to alkali and alkaline-earth metal ions when strong acids are used as eluents. The determination of heavy metals by the standard approach is complicated or impossible because of the precipitation of the metal hydroxides on the suppressor column in the hydroxide form. Thus, special conditions are necessary to determine heavy metals.

Several approaches have been described for the determination of heavy metals as cations, with and without a suppressor column, but using a conductivity detector. Alkaline earth metals have been determined with the use of silver(I) salt solutions as eluents [1]. The determination of some metals with the help of barium and lead salt solutions as eluents has also been reported [5]; the drawback of this method is the difficulty of regenerating the suppressor column. The alkaline earth elements have been separated with solutions of nitric acid containing zinc ions as eluent [6]; a suppressor column in the OH^--form was used. For the determination of cadmium in the presence of Ba, Ca, Cu, Co, Hg, Ni, Pb, Sr and Zn, solutions of hydrochloric acid containing aluminium can serve as eluents [7], again with the suppressor column in the OH^--form. To determine cations without a suppressor column [8, 9], organic eluents with low equivalent conductance have been suggested with the addition of complexing organic anions to the eluents. Thus, for determining alkaline earth and some heavy metals, ethylenediammonium tartrate has been recommended [9]. The drawback of determinations without a suppressor column is the low sensitivity caused by the comparatively high background eluent signal.

0003-2670/85/$03.30

In the work reported here, a similar approach was adopted, but with the application of a suppressor column (OH^--form) to increase the sensitivity. The behaviour of alkali and alkaline earth metals, Cd, Cu, Mn, Ni, Pb and Zn was studied when solutions of ethylenediamine with the addition of tartaric, hydrochloric or nitric acid were used as eluents.

Experimental

A Biotronik IC-1000 ion chromatograph was used. A cation-exchange column (3 × 100 mm) was applied as the separator column (capacity 0.032 meq ml^{-1}). The anion-exchange suppressor column was 3 × 100 mm. The sample loop volume was 50 μl, and the eluent flow rate was 1.0—1.6 ml min^{-1}.

Results

Without a suppressor column and with tartrate as the complexing anion, the results obtained here were similar to those reported earlier [9]; all the listed metals gave negative peaks with different retention times on the chromatograms. When the OH^--form suppressor column was used, the most successful eluents were solutions of ethylenediammonium chloride or tartrate. When nitrate was used, the cations were eluted as broad peaks with long retention times, and lead was not eluted at all. Obviously, this is connected with the low complexing ability of nitrate for these metal ions.

The order of cation elution from the separator column, when ethylenediammonium chloride or tartrate was used, was the same (Na + K, Zn, Ni, Mn, Cu, Cd, Ca, Sr, Pb, Ba) but in the case of chloride the retention times were rather shorter.

Chemistry of the processes. The reactions which take place on the column when ethylenediammonium is used as the eluent can be described as follows: on the separator column,

$$R_2{-}M^{2+} + AmH_2^{2+} = R_2{-}AmH_2^{2+} + \underset{\underset{ML}{\uparrow\downarrow}}{M^{2+}}\ L^{2-} \qquad (1)$$

and on the suppressor column,

$$2R{-}OH^- + L^{2-} = R_2L^{2-} + 2OH^- \qquad (2)$$

$$AmH_2^{2+} + OH^- = AmH^+ + H_2O \qquad (3)$$

Here AmH_2^{2+} represents ethylenediammonium, M^{2+} a metal ion, L^{2-} doubly-charged tartrate, and R the ion-exchange resin. The elution from the separator column, obviously, has two facets: metal ions are replaced by the ethylenediammonium ion AmH_2^{2+}, which has a higher affinity for the resin, and metal complexes are formed with tartrate or chloride.

The pH of the eluent plays an important rôle in the elution of cations from the separator column, as the pH value controls the equilibrium concentrations of AmH_2^{2+} and L^{2-} in the eluent. It was calculated that ethylenediamine exists mainly as AmH_2^{2+} ions at pH $\leqslant$ 6.0. When chloride serves as the

complexing anion, it is possible to use all the range pH $\leqslant 6.0$. According to the calculated and experimental data, it was found that when ethylenediammonium chloride is used, the optimal molar ratio of ethylenediamine to HCl is $\geqslant 1:4$ for the determination of metals. At lower concentrations of hydrochloric acid, the pH value becomes >6.0, which makes the peaks broader because the AmH_2^{2+} ion exists in other forms.

Tartaric acid exists mainly as L^{2-} at pH $\geqslant 5.0$. Obviously, the optimal range of pH for ethylenediammonium tartrate is 5.0—6.0; ethylenediamine and tartrate are then both present mainly as doubly-charged ions, the necessary condition for the separation and determination of the metals. The optimal molar ratio of ethylenediamine to tartaric acid was found to be 1:1.5. The pH of the eluent was then 5.5, which corresponds to the existence of 95% of ethylenediamine as AmH_2^{2+} and 90% of tartaric acid as L^{2-}. If the concentration of tartaric acid in the eluent is decreased, the eluent pH, as in the case of chloride, becomes >6.0 and the AmH_2^{2+} ion is converted to other forms. But if the concentration of tartaric acid is increased, the pH of the eluent decreases, which leads to a decrease in the equilibrium concentration of tartrate and so to decreased complex formation between tartrate and the metals.

On the suppressor column, the doubly-charged ethylenediammonium ion turns into AmH^+ (Eqn. 3) because of the interaction with hydroxide groups, which are replaced here by chloride or tartrate (Eqn. 2). The pH value of the eluent after the suppressor column is 7.8—8.0, which corresponds to the existence of the singly-charged ethylenediammonium cation.

Chromatograms. In both cases, if the above eluents, ethylenediammonium tartrate or ethylenediammonium chloride, and the suppressor column are used, Ba^{2+}, Sr^{2+}, Ca^{2+}, Cd^{2+}, Ni^{2+}, and Cu^{2+} give positive peaks on the chromatogram (Figs. 1 and 2); in contrast, Zn^{2+}, Mn^{2+} and Pb^{2+} give negative peaks (Fig. 3) because they are not eluted from the suppressor column. The negative peaks are due to deionized water passing through the conductivity detector; the water is produced when the metals are retained on the suppressor column as their tartrate or chloride complexes. The increase in retention time for lead and the broader peak formed from chloride solutions than from tartrate solutions (10.2 and 6.6 min, respectively) can be explained by the low solubility of lead chloride.

The behaviour of these two eluents also differs with respect to copper. In the case of tartrate, the peak height and retention time for copper depend on the degree of loading of the suppressor column; the longer the suppressor column works, the broader is the peak. This is obviously connected with the formation of very stable tartrate complexes of copper; the more hydroxide ions are replaced by tartrate on the suppressor column, the more copper is retained on it as the tartrate complexes. If the ethylenediammonium chloride is used, nothing of this kind is observed.

Determination of metals. The above investigations of eluents containing ethylenediamine and tartaric or hydrochloric acid in different concentrations

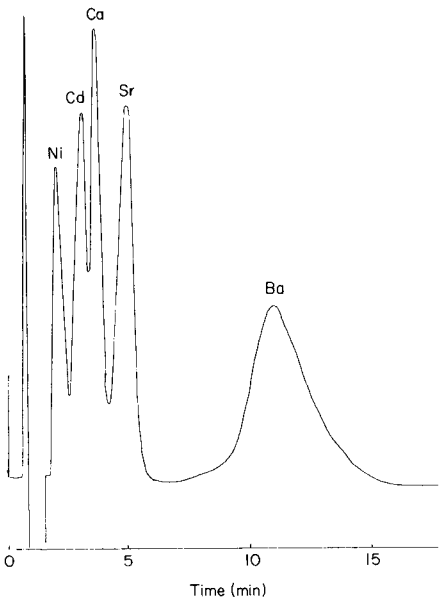

Fig. 1. Chromatogram of a solution containing nickel, cadmium, calcium, strontium and barium. Eluent, 4×10^{-4} M ethylenediamine/6×10^{-4} M tartaric acid; $C_{Ni} = C_{Cd} = C_{Sr} = C_{Ba} = 5$ mg l^{-1}; $C_{Ca} = 0.5$ mg l^{-1}; eluent flow rate 1.4 ml min^{-1}; sensitivity of conductivity detector 10 μS.

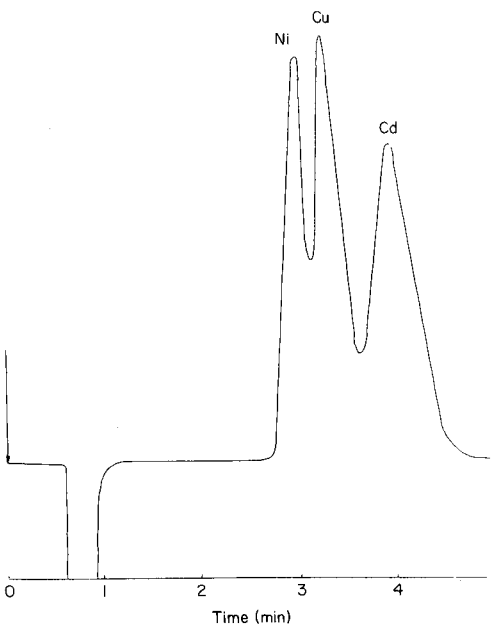

Fig. 2. Chromatogram of a solution containing nickel, copper and cadmium. Eluent, 4×10^{-4} M ethylenediamine/1.6×10^{-3} M hydrochloric acid; $C_{Bi} = C_{Cu} = C_{Cd} = 5$ mg l^{-1}; eluent flow rate 1.4 ml min^{-1}; sensitivity of conductivity detector 10 μS.

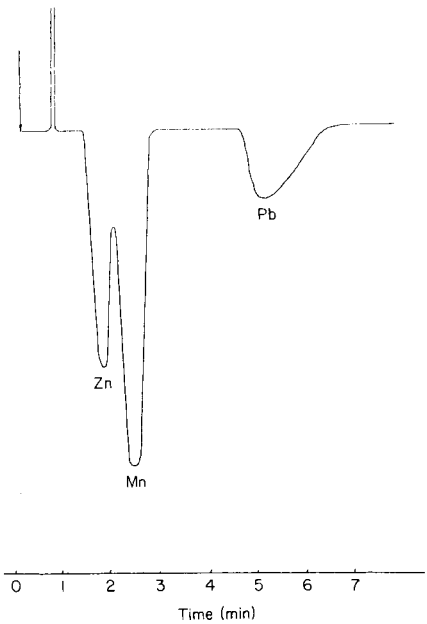

Fig. 3. Chromatogram of a solution containing zinc, manganese and lead. Eluent, flow rate and sensitivity as for Fig. 1; $C_{Zn} = C_{Mn} = C_{Pb} = 5$ mg l^{-1}.

and ratios, and of pH effects, made it possible to select optimal eluent conditions. For the determination of metals, the following eluents are the most suitable: 4×10^{-4} M ethylenediamine/1.6×10^{-3} M hydrochloric acid or 4×10^{-4} M ethylenediamine/6×10^{-4} M tartaric acid. With these eluents Ba, Ca, Cd, Cu, Ni and Sr can be determined by their positive peaks and Mn, Pb, Zn by their negative peaks.

The detection limits were calculated from the calibration graphs (3σ criterion) for each metal. The values found were (in μg l^{-1}) for Ba 1.4, for Ca 0.045, for Cd 0.6, for Cu 0.3, for Mn 0.8, for Ni 0.5, for Pb 6.3, for Sr 0.3, and for Zn 1.2. These detection limits are on average two orders lower than the detection limits reported earlier [9]. The reproducibility of the separate determinations of cadmium, nickel, lead and zinc (20 mg l^{-1}) eluted with 4×10^{-4} M ethylenediamine/4×10^{-3} M tartaric acid at 1 ml min^{-1} was established; the relative standard deviations were 0.017, 0.015, 0.046 and 0.051, respectively ($n = 5, p = 0.95$).

The determination of the metals studied is not affected by alkali metals or iron(III) which are not retained on the columns. Aluminium and mercury also do not interfere because they are not eluted from the column at all. Barium and lead do not influence the determination of the other metals because they have comparatively long retention times.

It can be seen from Figs. 1—3 that in some cases studied, the metals are

TABLE 1

Tolerable molar ratios of the metals determined giving a resolution R of 0.3 (eluent, 4×10^{-4} M ethylenediamine/1.6×10^{-3} M tartaric acid)

Metal	Interfering metals							
	Ba	Ca	Cd	Mn	Ni	Pb	Sr	Zn
Ba	—	2000	4000	100 000	7000	100 000	400	100 000
Ca	1 000 000	—	10	300	30	35 000	20	2 500
Cd	20 000	0.1	—	1	1.5	100 000	5	6
Mn	25 000	30	1	—	0.2	150 000	200	1.5
Ni	50 000	0.3	1.5	0.5	—	250 000	60	5
Pb	4 000	30	1000	2 000	1500	—	3	4 000
Sr	8 000	1.5	20	2 000	150	1 000	—	1 500
Zn	100 000	40	1.5	1	0.8	100 000	300	—

not separated ideally. The mutual effect can be rather high and positive and negative peaks may overlap. In Table 1 are listed the molar ratios of the elements that give peaks overlapping by more than 50% (criterion of separation, R = 0.3). The calcium determination is affected by a 10-fold amount of cadmium and a 20-fold amount of strontium. Even small amounts of calcium and comparable quantities of nickel and manganese interfered with the cadmium determination. Small amounts of nickel and comparable amounts of cadmium or zinc affect the manganese determination. Nickel can be determined in the presence of only small quantities of calcium or manganese and comparable quantities of cadmium and zinc. The determination of strontium is influenced by similar amounts of calcium, while large amounts of other metals can be tolerated. The determination of zinc suffers interference from comparable amounts of cadmium, nickel and manganese.

REFERENCES

1 H. Small, T. S. Stevens and W. C. Bauman, Anal. Chem., 47 (1975) 1861.
2 F. C. Smith and R. C. Chang, Crit. Rev. Anal. Chem., 9 (1980) 197.
3 O. A. Shpigun and Yu. A. Zolotov, Zavodsk. Labor., 48 (1982) No. 9, 4.
4 C. A. Pohl and E. L. Johnson, J. Chromatogr. Sci., 18 (1980) 442.
5 F. R. Nordmeyer, L. D. Hansen, D. G. Eatough, D. K. Rollins and J. D. Lamb, Anal. Chem., 52 (1980) 852.
6 J. W. Wimberley, Anal. Chem., 53 (1981) 2137.
7 O. A. Shpigun, L. A. Bubchikova, O. D. Choporova and Yu. A. Zolotov, in Methods of environmental samples analyses, Abstracts of the papers of All-union conference, Moscow, 1983.
8 J. S. Fritz, D. I. Gjerde and R. M. Becker, Anal. Chem., 52 (1980) 1519.
9 G. J. Sevenich and J. S. Fritz, Anal. Chem., 55 (1983) 12.

Analytica Chimica Acta, 172 (1985) 347—352
Elsevier Science Publishers B.V., Amsterdam — Printed in The Netherlands

Short Communication

THE USE OF SILICALITE AS A COLUMN PACKING FOR STEAM-SOLID CHROMATOGRAPHY

DUNCAN J. CAMPBELL, BARRIE M. LOWE, ALAN G. ROWLEY* and RUTH WILLIAMS
Department of Chemistry, University of Edinburgh, West Mains Road, Edinburgh EH9 3JJ (Great Britain)

(Received 3rd November 1984)

Summary. Chromatographic-grade silica gel can be converted to a form of the high-silica zeolite silicalite-1, which is suitable for use as a gas chromatographic column packing and can be used with steam as carrier gas in a suitably modified chromatograph. The material has the expected molecular sieve properties and lends itself to some novel separations based on molecular size and shape. The behaviour of lower aliphatic alcohols and chlorohydrocarbons, acetone and xylenes is reported.

Steam or a steam/nitrogen mixture has been used as a carrier gas in gas chromatography; Teply and Dressler [1] reviewed the field fairly recently. The addition of a little steam to the nitrogen carrier reduces the tailing of peaks from polar compounds but otherwise the chromatography seems to be largely unaffected [2], whereas the chief reported advantage of steam as the main component of the carrier gas is to allow the injection of relatively large volumes of aqueous samples onto the column without serious perturbation in the chromatography [1]. The latter aspect was of particular interest here; it was considered that the use of a polar carrier gas might, with suitable stationary phases, allow some interesting separations.

Analysis for organic contaminants in water by gas chromatography normally requires liquid-liquid extraction of the analytes before injection. This procedure serves not only to avoid any effect of water on the chromatography but also as a pre-concentration step, particularly if the bulk of the extraction solvent is removed by distillation. This type of technique is not suitable, however, if the analytes are very polar and/or volatile because the extraction may be inefficient and the removal of the solvent may lead to sample loss. Some potential contaminants in waste waters fall into these categories, e.g., the lower aliphatic alcohols and ketones.

Steam-solid chromatography seemed to offer an alternative to liquid-liquid extraction but it was necessary to find a suitable stationary phase. The requirements are stringent because the material must be stable in super-heated steam and have a high affinity for organics, including some highly polar

0003-2670/85/$03.30

compounds, even when elution is done with a highly polar carrier gas. This is an unusual situation in gas chromatography where the mobile phase is normally very inert.

The most successful stationary phases reported to date for steam-solid chromatography [1] seem to be porous silicas such as Porasil F, either pretreated with phosphoric acid or used as manufactured; however, the ability of such materials to retain and separate even highly polar molecules is often poor. The high-silica zeolites were considered for stationary phases for this type of chromatography because they are stable in aqueous environments at high temperature and are well known [3] to adsorb even highly polar organics from water. In addition, it seemed possible that the molecular-sieve properties of the zeolites might admit of some interesting chromatographic variations.

For these investigations, the silica molecular sieve, silicalite-1, was chosen; this is the "aluminium-free" form of the high-silica zeolite ZSM-5 [4]. It has been claimed that when prepared with tetrapropylammonium fluoride as a template, the resulting silicalite can be used as a column packing for gas and liquid chromatography; this claim has been exemplified by the chromatographic separation of low-molecular-weight alcohols [5]. However, as conventionally prepared with tetrapropylammonium hydroxide as the template, the crystals are usually too small ($<10\ \mu m$) for use in gas chromatography. To circumvent this problem, an attempt was made to convert chromatographic-grade silica gel to silicalite-1 without changing the overall particle morphology.

Experimental

The conversion of Kieselgel 60 (35—70 mesh ASTM; Merck) to silicalite was effected by heating it for 9 days at 150° C with an aqueous solution of piperazine hexahydrate (PIPZ 98%; Aldrich) and tetrapropylammonium bromide (TPABr; 98%, Aldrich) in a stirred (50 rpm) stainless-steel autoclave. The overall composition of the reaction mixture was: 10 PIPZ, 2 TPABr, 20 SiO_2, 1000 H_2O. The product was filtered off, washed with distilled water and dried at 100° C. The organic component was removed by calcination at 500° C for 16 h and the product was treated with 0.1 M hydrochloric acid (10 ml g^{-1} of silicalite) for 30 min at room temperature. It was then washed with water and dried at 100° C. The materials before and after calcination were examined by x-ray powder diffraction (Philips diffractometer) with Cu K_α radiation and by scanning electron microscopy on a Cambridge Instruments 604 microscope.

For examination of their chromatographic properties, the materials were packed into glass columns (1.5 m × 4 mm i.d.). A Pye 104 chromatograph fitted with a flame ionisation detector was modified for use with steam as the carrier gas. This was done as reported by Teply and Dressler [1] except that a facility was included to warm and cool the column with nitrogen as carrier gas and steam was used only when the operating temperature, normally 140—160° C, had been reached. This prevented build-up of water on the

column and corrosion of the detector. The nitrogen/steam circuit is shown in Fig. 1.

Results and discussion

Silicalite column packings. The preparation of the column packings was repeated several times. In every case, the product before and after calcination was highly crystalline and had the x-ray powder diffraction pattern of silicalite-1. Scanning electron microscopy showed that the overall morphology of the gel particles was maintained, although deep fissures were formed along their original sharp edges. The external flat surfaces were seen to be composed of tiny crystallites (<1 μm) and the insides of the particles as seen in the fissures were entirely composed of larger (2–6 μm) crystals. Thus it appeared that the whole of the silica gel particles had been converted to silicalite without change in their external morphology. It is believed that this is the first time that such a conversion has been achieved. One reason for the immediate success of the preparation is probably the use of an amine to provide alkalinity and to control the pH of the reaction mixture [6]. However, it is likely that with suitable compositions, similar conversions could be achieved with strong bases.

Chromatographic performance. All the materials were tested with the standard mixture shown in Table 1; a typical chromatogram is shown in Fig. 2. The peak shapes were excellent, even for the most polar materials,

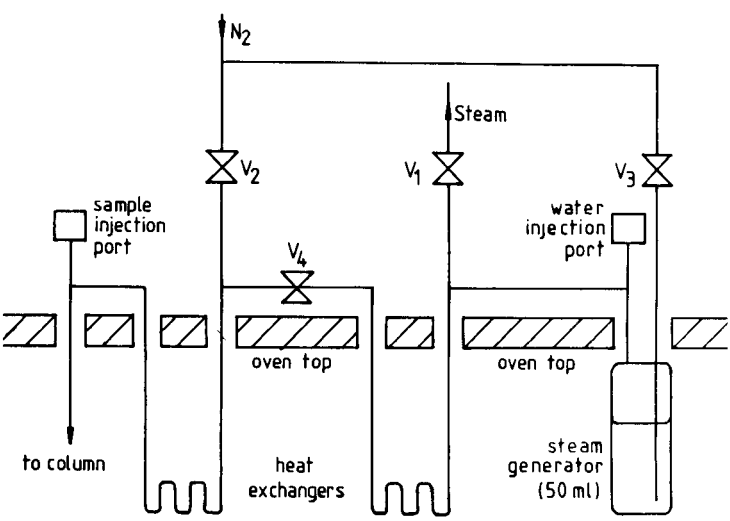

Fig. 1. Schematic diagram of the steam generator for Pye 104 chromatograph. When nitrogen is used, V2 is open to admit nitrogen, V4 is closed, and V1 is open to vent steam. For steam operation, V2 and V1 are closed with V4 open to admit steam to the column. At all times, V3 is adjusted to admit a steady stream of bubbles into the steam generator vessel to promote steady boiling.

TABLE 1

Comparison of retention times with steam or nitrogen as carrier gas at 168° C on a silicalite column packing

Compound	Retention time (min)		Compound	Retention time (min)	
	Steam	Nitrogen		Steam	Nitrogen
Methanol	0.8	—[a]	*p*-Xylene	4.2	3.0
Dichloromethane	2.1	2.8	Acetone	6.2	—[a]
Ethanol	2.8	—[a]	Propanol	9.9	—[a]
Chloroform	2.8	4.2			

[a]Not eluted after 30 min.

and resolution, although not to the baseline in all cases, was generally acceptable. The material did, indeed, have the properties to be expected from a molecular sieve. This was confirmed by the chromatography of the three isomeric xylenes; the 1,2- and 1,3-isomers were both eluted within 0.25 min, whereas the more symmetrical 1,4-isomer had a retention time of 4.2 min. This is exactly the behaviour to be expected of silicalite-1 because only the 1,4-xylene can gain ready access to the cavities, the other isomers being sorbed slowly because of their shape and size [7]. Further confirmation was obtained by chromatography of the xylenes on a silica gel column, again with a steam carrier gas; all three isomers eluted as one poorly resolved peak with a retention time of 3 min.

Studies were also conducted with ethylene glycol and glycerol, neither of which would be expected to have a particularly high affinity for the essentially non-polar cavities in the zeolite. It was hoped, therefore, that these materials would elute rapidly because they would be expected to have a high affinity for the steam. In the event, they were both eluted after more than 30 min as very broad peaks. This indicates that there are chromatographically active sites on the surface of the zeolite, possibly free hydroxyl groups, and that the polyhydric alcohols are strongly adsorbed. In order to try to confirm this, ethylene glycol and glycerol were chromatographed on a silica column, with steam carrier gas, and the results were identical to those obtained with the zeolite packing. This suggests that surface sites may be involved in the adsorption. Attempts to deactivate the zeolite surface by silylation resulted in degradation of the material to a fine powder which was quite unsuitable for use as a gas chromatographic packing. This aspect is the subject of further investigations.

The properties of the zeolite with a nitrogen carrier were studied in order to try to elucidate the role of the steam. With a nitrogen carrier gas, the highly polar materials such as the alcohols and ketones were not eluted at all, whereas the xylenes and chlorohydrocarbons gave peaks with retention times similar to those obtained with steam. When the carrier gas was changed to

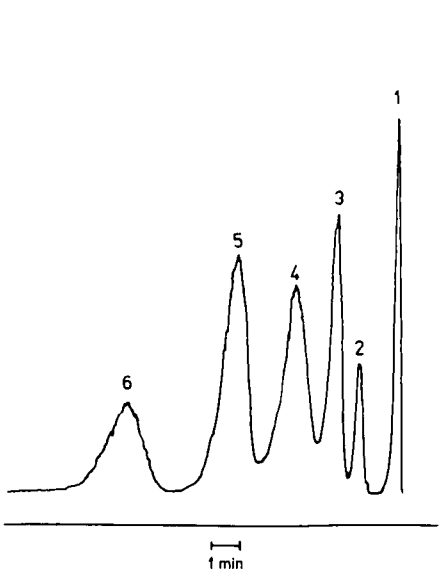

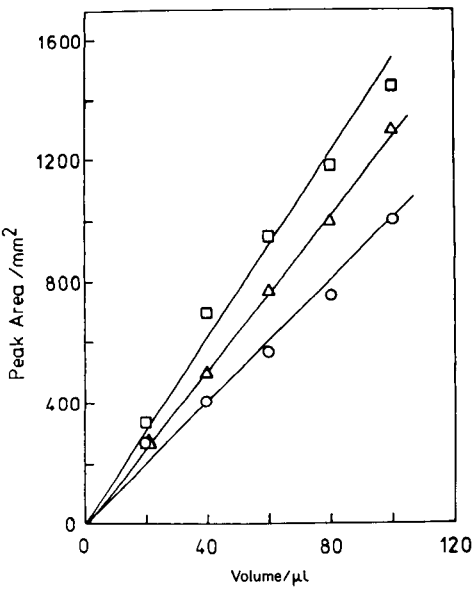

Fig. 2. Chromatogram obtained with steam and silicalite at 168° C. Peaks: (1) methanol; (2) dichloromethane; (3) ethanol; (4) *p*-xylene; (5) acetone; (6) propanol.

Fig. 3. Relationship between volume of aqueous 1000 mg l^{-1} solutions injected and peak area: (○) methanol; (□) ethanol; (△) acetone. Conditions as Fig. 2.

steam, however, the polar materials were eluted with the retention times that they would have had if injected at the time that the steam was introduced. The effect of injecting the polar analytes under nitrogen is similar to that of a stopped-flow injection. The possibility opens up of using the system in a new way by eluting all the non-polar materials with nitrogen and then changing to steam to examine the chromatogram of the polar components of a mixture. To illustrate this possibility, the separation of chloroform and ethanol, which are unresolved by the steam carrier gas, was examined. Injection of the mixture under nitrogen gave a peak for chloroform, the carrier gas was then changed to steam, and the ethanol was eluted. This would seem to be a technique with some potential, being somewhat akin to gradient elution in liquid chromatography.

Detection limits, linearity and injection size. The detection limit of the technique was rather disappointing. The performance of the flame ionisation detector is reduced when steam is the carrier gas [1], but this is mitigated to some extent when aqueous samples are used because the volume injected can be comparatively large. In practice, it was possible to inject up to 500 μl of aqueous solutions before the time taken for the injection itself became so long as to degrade the separation. With this injection volume, it was possible to detect all the components of the test mixture down to concentrations of 0.5 mg cm^{-3}.

The results of a linearity study with ethanol, methanol and acetone are shown in Fig. 3. The linear range is acceptable, although rather poorer for ethanol than the other two components. The effect of the injection volume on linearity of response was also checked and found to be satisfactory. For example, a 500-μl injection of aqueous 100 mg l^{-1} methanol solution gave the same peak area, within 3%, as a 50-μl injection of a solution with 1000 mg l^{-1} methanol.

Conclusions

It is possible to convert chromatographic-grade silica gel to highly crystalline aggregates of silicalite without changing the overall morphology of the particles. This crystalline packing material is particularly suitable for steam-solid chromatography, but it may also be used for conventional gas chromatography. It should be possible, by similar procedures, to produce highly crystalline aggregates of other silica molecular sieves (e.g., ZSM-48 [8]) and high-silica zeolites, each suitable for particular chromatographic separations by steam-solid chromatography.

REFERENCES

1 J. Teply and M. Dressler, J. Chromatogr., 191 (1980) 221.
2 H. S. Knight, Anal. Chem., 30 (1958) 2030.
3 N. B. Milestone and D. M. Bibby, J. Chem. Tech. Biotechnol., 31 (1981) 732.
4 E. M. Flanigen, J. M. Bennet, R. W. Grose, J. P. Cohen, R. L. Patton, R. M. Kirchner and J. V. Smith, Nature (London), 271 (1978) 512.
5 T. P. J. Izod and J. A. Duisman, U.S. Patent 4375568 (1983).
6 S. G. Fegan and B. M. Lowe, paper in preparation.
7 P. Wu, A. Debebe and Y. H. Ma, Zeolites, 3 (1983) 118.
8 A. Araya and B. M. Lowe, J. Catal., 85 (1984) 135.

Analytica Chimica Acta, 172 (1985) 353—357
Elsevier Science Publishers B.V., Amsterdam — Printed in The Netherlands

Short Communication

DETERMINATION OF IRON(III) AND ALUMINUM IN SOLUTION WITH A PIEZOELECTRIC QUARTZ CRYSTAL COATED WITH SILICONE OIL

T. NOMURA* and M. ANDO

Department of Chemistry, Faculty of Science, Shinshu University, Asahi, Matsumoto 390 (Japan)

(Received 28th August 1984)

Summary. The frequency of the crystal connected to an integrated circuit oscillator changed on absorption of iron(III) or aluminum at pH 3.8—5.8 and 5.0—6.0, respectively. Absorption of iron(III) at pH $\geq$ 5.0 was prevented by addition of excess of sulfate. Iron(III) was determined at pH 4.7; 5—100 μM solutions of both species may be determined with a r.s.d. of $\leq$3%.

Piezoelectric quartz crystals have been tested extensively for analytical purposes since Sauerbrey [1] reported that the frequency F (MHz) of such a crystal having electrode area A (cm^2) changes with the weight change ΔW (g) of the electrode according to the equation $\Delta F = -2.3 \times 10^6 F^2 \Delta W/A$, where ΔF is the frequency change (Hz). Generally, it has been supposed that the crystal oscillates only when dry. Thus substances in solution are determined by the frequency difference before and after the reaction of the crystal electrode with the substance in solution, obtained after drying the crystal. The determination is thus time-consuming and the reproducibility poor [2].

A piezoelectric crystal connected to a transistorized oscillator is able to oscillate in solution and the frequency changes with changes in the specific conductivity and specific gravity of the solution. The crystal, therefore, can be used to determine, in situ, substances in solution if the solution properties are maintained constant with a buffer solution [3]. Because there is an electrical potential between the electrodes on the crystal, some metal ions electrodeposit spontaneously onto the electrodes [4]. The resulting frequency change, however, could only be measured by using a cell in which the solution was in contact with one of the electrodes [4]. Only silver and mercury were found [5] to deposit spontaneously onto the electrodes of a crystal connected to an integrated circuit (i.c.) oscillator [6]. Silicone oil coated on such a crystal is sufficiently insoluble in water to give a constant frequency. It absorbs iron(III) and aluminum from aqueous solution, which forms the basis for the sensitive determination of these metal ions described in this communication.

0003-2670/85/$03.30

Experimental

Apparatus and reagents. The piezoelectric quartz crystal used was a 9-MHz, AT-cut crystal (Toyo Craft) having a platinum-plated gold electrode (5-mm diameter) on each side. The crystal was rubbed with silicone oil (Sanwa Kasei, ST-200) on soft paper, resulting in a frequency decrease in water of 1—2 kHz. The crystal was set in a flow cell [5] and directly connected to an i.c. oscillator [6] supplied with 4.5 V by a variable transformer (Metronix 521C). The peristaltic pump (Tokyo Rikakikai, MP-3), the sample and reagent blank vessels and the oscillator were assembled in an air bath thermostated at 25 ± 0.5°C. The cell temperature was controlled with circulating thermostated water (20 ± 0.1°C) from a water bath (Taiyo Thermo Unit, C-650). The frequency change was monitored by a digital counter (Takeda Riken, TR-5143G) and recorder (Nippon Kagaku, U-228).

Iron(III) and aluminum(III) stock solutions (0.01 M) were prepared by dissolving their nitrates in dilute nitric acid, and were standardized with 0.01 M EDTA.

Procedure. Transfer the sample or standard solution, 0.01 M in acetate buffer (pH 4.7 for iron(III), pH 5.7 for aluminum) and 0.5 mM in sodium sulfate (to prevent interference from iron(III) in aluminum determinations) and leave for ca. 40 min for iron(III) or 20 min for aluminum and the reagent blank, in their respective containers. Pass the reagent blank solution through the cell at 6.1 ml min^{-1}. When the crystal frequency has become constant (F_1), pass the sample solution for exactly 5 min and then the reagent blank solution until the frequency is again constant (F_2). Measure the frequency change, $\Delta F = F_1 - F_2$, which is proportional to the concentration of iron(III) or aluminum. A calibration graph is constructed on this basis. After each series of runs, pass 0.01 M citric acid through the cell for about 5 min to remove metal ions (see below).

Results and discussion

Absorption of iron(III) or aluminum on the silicone oil coating. Iron(III) or aluminum solution containing 0.01 M acetate (pH 5.5) changed the frequency of the uncoated crystal, which has platinum-plated gold electrodes, but the change was observed only during the first run unless 0.01 M citric acid was passed through the cell between runs to remove the absorbed substance. However, the crystal coated with silicone oil changed frequency on each repeated run without citric acid washing and had a larger frequency change than the uncoated crystal. Almost the same frequency change was observed for a crystal connected to an oscillator which had its power cut off while the solution was passing through the cell. In addition, the frequency change was observed on a crystal, one electrode of which was covered to prevent electrolysis [4]. The pH values at which absorption of these metal ions occurred were in agreement with the pH values at which their hydrated oxides precipitate, as calculated from the solubility products. It may be concluded, therefore, that the frequency change results from the preferential

absorption of hydrated iron(III) or aluminum oxides into the silicone oil. Iron(III) or aluminum absorbed in this way could partly be removed by passing 0.01 M hydrochloric acid through the cell for about 5 min, but completely removed with 0.01 M citric acid for 5 min.

The amount of silicone oil coated on the crystal affected the frequency change caused by the absorption of iron(III) or aluminum, as shown in Fig. 1. The crystal oscillated in solution even when it did not oscillate in air, when coated with large amounts of silicone oil. The best amount of silicone oil was in the range corresponding to a frequency decrease of 1—2 kHz in solution. The crystal was cleaned by dissolving the silicone oil in chloroform and recoated when signals became irreproducible.

Effects of experimental variables. The frequency changes resulting from absorption of iron(III) and aluminum at various pH values are shown in Fig. 2. The frequency change at ca. pH 5.8 for iron(III) had poor reproducibility. Iron(III) could be determined without interference from aluminum when the pH was ca. 4.7. Aluminum was absorbed only above pH 5.0, as was iron, but the total frequency changes caused by iron(III) and aluminum were not additive. Thus aluminum should be determined under conditions of no interference by iron(III) (see below). Above ca. 5 ml min^{-1}, the flow rate of iron(III) solution had almost no effect on the frequency change for 0.1 mM iron(III); at lower flow rates, the frequency change was also lower. The formation of the hydrated oxide was complete ca. 25 min after mixing the buffer and iron(III). Standing times of 25—180 min gave rise to a constant

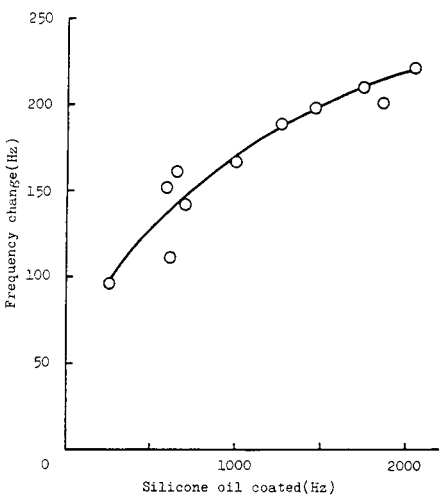

Fig. 1. Dependence of frequency change on the amount of silicone oil coated on the crystal. Conditions: 0.1 mM Fe(III), pH 4.7 (0.01 M acetate), flow rate 6.1 ml min^{-1}, reaction time 5 min.

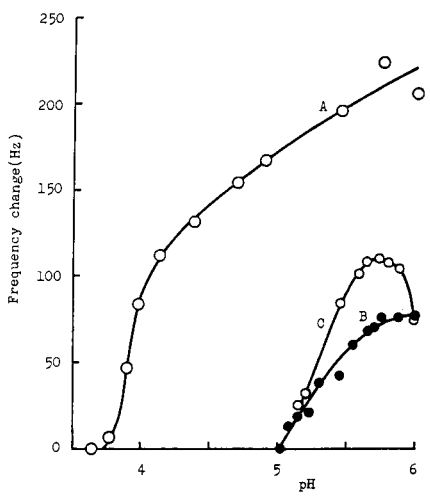

Fig. 2. Dependence of frequency change on pH: (A) for 0.1 mM Fe(III); (B) for 50 μM Al; (C) for 50 μM Al(III) with 0.5 mM sulfate. Other conditions as in Fig. 1.

frequency change. After ca. 3 h, the precipitate adhered to the wall of the glass vessels, resulting in decreasing frequency changes with increasing standing times.

Determination of aluminum. Aluminum could not be determined from the difference between the frequency changes found at pH 4.7 and pH 5.7, because, as mentioned above, the frequency changes were not additive. However, interference from iron(III) could be avoided by adding sulfate. Sulfate (50 mM) added to the aluminum sample caused an increased frequency change, as shown in Fig. 3; this frequency change increased with standing time for 10 min, was constant for a further 20 min and decreased thereafter by 1 Hz min^{-1}. It was presumed that aluminum gradually formed a hydrated basic sulphate which absorbed on the crystal and then on the vessel walls. Consequently the measurement was made 20 min after mixing.

Calibration and reproducibility. The calibration graphs of ΔF vs. iron(III) or aluminum concentration were linear over the range 5—100 μM, and are described by the equations [Fe(III)] = $(\Delta F/18.8) \times 10^{-5}$ M, and [Al] = $(\Delta F/22.9) \times 10^{-5}$ M, where ΔF is in Hz. The standard deviations were 2.80 Hz (2.98%) or 2.83 Hz (2.47%) for 8 determinations of 50 μM iron(III) or aluminum, respectively.

Effect of other ions. The effects of various ions on the determination of 0.1 mM iron(III) or aluminum were investigated. Frequency changes of >5% (i.e., 2σ) were considered to result from interferences. Sulfate, phosphate or chromate in equimolar amounts interfered in the determination of iron(III) at pH 4.7. These ions as well as lead and iron(III) interfered with the determination of aluminum at pH 5.7. The anion interferences were caused by the formation of precipitates. Lead(II) was probably absorbed as its basic acetate, resulting in high recoveries; the interference could be eliminated by precipitation of lead sulfate at pH <3 and filtration.

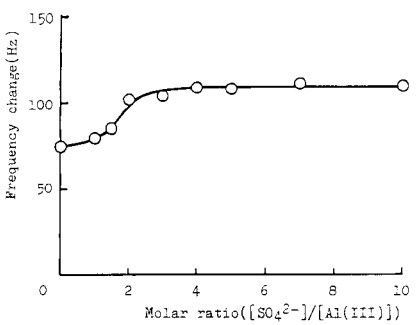

Fig. 3. Dependence of frequency change for 50 μM aluminum on its molar ratio to sulfate. Other conditions as in Fig. 1.

The authors gratefully acknowledge the financial support of research grants from the Education Ministry of Japan.

REFERENCES

1 G. Sauerbrey, Z. Phys., 155 (1959) 206.
2 J. L. Jones and J. P. Mieure, Anal. Chem., 41 (1969) 484.
3 T. Nomura and A. Minemura, Nippon Kagaku Kaishi, 1980 (1980) 1621.
4 T. Nomura and M. Maruyama, Anal. Chim. Acta, 147 (1983) 365.
5 T. Nomura and K. Tsuge, Anal. Chim. Acta, 169 (1985) 257.
6 S. Nakajima, Transistor Gijutsu, 19 (1982) 348.

Analytica Chimica Acta, 172 (1985) 359—364
Elsevier Science Publishers B.V., Amsterdam — Printed in The Netherlands

Short Communication

DETERMINATION OF GOLD IN LEACH LIQUORS BY ANODIC STRIPPING VOLTAMMETRY IN NON-AQUEOUS MEDIUM

KAREL JAKUBEC* and ZDENĚK ŠÍR

Institute of Chemical Process Fundamentals, Czechoslovak Academy of Sciences, Rozvojová 135, 165 02 Prague 6 — Suchdol (Czechoslovakia)

(Received 29th November 1984)

Summary. The anodic stripping voltammetry of gold in butyl acetate/methanol (2 + 1) mixture is reported. The tetrachloroaurate(III) complex is extracted into butyl acetate, lithium perchlorate in methanol is added, and gold is deposited on a glassy carbon rotating disk cathode at —0.6 V vs. SCE. The deposited gold is stripped in the same medium at a scan rate of 50 mV s^{-1}. The method is suitable for the determination of gold (0.1—1 mg l^{-1}) in chloride leach liquors.

Stripping voltammetry is especially suitable for the determination of traces of metals. The determination of gold by this method is awkward because its high dissolution potential excludes the application of a mercury electrode. Only solid working electrodes have been recommended in the literature [1—11]. Suitable electrode materials are a graphite paste [1—3, 5, 6], graphite impregnated by paraffin [1, 7—9], glassy carbon [1, 4, 10] or platinum [8]. The electrodeposition of gold has been done in 0.1—1 M hydrochloric acid solutions [1, 2, 5—8, 10] or in acidified potassium bromide solutions [1, 3, 4, 9] at a potential ranging from —1.0 to +0.4 V vs. SCE. The electrodeposition time varies from 30 s to 2 h, depending on the gold concentration.

The use of non-aqueous media has been described [4, 10, 11]. Peták and Vydra [4] reported on gold determination, using a chloroform/methanol (4 + 1) mixture containing 5% (w/v) methyltrioctylammonium chloride and potassium nitrate. Nghi and Vydra [10] used 60% tributyl phosphate solution in benzene with a methanolic 0.5 M solution of lithium chloride added.

Direct stripping voltammetry of gold in the acidic leach solutions from auriferous rock is not possible, because of the high concentrations of other metals, especially iron. The extraction of the tetrachloroaurate(III) complex from 6 M hydrochloric acid by butyl acetate is a convenient method for gold separation [12]; back-extraction of the organic extract with 2 M hydrochloric acid removes all interfering ions except antimony and thallium.

This communication reports on the determination of gold in butyl acetate extracts by anodic stripping voltammetry in the d.c. mode at a glassy carbon rotating disk electrode.

0003-2670/85/$03.30

Experimental

Chemicals and equipment. All the chemicals used were of analytical grade, except for iron(III) chloride which was of technical grade. An OH-102 polarograph (Radelkis, Hungary) and a rotating disk electrode assembly (Laboratorní přístroje, Czechoslovakia) were used in anodic stripping measurements. The three-electrode system consisted of a working glassy carbon rotating electrode, an auxiliary platinum electrode and a saturated calomel reference electrode. The working electrode was a 2-mm glassy carbon rod (Tokai Electrode, Japan) fitted into a teflon sleeve. The surface of the glassy carbon electrode was polished with Schröder PC 6/OF emery paper.

Spectrometric measurements were made with a DK-2A spectrophotometer (Beckman) and an Atomspek atomic absorption spectrometer (Rank Hilger).

Recommended procedure. A 5.00-ml sample of leach liquor containing 0.5—5 μg of gold and less than 300 mg of iron is mixed with 20 ml of 6 M hydrochloric acid in a 50-ml separating funnel and then 5 ml of 7 M hydrochloric acid saturated with chlorine is added. After 5 min, the benzidine test is used to check for free chlorine. If chlorine is absent, another portion of the hydrochloric acid solution saturated with chlorine is added. When chlorine is detected, the mixture is extracted with two 10.00-ml portions of butyl acetate, and the combined extracts are washed with 20-ml portions of 2 M hydrochloric acid until the organic phase is colourless.

The organic extract is transferred to the polarographic cell, 10.00 ml of 0.5 M lithium perchlorate in methanol is added and the mixture is purged with nitrogen (20—30 min) until free chlorine is completely removed (benzidine test). During this period, the potential of the working electrode is maintained at −0.6 V without rotation. After the chlorine has been removed, the nitrogen flow is stopped and the potential of the working electrode is changed at a rate of 50 mV s^{-1} up to +0.8 V with simultaneous recording of the voltammetric curve. If the dissolution peak of gold at +0.5 to +0.7 V does not appear, the electrolysis with nitrogen bubbling is repeated at −0.6 V. As soon as a dissolution peak is recorded, five successive measurements of the same sample are done under the following conditions: working electrode potential −0.6 V, 2500 rpm rotation rate, deposition time 5 min, rest time 30 s, recording of the stripping curve on the non-rotating electrode at a scan rate of 50 mV s^{-1} and a sensitivity of 1.2×10^{-7} A/div. From the five measurements, the average peak height is calculated and the gold content is evaluated from a calibration curve that was obtained in a similar manner by using standard samples. Prior to the analysis of each new sample, the surface of the working electrode is polished as described above.

Results and discussion

Separation of gold from chloride solutions. The distribution coefficients of gold(III) and iron(III) between butyl acetate and 6 M hydrochloric acid are 80 and 12, and between butyl acetate and 2 M hydrochloric acid

15 and 1, respectively [13]. As the leach liquors to be analyzed could contain up to 1 M iron(III) ions, the earlier procedure for separating gold from the other metal ions [12] was modified as outlined above. The organic extract obtained contains all the gold, antimony, thallium and minute amounts of iron that do not interfere in the further procedure.

This extract is not, however, sufficiently conductive for electroplating, thus 10.00 ml of 0.5 M lithium perchlorate in methanol is added as supporting electrolyte. Preliminary experiments showed that reproducible results were obtained only when the dissolved chlorine was removed completely from the solution and when the first gold layer or at least active gold centres were formed on the surface of glassy carbon electrode. The dissolved chlorine was removed by passing nitrogen through the solution, and the first gold layer was formed by a preelectrolysis step at −0.6 V applied to the stationary working electrode. If a scan to +0.8 V did not produce a peak at +0.5 to +0.7 V, characterizing the dissolution of a gold deposit, then the purging and preliminary deposition procedure was repeated on the same solution. A typical shape of the dissolution peak is represented in Fig. 1.

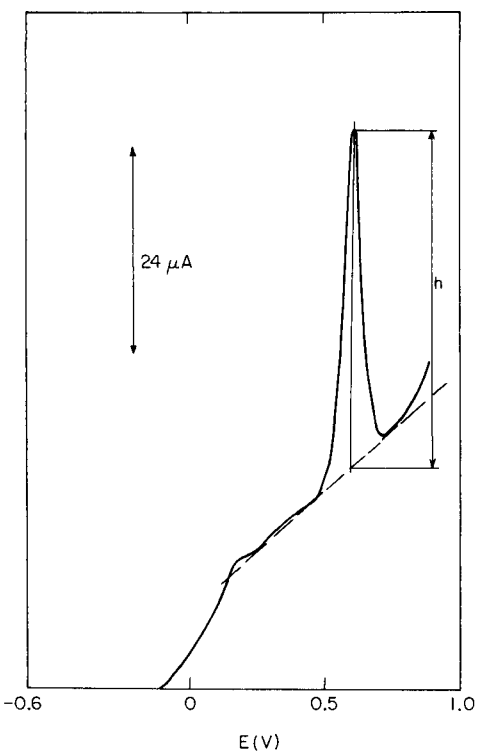

Fig. 1. A typical dissolution peak of deposited gold. Conditions: 20 ml of butyl acetate and 10 ml of 0.5 M $LiClO_4$ in methanol; 5 μg Au; E_d = −0.6 V; t_d = 5 min; 2500 rpm.; 50 mV s^{-1}.

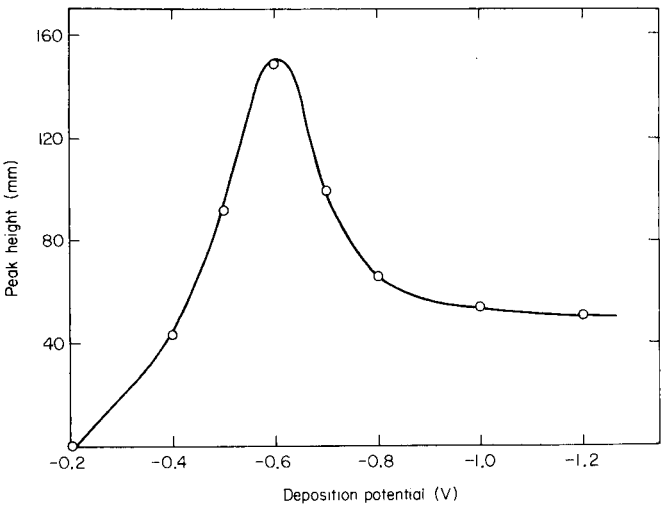

Fig. 2. The dependence of the peak height on the deposition potential. Conditions as for Fig. 1, except for E_d.

Optimum conditions for electrodeposition. To ensure the maximal electroplating rate, the optimal deposition potential was determined. A 5.00-ml sample of 0.3 M iron(III) chloride containing 5 μg of gold was extracted with butyl acetate, and the extract was placed in the polarographic cell and treated as described above. The potential applied to the working electrode was varied successively within the range −1.2 to −0.2 V. For each potential, the electrolysis was allowed to proceed for 5.00 min with the electrode rotating at 2500 rpm, then the rotation was stopped, and after 30 s the voltammetric curve was recorded at a scan rate of 50 mV s^{-1} to +0.8 V. Figure 2 shows the dependence of the height of the dissolution peak on the potential of the electrolysis; the optimum deposition potential is −0.6 V.

The electrodeposition time was studied in an analogous manner over the range 1—10 min. As shown in Fig. 3, the reproducibility of the dissolution peak height was poor for deposition times shorter than 5 min; this is obviously caused by the slow formation of active centers on the electrode surface. For longer deposition times (5—10 min) the dependence was essentially linear.

When the rotation speed of the working electrode was varied over the range 0—2500 rpm, the height of the stripping peak increased quickly up to 1000 rpm, but further increases in the rotation speed had little effect (Fig. 4). Further measurements were made at 2500 rpm.

Data evaluation. In a series of repeated measurements on the same organic extract, the height of dissolution peak first increased and then remained constant or slowly decreased. This can be attributed to the changing character of the electrode surface during the electrodeposition and subsequent

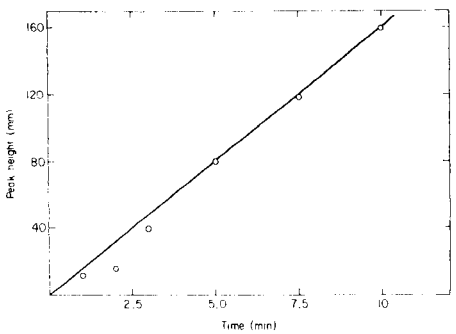

Fig. 3. The dependence of the peak height on the deposition time. Conditions as for Fig. 1, except for t_d.

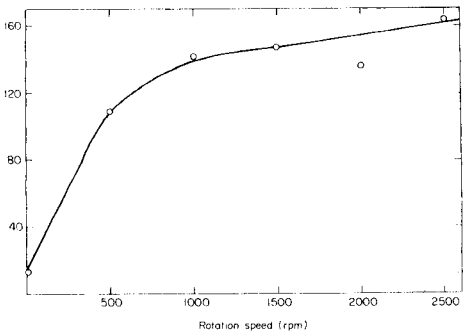

Fig. 4. The dependence of the peak height on the rotation speed. Conditions as for Fig. 1, except for speed.

stripping steps. Therefore, the optimum value to be used for determining the gold content in the sample was tested, i.e., the use of the maximum peak height in a series of successive measurements or the average peak height from this series. The linearity of the calibration graph was the criterion used.

A total of 12 samples containing 1—5 μg of gold and 0.3—1.0 mol l^{-1} iron(III) chloride were analysed and at least 5 voltammetric curves were recorded for each sample without mechanical cleaning of the electrode surface. However, prior to the analysis of another sample, the electrode was polished as described above. For each sample the average and the maximum peak height were obtained. The linear regression of these values to the gold content in the sample gave the following correlation coefficients: 0.96 for the average peak height and 0.92 for the maximum peak height. Therefore, the average of several measurements of each sample is better.

Precision and accuracy. The precision and accuracy of the method were tested by analysing a series of leach liquors. These were obtained by leaching auriferous rocks with solutions containing 0.3—1.5 mol l^{-1} iron(III) chloride and 0.1—2 mol l^{-1} hydrochloric acid. The content of gold in these samples was 0.1—1.0 mg l^{-1}. Each sample was divided into three portions, of which one was analysed by atomic absorption spectrophotometry (a.a.s.) [14], the second spectrophotometrically with the use of Rhodamine B, and the third by stripping voltammetry. The results are presented in Table 1. The results obtained by a.a.s. can be taken as more accurate than the spectrophotometric results because Rhodamine B is also sensitive to antimony in the sample. The agreement between the a.a.s. results and those obtained by the proposed method is relatively good.

Conclusion

The method described is advantageous, especially if only small samples are available. The a.a.s. and spectrophotometric methods require much

TABLE 1

Determination of gold content (mg l^{-1}) in leach liquors from auriferous rocks by a.a.s., spectrophotometry and stripping voltammetry

Sample	Gold found (mg l^{-1})		
	a.a.s.	Spectro-photometry	Stripping voltammetry
I	0.110	0.197	0.150 ± 0.028[a]
II	0.265	0.220	0.280 ± 0.051
III	0.503	0.607	0.500 ± 0.092
IV	1.020	1.040	0.996 ± 0.216

[a]Standard deviations from six parallel analyses of the same sample.

larger volumes of the sample. The sensitivity of the method can be increased if 50 ml of the sample is taken or if the deposition time is prolonged; solutions containing 0.01—0.1 mg l^{-1} gold can then be analysed. Such sensitivity is difficult to achieve by other methods. The disadvantages of the method is that it is time-consuming and that the scatter of the results can reach about 20%.

REFERENCES

1 F. Vydra, K. Stulik and E. Julakova, Electrochemical Stripping Analysis, Horwood, Chichester, 1976, pp. 243—245.
2 S. I. Sinyakova and L. S. Chulkina, Zh. Anal. Khim., 23 (1968) 841.
3 H. Monien, Z. Anal. Chem., 237 (1968) 409.
4 P. Peták and F. Vydra, Collect. Czech. Chem. Commun., 39 (1974) 943.
5 V. A. Zarinskii, L. S. Chulkina and N. N. Baranova, Zh. Anal. Khim., 32 (1977) 530.
6 L. N. Vasileva and T. A. Koroleva, Zh. Anal. Khim., 28 (1973) 2107.
7 E. Ya. Neiman and M. F. Sumenkova, Zh. Anal. Khim., 31 (1976) 912.
8 B. S. Bruk, M. I. Pozina and E. I. Rozenfeld, Zh. Anal. Khim., 34 (1979) 1095.
9 Kh. Z. Brainina, T. D. Gornostaeva and V. A. Pronin, Zh. Anal. Khim., 34 (1979) 1081.
10 T. V. Nghi and F. Vydra, J. Electroanal. Chem., 64 (1975) 163.
11 F. Vydra, Chem. Listy, 70 (1976) 337.
12 P. Hannaker and T. C. Hughes, Anal. Chem., 49 (1977) 1485.
13 Z. I. Nikolotova and N. A. Kartashova, Spravochnik po Ekstrakcii Part 1, Atomizdat, Moskva, 1976.
14 K. Jakubec, Z. Sir and J. Vilimec, Anal. Chim. Acta, 173 (1985) 97.
15 B. J. MacNulty and L. D. Woollard, Anal. Chim. Acta, 13 (1955) 154.

Analytica Chimica Acta, 172 (1985) 365—370
Elsevier Science Publishers B.V., Amsterdam — Printed in The Netherlands

Short Communication

POTENTIOMETRIC STRIPPING ANALYSIS FOR TIN WITH A GOLD FILM ELECTRODE FORMED IN SITU ON GLASSY CARBON

ER-KANG WANG* and WENTA SUN

Changchun Institute of Applied Chemistry, Academia Sinica, Changchun, Jilin 130021 (People's Republic of China)

(Received 15th July 1984)

Summary. A gold film electrode formed in situ on glassy carbon is used as the working electrode for the determination of tin over the range 0.1—10 $\mu g\ ml^{-1}$. Gold(III) added to the solution provides the film and serves as the oxidant for stripping. Two stripping curves corresponding to Sn(Au) → Sn(II) and Sn(II) → Sn(IV) were observed; either can be used for determinations of tin. The equations for the transition time (i.e., stripping signal) and stripping curve derived were verified experimentally.

Potentiometric stripping analysis (p.s.a.) [1—3] has developed rapidly as a practical technique. Recently, a gold film electrode formed in situ at glassy carbon substrate has been described as the working electrode in p.s.a. [4]; the gold(III) present in the solution also serves as the oxidant, and copper(II), bismuth(III), antimony(III) and lead(II) can be determined simultaneously [4]. In this communication, a similar procedure is used to determine tin. Tin(II,IV) is first preconcentrated (through pre-electrolysis) on the gold film electrode and then stripped by chemical re-oxidation with gold(III). Two potentiometric stripping curves represented by Sn(Au) → Sn(II) and Sn(II) → Sn(IV) were studied to verify the theoretical equations. The method was applied for the determination of tin in rocks and waste plating solutions.

Theory

Potentiometric stripping analysis for tin with the in-situ gold film electrode consists of two steps. The deposition step is

$$Au(III) + Sn(II) + 5e^- \rightarrow Sn(Au) \quad (1)$$

and any tin(IV) in the solution is first reduced to tin(II) at the electrode prior to this reaction. Then in the stripping step, the reactions are

$$3\ Sn(Au) + 2\ Au(III) \rightarrow 3\ Sn(II) + 5\ Au \quad (2)$$

$$3\ Sn(II) + 2\ Au(III) \rightarrow 3\ Sn(IV) + 2\ Au \quad (3)$$

Thus gold(III) present in the solution serves not only to form the gold film electrode in the deposition step but also as the oxidant in the stripping step.

0003-2670/85/$03.30

If the reaction rate for Eqn. 2 is not very slow, the concentration of gold(III) at the electrode surface during stripping will approach zero, and the transition time (i.e., stripping signal) can be expressed [4] as

$$\tau = 3/2(D_{Sn(II)}/D_{Au(III)})^{2/3}(\omega_p/\omega_s)^{1/2}(C_{Sn(II)}/C_{Au(III)})t_p \quad (4)$$

where $D_{Sn(II)}$ and $D_{Au(III)}$ are the diffusion coefficients, ω_p and ω_s are the angular velocity of the rotating disk during the pre-electrolysis and stripping steps, respectively, $C_{Sn(II)}$ and $C_{Au(III)}$ are the bulk concentrations of the relevant species, and t_p is the pre-electrolysis time. The equation for the potentiometric stripping curves can be expressed [4—6] by

$$E = E_0' + (RT/nF) \ln [t^{1/2}/(\tau - t)] \quad (5)$$

Experimental

Equipment and chemicals. The laboratory-built apparatus for p.s.a. was the same as before [4]. A rotating glassy carbon electrode (0.40 cm diameter) was used as the support for the gold film. A silver/silver chloride (saturated KCl) electrode was used as reference; all potentials are referred to this electrode.

All chemicals were of analytical or guaranteed grade. Deionized water was distilled twice in quartz.

General procedure. Unless otherwise stated, 3 M hydrochloric acid was used as supporting electrolyte, the pre-electrolysis time was 4 min, the pre-electrolysis potential was fixed at —0.7 V, the concentration of gold(III) used was 20 μg ml^{-1}, and 5 μg ml^{-1} tin(II) was used. Solutions were deoxygenated with argon.

Procedure for rocks. Weigh exactly 0.500—1.000 g of rock sample into a porcelain crucible containing 2 g of sodium peroxide, and cover with another 2 g. Fuse over a burner until a clear melt is obtained or place in a furnace at 700°C for about 10 min. Immerse in hot water in a beaker, dissolve the hydrated iron(III) oxide completely with (1:1) sulphuric acid and add 8 ml more. Heat to boiling, add 5—6 drops of 10% (w/v) barium chloride solution, filter into a volumetric flask and dilute to the volume. Prepare a blank solution in the same way.

For samples with low iron content, transfer 0.2—1.0 ml of sample solution to a small beaker, evaporate to dryness, cool, add 10 ml of 3 M hydrochloric acid and gold(III) to give a 5—10 μg ml^{-1} solution. Then proceed with pre-electrolysis at —0.7 V for 10 min and record the stripping curves. The standard addition method was used to determine tin.

Procedure for waste plating solutions. Pipette 1 ml of sample solution into a small beaker, add 1 ml of (1:1) hydrochloric acid and 1 ml of (1:1) nitric acid, and heat to near dryness. Cool, add 10 ml of 3 M hydrochloric acid, and heat gently to dissolve. Then add 20 μg ml^{-1} gold(III), deoxygenate and proceed to pre-electrolysis at —0.7 V for 2 min, and record the stripping curves.

Results and discussion

Choice of medium and experimental conditions. Hydrochloric acid was chosen as supporting electrolyte. Table 1 shows the effect of the concentration of hydrochloric acid on the stripping signal. The tin deposited during the pre-electrolysis yields two waves or peaks corresponding to the oxidation to tin(II) and then tin(IV) as in Eqns. 2 and 3 (Fig. 1). The dependence of the stripping signal of tin on the concentration of gold(III) is shown in Fig. 2; a concentration of 20 μg ml^{-1} gold(III) is suitable. Figure 3 indicates that for the first stripping step (Eqn. 2), a pre-electrolysis potential between —0.6 and —0.9 V is suitable while for the second step, the potential should be —0.7 to —1.0 V. Hydrogen ion is probably reduced at more negative potentials. The stripping signals are directly proportional to the pre-electrolysis time up to 20 min (Fig. 4) and to the concentration of tin(II, IV) in the

TABLE 1

Effect of the concentration of hydrochloric acid on the stripping signals (τ) of tin

Wave	Stripping signal (s) with different HCl concs. (M)					
	1.0	2.0	3.0	4.0	5.0	6.0
Sn → Sn(II)	2.25	5.0	5.50	4.50	5.25	5.25
Sn(II) → Sn(IV)	2.75	3.25	2.50	2.25	2.50	3.00

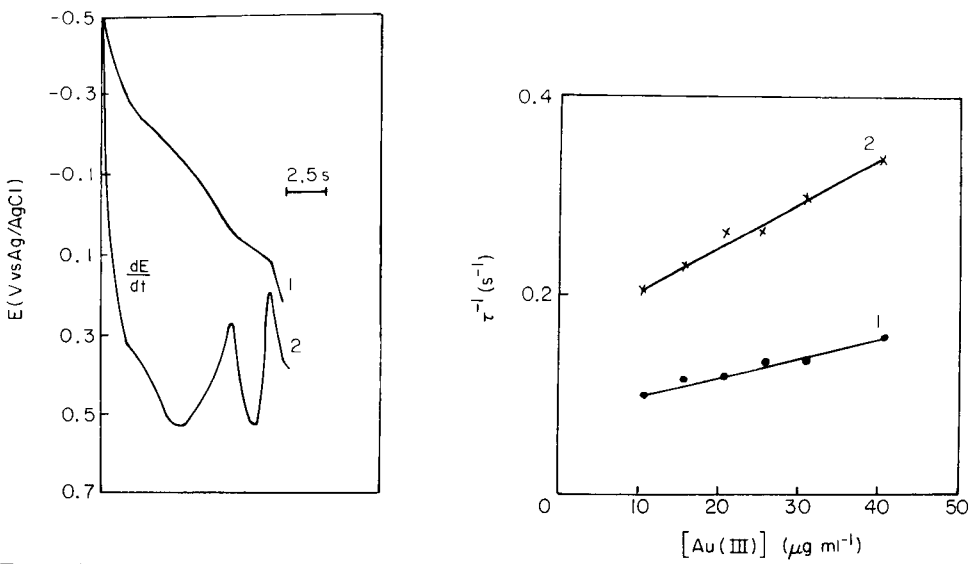

Fig. 1. Potentiometric stripping curve with the in-situ gold film electrode obtained after deposition for 4 min at —0.7 V in 3 M HCl containing 5 μg ml^{-1} tin(IV). Curves: (1) normal stripping; (2) derivative plot.

Fig. 2. Dependence of the stripping signal of tin on the concentration of the oxidant: (1) first signal; (2) second signal. Conditions as for Fig. 1.

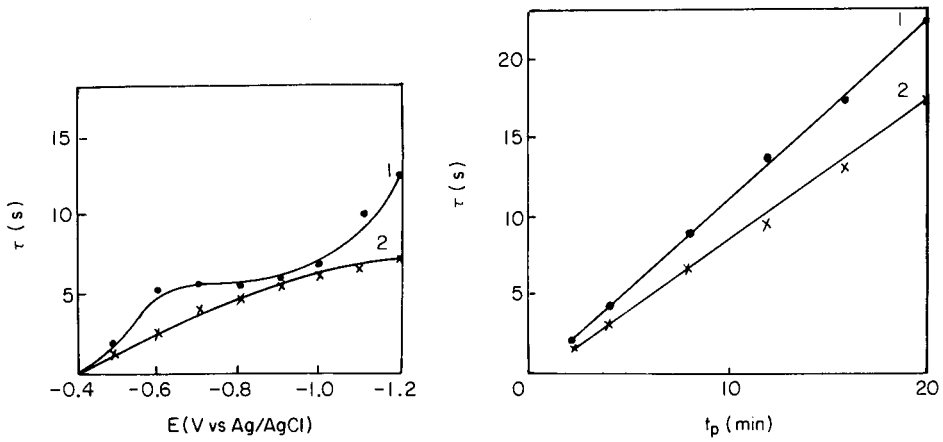

Fig. 3. Dependence of the stripping signal of tin on the pre-electrolysis potential. Curves 1 and 2 and conditions as for Fig. 2.

Fig. 4. Dependence of the stripping signal of tin on the pre-electrolysis time. Curves 1 and 2 and conditions as for Fig. 2.

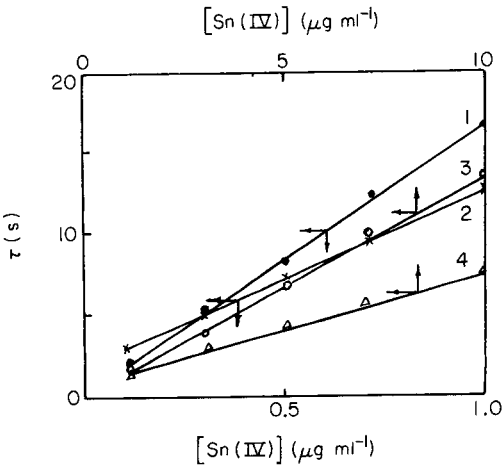

Fig. 5. Dependence of the stripping signal on the concentration of tin. Curves: (1, 2) 5 μg ml^{-1} gold(III), pre-electrolysis at −0.7 V for 10 min; (3, 4) 20 μg ml^{-1} gold(III), pre-electrolysis for 4 min. (1, 3) First signal; (2, 4) second signal.

range 0.1—1.0 μg ml^{-1} (Fig. 5). The sensitivity of the determination can be increased by prolonging the pre-electrolysis time and by decreasing the concentration of gold(III). The dependence of the stripping signals on the angular velocity of the rotating disk electrode (either ω_p or ω_s) is shown in Fig. 6. Figure 7 shows the linear relationship of E vs. log $[t^{1/2}/(\tau - t)]$.

The above experimental results (Figs. 1—7) are in good agreement with Eqns. 4 and 5. Tin is stripped in two steps (Eqns. 2 and 3) and the Sn(II)

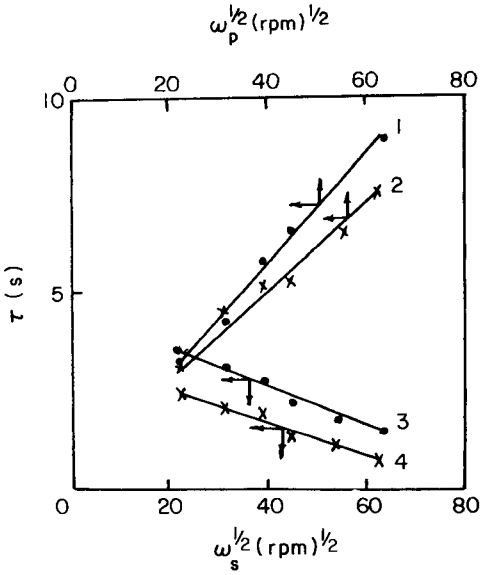

Fig. 6. Dependence of the stripping signal of tin on ω_p and ω_s: (1, 3) first signal; (2, 4) second signal.

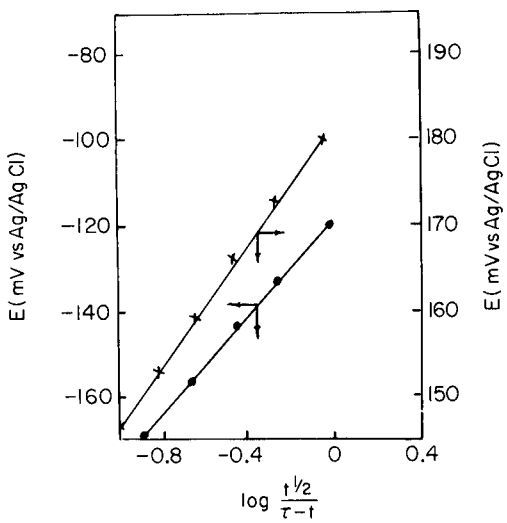

Fig. 7. Dependence of E on log $[t^{1/2}/(\tau - t)]$ for tin.

species formed during the first step must remain around the working electrode. However, the stripping signal of the first step is always larger than that of the second step (see Figs. 1—6), probably because of slow diffusion (compared to stripping) of the tin(II) species away from the working electrode

during the stripping. This is verified experimentally by the relationship between the stripping signals and ω_p and ω_s (Fig 6).

Interferences. Lead(II) yields a stripping curve overlapping the first step for tin but does not interfere with the second step. Silver(I) and mercury(II) yield stripping curves overlapping the second step for tin, causing positive errors. Iron(III) and chromium(VI), being oxidants, decrease the stripping signal for tin. Copper(II) interferes with the second signal for tin. It is not known if intermetallic compound formation is involved.

Applications. The method was applied to the determination of tin in two rock samples; the tin contents found were 0.34% and 0.064%, to be compared with 0.35% and 0.05% obtained by cathode-ray polarography. The result obtained for tin in a waste plating solution was 0.067 g l^{-1}, compared with 0.068 g l^{-1} by cathode-ray polarography.

Conclusions

The in-situ gold film electrode is useful for the potentiometric stripping determination of tin. Tin can also be determined by stripping analysis at a mercury film electrode [2], which provides better sensitivity than the above method. However, the proposed method avoids the toxicity of mercury, and illustrates further the possibilities of gold film electrodes in potentiometric stripping analysis [4].

REFERENCES

1 D. Jagner and A. Granéli, Anal. Chim. Acta, 83 (1976) 19.
2 D. Jagner, Trends Anal. Chem., 2 (1983) 53.
3 D. Jagner, Analyst (London), 107 (1982) 593.
4 Er-kang Wang Wen-ta Sun and Yun-fa Yang, Anal. Chem., 56 (1984) 1903.
5 Tuen Chi Chau, De Yu Li and Ying Liang Wu, Talanta, 29 (1982) 1083.
6 Zu-xun Zhang and Qi Zhou, Acta Chim. Sinica, 41 (1983) 403.

Analytica Chimica Acta, 172 (1985) 371—375
Elsevier Science Publishers B.V., Amsterdam — Printed in The Netherlands

Short Communication

AMPEROMETRIC DETECTION OF ACETYLCHOLINE AND CHOLINE IN A LIQUID CHROMATOGRAPHIC SYSTEM WITH AN IMMOBILIZED ENZYME REACTOR

TOSHIO YAO* and MINORU SATO

Department of Applied Chemistry, College of Engineering, University of Osaka Prefecture, Mozu-Umemachi, Sakai 591 (Japan)

(Received 6th December 1984)

Summary. Acetylcholinesterase and choline oxidase were co-immobilized by reaction with glutaraldehyde onto alkylamino-bonded silica, which was incorporated as the enzyme reactor in an h.p.l.c. system for the determination of acetylcholine and choline. The hydrogen peroxide produced enzymatically in the enzyme reactor, after the separation of acetylcholine and choline by the reverse-phase column, was monitored amperometrically. The detection limits were 1.2 pmol for choline and 1.8 pmol for acetylcholine.

Acetylcholine is an important neurotransmitter. Gas chromatographic [1, 2] and radioisotope [3—6] methods for its determination have been developed in recent years. However, these methods involve some complicated and time-consuming procedures, and some require expensive equipment. More recently, Potter et al. [7] developed a usable, simple, specific and sensitive method utilizing high-performance liquid chromatography (h.p.l.c.) with electrochemical detection for determination of acetylcholine and choline. The method is based on the separation of the two compounds by reverse-phase h.p.l.c., mixing the effluent in a reaction coil with soluble acetylcholinesterase (AChE) and choline oxidase (ChO), followed by the amperometric detection of hydrogen peroxide produced from both endogenous choline and that generated from acetylcholine in the reaction coil. The reactions involved are

$$\text{acetylcholine} + H_2O \xrightarrow{\text{AChE}} \text{choline} + \text{acetic acid}$$

$$\text{choline} + 2O_2 + H_2O \xrightarrow{\text{ChO}} \text{betaine} + 2H_2O_2$$

However, the limited stability and high cost of the soluble enzymes have appreciably restricted the application of this method in routine work.

Recent progress in the chemistry of enzyme bonding permits the preparation of immobilized enzymes, which can be used repeatedly. Besides providing economic advantages, the use of immobilized enzymes decreases some problems of instability which occur with soluble enzymes. This communica-

tion describes the use of immobilized enzymes as a packed-bed reactor in a h.p.l.c./electrochemical system for the specific determination of acetylcholine and choline.

Experimental

Reagents. Acetylcholine chloride and choline chloride (Wako Pure Chemical Co.) were dried in a vacuum over phosphorus pentoxide. The enzymes used were acetylcholinesterase (EC 3.1.1.7., from electric eel, 1400 IU mg^{-1}, Type V-S; Sigma Chemical Co.) and choline oxidase (EC 1.1.3.17., from *Alcaligenes* sp., 14.3 IU mg^{-1}; Toyobo Co.). Tetramethylammonium chloride (TMA) and sodium octyl sulfate (SOS) were obtained from Wako Pure Chemical Co. and Aldrich Chemical Co., respectively. Ethylhomocholine (EHC) was prepared as previously described [7] and was used as an internal standard. All other chemicals were of analytical reagent grade. Stock solutions (0.1 M) of the three cholines were prepared in 0.02 M acetate buffer (pH 5.0).

Preparation of immobilized enzyme reactor. The method was similar to that described previously [8]. The alkylamino-bonded silica (LiChrosorb NH_2; Merck) was packed into a stainless steel column (20 mm × 0.2 mm i.d.), and glutaraldehyde solution (5 v/v%) in sodium hydrogencarbonate (0.1 M, pH 8.5) was pumped for activating the silica at 1 ml min^{-1} for 1.5 h. After the column had been washed with phosphate buffer (0.1 M, pH 8.0) for 2 h, enzymes were loaded onto the column by circulating a 20-ml solution of enzymes (0.2 mg AChE and 3.0 mg ChO) in sodium phosphate buffer (0.1 M, pH 8.0) through the column at 1.5 ml min^{-1} for 2.5 h at room temperature. The excess of enzymes was washed out with the phosphate buffer (0.1 M, pH 8.0) for 2 h and the column was stored at ca. 5°C in the same buffer when not in use. The amount of enzymes loaded onto a reactor was 1.7 mg.

System and procedures. The h.p.l.c. system is shown schematically in Fig. 1. The immobilized enzyme reactor was inserted as shown. The apparatus consisted of a high-performance liquid chromatograph (Yanagimoto L-5000), a voltammetric detector equipped with a flow-through platinum electrode (Yanagimoto VMD-101), an intermediate pressure pump (Yanagimoto RP-203) for pumping the reagent solution, a strip-chart recorder, a teflon mixing coil (20 m, 0.25 mm i.d.), and a Yanagimoto ODS-120T reverse-phase column (250 mm, 4 mm i.d.).

When the mobile phase and the reagent solution were pumped at 1.0 and 0.5 ml min^{-1}, respectively, and mixed in the teflon coil, the pH of the combined solution was 8.2, which was near the optimum pH for activity of the immobilized enzyme reactor. Enzymatic reactions of choline and acetylcholine proceeded in the reactor, and the hydrogen peroxide produced was monitored amperometrically at 0.5 V vs. a Ag/AgCl reference electrode.

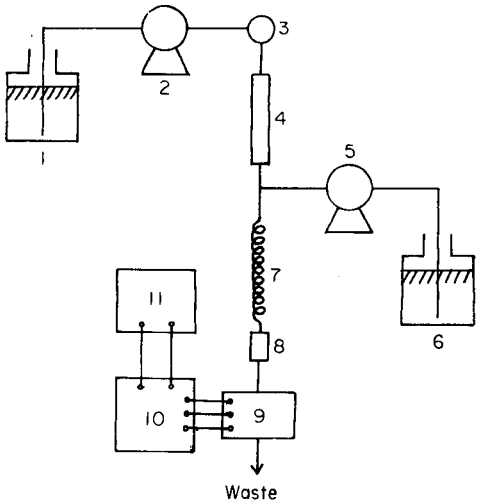

Fig. 1. An h.p.l.c. system for amperometric detection of acetylcholine and choline with the immobilized enzyme reactor: (1) mobile phase (0.01 M sodium acetate buffer, pH 5.0, containing 10 mg l^{-1} sodium octyl sulfate and 1 mM tetramethylammonium chloride); (2) h.p.l.c. pump, 1.0 ml min^{-1}; (3) injector; (4) ODS-120T column; (5) pump, 0.5 ml min^{-1}; (6) 0.3 M phosphate buffer, pH 8.5, containing 5×10^{-4} M EDTA; (7) mixing coil; (8) immobilized enzyme column; (9) flow-through platinum electrode; (10) potentiostat; (11) recorder.

Results and discussion

Enzymatic conversion of acetylcholine and choline to hydrogen peroxide. Experiments were first conducted to establish the optimum pH, under flow-injection conditions, without the h.p.l.c. column and the pump for the reagents, for the detection of choline and acetylcholine. Phosphate and pyrophosphate buffers (0.1 M) at various pH values were used as the carrier solution. Figure 2 shows the effect of pH on the peak current; maximum response for choline and acetylcholine was obtained at pH 8.0—8.5 which is near the optimum pH of 8.0 for soluble choline oxidase.

After complete enzymatic conversion, 2 mol of hydrogen peroxide should be produced for every mole of choline or acetylcholine. Figure 3 evaluates the conversion efficiencies at various flow rates. As the flow rate increased, the conversion efficiency of choline to hydrogen peroxide decreased; but the decrease was slight at higher flow rates. In contrast, conversion of acetylcholine to choline was ca. 100% at every flow rate tested at room temperature.

Separation of choline and acetylcholine. To the 0.01 M sodium acetate buffer (pH 5.0) as the mobile phase, sodium octyl sulfate was added as an ion-pairing agent to retard the elution of choline, and TMA was added to avoid strong adsorption of acetylcholine on the ODS column. The effect of TMA on the activity of the immobilized enzymes was tested, because TMA inhibited soluble choline oxidase [7]; TMA below 5 mM had no effect on

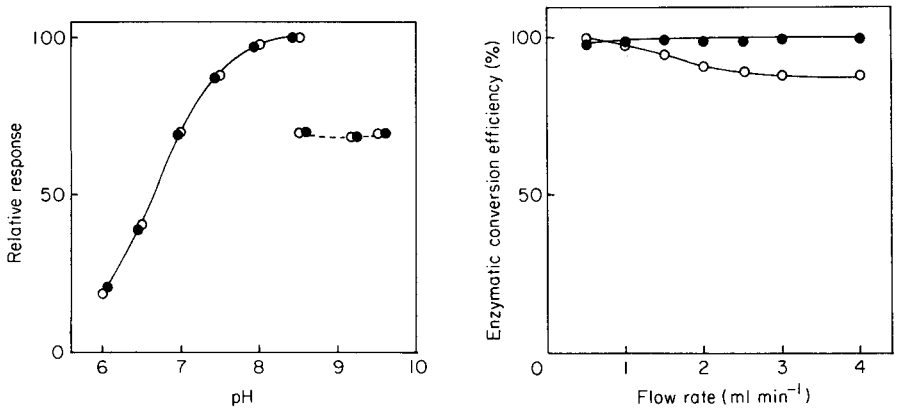

Fig. 2. Effect of pH on the peak current: (——) phosphate buffer (0.1 M); (----) pyrophosphate buffer (0.1 M). Compound: (○) choline chloride; (●) acetylcholine chloride.

Fig. 3. Effect of flow rate on the enzymatic conversions: (○) choline to hydrogen peroxide; (●) acetylcholine to choline.

the two enzymatic conversions, but it had a slight detrimental effect on the long-term stability of the enzyme reactor.

The sensitivity of the platinum electrode to hydrogen peroxide decreased gradually during long periods (several hours) of operation. Therefore, to compensate for this, ethylhomocholine was added to sample solutions as an internal standard which is also enzymatically oxidized to produce hydrogen peroxide. Figure 4A shows a typical chromatogram for a solution containing

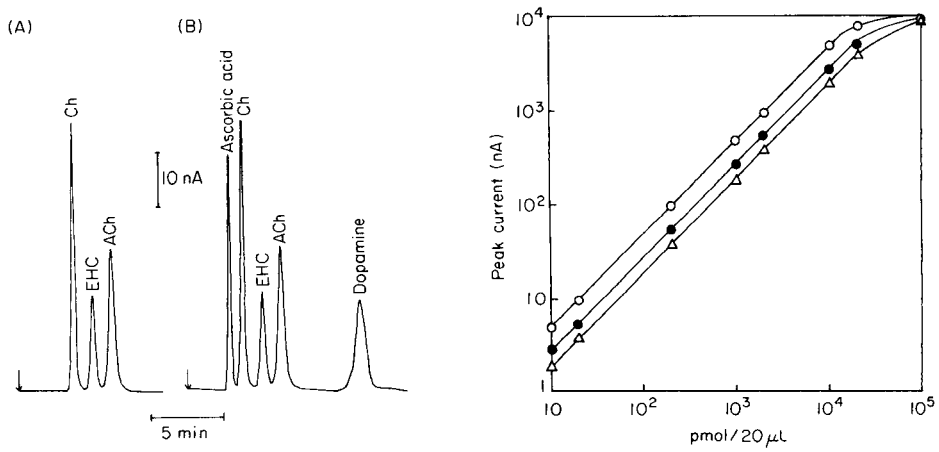

Fig. 4. Chromatograms of standard solutions (200 pmol of each compound): (A) choline, acetylcholine and ethylhomocholine; (B) as for A plus ascorbic acid and dopamine.

Fig. 5. Calibration graphs: (○) choline chloride; (●) acetylcholine chloride; (△) ethylhomocholine.

200 pmol each of the three cholines; elution was complete within 7.5 min. Electroactive species other than hydrogen peroxide produced enzymatically, such as ascorbic acid and dopamine, were oxidized at the platinum electrode at the same potential (0.5 V). However, ascorbic acid eluted with the void volume and dopamine at 11.6 min (Fig. 4B); therefore neither compound interfered in the measurements.

Figure 5 shows calibration graphs for choline, acetylcholine and ethylhomocholine, obtained by measurements of peak current. The graphs were linear from 10 to 2×10^4 pmol per 20-μl injection for all three compounds. The lower limits of detection were 1.2 and 1.8 pmol for choline and acetylcholine, respectively (S/N = 2).

Long-term stability of the reactor. The immobilized enzyme reactor was used repeatedly to confirm its stability over three months; it was stored at ca. 5°C in 0.1 M phosphate buffer (pH 8.0) when not in use. The immobilized enzyme retained more than 95% of its original activity even after three months, while soluble enzymes lost most of their activities in about 4 days. When the enzyme reactor was stored in the dried form, however, its activity decreased gradually from day to day.

We thank H. Nishino and T. Kurahashi (Yanagimoto Mfg. Co., Kyoto) for providing us with the facilities to conduct this study.

REFERENCES

1 D. J. Jenden, B. Campbell and M. Roch, Anal. Biochem., 35 (1970) 209.
2 I. Hanin and R. F. Skinner, Anal. Biochem., 66 (1975) 568.
3 W. D. Reid, D. R. Haubrich and G. Krishna, Anal. Biochem., 42 (1971) 390.
4 R. E. McCaman and J. Stetzler, J. Neurochem., 28 (1977) 669.
5 D. R. Haubrich, N. Gerber, A. B. Pflueger and M. Zweig, J. Neurochem., 36 (1981) 1409.
6 M. L. Gilberstadt and J. A. Russell, Anal. Biochem., 138 (1984) 78.
7 P. E. Potter, J. L. Meek and N. H. Neff, J. Neurochem., 41 (1983) 188.
8 T. Yao, Y. Kobayashi and S. Musha, Anal. Chim. Acta, 138 (1982) 81.

Analytica Chimica Acta, 172 (1985) 377—379
Elsevier Science Publishers B.V., Amsterdam — Printed in The Netherlands

Short Communication

A SIMPLE METHOD FOR CORRECTING BASELINE ARTIFACTS IN NUCLEAR MAGNETIC RESONANCE SPECTROSCOPY

WERNER STOREK

Central Institute of Physical Chemistry of the Academy of Sciences of the GDR, 1199 Berlin (German Democratic Republic)

(Received 12th December 1984)

Summary. A simple baseline correction program is described. It depends on an adjustable threshold for initiation of a data-sorting process between the signals and baseline of a computer-stored n.m.r. spectrum. An application is discussed.

Imperfect baselines are a nuisance in practical nuclear magnetic resonance spectroscopy (n.m.r.). Their sources are several: (a) imperfect instrument conditions or bad choice of parameters for measurements, which affect the baseline mainly in the lengthy data accumulations needed for low concentrations in samples; (b) dynamic range problems, e.g., when solvent signals are intense and the desired signals are weak; (c) manipulations of spectra by various computer procedures. Point (c) may be illustrated by the result of extreme resolution enhancement, when signals appear to sit in little troughs [1—5]. Another example is given in Fig. 1A, which shows the almost periodic baseline distortions caused by the large phase corrections necessary when the single-pulse J-modulation technique (attached proton test, APT, or delayed decoupling test) is used with early single-pulse F.t.n.m.r. spectrometers to improve the data for structural studies of organic compounds [6—10]. Under these circumstances, the use of earlier procedures for baseline flattening [11, 12] is not successful. This communication describes a new computer program for the correction of badly distorted baselines.

Program description

The proposed algorithm extracts the distorted baseline from the spectrum, and produces the baseline-corrected spectrum from the difference in a second step. First, the mean value $\bar{Y}$ of the noise in a spectral range free of any n.m.r. signal for m selected data points Y_i of the digitized spectrum is calculated: $\bar{Y} = (1/m) \sum_{i=1}^{m} Y_i$. Then the mean value of the absolute deviation from $\bar{Y}$ is calculated for the same spectral range: $\Delta\bar{Y} = (1/m) \sum_{i=1}^{m} |Y_i - \bar{Y}|$. This value of $\Delta\bar{Y}$ serves as a threshold for a sorting procedure between signals and baseline; by means of $\Delta\bar{Y}$, it is possible to produce a test value

$$\Delta Y_i = |Y_{i+1} - Y_i| - n\Delta\bar{Y} \quad (1)$$

0003-2670/85/$03.30

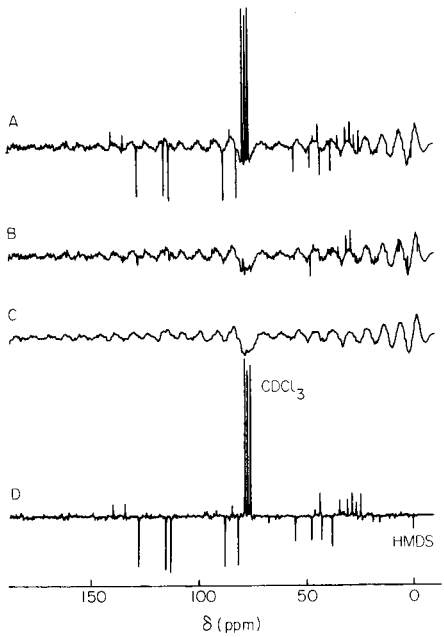

Fig. 1. (A) An APT ^{13}C-n.m.r. spectrum at 25.15 MHz from a saturated solution of estra-1,3,5(10)-trien-16β,17α-diol-3-methylether in $CDCl_3$ [13] measured with a high-resolution Jeol PFT-100 spectrometer at 24°C (4 K spectrum, 5 kHz sweep width, 17 μs (45°) pulse width, 0.9 s repetition time, 86 300 scans, 5133 μs predelay time, frequency-dependent phase correction of 9240 $^{-}$). (B) The extracted baseline of A; n = 2 and m = 300 were chosen for the leftward data points of spectrum A. (C) Same as B but with n = 0.5 and with smoothing of the extracted baseline. (D) The baseline-corrected spectrum obtained by the subtraction A — C.

The level of this threshold in Eqn. 1 may be changed by suitable choice of the positive factor n. The ΔY_i values are calculated for the whole set of N data points of the digitized spectrum and are the basis for decision by the program.

If $\Delta Y_i < 0$, then the data point Y_i is transferred to a second data block in the computer memory. If $\Delta Y_i \geqslant 0$ for a particular data point $Y_i = Y_s$, then Y_s is stored temporarily. If $\Delta Y_i \geqslant 0$ is found again for another data point $Y_{s'}$, then the program asks if $s' = s + 1$. If $s' \neq s + 1$, the data point Y_s is stored at its initial location in the second data block. If $s' = s + 1$, the program interprets the immediately adjacent data points Y_s and $Y_{s'}$ as "signals". Then $Y_{s'}$ is also stored temporarily and is replaced, if a new immediately adjacent data point is selected. This procedure is interrupted for the first actual Y_i with $\Delta Y_i < 0$. In this case, a programmed jump is made to a "straight line" subroutine.

This subroutine produces a straight line by simple interpolation. If j data points are selected, then a value

$$h = (Y_{i+j} - Y_i)/j \qquad (2)$$

is calculated and a straight line, formed by the data points Y_s, $Y_s + h$, $Y_s + 2h$, ..., $Y_s + jh$ is stored in the second data block. Consequently, the distorted baseline together with the rectilinear sections instead of signals is extracted from the spectrum and stored separately. The quality of this sorting process may be improved by an appropriate choice of n, done visually from a display (compare Fig. 1B and 1C). In the final step, the separated baseline is subtracted from the distorted spectrum, which produces the baseline-corrected spectrum (Fig. 1D).

The program was written in the NIC-assembly language for a Nicolet 1085 computer*. The time needed for calculation of a single run for $N = 4096$ data points of a digitized spectrum was about two seconds.

Discussion

The original signal/noise ratio is little affected by the proposed procedure. To avoid a large number of zero-filled data channels in the final spectrum, a conventional smoothing procedure may be applied to the extracted baseline before subtraction from the original spectrum. The program is satisfactory for acceptable signal/noise ratios and sufficiently narrow line widths of resolved n.m.r. signals. If these conditions are fulfilled, then the proposed method is not limited to application in high-resolution n.m r. spectroscopy.

The use of this program has not only a cosmetic effect but is useful for achieving more reliable signal integration in quantitative studies or for comparison of intensities from peak printouts. If the original baseline is perfect, then the program may be used to discriminate between broad (and noisy) and sharp n.m.r. signals. The program can also serve as a rigorous smoothing procedure for broad signals which are hidden in noise.

REFERENCES

1 R. R. Ernst, in J. S. Waugh (Ed.), Advances in Magnetic Resonance, Vol. 2, Academic Press, New York, 1966, p. 1.
2 A. De Marco and K. Wüthrich, J. Magn. Reson., 24 (1976) 201.
3 B. Clin, J. De Bony, P. Lalanne, J. Bias and B. Lemanceau, J. Magn. Reson., 33 (1979) 457.
4 J. C. Lindon and A. G. Ferrige, J. Magn. Reson., 36 (1979) 277.
5 K. Roth and B. J. Kimber, Org. Magn. Reson., 18 (1982) 197.
6 C. Le Cocq and J. Y. Lallemand, J. Chem. Soc. Chem. Commun., (1981) 150.
7 S. L. Patt and J. N. Shoolery, J. Magn. Reson., 46 (1982) 535.
8 R. Radeglia, J. Prakt. Chem., 325 (1983) 642.
9 D. Zeigan, R. Radeglia and G. Engelhardt, J. Prakt. Chem., 325 (1983) 651.
10 P. Bigler, J. Magn. Reson., 55 (1983) 468.
11 G. A. Pearson, J. Magn. Reson., 27 (1977) 265.
12 W. Dietrich and R. Gerhards, J. Magn. Reson., 44 (1981) 229.
13 G. Engelhardt, D. Zeigan and B. Schönecker, Org. Magn. Reson., 12 (1979) 628.

*The program is available from the author upon request.

Analytica Chimica Acta, 172 (1985) 381—386
Elsevier Science Publishers B.V., Amsterdam — Printed in The Netherlands

Short Communication

APPLICATION OF A FUNDAMENTAL PARAMETER TECHNIQUE FOR SOLVING PEAK-OVERLAP PROBLEMS IN QUANTITATIVE ENERGY-DISPERSIVE X-RAY FLUORESCENCE SPECTROMETRY

NIELS PIND

Department of Chemistry, Aarhus University, Langelandsgade 140, 8000 Aarhus C (Denmark)

(Received 7th December 1984)

Summary. The procedure exploits the fundamental parameter technique for mono-energetic excitation. The algorithm describes each peak as a sum of line intensities, thus intensities from unresolved lines are included directly in the equations. The procedure includes the condition that the sum of all weight fractions equals unity, and so is valid only when all elements are measured by x-ray fluorescence spectrometry, e.g., in steel alloys. The procedure is tested with a set of theoretically calculated x-ray fluorescence intensities, and for two NBS standard steel alloys.

In complex energy-dispersive x-ray fluorescence (x.r.f.) spectra, overlapping peaks are the rule rather than the exception, which complicates the calculation of each line intensity. To some extent, the problem can be solved by a linear least-squares filter-fit method [1] or by non-linear least-squares peak fitting [2, 3]. A numerical solution based on a fundamental parameter technique was used by Jensen et al. [4]. The present communication outlines a new numerical solution based on a fundamental parameter technique for mono-energetic excitation. The recent work by Jensen et al. [5] is expanded to include fluorescence peak intensities which consist of intensities of several lines from different elements. As before [5], this approach leads to a set of linear equations, which are closely related to the Lachance -Traill [6, 7] equations. The equations are given as a quadratic matrix, where some of the matrix elements are updated during an iterative procedure.

The procedure is based on the condition that the sum of all weight fractions be unity. Thus, the equations are valid only if all elements in the sample are determined simultaneously. The use of the normalization condition means that quantitative calculations are possible without absolute calibration of the x-ray spectrometer.

Theory

In the case of a mono-energetic excitation source and an infinitely thick sample, the equations used in the fundamental parameter approach are considerably reduced, as described in detail by Sparks [8]. Severe peak

0003-2670/85/$03.30

overlap occurs when an experimental fluorescence peak consists of fluorescence lines from more than one element. The total peak intensity, I_r, is given by the sum of the individual elemental line intensities, I_i

$$I_r = \sum_i I_i = \sum_i \{[G K_i (1 + H_i) W_i \sin \psi_1] / [\sum_s^N W_s (\mu_s^0 + \mu_s^i \sin \psi_1 / \sin \psi_2)]\} \quad (1)$$

where G is the absolute calibration factor, which includes the geometry factor and the primary excitation intensity. For each element i, K_i is the combined excitation and detection efficiency, H_i corrects for enhancement effects and W_i is the weight fraction; ψ_1 and ψ_2 are the angles of incidence and exit of exciting and fluorescent radiation, respectively; μ_s^0 is the mass absorption coefficient for the element s with respect to the excitation energy; μ_s^i is the mass absorption coefficient for the element s with respect to the fluorescence energy of element i. In the case of overlapping lines, the line energies are nearly equal, thus the corresponding μ_s^i values are assumed to be equal. Further, in this case, the value of μ_s^i is given corresponding to one of the elemental line energies, and the superscript, i, is replaced by r'. Hence Eqn. 1 is rewritten, and by combination with the normalization condition $\Sigma_s^N W_s = 1$, it is found that

$$\sum_s^N b_{r,s} W_s = 1 \quad (2)$$

where $b_{r,s} = a_{r,s} + 1 - [\mu_s^0 + \mu_s^{r'} \sin \psi_1 / \sin \psi_2] / [\mu_s^0 + \mu_r^{r'} \sin \psi_1 / \sin \psi_2]$ (2a)

and if the element s contributes to I_r then

$$a_{r,s} = [G K_s (1 + H_s) \sin \psi_1] / I_r \, [(\mu_r^0 + \mu_r^{r'} \sin \psi_1) / \sin \psi_2] \quad (2b)$$

In all other cases $a_{r,s} = 0$. The subscript r in Eqns. 2a and 2b indicates that the element is related to the energy r'. This symbolism is chosen in order to demonstrate the similarity with the Lachance-Traill equations [6, 7].

The present equations are an extension of the equations given by Jensen et al. [5], where details for the calculation of K_s, H_s and G are given. Because H_s depends on the sample composition, the quantitative calculation is done iteratively, where the $a_{r,s}$ values, and thereby the $b_{r,s}$ values, are updated during each iteration. The indirect use of the normalization condition means that the absolute calibration factor, G, can be calculated during each iteration; separate absolute calibration is then redundant.

The resulting concentrations can be checked by calculating theoretical fluorescence intensities from Eqn. 1, and comparing these with the experimentally obtained intensities. Finally, the sum of calculated weight fractions should not differ considerably from unity.

Experimental

Apparatus and samples. The equipment used was described recently [9], as were the excitation chamber and the software for the spectrometer [4, 10]. Two standard reference materials were examined: SRM 1198 (Incoloy 901) and SRM 1201 (Hastelloy X), both from the U.S. National Bureau of Standards. The spectrometer was operated at 10 mA and 45 kV with the silver secondary target for 2000 s. Each SRM sample was measured four times.

Programs and calculations. For intensity calculations, the PROFIT program [4] was used; the intensities are found by a non-linear χ^2 minimization procedure, which assigns Gaussians to the fluorescence lines. Two programs, VAP [4] and IMELF, which exploit the fundamental parameter technique, were used for quantitative calculations. Element parameters used in VAP and IMELF were taken from tables [11—13]. The VAP program uses the numerical peak-overlap procedure described by Jensen et al. [4], and IMELF uses the procedure outlined above. Theoretical fluorescence intensities were calculated by using either IMELF or VAP. For the theoretical investigation, G was known in advance. For the analysis of the NBS samples, the determination of G was included in both quantitative programs. All three programs are coded in VAX-11 FORTRAN and were executed on the VAX 11/780.

Results and discussion

The procedure outlined by Jensen et al. [5] was used to calculate the theoretical K_α, K_β, L_α and L_β intensities for several hypothetical samples in which severe peak overlap occurred, e.g., samples of Ti, V and Ba, samples of Fe, Co and Ni, or samples containing As and Pb. In order to obtain the originally chosen weight fractions, the IMELF program was in turn applied to the calculated intensities. The main purpose of these calculations was to investigate the influence of the representative mass absorption coefficient μ_s^r. For comparison, the procedure proposed by Jensen et al. [4] (also included in VAP) was also applied to the calculated intensities. Only representative results obtained from the calculations on samples of Ti/V/Ba and Fe/Co/Ni are given here.

For the Ti/V/Ba sample, in which concentrations were selected arbitrarily (see Fig. 1), theoretical fluorescence intensities were calculated; part of the theoretical spectrum (Gaussian line shapes and FWHM = 156 eV) is given in Fig. 1. Peak overlap was assumed for Ba L_α/Ti K_α and for Ba L_β/Ti K_β/V K_α. The V K_β intensity was used for the last intensity equation. Thus, theoretical intensities were summed and used for I_r in Eqn. 2. Concentrations were calculated for six different combinations of the representative mass absorption coefficients, μ_s^r. The results are given in the first part of Table 1; results obtained by the VAP program [4] are included. Here, correction for V K_α on Ba L_β was included in VAP. The results show that the IMELF program is able to handle three overlapping peaks. However, the concentrations found

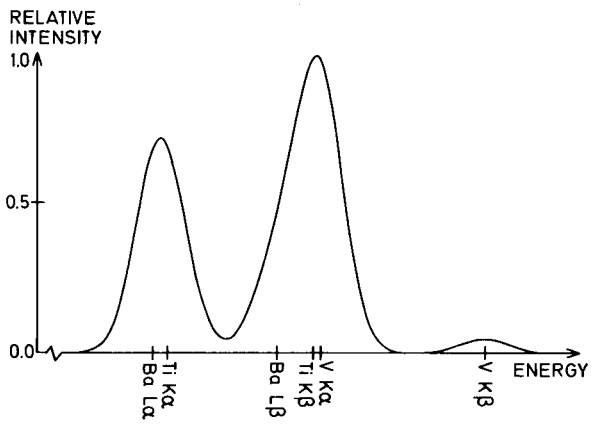

Fig. 1. Calculated energy-dispersive x-ray spectrum for Ti/V/Ba sample (27%, 33% and 40% w/w, respectively). The excitation energy is 17.806 keV Line shapes are assumed to be Gaussian, and a constant energy resolution, FWHM = 156 eV, is used.

are strongly dependent on the values chosen for $\mu_s^{r'}$. It can be seen that the mean values obtained from all combinations of $\mu_s^{r'}$ agree with the initial concentrations. In the case of the numerical procedure used in VAP, the results are almost useless.

Subsequently, it was assumed that only Ba L_α/Ti K_α and Ti K_β/V K_α were overlapping peaks, and the Ba L_β line was used as the third intensity equation. The concentrations thus obtained are listed in the second part of Table 1. The results of a similar calculation for a hypothetical sample consisting of Fe, Co and Ni (40:1:59% w/w) are also shown in Table 1; peak overlap was assumed for Co K_α/Fe K_β and Ni K_α/Co K_β. For both IMELF and VAP, these results agree with the initial concentrations. Again, IMELF indicates independence on the choice of $\mu_s^{r'}$.

Finally, experimental results from two NBS standards, SRM 1198 and SRM 1201, were examined by both quantitative programs. In the x.r.f. spectra of the samples, severe peak overlap occurs for Mn K_α/Cr K_β, Fe K_α/Mn K_β, Co K_α/Fe K_β and Ni K_α/Co K_β, but because of the small Mn and Co concentrations, no corrections for Mn K_β on Fe K_α and Co K_β on Ni K_α were included in either program. The results are listed in Table 2. In the mean values obtained by IMELF, all combinations of $\mu_s^{r'}$ were used for the overlapping lines. The concentrations calculated by VAP and IMELF agree well with each other. For most of the major elements, the difference between the certified concentrations and the concentrations obtained here is less than 3%.

TABLE 1

Influence of the representative mass absorption coefficient $\mu_s^{r'}$ for the quantitative calculation by IMELF in the case of a Ti/V/Ba sample and a Fe/Co/Ni sample (theoretically calculated intensities were obtained as described earlier [5])

Representative mass absorption coefficients used			Elemental concentration (% w/w)		
			Ti 27[a]	V 33[a]	Ba 40[a]
Assumed overlapping lines: Ba L_α/*Ti* K_α *and Ba* L_β/*Ti* K_β/*V* K_α					
μ(Ba L_α)	μ(Ba L_β)		26.15	34.04	43.44
μ(Ba L_α)	μ(Ti K_β)		31.94	29.75	27.17
μ(Ba L_α)	μ(V K_α)		32.20	29.56	26.42
μ(Ti K_α)	μ(Ba L_β)		26.77	33.95	42.63
μ(Ti K_α)	μ(Ti K_β)		26.63	32.75	38.71
μ(Ti K_α)	μ(V K_α)		26.56	32.10	38.13
		Mean[b]	28.0(3.0)	32.2(1.9)	36.0(7.0)
		VAP mean[c]	13.15	18.35	68.50
Assumed overlapping lines: Ba L_α/*Ti* K_α *and Ti* K_β/*V* K_α					
μ(Ba L_α)	μ(Ti K_β)		27.43	33.18	39.75
μ(Ba L_α)	μ(V K_α)		27.50	32.87	39.85
μ(Ti K_α)	μ(Ti K_β)		26.66	33.35	40.01
μ(Ti K_α)	μ(V K_α)		26.65	33.06	40.12
		Mean[b]	27.1(0.5)	33.1(0.2)	39.93(0.17)
		VAP mean[c]	27.00	33.00	40.00
Assumed overlapping lines: Co K_α/*Fe* K_β *and Ni* K_α/*Co* K_β					
			Fe 40[a]	Co 1[a]	Ni 59[a]
μ(Co K_α)	μ(Ni K_α)		40.01	1.09	59.00
μ(Co K_α)	μ(Co K_β)		40.10	1.09	57.05
μ(Fe K_β)	μ(Ni K_α)		40.00	0.98	59.01
μ(Fe K_β)	μ(Co K_β)		40.09	0.98	57.06
		Mean[b]	40.05(0.05)	1.04(0.06)	58.0(1.1)
		VAP mean[c]	39.96	1.00	59.04

[a]Initial values. [b]Mean value with standard deviation in parentheses. [c]Value obtained by the VAP procedure.

In conclusion, the proposed procedure for solving peak-overlap problems in energy-dispersive x.r.f. spectra by a fundamental parameter technique proved to work well when the fluorescence peak consisted of only two fluorescence lines, which did not differ much in energy. In all cases, it is recommended to use all possible values of $\mu_s^{r'}$ in quantitative calculations and then to calculate the mean values and standard deviations.

TABLE 2

Quantitative analysis of NBS SRM 1198 and SRM 1201 (mean values and standard deviation of four independent measurements are given)

Element	Element concentration (% w/w)		
	Quantitative algorithm		Certified
	VAP	IMELF	
SRM 1198			
Ti	2.84(0.07)	2.84(0.06)	2.59(0.01)
Cr	13.10(0.02)	13.08(0.03)	12.9(0.1)
Mn	1.07(0.02)	1.07(0.03)	0.49[a]
Fe	36.54(0.04)	36.57(0.06)	36.2(0.1)
Co	1.655(0.016)	1.70(0.13)	0.70(0.01)
Ni	39.19(0.07)	39.14(0.09)	40.1(0.1)
Zr	0.0201(0.0013)	0.0201(0.0012)	0.014[a]
Mo	5.584(0.017)	5.579(0.016)	6.08(0.05)
SRM 1201			
Cr	20.93(0.02)	20.90(0.03)	20.7(0.1)
Mn	0.637(0.019)	0.65(0.03)	—
Fe	23.66(0.01)	23.69(0.03)	23.2(0.1)
Co	1.409(0.014)	1.44(0.10)	0.56(0.01)
Ni	45.00(0.02)	44.96(0.06)	45.7(0.1)
Mo	8.371(0.014)	8.362(0.014)	9.18(0.05)

[a]Not certified; additional information.

The author is grateful to the Danish Technical Research Council for financial support (grant no. 16-1866) and to S. E. Rasmussen for his advice on the preparation of the paper.

REFERENCES

1 J. J. McCarthy and F. H. S. Chamber, in K. F. J. Heinrich (Ed.), Energy-Dispersive X-ray Spectrometry, NBS Special Publication 604, PB 81-226334, Washington, DC, 1981, p. 273 ff.
2 P. Van Espen, H. Nullens and F. C. Adams, Z. Anal. Chem., 285 (1977) 215.
3 E. Marageter, W. Wegscheider and K. Müller, Nucl. Instrum. Meth. Phys. Res., B1 (1984) 137.
4 B. B. Jensen, J. N. Marcussen and N. Pind, Anal. Chim. Acta, 161 (1984) 175.
5 B. B. Jensen, J. N. Marcussen and N. Pind, Anal. Chim. Acta, 167 (1985) 305.
6 G. R. Lachance and R. J. Traill, Can. Spectrosc., 11 (1966) 43.
7 R. J. Traill and G. R. Lachance, Can. Spectrosc., 11 (1966) 63.
8 C. J. Sparks Jr., Adv. X-ray Anal., 19 (1976) 19.
9 B. B. Jensen and N. Pind, Anal. Chim. Acta, 171 (1985) 101.
10 L. H. Christensen, S. E. Rasmussen, N. Pind and K. Henriksen, Anal. Chim. Acta, 116 (1980) 7.
11 W. H. McMaster, N. Kerr Del Grande, J. H. Mallett and J. H. Hubbell, Compilation of X-ray Cross Sections, Sec. 2, Rev. 1, 1969, UCRL-50174.
12 M. O. Krause, J. Phys. Ref. Data, 8 (1979) 307.
13 J. H. Scofield, At. Data and Nucl. Data Tables, 14 (1974) 121.

Analytica Chimica Acta, 172 (1985) 387—391
Elsevier Science Publishers B.V., Amsterdam — Printed in The Netherlands

Short Communication

ROUTINE THERMOMETRIC TITRATION OF TRICYCLIC ANTIDEPRESSANT DRUGS AND THEIR FORMULATIONS

E. J. GREENHOW*,[a] and O. LADIPO[b]

Department of Chemistry, Chelsea College, University of London, Manresa Road, London, SW3 6LX (Great Britain)

(Received 7th November 1984)

Summary. A rapid procedure is described for the routine assay of amitryptyline, imipramine and clomipramine hydrochlorides and trimipramine maleate. The weakly basic drugs are titrated with perchloric acid in anhydrous acetic acid; the heat output of the proton-catalysed acetylation of 4-hydroxy-4-methylpentan-2-one with acetic anhydride indicates the equivalence point. For milligram amounts of the drugs, accuracy is good and relative standard deviations are usually better than 1%; sub-milligram amounts can also be assayed. Four commercial formulations were found to be within the British Pharmacopoeia 1980 specifications.

The tricyclic antidepressant drugs investigated here are well-established psychotherapeutic agents. Their mass production demands rapid procedures for quality control. Several methods have been proposed for quantifying such drugs. These include the British Pharmacopoeia (B.P.) titrimetric method [1] and spectrophotometric [2], gas-liquid chromatographic (g.l.c.) [3, 4] and high-performance liquid chromatographic (h.p.l.c.) methods [5, 6]. The official B.P. methods are for the assay of both the pure drugs and the drugs in pharmaceutical preparations. Since the exploitation of tricyclic drugs as antidepressant agents, g.l.c. and h.p.l.c. seem to be the most popular, as the major concern is with determination of low levels of unchanged drugs in the presence of many metabolites in biological fluids.

In the proposed titrimetric method, an esterification indicator reaction [7] is applied. The slight excess of perchloric acid titrant after the weakly basic drug has reacted in dry acetic acid/acetic anhydride mixture (2:3) catalyses the acetylation of 4-hydroxy-4-methylpentan-2-one, which generates heat; this produces a sharp end-point. The speed and sensitivity of the catalytic end-point in the thermometric technique coupled with its simple instrumentation [8] make it useful for the routine work needed in quality control. Other advantages of the technique are that it is not usually necessary

[a]Present address: Chemistry Department, Birkbeck College, Malet Street, London WC1E 7HX, Great Britain.
[b]Present address: Department of Chemistry, Faculty of Science, University of Lagos, Lagos, Nigeria.

0003-2670/85/$03.30

to separate the active ingredient from the powdered sample as in the B.P. [1] methods, and that the high sensitivity permits the use of individual tablets for several replicate assays. There is no need to add mercury(II) acetate when acid halide salts of the drugs are determined [8].

Experimental

Apparatus. The apparatus has been described [8]. A motor-driven micrometer syringe was used to deliver the titrant to the sample solution in a 10-ml Dewar flask at a nominal rate of 0.11 ml min^{-1}; both solutions were initially at room temperature. The temperature changes were recorded as the imbalance voltage from a Wheatstone bridge with a thermistor as one of the arms.

Chemicals. The tricyclic antidepressants tested were: amitriptyline hydrochloride [3-(3-dimethylaminopropylidene)-1,2,5-dibenzocyclohepta-1,4-diene hydrochloride; Merck, Sharp and Dohme], imipramine hydrochloride [10,11-dihydro-*N*,*N*-dimethyldibenzo(b,f)azepine-5-propanamine hydrochloride], clomipramine hydrochloride [3-(3-chloro-10,11-dihydro-5H-dibenzo(b,f)azepin-5-yl)-*N*,*N*-dimethylpropylamine hydrochloride] (both from Ciba-Geigy), and trimipramine maleate [5-(3-dimethylamino-2-methylpropyl)-10,11-dihydrodibenzo(b,f)azepine hydrogenmaleate; May and Baker, Dagenham, Great Britain).

Potassium hydrogenphthalate (AnalaR grade) was dried to constant weight at 110°C. Perchloric acid, glacial acetic acid and acetic anhydride were of analytical-reagent grade. Anhydrous acetic acid was prepared by adding the theoretical amount of acetic anhydride to glacial acetic acid of known water content (determined by the Karl Fischer method) and leaving overnight. 4-Hydroxy-4-methylpentan-2-one was of laboratory reagent grade.

Stock solutions. Perchloric acid solution (0.1 M) in anhydrous acetic acid was prepared by measuring 98.5 ml of perchloric acid (71.0—73.0%) into a 1-l volumetric flask, adding 100 ml of anhydrous acetic acid and 15 ml of acetic anhydride with constant stirring and cooling, and diluting to the mark with anhydrous acetic acid, and leaving for 24 h in the dark. The solution was standardised against potassium hydrogenphthalate solution in anhydrous acetic acid, by the thermometric method. It was also standardised by the classical visual procedure with crystal violet indicator. Other standard solutions of perchloric acid were prepared by suitable dilution with anhydrous acetic acid.

Pure tricyclic drug stock solutions (0.01 M) were prepared in anhydrous acetic acid and protected from light for storage. Dilute (0.001 M) solutions were prepared by diluting with anhydrous acetic acid.

Tablet stock solutions (1 ml ≡ 1 mg of the drug nominally) were prepared by dissolving powdered tablets in anhydrous acetic acid. Capsule stock solutions (1 ml ≡ 1 mg of the drug nominally) were prepared by dissolving the contents of two 10-mg capsules of clomipramine hydrochloride in anhydrous acetic acid.

Procedures. An aliquot of the test solution containing the required quan-

tity (e.g., 0.01 mmol or 1 mg (ml^{-1})) of the active ingredient in anhydrous acetic acid was pipetted into the Dewar flask. The volume was adjusted to 2.0 ml with anhydrous acetic acid and 3.0 ml of acetic anhydride and 0.5 ml of 4-hydroxy-4-methylpentan-2-one were added. The flask was covered with a polyethylene cap bearing the thermistor and the polyethylene titrant delivery tube. The solution was stirred magnetically for 1—2 min until thermal equilibrium was attained; the recorder range was set at 100 mV with a chart speed of 10 mm min^{-1}.

The pure 0.01 M drug solutions were titrated with the standardised 0.1 M perchloric acid whereas the 0.001 M solutions and the tablet and the capsule stock solutions were titrated with 0.01 M perchloric acid. The use of titrant concentrations at least 10 times greater than the drug concentration ensures that extraneous heat from mixing and dilution is minimised. During the titration, the temperature change was recorded; there was a gradual increase in temperature up to the end-point, at which stage the temperature rose sharply.

Results and discussion

The results are summarised in Tables 1 and 2. It is evident from these results that anhydrous acetic acid/acetic anhydride (2:3) is a satisfactory solvent system for the assay of these weakly basic drugs. The excess of acetic anhydride in the mixture eliminates the unfavourable thermal effects of traces of water previously reported [9]. The sharp change in slope of the enthalpogram is due to the acetylation reaction catalysed by the slight excess of the titrant at the equivalence point. Preliminary investigation and a previous report on the assay of barbiturates [10] suggest that the occasional slight curvature at the end-point when 0.01 M perchloric acid is used,

TABLE 1

Thermometric determination of tricyclic antidepressant drugs

Compound	Mass of drug (mg)						
	Taken	Found[a]	Compound		Taken	Found[a]	
Amitriptyline	6.28	6.22	(0.2)[b]	Trimipramine	8.2	8.15	(0.7)[b]
hydrochloride	3.14	3.11	(0.6)[b]	maleate	4.11	4.15	(1.4)[b]
	0.63	0.63	(1.6)[c]		2.05	2.03	(1.0)[b]
	0.31	0.31	(6.4)[c]		0.82	0.82	(2.4)[c]
	0.16	0.16	(6.3)[c]		0.41	0.41	(7.3)[c]
Imipramine	6.34	6.34	(0.2)[b]	Clomipramine	7.02	7.02	(0.3)[b]
hydrochloride	3.17	3.14	(0.3)[b]	hydrochloride	3.51	3.47	(0.6)[b]
	1.58	1.57	(1.3)[b]		1.75	1.74	(0.6)[b]
	0.63	0.63	(1.6)[c]		0.70	0.71	(2.8)[c]
	0.32	0.32	(3.1)[c]		0.35	0.36	(5.6)[c]
	0.16	0.16	(6.2)[c]		0.18	0.18	(5.6)[c]

[a]Mean of 4 determinations with relative standard deviation (%) in parentheses. [b]Titrated with 0.1 M perchloric acid. [c]Titrated with 0.01 M perchloric acid.

TABLE 2

Percentage recovery of the drugs from formulations

Product	Mass of drug (mg)		Nominal recovery (%)
	Taken[a]	Found[b]	
Amitriptyline tablet	1.0	1.0(1.0)	100
	0.5	0.53(3.8)	106
	0.25	0.25(4.0)	100
	0.13	0.14(7.1)	107.7
Imipramine tablet	1.0	1.01(1.0)	101
	0.50	0.50(2.0)	100
	0.25	0.24(8.3)	96
	0.1	0.1(10.0)	100
Trimipramine maleate tablet	2.0	1.9(1.1)	95
Clopramine HCl capsule	1.0	1.04(2.9)	104
	0.25	0.26(7.7)	104

[a]Nominal mass of active constituent. [b]Mean of 4 determinations with relative standard deviation (%) in parentheses. All titrations with 0.01 M perchloric acid.

relates partly to the overall sensitivity of the potentiometric recorder used and cannot be attributed solely to the titrant concentration. In all cases, end-points are easily evaluated by extrapolation of the linear sections of the plot.

The method is accurate, sensitive and reproducible, and requires only dissolution of samples. It is therefore suitable for routine quality control. The lower limit of determination is governed by the titrant concentration, i.e., by the temperature change obtainable at the equivalence point (see Table 1). The upper limit of determination is unrestricted except by thermal capacity considerations.

The proposed method was applied for routine assay of single dosage forms of different formulations. The results in Table 2 are within the B.P. specifications of 92.5—107.5% [1], thus the excipients do not appear to cause overestimation of the nominal values. The sensitivity of the method means that a single tablet or capsule can be used for several titrations, which enhances the convenience of the method.

The authors thank Merck, Sharp and Dohme, Ciba-Geigy, and May and Baker for providing the drugs tested.

REFERENCES

1 British Pharmacopoeia, 1980 H.M. Stationary Office, London, 1980, pp. 29, 238 and 466; 732, 779 and 831.
2 E. Hamilton, J. E. Wallace and K. Blum, Anal. Chem., 47 (1975) 1139.
3 G. Norheim, J. Chromatogr., 88 (1974) 403.
4 L. A. Gifford, P. Turner and C. M. B. Pare, J. Chromatogr., 105 (1975) 107.

5 A. G. Butterfield and R. W. Sears, J. Pharm. Sci., 66 (1977) 1117.
6 D. Watson and M. J. Stewart, J. Chromatogr., 132 (1977) 155.
7 E. J. Greenhow, Analyst (London), 102 (1977) 584.
8 E. J. Greenhow and L. E. Spencer, Analyst (London), 98 (1973) 81, 98.
9 V. J. Vajgand, F. F. Gaal and S. S. Brusin, Talanta, 17 (1970) 415.
10 L. S. Bark and O. Ladipo, Analyst (London), 101 (1976) 203.

Analytica Chimica Acta, 172 (1985) 393–396
Elsevier Science Publishers B.V., Amsterdam — Printed in The Netherlands

Announcement

WORKING PARTY ON ANALYTICAL CHEMISTRY (WPAC), FEDERATION OF EUROPEAN CHEMICAL SOCIETIES (FECS)

EUROPEAN ANALYTICAL COLUMN 8

In January 1985 the Working Party on Analytical Chemistry (WPAC) consisted of 28 chemical societies from 23 European countries personally represented by 26 delegates. The Greek and the Turkish Chemical Societies are in correspondence with the secretariat; only the Society of Luxembourg Chemists and the Pancyprian Union of Chemists among the FECS members are not yet active in the WPAC. The chemical societies of Egypt, the German Democratic Republic, Israel and Rumania as well as IUPAC have observer status.

The 15th meeting of the WPAC was held in Cracow, August 26, 1984, during the Euroanalysis V Conference. At this meeting, Prof. Dr.Dr.h.c. Ernö Pungor was unanimously re-elected as chairman of the WPAC for his second term, 1984–1987.

The following WPAC activities were discussed.

Euroanalysis Conferences

Euroanalysis V, August 26–31, 1984, Cracow, Jagellonian University, Poland. Host society: Polish Chemical Society. Conference president: Prof. A. Hulanicki. Presidium members: Prof. E. Pungor, Prof. E. Roth, Prof. L. Niinistö. Secretary: Prof. Z. Kowalski. There were 619 participants from 30 countries at this successful international conference with 14 invited lectures. 121 discussion papers and 320 posters. The contributions were presented in 18 sessions including special sessions on computer-based analytical chemistry (COBAC III) and on speciation in water analysis and air analysis. The invited lectures will be published as the Proceedings of the Euroanalysis V Conference in the series "Review on Analytical Chemistry", editor A. Hulanicki, printed and distributed by Akademiai Kiado, Budapest, 1985.

Euroanalysis VI, September 7–11, 1987, Paris, France. Conference presidium: Prof. E. Roth, Prof. E. Pungor; Prof. A. Hulanicki and Prof. H. Malissa. It is planned to maintain the successful broad-spectrum type of conference and to have another special session in the COBAC series. For further information please contact Prof. E. Roth.

Euroanalysis VII, 1990. At the Cracow meeting of the WPAC, Vienna was selected as the venue for Euroanalysis VII (host: Austrian Society for Microchemistry and Analytical Chemistry).

Events sponsored or supported by WPAC/FECS in 1984

Symposium on "New Trends in Chemistry — The Role of Analytical Chemistry to National Development", January 3—7, 1984, Cairo, Egypt. Host society: Egyptian Chemical Society. There were very successful discussions between 200 Egyptian analytical chemists and 9 specialists from some European societies of analytical chemistry. As one consequence, an independent society of analytical chemistry has been created and several ways of cooperation with European countries have been designed (joint supervision programs, workshops, etc).

Fourth Scientific Session on Ion-Selective Electrodes, October 8—12, 1984 (72nd event of FECS), Matrafüred, Hungary. Chairman: Prof. E. Pungor. Ninety-five scientists from U.S.A., Europe, China and Japan attended. Proceedings are to be prepared (contact Prof. E. Pungor).

Further events sponsored or supported by WPAC/FECS

Twelfth International Competition in Analytical Chemistry, May 13—15, 1985, University of Veszprem, Hungary. Chairman: Prof. J. Inczedy. Students at European universities are invited to take part in these traditional competitions in the theory and practice of chemical analysis. Costs of accommodation for 3 competitors and one group leader per university will be covered by the organizers.

First International Symposium on Philosophy and History in Analytical Chemistry, Schallaburg/Vienna, Austria, November 22—23, 1985. Chairmen: Prof. H. Malissa and Prof. F. Szabadvary. This joint venture with the Working Party on the History of Chemistry is organized by the Austrian Society of Microchemistry and Analytical Chemistry to discuss the impact and the importance of selected periods of time in the development of analytical chemistry.

COBAC IV, 1986, Graz, Austria. Host society: Austrian Society of Microchemistry and Analytical Chemistry with Society of Austrian Chemists. Chairmen: Doz. W. Wegscheider and Doz. K. Varmuza. It is planned to have this specialist meeting in addition to the more open COBAC meetings at the Euroanalysis VI and VII conferences.

Final evaluation of the questionnaire on "Education in Analytical Chemistry at University Level — 1983/84"

By December 31, 1984, 229 universities from all 23 member countries of the WPAC contributed to this activity. Separate evaluations have been done for institutions with and without a chair or department of analytical chemistry. The result quantifies for the first time what has only been felt before. The total teaching time available as well as the distribution over the six major areas of analytical chemistry is much better in institutions with a separate chair in analytical chemistry (Fig. 1) than in those without one (Fig. 2). Institutions without a chair in analytical chemistry tend to preserve the traditional structure of the courses and to neglect new developments. As

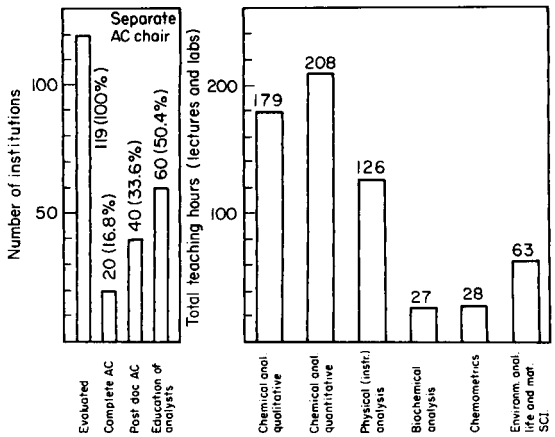

Fig. 1. Education in analytical chemistry in Europe (1983/84) showing total teaching hours for chemical, physical and biochemical analysis, chemometrics, environmental analysis, and analytical chemistry in life and material sciences. The mean values are based only on those universities evaluated with a separate chair, group or department in analytical chemistry.

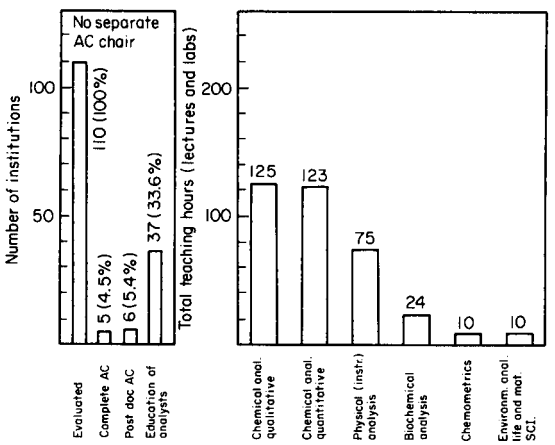

Fig. 2. Total teaching hours for chemical, physical and biochemical analysis, chemometrics, environmental analysis and analytical chemistry in life and material sciences. The mean values given are based only on those universities without a separate chair, group or department in analytical chemistry.

a consequence, teaching time in conventional fields (classical chemical analysis) is drastically cut back without extension to modern fields of analytical chemistry (physical methods, chemometrics, biological methods, environmental analysis, etc.).

Next (16th) meeting of the WPAC

The Austrian Society of Microchemistry and Analytical Chemistry has invited the WPAC to hold its 16th meeting in Vienna, November 24, 1985, in connection with the 1st International Symposium on Philosophy and History in Analytical Chemistry (see above).

For any information related to WPAC activities, pleast contact the secretary: Prof. Dr. R. Kellner, Institut für Analytische Chemie, Technische Universität Wien, A-1060 Wien, Getreidemarkt 9, West Germany.

ANALYTICA CHIMICA ACTA, VOL. 172 (1985)

AUTHOR INDEX

ACA announcements

PRIZE

PRIZE BIOCHEMICAL ANALYSIS 1986

The German Society for Clinical Chemistry awards the prize BIOCHEMICAL ANALYSIS every two years at the symposium: Analytica 86, 10th International Trade Exhibition, 10th International Conference Biochemical Analytics", held June 3–6, 1986 in Munich, F.R.G.

The prize of DM 10 000.00 is donated by BOEHRINGER Mannheim GmbH for outstanding and novel work in the field of biochemical analysis or biochemical instrumentation or for significant contributions to the advancement in experimental biology especially relating to clinical biochemistry.

Competitors for the prize 1986 should submit papers concerning one theme, either published or accepted for publication between October 1st 1983 and September 30th 1985, before November 15th 1985, to: Prof. Dr. H. Feldmann, Secretary of the prize BIOCHEMICAL ANALYSIS; Institut für Physiologische Chemie der Universität, Goethestrasse 33, D-8000 München 2, F.R.G.

If several authors are involved in this work, please, indicate the name(s) of the candidate(s).

ANNOUNCEMENTS OF MEETINGS

12th ANNUAL MEETING OF THE FEDERATION OF ANALYTICAL CHEMISTRY AND SPECTROSCOPY SOCIETIES, PHILADELPHIA, PA, U.S.A., SEPTEMBER 29–OCTOBER 4, 1985

The 12th annual meeting of the Federation of Analytical Chemistry and Spectroscopy Societies (FACSS) will be held at the Philadelphia Marriott Hotel, in Philadelphia, PA, U.S.A. The sponsoring organizations for the meeting are: the Society for Applied Spectroscopy; the Division of Analytical Chemistry of the American Chemical Society; the Association of Analytical Chemists, Inc. (Anachem); the Analysis Instrumentation Division of the Instrument Society of America; and the Chromatography Forum of the Delaware Valley. Approximately 40 symposia, with 450 papers, covering all areas of analytical chemistry, are planned for the four and a half day meeting.

Contact: Richard J. Knauer, Publicity Chairman, Armco, Inc., P.O. Box 1697, Baltimore, MD 21203, U.S.A.

2nd SYMPOSIUM ON HANDLING OF ENVIRONMENTAL AND BIOLOGICAL SAMPLES IN CHROMATOGRAPHY, FREIBURG, F.R.G., OCTOBER 24–25, 1985

The organisation of this second event – the first was held in Lausanne, Switzerland in 1983 – is in the hands of the International Association of Environmental Analytical Chemistry and sponsored by national bodies. A strong industrial participation is planned. It is the intention to bring together specialists in this field who can give a good account of the state-of-the-art in their respective specialty and to present first-hand experience in sample handling. Continous flow extraction techniques, solid surface sample handling with pre-column technology (on-line and off-line), pre-chromatographic use of derivatization techniques, column switching methodology for handling of complex samples are some of the topics that will be treated and extensively discussed. Special emphasis will be placed on techniques with automation potential and actually automated procedures suitable for routine handling of large series of biological (urine, blood, tissue, plant material) and enviromental samples (water, waste water, air).

Contact: Workshop Office IAEAC, M. Frei-Hausler, Postfach 46, CH-4123 Allschwil 2, Switzerland.

III CAC – MEETING OF THE CHEMOMETRICS SOCIETY, LERICI, ITALY, MAY 26–29, 1986

An international conference on chemometrics in analytical chemistry and optimization will be held at Villa Marigola in Lerici, Italy, on May 26–29, 1986. The conference is being organized under the auspices of the Analytical Division of the Italian Chemical Society and of the Chemometrics Society.

Topics will include: application and development of techniques for design, optimization and evaluation of analytical procedures and results, application of chemometrical techniques (pattern recognition, operations research, information theory, artificial intelligence, robotics, . .) in analytical chemistry with a special reference to food chemistry and clinical chemistry, computerized signal- and data processing; education in chemometrics.

The programme will include invited plenary lectures and submitted research papers. Papers are to be refereed for publication in a special issue of *Analytica Chimica Acta.*

Further information can be obtained from: Prof. M. Forina, Istituto di Analisi e Tecnologie Faemaceutiche ed Alimentari, Via Brigata Salerno (ponte), I-16147 Genova, Italy. Tel.: (010) 3993656.

10th INTERNATIONAL CODATA CONFERENCE, OTTAWA, CANADA, JULY 14–17, 1986

The Tenth International Conference on Computer Handling and Dissemination of Data will be held at the Westin Hotel, Ottawa, Ontario, Canada, at the invitation of The National Research Council of Canada with the collaboration of The Royal Society of Canada and The Government of Ontario, Ministry of Industry and Trade.

The conference will be organized around a number of multi-disciplinary and discipline-oriented symposia in the area of scientific and technical data. Major themes will be: computerized databases – technology and management; computer techniques in data and systems analysis; numerical information systems in materials science, technology and industry; numerical information processing in the biosciences; numerical data processing and dissemination in the geosciences; data needs in industry.

CODATA, an interdisciplinary Scientific Committee of ICSU (International Council of Scientific Unions) deals with data of importance to science and technology, quantitative data on properties and behavior of matter, quantitative data and characteristic values of biological, geological, and atronomical systems, and other experimental and observational values in all areas of science represented by the member Unions of ICSU. Many of its activities bear upon problems which are common to the various disciplines.

Further information: Mrs. Lois Baignée, Executive Secretary CODATA '86, Conference Services, National Research Council of Canada, Montreal Road, Ottawa, K1A OR6 Canada.

4th CONFERENCE ON COMPUTER BASED ANALYTICAL CHEMISTRY, GRAZ, AUSTRIA, SEPTEMBER, 1986

The Austrian Society for Microchemistry and Analytical Chemistry together with the Working Group "Computers in Chemistry" (Chairman: Univ. Doz. Dr. Kurt Varmuza) of the Austrian Chemical Society plans to organize the 4th COBAC Conference.

The earlier Conference in Portoroz (Yugoslavia), Munich (F.R.G.) and Crakow (Poland) have all been well received by the scientific community so that the Graz Conference is intended to attract specialists in our field. In this sense the tradition of Portoroz is followed by holding a separate meeting that is not part of another general analytical conference.

To establish international contact and to profit from your experience that is believed to be essential to make such an undertaking work out you are invited to join the organizers as a member of the "International Liaison Board".

In order to make the most of your effort the members of this board will be invited at a later date to organize and chair sessions, that feature the most relevant developments. At this time you will be asked to consider your cooperation with the Organizing Committee and prepare a suggestion for an eminent topic together with a short statement of its current and future relevance. In doing so you can help to make sure that the meeting in Graz will scientifically be successful.

In an attempt to encourage also non-specialists, particularly from industry, the support of both software houses and computer companies will be solicited. It is felt that those have to offer so much that room should be given to the companies to explain products and computer procedures.

For suggestions in this direction as well as any input you might be willing to give, please contact: Dr. Wolfhard Wegschneider, Institut für Analytische Chemie, Mikro- und Radiochemie, Technische Universität, Technikerstrasse 4, A-8010 Graz, Austria. Tel.: (0316) 7061-8300/8301.

XXV COLLOQUIUM SPECTROSCOPICUM INTERNATIONALE, TORONTO, CANADA, JUNE 21–26, 1987

The XXV Colloquium Spectroscopium Internationale, sponsored by the Spectroscopy Society of Canada, the Society for Applied Spectroscopy (U.S.A.) and the National Research Council of Canada, will be held at the Hilton Harbour Castle, Toronto, Canada from June 21 to 26, 1987.

The core of the scientific programme will consist of two plenary lectures, by Nobel Laureates Dr. Gerhard Herzberg and Professor Arthur L. Schawlow, and about thirty-five invited lectures by young scientists. The other lectures will be selected from submitted abstracts. There are no plans for poster sessions. The invited and submitted presentations will be based on recent research, rather than reviews of past work. There will be eight to ten simultaneous sessions, many beginning with invited lectures. For further information, contact: Dr. J.D. Winefordner, Department of Chemistry, University of Florida, Gainesville, FL 32611, U.S.A. Tel.: (904) 392-0556.

The second circular with a call for papers will be published in Spring 1986. Anyone wishing to receive additional general information on the Colloquium should contact: Mr. L. Forget, Executive Secretary CSI XXV, National Research Council of Canada, Ottawa, K1A 0R6 Canada. Tel.: (613) 993-9009, telex: 053-3145.

CALENDAR OF FORTHCOMING MEETINGS

Sept. 8–13, 1985 Madrid, Spain	**17th European Congress on Molecular Spectroscopy** Contact: Organizing Committee EUCMOS XVII, Instituto de Optica, C.S.I.C. Serrano, 121 Madrid-6, Spain.
Sept. 8–13, 1985 Chicago, IL, U.S.A.	**190th National Meeting of the American Chemical Society** Contact: Meetings Department, American Chemical Society, 1155 Sixteenth Street, NW, Washington, DC 20036, U.S.A.
Sept. 9–13, 1985 Manchester, U.K.	**30th International Congress of Pure and Applied Chemistry** Contact: The Royal Society of Chemistry, Burlington House, London W1V 0BN, U.K. (Further details published in Vol. 155.)
Sept. 10–13, 1985 Guildford, U.K.	**6th International Bioanalytical Forum** Contact: Dr. E. Reid, Guildford Academic Associates, 72 The Chase, Guildford, Surrey GU2 5UL, U.K. Tel.: 0483-65324. (Further details published in Vol. 169.)
Sept. 15–19, 1985 San Francisco, CA, U.S.A.	**14th North American Thermal Analysis Society Meeting** Contact: John Elder, University of Kentucky, Institute for Minerals & Mining, Iron Works Pike, P.O. Box 13015, Lexington, KY 40583, U.S.A. Tel.: (606) 252-5535.
Sept. 15–21, 1985 Garmisch–Partenkirchen, F.R.G.	**Colloquium Spectroscopicum Internationale XXIV** Contact: CSI XXIV, Organisationsbüro, Institut für Spektrochemie und angewandte Spektroskopie, Postfach 778, D 4600 Dortmund 1, F.R.G. (Further details published in Vol. 169.)
Sept. 16–19, 1985 Bradford, U.K.	**Particle Size Analysis 1985** Contact: Dr. T. Allen, School of Powder Technology, University of Bradford, Bradford, West Yorkshire BD7 1DP, U.K. Tel.: (0274) 733466 etx. 382/380.
Sept. 29–Oct. 4, Philadelphia, PA, U.S.A.	**12th Annual Meeting of the Federation of Analytical Chemistry and Spectroscopy Societies** Contact: Alan Ullman, Procter & Gamble Co., 6250 Center Hill Road, Cincinnati, OH 45224, U.S.A. Tel.: (513) 659-6445.

Oct. 9–11, 1985 Gaithersburg, MD, U.S.A.	**1st International Symposium on Fire Safety Science** Contact: J. Quintiere, A345 Polymers Building, NBS, Gaithersburg, MD 20899, U.S.A. Tel.: 301/921-3242.
Oct. 20–23, 1985 Boston, MA, U.S.A.	**3rd International Symposium on Laboratory Robotics** Contact: Gerald Hawk, Zymark Center, Hopkinton, MA 01748, U.S.A. Tel.: (617) 435-9501.
Oct. 20–24, 1985 Knoxville, TN, U.S.A.	**4th Symposium on Separation Science and Technology for Energy Applications** Contact: J.T. Bell, Oak Ridge National Laboratory, P.O. Box X, Oak Ridge, TN 37831, U.S.A.
Oct. 24–25, 1985 Freiburg, F.R.G.	**2nd Symposium on Handling of Environmental and Biological Samples in Chromatography** Contact: Workshop Office IAEAC, M. Frei-Hausler, Postfach 46, CH-4123 Allschwil 2, Switzerland (Further details published in Vol. 162.)
Nov. 4–6, 1985 Toronto, Canada	**5th International Symposium on HPLC of Proteins, Peptides and Polynucleotides** Contact: Ms. S.E. Schlessinger, Symposium Manager, 5th International Symposium on HPLC of Proteins, Peptides, and Polynucleotides, 400 East Randolph, Chicago, IL 60601, U.S.A. Tel.: (312) 527-2011.
Nov. 11–16, 1985 Yalta, U.S.S.R.	**5th Danube Symposium on Chromatography** Contact: Dr. L.N. Kolomiets, The Scientific Council of Chromatography, Academy of Sciences of the U.S.S.R., Institute of Physical Chemistry, Lenin-Prospect 31, Moscow 117312, U.S.S.R.
Nov. 19–22, 1985 New York, NY, U.S.A.	**Eastern Analytical Symposium** Contact: Dr. S. David Klein, EAS Publicity, Merck & Co., Inc., P.O. Box 2000/R80L-106, Rahway, NJ 07065, U.S.A. Tel.: (201) 846-1582. (Further details published in Vol. 169.)
Jan. 2–8, 1986 Maui, HI, U.S.A.	**1986 Winter Conference on Plasma Spectrochemistry** Contact: 1986 Winter Conference, c/o ICP Information Newsletter, Department of Chemistry, GRC Towers, University of Massachusetts, Amherst, MA 01003-0035, U.S.A. Tel.: (413) 545-2294.
March 10–14, 1986 Atlantic City, NJ, U.S.A.	**37th Pittsburgh Conference and Exposition on Analytical Chemistry and Applied Spectroscopy** Contact: Mrs. Alma Johnson, Program Secretary, 12 Federal Drive, Suite 322, Pittsburgh, PA 15235, U.S.A.
Apr. 21–23, 1986 Neuherberg, F.R.G.	**4th International Workshop on Trace Element Analytical Chemistry in Medicine and Biology** Contact: Dr. P. Schramel, Gesellschaft für Strahlen- und Umweltforschung mbH, Institut für Angewandte Physik, Physikalisch- Technische Abteilung, Ingolstädter Landstrasse 1, D-8042 Neuherberg, F.R.G.
Apr. 22–24, 1986 Noordwijkerhout, The Netherlands	**Anatech '86 – An International Symposium on Applications of Analytical Chemical Techniques to Industrial Process Control** Contact: Prof. W.E. van der Linden, Laboratory for Chemical Analysis, Department of Chemical Technology, Twente University of Technology, P.O. Box 217, 7500 AE Enschede, The Netherlands. (Further details published in Vol. 169.)
Apr. 24–25, 1986 Neuherberg, F.R.G.	**2nd International Symposium on Biological Reference Materials** Contact: Dr. W.R. Wolf, Beltsville Human Nutrition Research Center, Beltsville, MD 20705, U.S.A.

May 18–23, 1986 San Francisco, CA, U.S.A.	**HPLC '86. New Frontiers in HPLC. 10th International Symposium on Column Liquid Chromatography** Contact: Ms. Shirley Schlessinger, 400 E. Randolph Drive, Chicago, IL 60601, U.S.A. (Further details published in Vol. 169.)
May 26–29, 1986 Lerici, Italy	**III CAC – Meeting of the Chemometrics Society** Contact: Prof. M. Forina, Istituto di Analisi e Tecnologie Farmaceutiche ed Alimentari, Via Brigata Salerno (ponte), I-16147 Genova, Italy. Tel.: (010) 3993656.
May 27–30, 1986 Brussels, Belgium	**2nd International Symposium on Drug Analysis** Contact: Mrs. C. van Kerchove, c/o Société Belge des Sciences Pharmaceutiques, Rue Stévinstraat 137, B-1040 Brussels, Belgium. Tel: (02) 230 26 85, ext. 33.
June 10–12, 1986 Dublin, Ireland	**Electroanalysis na h'Eireann** Contact: Dr. Malcolm R. Smith, School of Chemical Sciences, National Institute for Higher Education, Glasnevin, Dublin 9, Ireland.
June 23–27, 1986 Copenhagen, Denmark	**Modern Trends in Activation Analysis, 7th International Conference** Contact: Dr. K. Heydorn, General Chairman MTAA-7, Risø National Laboratory, Post Box 49, DK-4000 Roskilde, Denmark. (Further details published in Vol. 169.)
July 7–10, 1986 Bordeaux, France	**2nd International Meeting on Chemical Sensors** Contact: Dr. Claude Lucat, 2nd International Meeting on Chemical Sensors, Université de Bordeaux I, 351, cours de la Libération, 33405 Talence, Cedex, France.
July 14–17, 1986 Ottawa, Canada	**10th International CODATA Conference** Contact: Mrs. Lois Baignée, Executive Secretary CODATA '86, Conference Services, National Research Council of Canada, Montreal Road, Ottawa, K1A OR6 Canada.
July 20–26, 1986 Bristol, U.K.	**SAC 86 – International Conference and Exhibition on Analytical Chemistry** Contact: Miss PE. Hutchinson, Royal Society of Chemistry, Analytical Division, Burlington House, London W1V 0BN, U.K. Tel.: (01) 734-9971, (Further details published in Vol. 169.)
Aug. 10–17, 1986 Ottawa, Canada	**6th International Congress of Pesticide Chemistry** Contact: T.H.G. Micheal, Chemical Institute of Canada, 151 Slater Street, Suite 906, Ottawa, Ontario, Canada K1P 5H3. Tel.: (613) 233-5623. Telex: 053-4306 AIC.
Aug. 25–29, 1986 Antwerp, Belgium	**10th International Symposium on Microchemical Techniques** Contact: Dr. R. Dewolfs, University of Antwerp, Department of Chemistry, Universiteitsplein 1, B-2610 Wilrijk, Belgium. Tel.: 03/828.25.28 (ext. 204). Telex: 33646. (Further details published in Vol. 169.)
Sept., 1986 Graz, Austria	**4th Conference on Computer Based Analytical Chemistry** Contact: Dr. Wolfhard Wegschneider, Institut für Analytische Chemie, Mikro- und Radiochemie, Technische Universität, Technikerstrasse 4, A-8010 Graz, Austria. Tel.: (0316) 7061-8300/8301.
Sept. 8–10, 1986 Freiburg, F.R.G.	**4th International Symposium on Bioluminescence and Chemiluminescence** Contact: Dr. J. Schölmerich, Medizinschi Universitätsklinik, D-7800 Freiburg, F.R.G.

Sept. 9–12, 1986 London, U.K.	**5th Meeting of the International Electrophoresis Society, "Electrophoresis '86"** Contact: Dr. M.J. Dunn, Muscle Research Unit, Royal Postgraduate Medical School, DuCane Road, London W12 0HS, U.K., Tel.: 01-743-2030 ext. 338.
June 21–26, 1987 Toronto, Canada	**XXV Colloquium Spectroscopium Internationale** Contact: Mr. L. Forget, Executive Secretary XXV CSI, National Research Council of Canada, Ottawa, K1A 0R6 Canada. Tel.: (613) 993-9009, telex: 053-3145.

(*Continued from inside back cover*)

(*Continued from outside back cover*)

(*Continued on facing page*)

CONTENTS

(Abstracted, Indexed in: Anal. Abstr.; Biol. Abstr.; Chem. Abstr.; Curr. Contents Phys. Chem. Earth Sci.; Life Sci.; Index Med.; Mass Spectrom. Bull.; Sci. Citation Index; Excerpta Med.)

(Continued on inside back cover)